DOE/NASA/0058-79/2 – Vol. I
NASA CR-159495

MOD-1 WIND TURBINE GENERATOR ANALYSIS AND DESIGN REPORT

General Electric Company
Space Division

March 1979

Prepared for
NATIONAL AERONAUTICS AND SPACE ADMINISTRATION
Lewis Research Center
Under Contract NAS 3-20058

for
U.S. DEPARTMENT OF ENERGY
Office of Energy Technology
Division of Distributed Solar Technology

NOTICE

DOE/NASA/0058-79/2-Vol I
NASA CR-159495

MOD-1 WIND TURBINE GENERATOR ANALYSIS AND DESIGN REPORT

General Electric Company
Space Division
Advanced Energy Systems
Philadelphia, Pennsylvania 19101

March 1979

Prepared for
National Aeronautics and Space Administration
Lewis Research Center
Cleveland, Ohio 44135
Under Contract NAS 3-20058

for
U. S. DEPARTMENT OF ENERGY
Office of Energy Technology
Division of Distributed Solar Technology
Washington, D. C. 20545
Under Interagency Agreement EX-77-A-29-1010

TABLE OF CONTENTS

Section

Section Page

SECTION 1

INTRODUCTION

SECTION 1

INTRODUCTION

Background

The extraction of power from the wind is not a new concept, especially in the application of mechanical power to pump water or to mill grains. However, the generation of electrical power from the wind dates only from the turn of the century. Wind turbine generators achieved a measure of technical and economic practicality in rural and remote areas of the country during the 1920's, but the gradual extension of electrical utility networks and the availability of low cost fossil fuels led to their abandonment by the 1940's.

The early wind turbine generators were generally limited to power levels below 10 kilowatts and were operated independently of an electric utility network. The Smith-Putnam machine of the 1940's was the singular attempt in this country to develop a large-scale unit with the capability of being connected to an electric utility network. Interest in wind power waned until the 1970's when shortages in energy and the increasing costs of fossil fuels forced the nation to reassess all forms of available energy. A national wind energy program was established to develop the technology necessary to enable wind energy systems to be cost competitive with conventional power generation systems and to be capable of rapid commercial expansion for producing significant quantities of electrical power. As part of that program, General Electric's Space Division was contracted to design and build, under the direction of NASA - Lewis Research Center and sponsored by the Department of Energy, a wind turbine generator having a nominal rating of 1.8 megawatts, designated Mod 1.

History of the Mod 1 Program

The Mod 1 program is being conducted in six phases: Analysis and Preliminary Design (culminating in a Preliminary Design Review), Detail Design (ending with a Final Design Review), Fabrication and Assembly, System Testing, Site Preparation, and Installation and Checkout. Major milestone dates for these phases are shown in Table 1-1. This report is intended to describe only the results of the first two phases; that is, activities leading to the completion of Detail Design. Although this report places emphasis on a description of the design as it finally evolved, it is of some interest to trace the steps through which the design progressed in order to understand the major design decisions.

The design requirements specified by NASA for the Mod 1 wind turbine generator in the contract Statement of Work reflected the conclusions of two previous design studies by contractors, as well as the experience of NASA-LeRC in designing, building, and operating the Mod 0 unit. These specifications, summarized in Table 1-2, were utilized as the design starting point. Therefore, during the Analysis and Preliminary Design phase, only certain parameters were optimized and certain design options were investigated. A major decision was the selection of a rigid rotor hub as opposed to a teetered hub. A trade-off study was conducted in which the effects on rotor hub, supporting structure, and tower as a result of load reduction from teetering were weighed against the increased complexity and programmatic risks of a teetered hub design. Supporting this study, detailed layouts were prepared of rigid hub and teetering hub

concepts, with corresponding load analyses for selected critical wind and gust conditions. In the process of conducting this study, it was discovered that the pitch control mechanism, because of its required location and its role in determining blade torsional stability, had to be much more robust than had been anticipated and greatly influenced the size, weight, and cost of all adjoining mechanical components. As a result, an in-depth design study was initiated to evaluate various mechanism concepts, resulting in selection of the system that will be described later. Undoubtedly, the size and complexity of the pitch control mechanism was the deciding factor that made it difficult to incorporate a teetering feature and so tipped the scales in favor of a rigid hub design.

A major analytical task of the first program phase was the verification of analytical computer codes used for dynamic simulation and load analyses. The results of this task are reported in Appendix "A". The results of this and other analytical tasks, as well as the conclusions of the teetered hub study, were orally presented to NASA at a First Phase Formal Review, just prior to the Preliminary Design Review (PDR).

At PDR, the results of the Analysis and Preliminary Design tasks were presented as follows:

a. Design features were described.
b. Analyses, completed and planned were discussed.
c. Any design deficiencies established by analysis were identified.
d. Failure modes were reviewed.
e. Material selection and justification were discussed.
f. Fabrication procedures were discussed.
g. Inspection and testing techniques and criteria were discussed.
h. Approval to deviate from specifications was obtained, where required.
i. Approval for procurement of long-lead items was obtained.

Approval of the Preliminary Design permitted the next phase, Final Design, to proceed.

During Preliminary Design and through the initial stages of Final Design, responsibility for the blade, rotor hub, and pitch control mechanism was subcontracted to Hamilton-Standard in Windsor Locks, Conn., along with related analytical tasks. Hamilton-Standard proposed a filament wound, glass fiber reinforced plastic blade with fabrication in turn subcontracted to Allegheny Ballistics Laboratory. When it became evident that the filament wound blade would not live up to its expectations, a back-up design study for a metal blade was initiated with Lockheed Aircraft Co. Subsequently, Hamilton-Standard's participation was terminated and the design and fabrication of a metal blade was subcontracted to Boeing Engineering Company.

At this stage in the program, the opportunity was taken to reassess the design requirements at a point when the final design had not been frozen. Among the requirements re-examined at this time were rated power, rated wind speed, blade ground clearance, design gust conditions, blade profile, downwind rotor placement, and ambient temperature extremes. As a result, recommendations to change certain of the requirements were made to NASA and the negotiated changes are reflected in Table 1-2. A review of the total program costs at this time

resulted in the cancellation of the option to fabricate a second unit.

While a new metal blade design was initiated, final design of the remainder of the wind turbine generator system was completed and a Final Design Review was held. However, final drawing releases of some components whose design depended on the blade were delayed until the required information was available. The blade design progressed through PDR and FDR, similar to the steps taken for the remainder of the system.

Two tasks that supplemented the Detail Design tasks were the Safety Review and the Failure Modes and Effects Analysis (FMEA). The Safety Review was imposed as an internal General Electric-Space Division requirement, a prerequisite to approval of the final design. This review was conducted by qualified specialists within the Space Division but not associated with the Mod 1 program. The FMEA was directed towards prevention of failures that presented a hazard to operating personnel or the general public, and failures resulting in major damage to the wind turbine generator. Results of the FMEA are presented in a separate report but the highlights are in the next sub-section.

Table 1-1

Mod 1 Program Milestones

Program Go-Ahead	July, 1976
First Phase Formal Review	December, 1976
Preliminary Design Review (less blade)	January, 1977
Reassessment of Design Requirements	June, 1977
Final Design Review	August, 1977
Metal Blade Go-Ahead	September, 1977
Blade Preliminary Design Review	December, 1977
Blade Final Design Review	March, 1978
Assembly Start	May, 1978
Site Preparations Start	June, 1978
System Test Start	August, 1978
Shipment to Site (less blade)	September, 1978
Sub-system Checkout	March, 1979
Blade Shipment to Site	April, 1979
System Checkout	May, 1979

Table 1-2

Summary of Design Parameters

Rated Power	2000 kWe @ 11.4 m sec^{-1} (25.5 mph) 1800 kWe @ 11.0 m sec^{-1} (24.6 mph)
Cut-In Wind Speed	5 m sec^{-1} (11 mph) max.
Cut-Out Wind Speed	15.9 m sec^{-1} (35 mph)
Maximum Design Wind Speed	67 m sec^{-1} (150 mph at shaft center line - assume no wind shear)
Rotors per Tower	1
Location of Rotor	Downwind of Tower
Direction of Rotation	CC (looking upwind)
Blades per Rotor	2
Cone Angle	9^{o}
Inclination of Axis Rotation	None
Rotor Speed Control	Variable Blade Pitch
Rotor Speed	34.7 RPM
Blade Diameter	61 meters nom. (200 ft. nom.)
Airfoil	44XX series
Blade Twist	11^{o} Linear
Tower	Steel Truss
Blade Tip to Ground Clearance	12 meters (40 ft.)
Hub	Rigid
Transmission	Fixed Ratio Gear
Generator	60 Hz/Synchronous
Yaw Rate	$.25^{o}$/sec
Control System	Electro Mechanical/Microprocessor
System Life :	
Dynamic Components	30 years (with maintenance)
Static Components	30 years (with maintenance)

NOTE :

1. All wind velocities measured at 9 meters (30 ft.) elevation.

Failure Modes and Effects Analysis

The FMEA was directed primarily at identifying those critical failure modes that would be hazardous to life or would result in major damage to the system. As a result, the analysis was conducted from the "top down", minimizing the extent of analysis that would lead to trivial conclusions, had the analysis been approached from the "bottom up". For example, a component-by-component analysis of the lubrication system was not pursued, once it had been established that all single lubrication system failures lead to the same, non-critical conclusion.

The criteria used for evaluation during the FMEA is that none of the following injuries or damage shall occur because of a single failure or a single failure following an undetected failure of the wind turbine system.

Category I: Failures which would result in death or serious injury to the operator or general public.

Category II: Failures which would result in major or significant damage to the wind turbine system, extended outage, or damage to the connected utility.

The FMEA worksheets went through several stages of review, including review by qualified GE specialists outside of the Mod 1 program and two reviews by knowledgeable NASA LeRC personnel. Corrective action was taken whenever recommended.

Maintainability

This topic was addressed on a continuing basis during the design phase, and provisions were built-in for ease of maintenance. Whenever possible, standardized off the shelf components were chosen for minimum maintenance, with the normal maintenance cycle initially set at 6 months.

SECTION 2

SYSTEM DESCRIPTION

SECTION 2

SYSTEM DESCRIPTION

2.1 GENERAL CONFIGURATION

The general configuration of the Mod 1 wind turbine generator is shown in Figure 2-1. The two-bladed rotor is approximately 200 feet (61 m) in diameter and is located downwind of the tower 140 feet (46 m) above the ground. The nacelle, enclosing all equipment mounted on top of the tower, is driven to rotate about the vertical axis of the tower in response to changes in the wind direction. The truss tower is made up of tubular and channel structural shapes with bolted joints. It is 12 feet (4 m) square at the top and 48 feet (16 m) square at the bottom, and is anchored to reinforced concrete footings at each leg. At ground level is located an environmentally controlled enclosure for sensitive control and power generation equipment as well as elements of the data system. Within the fenced area are also located the back-up battery system, the step-up transfomer connecting to the utility, and the lift device that provides access to the top of the tower.

The total weight of all equipment above ground level is approximately 650,000 pounds (290,000 kg) of which 310,000 pounds (140,000 kg) is the weight of the tower. In order to facilitate transportation and erection, the system is designed to permit shipment in a number of subassemblies not exceeding 100,000 pounds (45,000 kg) each. The approach requires more high elevation assembly, but eliminates the need for a costly, high capacity crane at the site. See Table 2-1.

Equipment mounted on top of the tower is shown in more detail in Figure 2-2. Major components identified below are also discussed in more detail in subsequent sections of this report.

2.2 ROTOR

The steel blades are attached to the hub through a three-row roller bearing that permits the pitch angle of each blade to be varied 105 degrees from feather to full power. Blade pitch is controlled by hydraulic actuators operating through a mechanical linkage with sufficient capacity to feather the blades at a rate of 14 degrees per second. The rotor is supported by a single bearing with two rows of tapered rollers.

2.3 DRIVE TRAIN

Torque from the rotor is carried by a floating shaft to a speed increaser gearbox. The gearbox increases the speed through three stages to match the 1800 rpm synchronous generator, also connected to the gearbox through a floating shaft with flexible gear couplings. The high speed shaft incorporates a dry disk slip clutch protecting against torque overloads, and a disk brake that stops the rotor and holds it in a parked position. The gearbox lubrication system also provides oil to the rotor bearing and dissipates waste heat by means of a passive cooler suspended below the nacelle.

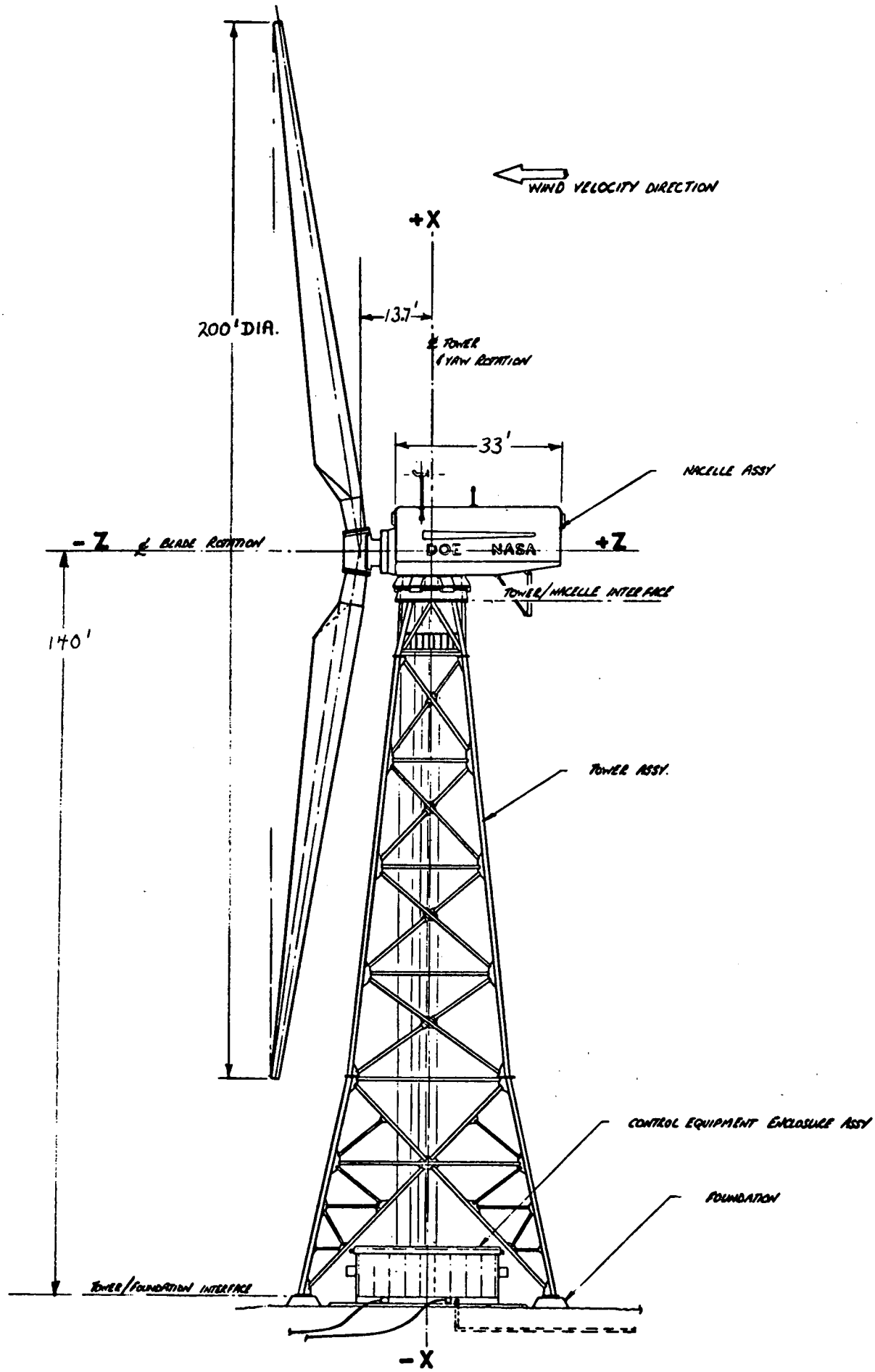

Figure 2-1 Mod 1 WTG General Configuration

TABLE 2-1

SYSTEM WEIGHT BREAKDOWN

ROTOR ASSEMBLY		103,000 lb
Hub	15,000	
Blades	36,000	
Bearings, supports	29,000	
Pitch Control Mechanism	11,000	
Pitch Control Hydraulics	12,000	
NACELLE ASSEMBLY		171,000 lb
Bedplate	68,000	
Fairing	5,000	
Generator	14,000	
Power Generation Equipment	1,000	
Shafts and Couplings	18,000	
Gearbox	58,000	
Lube, Hydraulic System	4,000	
Control and Instrumentation	1,000	
Cables, Lights, etc	2,000	
YAW ASSEMBLY		56,000 lb
Yaw Structure	34,000	
Bearing	13,000	
Yaw Brake	1,000	
Yaw Frive	8,000	
TOWER ASSEMBLY		320,000 lb
Structure	313,000	
Lift Device	1,000	
Cable, Conduit	6,000	
TOTAL (Excluding Ground Equipment)		650,000 lb
GROUND EQUIPMENT (Including Transformer)		54,000 lb
TOTAL		704,000 lb

The low speed shaft and the gearbox first stage shaft are hollow to permit passage of electrical cables from the rotor to a slip ring assembly.

2.4 POWER GENERATION EQUIPMENT

A synchronous ac generator is driven at 1800 rpm by the high speed shaft. A shaft-mounted, brushless exciter, controlled by a solid-state regulator and power stabilizer, provides voltage control. Generator output at 4160 volts is brought by cables and a slip ring at the yaw bearing down the tower to the ground enclosure. Surge capaciters and related power generation equipment are mounted in a caged enclosure below the generator.

2.5 NACELLE STRUCTURE

The welded steel bedplate is the primary nacelle structure, supporting all equipment mounted on top of the tower and providing a load path between the rotor and the yaw structure. Equipment mounted on the bedplate includes the pitch control and yaw drive hydraulic packages, the control and data system units, access ladders and walkways, oil coolers, lubrication pumps, hydraulic plumbing, and cables for electrical power and instrumentation. A removable fairing encloses the nacelle, incorporating inlet and outlet louvers for cooling air. The fairing also provides mounting for wind sensors, obstruction lights, and interior lighting.

2.6 YAW DRIVE

Rotation of the nacelle about a vertical axis is provided by the yaw drive system, consisting of upper and lower structures, a cross-roller bearing, dual hydraulic drive motors, and six hydraulic brakes. Each yaw motor drives a pinion meshing with a gear on the inner race of the yaw bearing. The yaw brakes control dynamic excitations in yaw by maintaining a rigid connection, and assist in damping yaw motions while the nacelle is being driven. Power and signal data are transferred to the tower-mounted cables by slip-rings.

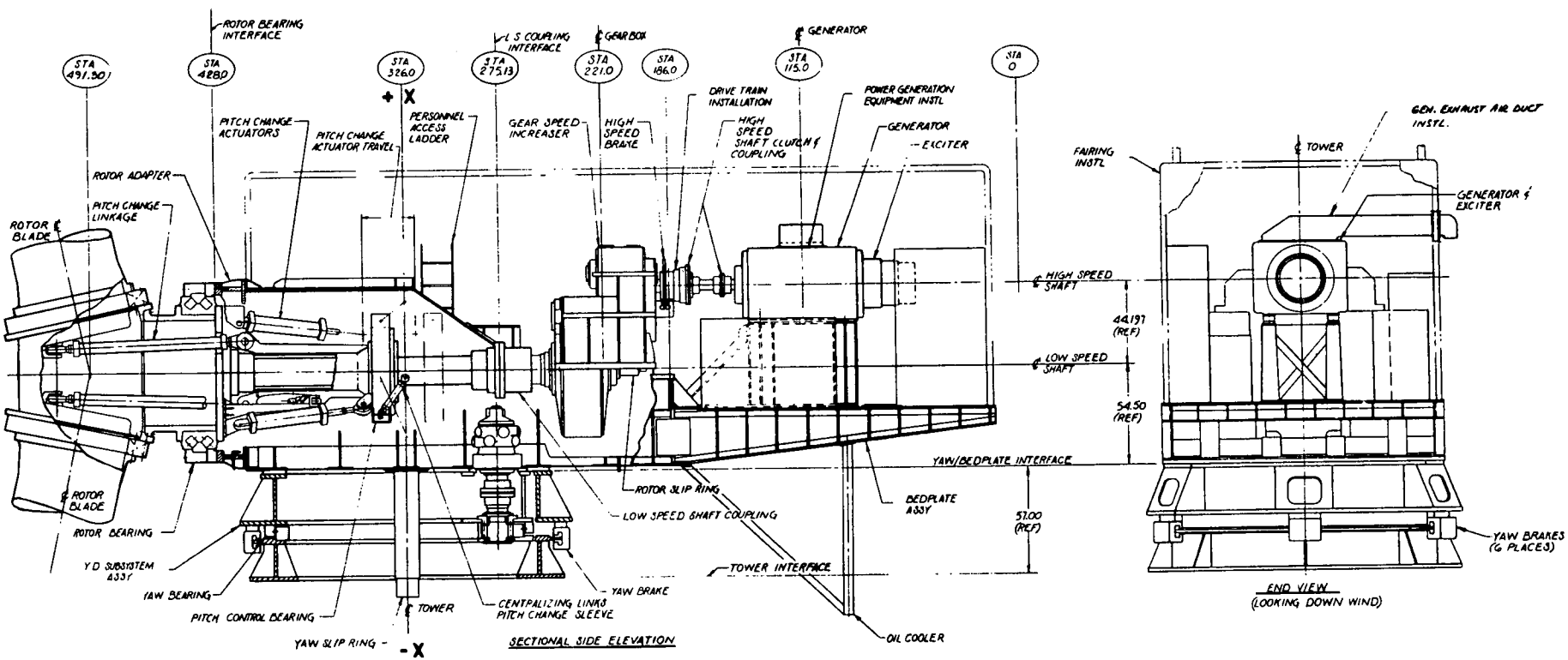

Figure 2-2. Nacelle Installation

SECTION 3

STRUCTURAL DYNAMICS

SECTION 3

STRUCTURAL DYNAMICS

3.1 REQUIREMENTS/OBJECTIVES/APPROACH

The objective of the structural dynamic analysis is to assure the dynamic adequacy of the system design for the range of operating conditions experienced in service. Key factors which influence the system dynamic design adequacy are:

1. Accurate prediction of operational loads and deflections
2. Proper system resonant frequency placement
3. Selection of a design approach which minimizes sensitivity to variations in parameters and alleviates dynamic loading

Because of the many dynamic interactions within the WTG system, proper placement of the system resonant frequencies is not directly related to the subassembly dynamic characteristics. Similarly, the design loads can be amplified by the structural response to cyclic excitation. The design approach can provide parameters which are variable and difficult to predict, and can increase dynamic loading. By analyzing the system dynamic characteristics for specified subassembly characteristics considering the variability of key parameters, the dynamic adequacy of the system can be evaluated early in the design phase and modifications made to assure the adequacy of the final design. The purpose of the dynamic analysis is to examine the system dynamic characteristics and to assure the compatibility of the system with the service conditions.

The frequency placement and operational design load requirements for the Mod-1 Wind Turbine Generator are summarized in Table 3-1. The frequency requirements are an outgrowth of the original NASA specification and frequency placement sensitivity studies, which are discussed in Paragraph 3.3. The fatigue design is based on the Case A loading conditions. Because of the high number of cycles accumulated over 30 years at the high wind speeds, the cyclic loads at the cut-out speed (35 mph) are used to design the system for infinite life. The steady state vibratory loads calculated at this speed are multiplied by dispersion factors to account for gusts and wind directional changes. Cases B through D represent limit loading conditions which the system must withstand.

The approach used to analyze the system dynamic behavior is to synthesize the system from substructures and analyze the system for anticipated operating conditions in service. Modal synthesis is used to assemble the WTG system from its major substructures: the tower, bedplate, shaft, hub and two blades shown in Figure 3-1. The mode shapes and resonant frequencies of these substructures are combined using stiffness coupling. Finite element models of the substructures are used for both stress and dynamic analysis and are sufficiently detailed to capture the dynamic behavior of component structures. By using this substructure definition, the system characteristics can readily be determined for various yaw and rotor positions. In addition, the bearing stiffness, which is difficult to predict, can be readily varied to determine its influence on the structural response characteristics.

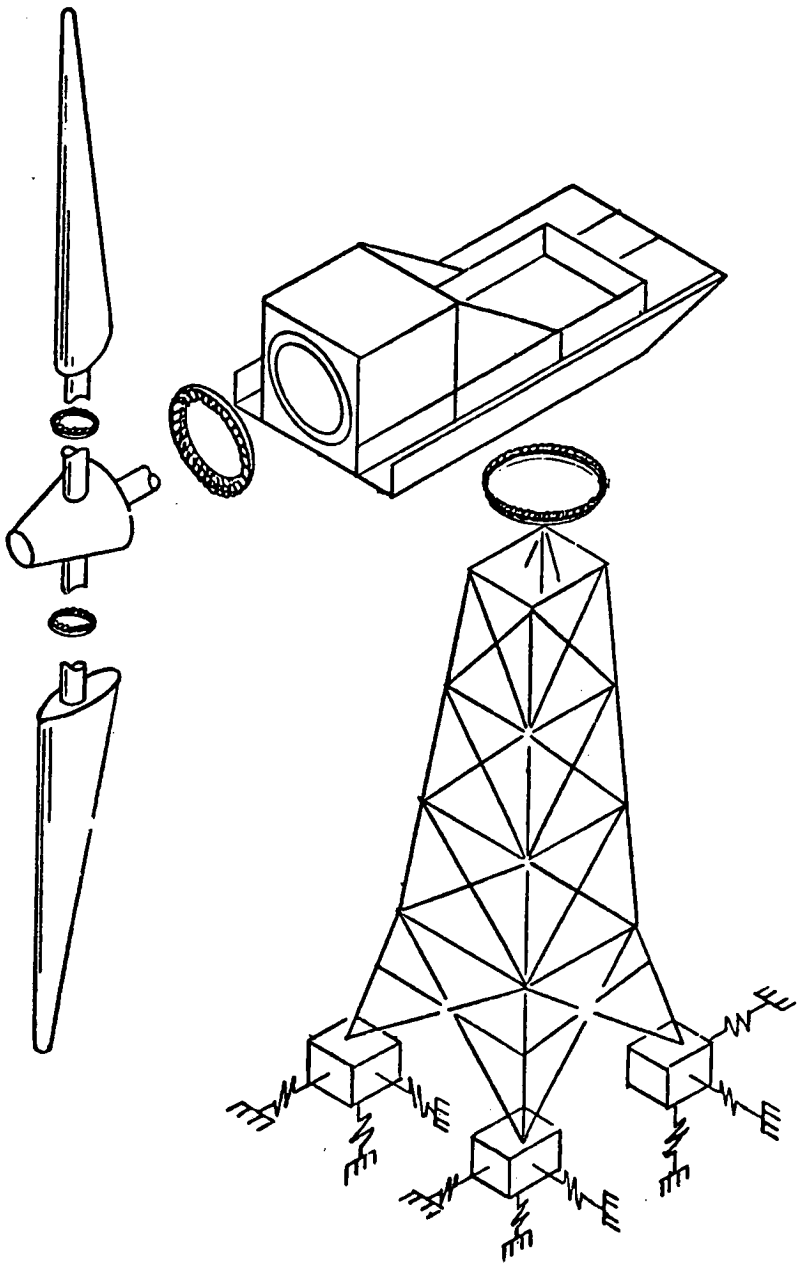

Figure 3-1 WTG Analytical Model Synthesized from Substructures

Table 3-1

WTG Frequency Placement and Operational Design Load Requirements

Frequency Placement

1.	Blade Flapwise	2.15-2.7P
2.	Blade Edgewise	4.15-4.7P
3.	Tower Bending	> 2.8P
4.	Tower Torsion	> 6.5P

All blade modes are to be removed from integers of per Rev. (i.e., 1P, 2P, 3P, etc.).

All tower modes are to be removed from even integers of per Rev. (i.e., 2P, 4P, 6P, etc.).

Load Cases

Case A - Accumulated fatigue over entire wind duration regime from cut-in to cut-out velocity. Inflow angles to 20^{o} included. Above is met by basing fatigue design on dispersed cyclic loads at cutout, 35 mph

Case B - Maximum upgust 35-50 mph, rotor disk fully immersed. Blade pitch at trim for 35 mph, $\pm$ 41^{o} inflow.

Maximum downgust 35-20 mph, rotor disk fully immersed. Blade pitch at trim for 35 mph, $\pm$ 41^{o} inflow.

Case C - Overspeed (Emergency Feather). 15% overspeed, zero torque at 50 mph.

Case D - Hurricane, parked at 120 mph.

The dynamic response of the system is determined using piecewise linear models to represent the system at various rotor blade positions, see Figure 3-2.

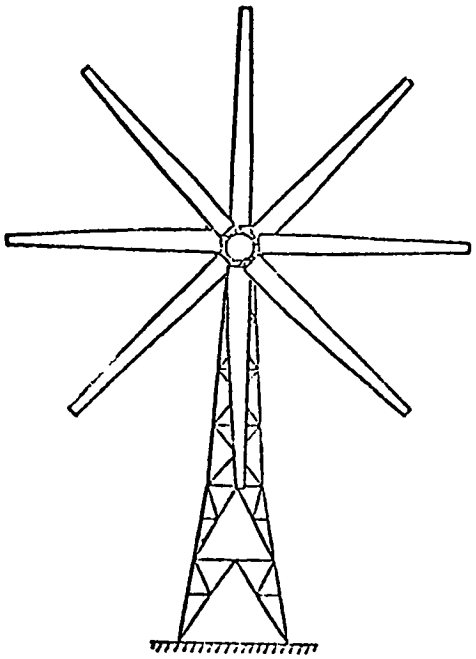

Figure 3-2. Piecewise Linear Model

Sensitivity to the number of models has been studied and it was found that 45-degree increments of rotor position are sufficient for design purposes. The model is switched using the modal responses of the previous model to determine the initial conditions for the next model. This provides a readily understood representation of the system. Critical modes and couplings can be identified as the system is excited and responds. By examining the system mode shapes and modal responses, changes to the system can be determined to improve the dynamic response characteristics. By evaluating the complete system, the interactions of all the substructures can be accurately modeled and included in the simulation.

The system design includes several features which should alleviate dynamic loading. The tower is of tubular construction which minimizes tower blockage. The nacelle is yawed while a brake is applied, which eliminates free play in the yaw drive system.

These characteristics enhance the accuracy of the loads predictions and should reduce dynamic amplifications within the system.

Since the final blade design was not complete at the time of this analysis, preliminary blade physical properties were used which allow for growth to 20,000 pounds. For an actual blade weight of less than 20,000 pounds, the predicted loads are conservative.

3.2 SYSTEM SYNTHESIS

3.2.1 SYSTEM DYNAMIC ANALYSIS

The analysis of the WTG system by substructures was accomplished by the separation of the system into major substructural segments. This system naturally divided at: the bearing attachments located at each rotor blade, at the hub, the low and high-speed drive shaft supports, and the bedplate/tower interface. A natural division was also made at the the blade pitch actuator attachment and the yaw drive/brake mechanism. This division resulted in five major substructures: the tower, bedplate, hub/shaft and two rotor blades.

Each major substructure was then analyzed separately, using finite element models to obtain substructure vibration mode shapes and frequencies with free attachment coordinates. Then, the stiffness coupling method of modal synthesis was used to assemble the complete structure through stiffness links (stiffness matrices) representing the bearings and drive mechanisms. This assembly of component modes and frequencies through flexible links was then used to derive the eigenvalues and corresponding eigenvectors representing the system dynamic model.

The flow of the dynamic model assembly is shown in the block diagram of Figure 3-3. This diagram gives the sequence of assembly for the model and the subsequent input of the modal parameters into the response and dynamic loads analysis programs. Revisions to the dynamic model were made after frequency placement checks and preliminary stress analysis, where necessary, to meet the design criteria. Results of the dynamic loads analysis were then used to check the loads used in the final stress analysis.

3.2.2 ANALYTICAL SUBSTRUCTURE DESCRIPTIONS

Finite element models were developed for each of the five substructures identified in Figure 3-3. Each of these substructure models is described as follows:

1. Tower. The tower model consisted of approximately 250 curved and straight beam elements representing each tubular member connected at 120 nodes. This representation provided the structural detail necessary to describe the dynamic behavior of the tower structure. Through nodal compression methods, it was possible to reduce the quantity of nodes used in the substructure eigenvalue solution to 16 nodes, each with three linear degrees of freedom.

2. Bedplate. The bedplate model consisted of approximately 400 curved and straight beam elements representing the I-beam and channel basic frame members and plate elements representing the closed frame sections. Large mass component mounts were also represented explicity to provide realistic mass loading points. These components included the gearbox, generator and the yaw and hub bearings. This representation resulted in 196 nodes which were reduced to 27 nodes with a total of 96 degrees of freedom.

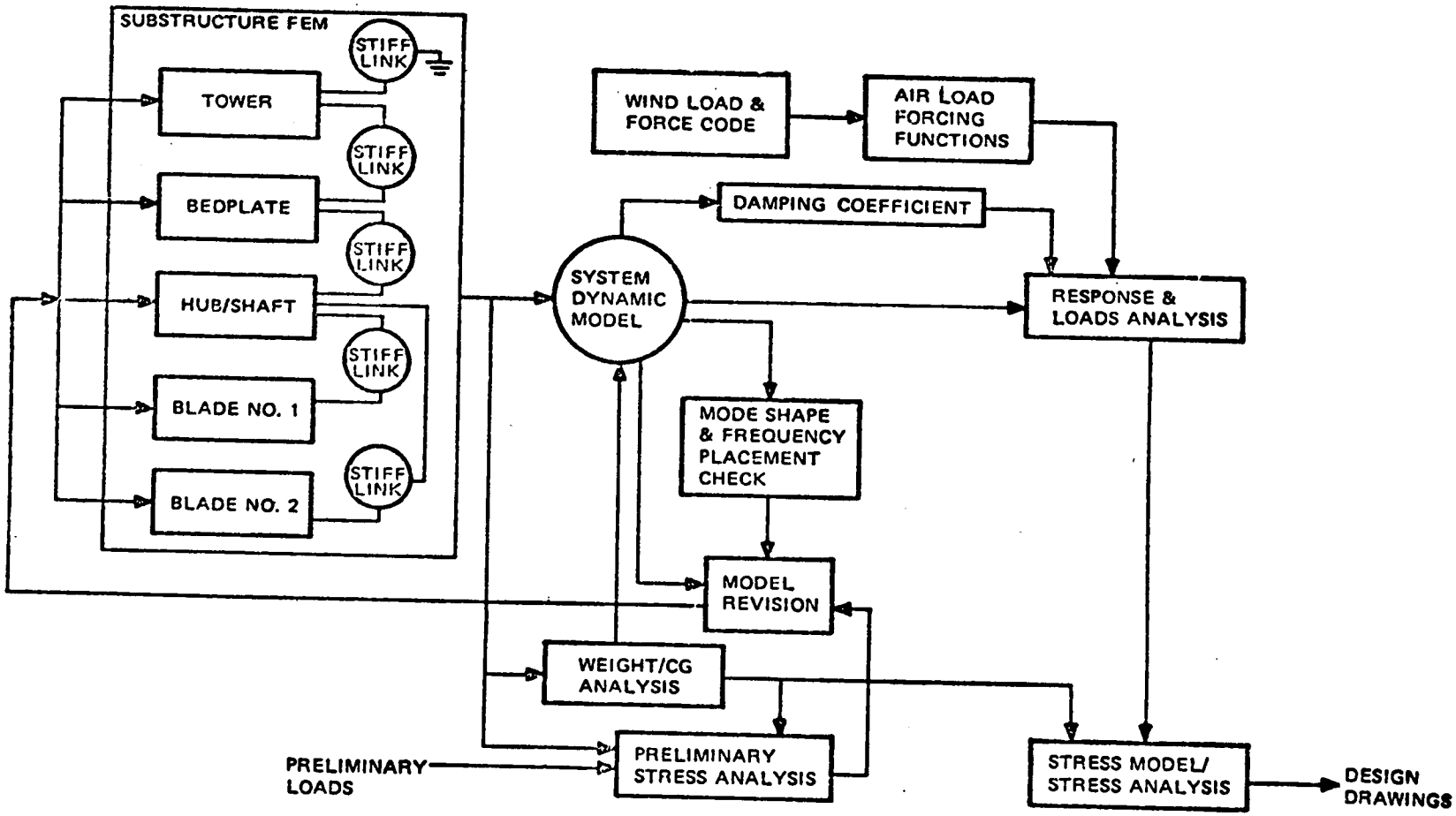

Figure 3-3. Mod-1 Analysis Flow

3. Hub/Shaft. The hub was modeled using NASTRAN as described in Paragraph 5.2, Stress Analysis; while the high and low-speed shafts were modeled by straight beam elements. Nodes were selected to correspond to the bearing attachment locations, flex-coupling, gearbox, bearing support and other mass loading points. Gearbox flexibility was included in the form of beam elements which considered effects of gear ratio. Eighteen nodes were used to represent this complete assembly from the hub to the generator.

4. Rotor Blades. Rotor blade mass and stiffness properties received from Boeing were used as input data for a vibration analysis computer program, STRAP. This program calculated free mode shapes and frequencies of the blade considering twist angle and centrifugal stiffening. Twelve nodes with six degrees of freedom each were used to represent a single blade. The analytical modes obtained were rotated 180° to obtain the modal deflections for the second rotor blade.

3.2.3 STIFFNESS LINKS

The stiffness links used to assemble the WTG system consisted of several stiffness matrices which contained the actual stiffness properties of the bearings that physically connect the substructures. It also included flexibility of the blade pitch change mechanism and the yaw drive/brake flexibility as used in the physical assembly. These stiffness matrices thus related each substructure at the attachment coordinates.

1. Blade to Hub. A single blade retention bearing was used to attach the blade to the hub. This bearing provided linear restraint in three directions (one axial and two radial), and rotational restraint about the two radial axes. Rotational restraint about the blade axial direction was defined by the stiffness of the pitch change mechanism.

2. Hub Shaft to Bedplate. A single hub retention bearing was used to attach the hub segment of the hub/shaft assembly to the bedplate. Rotational stiffness about the two radial axes were derived from the linear values and rotational stiffness about the axial direction, which was set to zero to permit free rotation of the hub/shaft.

   A rotational stiffness about the axial direction was included at the generator to represent the on-line configuration. This rotational stiffness was set to zero for off-line evaluation.

3. Bedplate to Tower. Assembly of the bedplate structure to the tower is accomplished by a 12-foot yaw drive bearing. This bearing provides restraint in all degrees of freedom except rotation about the yaw axis. Bearing stiffness data, obtained directly from the bearing vendor, was used for the stiffness matrix. For the yaw axis rotational restraint, the brake was

considered to be "on" such that the yaw drive system flexibility was shorted. Rotational stiffness for this condition was assumed to be sufficiently high to place the first bedplate mode (bedplate rotation about yaw axis) greater than the tower first torsion mode (7.2 P).

4. Tower to Ground. The tower assembly was modeled considering the tower base cantilevered to the ground through linear springs attached to each of the four tower legs. These springs represented soil flexibility derived from down loads (soil compression) and up-loads (pier shear of the foundation). The lowest stiffness values from a range of values was selected from calculations based on concrete footing and pier area. These values were used in the stiffness matrix relating the tower attachment coordinates to ground. Bearing stiffnesses are summarized in Table 3-2.

Table 3-2

Bearing Stiffnesses

Component	Stiffness (lb/in or in-lb/rad)		Source
Yaw Bearing	Axial	$2.47X10^{8}$	Messinger Bearing Co.
	Radial	$1.37X10^{8}$	
	Bending	$6.62X10^{11}$	
	Torsion Brake on	$6.4X10^{11}$	GE Analysis
	Torsion Brake off	$4.5X10^{9}$	
Hub Bearing	Axial	$2.48X10^{7}$	J. Rumbarger (Franklin Institute)
	Radial	$1.73X10^{7}$	
	Bending	$2.25X10^{10}$	
	Torsion	0	
Blade Retention Bearing	Axial	$4.38X10^{7}$	J. Rumbarger & GE Analysis
	Radial	$8.0X10^{6}$	
	Bending	$2.52X10^{10}$	
	Torsion	$1.2X10^{8}$ (Pitch Actuator)	
Generator Bearing Elec. Field	Radial	$2.5X10^{7}$	GE Analysis
	Torsion	$2.88X10^{5}$	

3.2.4 COUPLED DYNAMIC MODEL

The modal synthesis method selected for the WTG analysis is a technique that has been used extensively at the General Electric Space Division for spacecraft analysis. The method uses the free substructure vibration modes and frequencies to determine the coupled system modes of the entire system. These substructures, as defined by the stiffness coupling method, have no common degrees of freedom and are coupled together by the stiffness links described which relate the free attachment coordinates of the substructures.

In other methods of modal synthesis, the stiffness coupling method provides an approximate coupled solution where high frequency modes are truncated. Instead of truncating (or omitting the high frequency modes), a Dynamic Transformation is used to include modes in the solution that would otherwise be truncated. This transformation relates the unused (truncated) modes to the retained modes at a selected system frequency. This transformation is then used to reduce the generalized mass and stiffness matrices which describe the dynamic behavior of the coupled system. Details of the dynamic transformation are documented in Reference 1.

The wind turbine generator was assembled using a computer program, SCAMP (Stiffness Coupling Approach to Modal-Synthesis Program), which contained the stiffness coupling method with the Dynamic Transformation. The complete WTG model consisted of 423 degrees of freedom, of which 235 were used to synthesize the coupled model. The final size of the coupled eigenvalue problem (60 DOF) was determined from the total number of "modes kept". Selection criterion for the number of modes "kept" was determined on the basis of participation factors. System modes were thus calculated for the four rotor positions (0°, 45°, 90°, 135°) depicted for the piecewise linear model in Figure 3-2. Of the 60 modes, the first 20 were used to calculate the system forced response.

3.2.5 DETERMINATION OF FORCED RESPONSE

The flow of the system loads analysis is shown in Figure 3-4. The specified wind conditions are first used to define the system forces considering the system to be rigid. These rigid system loads are used as preliminary design loads for initial sizing of the tower and bedplate structures. The forced response analysis is then performed using the rigid system forces with motion-dependent aerodynamic coefficients to excite the system modes from SCAMP, described in Paragraph 3.2.4. The modal responses are then used to determine critical interface loads, accelerations and deflections for evaluation of the structural adequacy.

The WINDLD code determines the aerodynamic and inertial forces acting on the system as a function of rotor position. The aerodynamic forces are determined at ten stations along each blade using quasi-steady aerodynamics based on smooth airfoil characteristics. The wind shear profile is included as a power function with an exponent of 0.167 as indicated in the Statement of Work. The tower shadow

---

[1]Kuhar, E.J., "Selected System Modes Using the Dynamic Transformation With Modal Synthesis," Shock & Vibration Bulletin, August 1974, pp. 91-102.

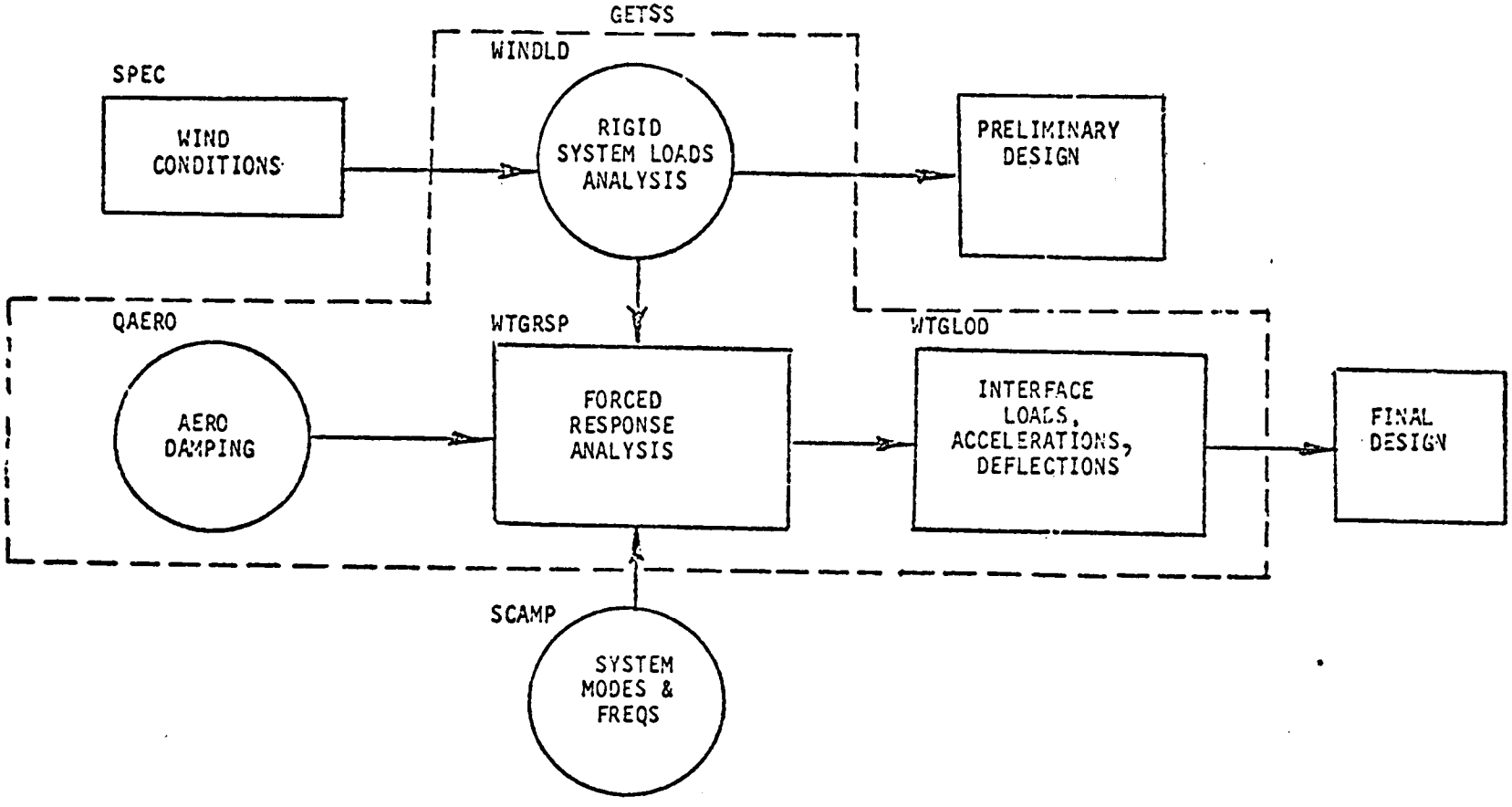

Figure 3-4. Flow of System Loads Analysis

is defined in system coordinates by a series of cosine functions aligned with the tower geometric position, providing a three dimensional velocity retardation that permits initial entry of the inboard blade section, Figure 3-5. With inflow, the shadow is shifted laterally to align the edges of the shadow with the projected edges of the tower, accounting for the downstream position of the rotor. The centrifugal and gravitational forces are also determined at each blade station. The forces are calculated in system coordinates for one revolution of the rotor. For initial design of the system, the integrated hub forces and moments are also calculated. For the forced response analysis, the forces at each of the ten stations on the two blades are used to excite the system.

The QAERO code determines the modal damping for the system modes considering the aerodynamic forces on the blades. The code uses a linearized solution based on the angle of attack at each blade station for each system model calculated in the WINDLC code. The fully coupled modes (i.e., flap, lag, and torsion) are used to determine the quasi-steady aerodynamic forces proportional to the generalized coordinate velocities. Then, modal damping ratio is determined from the integrated aerodynamic forces considering the total kinetic energy of the system, including the bedplate and tower structure. Additional structural or electrical damping of a selected value is then added to the aerodynamic damping.

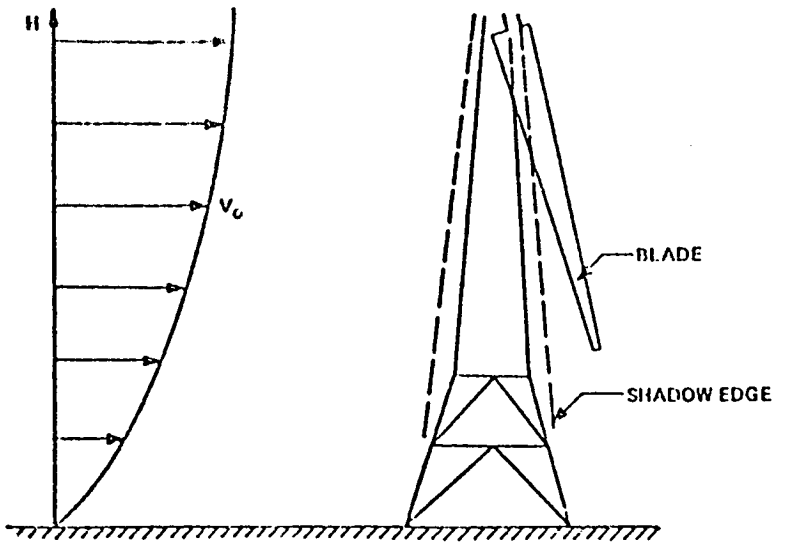

WIND SHEAR

$V_o = V_R \left(\frac{H}{H_R}\right)^{.167}$

V_R = REFERENCE VELOCITY

H_R = REFERENCE HEIGHT = 30'

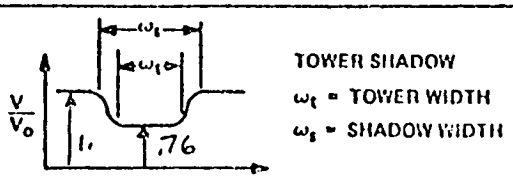

Figure 3-5. Tower Shadow Representation

The modal response to aerodynamic and inertial excitation is calculated using the WTGRSP code. The analysis considers the system to be piecewise linear for each model position. The solution for a 45° interval is obtained using the subroutine MERTA (Matrix Extra Routine for Transient Analysis). MERTA provides a closed form Laplace solution in modal coordinates treating the excitation forces as a series of ramp functions. For the WTG analysis, time increments corresponding to three degree rotor positions are used to define the forcing function. The initial conditions at the model switching positions are determined using the modal displacements and velocities at that time step for the previous model. A sufficient number of revolutions is analyzed to achieve a steady-state condition. The generalized coordinate displacements, velocities and accelerations determined at each time step for each model are the output from this code.

The WTGLOD code processes the modal responses from the WTGRSP code to determine the interface loads, accelerations and deflections at selected points of the WTG system. The code uses the modal displacement method. The load coefficients are determined on a modal basis to calculate the loads at nine interfaces. The interfaces consist of the 25%, 50%, and 75% blade stations, the blade root, the rotating shaft, the stationary shaft, the main rotor bearing, the yaw bearing and the tower base. To aid in understanding the results, the maximum modal contributions to each interface load are tabulated with the associated rotor angular position. In addition, the major mode contributing to the maximum interface load is also tabulated.

3.2.6 CODE VERIFICATION

A key element in the program was the development and verification of the GETSS (GE Turbine System Synthesis) computer code. Cost effective design of the WTG requires the accurate determination of the loads throughout the structure and the influence of critical resonant frequency placement. These data are provided by the GETSS code which was verified by comparing analytical predictions with measured results for the Mod-0 WTG under various operation conditions. The development of the Mod-0 dynamic model followed the same methods used in the Mod-1 analysis.

The final solution resulted in 20 modes under 10 Hz. These modes were used to compare directly with the results reported in NASA TMX-71879, 3426, and the final report by the University of Cincinnati on the modal testing. This comparison showed agreement in modal frequency within less than 1 percent for the first tower bending (N-S), first tower torsion and second tower bending (N-S). The first rotor flatwise and edgewise modes differed by only 3 to 4 percent and the others by not greater than 9 percent. A check of modal displacements also showed good agreement for the tower bending modes (Modes 4 and 5). The upper bay motion showed similar diagonal motion as that measured on the test, along with a similar amount of displacement.

The procedure used to verify the GETSS computer code is presented in Appendix A.

3.3 SENSITIVITY ANALYSIS AND FREQUENCY PLACEMENT

The coupling between the various WTG structures is significant and makes the influence of component structural changes on the system dynamic response a complex problem for analysis. The structural coupling exists between the rotor, shaft, bedplate, and tower such that as the rotor position changes, the dynamic characteristics of the system change. An understanding of the system sensitivity to these interactions was aided considerably by the modal synthesis approach which was used in the evaluation of the modal contributions to the dynamic loads. The identification of critical tuning parameters thus comprised a major contract study effort. The parameters investigated included blade/tower frequence placement and bearing stiffness variations at the major interfaces. The sensitivity to bearing stiffnesses are particularly important because these are difficult to predict accurately. The results of this study are summarized in Table 3-3.

Table 3-3. Summary of Sensitivity Analyses

- Soil Stiffness - Not Significant
- Yaw Drive Torsional Stiffness - Critical
- Tower/Blade Tuning - Critical
- Blade Retention Bearing Stiffness - Significant
- Main Rotor Bearing - Significant
- Yaw Bearing Stiffness - Not Significant
- Shaft Bearings - Not Significant
- Bedplate CG - Statically Significant

A brief discussion of the significant parameters follows:

1. Yaw Drive Torsional Stiffness. The variation in hub bending moment with yaw drive stiffness is illustrated in Figure 3-6. Large increases in flapwise moment are evident for decreases in yaw drive stiffness below the design value. Less dramatic increases in load occur at the yaw bearing and tower root. With the yaw brake engaged there is more than sufficient stiffness.

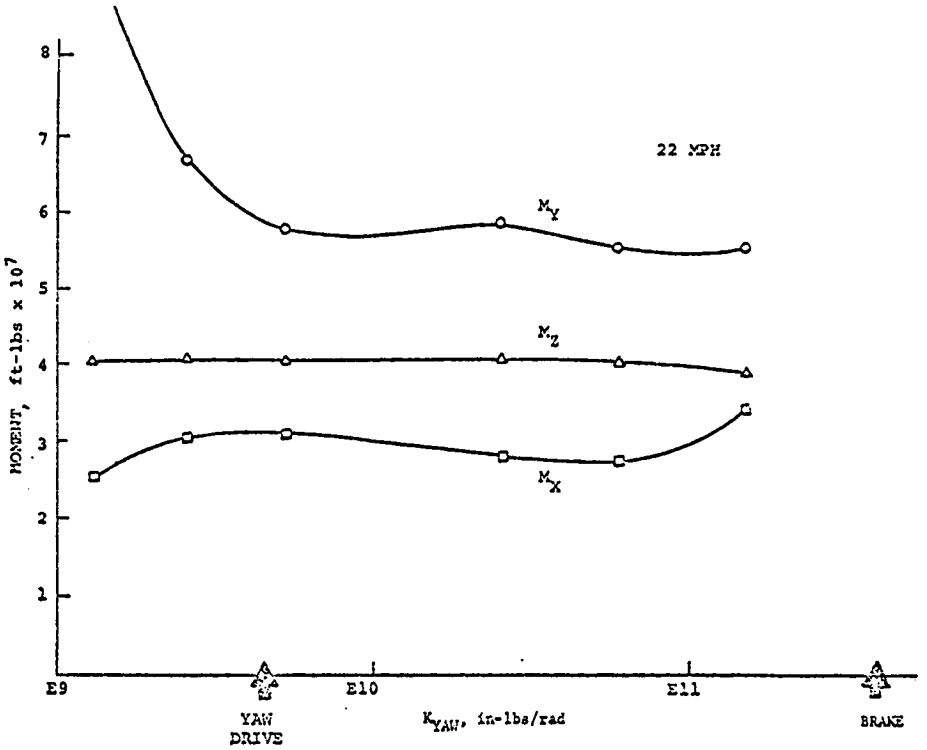

Figure 3-6. Load Variation with Yaw Drive Stiffness

2. Tower/Blade Tuning. A parametric study was performed to evaluate the sensitivity of system loads to tower stiffness. Coupling between the tower fundamental bending mode and the blade flapwise mode was investigated. Figure 3-7 shows the variation in cyclic moments with tower bending frequency, with the blade frequency fixed at 2.2P and at 2.6P. Moments are given at two major interfaces: the yaw bearing and at the base of the tower. For both values of assumed blade stiffness, there is a significant increase in loads when unfavorable coupling occurs between tower bending and blade flapping modes. Similar plots of cyclic moment are shown in Figure 3-8, for varying blade flapping frequency at constant values of tower bending frequency. It was concluded that with a blade flap frequency in the range of 2.15 to 2.7P (the actual value was unknown at the time of this analysis), unfavorable coupling could be avoided by ensuring that the tower bending frequency exceeded 2.8P. As a result, a change was made in the design requirements specified by NASA to raise the tower bending frequency placement from 2.2P to 2.8P.

3. Blade Retention Bearing Stiffness. Shear and axial stiffness variations were found to have negligible effect on system loads, while a reduction in bending stiffness by a factor of 24 produced a decrease in most of the system cyclic loads. The only significant increase was a 12% growth in tower base cyclic yaw moment.

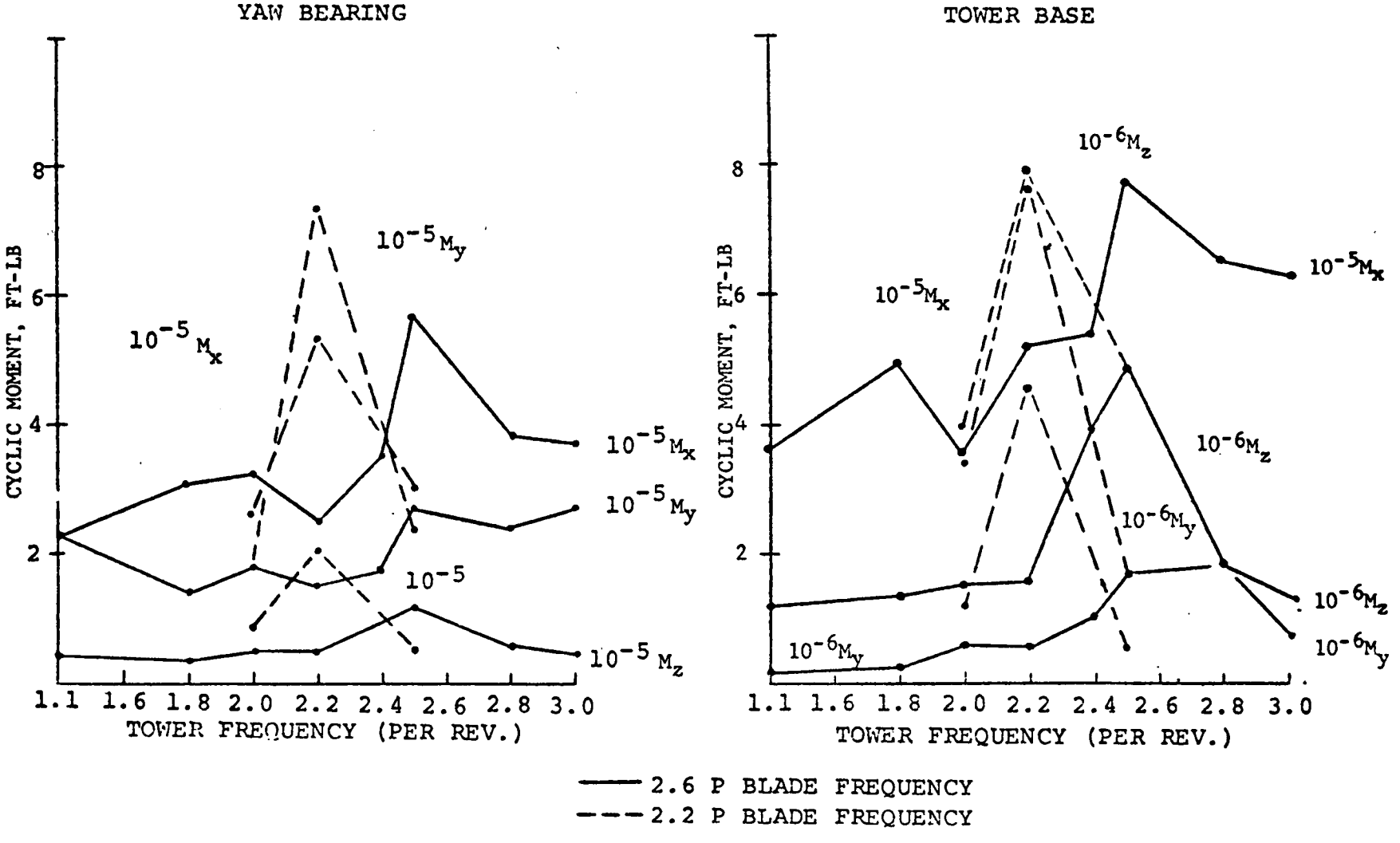

Figure 3-7. Cyclic Moments vs. Tower Frequency

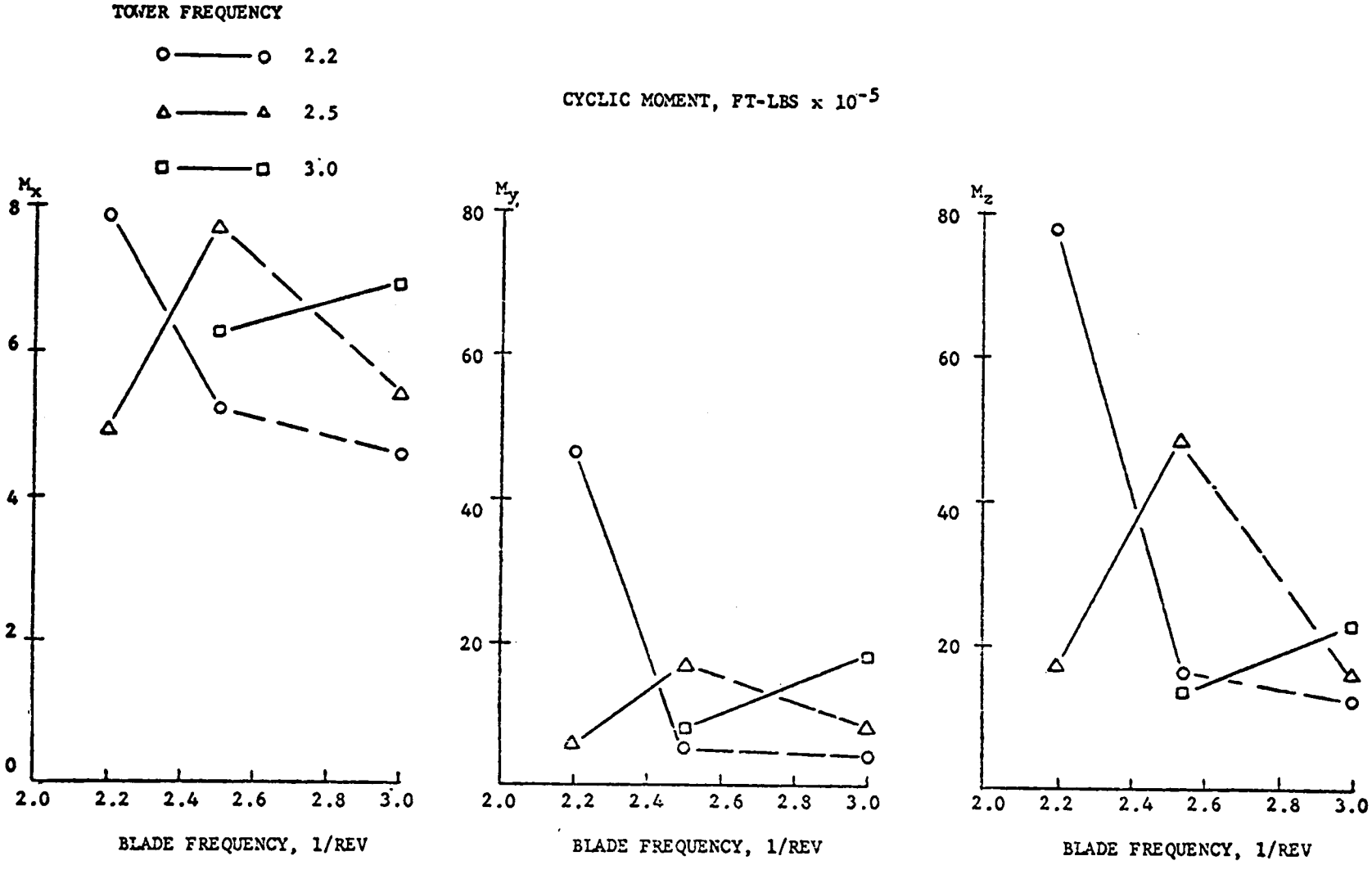

Figure 3-8. Cyclic Moments vs. Blade Flap Natural Frequency

4. Main Rotor Bearing Stiffness. Loads were relatively insensitive to changes in radial and axial stiffnesses; reductions by a factor of 100 were necessary to produce any noticeable change. A decrease in bending stiffness from the design value of 2.25×10^{10} to 4.0×10^{9} did not significantly affect the majority of the loads; some reductions were noted. The largest change was a 65% increase in tower base cyclic bending moment.

5. Foundation Stiffness. A parametric study was performed to evaluate the effects of soil or foundation stiffness. Tower natural frequencies were computed for a range of foundation stiffnesses that varied from approximately one-half to twice the anticipated values, laterally as well as vertically, as shown in Table 3-4. The results are summarized in Table 3-5, which shows tower frequencies for the first ten modes varied less than 5% from the expected value.

Table 3-4
Foundation Stiffnesses used for Parametric Analysis

	Vertical (lb/in)	Lateral (lb/in)
Low	8.58×10^6	7.33×10^6
Mid Range	14.33×10^6	12.17×10^6
High	28.58×10^6	24.42×10^6

Table 3-5
WTG 1500-MOD 1 Tower Natural Frequencies

Mode No.	Description	Natural Frequency, Per Rev.		
		Low K	Mid-Range K	High K
1	Tower Bending-Y axis	2.9260	3.0384	3.1306
2	Tower Bending-Z axis	2.9405	3.0543	3.1478
3	Tower Torsion	7.3405	7.3484	7.3542
4	Tower 2nd Bending-Y axis	11.868	12.002	12.108
5	Tower 2nd Bending-Z axis	13.848	14.151	14.397
6	Tower Axial-X axis	15.931	16.748	17.376
7	Tower 2nd Torsion	17.592	17.974	18.306
8	Tower 3rd Bending-Y axis	19.485	19.580	19.639
9	Tower 3rd Bending-Z axis	19.793	20.013	20.207
10	Tower 3rd Torsion	30.843	30.993	31.054

3.4 SYSTEM NATURAL FREQUENCIES AND LOADS

The final design coupled system natural frequencies at the four rotor azimuth positions needed for the piecewise linear model are contained in Table 3-6. Selected mode shapes appear in Figure 3-9A through 3-9G.

Table 3-6

Systems Frequencies and Modes

	Mode Description	Freq (/Rev)				Criteria
		0°	45°	90°	135°	
1.	Rotor Rotation	.67	.67	.67	.67	
2.	1st Rotor Flapwise Cyclic	2.4	2.7	2.3	2.3	2.15-2.7
3.	1st Rotor Flapwise Collect	2.6	2.6	2.6	2.6	
4.	Tower Bending - Y	3.1	3.1	3.2	3.1	2.8
5.	Tower Bending - Z	3.3	6.0	3.3	3.3	2.8
6.	1st Rotor Edgewise Cyclic	4.2	4.0	4.2	4.4	4.15-4.7
7.	2nd Rotor Flapwise Cyclic	5.6	5.4	5.0	5.0	
8.	Shaft Torsion	6.9	6.9	6.9	6,9	
9.	2nd Rotor Flapwise Collect	6.2	6.2	6.2	6.2	
10.	Tower Torsion	7.2	7.2	7.9	7.5	6.5
11.	2nd Rotor Edgewise Collect	12.9	12.9	12.9	12.9	
12.	3rd Rotor Flapwise Cyclic	11.0	11.7	11.6	11.7	
13.	3rd Rotor Flapwise Collect	11.3	11.3	11.3	11.3	
14.	Tower 2nd Bending Z	14.7	14.3	14.1	14.2	
15.	Tower 2nd Bending Y	14.9	15.0	15.0	14.9	
16.	Blade Torsion Antisymmetric	11.6	11.6	11.5	11.6	
17.	Blade Torsion Symmetric	11.6	11.6	11.6	11.6	
18.	2nd Rotor Edgewise Cyclic	15.6	15.2	14.8	15.1	
19.	Tower Longitudinal	16.4	17.7	17.2	17.2	
20.	Tower 2nd Torsion	17.0	16.4	16.5	16.5	

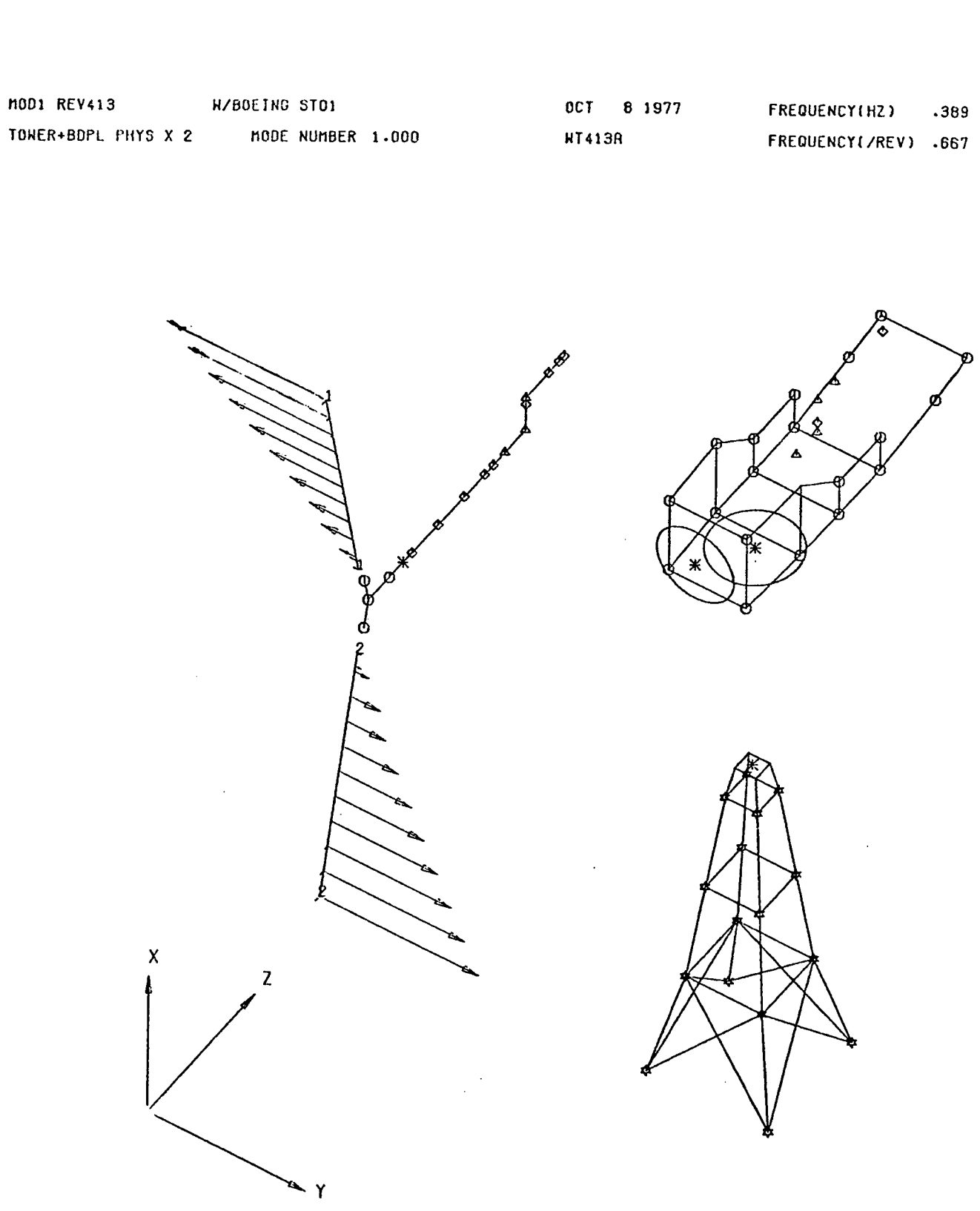

Figure 3-9A. Rotor Rotation

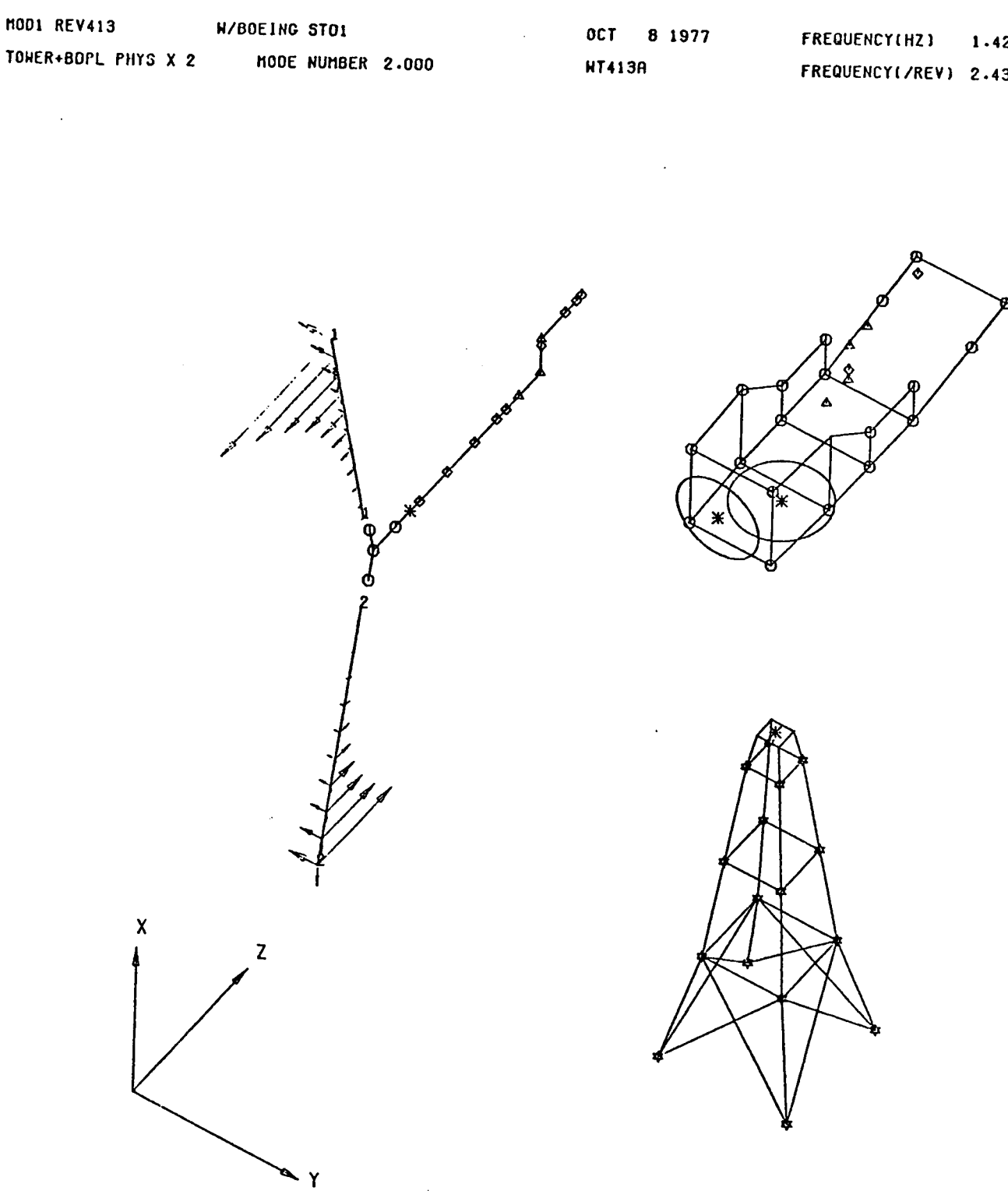

Figure 3-9B. First Rotor Flatwise, Cyclic

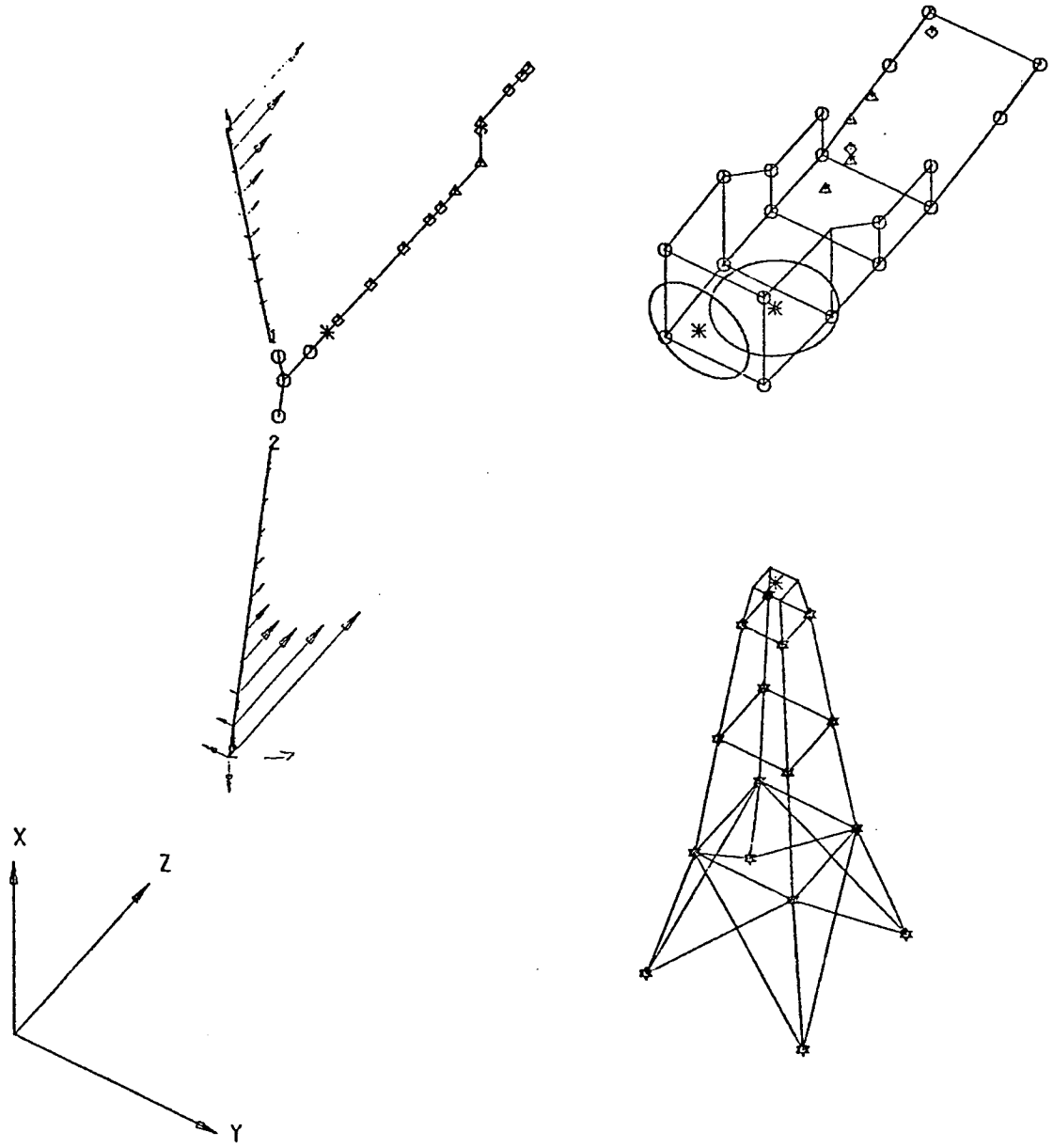

Figure 3-9C. First Rotor Flatwise, Collect

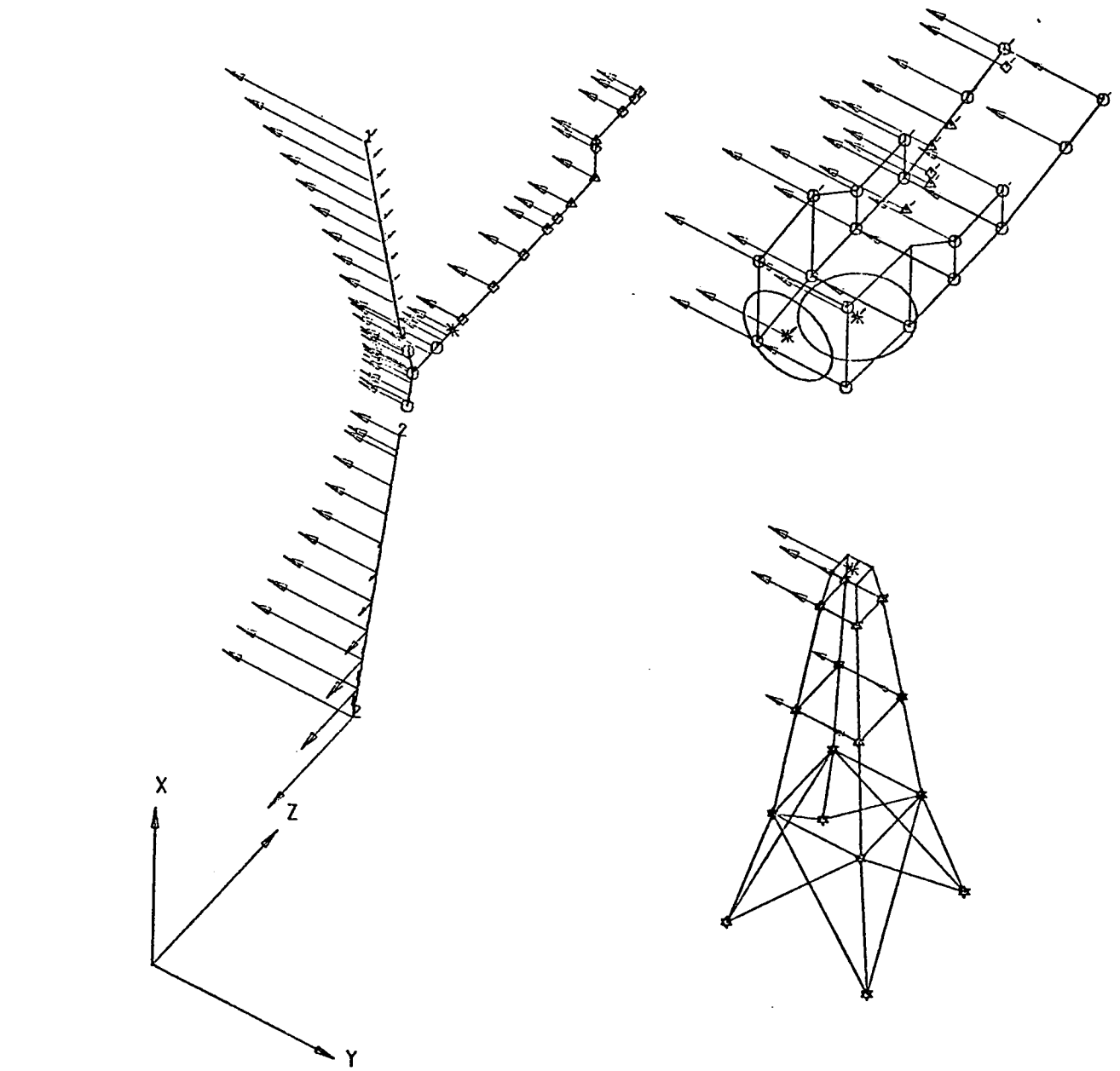

Figure 3-9D. Tower Bending, Y-Axis

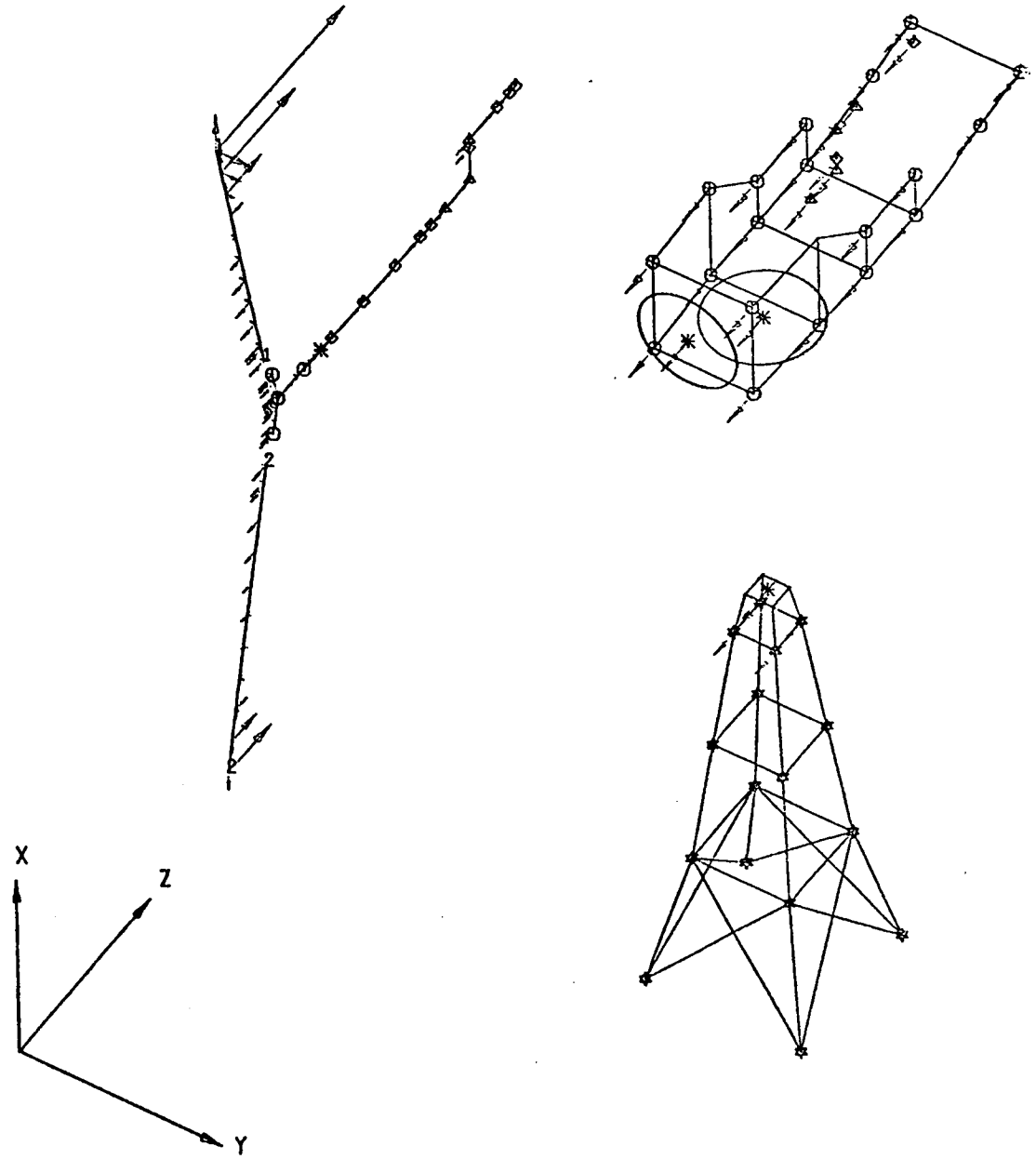

Figure 3-9E. Tower Bending, Z-Axis

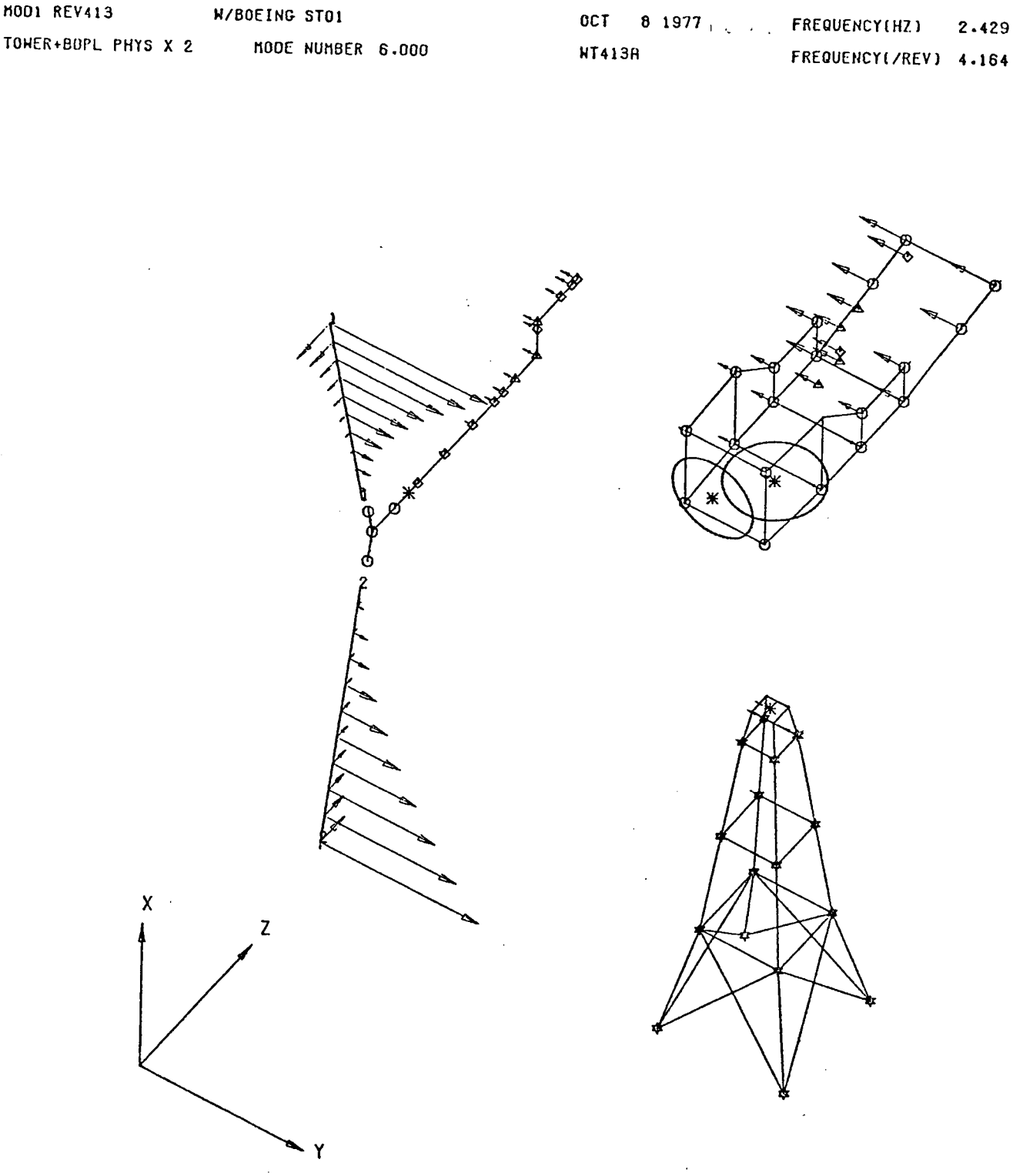

Figure 3-9F. First Rotor Edgewise, Cyclic

MOD1 REV413 W/BOEING ST01 OCT 8 1977 FREQUENCY(HZ) 4.179

TOWER+BDPL PHYS X 2 MODE NUMBER 10.000 WT413A FREQUENCY(/REV) 7.164

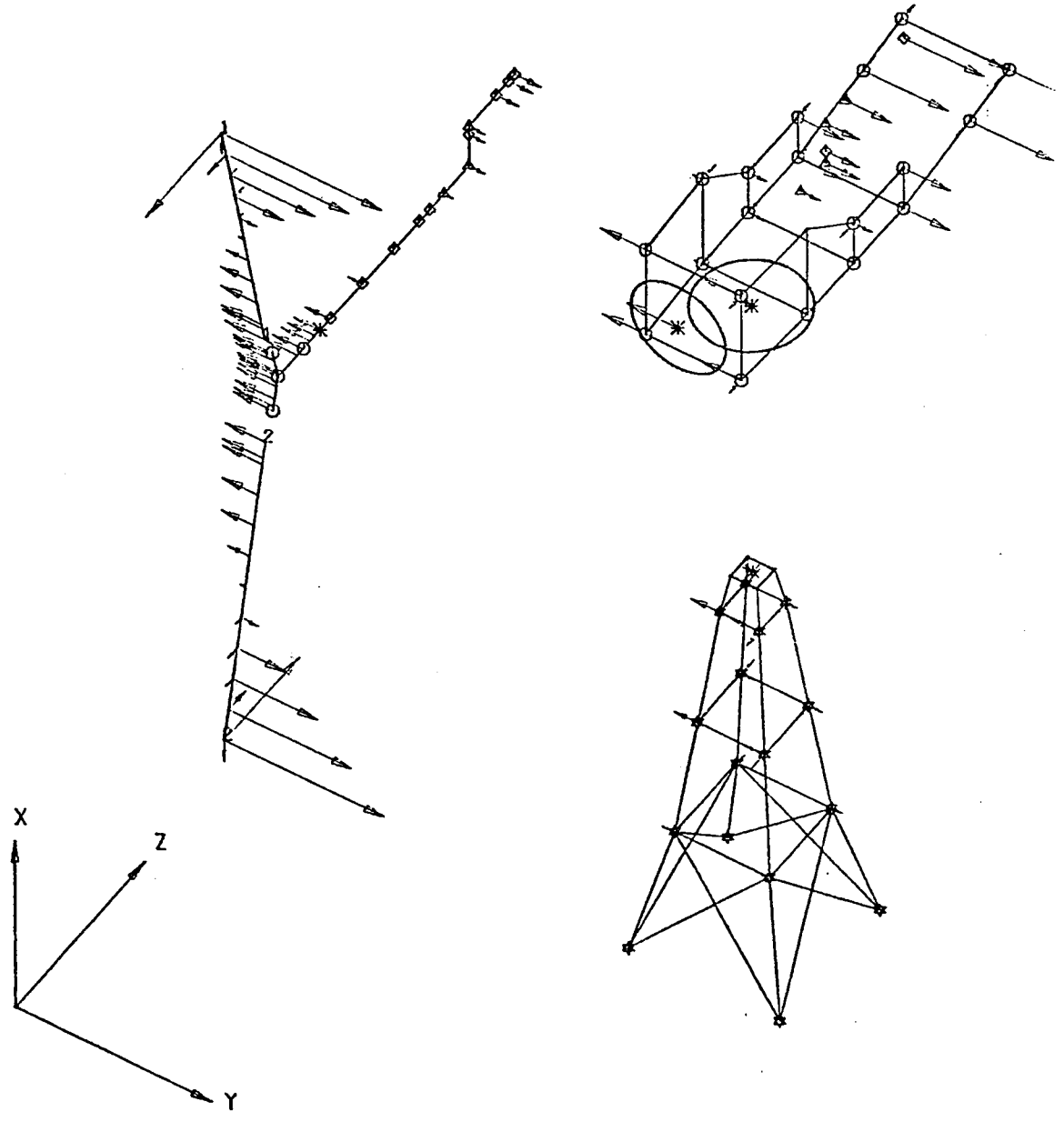

Figure 3-9G. Tower Torsion

The final design loads, for Cases A through D of Table 3-1, are contained in PIR WTG 1500-77-015 in Appendix B. These loads were generated before the blade precone change from 12° to 9° cone angle was made. The additional precone associated with these loads will not effect the cyclic loads. The steady loads for Cases B through D will be relieved somewhat.

3.4.1 DISPERSION FACTORS

3.4.1.1 Blade Loads

Analysis of measured data from Mod-0 revealed significant scatter of the blade cyclic load amplitudes. This scatter was observed to occur at any given wind speed as illustrated in Figure 3-10. The variation of these cyclic moments at various wind speeds is indicated by the shaded band of data in the figure. Evaluation of these measurements showed that the mean of the scatter band (broken line) was governed by the tower shadow, wind shear and gravity (which are always present) while dispersion from the mean was attributed to atmospheric turbulence (gusts).

To assure the regularity of the dispersion of the cyclic moments (illustrated by the band of data in Figure 3-10) from its mean, a probability plot was constructed from the Mod-0 cyclic flap bending histograms. This plot, which is given in Figure 3-11, contains data for five velocity bands and has a log normal distribution as indicated by the straight line characteristic at each windspeed group. From this plot it can be seen that the flap bending load at the 99.8 percentile (3σ) is approximately twice the load at the 50th percentile.

Referring back to the Mod-0 data given in Figure 3-10, it is observed that the General Electric GETSS program predicts the mean of the scatter. A data point at 25 mph, which is plotted in the figure, illustrates this characteristic. Since standard practice for design to random loading is to base stress calculations on the 99.8 percentile loads (3σ for a normal distribution), those loads predicted by GETSS (which are at the 50th percentile) would have to be multiplied by a factor to produce the maximum of the load dispersion observed on the Mod-0 data. Accordingly, these factors must be consistent with the data in Figure 3-1 to produce the final load, which includes the effect of atmospheric turbulence.

For the Mod-1 design, the dispersion factors determined by the Figure 3-11 data were found to be 1.9 for the flap bending cyclic loads. Chord bending data which were similarly plotted suggested a factor of 1.5 for a cyclic load dispersion factor. Since these factors are relatively insensitive to wind speed (as evidenced by the nearly parallel lines in Figure 3-11) the same factors were used in all of the blade load cases.

3.4.1.2 Structure Loads

It is clear that loads at other points in the structure would have different dispersion factors. Unfortunately, only blade data have been extensively analyzed on Mod-0 so a means had to be developed to approximate the dispersion factors at

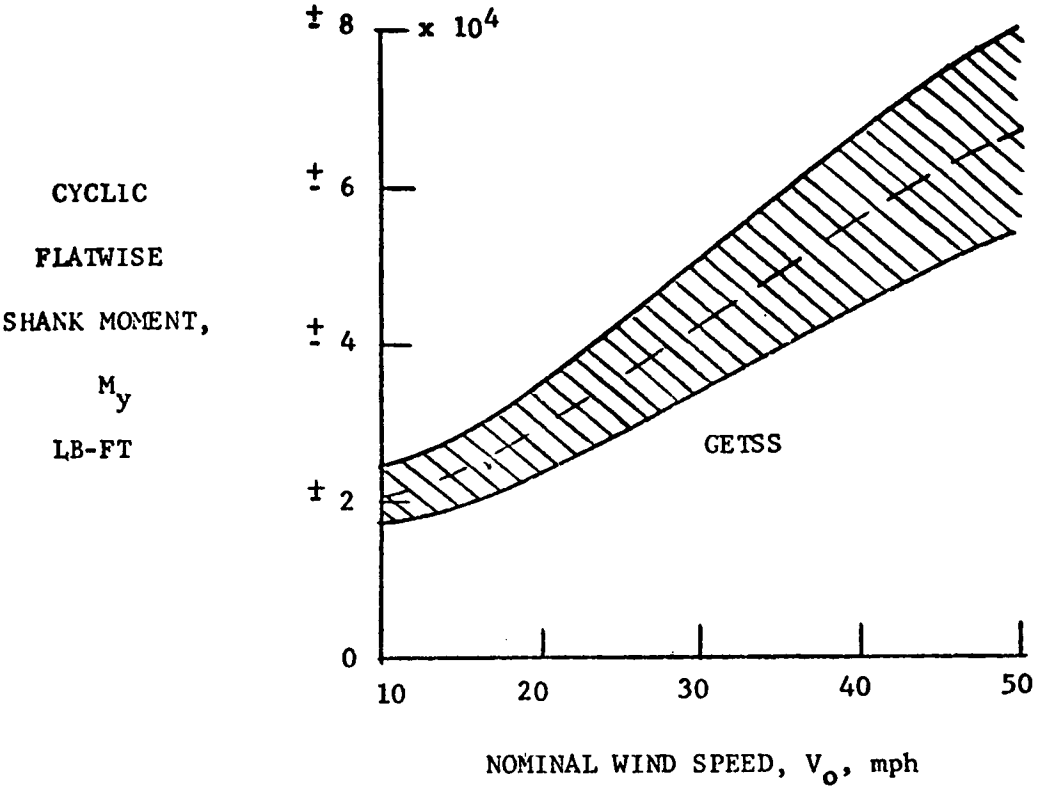

Flatwise moment load (tower without stairs; locked yaw drive)

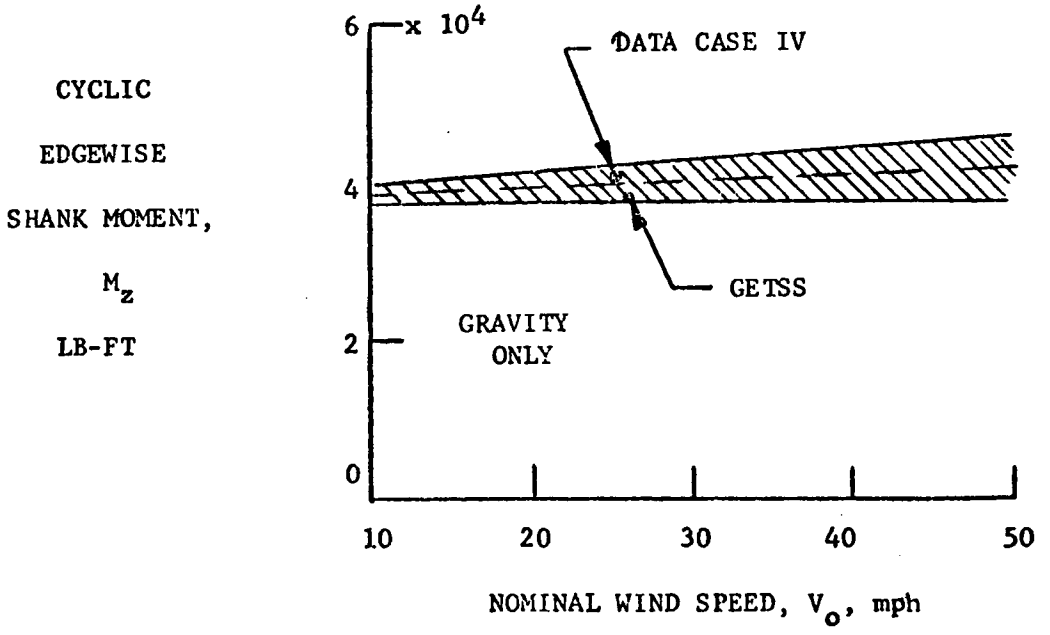

Edgewise moment load (tower without stairs; locked yaw drive)

Figure 3-10. Mod-0 Blade Loads

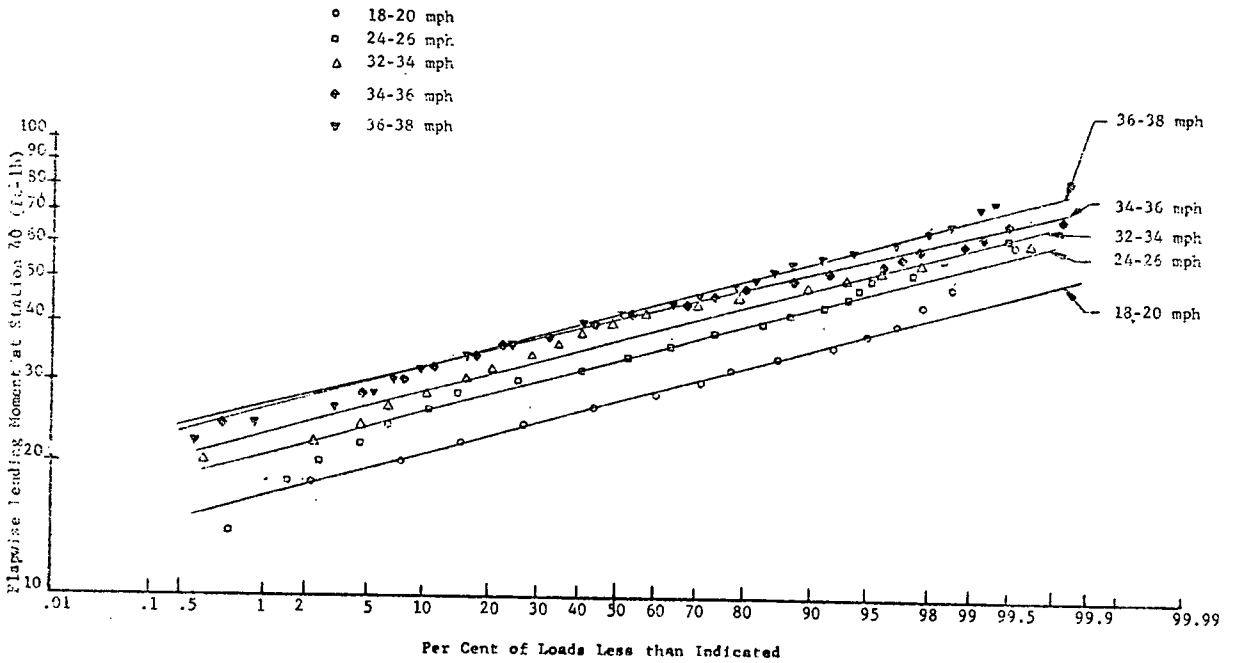

Figure 3-11. Mod-0 Blade Bending Moment Dispersions

the various interfaces of the Mod-1 structure. The approach taken was to define (and then analyze) a "design gust condition" that satisfied the following criteria.

1. Consistent with Mod-0 data - predicts "3σ" blade loads
2. Consistent with wind data supplied by Professor Dutton (Reference 2)
3. Compatible with existing analytical capabilities

These conditions were met by the change in steady-state loads that occur in going from 25 to 35 (or 35 to 25) mph with an inflow range from -32° to +32°. This corresponds to a fully immersed, fully compensated gust of 10 mph. The two wind speeds, 25 and 35 mph, correspond to the rated and cut-out velocities of the Mod-1, so that the design condition is not unreasonable for actual operation.

---

[2]Dutton, J.A., Private Communication to S.L. Macklis, May 16, 1977.

The calculation of the dispersed load factor was then determined by the range of the load between these two steady-state cases. This determination of the dispersion factors is depicted schematically in Figure 3-12. The dispersion factors calculated by this procedure were applied to the loads predicted by GETSS at 35 mph to generate the fatigue loads contained in Appendix B. Most of the dispersion factors thus obtained were below 2.0; however, a minimum dispersion factor of 1.5 was set regardless of the factor which was calculated. Limit loads in Appendix B, of course, contain no dispersion factors.

3.4.1.3 Discussion

Loads calculated for the blade design and the Mod-1 structure by the GETSS program were dispersed by factors to account for atmospheric turbulence. The basis of the factors was correlation with Mod-0 data measurements and with the wind data analysis supplied by Professor Dutton of Penn State. It is recognized that this procedure is not the most desirable way to handle gust loads (and changes in wind direction); what is needed is an analytical model which uses statistical wind characteristics (e.g., cross-spectra) to predict the statistical properties of the WTG dynamic response. At present, neither the wind data nor the analysis is available. In this light, it is felt that the most solid design approach now possible has been adopted, with its roots based on Mod-0 experience. If anything, the approach adopted is conservative because the Mod-1 has a larger rotor than the Mod-0 and hence should be less sensitive to partially immersed gusts of a given physical dimension.

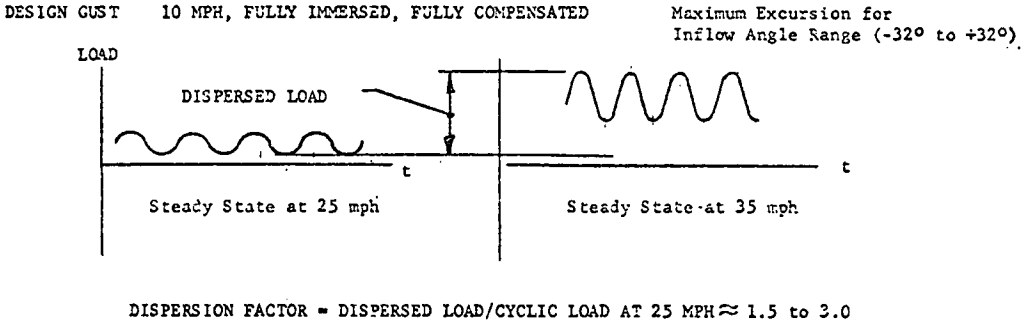

Figure 3-12. Determination of System Load Dispersion Factors

3.5 CONCLUSIONS OF THE STRUCTURAL DYNAMICS ANALYSIS

The following major objectives of the structural dynamics analysis have been met:

1. A computer code (GETSS) has been developed to accurately predict system dynamic response in service. The code has been verified against Mod-0 test data. Mod-1 design operational loads have been computed to enable a detailed component stress analysis.

2. Favorable resonant frequence placements have been implemented into the design in order to minimize dynamic loads.

3. System sensitivity to variations in bearing stiffnesses have been established and critical parameters were identified.

SECTION 4

STABILITY ANALYSIS

SECTION 4

STABILITY ANALYSIS

This section describes the model and the analysis utilized in determining analog control system performance and stability. Both frequency and time domain regimes are examined. The power transfer path is examined from the wind to the rotor, then through the drive train shafts and gearbox to the generator and the utility grid.

4.1 REQUIREMENTS, OBJECTIVES AND APPROACH

4.1.1 STATEMENT OF WORK AND DERIVED REQUIREMENTS

A controls and performance analysis is specified by the following paraphrased requirements from NAS 3-20058, the MOD-1 SOW:

Exhibit A

Task II - 8 Controls Analysis - Details of model, large and site systems, graphical format.

Exhibit B

1.3.2	-	Gust model time histories
2.2.1.1	-	8 Degrees per second pitch change rate
2.5.6	-	Stability to wind gusts
2.7.1.1	-	Safe starting and synchronization
2.7.1.2	-	Maintain electrical stability
2.7.1.4.1	-	Minimize torque variation

Two important derived requirements, voltage dip response and connection impedance range, are the result of electric utility standards and practice at the distribution voltage level near 15 kV where Mod-1 will connect to an existing grid.

Voltage deviation is objectionable for a variety of reasons such as incandescent lamp flicker and television picture changes. Figure 4-1 is a typical flicker chart of voltage magnitude versus frequency of occurrence. The derived Mod-1 requirement of ± 5 percent for infrequent occurrences down to ± 1.5 percent at tower shadow frequency is indicated. This voltage performance is at a critical customer voltage measurement location, not at the generator terminals.

Electrical systems tied to a utility grid with generation are typically represented as having an impedance (resistance and inductive reactance) connection to a constant voltage, constant frequency source or infinite bus. Large-scale system analyses take one generator as reference and permit all voltages to vary magnitude and relative phase to the reference. In comparison with fossil or nuclear-powered generators in the hundreds of megawatts or gas turbine-powered units from 20-60 megawatts, the 2 megawatt Mod-1 generator connecting to a radial feeder can be considered analytically as just the generator system, a connection impedance, and the reference infinite bus. Loss of detail due to

condensing the network to an impedance is very small. A range of connection reactance from 0.1 to 0.4 pu (1 pu = 9.23 Ohms) is considered typical for this type system with resistance to reactance ratios varying from 0.1 to 0.5.

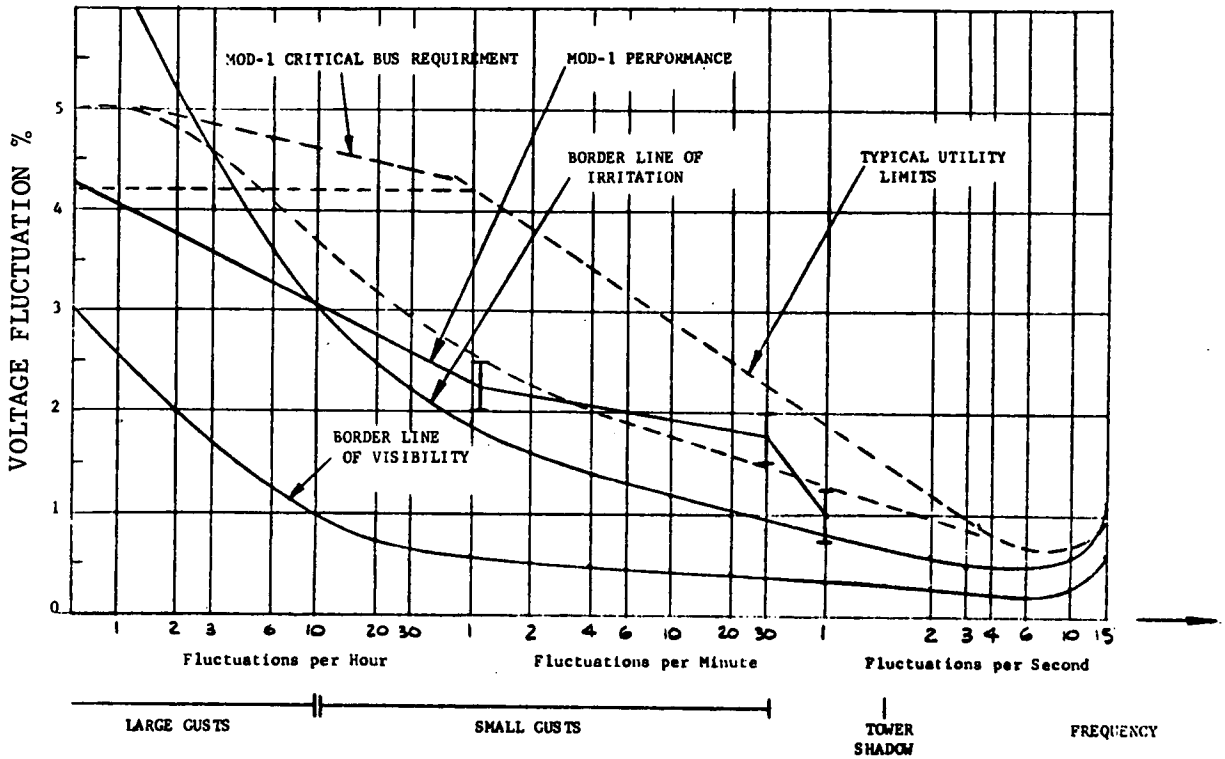

Figure 4-1, Voltage Flicker Characteristics

For maximization of energy capture, operation can be over the full power range of the generator. As the dynamic stiffness of the generator air gap is a function of real and reactive power level and connection impedance, a broad range of conditions is required to assess stability. The system range of conditions, without specific data on a site and nearby generation, is accommodated by the range of connection impedance. At the site on Howard Knob near Boone, NC, the effective impedance, is at the lower, more stable, end of the examined range.

4.1.2 WIND CHARACTERIZATION

Wind is an uncontrolled source of power that has large fluctuations in both amplitude and direction. The torque produced by the wind rotor and the structural response of the entire wind turbine is strongly influenced by the variability of the wind.

Three-time domain forms of wind forcing function amplitude-histories were used during the course of design and analysis:

1. 1-Cosine Model - from original SOW with amplitude envelope shown in Figure 4-2.

2. Probabilistic Time History - from present SOW shown in Figure 4-3.

3. Random Noise - based on probabilistic data with typical time history shown in Figure 4-4.

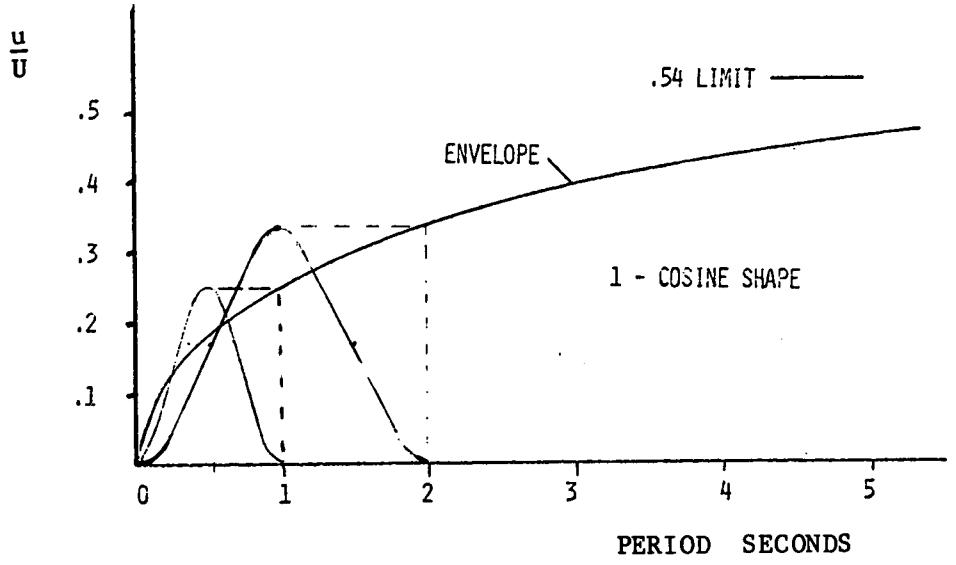

Figure 4-2. 1-Cosine Wind Model

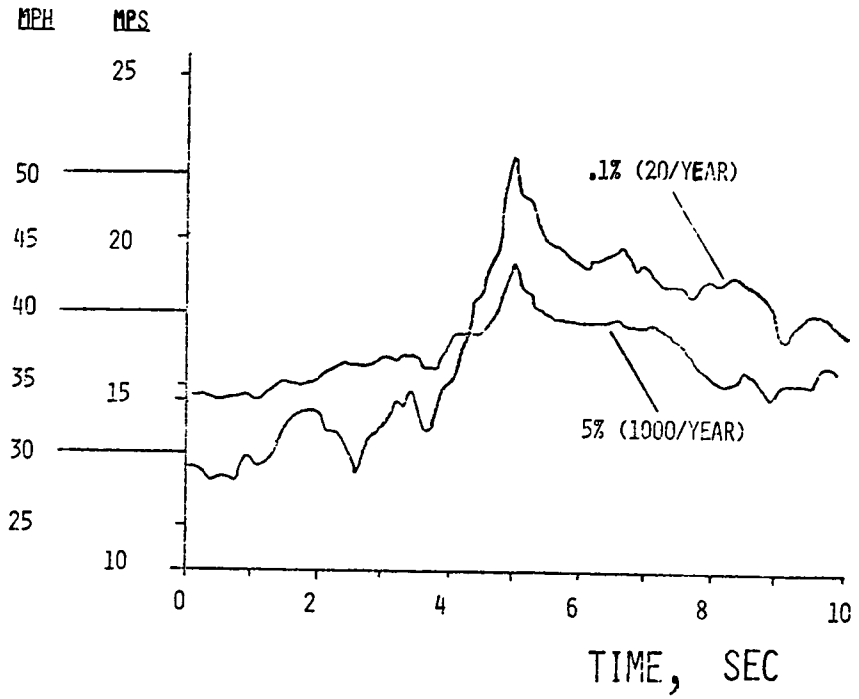

Figure 4-3. Probabilistic Wind Model

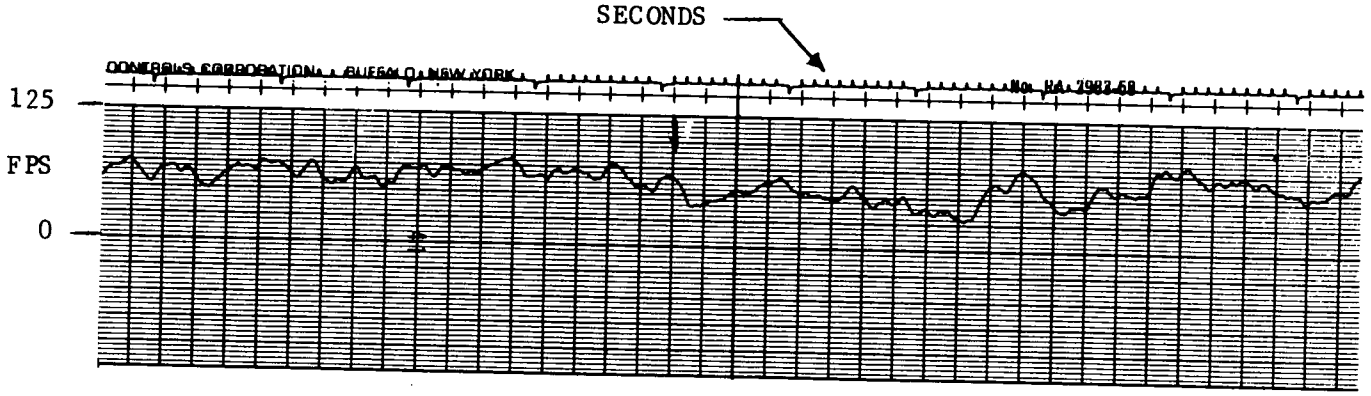

Figure 4-4. Typical Random Wind Model

Model (1), while based on extensive wind records, has a smoothed amplitude-time characteristic that does not represent actual wind disturbances as well as Model (2), also based on a large amount of actual wind data. Ranking of severity and probability of occurrence is based on amplitude and rate of change of amplitude. Model (3) is used for runs of several minute duration using random noise filtered as in Figure 4-5. The ideal filtering characteristics are based on a power spectral density (PSD) of the same data from which Model (2) is extracted. The actual filter is 2nd order, with the gain adjusted to intersect the PSD curve at the rotor diameter, giving conservative results for full immersion gusts.

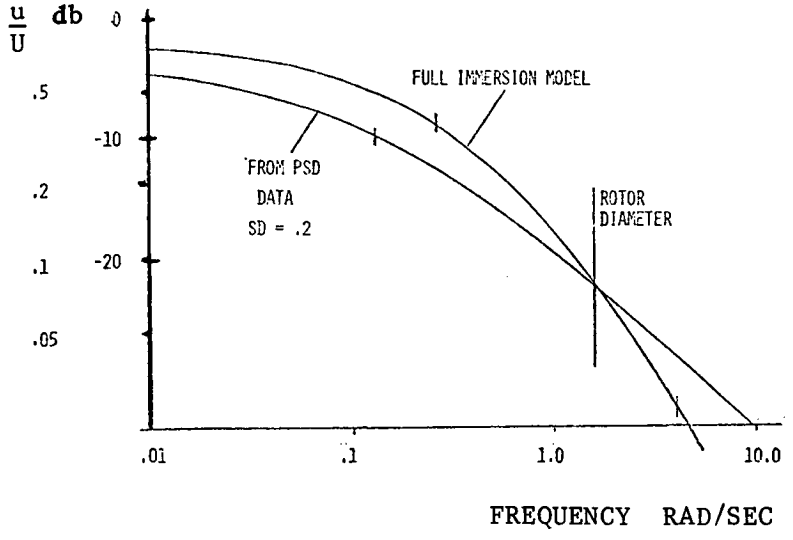

Figure 4-5. Random Wind Filtering

4.1.3 OBJECTIVES

The primary objective of the analysis is to ascertain stability. Stability of a control system and simulation may be defined in three ways:

1. Classic Stability. Frequency domain based criteria of no positive real eigenvalues for the system with a small signal linearized around a variety of operating points.

2. Dynamic Stability. Time domain-based criteria of maintaining synchronism and acceptable voltage performance on the non-linear system simulation for large gusts or electrical faults.

3. Deviational Stability. Time domain-based criteria of minimal deviations from constant power and voltage output when driven by nominal wind and tower shadow effects.

All three definitions were examined during the course of analysis.

As analysis and design are difficult to separate for a control system, additional objectives were to identify filtering and inner control loop characteristics required to improve stability.

A responsive, high crossover frequency, closed loop system with adequate phase and gain margin for both an off-line speed control and an on-line power control outer loop is required.

Control of rotor torque is by servovalve-controlled hydraulic actuators with spool and blade position feedback loops. Gains, frequency response characteristics, and signal filtering requirements must be identified to the electronics design group based on the simulation results.

4.1.4 APPROACH

The first task was development of suitable analytical models for rotor behavior and pitch change mechanism dynamics. Next, the results of the structural dynamics analysis were examined for modes significant to rotor torque and drivetrain behavior which were then incorporated primarily as blade flapwise bending. Yaw motion and inflow angle were assumed unimportant for drivetrain effects.

An overall simulation model was developed by combining a standard generator and grid model, drivetrain dynamics, and various control loop transfer functions. The model was coded for digital computer use for eigenvalue analysis and short-time response runs. Additionally, a hybrid (analog-digital) setup was patched and coded for interactive real time analysis and longer time runs.

Root locus plots from the digital model frequency analysis were used to set initial gains and time constants on the hybrid, then the hybrid model was used to add time responsive filtering and determine dynamic margins by increasing gains until instability was reached.

4.2 MODELING AND BLOCK DIAGRAMS

4.2.1 OVERALL MODEL

A simplified model configuration is shown in Figure 4-6, and the following sections detail transfer functions for subloops in the model.

Flow through the model starts with the wind, which is modified to reflect shear and tower shadow, then impressed on the rotor. Blade torque uses a torque coefficient curve computation and hub torque depends on the blade response with flapwise and drivetrain flexibilities included. After drivetrain response, the generator dynamics produce an electrical power output relative to an infinite bus voltage phasor. Output power is used to get an error signal through the controller to modulate blade pitch angle with a wind feed forward signal added in. Generator excitation is modulated by voltage, acceleration, and reactive power level. When off line, speed is used as the variable to control blade pitch.

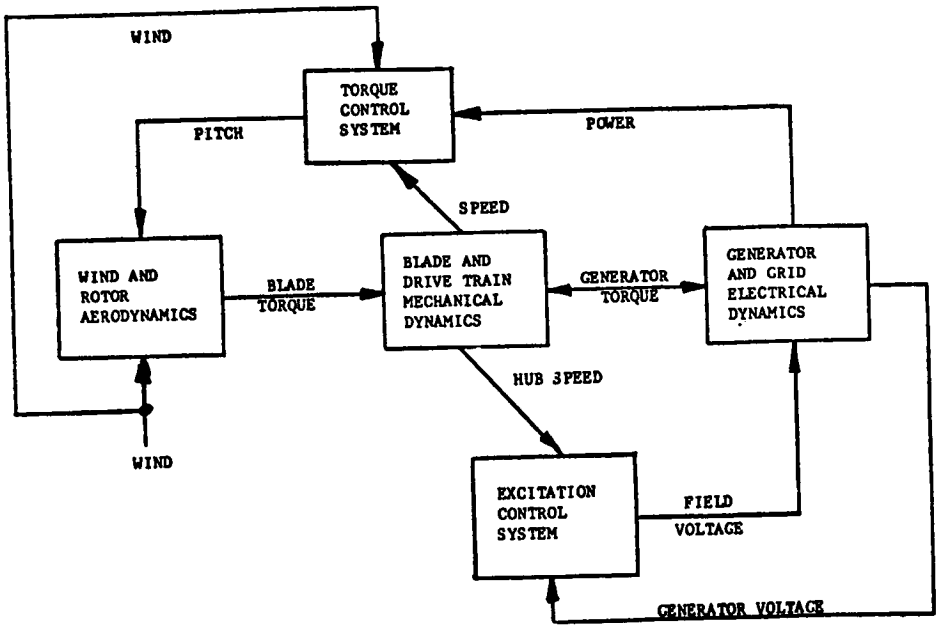

Figure 4-6. Basic Model Block Diagram

4.2.2 GENERATOR

The generator model is shown in Figure 4-7. Three integrators are used to represent the field and direct and quadrature axis rotor damper circuits. The model provides output voltage and current amplitudes but not the full 60 hertz waveform and is valid over the dynamic frequency range of interest. This is a conventional model used for detail power system analysis with saturation of the field circuit implemented. Values and the saturation characteristic are shown in Table 4-1 and Figure 4-8. Per unit reference is 1875 kVA.

4.2.3 EXCITATION SYSTEM

The generator excitation system has a 25 kW brushless exciter and solid state voltage regulator capable of negative field forcing shown in Figure 4-9. Exciter saturation is shown in Figure 4-10.

4.2.4 UTILITY GRID CONNECTION

As described in Paragraph 4.1.1, an impedance connection to an infinite bus was utilized for the majority of analysis. This is shown in Figure 4-11 which mates with the generator model in Figure 4-7.

A small radial system with two wind turbine generators was also examined with characteristics shown in Figure 4-12. This model was used to evaluate interaction between machines.

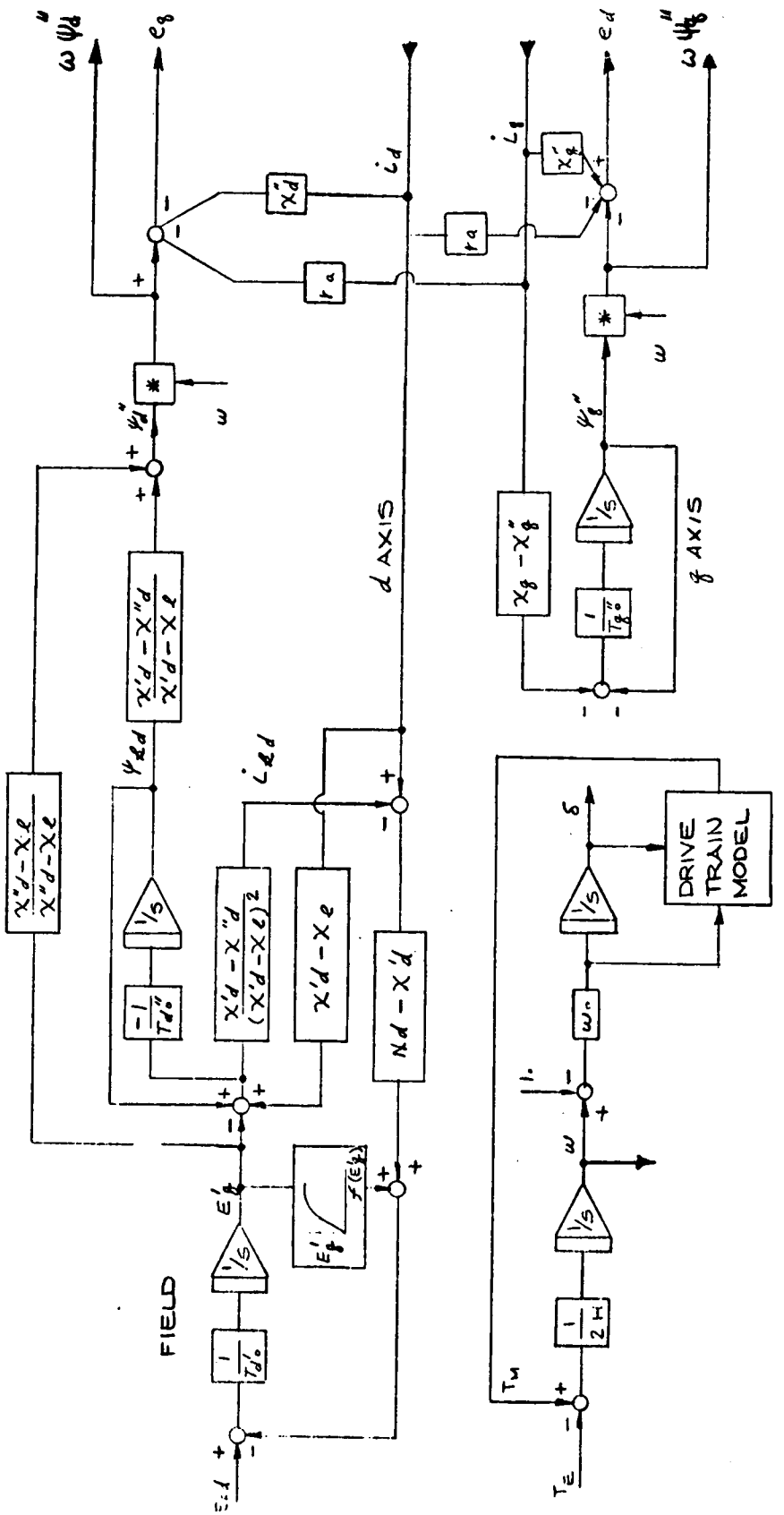

Figure 4-7 Generator Block Diagram

Table 4-1. Generator Values

General Electric Custom 8000 - 9.28 Ohms = 1 (PU) 1875 kVA Base

Rating: ATI - 4 Pole, 1800 rpm, 8409 Frame, 2188 kVA, 3 Phase, 60 Hz, 4160 Volts, .8 Power Factor

1.	Synchronous Reactance (Xd) Direct Axis (PU)	2.552
2.	Synchronous Reactance (Xq) Quadrature Axis (PU)	1.52
3.	Transient Reactance (X'd) Direct Axis (PU)*	0.311
4.	Transient Reactance (X'q) Quadrature Axis (PU)	1.52
5.	Sub-Transient Reactance (X"d) Direct Axis (PU)*	0.230
6.	Sub-Transient Reactance (X"q) Quadrature Axis (PU)	0.341
7.	Negative Sequence Reactance (X_2) (PU)	0.275
8.	Zero Sequence Reactance (Xo) (PU)	0.0908
9.	Armature Resistance (Ra) (PU), L-L at 25°C DC-OHMS	Y Conn. 0.1268
10.	Open Circuit Transient Time Constant (T'do) (SEC)	3.36
11.	Transient Time Constant (T'd) Direct Axis (SEC)	0.455
12.	Sub-Transient Time Constant (T"d) Direct Axis (SEC)	0.023
13.	Sub-Transient Time Constant (T"q) Quadrature Axis (SEC)	0.037
14.	Speed of Response of Exciter (R) (SEC) Te = Open Circuit	0.52
15.	No Load Field Current for Rated Voltage (IFC) (AMPS)	28.7
16.	Field Current at Ceiling Excitation, Rated Conditions (IFR)	195 Amps
17.	Short Circuit Ratio (SCR)	0.45
18.	Efficiencies (4/4) Load Fraction, calculated (3/4) (1/2)	95.5 95.4 95.0

*Tolerance of ± 15%

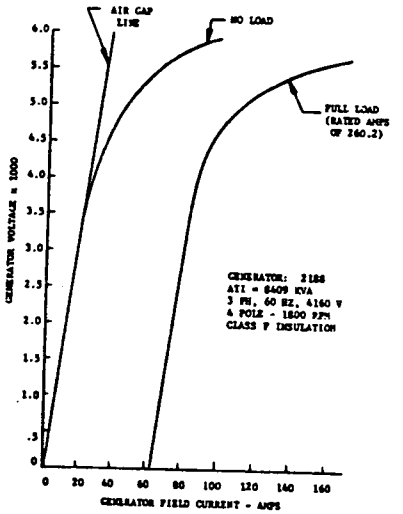

Figure 4-8. Generator Saturation

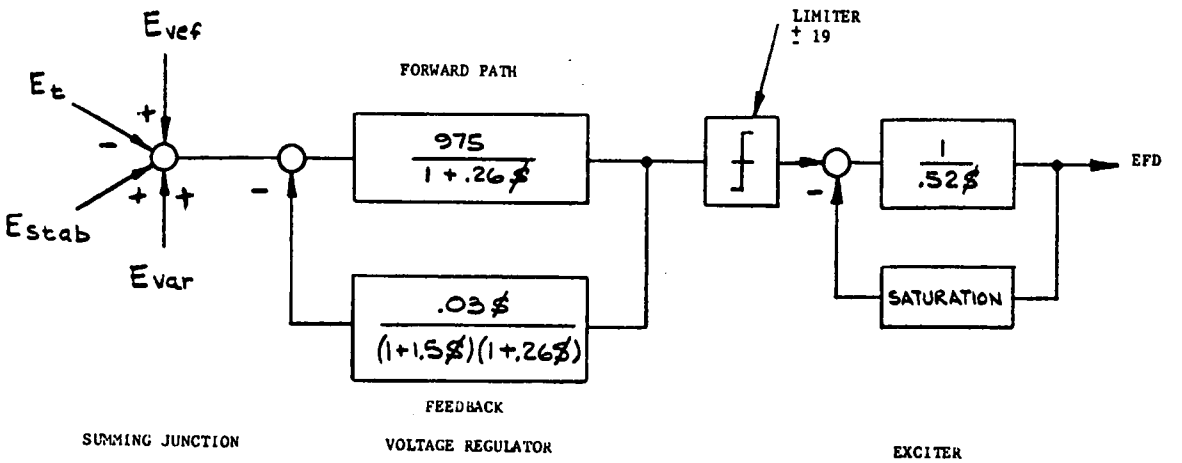

Figure 4-9. Excitation Block Diagram

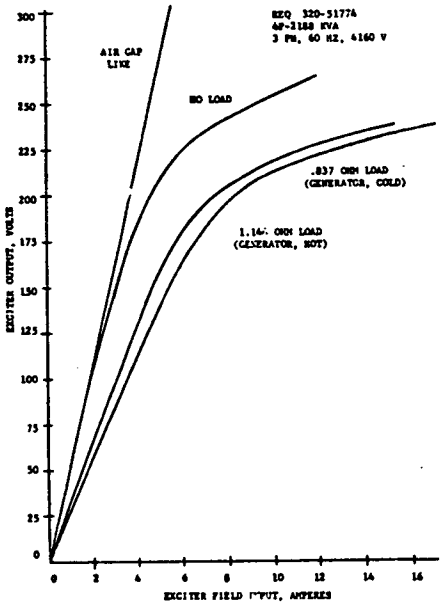

Figure 4-10. Exciter Saturation

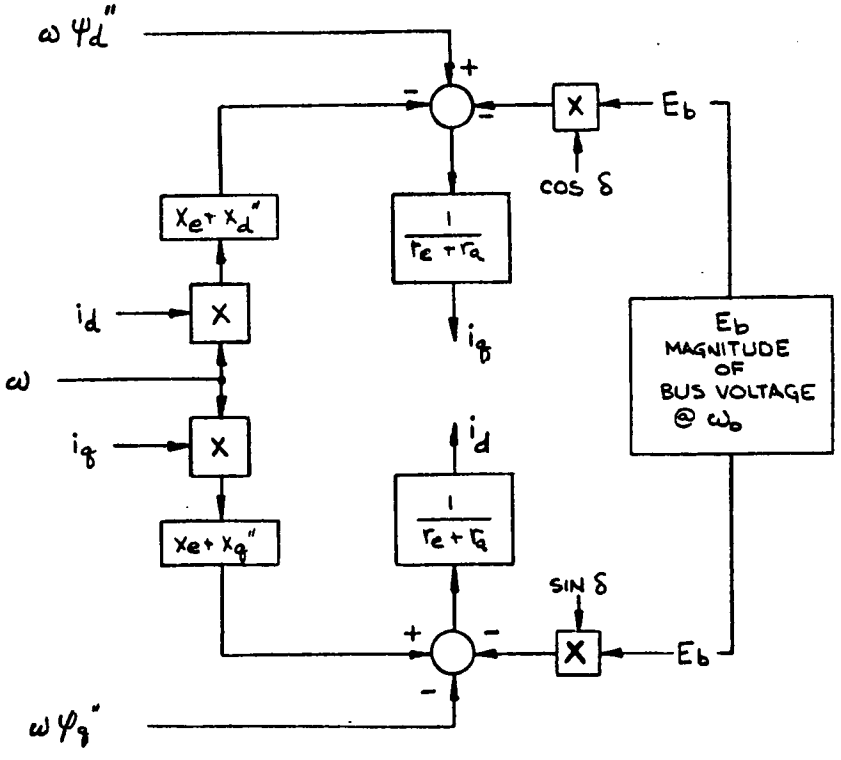

Figure 4-11. Utility Block Diagram

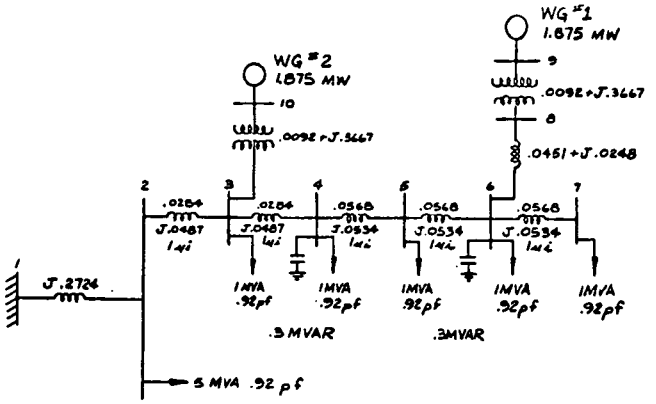

12.5 KV DISTRIBUTION NETWORK

Figure 4-12. Small Utility System

At the site, the impedance and loads have been provided by Blue Ridge Electric Membership Cooperative (BREMC), the connecting utility, as shown in Figure 4-13.

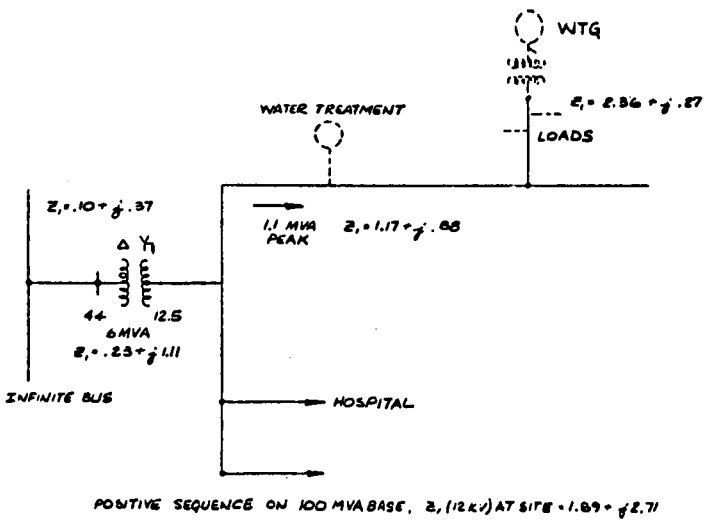

Figure 4-13. Site Utility System

4.2.5 WIND

The wind model used on the hybrid system permitted addition of step, 1-cosine random, or wind tape perturbations to a mean hub wind level. Next, for each blade, wind shear and tower shadow variations were superimposed on the hub full immersion model wind in order to obtain a single blade time phased wind for blade torque computation.

A wind shear exponent of .167 specified in the SOW was used as site data was not available. Tower shadow was modeled as a 60-degree half sinusoid with 35% maximum deficit in wind velocity. The shadow values are conservative.

4.2.6 AERODYNAMIC TORQUE

A torque coefficient polynomial evaluation as a function of pitch angle and tip velocity ratio was utilized to compute the forcing torque of each blade. The conventional power coefficient plot of the polynomial is shown in Figure 4-14, and a power versus wind velocity plot at rated speed is shown in Figure 4-15.

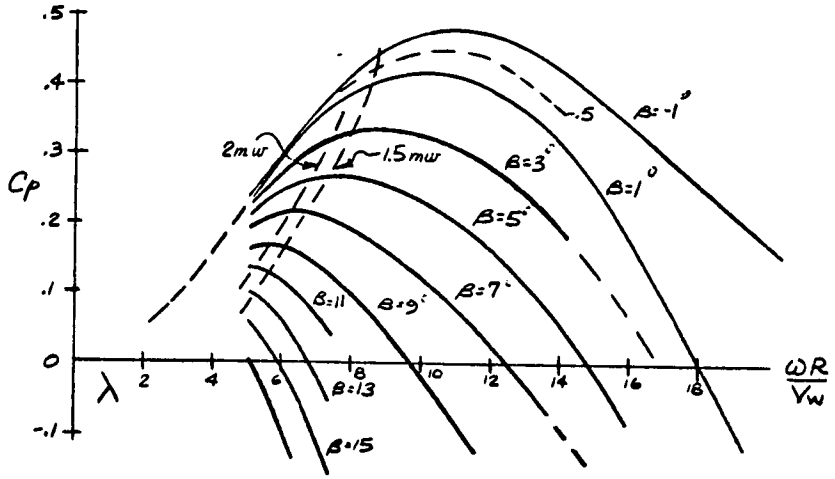

Figure 4-14. Blade Power Coefficient

While this characteristic is not perfectly representative of the actual blade characteristic, the deviation is small enough to be ignored in the positive coefficient range. In the negative coefficient range, there is insufficient data on actual blade characteristics to evaluate deviation, but the model is believed to be reasonable.

4.2.7 ROTOR

A three-degree of freedom model is used to represent the torsional dynamics of the rotor plus an additional degree of freedom to represent pitch change dynamics. The model is shown in Figure 4-16. A central hub and blade inertia

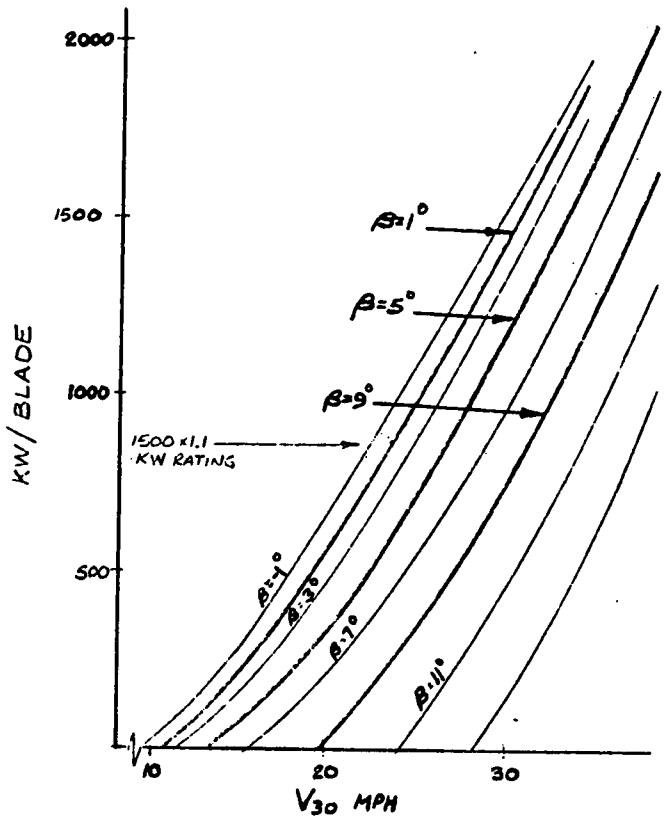

Figure 4-15. Blade Power

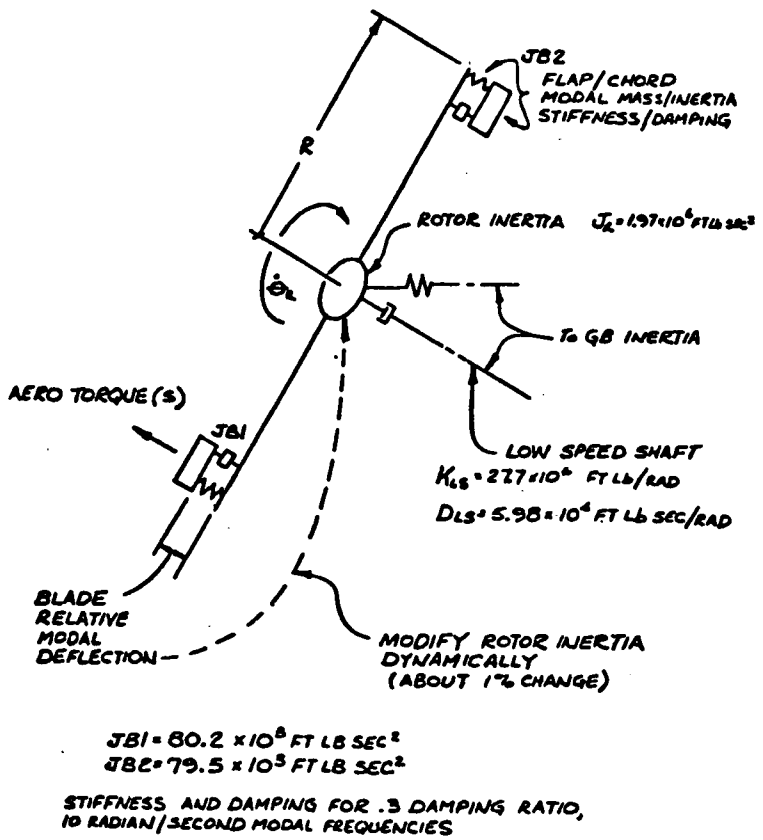

Figure 4-16. Rotor Model

has individual blade modal inertias to which the aerodynamic torques are applied. The central inertia is varied as a function of blade modal deflections, but the inertia change is quite small.

Initial analysis utilized the first blade edgewise (in-plane) mode to determine the modal values, but drivetrain response was significantly different in frequency content when compared with the more detailed structural dynamics model response. Based on the hypothesis that blade flap behavior dominates rotor torque, the modal stiffness and damping values were adjusted to represent the fundamental blade flap frequency and the resulting drivetrain response showed good agreement with the structural dynamics results. Based on the agreement in tower shadow response results, and the fact that wind gusts practically dominate response, the simplified model with a single degree of in-plane freedom per blade at flap frequency was utilized to represent the rotor dynamics.

This portion of the model behaves as a flexible blade, flexible hub configuration. The pitch change degree of freedom is treated as not coupled with the modal degree of freedom in flap.

4.2.8 DRIVE TRAIN

The balance of the drive train from the rotor hub through the generator is represented by gearbox and generator inertia nodes with inter-node coupling as shown in Figure 4-17. Hub-to-gearbox stiffness is predominantly from the low-speed shaft and gearbox to generator flexibility is predominantly from the gearbox internal components. Electrical air gap torque loads the generator inertia when on-line. This system adequately represents important torsional dynamics. Backlash and losses were not modeled.

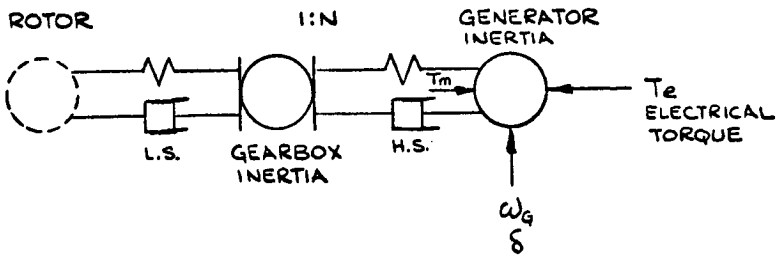

GEAR BOX RATIO N = 51.9	1800/34.7 rpm
GEAR BOX INERTIA	15.7×10^3 lb ft sec^2
H.S. STIFFNESS (MOSTLY GEAR BOX)	22×10^3 ft lb/rad
GENERATOR INERTIA	50.5 ft lb sec^2
H.S. DAMPING	NONE USED

Figure 4-17. Drive Train Model

4.2.9 PITCH CHANGE MECHANISM

The pitch change mechanism is modeled as shown in Figure 4-18. A hydraulic actuator drive inertia is connected to the blade pitch change degree of freedom and the hydraulic flow and servo valve spool dynamics are included in the model. Amplifier elements close the spool and actuator position loops and filter the input to avoid exciting the pitch mechanical degree of freedom, or responding to rated speed tower shadow excitation.

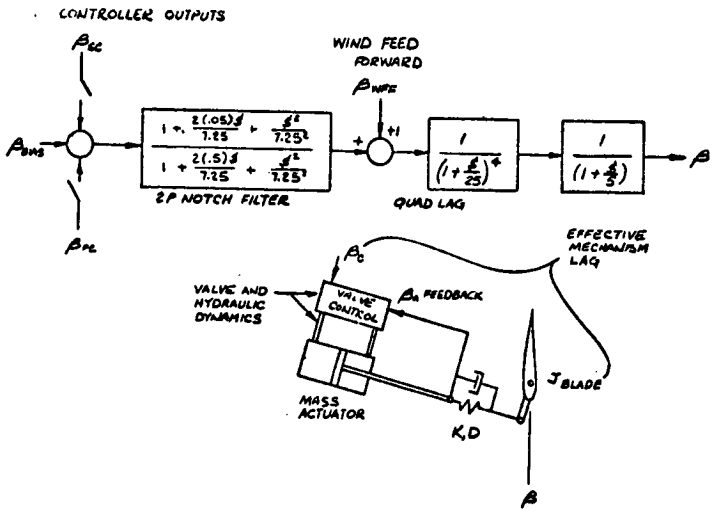

Figure 4-18. Pitch Mechanism Model

4.2.10 SPEED CONTROLLER

For off-line speed control, a governor controller with proportional and integral characteristics plus a biquadratic notch filter at the rated speed fundamental is used as shown in Figure 4-19.

4.2.11 POWER CONTROLLER

When on line, the grid controls frequency (speed) and a power controller loop is used. The block diagram is shown in Figure 4-20, with a 10.0 radian per second transducer response utilized for power feedback. The error signal transfer function has a complex numerator to notch filter , attenuate the drivetrain response resonance and a pair of real lags. This behaves as an integral characteristic below the notch and a derivative characteristic above it with flat response below and above the pair of lags.

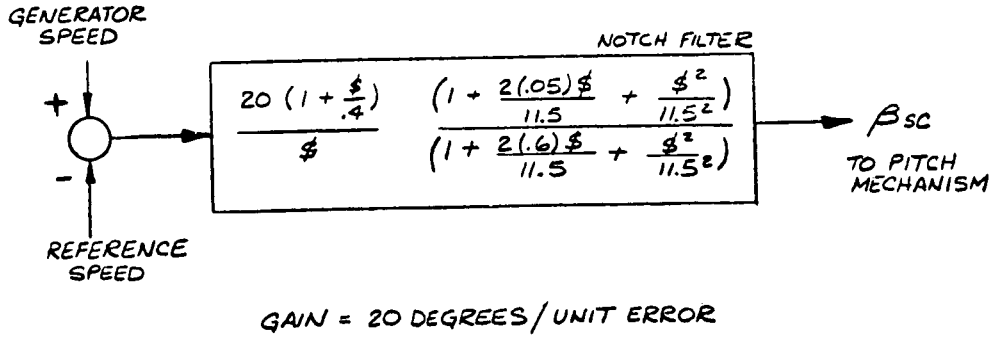

Figure 4-19. Speed Controller Block Diagram

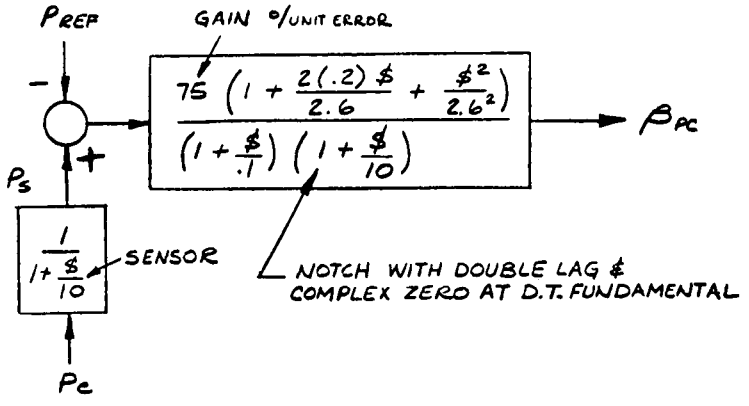

Figure 4-20. Power Controller Characteristic Block Diagram

4.2.12 WIND FEED FORWARD

A wind signal from an up-wind sensor arrangement for feed forward purposes is modeled as shown in Figure 4-21. The sensor lag and upwind distance lead vary with wind velocity but were more simply modeled as fixed values with a constant .4 second lead time on the hybrid.

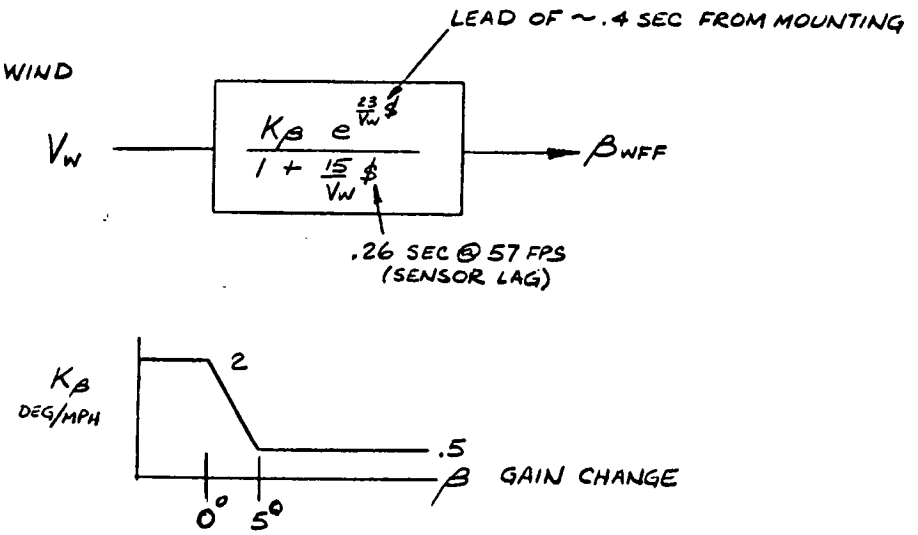

Figure 4-21. Wind Feed Forward Block Diagram

4.2.13 SPEED STABILIZER

Use of a speed derived signal to produce generator torque modulation in phase with speed as a damping source is used on large power systems under the name of power system stabilizer (PSS). Such a system is adopted to Mod-1 as shown in Figure 4-22 in order to improve the on-line fundamental frequency damping. The characteristic has a rate and washout plus double lead-lag and biquadratic filtering for dominant time excitations.

4.2.14 REACTIVE POWER CONTROLLER

A Var controller shown in Figure 4-23 is used to control the reactive power level by biasing the voltage regulator output based on power factor or reactive power reference settings.

4.2.15 MISCELLANEOUS

Hybrid logic was included to simulate synchronization, loss of load, and pull out of synchronization transients. All hybrid results are for .2 pμ reactance.

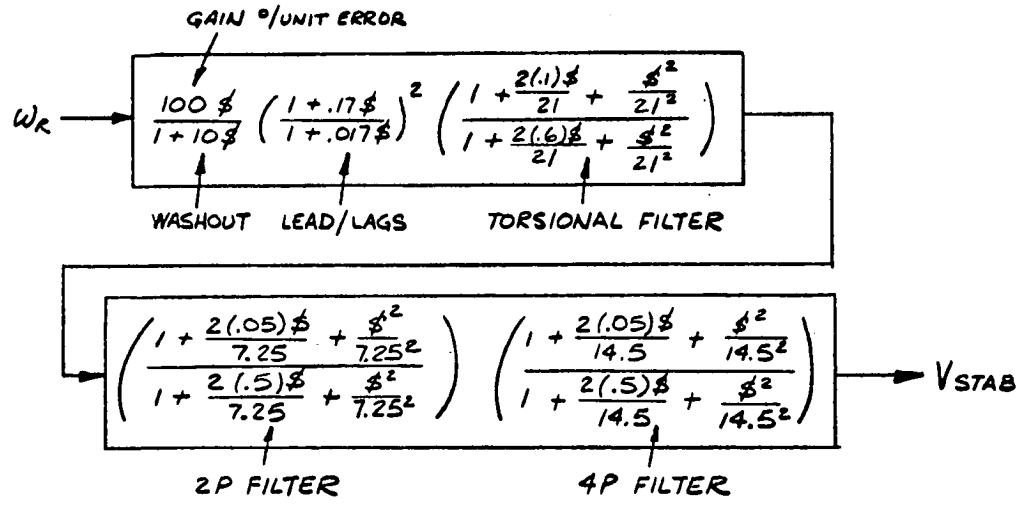

Figure 4-22. Speed Stabilizer Block Diagram

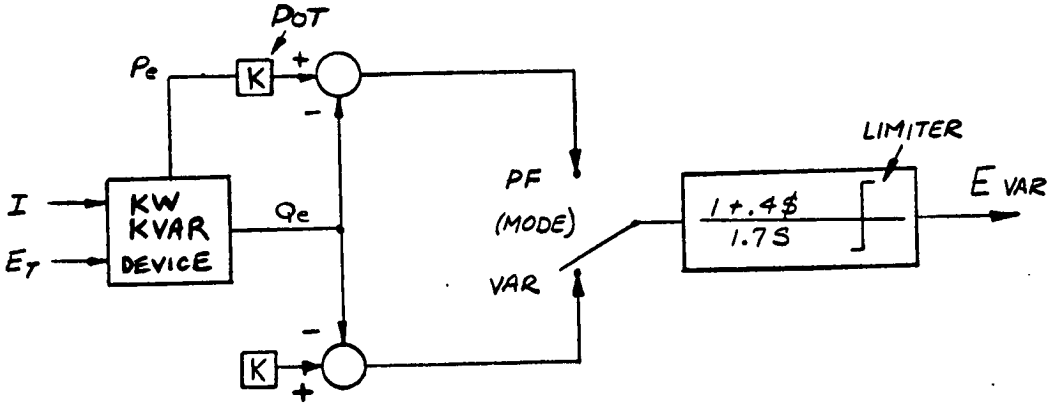

Figure 4-23. VAR Controller Block Diagram

4.3 SUBSYSTEMS ANALYSIS CASES

4.3.1 FREQUENCY DOMAIN

Prior to defining wind and electrical transient load cases, inner loop analysis and outer loop frequency domain analysis were performed. Small signal linearizations of the system variables about selected operating points were subjected to eigenvalue analysis to generate root locus plots and transfer functions.

4.3.2 PITCH MECHANISM AMPLIFIER

Amplifier characteristics shown in Figure 4-18 were determined by the following criteria.

1. Avoid excitation of the mechanical degree of freedom around 54 radians/second (r/s) due to pitch inertia and mechanism stiffness.

2. Retain as high a crossover frequency as practical to reduce the effective time constant.

The values provide for inner loop (spool) crossover at 250 r/s and outer loop (actuator) crossover at 5 r/s with a quad lag filter at 25 r/s for rapid attenuation before the blade frequency is reached. Crossover at 10 r/s with less margin is possible.

4.3.3 ROOT LOCUS VARIABLES

Gains were varied over the following ranges for frequency domain analysis:

1.	Real Power	0 to 2000 kW
2.	Reactive Power	0 to 1000 KVA
3.	Connection Reactance	.1 to .4 pu
4.	Power Controller Gain	0 to 200 degrees/pu error
5.	Speed Controller Gain	0 to 1000 degrees/pu error
6.	Stabilizer Gain	0 to 200 pu/pu

Result plots are shown in Paragraph 4.5.

4.3.4 DEVIATIONAL RESPONSE VARIABLES

For determination of steady state time response, the following variations were made:

1.	Mean Wind	20 to 90 fps at rotor (10 to 45 mph)
2.	Tower Shadow	30 degrees by 35 percent to 60 degrees by 70 percent
3.	Inertia Change Coupling (Rotor)	5 to 1 range
4.	Rotor Inertia	1 to 2 million lb-ft-sec^2
5.	Shaft Stiffness	4 to 1 range
6.	Random Wind	0 to .1 pu gustiness (pp)
7.	Stabilizer Gain	0 to 100 pu/pu
8.	Multiple Loops	With and without wind feed forward, stabilizer and VAR controller

4.3.5 TRANSIENT RESPONSE VARIABLES

To determine response for large, infrequently occurring transients, the following variations were made:

1.	Step Wind	.25 pu step
2.	Continuous Frequency Wind	.2 pu at 2.5 r/s (.4 Hz)
3.	Step Voltage	.1 pu
4.	Random Wind	To .5 pu (peak to peak)
5.	Probabilistic Wind	0.1 percent gust (worst)
6.	Synchronization	On and off transients
7.	Emergency Overspeed and Speed Control Step	.8 pu step wind plus load loss

4.3.6 SMALL SYSTEM ANALYSIS

Frequency and 1-cosine time analysis was performed on the small radial system described in Paragraph 4.2.4. Voltage dips along the system and critical clearing time for a bus fault were analyzed.

4.3.7 SITE ANALYSIS

Detailed site behavior analysis had not been made at the time this report was prepared. The effective site impedance to an infinite bus from the generator terminals is .05 + j.11 pu which represents a stable system connection at the low end of the range analyzed. It is unlikely that significant detailed site analysis is required and component parameter adjustment ranges are adequate to accommodate the site values.

4.4 COMPENSATION

4.4.1 FILTERING

In most loops, when a need to attenuate response at a particular frequency had been identified, a filter with second order zero and pole characteristics was specified to provide a "notch". This type of design is conventional and readily adjustable over a limited range via potentiometer and fixed resistance changes. A typical Bode diagram for such a filter is shown in Figure 4-24.

4.4.2 WIND FEED FORWARD (WFF)

The injection of a signal to control blade pitch angle at the same time a wind disturbance arrives at the rotor is a form of compensation. Data from Mod-0 at NASA Lewis Research Center's Plumbrook Station indicates a benefit in practice with a single wind sensor below 1 r/s (0.15 Hz) with analytical results predicting a benefit a decade higher. This is reasonable because the rotor responds to a much larger wind field and the sensor signal may represent local gustiness that does not affect the entire blade area.

On Mod-1, the average of multiple wind sensors is utilized as the control signal with computer controlled switching of the signal into the control loop. The WFF does not effect classical stability and in the nonachievable theoretical limit would provide constant rotor torque.

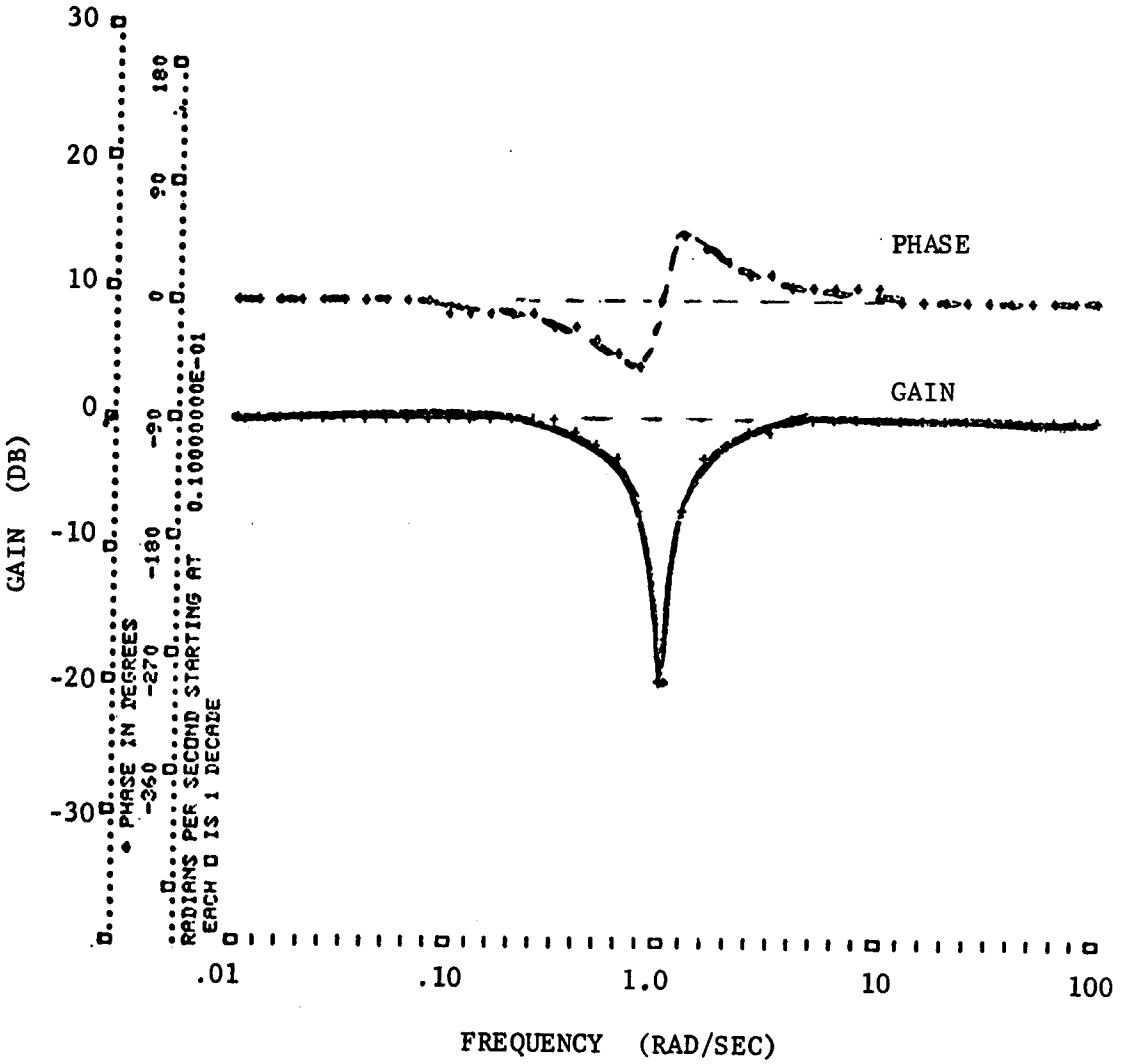

Figure 4-24 Filter Gain-Phase Diagram

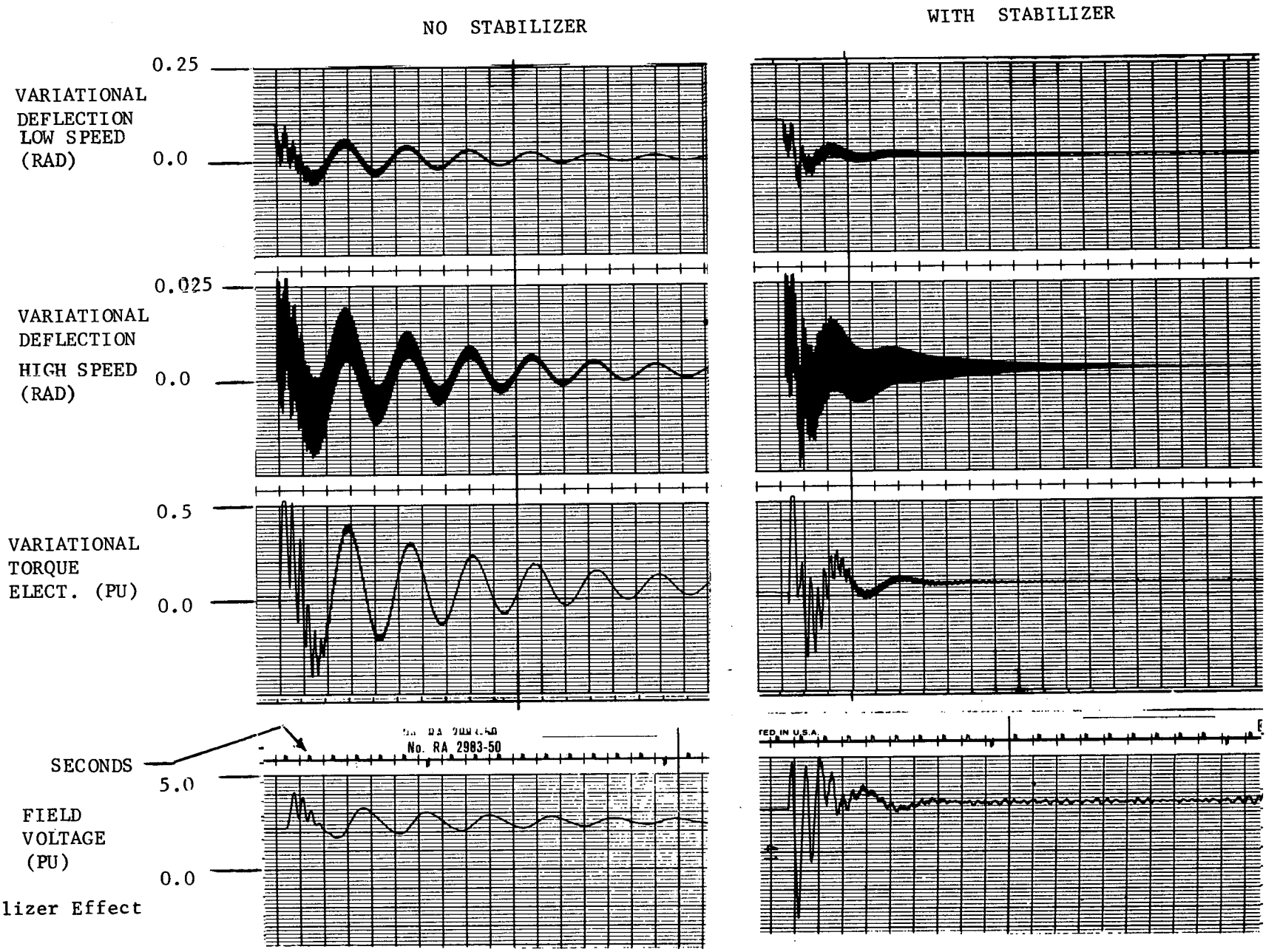

Stabilizer Effect

Figure 4-25.

4.4.3 SPEED STABILIZER

A speed stabilizer or power system stabilizer (PSS) is utilized to increase on-line fundamental torsional frequency damping to 30 percent of critical. This compensation provides nearly three times the damping available from just adjusting the voltage regulator by modulating the generator field, and thus air gap torque.

This compensation has filtering applied to minimize response to tower shadow-produced steady state excitations. An increase in steady state and dynamic voltage fluctuation and reactive power flow is an undesirable byproduct of the stabilization but the amplitudes are not objectionally increased and the benefit is considerable.

Time responses of drivetrain, both without and with the stabilizer, are shown in Figure 4-25. An initial unbalanced drivetrain deflection representing 0.5 per unit torque is released at the start of the response traces and the more rapid decay in response due to the stabilizer augumented damping is readily evident.

Utilization of a fluid coupling was considered on Mod-1 in the preliminary design stage and after one was added to Mod-0. This device behaves as a series damper in the drive train with steady state loss comparable to slip speed. A Mod-1 sized device would weigh, cost as much and take up the same space as another generator in addition to having a need for coolant flow to dissipate 2-3 percent of total power. The stabilizer is a more cost-effective means of getting added damping on Mod-1 and is used instead of a mechanical loss element.

4.5 RESULTS

4.5.1 SPEED CONTROL LOOP

4.5.1.1 Frequency Analysis

The basic speed control block diagram is shown in Figure 4-26. An off-line fundamental frequency at 11.5 r/s (1.83 Hz, 3.2 P) limits crossover of the loop as does the pitch mechanism effective lag at 5 r/s (.8 Hz). An integral plus proportional controller characteristic is designed to crossover around 1 r/s (.16 Hz).

Closed loop step response for a gain of 250 degrees/radian is shown in Figure 4-27, a Bode plot of the transfer function of generator speed to wind velocity. The blade torque characteristic has been approximated as linear with wind velocity and pitch angle by:

$$TA = K1 + K2 * VW + K3 * B$$

where

TA = Rotor Torque in ft-lb
K1 = - 483086 ft-lb

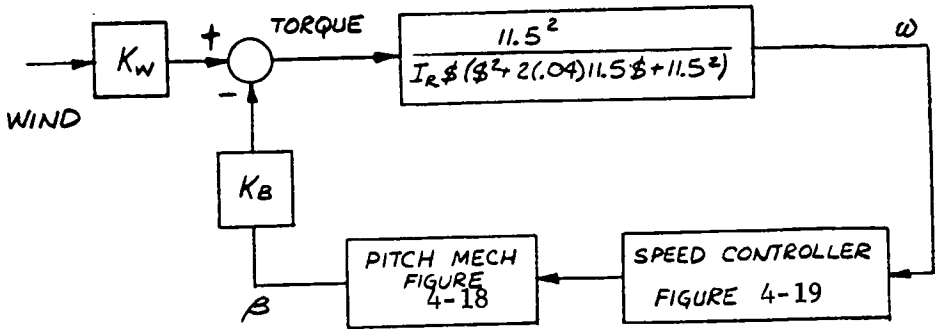

I_R = 2 x 10^6 Ft-lb sec^2

K_W = 36536 Ft-lb/mph

K_B = 28417 Ft-lb/degree

Figure 4-26. Speed Control Loop

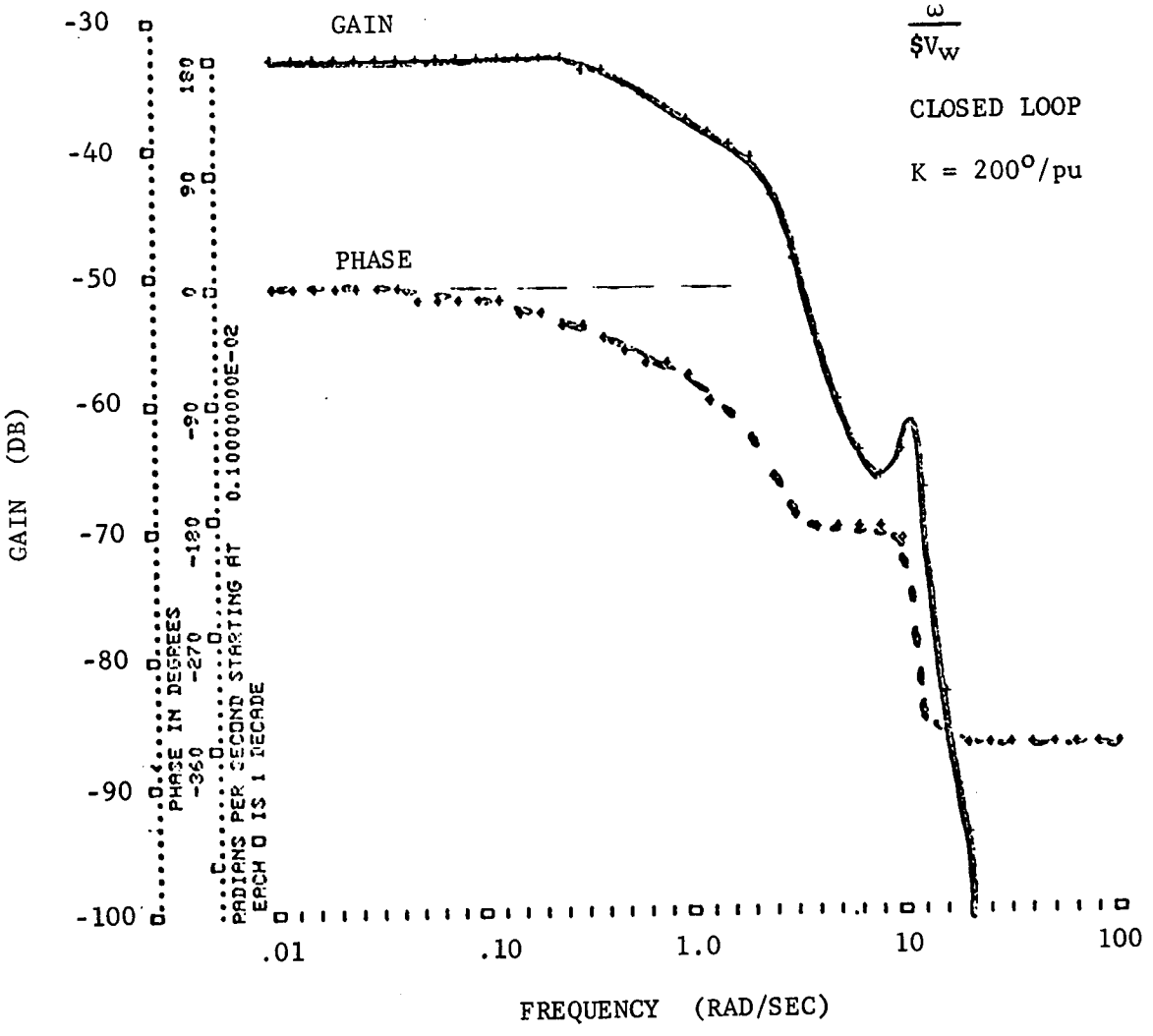

Figure 4-27 Speed Loop Gain-Phase Diagram

K2 = +36536 ft-lb/mph
VW = 30 ft wind velocity in mph
K3 = 28417 ft-lb/degree
B = 3/4 radius pitch angle in degrees

4.5.1.2 Time Analysis

Step response of the system described in Paragraph 4.5.1.1 is shown in Figure 4-28. Response of the same system with gain at 20 degrees/radian on the hybrid full simulation with loss of load from 1500 kW and shift to speed control rather than emergency feather rate is shown in Figure 4-29.

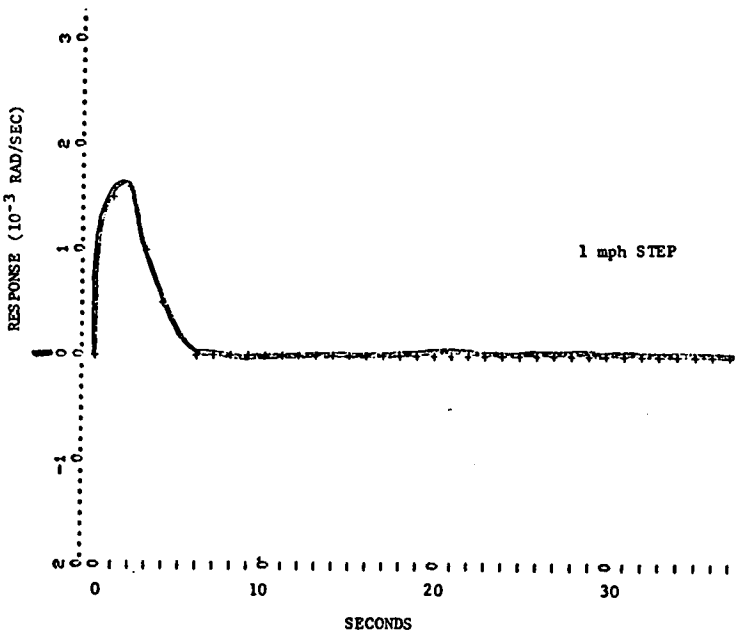

Figure 4-28 Speed Loop Step Response

The full simulation case limits overspeed on loss of load to only 2.0 percent. A limiting-type condition is represented in Figure 4-30 which combines loss of load with a step increase in wind velocity from 50 to 90 fps at the hub with a maximum overspeed of 10 percent.

4.5.2 EXCITATION SYSTEM

4.5.2.1 Frequency Analysis

Responsive control of terminal voltage and use of the excitation system to improve drive train damping require a moderately fast response voltage regulator and exciter with forcing capability to aid transient stability for large torque changes. A Basler SRN4 voltage regulator is utilized with special modifications for adjustment of forward and feedback gains. A Bode diagram of the regulator response with nominal settings is shown in Figure 4-31.

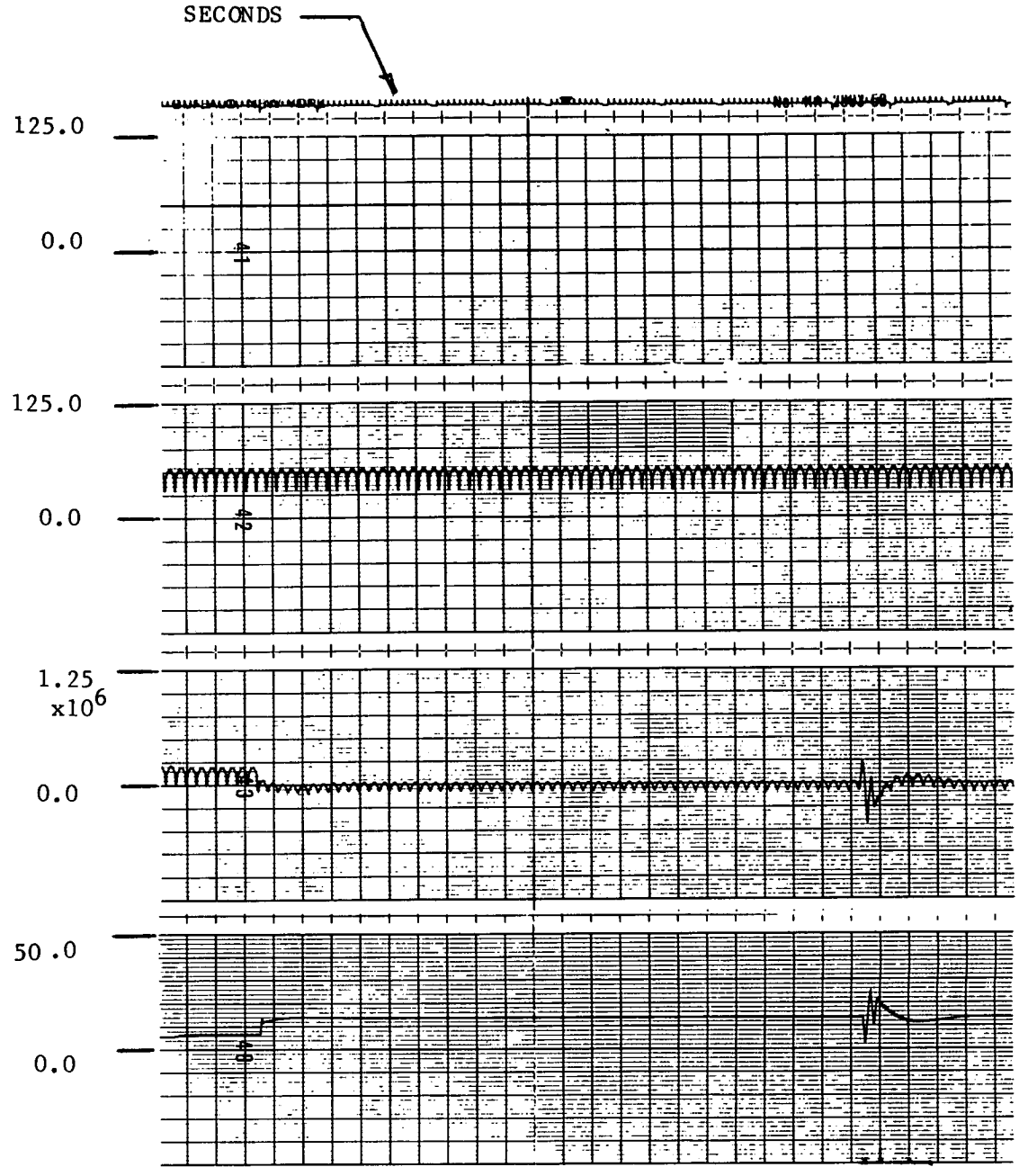

Speed Loop Load Loss Response

Figure 4-29. A

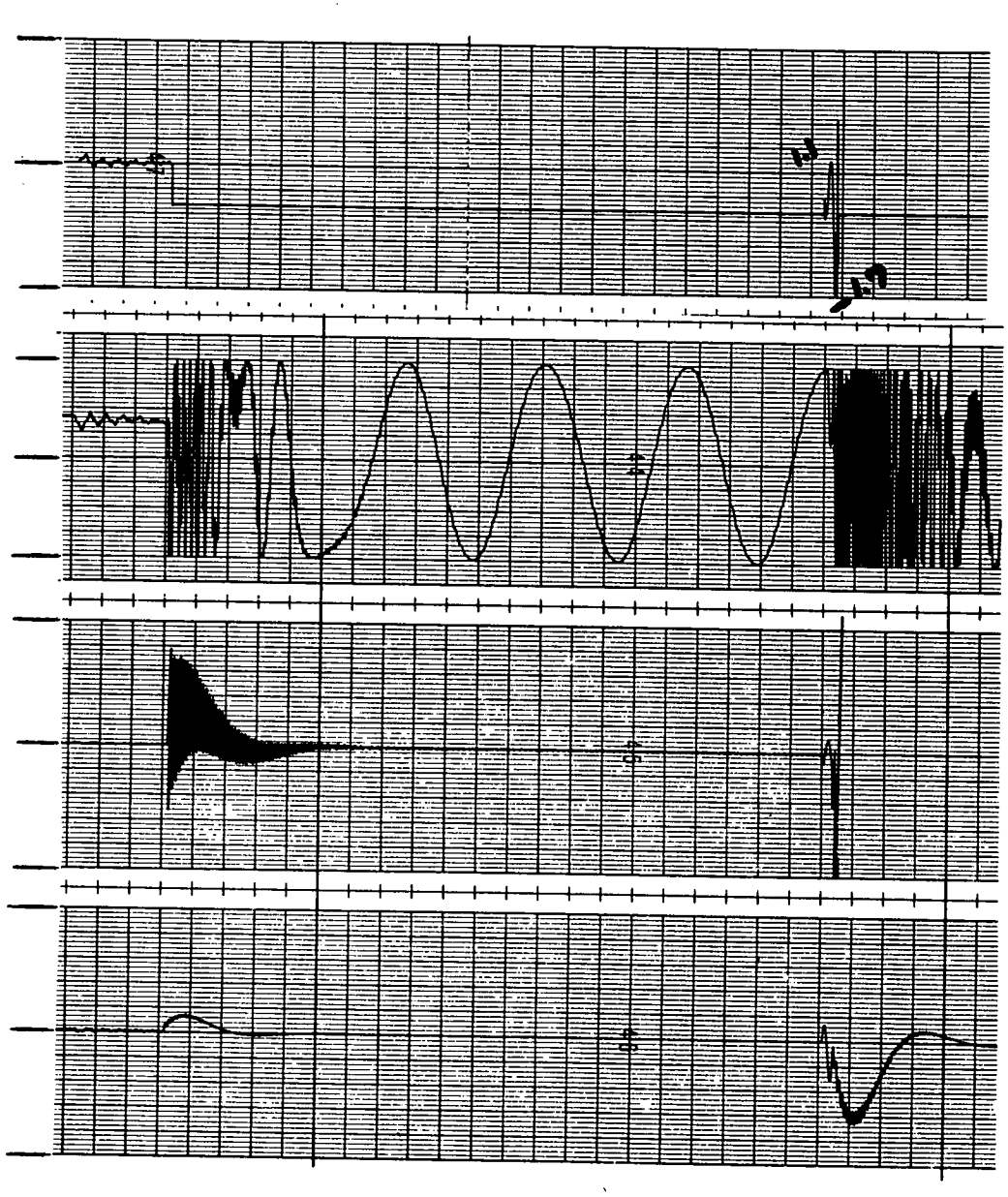

Speed Loop Load Loss Response

Figure 4-29. B

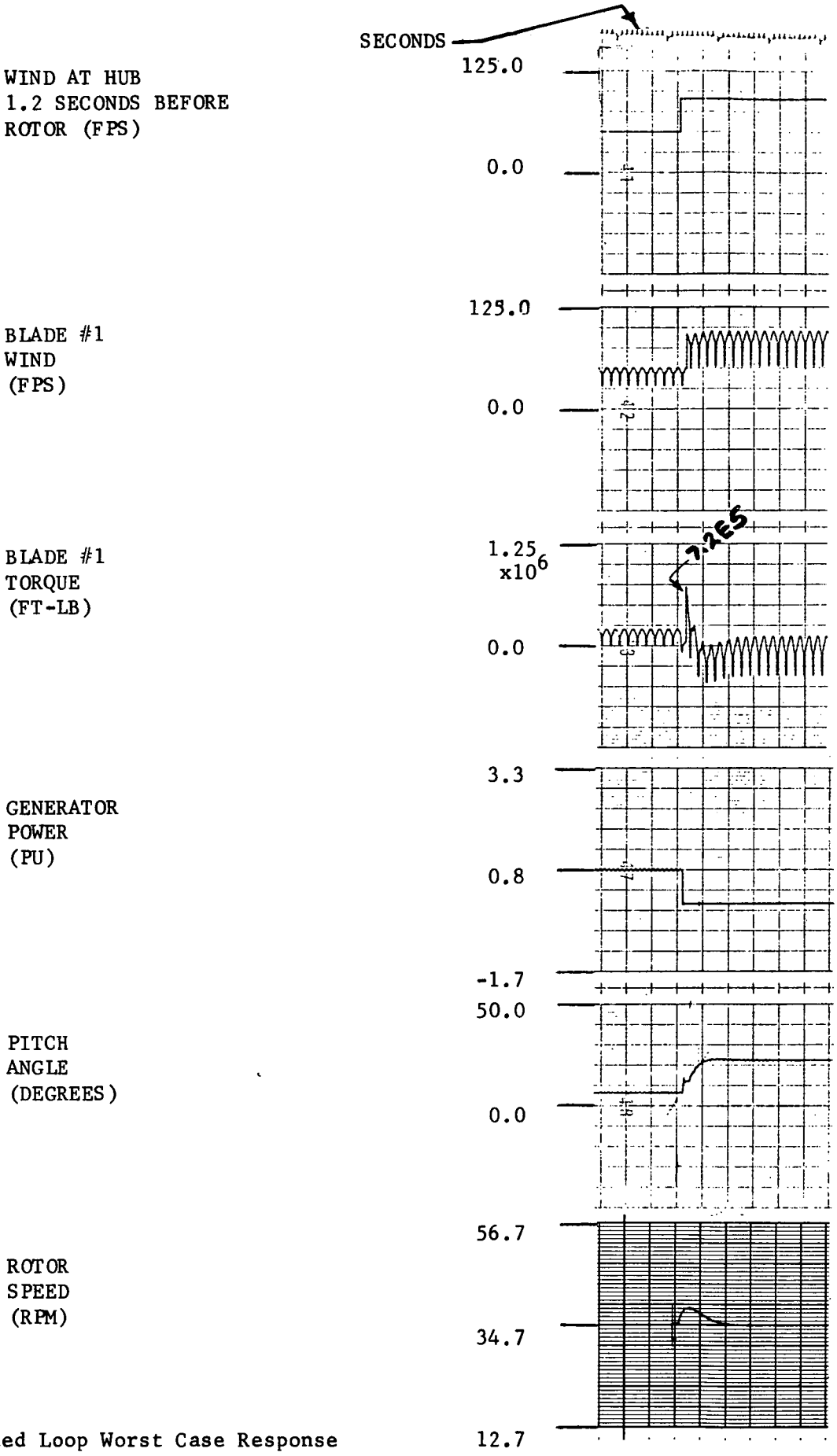

Speed Loop Worst Case Response

Figure 4-30.

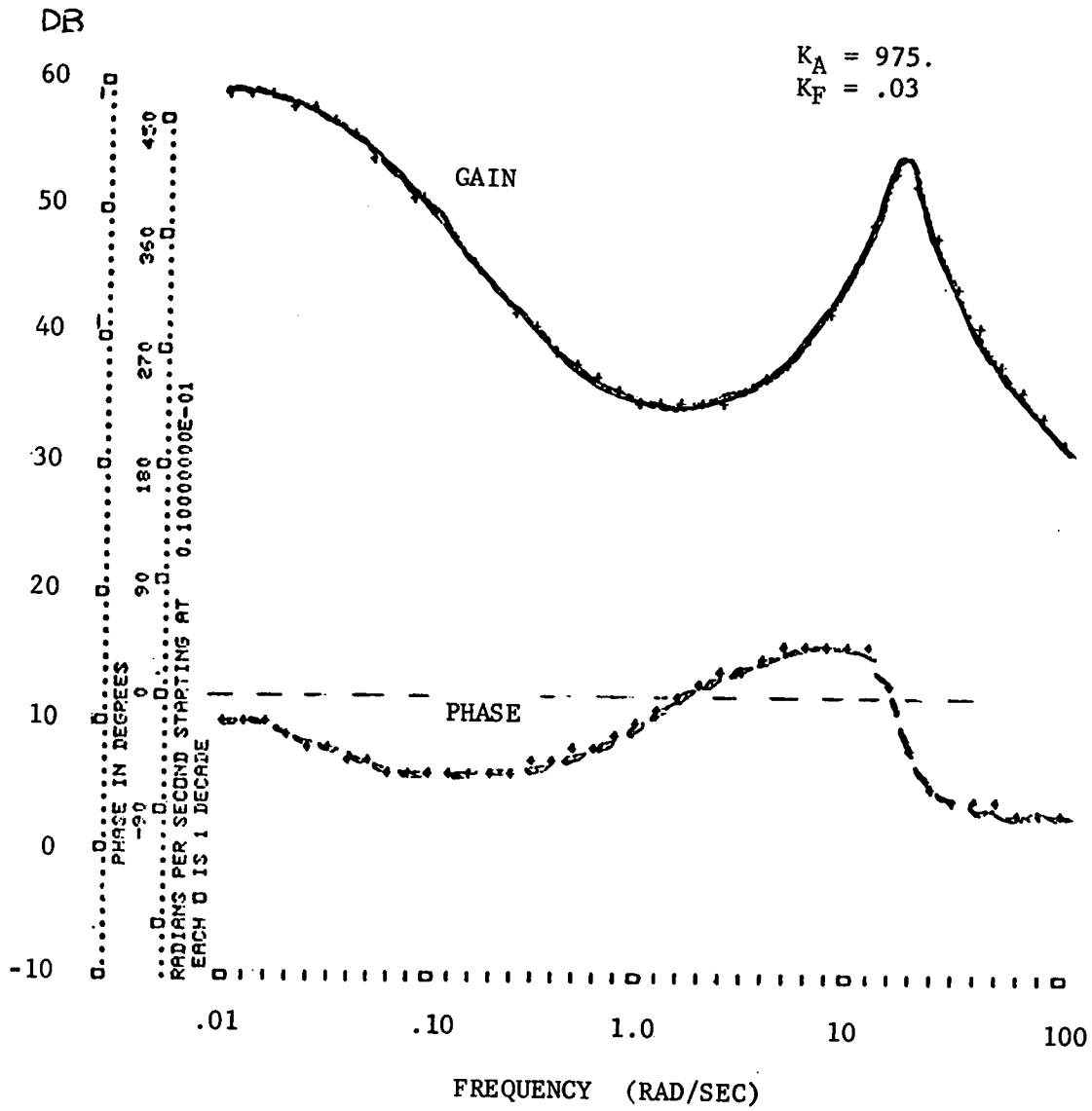

Figure 4-31 Regulator Gain-Phase Diagram

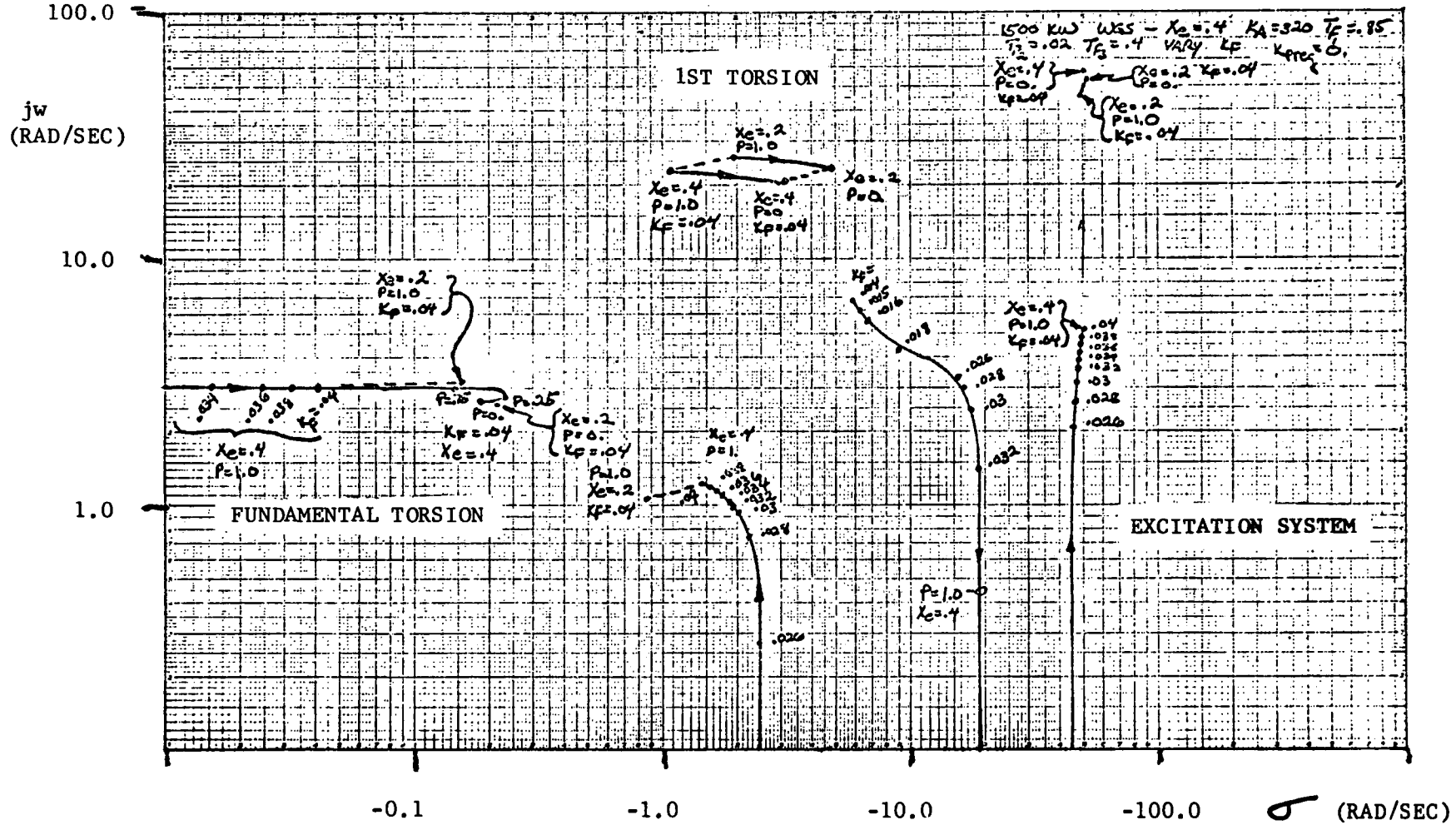

Figure 4-32. System Root Locus

A system multivariable root locus plot varying regulator feedback gain setting for the system through frequencies of interest is shown in Figure 4-32. Root migration with power level and connection impedance is also shown in Figure 4-32.

4.5.2.2 Time Analysis

Response of the full simulation to a change in reference voltage at 1500 kW is shown in Figure 4-33 for a 1.5 percent step. This closed loop loaded response includes saturation and is typical of an IEEE Type 2 brushless exciter and solid state voltage regulator system.

4.5.3 STABILIZER

4.5.3.1 Frequency Analysis

Stabilizer compensation design started by using generator speed as the control signal, but insurmountable difficulties occurred involving destabilization of the first torsional mode occurring while the fundamental mode was showing added damping. The reason became evident from examination of mode shapes with the generator inertia having the greatest participation in the first torsional mode.

A shift in speed sensor reference to the rotor bypassed the difficulty with the slight penalty of lower resolution due to a 52:1 speed difference. The rotor hub is essentially a node for all drive train related frequencies except the fundamental.

Figure 4-34 shows the stabilizer loop block diagram and Figure 4-35 shows root migration with gain change on both a high impedance connection system of .4 pu, and a medium impedance connection system of .2 pu. The desired effect of almost pure increase in magnitude of negative real part of the fundamental root is evident with damping at 30 percent of critical for a 100 pu/pu gain. These plots reflect a lower inertia system with fundamental frequency near 3.5 r/s rather than presently calculated 2.5 r/s but the effect is essentially identical.

4.5.3.2 Time Analysis

Reference to Figure 4-25 will demonstrate the full simulation effect of the stabilizer. Also, in Figure 4-36, a random wind input time response is shown with and without the stabilizer loop closed. A filter in the power controller loop attenuates response at the fundamental frequency to permit improved performance at all other frequencies, but this makes the power controller "blind" to this input frequency.

Quasi-resonant response buildups and decays are evident without the stabilizer due to the blindness. With the added stabilizer damping, however, the buildup is less and the decay is more rapid which provides reduced fatigue loading on the gearbox and smoother power.

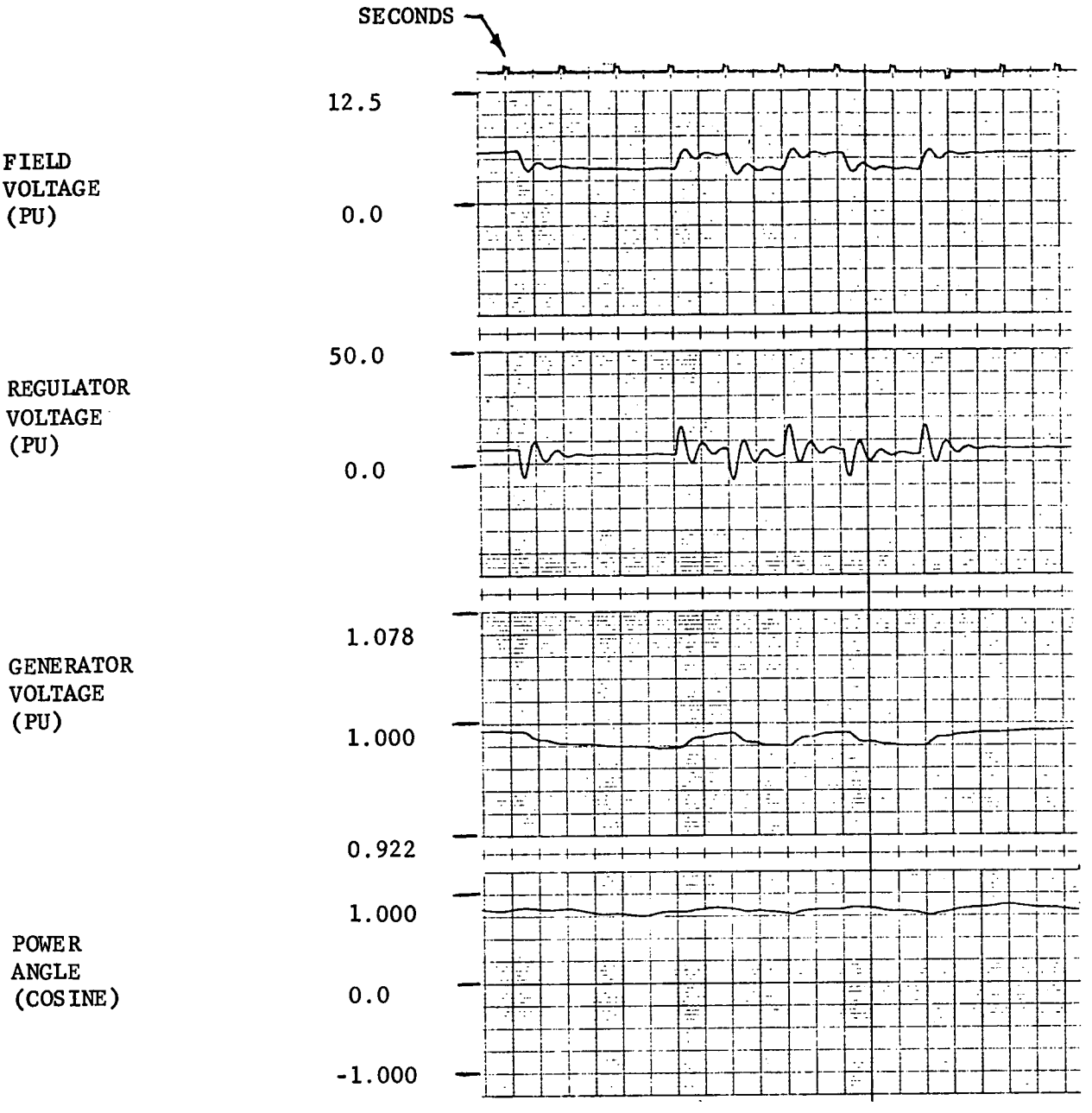

Figure 4-33. Excitation Step Response

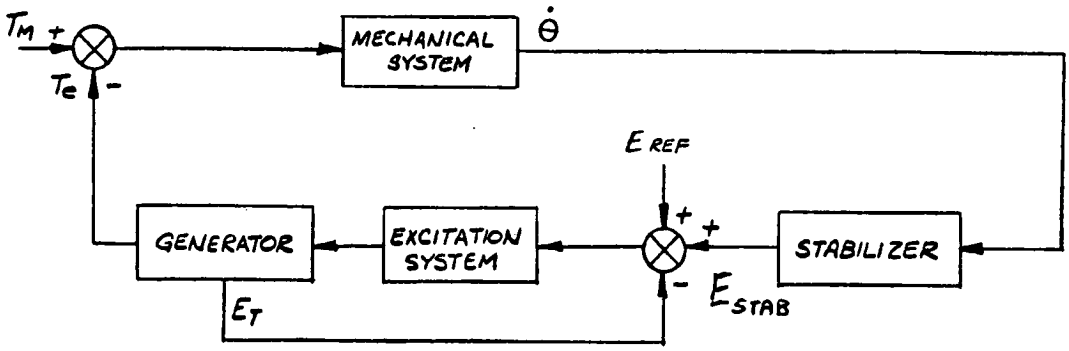

Figure 4-34. Stabilizer Control Loop

4.5.4 POWER CONTROL AND COMBINED LOOPS

4.5.4.1 Frequency Analysis

Figure 4-37 is a Bode diagram of electrical torque (or power at constant speed) relative to rotor torque. Without the stabilizer, the poorly damped pole at 2.5 r/s would severely limit crossover frequency for an integral control characteristic. Utilizing a complex zero, double real pole characteristic minimizes the mechanical pole effect and provides an integral characteristic below the pole and improved gain above it relative to a straight integral function as shown on the Bode diagram of Figure 4-38.

A block diagram of the power control loop in Figure 4-39 shows the main elements described in the previous paragraph in addition to a second torsional frequency and the wind feed forward loop. Closed loop performance of the system to an impulse in wind velocity is shown in the Bode diagram of Figure 4-40.

Power controller gain variation root migration is shown in Figure 4-41 for the system.

4.5.4.2 Time Analysis

Single 1-cosine disturbances in wind velocity for various combinations of control loops are shown in Figure 4-42. The behavior is consistent with

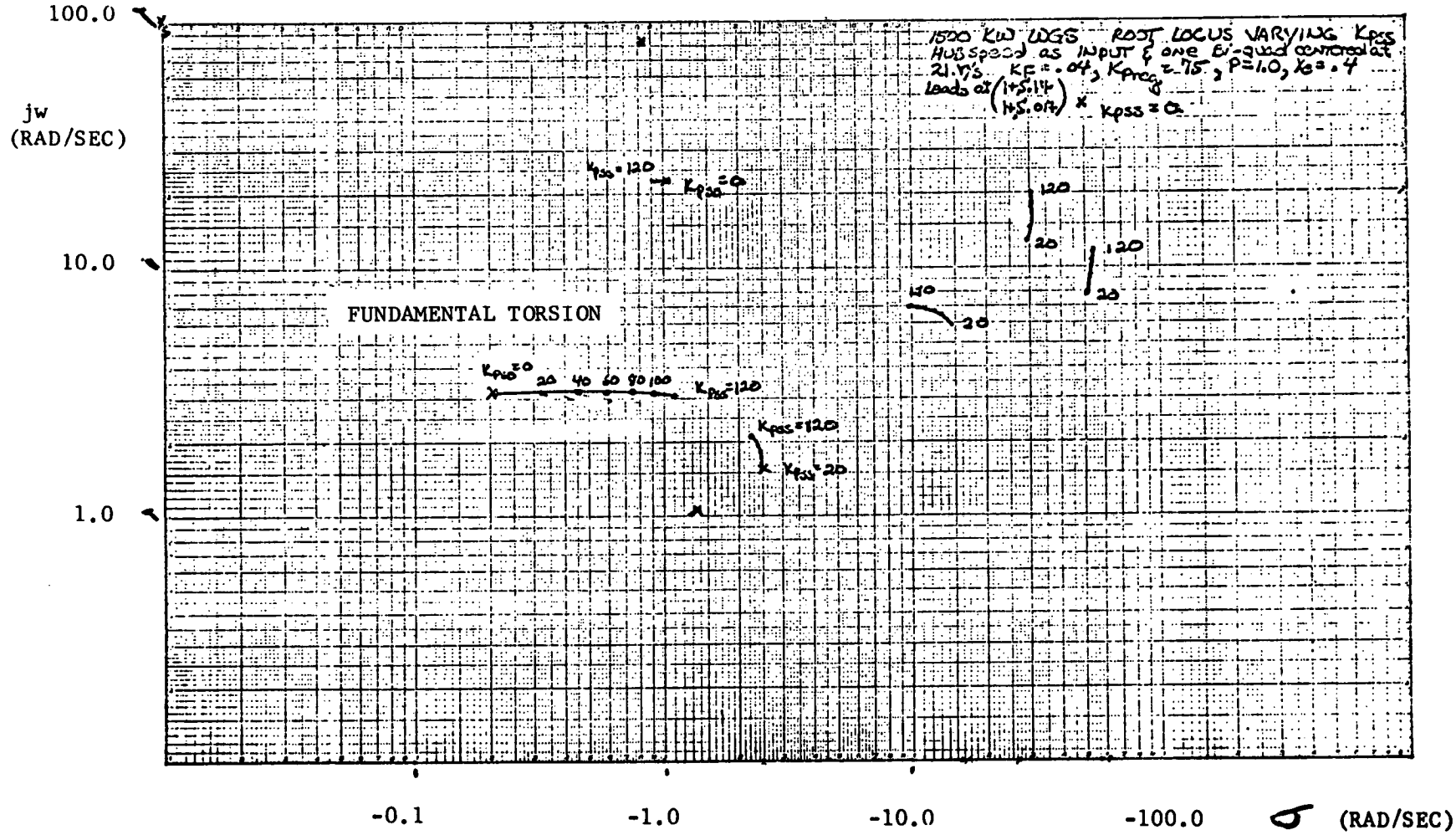

Figure 4-35. Stabilizer Root Locus

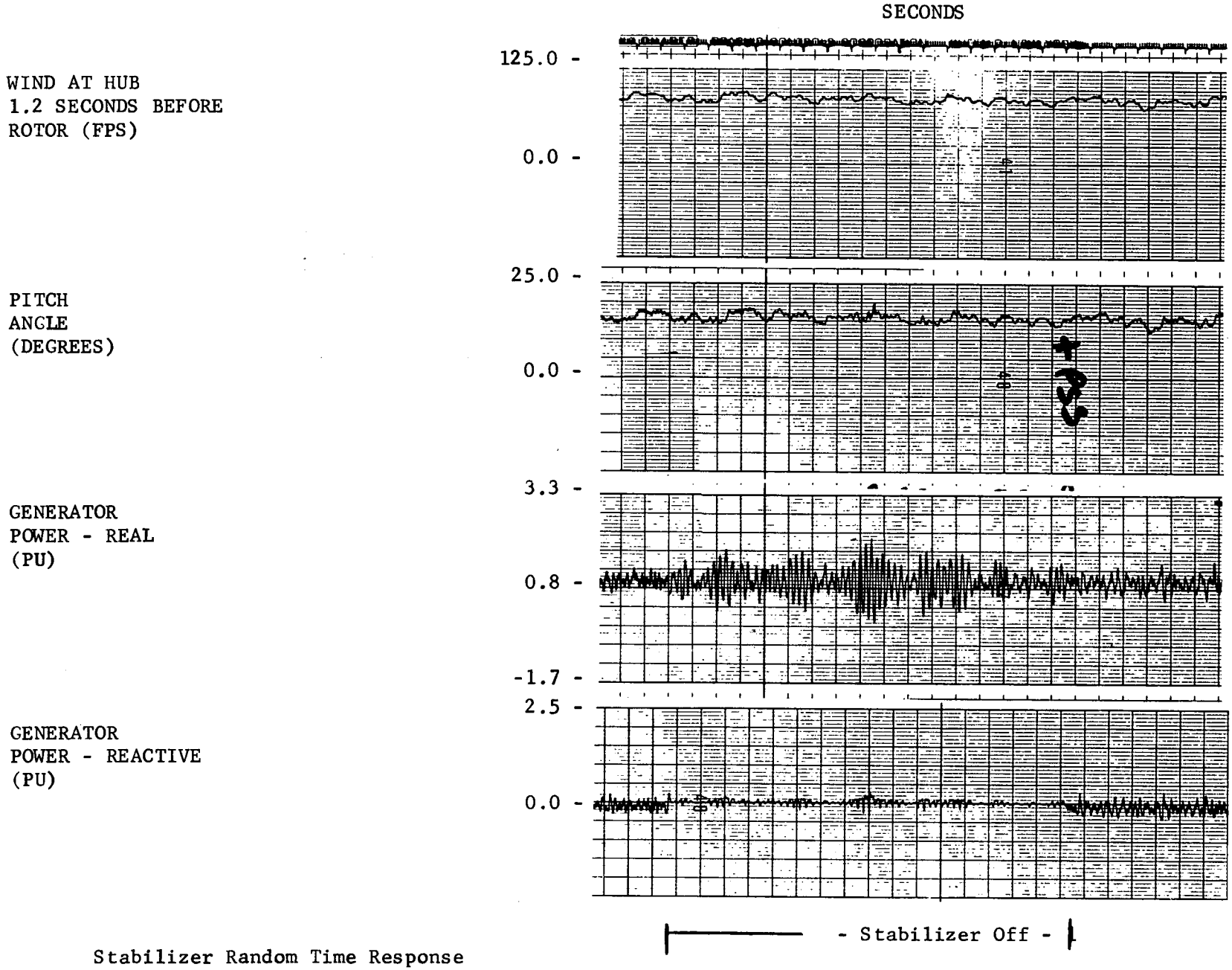

Stabilizer Random Time Response
Figure 4-36. A

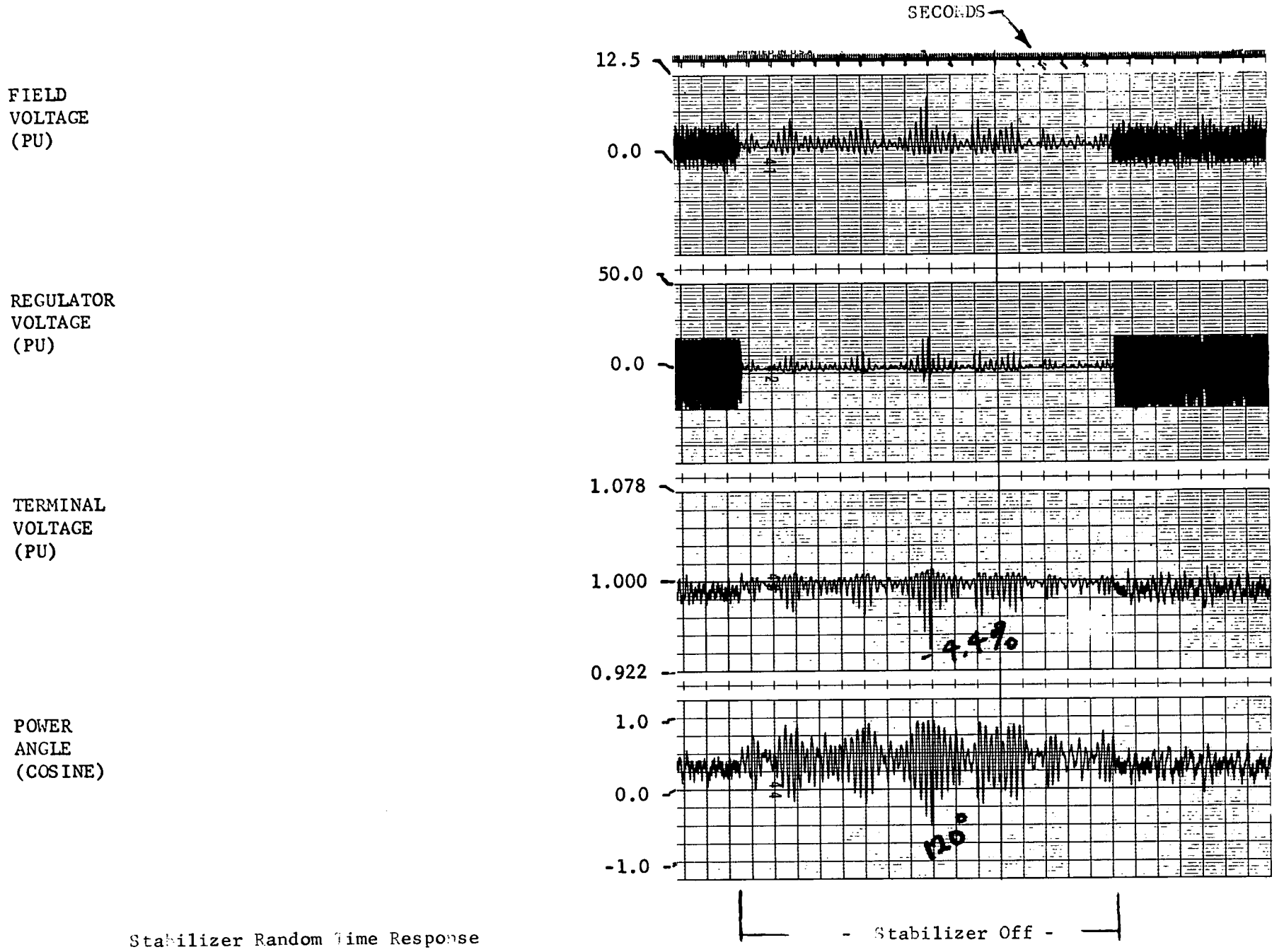

Stabilizer Random Time Response
Figure 4-36. B.

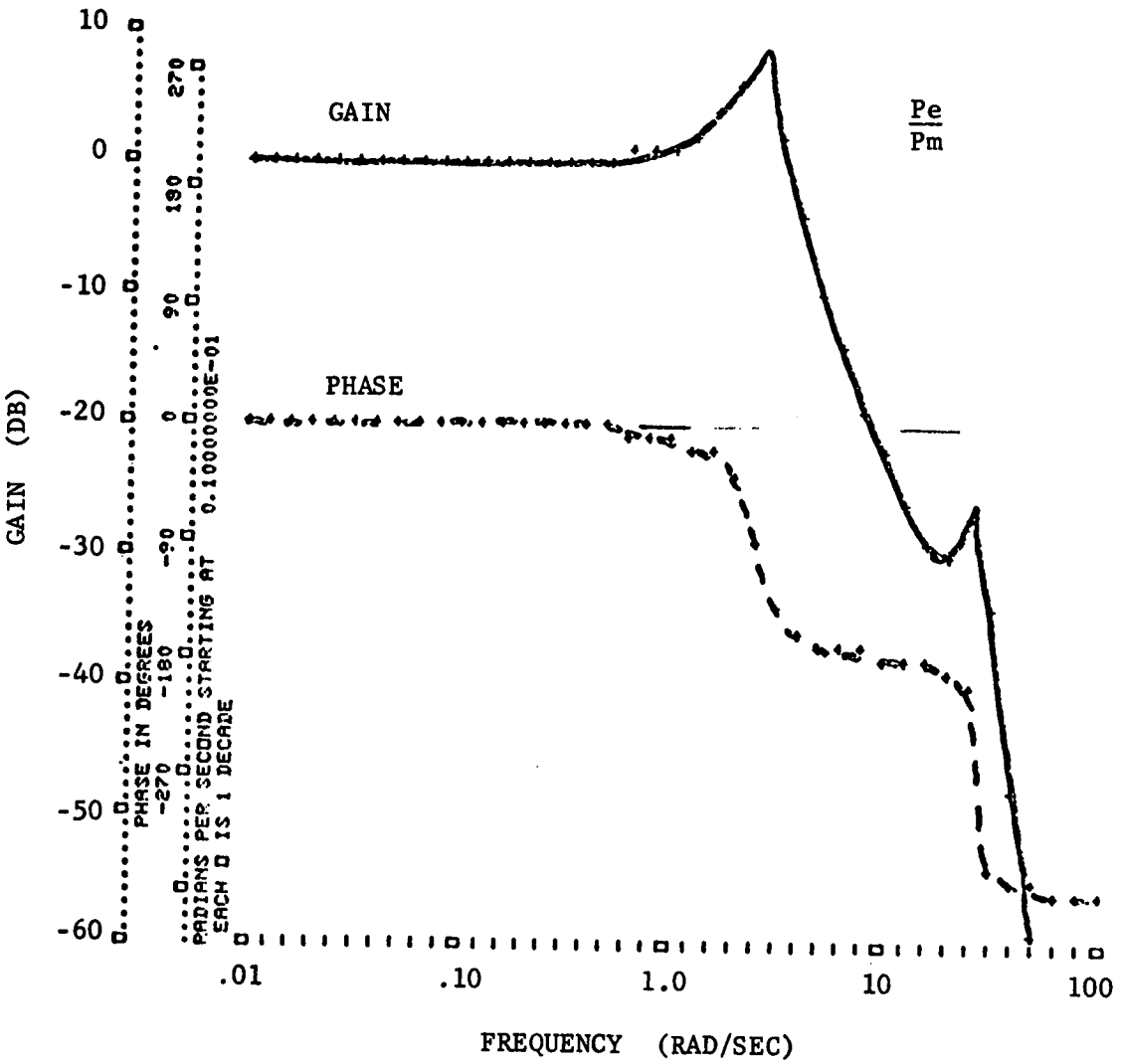

Figure 4-37 Torque Gain-Phase Diagram

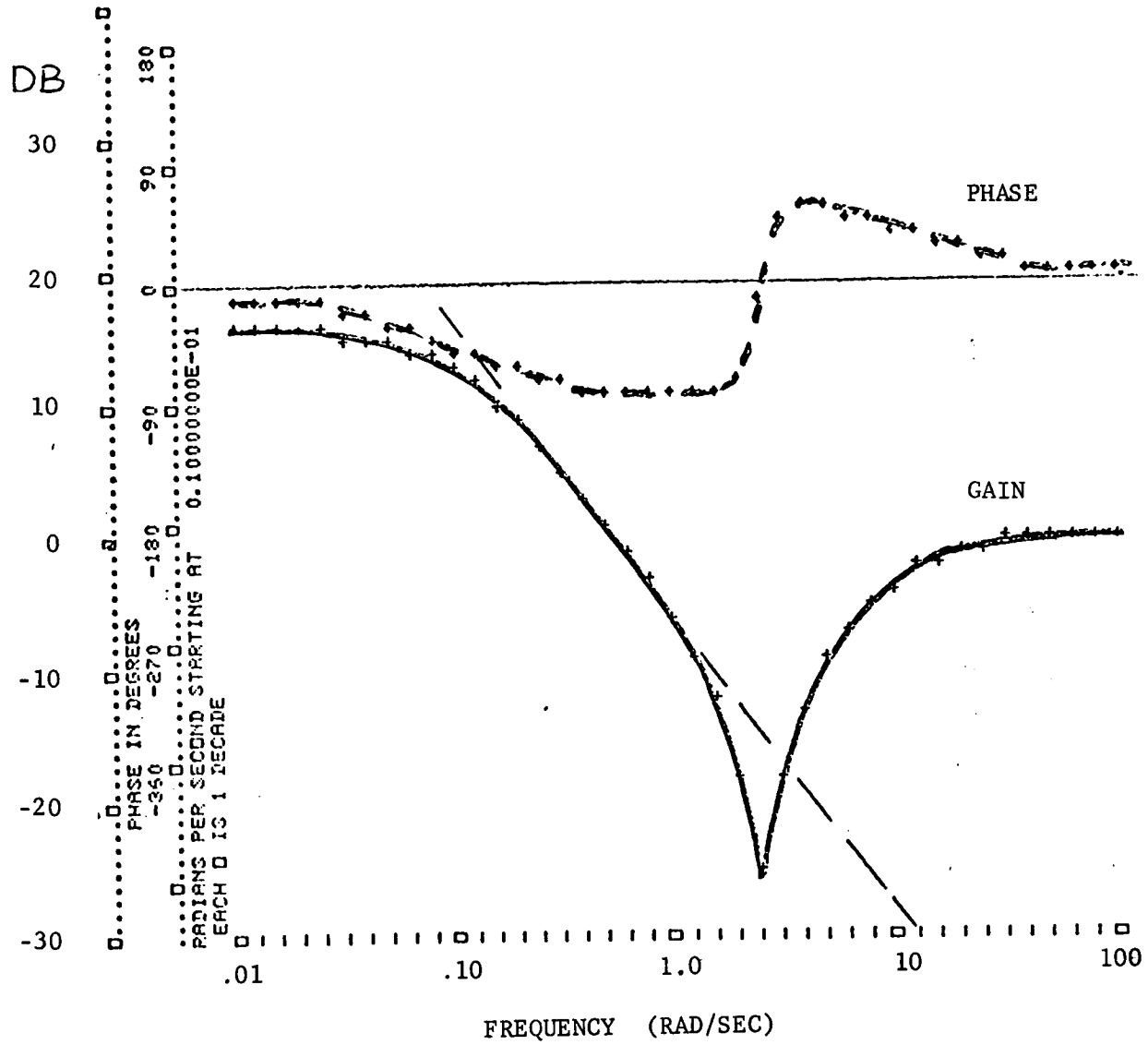

Figure 4-38 Controller Gain-Phase Diagram

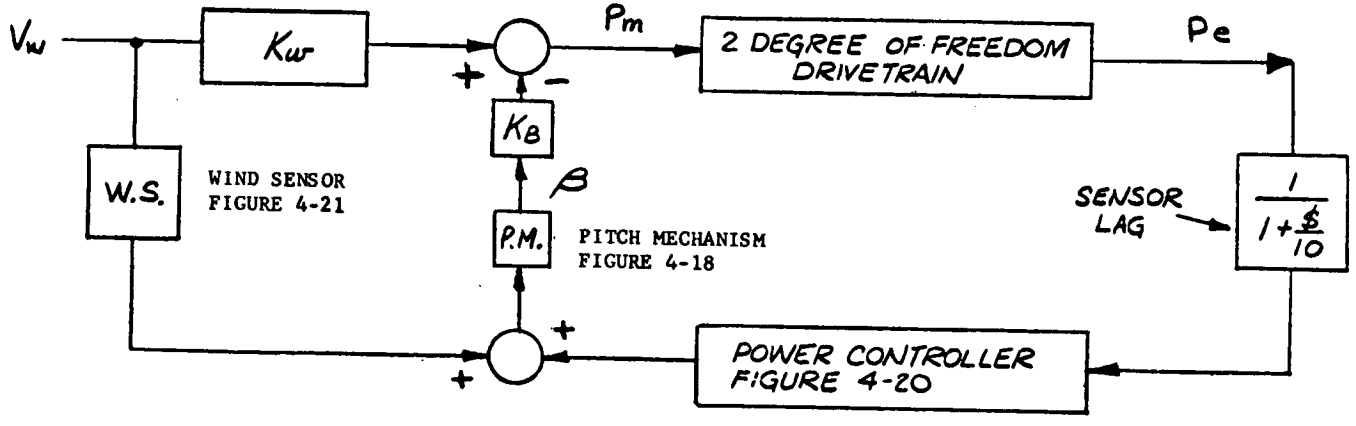

Figure 4-39. Power Control Block Diagram

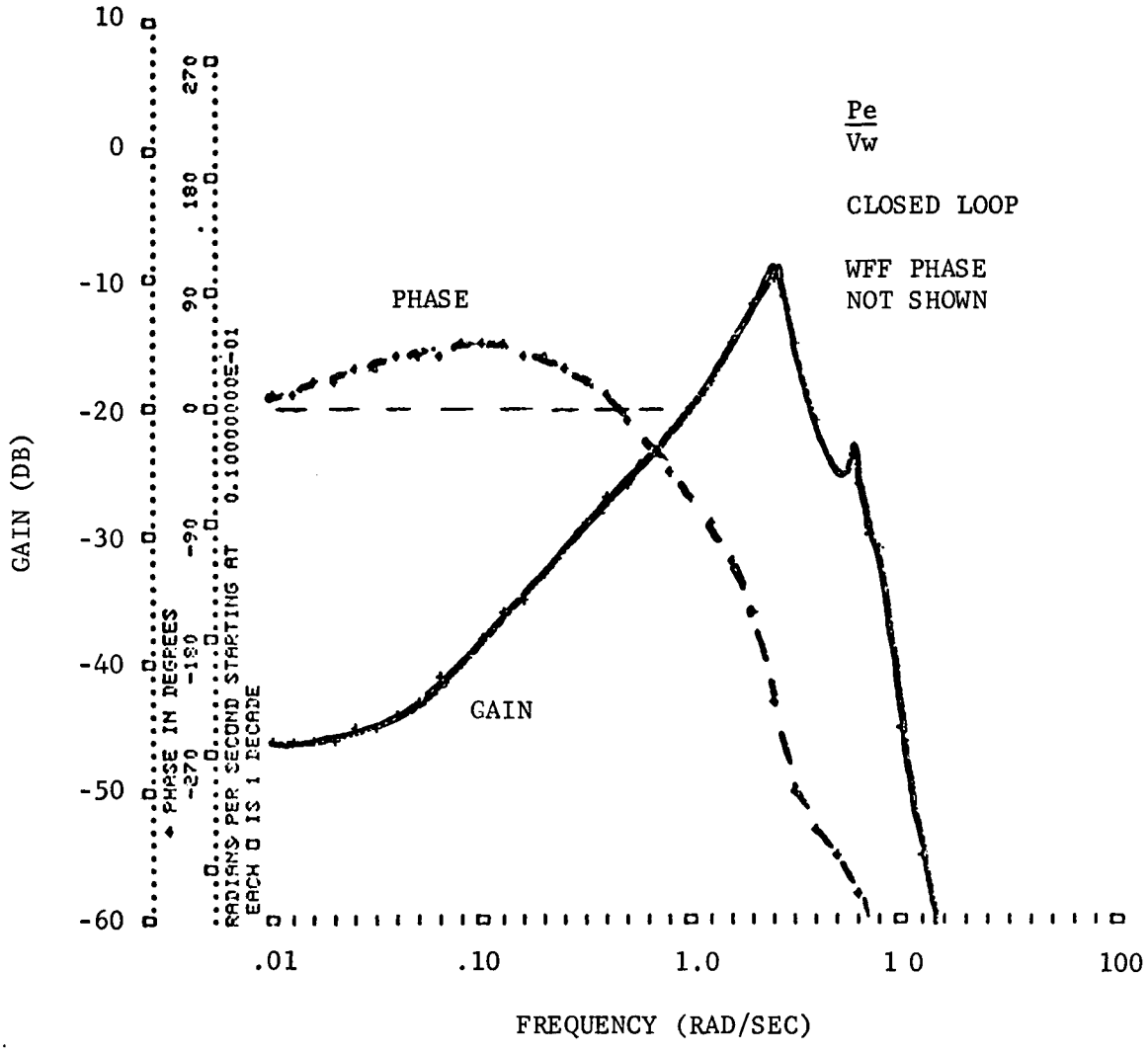

Figure 4-40 Power Loop Gain-Phase Diagram

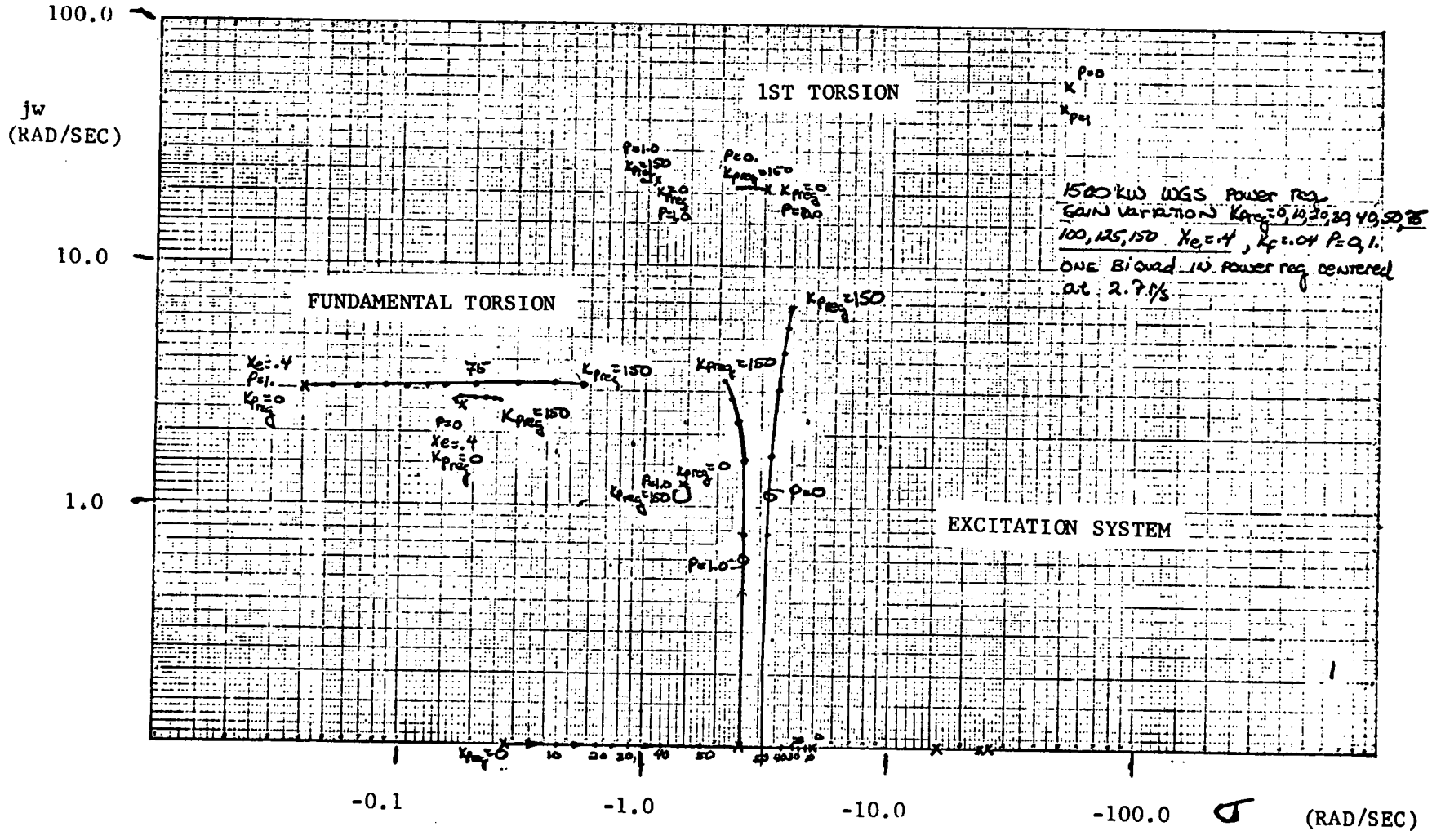

Figure 4-41. Power Control Root Locus

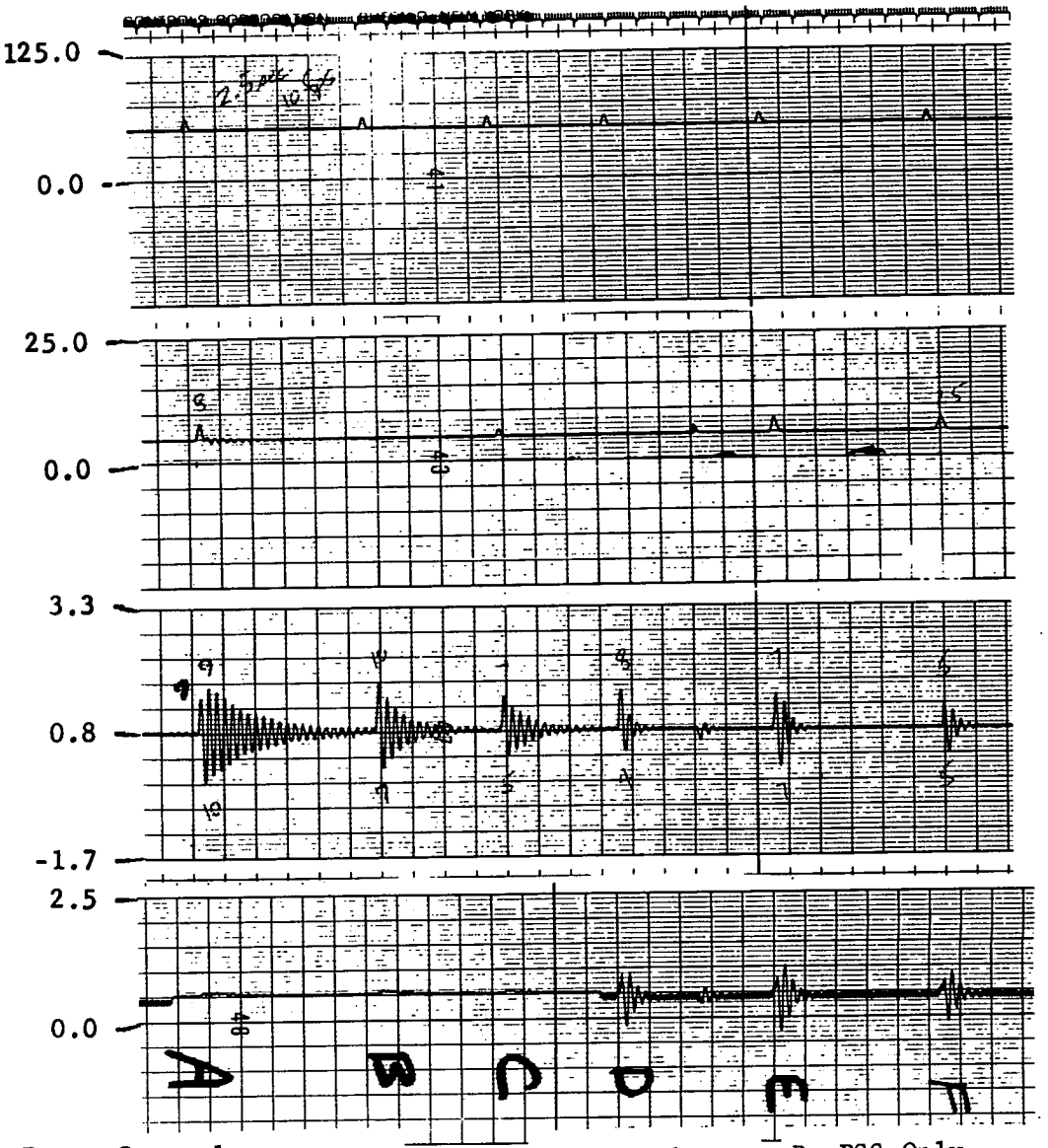

PC = Power Control
PSS = Power System Stabilizer
WFF = Wind Feed Forward

A- PC Only
B- No Control
C- WFF Only
D- PSS Only
E- PC and PSS
F- PC and PSS and WFF

Figure 4-42A System Gust Response

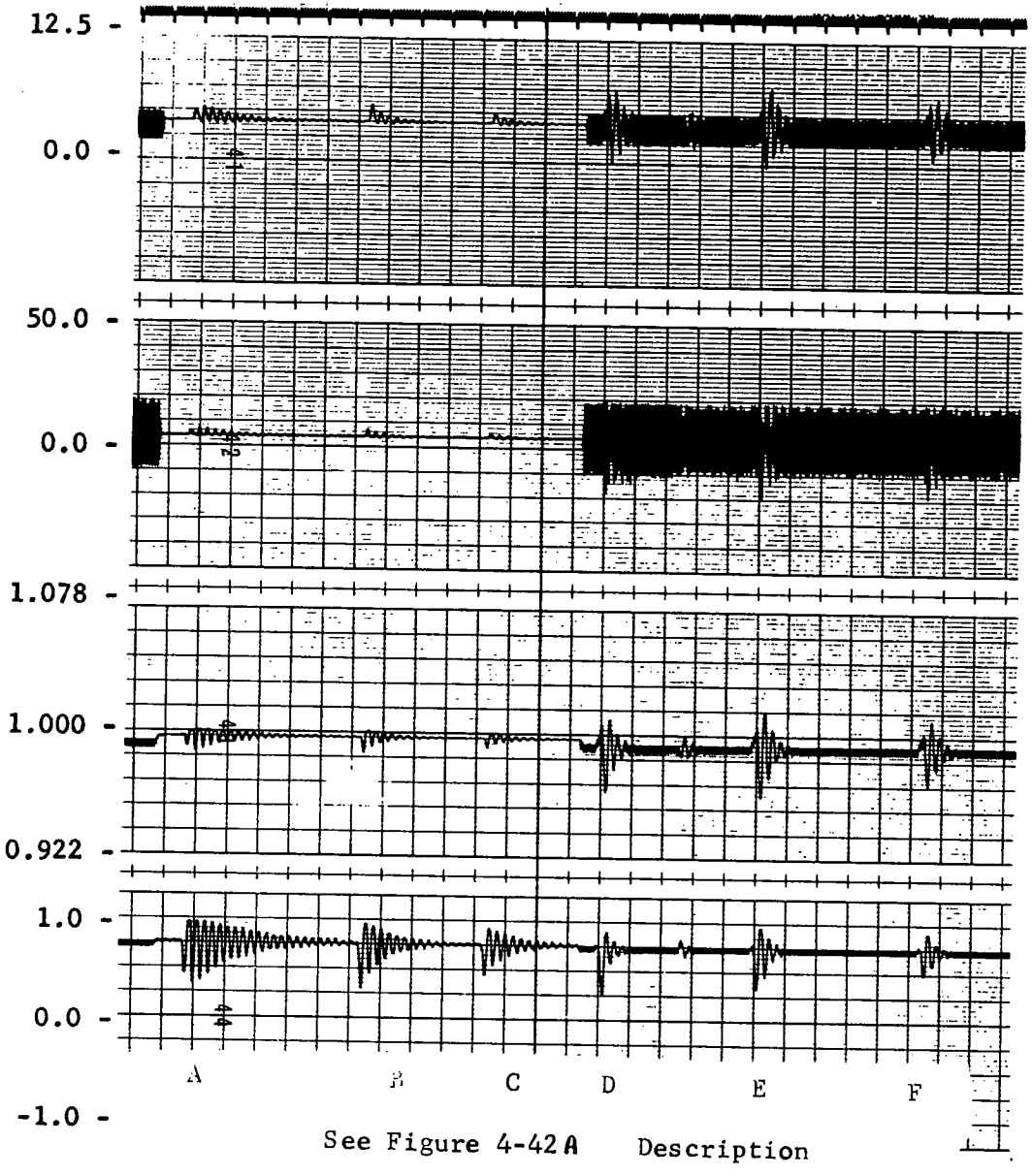

System Gust Response
Figure 4-42.

See Figure 4-42A Description

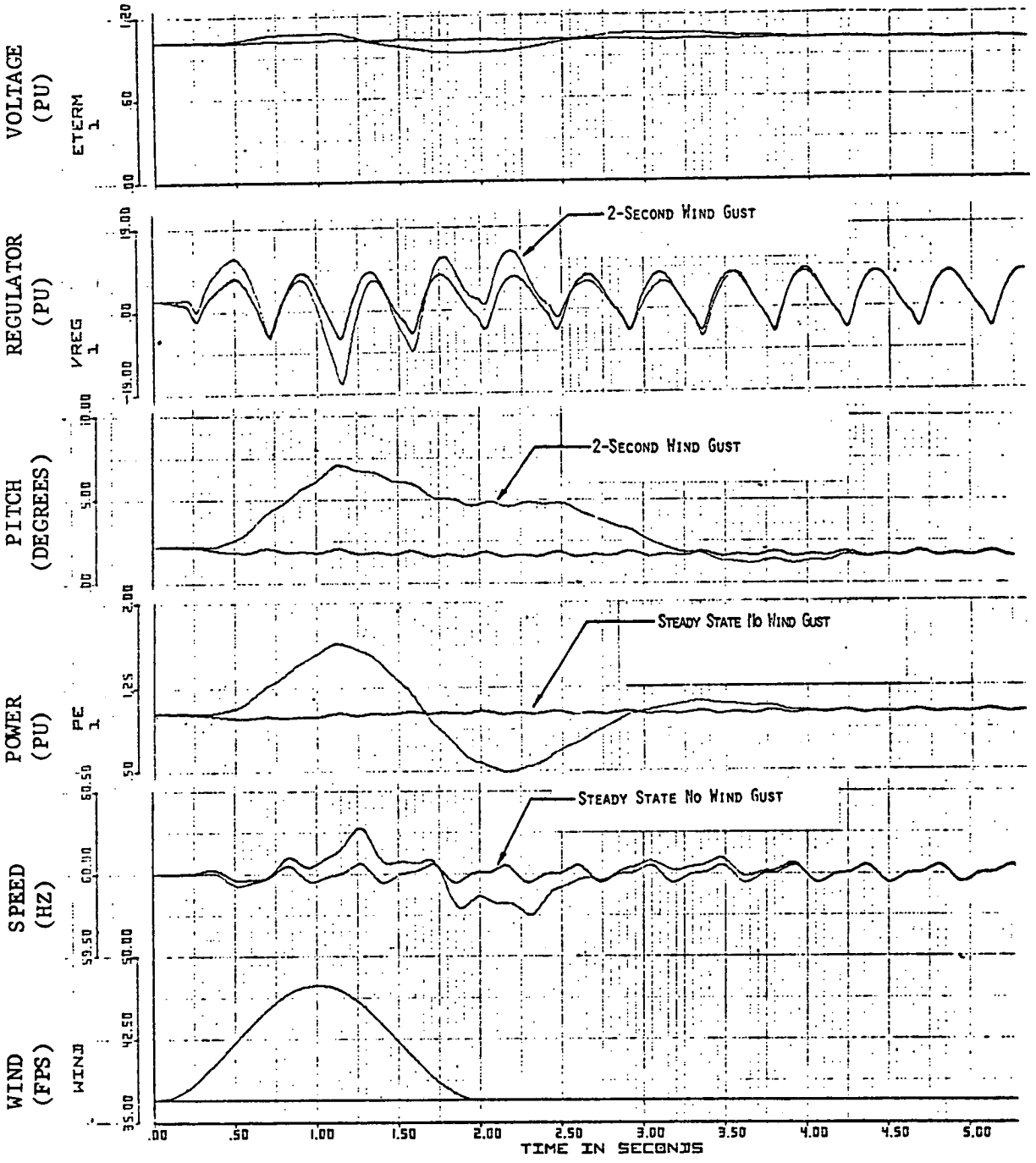

Figure 4-43 Small System 1-Cosine Response

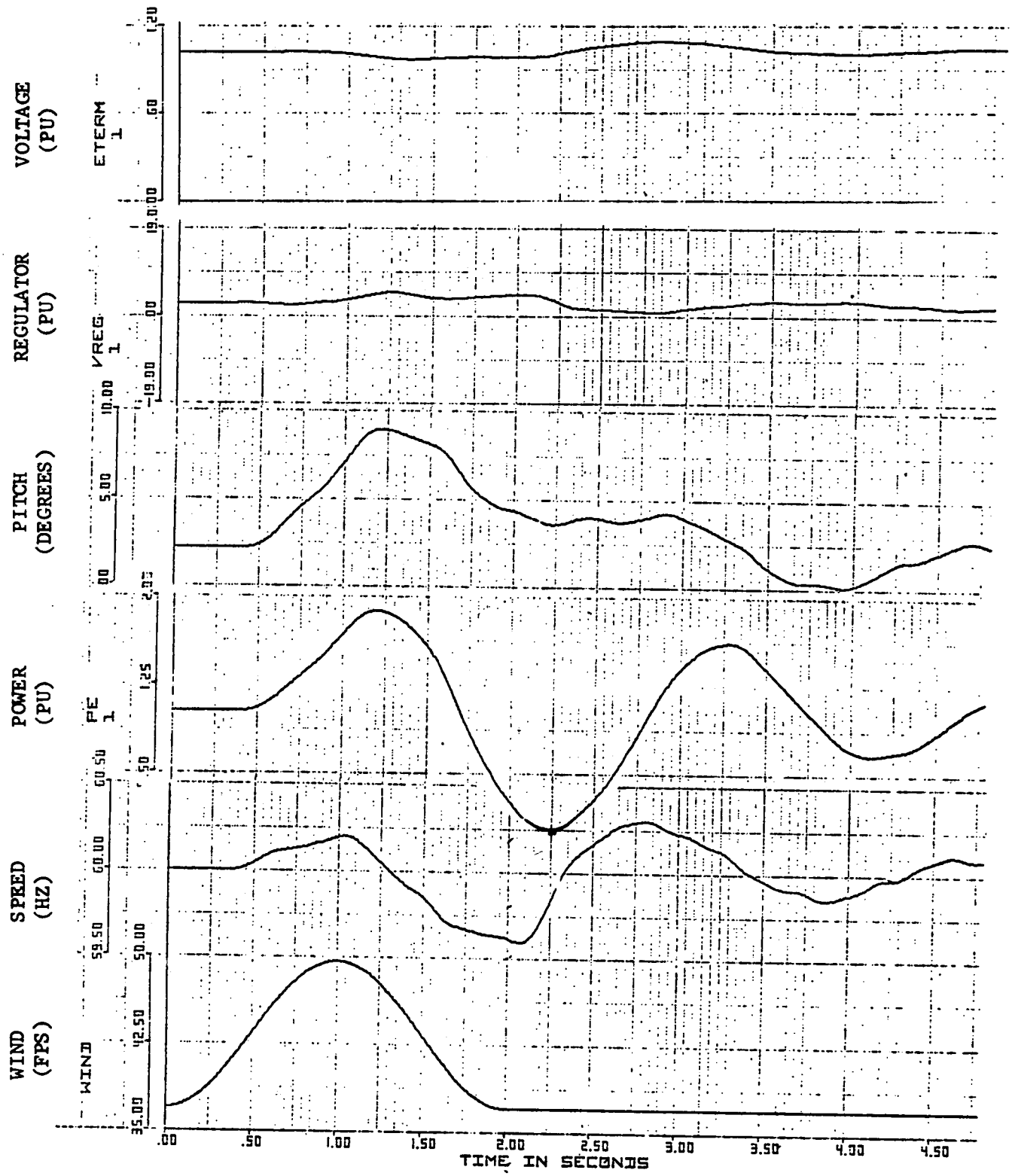

Figure 4-44 Small System Response Without Stabilizer

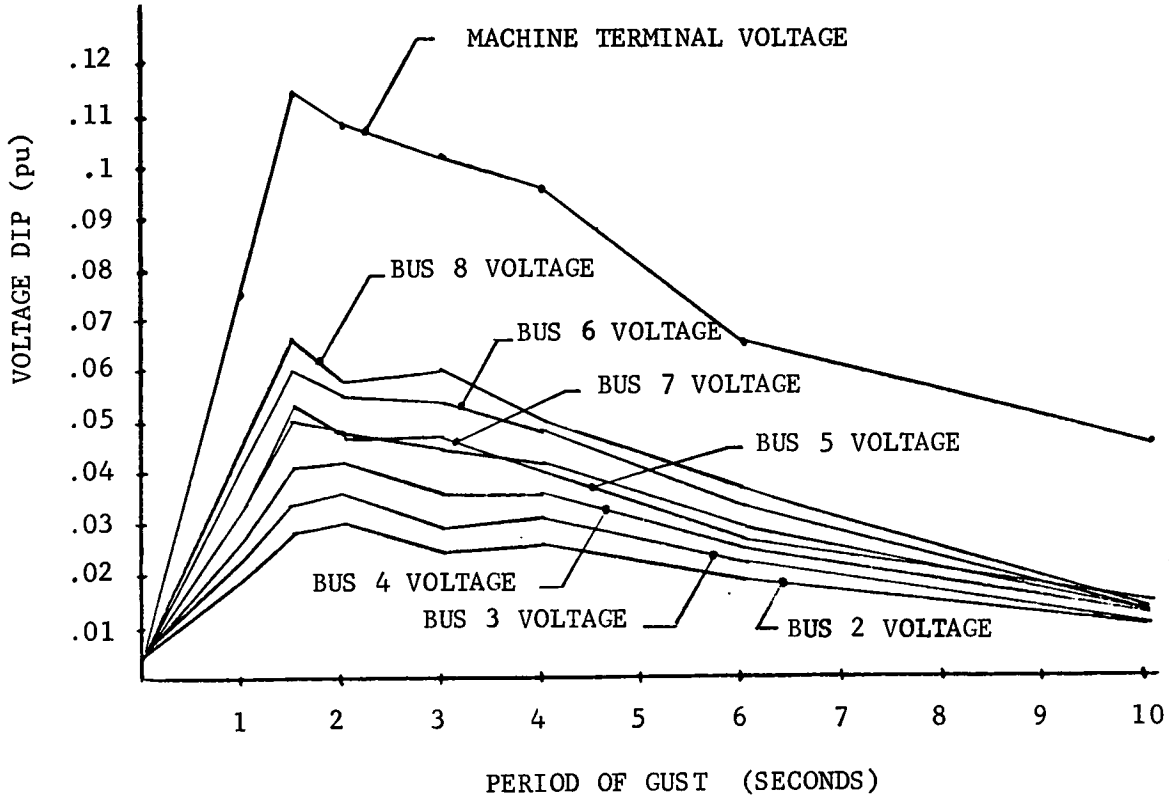

Figure 4-45 Voltage Dip Response

frequency analysis. A need for additional filtering at 2P and 4P in the power control and stabilizer loops was identified to decrease aggravated response to tower shadow induced continuous perturbations.

4.5.5 Transient Response

4.5.5.1 1-Cosine Gusts

The most severe period 1-cosine gust that can be applied has a period around 2 seconds, or the same as the on-line fundamental frequency of oscillation. In Figure 4-43, the response of the network of Figure 4-12 is shown to a 2-second gust. Note that interaction between machines is almost nonexistent but that a significant power swing occurs. This system has stabilizers but no wind feed forward control. Accelerating torque from the gust initially increases power, then action of the power controller changes pitch angle to decrease blade gain and reduce power. As the gust tails off, decelerating torque swings power low as the blade angle lags incoming torque.

Cases shown in Figure 4-42 are for:

A. Power Controller Only

B. No Control (No Pitch Change)

C. Power Control Plus Wind Feed Forward

D. Stabilizer Only (No Pitch Change)

E. Power Control Plus Stabilizer

F. Power Control Plus Stabilizer Plus Wind Feed Forward

Action of the stabilizer is evident in rapid damping of power oscillations in the time after 3 seconds. In Figure 4-44, the same case without the stabilizer is shown. Note the less well damped longer decay in oscillation of power.

As gust period increases, the control system is more able to correct blade gain at the same time that wind changes occur and less transient system disturbance results. Variations in WTG terminal voltage and system voltage versus gust period are shown in Figure 4-45.

4.5.5.2 Step Gusts

Step response analysis produced the same general results as discrete 1-cosine gusts. The long time steady state pitch angle will change to accommodate the new wind at the reference power, but the transient is similar to that resulting from a small period 1-cosine input.

System response is characterized by the relatively low 2.5 r/s (.4 Hz, .7P) fundamental frequency and small 1-cosine inputs look the same as a square pulse or an up step followed by a down step.

4.5.5.3 Probabilistic Gusts

Synchronism was maintained for the gusts of Figure 4-3 with all control loops active and even without the stabilizer and wind feed forward. Removal of the power control loop (fixed blade gain) caused loss of synchronism for the worst 0.1 percent gust.

4.5.5.4 Random Wind

Long time response to moderate amplitude random wind is illustrated in Figure 4-46. This extends the trace of Figure 4-36 with a stabilizer to the effect of adding the wind feed forward signal. Variation in output power is reduced to half the value resulting from not having wind feed forward. Wind field coherence variation was not modeled and site performance may not show as great a reduction.

Response to high amplitude random wind is shown in Figure 4-47 without the power control loop energized to simulate fixed pitch operation. The stabilizer permits retaining synchronism for a short time, but a significant increase in wind velocity drives the generator out of synchronism with resultant circuit breaker opening and loss of load causing oscillations or "ringdown" of the generator inertia about the rotor due to the sudden removal of drive-train torque.

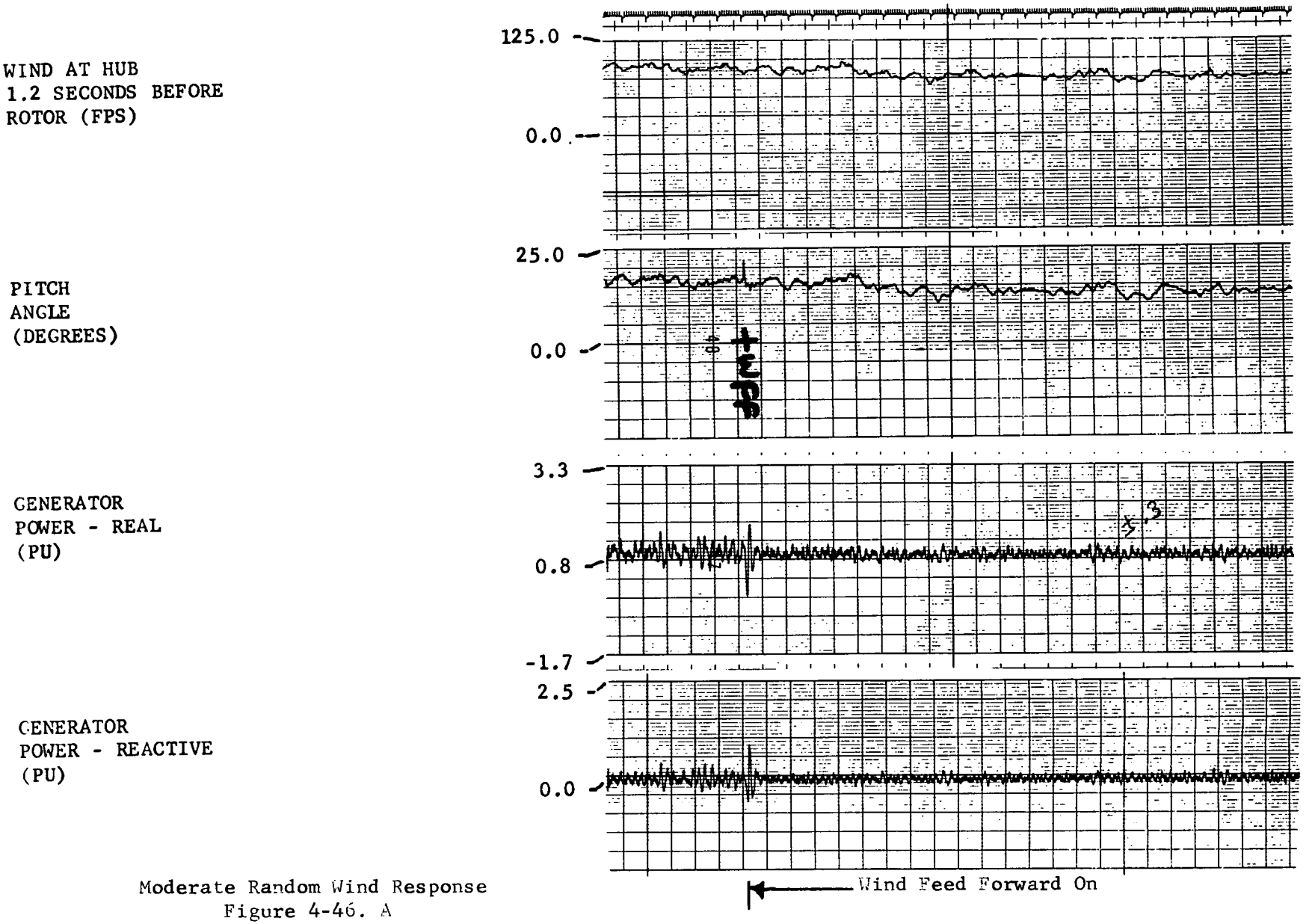

Moderate Random Wind Response
Figure 4-46. A

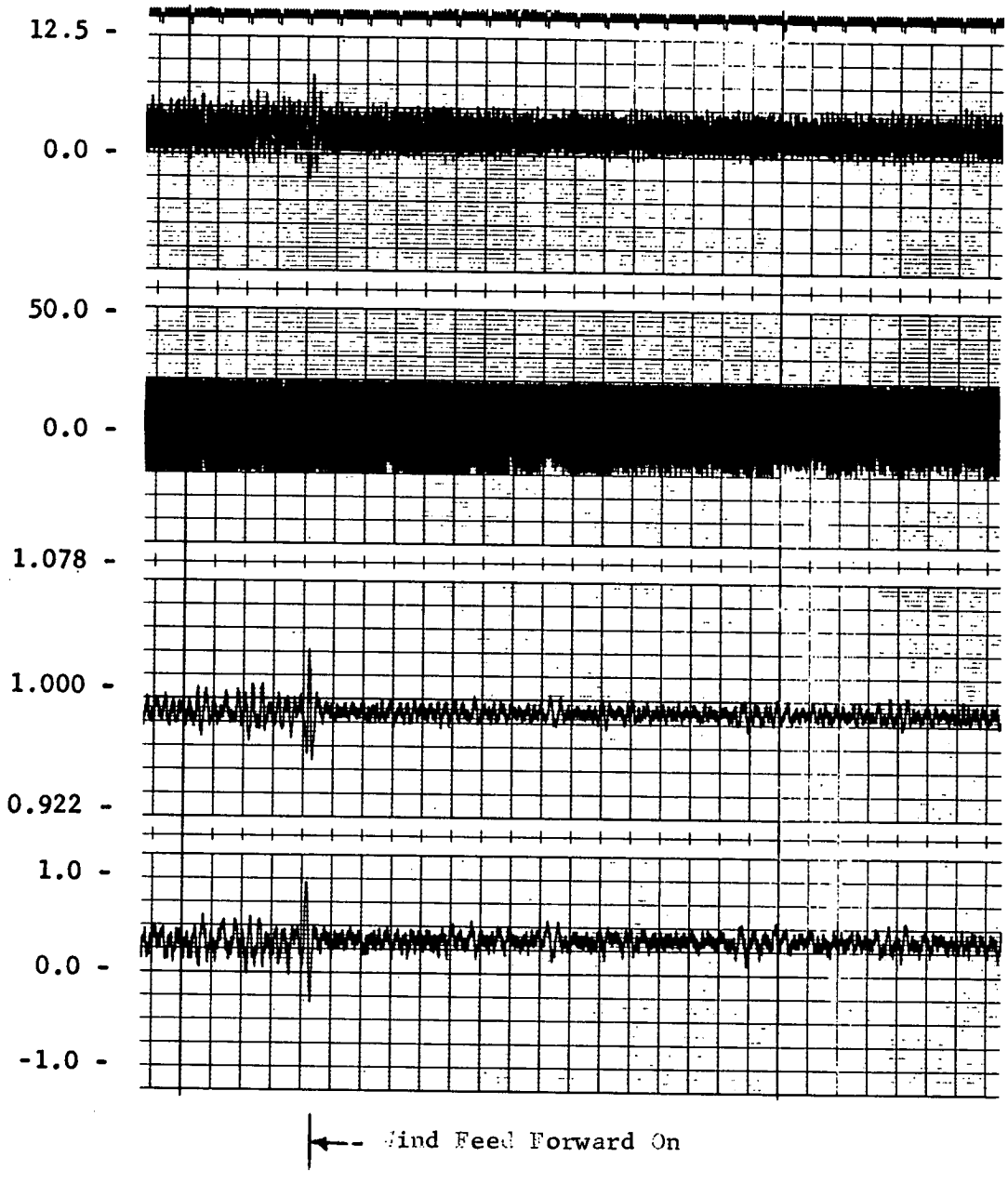

Moderate Random Wind Response
Figure 4-46. B

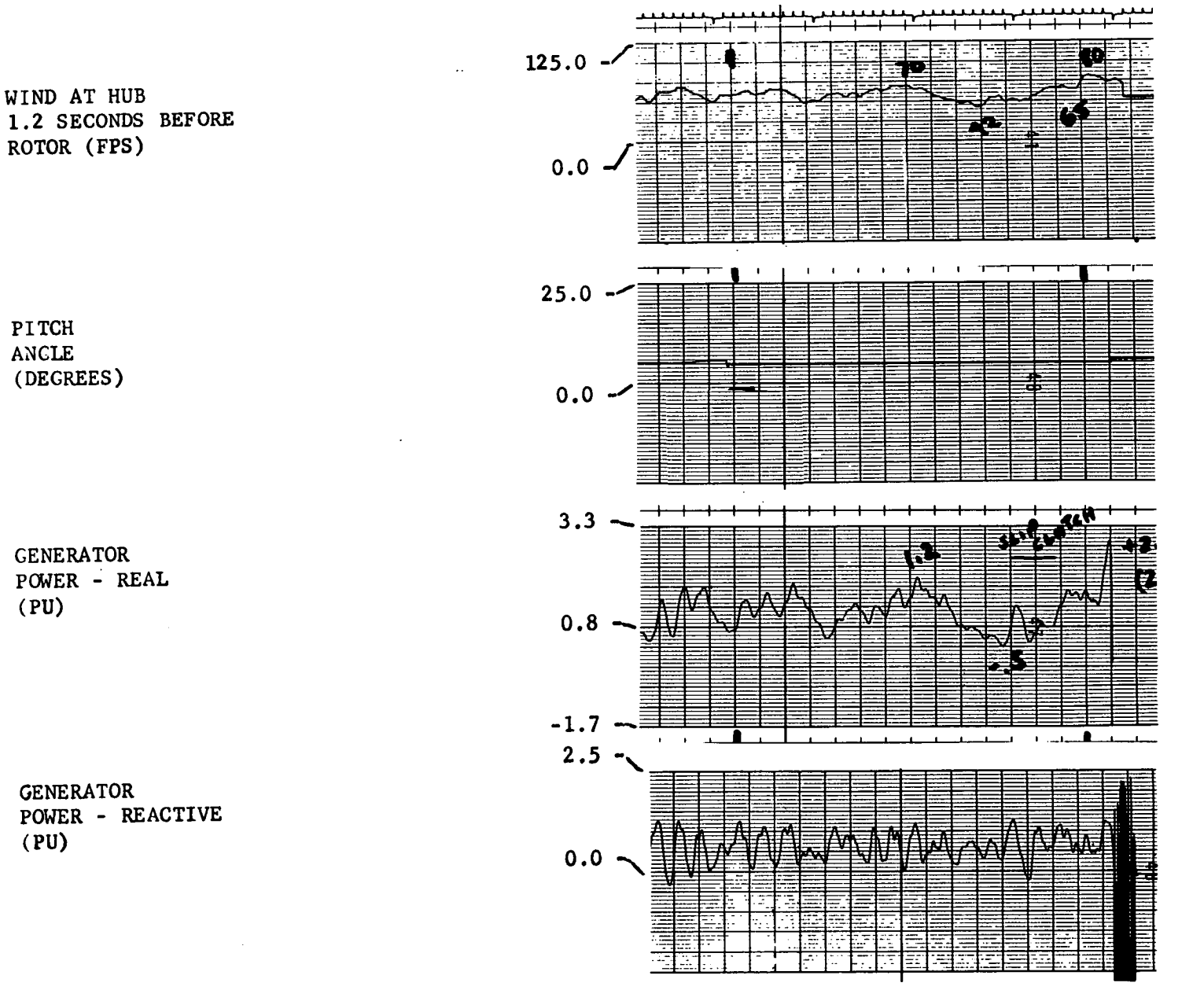

Fixed Pitch Random Wind Response
Figure 4-47 A.

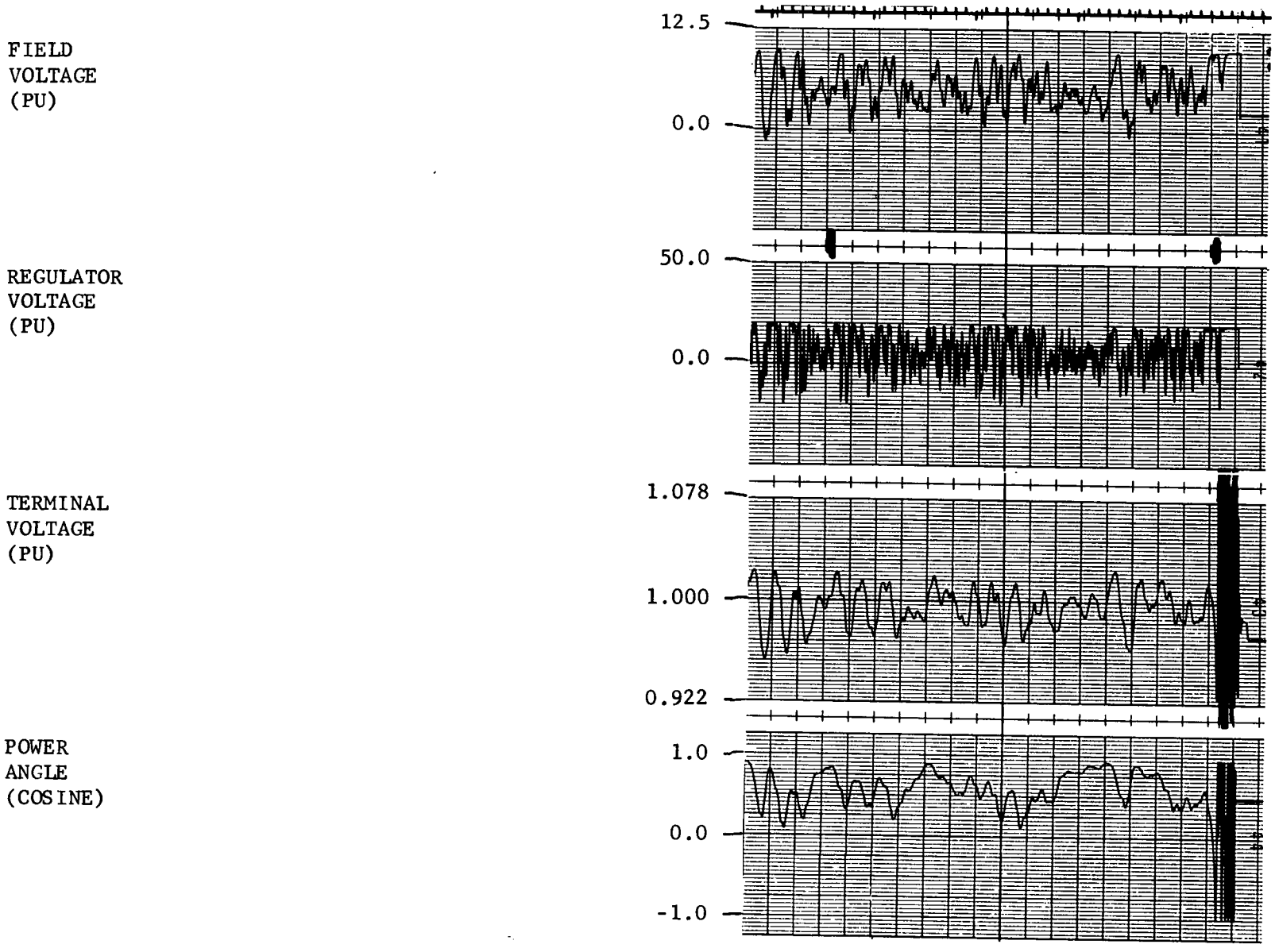

Fixed Pitch Random Wind Response
Figure 4-47. B

Loss of Synchronism

A lightly damped drive train model was used and site ringdown is expected to be better damped.

Voltage response at the generator terminals was generally within 5 percent on the .2 pu hybrid runs, although severe gust variations brought it as high as 10 percent. As the criteria of Figure 4-1 is defined at a critical bus removed from the terminals, the derived requirement is satisfied for this system.

Variation in power is anticipated to be $\pm$ 30 percent for moderately gusty winds with all control loops active. Large gusts will excite a few swings of greater amplitude, possibly reaching $\pm$ 100 percent. Constant wind produces $\pm$ 6 percent power response due to tower shadow.

4.5.5.5 Emergency Feather

A series of loss of load and step gust cases were simulated with various programmed pitch change rates in order to evaluate operation of the emergency feather system. Too rapid a change in pitch angle creates large decelerating torques that are undesirable from a blade-to-tower clearance standpoint. The results of a rate schedule with initial value at 14 degrees per second, then shifting to 2 degrees per second after 1.5 seconds, then further shifting to speed control at 80 percent of speed are shown in Figure 4-48.

4.5.6 Sensitivities

4.5.6.1 Wind and Tower Shadow

A change in shadow width directly effects response as energy content is effected. The 60-degree width utilized in the simulation is severe. An increase in velocity deficit beyond the 35 percent reduction level does not linearly increase torque deficit due to the blade aerodynamic characteristics. Higher mean wind produces a more severe tower shadow effect for the same reason because a larger torque change results from the same percent reduction.

4.5.6.2 Inertia and Shaft Stiffness

Rotor inertia change effects system stability in that response to changes in torque are more or less rapid from the viewpoints of both wind disturbance and blade power gain. Overall, a larger inertia is more beneficial in transient cases such as overspeed, where slower response time will reduce the maximum value for a given control strategy and time.

Shaft stiffness has a controlling effect on off-line frequency and contributes to the on-line fundamental and higher modes. A stiffer shaft is undesirable because it raises the on-line fundamental frequency closer to 1P. Any blade unbalance in aerodynamic characteristics will cause a 1P torque excitation and a natural frequency at 1P is undesirable. Soft shafts reduce the steady response to tower shadow but do not improve gust response. As soft shafting implies an elastomer, the main benefit is added damping but with a thermal dissipation problem.

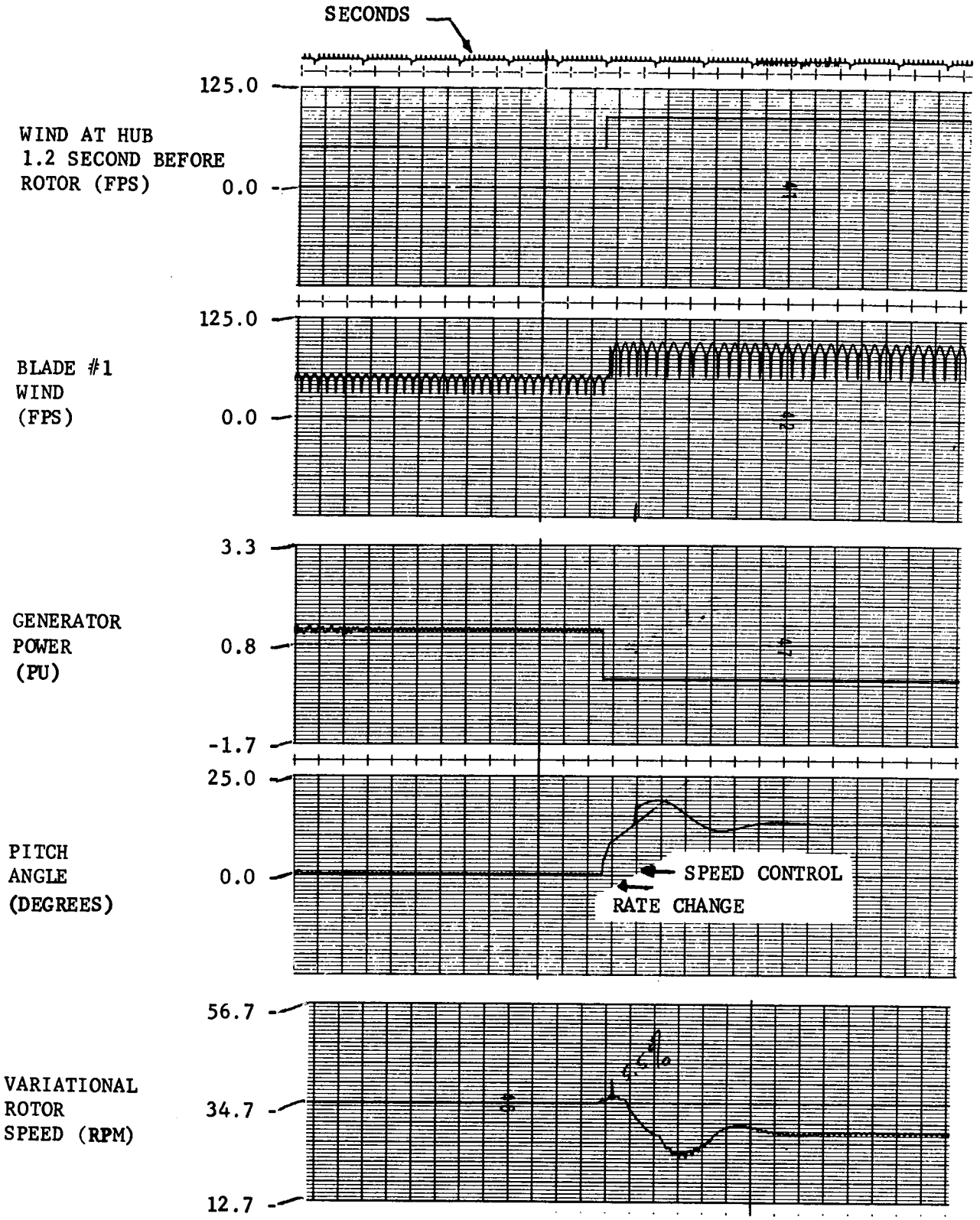

Figure 4-48. Emergency Feather

4.5.6.3 Reactive Power Controller

Various simulation runs utilized the reactive power controller in a power factor mode directly connected through the regulator. This system showed no benefit and had greater reactive power response. Operation in the VAR mode or through a motor-operated control to introduce a large time constant similar to Mod-0 is recommended and will be pursued.

4.5.6.4 Margins

Gain settings on the power and speed control loops provide over 10 DB gain margin and 60 degree-phase margin. Component value drift is expected to be minimal and not effect margins. Filtering was simulated at .1 to .2 r/s off ideal to approximate drift in frequency.

4.6 CONCLUSIONS

The requirements of the SOW are met and voltage response is predicted to be within desired limits. An effective multiloop control of blade gain and generator excitation has been applied to Mod-1 consistent with the state of the art in wind turbine as well as more conventional prime mover systems. Power fluctuations are relatively large due to the randomness of the wind and large blade gain but within reason and not predicted to be objectionable. Active control of excitation to improve damping is a cost-effective approach on a machine the size of the Mod-1 and it is utilized instead of a loss-type device. In any event, some form of damping augmentation is necessary for satisfactory performance.

SECTION 5

MECHANICAL SUBASSEMBLIES DESIGN

SECTION 5

MECHANICAL SUBASSEMBLIES DESIGN

5.1 BLADE

The Mod 1 WTG incorporates two blades in its rotor system, each of which is mounted to the hub via a pitch bearing and is capable of being controlled collectively in pitch by the pitch control mechanism.

5.1.1 REQUIREMENTS

Design requirements on the blade include the following:

Rotor Diameter	200 feet nominal
Blade Material	Steel with foam supported Trailing edge
Design Life	30 years
Weight and CG	20,000 lbs each; $\pm$1% variation between blades Chordwise CG: $\leq$ 35% chord
Sealing and Corrosion Protection	Spar Sealed Trailing edge - No cracks, openings Primer - all over Paint - outside (white and orange per schedule) Dissimilar metal protection required where applicable
Balancing Weights	Tip weights: 40 lb. increments to 500 lb. max. Location: Tip - either side quarter chord line Static Balance: $\leq$ 467 ft-lbs
Lightning	Provide conductive path to hub
Environment	Temp: -31°F to 120°F Other: snow, rain, hail, sand, dust, salt spray
Damage Tolerance Design	Multi-load path structure where economically feasible
Natural Frequencies	With blade cantilevered: 1st Flap: 1.17-1.45 Hz (2P-2.5P) 1st Chord: 2.80-2.98 Hz (4.8P-5.1P) 1st Torsion: $>$ 17.5 Hz (30P)
Twist	11°
Instrumentation	Monitor strains at max. stress points Obtain bending moment data Redundancy on inaccessible gages Internal wiring where possible Life: 5 years

Surface Condition	Upper surface: 125 max. microinches RMS Elsewhere: 150 ± 50 microinches RMS Waviness: per specified schedule
Lifting, Handling and Shipping	Provide for lift in horizontal attitude Handling: 4 attitude positions Shipping: Rail and highway
Loads	Fatigue, gust, emergency shutdown-overspeed, hurricane Detail definition: Para. 5.1.4.1
Stability	1.5% modal damping Detail definition: Para. 5.1.4.3

5.1.2 DESCRIPTION

The Mod 1 blade is 97.5 feet long, with a tapered planform and thickness. It utilizes a NACA 44XX series airfoil with a thickness ratio varying from 10% at the tip to 33% at the root, with an all steel hollow spar as prime load carrier. A description of the subassemblies of the blade follows.

5.1.2.1 Geometry

The overall blade geometry is shown in Figure 5.1-1. The blade is 1169.3 inches long, which includes the 81.3-inch transition section. The blade planform is tapered with a chord of 33.8 inches at the tip to a chord of 134.8 inches at Station 212. From Station 212 inboard to the blade/transition junction at Station 121, the trailing edge fairs to zero, resulting in a spar-only chord of 72 inches. From this point inboard, the transition section circularizes the spar to the 59.25-inch diameter bolt circle at Station 40.7. The blade thickness varies from 48.3 inches at Station 121 to 3.38 inches at the tip (Station 1210). The thickness to chord ratio (T/C) from the root to the tip is linear and equals .026/10% span. Blade twist is 11° from root to tip with a linear twist angle change versus span. When mounted, the 75% span section is the blade pitch angle reference with respect to the hub and pitch change mechanism.

The blade is assembled in six main sections each approximately 180 inches long. The spar welds are located at five station locations as are the trailing edge section splices. The transition section is welded to the spar at Station 121 and provides the blade continuity to the interface with the hub at Station 40.7.

5.1.2.2 Spar

The spar is a hollow, single cell, steel structure running continuously the entire length of the blade and is the major load carrying member. It is fabricated from A533 Grade B, Class 2 high strength, low carbon steel. A sketch of the spar is shown in Figure 5.1-2. The shape of the spar conforms to the NACA 44XX series airfoil from the leading edge rearward to the point where the trailing edge tie is effected. Thus, its shape varies from root to tip as the airfoil thickness varies from a T/C of 0.34 to a T/C of 0.10. From the spar leading edge to its trailing edge, its width is 50% of the local chord.

The spar consists of an upper and lower panel in each of six sections -- a total

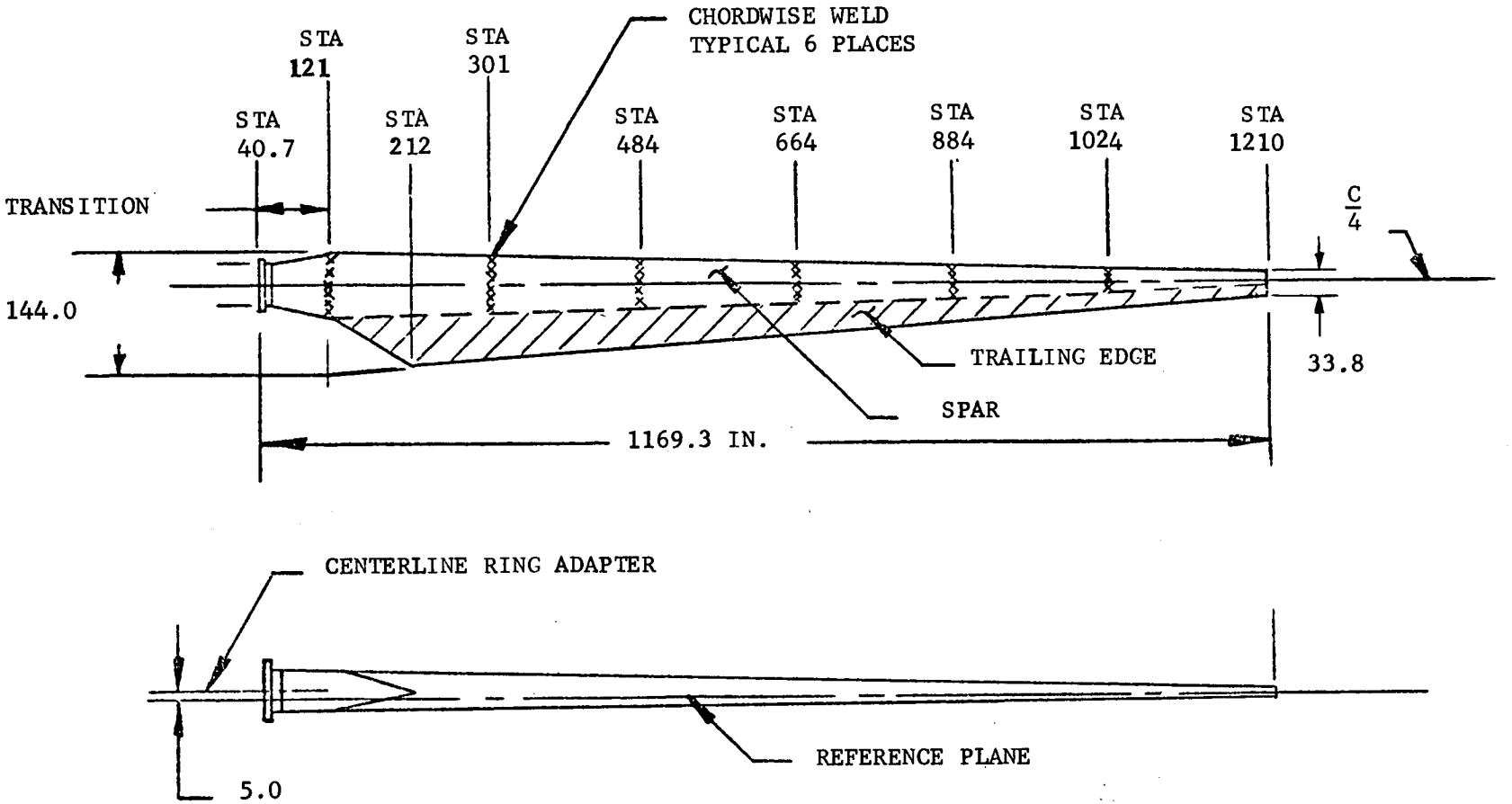

Figure 5.1-1 Blade Geometry

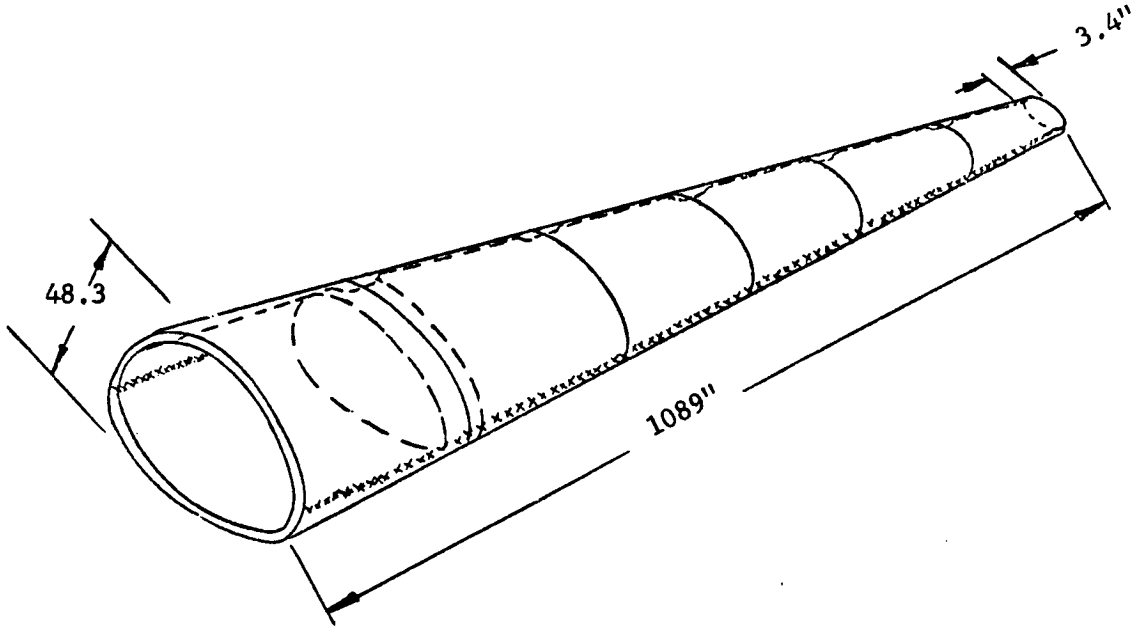

Figure 5.1-2. Spar Configuration

of 12 pieces. Each of the sections is approximately 180 inches long. The upper panels are joined to each other by means of chordwise welds as are the lower panels. Each half -- approximately 90-3/4 feet long -- is then welded spanwise at the leading and trailing edges. The spanwise welds are located close to the section flapwise neutral axis to minimize stress due to flap bending. The chordwise welds in the lower panels are subject to compressive stresses and consist of a double Vee weld ground smooth. The upper chord welds are in an alternating tension stress field and also consist of double Vees with the welds ground smooth. In addition, to minimize weight, the upper panels are machined thinner between weld stations, thereby generating lands of thicker material at the weld joints. The thickness of the two halves of the spar vary as shown in Figure 5.1-3.

Between Station 1144 and the tip, a pocket is formed in the spar for the installation of tip weight. Weights are located in this area to compensate for blade-to-blade static moment unbalance and for dynamic tuning. The tip weight installations are discussed in Paragraph 5.1.2.6.

At Station 121, the spar and transition section generate a change in angle which induces radial loads. A bulkhead is located on the blade side of this junction at Station 123.5 to react these kick loads. The bulkhead is fabricated from A533, Grade B, Class 2 steel and is welded to the land on the tension side of Station 121 and to the 0.37-inch thick panel on the compression side.

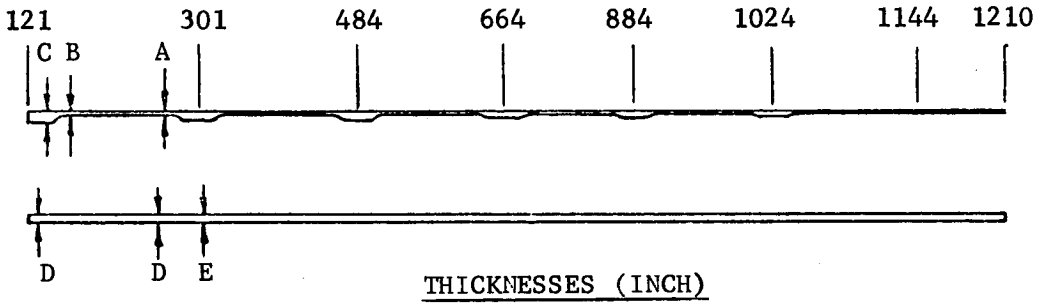

THICKNESSES (INCH)

Station	A	B	C	D	E
121	-	0.47	1.25	0.37	0.37
301	0.39	0.39	0.74	0.37	0.31
484	0.39	0.38	0.74	0.31	0.31
664	0.31	0.31	0.60	0.31	0.31
844	0.19	0.19	0.40	0.31	0.31
1024	0.19	0.19	0.40	0.31	0.25
1144	0.19	0.19	0.19	0.25	0.19

Figure 5.1-3. Spar Thickness Variation

5.1.2.3 Trailing Edge

The trailing edge consists of that portion of the blade which is aft of the spar. A sketch of a section of the trailing edge is shown in Figure 5.1-4. The interior of the trailing edge consists of four blocks of preformed foam with densities varying as shown in Figure 5.1-4. Each block is bonded to the other and to the .024-inch thick, 301 stainless steel skins with EC2216 (3M) adhesive. The foam-in-place foam is used adjacent to the spar to provide a continuous adherend joint between the interior foam and the spar. The structural continuity of the skin of the trailing edge is maintained by a spanwise splice to the spar. The splice material is .024-inch, 301 stainless steel with EC2216 adhesive used to bond it in place.

The trailing edge sections are the same span as the spar section to which they are joined. Chordwise splice plates are fastened mechanically at the T.E. (trailing edge) closure and run forward chordwise, around the leading edge of the blade, returning to the T.E. closure on the opposite side. Ten of these chordwise splice plates are bonded to the trailing edge sections and the spar to generate a redundant load path for the trailing edge sections in the event that a failure occurs in the T.E./spar attachment. The rearmost portion of the trailing edge is closed with a .024 Vee-shaped strip bonded to the upper and lower surfaces to close off the structure, and to prevent the entrance of moisture. Thin doublers are bonded and sealed over the spanwise splices for the same reason.

5.1.2.4 Transition

The transition section provides the structural link between the blade spar at the root end at Station 121 and the blade/hub interface at Station 40.7. A sketch of the transition section is shown in Figure 5.1-5. It consists of two A533, Grade B, Class 2 steel panels welded together near the flapwise neutral axis to minimize fatigue stress at the weld and an adapter ring. The upper half thickness tapers from 0.62 inch at the adapter ring to 0.47 inch at Station 121. The weld at both the adapter ring and at Station 121 is a double Vee with both weld surfaces ground smooth.

The adapter ring is a A508, Class 2 steel forging which is welded to the transition section at Station 50.98, and terminates with a flange at the blade/hub interface (Station 40.7). A sketch of the adapter ring is shown in Figure 5.1-6. An integral flange located near the junction with the transition section provides a surface for attachment of the bulkhead at Station 50. This bulkhead reacts the kick loads resulting from the angle change between the ring and the transition as well as providing a weather seal for the spar. In addition, the instrumentation connectors and pressure relief valves are mounted to the bulkhead. The bulkhead is removable to access the spar portion of the blade.

The ring increases in thickness toward the flange to react the moment resulting from the bolted attachment eccentricity. The flange is 2½ inches thick and contains fifty-six 1.31-inch diameter holes equally spaced on a 59.25-inch bolt circle.

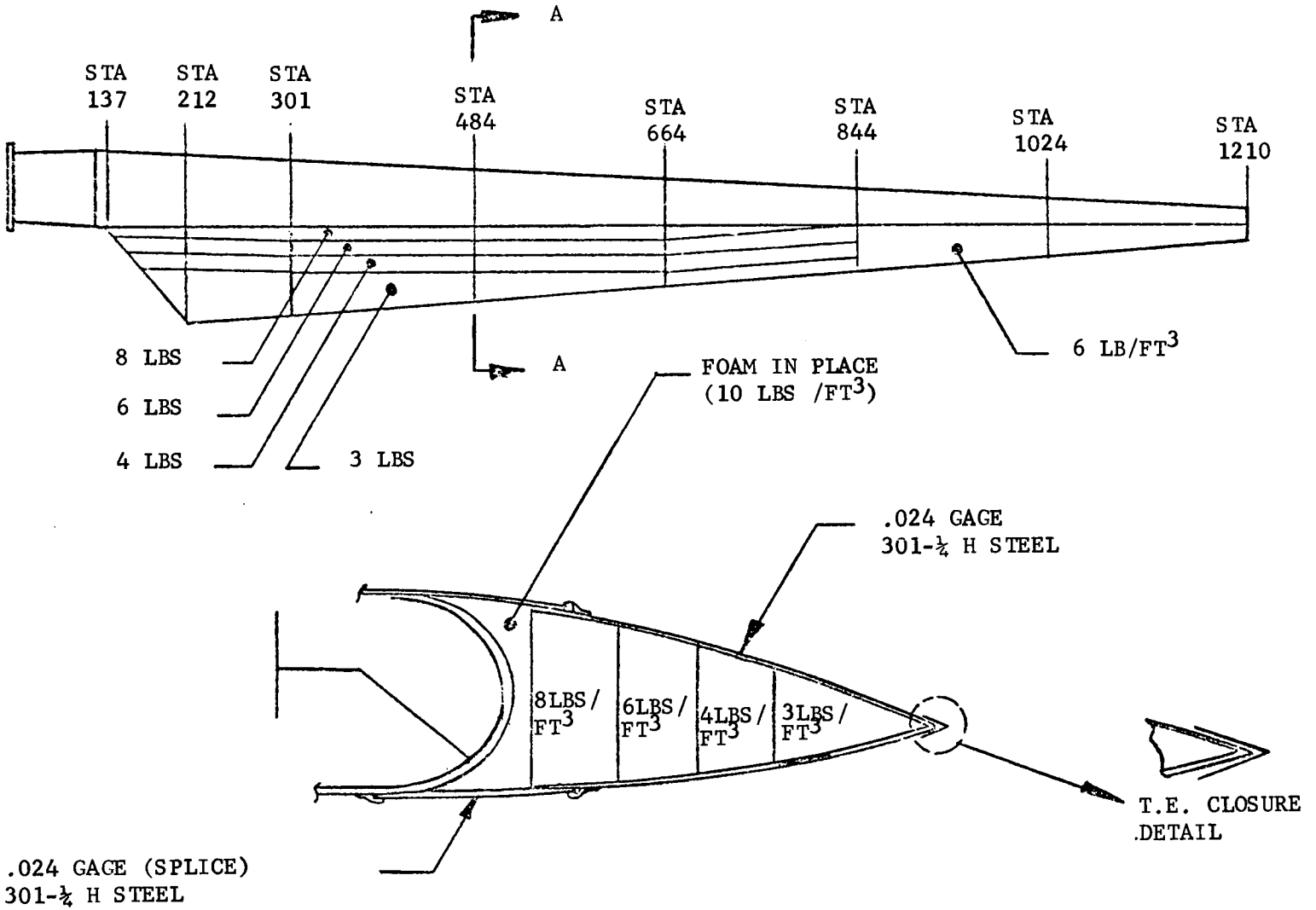

SECTION A-A

Figure 5.1-4 Trailing Edge

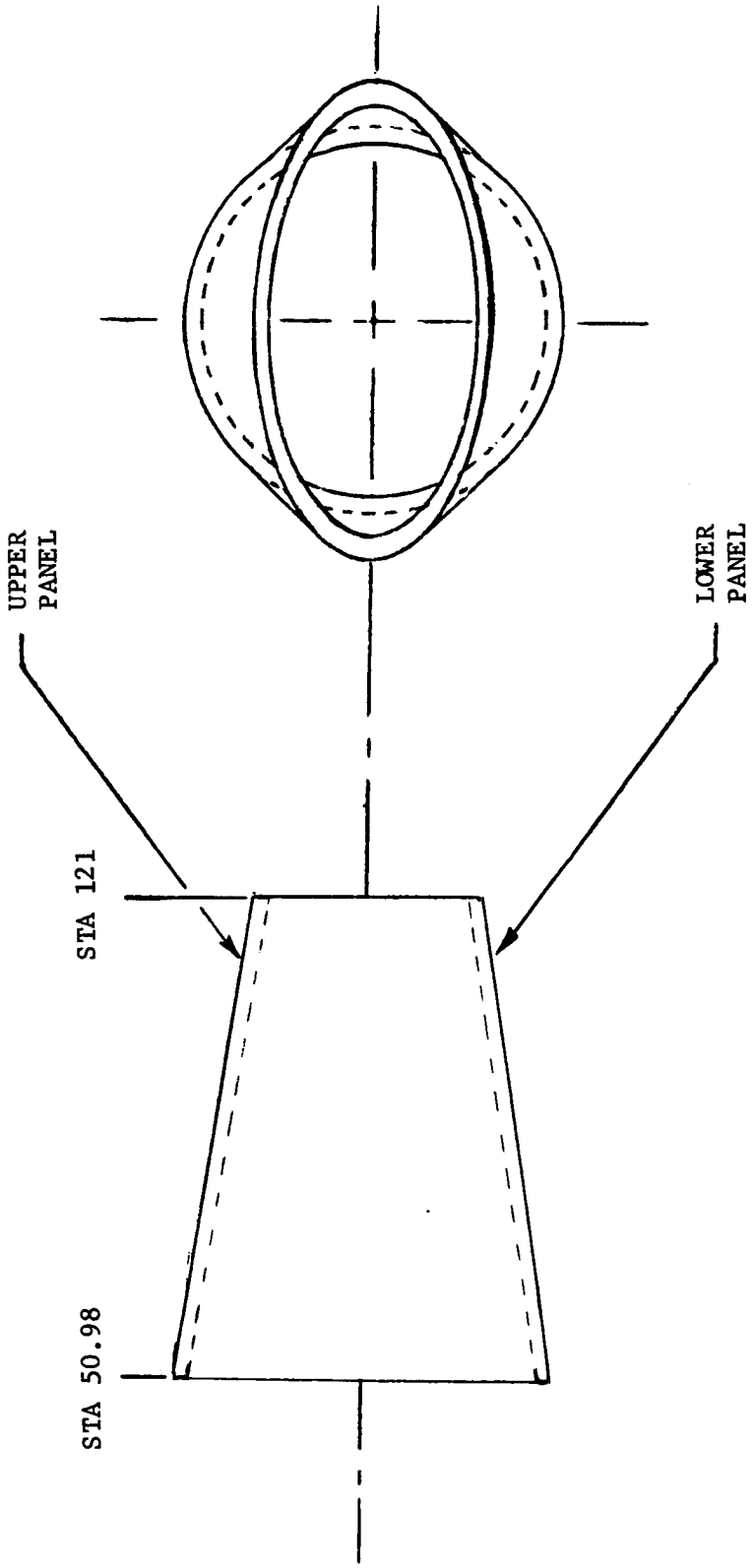

Figure 5.1-5 Transition Section

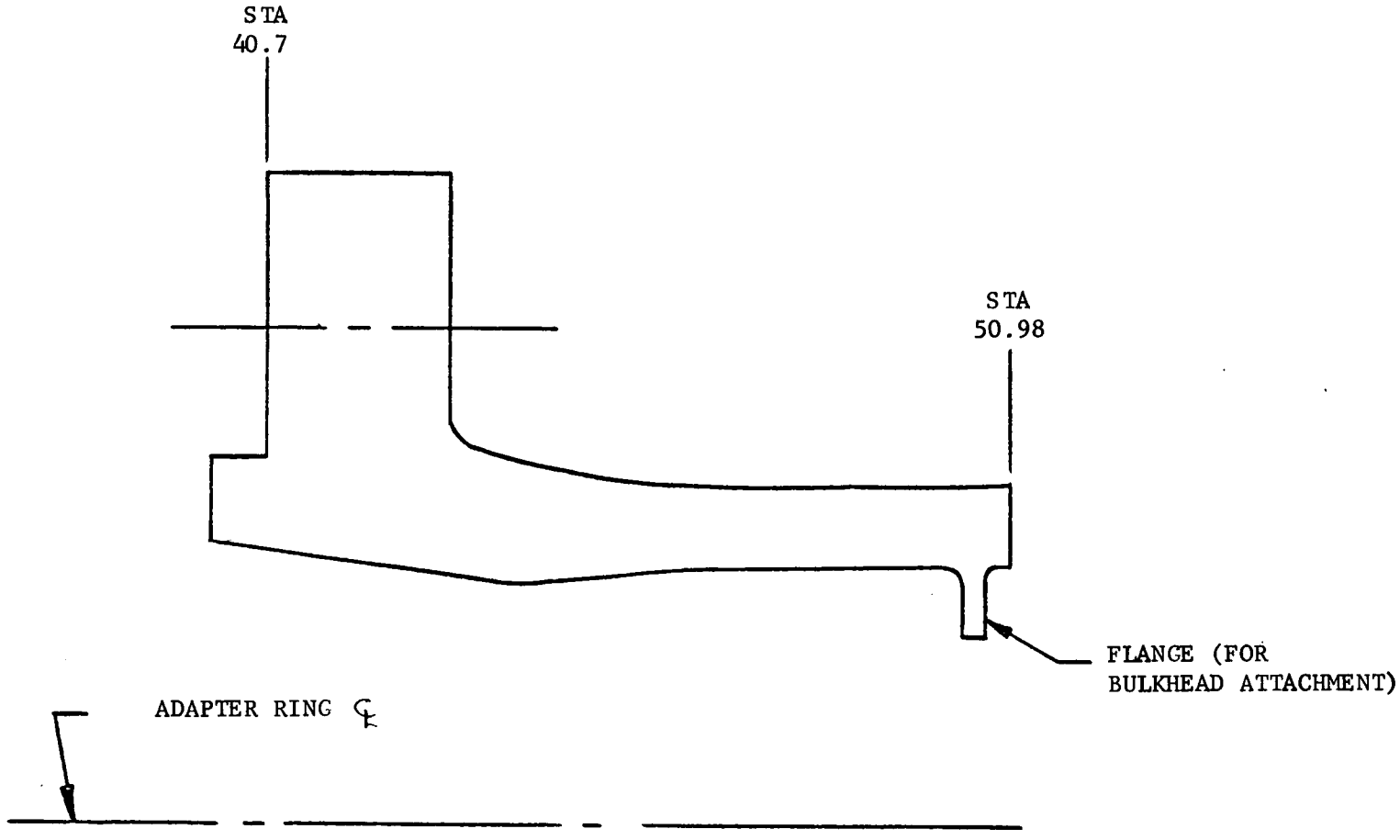

Figure 5.1-6 Adapter Ring

5.1.2.5 Tip Weights

Tip weights are installed as required in a pocket on the outboard end of the spar between Stations 1144 and 1210. Figure 5.1-7 is a sketch showing the installation of the tip weights.

For variances in blade-to-blade weight, provisions have been made for installing up to 60 pounds of tip weights. Two pockets are available for the installation of tip weights to tune flap and chord frequencies, as well as to provide some measure of chordwise CG control. These points are 4 inches forward and 4 inches aft of the 1/4 chord line and will retain up to 500 pounds in increments of 40 pounds. All blade tip weights are ASTM B23, No. 8. The pocket is protected from the environment by a cover with seal; the cover is attached to the blade with bolts.

5.1.2.6 Instrumentation

Engineering instrumentation for the blade is divided into two groups:

1. 28 Strain gages wired into 4-leg bridges to obtain bending moments

2. 28 Strain gages, either single axis or rosettes, for monitoring maximum stress at critical locations

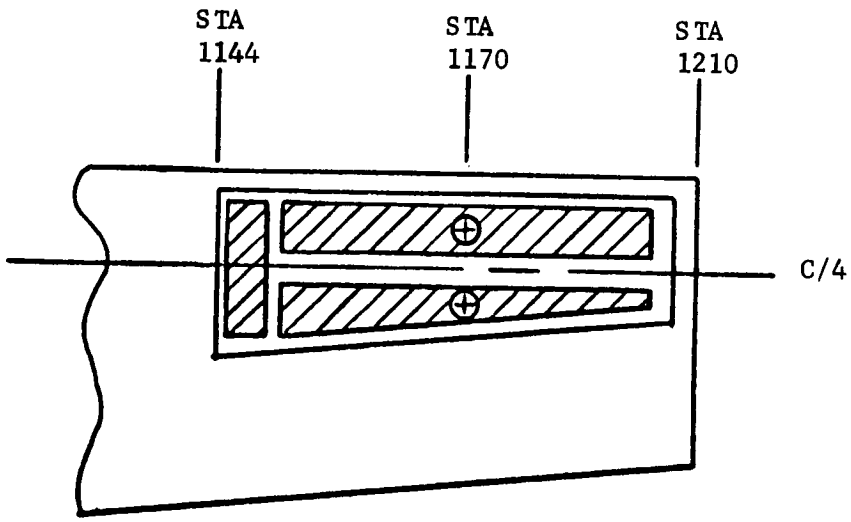

Figure 5.1-7. Tip Weight Installation

For bending moment gages in the first group, twenty-eight gages are planned. These will be wired into two 4-leg bridges for flap and chord moment determination for each of 3 locations -- Station 907.5 (75% span), Station 469 (39% span), and Station 120 (10% span). At Station 907.5, one set of gages is inaccessible, thereby requiring triple redundancy. The basic gages require 48 wires with 8 additional wires required for the redundancy. The bending gage wires will terminate in multiple pin potted connectors on the bulkhead at Station 50. The redundant wires will also terminate at the bulkhead with identifying numbers to be wired in if necessary.

The twenty-eight gages planned for monitoring the critical stress areas are noted on Table 5.1-1. Eighty-four wires are required (including the lead wire compensating leads), and these will terminate in additional connectors mounted to the same bulkhead as the bending gages.

Table 5.1-1. Critical Stress Instrumentation

Station	%C (LOC)	Type	Bridge/Wires	Purpose
844	56(U)	Axial	3 wires	Max. T.E. σ - skin
669	39(U)	Axial	3 wires	Max. spar σ
669	39(U)	Axial	3 wires	Redundant gage
664	39(U)	Axial	3 wires	Max. spar σ - weld
664	39(U)	Axial	3 wires	Redundant gage
649	39(U)	Rosette	9 wires	Max. spar σ
484	39(U)	Axial	3 wires	Max. spar σ - weld
469	39(U)	Rosette	9 wires	Max. spar σ
316	56(U)	Axial	3 wires	Max. T.E. σ - skin
301	37(U)	Axial	3 wires	Max. spar σ - weld
286	37(U)	Rosette	9 wires	Max. spar σ
120		Axial	3 wires	Max. spar σ - weld
120		Axial	3 wires	Redundant gage
106		Rosette	9 wires	Max. spar σ
101		Rosette	9 wires	Redundant gage
44	Intfce. Flange	Rosette	9 wires	Max. flange σ

Total: 84 wires

Notes: U = upper camber
Single axis gages require: 2 wires for gage
1 wire for lead compensation
Rosettes require: 6 wires for gage
3 wires for lead compensation

5.1.3 PERFORMANCE CHARACTERISTICS OF THE MOD 1 (BOEING) BLADE

5.1.3.1 Blade Airfoil and Geometry

A parametric study was carried out to provide a basis for the final blade design selection. At the time this was accomplished, weight of the Boeing blade had

been reduced to 18,000 pounds. It incorporated the 230XX series airfoil and captured 1,435 kW_e at 24.6 mph. This power was considerably less than 2,000 kW_e at 24.6 mph captured by the "Revised RFP" blade based on Lockheed's LS(1) design. The study was aimed at recovering as much performance as possible within the weight, frequency, life and other requirements.

A significant loss in performance could be attributed to the change in airfoil family section from LS(1) to the 230XX series which Boeing proposed because of ease of fabrication, i.e., the LS(1) has concave lower surfaces.

Evidence for this can be seen in the Baseline Column of Figure 5.1-8, where simply changing the airfoil family to 44 series and to LS(1) increases the captured power from 1435 kW_e to 1600 and 1650 kW_e, respectively.

It was reasoned that, to a certain extent, this loss in lift capability could be compensated for by increasing the chord. This increase was accomplished for Configurations 1 and 2, where the chord was everywhere increased over the baseline by 10% and 20%, respectively. The section thickness was held constant and consequently the thickness ratio decreased at the tip from 12% to 11% and 10%, respectively. Comparable changes occurred all along the blades (see the chart of Figure 5.1-8). The impact of the increase in chord on the captured electric power at rated wind speed was to increase it from 1435 kW_e to 1575 kW_e for the 10% increase and to 1680 kW_e for the 20% increase (all with the 230XX airfoil). Fourteen other combinations of geometrical changes were studied, but, of these, only three resulted in performance superior to Configuration 2 (chord increased by 20%). These were Configurations 6, 7 and 11. All of these cases involved reductions in the absolute thickness, usually an aerodynamically fruitful approach. However, the stresses on these thinner sections were unacceptable and therefore configuration 2 geometry was selected for the final design.

The effect of airfoil section was then analyzed by calculating the performance of Configuration 2 with 44XX and LS(1) series airfoils. The results show an increase from 1,680 kW_e for the 230XX series to 1,818 kW_e for the 44XX series and 1,871 kW_e for the LS(1). Fabrication of the 44XX series presented no problems, while forming the recurved lower surface of the LS(1) family projected some difficulties. Because Configuration 2 with the 44XX series airfoil family exceeded the specification performance requirement of capturing 1,800 kW_e at 24.6 mph, the 44XX series was selected for the final blade design. The aerodynamic performance of this configuration is shown in Figure 5.1-9.

Subsequent refinements in the computation for this configuration provide estimated power capture of 1,885 kW_e, but none of these estimates include the effects of compressibility. The tip Mach number of the Mod 1 at rated speed will be in the neighborhood of M = .33. Normally one does not anticipate compressibility effects at such low Mach numbers; however, because of the high operating lift coefficients, the outer sections of the blade may be reaching their critical speed. Approximate theoretical consideration indicates they do. If they do reach this speed, performance will be lost. In addition, there is evidence that high lift coefficient performance is degraded even before the attainment of the critical speed because

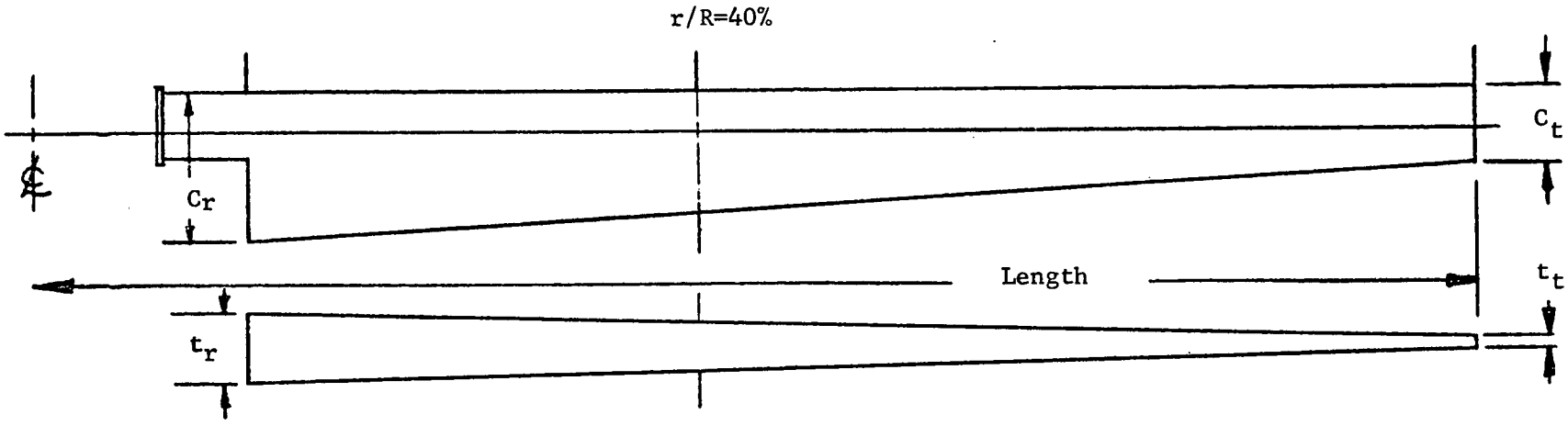

Geometry	Base-line	1	2	3	4	5	6	7	8	9	10	11	12	13	14	15	16
	Configurations																
Length	1210"	1210	1210	1210	1210	1198	1210	1210	1198	1210	1210	1210	1186	1164	1210	1210	1248
C_r	120"	132	144	132	132	132	144	114	144	120	132	144	144	144	120	120	120
C_t	28.2"	31	33.8	31	31	31	33.8	33.8	33.8	28.2	31	33.8	33.8	33.8	33.8	39.5	28.2
t_r	48.0"	48	48	48	48	48	48	48	48	48	45.6	43.9	43.9	43.9	48	48	48.0
t_t	3.38"	3.38	3.38	3.38	3.38	3.38	3.38	3.38	3.38	3.38	3.21	3.09	3.09	3.09	3.38	3.38	3.38
t/c	Lin. Ratio	Lin. Ratio	Lin. Ratio	Step	Step	Step	Step	Step	Step	Step	Lin. Ratio	Lin. Ratio	Lin. Ratio	Lin. Ratio	Lin. Ratio	Lin. Ratio	Lin. Ratio
t r/R=4	27.42"	27.42	27.42	26	24.7	24.7	26	24.7	24.7	24.7	26.05	25.09	25.09	25.09	27.42	27.42	27.42
t/c@40%	.307																.307
Power (KW_e) Series																	
230XX	1435	1575	1680	1602	1604	1557	1699	1719	1668	1487	1621	1724	1625	1533	1476	1516	
44XX	1600		1818				1831	1845									1724
LS(1)	1650		1871				1889	1905									

Figure 5.1-8 Blade Parametric Study

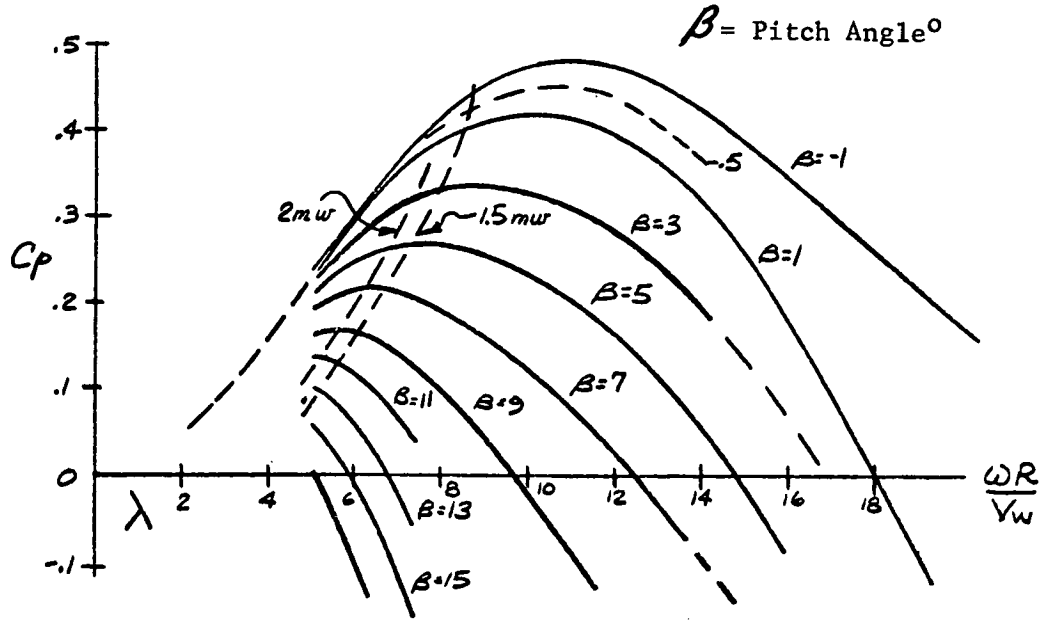

Figure 5.1-9. Wind Turbine Performance

of local steepening of the adverse pressure gradient and consequent earlier separation. Since our analysis does not include these effects, it was considered prudent not to anticipate performance above the initially estimated 1818 kWe.

5.1.3.2 Pre-Cone Angle

During the early stages of the program, a pre-cone angle of 12° was established for the rotor system primarily to provide blade tip/tower clearance for the WTG baseline fiberglass blades. With the introduction of the Boeing steel blade into the program the tip clearance increased. The pre-cone angle was then lowered to 9° to reduce the blade mean flap bending moment to permit weight reductions in the blade.

When the pre-cone angle was reduced from 12° to 9°, performance of the rotor was re-estimated. Two effects were noted. First, a minor improvement in the aerodynamic efficiency near rated wind velocity because of the reduced pre-cone angle. The second effect is due to the increased rotor radius from 98.63 to 99.59 feet. This 1% increase in radius causes a 1% increase in λ with a small efficiency rise and a 2% increase in power simply through the increased area. A further improvement is also effected through the increase in generator and transmission efficiency due to improved electromechanical efficiency attained at higher rotor power. The overall effect is an increase in power capture from 1,885 to 1,937 kW_e, a 2.8% improvement due to cone angle alone.

The parametric study was not repeated following the cone angle change since the trend results are valid for both angles.

5.1.4 ANALYSES

The GETSS computer program, described in Paragraph 3.2, is used to determine blade loads. The stresses associated with these loads, along with the physical properties of the blade are computed by Boeing. General Electric has, however, made independent checks on the Boeing calculations. Blade aeroelastic stability has been verified using the GE computer code GETSTAB, which is described in Paragraph 5.1.4.3.

5.1.4.1 Loads and Deflections

Blade loads and deflections have been calculated for the conditions which appear in Table 3-1 and Appendix B. The blades, like the rest of the WTG structure, are designed for infinite life at the 35 mph operating condition. Dispersion factors, which are based on Mod-0 data, are applied to the steady-state blade cyclid loads calculated by the GETSS program at 35 mph. These dispersion factors are: 1.9 for flap bending moments and 1.5 for chord bending moments. Figure 5.1-10 contains the undispersed flap and chord cyclic bending moments at the 35 mph condition. The fatigue design is based on these cyclic loads times the appropriate dispersion factor. When calculating stresses, the factors are not applied to the mean (steady) loads since these result primarily from steady

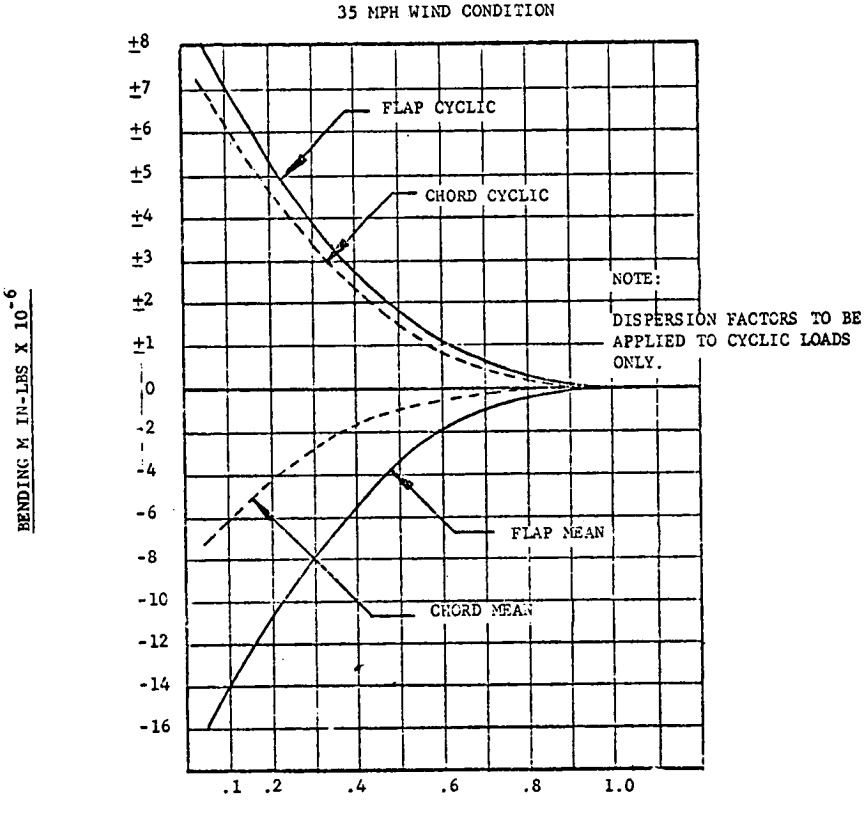

Figure 5.1-10 Blade Fatigue Loads

airloads and centrifugal force effects. The most critical of the limit loads was found to occur at the overspeed (emergency feather) condition. The peak loads associated with this condition are shown in Figure 5.1-11. A maximum blade tip deflection, 6.0 feet toward the tower, also occurred at this condition. The associated blade/tower clearance is 10 inches. The sign convention for blade loads is shown in Figure 5.1-12.

5.1.4.2 Stress, Weights, Margins of Safety

The strength philosophy adopted for the Mod-1 blade is predicated on the requirement that it will survive for 30 years. During this period it is expected to experience 4.5×10^8 stress cycles. Most of these cycles are low stress and repetitive in nature; however, a few loads occur on an infrequent basis which produce stress levels that are permitted to exceed those of the fatigue loading. The loads that produce these types of stresses are:

1. Severe positive gust - 35 mph to 50 mph
2. Severe negative gust - 35 mph to 20 mph
3. Hurricane condition - 120 mph @ 30 feet
4. Emergency feather - overspeed @ 39 rpm

Of the above four conditions, the emergency feather - overspeed is the most critical.

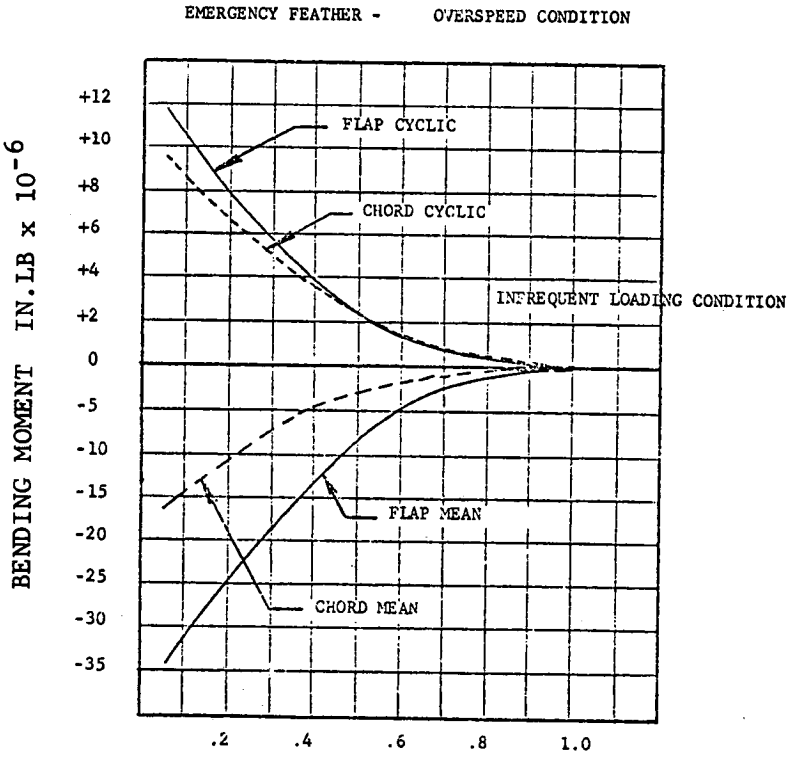

Figure 5.1-11. Peak Loads at Emergency Feather

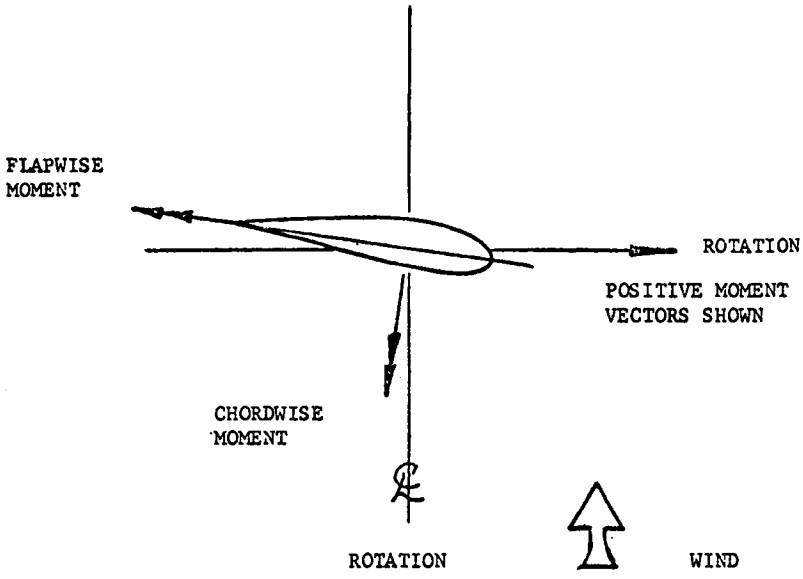

Figure 5.1-12. Sign Convention for Loads

The stresses resulting from the fatigue condition loads are limited to the crack growth threshold. With this approach, coupled with the NDT flaw acceptance criteria, no flaws will grow which are sufficiently small to be acceptable, thereby insuring 30 years operational life. The allowable stress range for the different category welds are shown in Table 5.1-2.

Table 5.1-2. Allowable Fatigue Stress Range*

Category	Allow Stress Range (ksi)
A' Base Metal (125 Finish)	28.6
A Base Metal (As Rolled)	24.2
B Ground Weld	16.0
C Fillet Weld	12.0
E Closeout Weld	5.0

*Stress Range = /S max - S min/

For the infrequent loading conditions (maximum positive and negative gusts, emergency feather, overspeed and the hurricane conditions), the allowable stress level is the proportional limit. In the case of the A533 steel, this is $.9F_{cy}$ or $.9F_{ty}$. In addition, there is a buckling factor of 1.25 which is used with the applied compression stress to account for the usual uncertainties in accurately predicting allowable compressive buckling stresses.

For the fatigue condition, no elastic buckling is allowed. The factor to be applied to the fatigue stresses to insure this is 1.44.

As of August 1, 1978, the blade design report had not been received from Boeing; therefore, the stress data presented at the FDR is included here. A summary of the induced stresses in the spar with margins of safety are shown in Table 5.1-3 for the fatigue condition and in Table 5.1-4 for the infrequent emergency feather condition. Table 5.1-5 presents the summary of the Trailing Edge Skin stresses.

In order to be assured that the blade ring adapter which retains the blade to the hub is structurally adequate, GE performed a finite element analysis of the ring. A three-dimensional model consisting of 765 elements and 1185 nodes was developed and the SAP V finite element computer program was used for the numerical determination. The mathematical model is shown in Figure 5.1-13, and boundary conditions and stress contours for the fatigue care are shown in Figure 5.1-14. As expected, the peak stresses in each case occurred at the root of the elliptical transition section on the outer surface of the ring, immediately adjacent to the bolt head location. For the fatigue case, the peak principal tensile (cyclic) stress was found to be 20,200 psi. For fatigue and emergency feather case, margins of safety were found to be +.416 and +.26, respectively. Also, the preload applied by the attachment bolts was not exceeded. The design on the WTG blade adapter ring is adequate.

The blade loads have been calculated with an extrapolated blade weight of 20,000 pounds. Current blade weight is 19,618 pounds (plus tip weights). A distribution of the blade weight is shown on Figure 5.1-15.

5.1.4.3 Dynamics

The final blade design will meet the following frequency and chordwise CG requirements:

1. 1st Flap Natural Frequency 1.17 - 1.45 Hz
2. 1st Chord Natural Frequency 2.80 - 2.98 Hz
3. 1st Torsion 17.5 Hz

(Above frequencies are for a Non-Rotating Cantilevered Blade)

The frequency requirements are to preclude resonant response and are based on

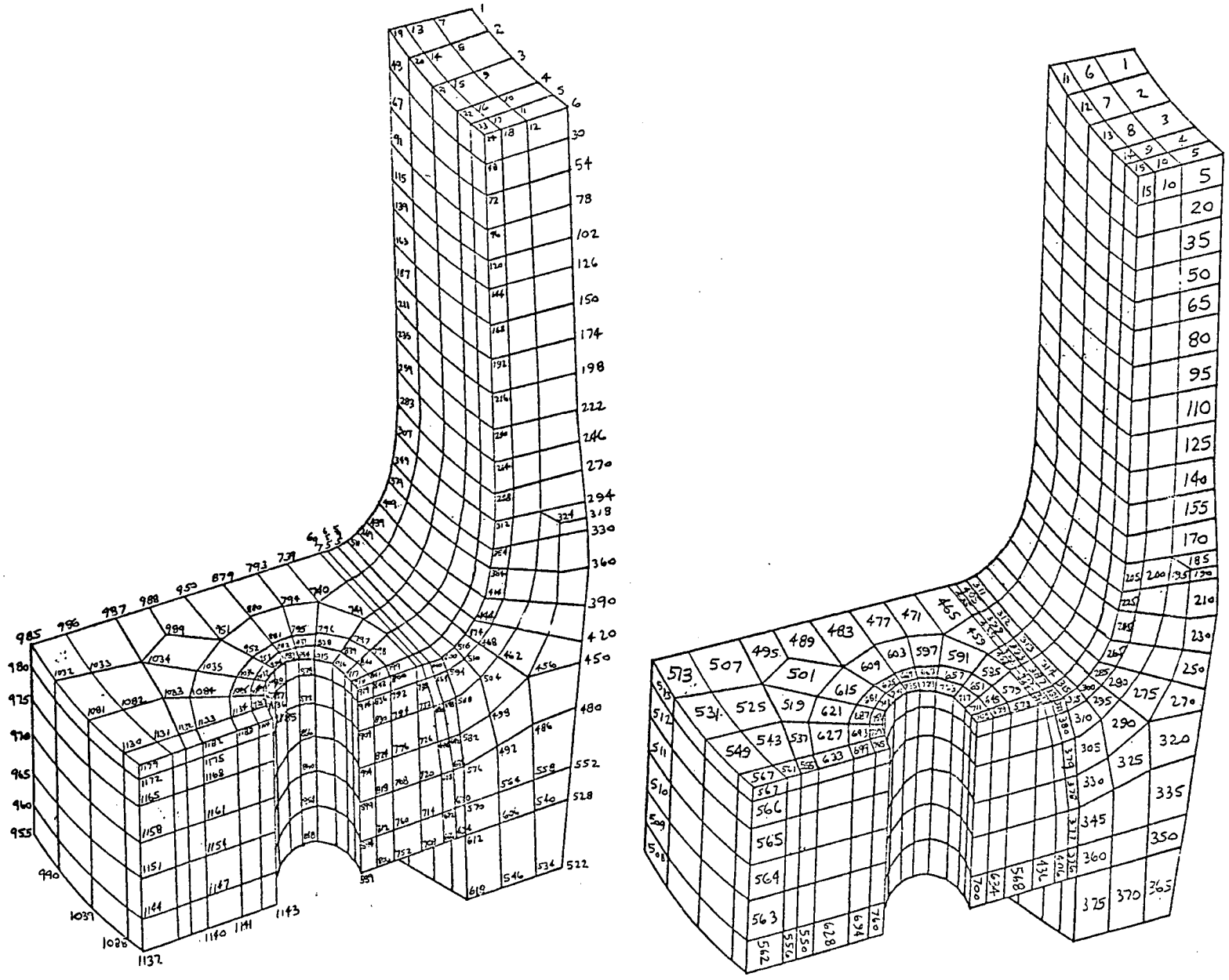

Figure 5.1-13. Finite Element Model of Blade Ring Adapter

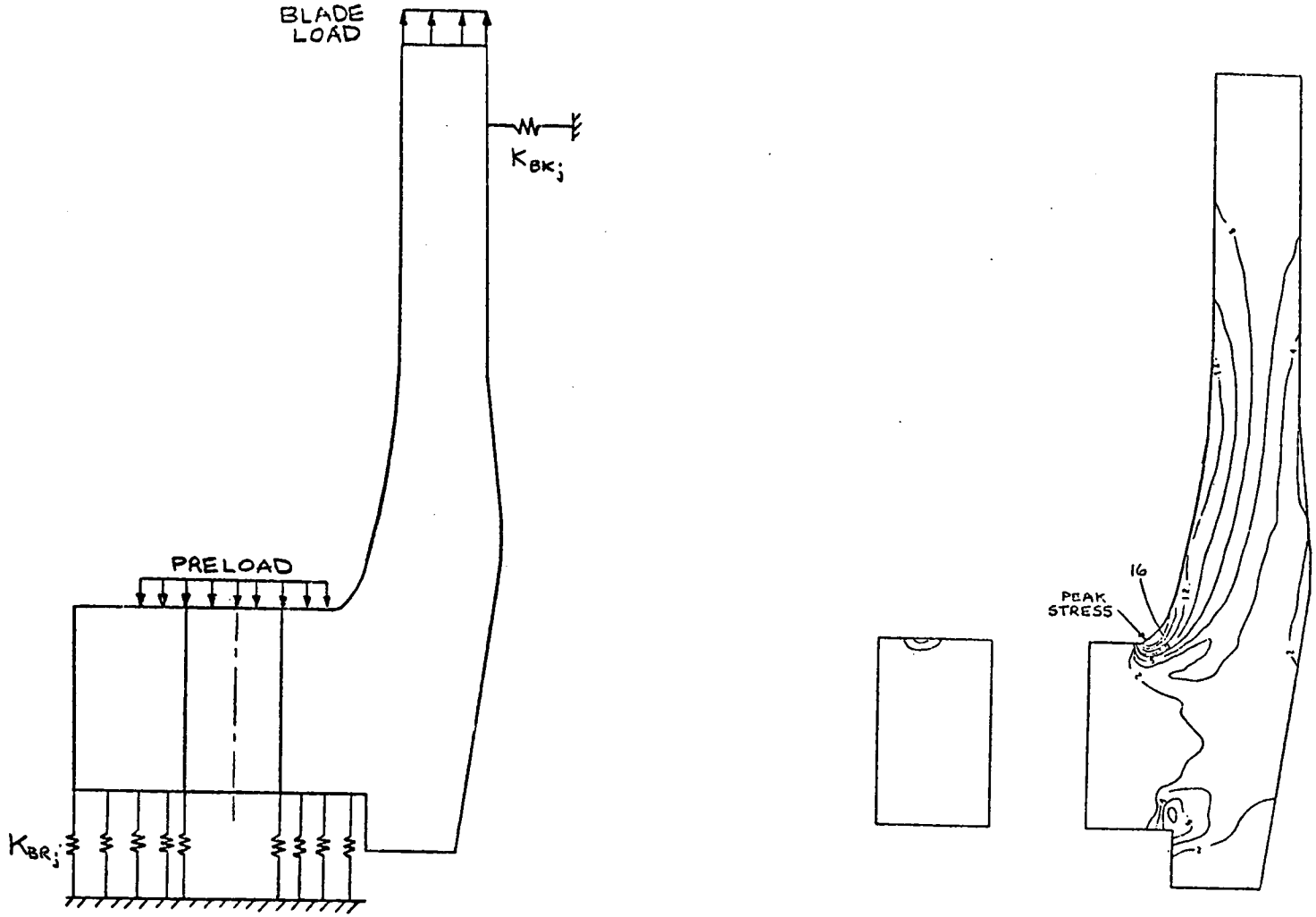

Figure 5.1-14 Boundary Conditions and Stress Contours

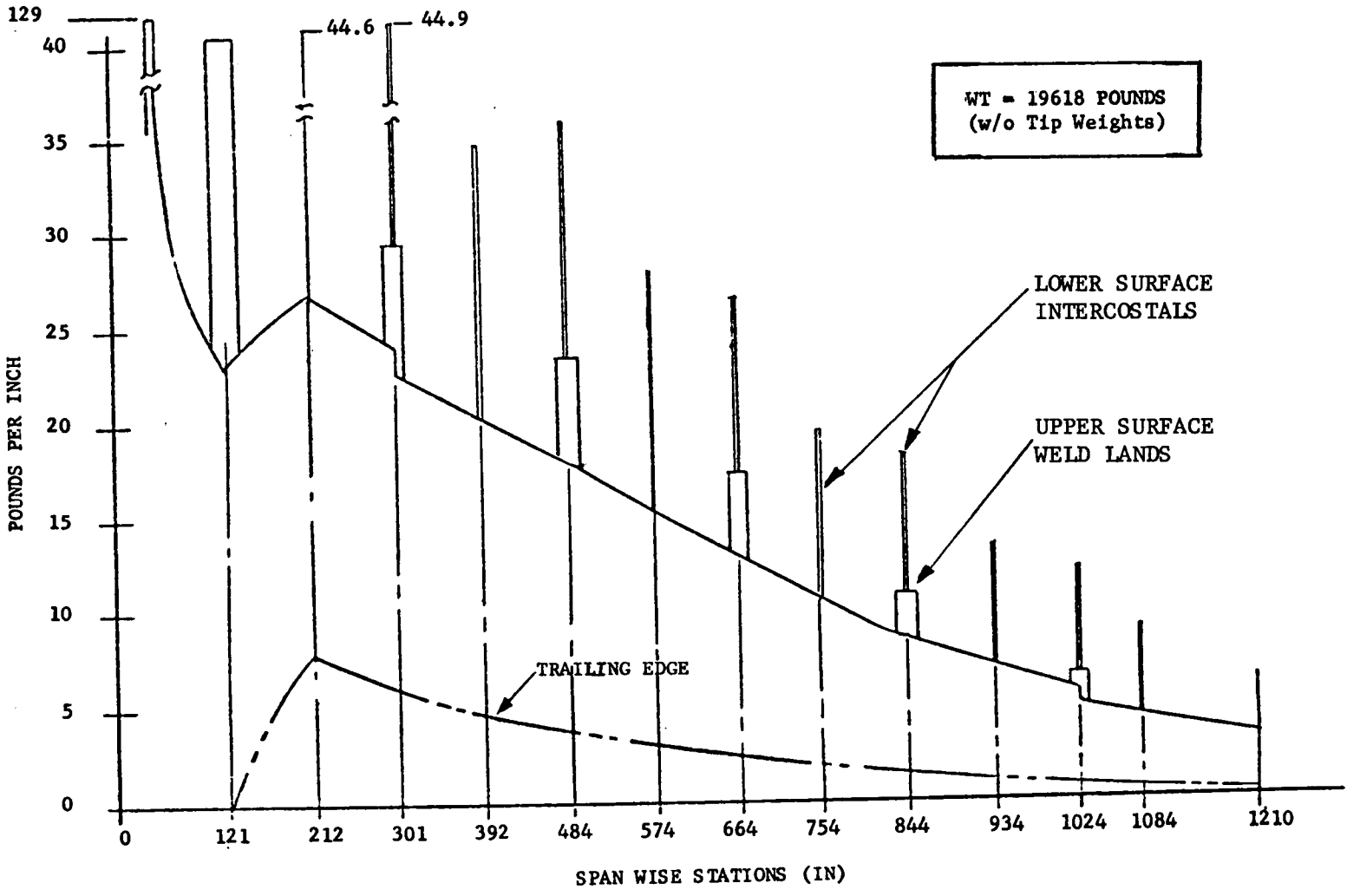

Figure 5.1-15 Blade Weight Distribution

Table 5.1-3. Stress Summary for the Fatigue Condition

Component	Drawing No. & Sheet	Area and/or Critical Location	Critical Load Condition	Failure Mode	Mat'l	Allowable Stress KSI	Calc. Stress KSI	M.S.
SPAR	276-10526	Upper Surface Basic Thickness						
	Sh. 9	Sta. 101.25	35 mph Wind	Fatigue	A533	F^*_{cyc}=28.6	27.7	.03
	10	121					26.5	.08
	11	301					26.7	.07
	12	484					27.0	.06
	13	664					27.2	.05
	14	844					20.7	.38
	15	1024					14.1	1.04
	15	1144					12.9	1.21
		Weld Land Sta. 50.98 --				F^*_{cyc}=16.0	14.2 --	.13 --
	10	121					10.2	.57
	11	301					14.3	.12
	12	484					14.2	.13
	13	664					14.2	.13
	14	844					11.3	.42
	15	1024					6.9	1.32
	Sh. 1	Longitudinal Weld	Intern. Press.	Skin Bending		F_{tp}=63	21.9	1.87

*F_{cyc} is Stress Range i.e. /S max - S min/

Table 5.1-4. Stress Summary for the Emergency Feather Condition

Component	Drawing No. & Sheet	Area and/or Critical Location	Critical Load Condition	Failure Mode	Mat'l	Allowable Stress KSI	Calc. Stress KSI	M.S.
SPAR	276-10526	Lower Surface						
	Sh. 2	Sta. 50.92	Emergency Feather	Buckling	A533	F_{crit}=63	19.8	2.17
	2	101.25				=63	40.7	.54
	3	121				=63	44.7	.41
	4	201				=50.5	49.4	.02
	5	484				=53.1	51.3	.04
	6	664				=55.9	51.0	.09
	7	844				=56.9	36.3	.57
	8	1024				=45.9	32.5	.41
	8	1144				=52.1	28.7	.81
		Upper Surface						
	Sh. 9	Sta. 50.98	Emergency Feather	Tension due to Bending	A533	F_{tp}=63.0	24.6	1.55
	9	101.25					52.2	.19
	10	121					47.7	.32
	11	301					52.6	.20
	12	484					54.6	.15
	13	664					58.7	.07
	14	884					58.5	.06
	15	1024					56.9	.24
	15	1144					42.7	.47

Table 5.1-5. Stress Summary on the Trailing Edge Skins

STATION	CONDITION	DIST. AFT LEADING EDGE	STRESS KSI	ALLOWABLE KSI	MARGIN OF SAFETY
301	35 MPH FATIGUE	73	27.9	28.6	.03
	EMERGENCY FEATHER	54 93	53.2 -13.2	62.1 -14.2	.17 .08
484	35 MPH FATIGUE	62.2	28.6	28.6	0
	EMERGENCY FEATHER	62.2 62.2	52.1 -11.8	62.1 -14.2	.19 .20
664	35 MPH FATIGUE	53.2	27.7	28.6	.03
	EMERGENCY FEATHER	40.7	55.6	62.1	.12
	120 MPH WIND	65.1	-13.4	-14.2	.06
844	35 MPH FATIGUE	35.7	24.3	28.6	.18
	EMERGENCY FEATHER	35.7	60.4	62.1	.03
	120 MPH WIND	40.7	-21.2	-23.3	.10
1024	35 MPH FATIGUE	24	14.3	28.6	1.0
	EMERGENCY FEATHER	24	22.8	62.1	1.12
	24.8 MPH WIND	24	-13.2	-23.3	.77

the sensitivity analyses described in Paragraph 3.3 and the NASA contract requirements. The chordwise CG requirement is to insure blade aeroelastic stability. Blade stability has been analyzed with the GETSTAB computer code which is described in the following paragraphs.

General Electric has developed a comprehensive rotor/tower aeroelastic stability analysis called GETSTAB. The program is capable of analyzing blade flap-lag pitch instability, classical flutter, divergence, whirl flutter, and other instabilities which may occur due to rotor/tower coupling. Blade elastic degrees of freedom are represented by fully-coupled, three-dimensional natural modes. The blades can have arbitrary twist, taper, and chordwise CG distributions along with any specified precone or prelag at the blade root. In addition, modes corresponding to general root boundary conditions, such as teetering wherein the motions of two separate blades are coupled, can be analyzed. Quasi-steady aerodynamic strip theory is used, incorporating the Theordorsen unsteady aerodynamic terms with C(k) = 1. Aerodynamic coefficients (C_L, C_D, C_M) are obtained from a table lookup as a function of angle of attack, and airloads are numerically integrated along the blade span. Tables corresponding to the airfoil characteristics at various radial stations may be input, thereby allowing for airfoil thickness taper distributions. Solutions are for perturbations from a trim condition and the use of stallable airfoil tables allows one to estimate the stability for a fully or partially stalled trim condition. The program can be used for isolated blade studies or for a two-bladed rotor coupled to a flexible tower, the latter being represented by general three-dimensional natural modes. The number of blade and tower modes can be varied to meet particular analysis needs and computer storage capabilities. The program is also capable of analyzing nonrotating blades.

The equations of motion are linearized and an eigenvalue solution is used to determine the stability of an isolated blade. Floquet theory is used to extract exponential decay rates for the coupled rotor/tower case because periodic coefficients arise for 2-bladed rotors.

The blade design has been analyzed for flap-lag-pitch instability and classical flutter. A typical plot of blade modal damping versus control system stiffness is shown in Figure 5.1-16. It is evident that there is ample margin of safety for the design control system stiffness of 120×10^6. The blade has been analyzed to be free of instability for the rpm operating envelope shown in Figure 5.1-17. The maximum rpm (52.5) is 1.5 times rated speed, although the maximum speed conservatively predicted at desynch is only 39 rpm, or 12% overspeed

5.1.5 TESTS

Three areas of testing have been planned for the Mod-1 blade. These are:

1. Engineering Development Tests. Tests performed on subelement structures to obtain early indication of design adequacy.

2. Blade Development Tests. Tests performed on full scale portions of the blade to ascertain structural adequacy. In most cases, the test data from these tests will be available after the final design is committed.

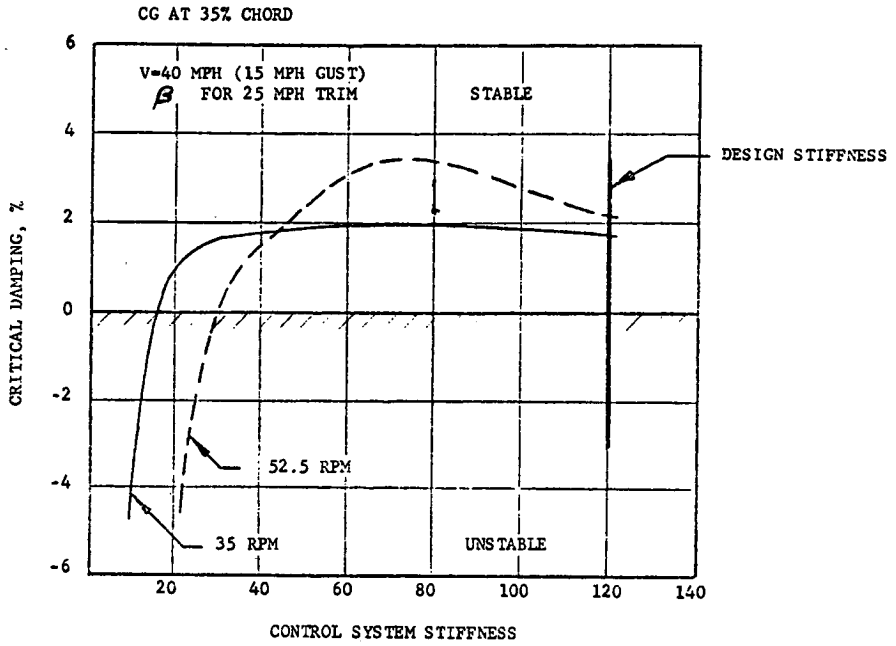

Figure 5.1-16. Blade Modal Damping vs. Control System Stiffness

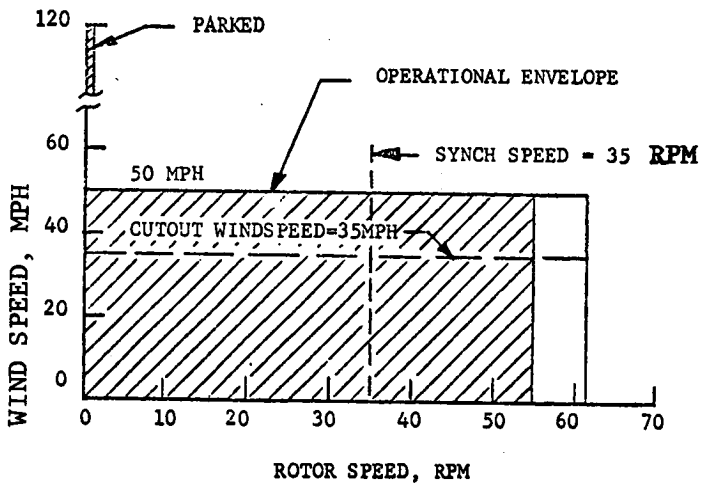

Figure 5.1-17 Operational Envelope Cleared for Stability

3. Blade Tests. Tests which will be performed on the completed blade to determine dynamic characteristics or basic property data such as elastic axis location, static moment, chrodwise CG locations, and stress and deflection data versus load.

These tests are discussed in the following paragraphs.

5.1.5.1 Engineering Development Tests

Subelement engineering tests were performed on trailing edge joint specimens to obtain data on the adhesive strength of the bonded joints. Twenty lap shear specimens for the stainless steel to stainless steel and the A533 steel to stainless steel joints were tested for static strength. Five tests each were run at room temperature and 140°F. Fatigue tests were performed on four specimens representing two bonded joints. Temperature and humidity were imposed during the testing which was run at 30 Hz. Duration of the test was 5×10^7 cycles. There were no failures.

5.1.5.2 Blade Development Tests

Development tests were performed on various size elements of the blade to establish:

1. Manufacturing methods, techniques and procedures

2. Static strength capability

3. Fatigue strength of welds and bonded joints

Forming, machining and welding techniques were initially established on a 4-foot section of the spar. The upper and lower panels were machined, formed and then checked with a template. The weld joint was then prepared and spanwise welds performed. This development test was completed successfully.

Next, four 8-foot long sections of the spar were machined and formed. Chordwise welds of the upper and lower panels were made. Each 16-foot panel was successfully fabricated, then the upper and lower panels were joined, with the proper twist induced. It was then instrumented, cantilevered off a fixture, and static tested. The area of interest in this test was the lower surface, critical in compression buckling.

Another specimen of the upper surface (including the weld lands with a length of base metal on either side) was formed, welded and coupons cut out across the weld joints for fatigue test. Six speciments were obtained including at least one with a weld repair and the others cut from areas determined by NDT to contain the most critical flaws. The test coupons were stressed for 1×10^8 cycles. There were no failures.

A fatigue test is also being run on a 6-foot section of the trailing edge attached to a simulated spar. The purpose of the test is to check the bonds within the trailing edge and the bond of the trailing edge to the spar. A steady plus a constant amplitude alternating load is being applied with the

spar loaded with its design bending moment at the section under test. The frequency of alternating load is 1 Hz resulting in 15 x 10^6 cycles in approximately 6 months.

5.1.5.3 Blade Tests

Tests planned for the completed blades include the following:

1. Weight and balance
2. Spanwise static moment
3. Chordwise CG location
4. Elastic axis determination
5. Static load tests including trailing edge bond verification.
6. Mode shapes, fundamental frequencies and structural damping measurements

The method of testing for each of the requirements listed are as follows:

1,2,&3. Weight (both blades)

The blade shall be weighed in a manner such that total weight, and the spanwise and chordwise centers of gravity can be determined. Two weighing devices can be attached to a fixture bolted to the hub, and one to a fixture bolted to the tip of the spar.

4. Elastic Axis (one blade)

To determine the elastic axis, the blade shall be rigidly fixed at the root, cantilevered in a horizontal position with the top of the airfoil up and the chord line at Station 844 horizontal. A fixture will be bolted to the tip of the spar in place of the lifting ring to apply the torsional loads. Deflection measurements shall be taken. Loads shall be applied in 20% increments. The structure shall not be flexure tested in either direction to more than 30% of the test requirement prior to the first test. The test shall be run three times in each direction.

5. Strain Gage Calibration (both blades) and Static Test (both blades)

The blade shall be rigidly fixed at the root as described above. A horizontal load of 5000 pounds shall be applied at the tip at the elastic center in increments of 10% of load. The direction of the load shall be toward the leading edge to cause a compressive stress in the leading edge. Deflection measurements shall be made at Stations 121, 301, 484, 664, 844, 1024 and 1210 at the leading edge. Deflection measurements shall also be taken at four points on the

bolting ring, two points in line with the load, and two points at right angles to the load application direction. Strain Measurements shall be made with the strain gages located on the blade in order to calibrate these gages.

With the blade in the same position, a vertical load down of 2400 pounds shall be applied at the tip at the elastic center and 5000 pounds at Station 844 in increments of 10% of the loads. Deflection measurements shall be made at Stations 121, 301, 484, 664, 844, 1024, and 1210 at the 25% chord and at the tip of the trailing edge. Deflection measurements shall also be taken at four points on the bolting ring, two points in line with the load, and two points at right angles to the load application direction. Strain measurements shall be made as described above.

In order to verify trailing edge (T.E.) bonds, the trailing edge skins will be inspected for evidence of wrinkling or local bucking after being loaded in compression during the static test. The T.E. lower surface will receive its compression load during the vertical down load test. The T.E. upper surface will receive its load by applying a 2500 pound aft acting horizontal load, while the blade is supported to cancel gravity loads.

6. Modal Survey (one blade)

The blade shall be rigidly fixed at the root, cantilevered in a horizontal position with the top of the airfoil up and the chord line at Station 844 horizontal. A modal survey shall be made using fixed and portable shaker pots as required and portable vibration pickups. The first three flapwise modes, the first two chordwise modes, and one torsional mode shall be determined. Modal data shall be measured at 15 equally space spanwise locations. Damping coefficients shall be determined and recorded.

5.2 ROTOR HUB

5.2.1 REQUIREMENTS

The rotor hub is all bolted construction, which avoids the limitations placed on weldments. Thus the structural requirements for the rotor hub are that the fatigue stresses not exceed the endurance limit for the material, and that peak operating loads, or other functional loads, will not cause stresses that exceed the allowable stresses specified in the AISC code. Loads for determining the operating stresses are in the Design Loads Definition, Appendix B.

The rotor lock can hold the blades vertically or horizontally. The rotor lock is required to hold the rotor from turning when feathered in the 6-12 o'clock position against a broadside 50 mph wind, including wind shear. Main bearing friction is disregarded and the load is calculated to be 71,500 ft. - lb. This is a "worst case" condition and could result if there is a failure of the parking logic to put the blade in the 3-9 o'clock position.

Other Functional Requirements are:

1. Oil seals shall be replaceable without disassembly of major components.

2. Fatigue critical threaded fasteners shall be selected from those produced for fatigue service, and preloaded hydraulically.

5.2.2 HUB

The hub carries the rotating blades and reacts the loads to the fixed bedplate. The hub consists of a cylindrical barrel with end rings at 9 degrees for blade coning. See Figure 5.2-1. The wall thickness of the barrel varies uniformly, and becomes thickest at the joint with the tailshaft. The tailshaft joins the barrel with a 120 degree saddle flange and a transition to the circular main bearing seat and flange. Both parts are machined from carbon steel forgings, ASTM A266, Grade 2. The fasteners around the joining flange are closely fit to transmit shear. Studs are installed through the circular flange because the distance to the bearing flange is not sufficient for the hydraulic tensioning device used to accurately preload the fasteners, nor will it allow bolts to be installed from that side. Bolts are used around the perimeter of the joining flange and along the straight flange. The forward end of the tailshaft is closed by the torque plate which secures the main bearing inner race and transmits the rotor torque to the smaller driveshaft coupling flange. The torque plate is machined from steel plate of ASTM A516, Grade 70 (as are all other parts unless noted otherwise) and is fastened to the end of the tailshaft with 42 studs. The clearance between the end of the tailshaft and the torque plate is shimmed so that a tension load equal to 44% of the stud's yield strength closes the gap to clamp the bearing. Further tension to 88% of yield strength provides the clamping friction for the driving torque. The connection to the drive shaft coupling is with 22 studs. The surface of the torque plate and coupling are grit blasted and a thin copper shim is installed in the joint to provide additional friction capability. The selection of the copper shim is based on good experience in a similar application. The outboard surface of the barrel has an access hole with a gasketed cover plate. All joints in the hub are sealed with polysulfide sealant. Holes in either side of the barrel, the

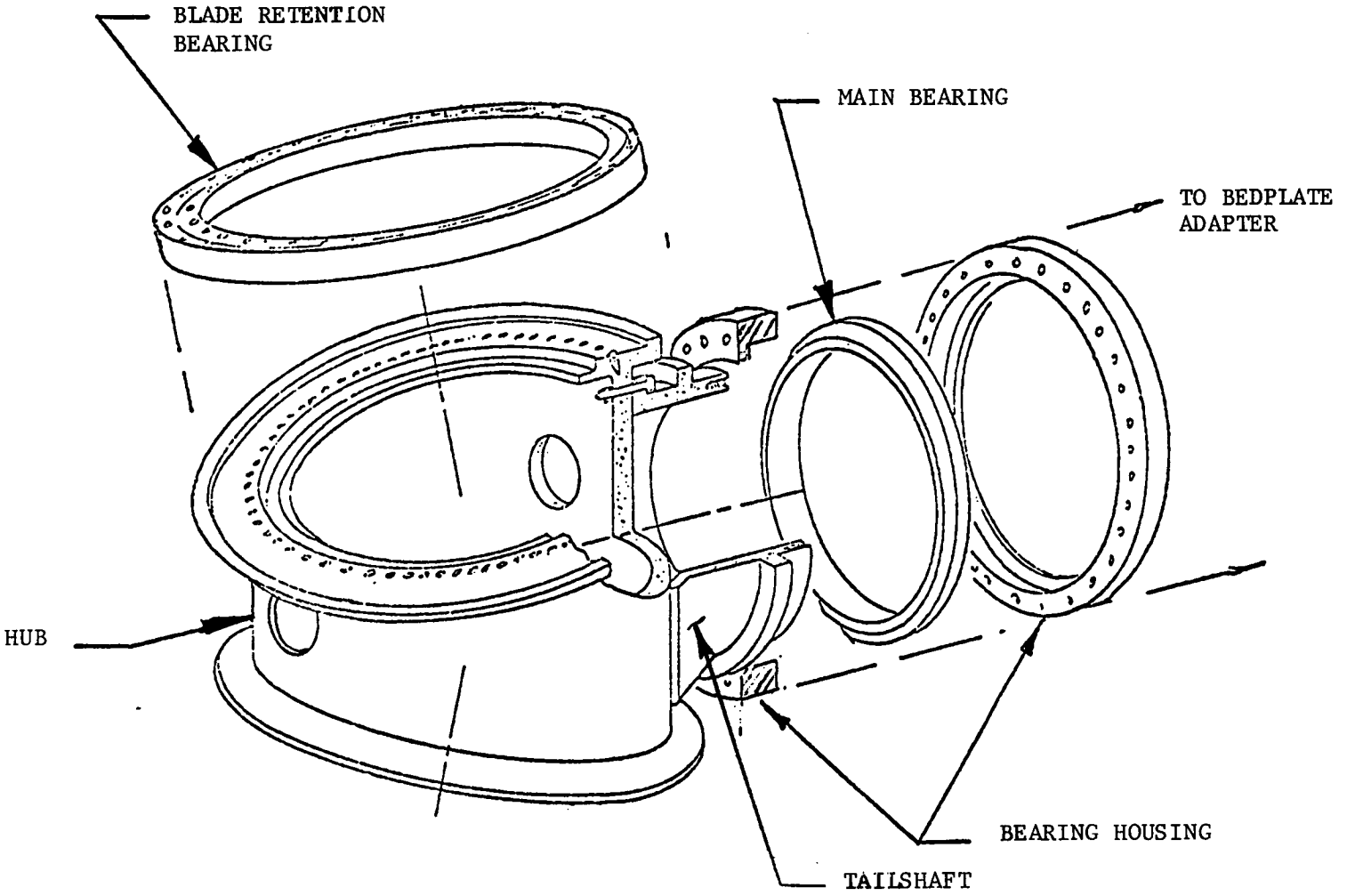

Figure 5.2-1 Rotor Hub

lowest point when the rotor is at the feathered position, allow condensate to drain.

All bolts and studs for the blade attachment through the tailshaft joint have UTS of 180,000 psi because of the substantial alternating loads. The torque plate bolts are to ASTM A490 (150,00 psi). All of these bolts and studs have radiused root rolled threads.

5.2.3 BLADE INTERFACE AND RETENTION BEARING

The blade retention bearing is a 3-row roller bearing with one inner and two outer races made of AISI 4150 steel. See Figure 5.2-2. The roller paths are case hardened and 56 axial holes through the races are provided for attachment. The three rows of rollers are all of different size to accommodate the loading; the thrust row that carries blade moment and centrifugal force is the largest, and the radial row is the smallest. Because of the limited rotation the bearing is grease lubricated with feed points at 8 places on each of the roller rows. The lubricant is grease to Specification MIL-G-81322, and it is applied at one point on the forward side of the torque plate. Two stages of volumetric distributors connected by steel tubing distribute the grease equally to 48 points on the two bearings. Integral grease seals can be replaced without major disassembly. Studs secure the bearing to the hub barrel and bolts secure the piloted blade flange to the bearing. The calculated life of the bearing is 30 years.

5.2.4 MAIN BEARING

The single main bearing is a two-row angular contact roller bearing with the high contact angle of 45 degrees. See Figure 5.2-3. The two separate inner races and the single outer race are made of AISI 52100 through-hardened steel. The inner races are a shrink fit on the tailshaft. Roller clearances are established by a precisely fit spacer between the two inner races. The inner races are clamped axially by the torque plate, with shims to limit the clamping force. The two housings clamp the outer race and are held together by 8 bolts until the bearing is attached to the bedplate rotor adaptor.

The high contact angle causes high end load of the rollers against the inner race. The induced friction heat load is more than grease can accommodate so oil lubrication is required. The lubrication system shown schematically in Figure 5.2-4 draws oil from the speed increasing transmission, and it is used to lubricate and cool the main bearing.

The flow is divided and 15 gallons per minute is fed to 6 points in the upper side of the outer race. An annular groove distributes the oil to radial holes through the outer race. The oil passes through the roller paths and extracts heat from the races and rollers, then it collects in the bottom of the bearing housing. A scavenging pump withdraws the oil at the rate of 17 to 18 gallons per minute. A vent line from the top of the housing to the speed increaser equalizes the volumetric flow. A magnetic inspection plug in the drain line permits checking for ferrous debris without draining the system. The rotating shaft is sealed by three elastomeric lip seals on each side running on a nickel-iron weld coating on the hub flange and torque plate. The two inner seals have spring fingers to assist in retaining the oil. The outer seal without

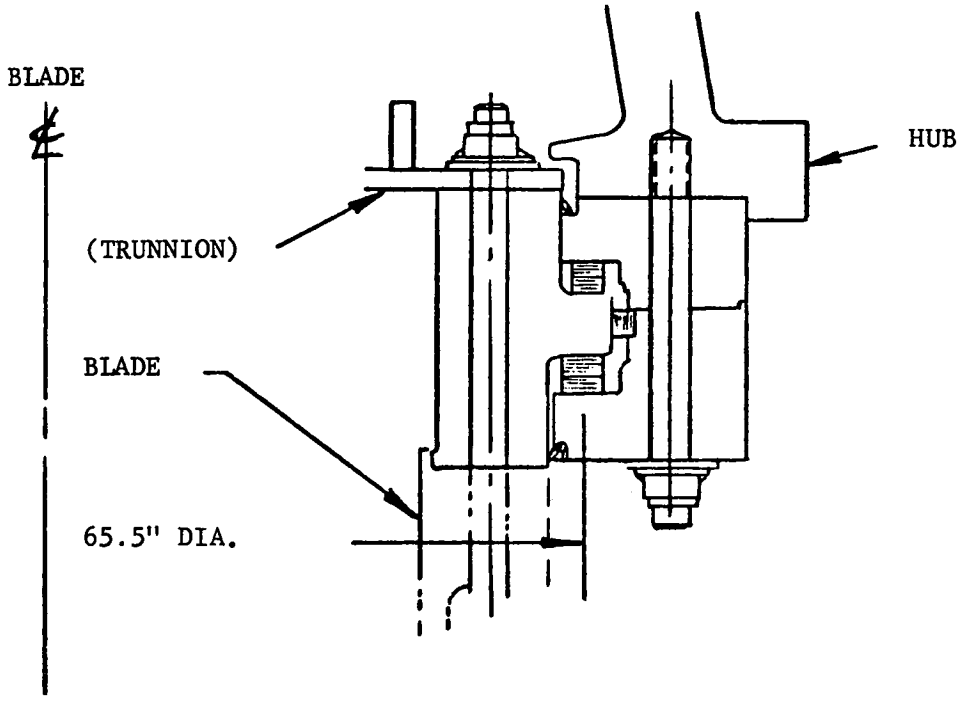

Figure 5.2-2 Blade Retention

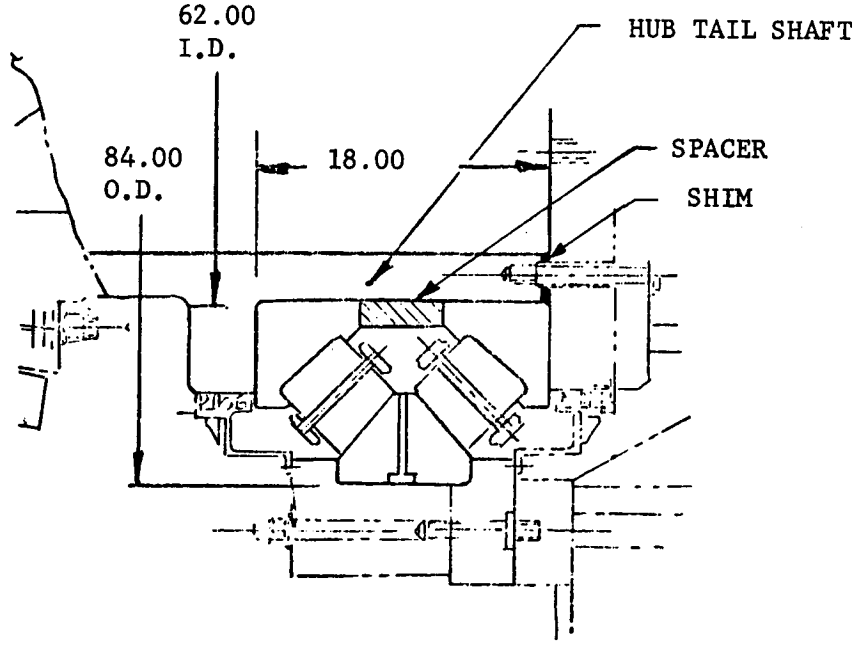

Figure 5.2-3 Main Rotor Bearing

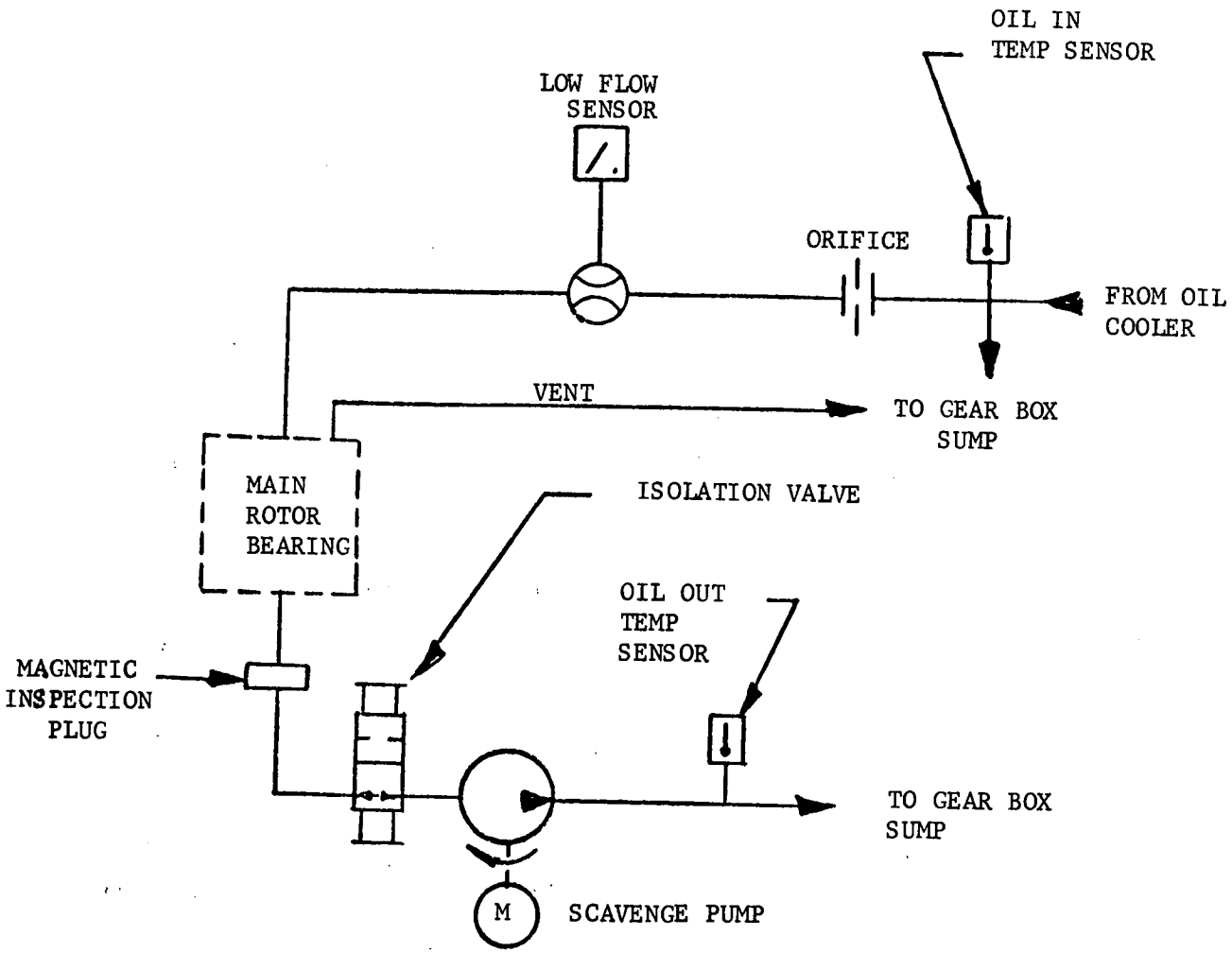

Figure 5.2-4 Rotor Bearing Lubrication System

spring fingers keeps debris out. Grease is injected at four circumferential points between the middle and outer seals to lubricate them and catch external debris. Grease for the forward and aft sides of the seal is piped separately, but both grease input points are accessable from within the nacelle.

5.2.5 ROTOR LOCK

The rotor lock is provided to disconnect elements of the drive train between the rotor and the highspeed brake, which normally locks the rotor when not operating. The rotor can be secured in any of four positions (blades horizontal or vertical) by manually installing eight 3/4 inch bolts between the locking plate on the upper aft side of the main bearing housing and the flange of the tailshaft. The locking plate is slotted so that the 8 bolts can be installed when the rotor stops within 5 degrees of normal.

5.2.6 INSTRUMENTATION

Operational Data Acquisition System (ODAS) instrumentation related to the rotor includes:

1. Rotor Bearing. Oil Flow. A flow switch in the oil line indicates 90% of oil flow rate.

2. Rotor Bearing Vibration. A single accelerometer installed on the main bearing housing with its sensitive axis skewed to the WTG principal axes.

3. Rotor Shaft Speed. Two induction pickups on opposite sides sense the passage of the toothed rim on the torque plate. (This speed sensor drives the backup Emergency Feather System).

Engineering Data Acquisition System (EDAS) Instrumentation includes:

1. Hub Strain Gages. Six locations on the hub for stress determination of critical locations.

2. Main Rotor Bearing Inner Race Temperature. A thermocouple probe contacts the forward face of the inner race on the rotor axis through the torque plate.

3. Main Rotor Bearing Outer Race Temperature. A thermocouple probe contacts the outer diameter on the lower side of the bearing through the housing.

4. Inlet Oil Temperature. A thermocouple in the oil line indicates the temperature of the oil supplied to both the rotor bearing and the transmission.

5. Rotor Bearing Oil Outlet Temperature. A thermocouple in the scavenge line indicates the temperature of the oil as it leaves the main bearing.

5.2.7 ROTOR HUB ANALYSIS

The rotor hub is analyzed by use of a NASTRAN finite element structures model combined with standard hand calculations. The critical design requirements are strength and fatigue life, per AISC code, and stiffness for blade retention bearing compliance requirements.

The hub structure is idealized with a NASTRAN finite element computer model. The structure is divided into plate and beam elements. The plate elements are used to define most of the hub structure including the bearing races, main hub body, and the tail shaft. Beams are used as connectors between the tail shaft and the main hub body and as a ring stiffener on the tail shaft.

The model consists of 776 grid points, 325 (CTR1A2) homogeneous trianglar plate elements, 528 (CQUAD2) homogeneous quadrilateral plate elements, and 64 (CBAR) beam elements.

An orthographic projection of element connections is shown in Figure 5.2-5.

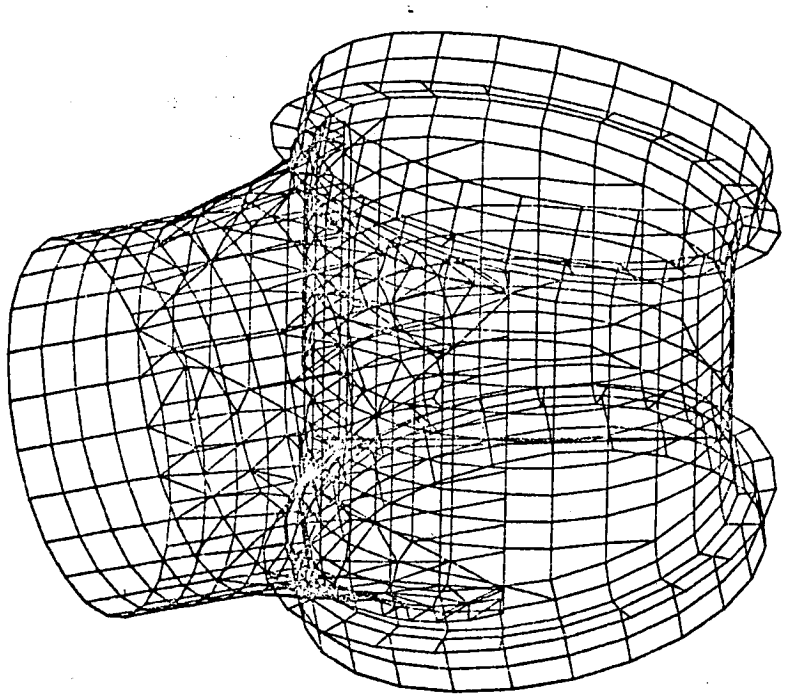

Figure 5.2-5 Rotor Hub Structural Analysis Model

Load Environment (Critical Design Loads)

The critical loading conditions are the following: (See Loads Appendix B for details).

1. Cyclic Loading (Case A).
   A spectrum loading determined by accumulated fatigue using Minor's rule, in combinations with a steel S-N curve shape.

2. Peak Loading (Cases B).
   Maximum up gust 35 to 50 mph +41° inflow and -41° inflow
   Maximum down gust 35 to 20 mph +41° inflow and -41° inflow
   with a fully immersed blade.

3. Emergency Feather (Case C).
   15% overspeed

4. Hurricane Loads (Case D) were not critical.

The key areas of concern are the following:

1. Attachment of the blade retention bearing to the hub

2. Stresses at the pitch rod holes

3. Attachment of the tail shaft to the main hub body

Description of Computer Programs

NASTRAN - is a generalized and well known finite element system.

HUBLDS - was written specifically to produce the 120 NASTRAN load cards required for each loading condition on the hub finite element model.

Stress Results - See Tabulation in Table 5.2-1 below.

Table 5.2-1

Hub Stress Analysis Summary

Component/Grid and Element Number	Maximum Stress	Allowable Stress	Critical Stress Type	Minimum Margin of Safety	Critical Condition
CTR1A 1087	<33,000	33,600	Bending & Tension	>+.02	Emergency Feather
CTR1A 506	27,382	33,600		+.23	
CTR1A 1569	24,341	33,600		+.38	
CTR1A 1508	21,676	33,600		+.55	
CTR1A 710	19,660	33,600		+.71	
CTR1A 1055	32,525	33,600		+.03	
CTR1A 1055	14,686	22,400	Shear	+.52	
CTR1A 1056	25,342	33,600	Bending & Tension	+.32	
CTR1A 1057	20,380	33,600		+.65	
CTR1A 1086	32,364	33,600		+.04	
CTR1A 1087	16,178	22,400	Shear	+.38	
CTR1A 1115	26,083	33,600	Bending & Tension	+.29	
CTR1A 1087	21,594	25,200		+.16	
CTR1A 1087	14,820	17,000	Shear	+.15	
Blade Retention Bearing Bolts					
Bearing to Hub	65,902	94,266	Tension	+.43	
Bearing to Blade	77,743	94,266	Tension	+.21	
Tail Shaft to Barrel Bolts	93,866	113,088	Shear	+.20	

5.3 PITCH CHANGE MECHANISM

5.3.1 REQUIREMENTS

5.3.1.1 Function

The function of the pitch change mechanism (PCM) is to position the pitch angle of blades in response to commands from the control system. In the power generation mode for example, this is such that the net aerodynamic torque on the rotor matches that required by the generator. Hydraulic fluid in four linear actuators provides the force and positions the blade angle as required through the PCM. The normal rate of change is one degree per second. During emergency feather however, the initial rate of change is 14 degrees per second, tapering off to 2 degrees per second to avoid over correction.

5.3.1.2 Structural Requirements

The structural requirements are established by the maximum force that the hydraulic actuators can exert against a jammed blade, and the alternating loads that fatigue the structure. The hydraulic pressure of 2,000 psi at zero flow causes a load of 308,000 pounds in the feather direction and 231,000 pounds in the opposite direction (piston rod area subtracted). This load is assumed to be reacted at the blade retention bearing. The eccentric loading is reacted by the swing links (see Figure 5.3-1).

The alternating pitch moment derived from the dynamic analysis is added to the friction torque of the blade retention bearing to determine the required alternating load from each bearing. The loads are summed at the actuator sleeve. Those loads that are in phase are reacted solely by the hydraulic actuators, while those out of phase are reacted solely by the swing links. The alternating load is $\pm$ 520,000 inch pounds; the reactions are shown in Figure 5.3-2 for the PCM limit loads and Figure 5.3-3 for the PCM fatigue loads.

5.3.1.3 PCM Stiffness and Travel

Blade stability analyses established critical stiffness requirements in the operating, startup, and nonoperating (hurricane) modes. With at least 100 percent margin, the respective stiffness requirements per blade are 120, 62 and 10.75 (each) x 10^6 inch - pound per radian. The stiffness of the Mod-1 PCM versus stroke is shown in Figure 5.3-4.

The blade pitch in the feathered position is -96 degrees, the angle of the 75 percent radius section chord line from the plane of rotation. In this position, the rotor aerodynamic shaft torque is essentially zero. The maximum blade pitch in the operating direction is 6 degrees, approximately 5 degrees greater than that required at rated wind speed. The mechanical stops at both extremes of travel are the bottoming of the piston at the ends of the actuator stroke.

5.3.1.4 Other Requirements

Other functional requirements include:

1. Manually operated lock secures the blades in the feathered position against hurricane winds when the pitch change mechanism is disconnected.

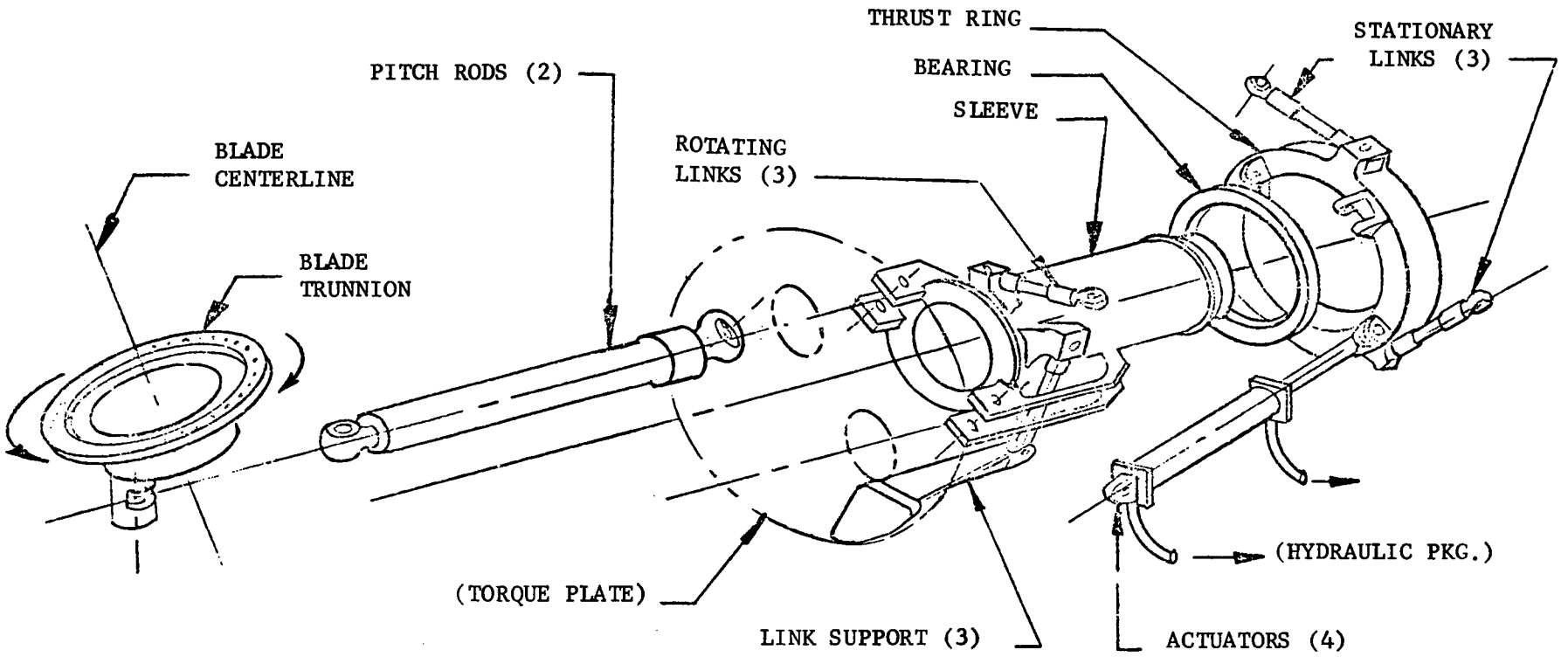

Figure 5.3-1 Pitch Change Mechanism

Figure 5.3-2
PCM Limit Loads (Lbs)

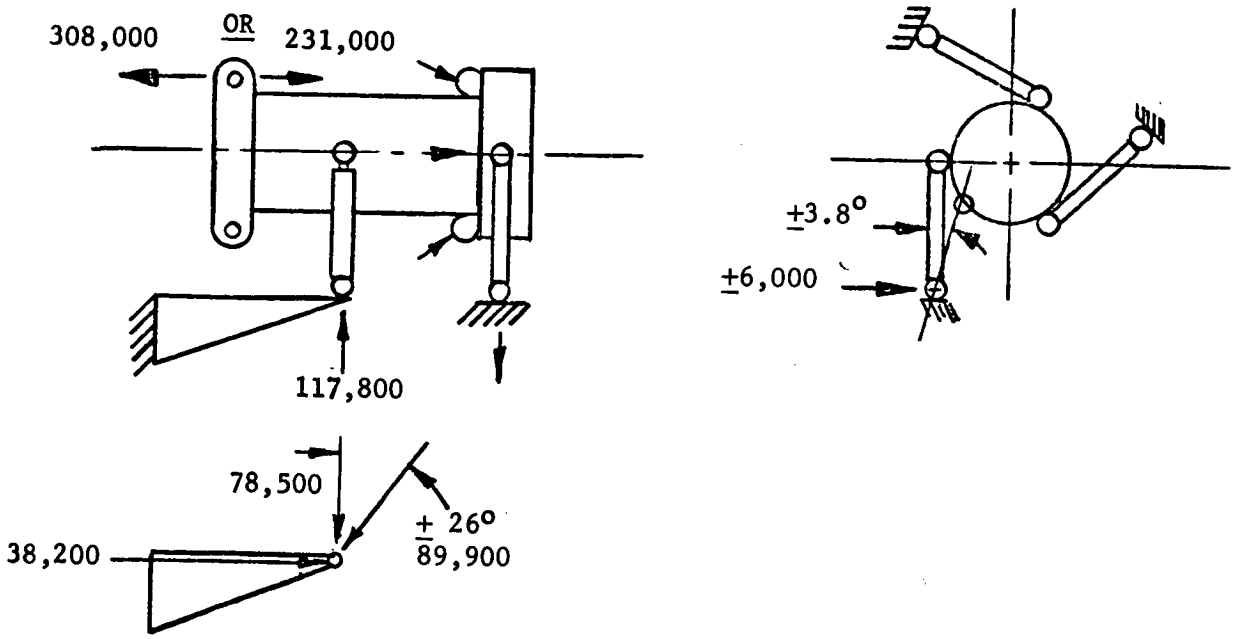

Figure 5.3-3
PCM Fatigue Loads (Lbs)

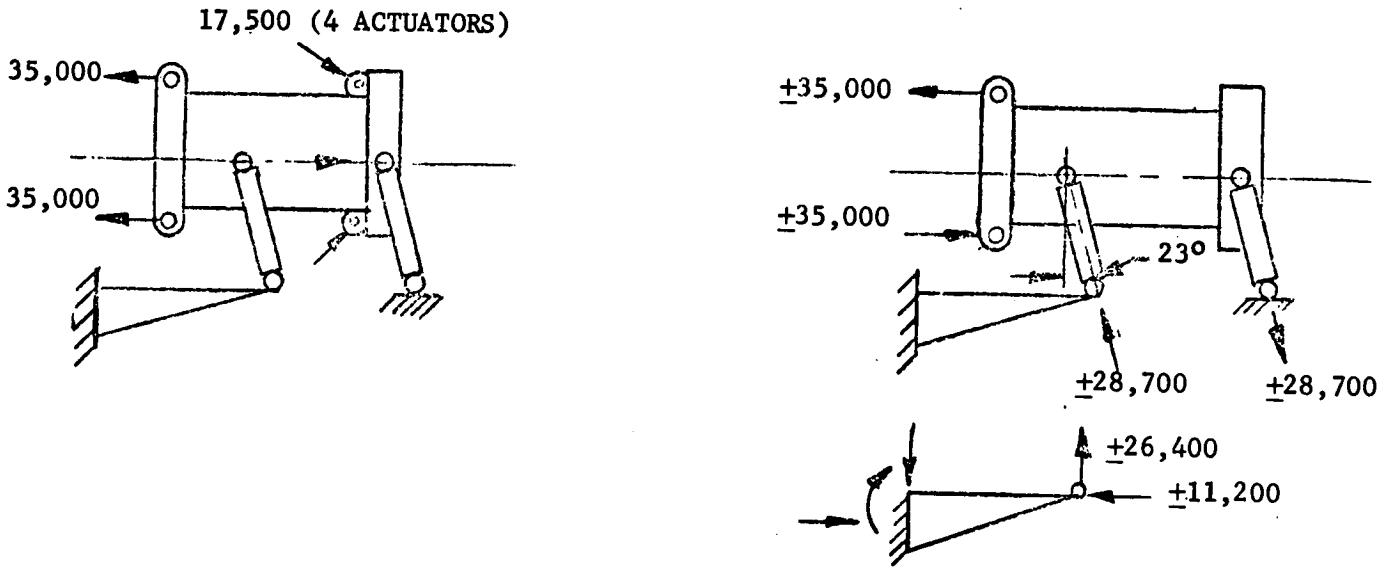

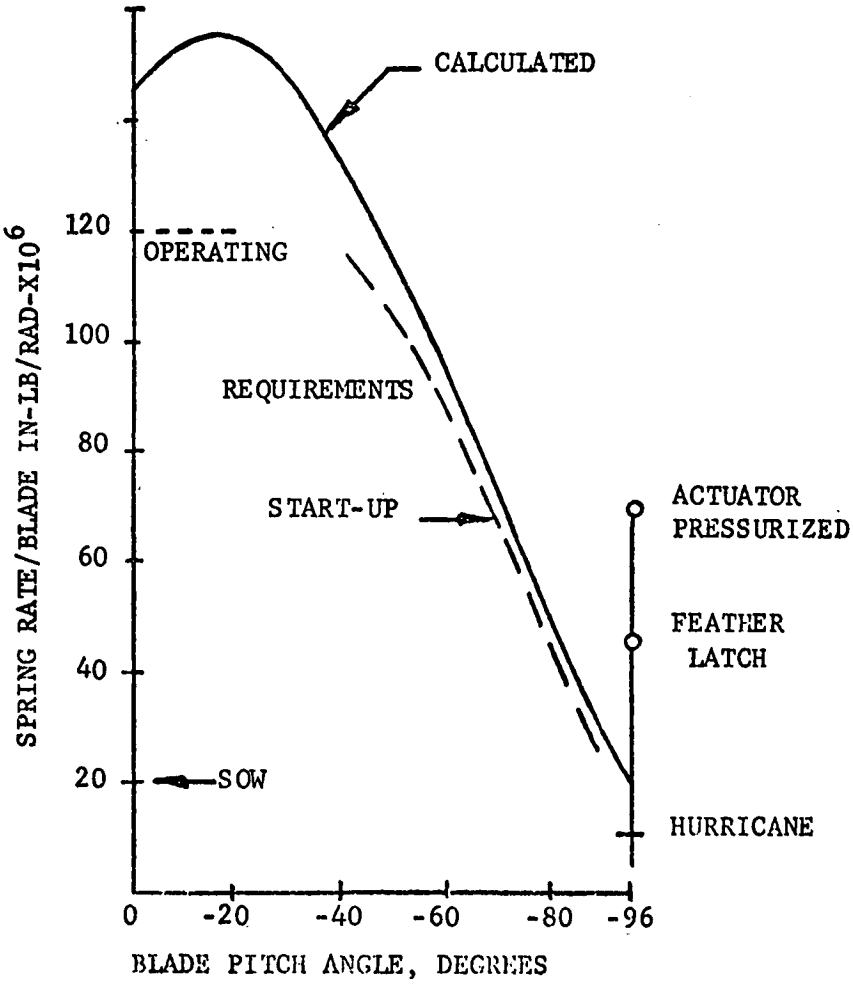

Figure 5.3-4

PCM Stiffness vs. Blade Pitch Angle

2. Mechanical feather lock secures the PCM in the feathered position when the hydraulic system is unpressured.

5.3.2 Description

5.3.2.1 Suspension

The suspension is the principal element of the pitch change mechanism that transmits the force and motion from the stationary actuators to the rotating blades. This element must have motion limited to one axis, while other directions are restrained. The suspension consists of two sets of 3 links each. The forward set supports the nonrotating outer race of the bearing from the bedplate, while the aft set supports the rotating inner race from the torque plate through cantilever beams. The corresponding ends of each set of links lie in a plane perpendicular to the direction motion, i.e., rotor Z axis. The links of a set are equidistant and tangential to the element it supports. As the moving element is displaced axially, it rotates about that axis in a varying helical motion. If the ends of the links are planar, equally spaced, and equidistant from the axis, the motion is concentric. Figure 5.3-5 shows variation of pitch angle with sleeve travel.

The displacement of the mechanism from the axis of rotation with axial displacement due to position errors of the ends of the links is shown in Figure 5.3-6. Displacement of one end of the mechanism in a direction different from the other will cause differential blade pitch change. This change, however, is less than .05 degrees in the operating range and is insignificant.

5.3.2.2 Actuator Sleeve

The actuator sleeve is a weldment of steel pipe, ASTM A 106, Grade 2, and end rings. The two pitch rod fittings are attached to the aft end with studs. The three lugs for the aft swing links are near the aft end. The pitch change bearing, Figure 5.3-7, is a double row tapered roller bearing similar to the main rotor bearing. The calculated life of this bearing is 30 years. The thrust ring is machined from plate and holds the outer race of the bearing. Both races are clamped by end rings. The four clevises which connect to the rod end of the actuators are bolted to the aft face of the thrust ring. Each side of the bearing is protected by two elastomeric lip seals. The grease lubricant is injected into nine radial passages through the thrust ring. The grease is further distributed around an annular groove in the outer race and then through radial holes into the roller paths. For relubrication, 16 plugs are removed from the thrust ring while grease is being injected. The contaminated grease is ejected from one row of rollers through these unplugged holes. The holes are plugged and the procedure repeated for the opposite side of the bearing.

5.3.2.3 Links

The swing links that suspend and guide the actuator sleeve are identical forward and aft. They consist of a 4340 steel bar which is internally threaded at both ends. Rod end bearings screw into the link with a retaining nut on the rod end shank. The nut is placed against the end of the link while 40,000 lb. tension is applied. Two set screws lock the nut. A bolt through the link and rod end is the key that prevents rotation of the rod end. The length of thread engagement allows each end to vary $\pm$ ½ inch. The bearing inserts consist of a stainless

Figure 5.3-5
Blade Pitch Angle vs. Sleeve Travel

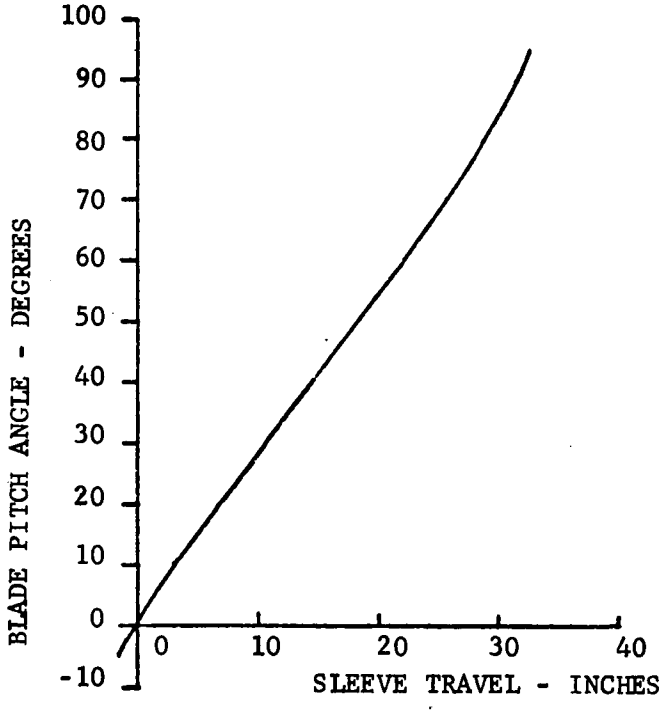

Figure 5.3-6
Effect of Suspension Tolerances
on Sleeve Displacement

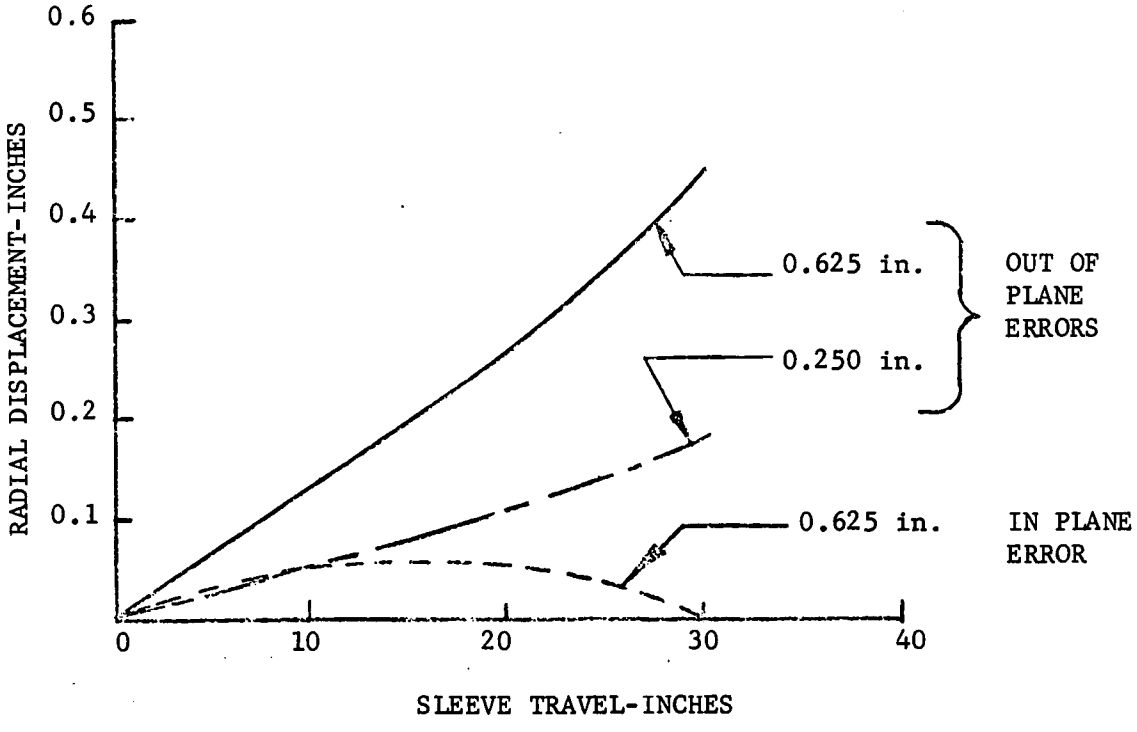

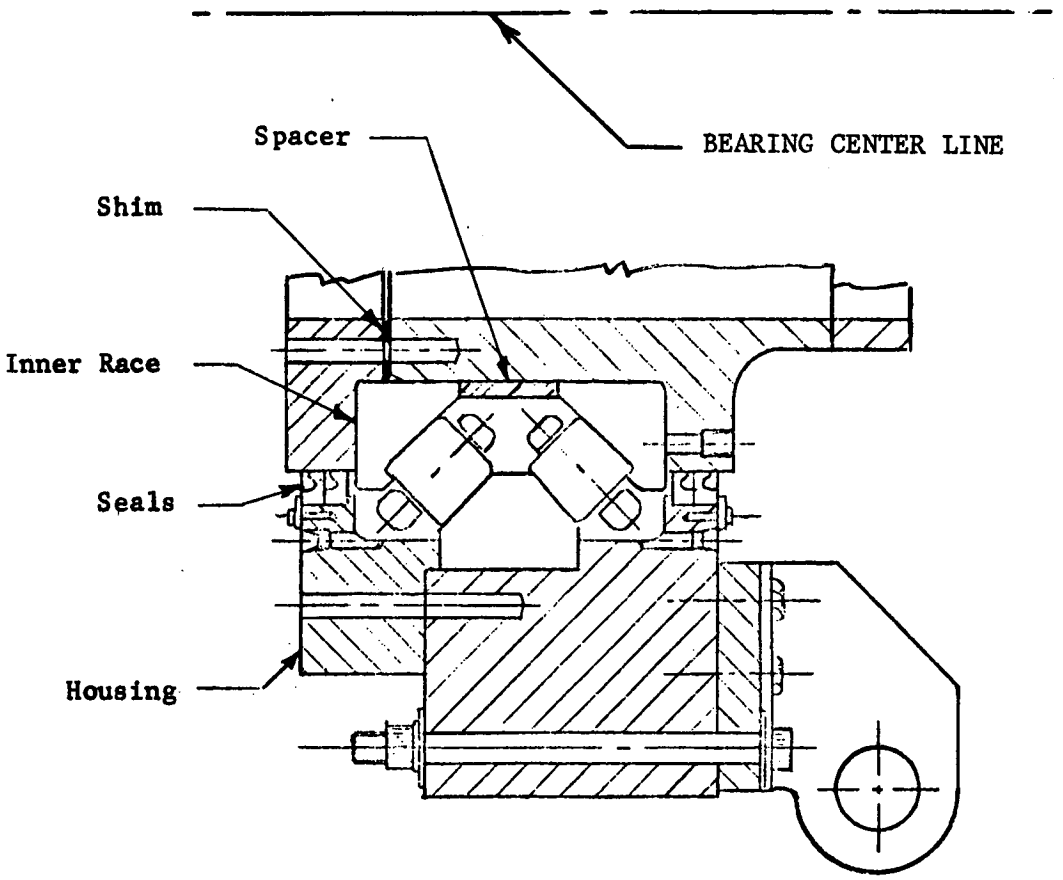

Figure 5.3-7 Pitch Change Bearing

steel ball turning in a woven TFE liner. These bearings require no lubrication. Maintenance consists of periodic inspection for wear.

The pitch rods consist of 4340 steel bar with internal threads, different at each end. The end of the rod at the actuator sleeve receives a differential threaded nut into which a rod end bearing is threaded.

The length of each rod may be varied by half turns of the differential nut. The threads are preloaded in tension by jack bolts between the differential nut and the link and rod ends. The adjustment of the rod length allows each blade to be adjusted over approximately 3.8 degrees in 0.14 degree increments from inside the nacelle. The aft end of the pitch rod inside the hub is similar except that there is no differential nut.

5.3.2.4 Instrumentation

Operational Data Acquisition System (ODAS) instrumentation related to the Pitch Control Mechanism includes:

1. (Blade) Pitch Angle No. 1 and No. 2. An RVDT at the attachment of two forward swing links to the bedplate measures the position of the swing link, which is calibrated to blade pitch angle.

2. Pitch Change Bearing Vibration. A single accelerometer installed on the thrust ring with its sensitive axis skewed in the plane of the bearing.

3. Feather Latch Position. A switch to indicate the position of the feather latch.

Engineering Data Acquisition System (EDAS) instrumentation includes:

1. Pitch Rods 1 & 2 Strain Gauges

2. Pitch Change Bearing Temperature TC probe on the inner race.

5.3.2.5 Pitch Control Mechanism Analysis

A schematic of the pitch control mechanism is shown in Figure 5.3-1 . The pitch control mechanism consists of statically-determinant components; stress margins and stiffness have been determined by means of conservative hand calculations employing standard classical methods of analysis. The system was broken into several smaller sections; each of these sections was analyzed separately to determine their capability to withstand the loading environments.

The detailed analysis of the PCM system shows that the critical design criteria is the compliance of the system rather than strength. The stress requirements are:

1. Fatigue stress below the endurance limit of the material and weld category.

2. Meet all structural requirements per the AISC code under maximum operating pressure in the actuators reached by a single jammed blade

retention bearing. This condition exceeds peak operating loads.

3. The critical design loads used in the analysis of the individual components of the pitch control mechanism were derived from "Design Loads Definition" Appendix B to this report. For pressurized components, a proof ultimate loading of 6000 psi was used.

Results

The analysis of the pitch control mechanism shows that all the substructures meet the specified compliance, and the strength requirements of the AISC code, including fatigue for 30 years of life.

Figure 5.3-8 summarizes the system compliance analysis, and Table 5.3-1 summarizes those components with Minimum Margins of Safety, none of which is negative.

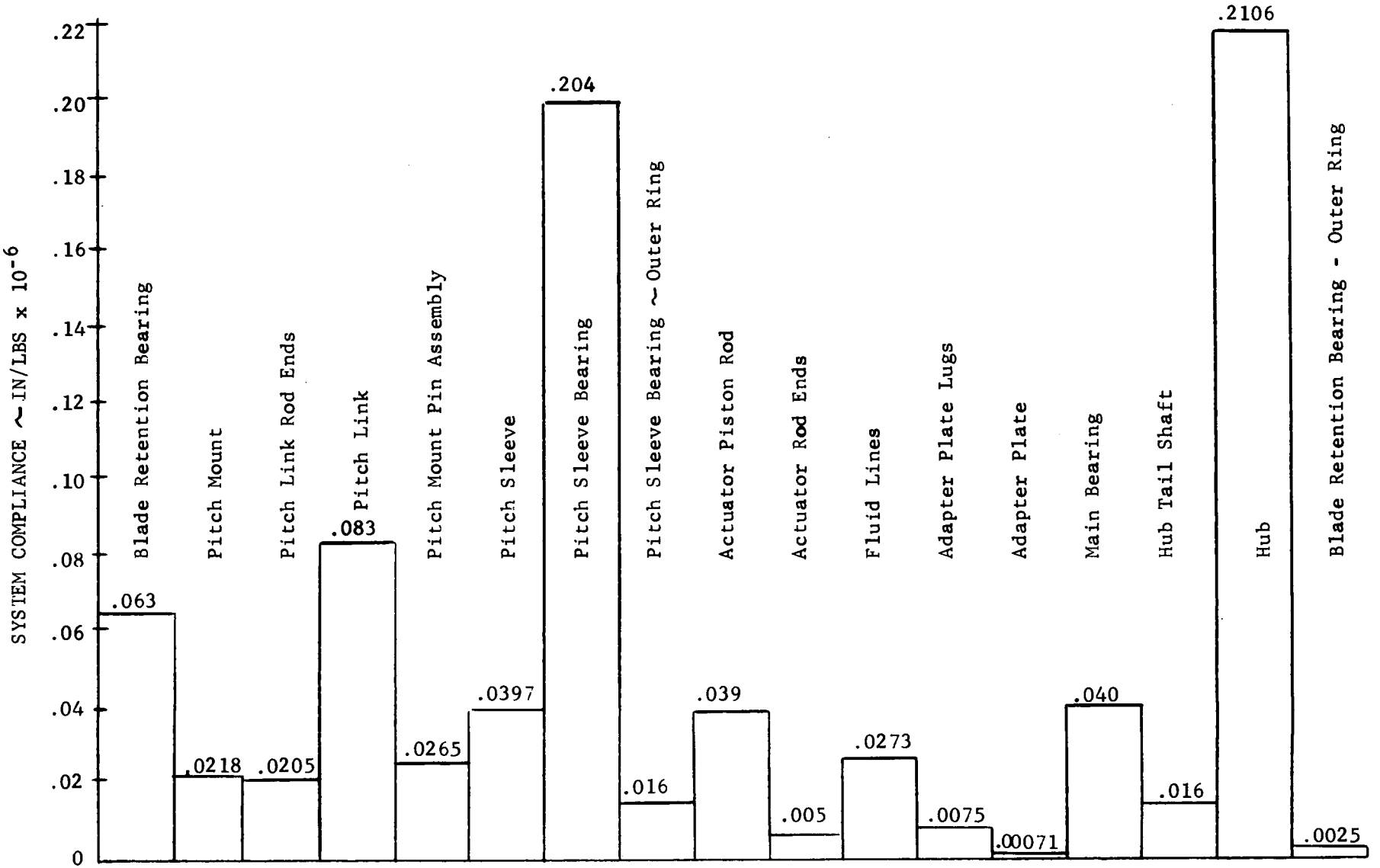

Figure 5.3-8 Component Contribution to Pitch Change Mechanism Compliance

Table 5.3-1

Pitch Change Mechanism Summary of Minimum

Margins of Safety

Part Description	Critical Stress	Allowable Stress	M.S. (+)
1. Pitch Links (As a Column)	21,224 psi	32,185 psi	+.52
2. Pitch Link to Actuator Sleeve Attachment Lugs			
A. Pin Bearing	28,880	32,400	+.12
3. Cantilever Support Beam			
A. Arm			
1) Fatigue	4,400	15,000	+2.4
2) Limit	20,000	22,800	+.14
B. Clevis			
1) Bearing (Y direction)	20,714	34,200	+.65
C. Base Plate bolts			
1) Bending (Limit Fatigue)	57,176	90,000	+.57
4. Swing Link to Actuator Sleeve Attachments	8,267	21,000	+1.5
5. Rotating Swing Links	28,648	74,619	+1.6
6. Actuator Sleeve			
A. Upper Lip	27,874	30,400	+.09
7. Thrust Ring			
A. Stationary Ring Lug			
1) Limit	20,100	22,800	+.12
B. Dowel Pin- Shear Limit	9,817	12,900	+.31
C. Actuator Lug Bolts	46,577	90,000	+.93
D. Actuator-Thrusting Lug			
1) Bending	11,917	22,800	+.91
E. Actuator	308,000 lbs	Pa=3X 10^6lbs	+11.5
H. Pin in Stationary Lug (Thrusting)	99,050 psi Tension	160,000 psi	+.62
8. Pitch Link Rotor Blade Mt.			
A. Top Plate			
1) Bearing Horizontal Load	34,200	34,200	+0
B. Bottom Plate Tension Vertical Load	9,661	17,100	+.77

5.4 DRIVE TRAIN

5.4.1 REQUIREMENTS

The function of the drive train is to transmit the power developed by the rotor to the generator. Specific requirements, including those of NASA defined in the SOW, as well as changes caused by uprating, are listed below.

1. Input speed 34.7 rpm
2. Output speed 1800 rpm
3. Fixed gear ratio
4. 30-year life (except for some gearbox components that require replacement at approximately 10-year intervals).
5. Startup and operation at -31°F to 120°F
6. Input power 2,945 hp
7. Maximum overload condition 5,520 hp (1,500 cycles in 30 years)
8. Minimum running efficiency 96%
9. Provide a slip clutch on the high speed drive shaft to protect the drive train from electrical faults.
10. Provide a rotor brake on the high speed drive shaft.
11. Maximum breakaway torque 45,000 in-lb. at the low speed shaft
12. Provide a 6 in. diameter hole through low speed shaft for rotor to slip ring cable passage.
13. Torsional stiffness, off-line $\sim$3.5P.

By definition, the drive train begins with the rotor tail shaft and the mating flange on the low speed shaft, continues through the gearbox, slip clutch, and ends at the interface between the high speed shaft and the generator. Included in the definition is the rotor brake and the lubrication/cooling system.

In mid-1977, it was ascertained that the 1,500 kW rating originally specified could be uprated to 2,000 kW. Since the gearbox design, material procurement and fabrication had already been started, an evaluation of the 1,500 kW design at the increased power was made. At the higher power rating, three gears have a calculated life of 10 years, two of 15 years, and 8 bearings have calculated lives between 15 and 22 years. Thus, by calculation, the gearbox has less than the 30-year life originally required; therefore, the condition of the gearbox must be monitored for wear and/or failure after 10 years of operation. Component

replacement, when required, will permit continued operation of the gearbox at the uprated power to provide a 30-year life.

The low and high speed shafts are not significantly affected by the increased power because they were originally designed to a mean of 2,209 hp and a ± 33% alternating load. Updated analyses indicate that the alternating load is only ± 10%, thus the net increase in peak loading seen by the shafts is only 10%. A fatigue stress analysis (using very conservative allowables) shows the low speed shaft and the high speed shaft to have positive margins of safety.

The rotor brake design criteria is as follows:

1. Brake from rotor speed of 5 rpm to zero
2. 100,000 braking cycles
3. Static torque capability of 112% at 2,000 kW rating (was 150% for 1,500 kW)

It was further assumed as a design criteria that the rotor blades would be feathered but would provide no aerodynamic braking.

The design criteria for the slip clutch is as follows:

1.	Speed	1,800 rpm
2.	Torque	8,212 ft-lbs
3.	Slip Torque	15,400 ft-lbs (1.88 x rated torque)

The design criteria for the low speed shaft is as follows:

1.	Speed	34.7 rpm
2.	Rated Torque	442,000 ft-lbs
3.	Max. Overload	995,000 ft-lbs (1.88 x 1.2 S.F. x rated torque)

5.4.2 DESIGN DESCRIPTION

5.4.2.1 Floating Shaft Assembly (Low Speed)

Connecting the rotor to the gearbox is a floating shaft assembly, consisting of a drive shaft with flexible couplings mounted on each end. This assembly is of a type available from several coupling manufacturers as a standard product line. Flexible gear hubs are mounted on each end of the drive shaft and mate with a rigid flange on the rotor and a rigid hub on the gearbox, allowing the shaft to float and accommodate angular and lateral misalignments as well as axial float. The assembly is shown in Figure 5.4-1 (Drawing 132D6268). The angular misalignment is limited to 1/2 degree per engagement plus a parallel off set of 0.50 inch. The gears are designed with a crown to accommodate these conditions.

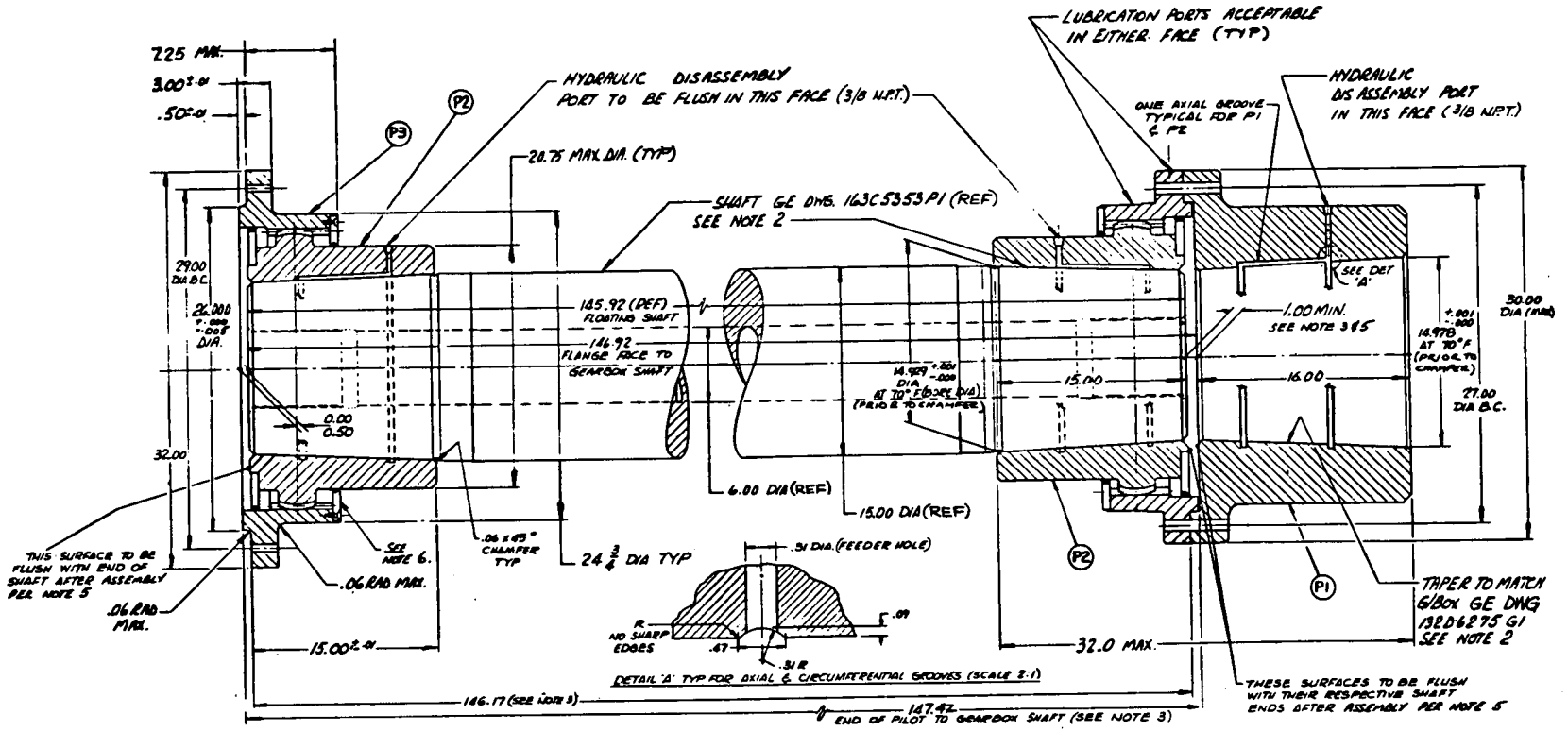

Figure 5.4-1 Low Speed Floating Shaft Assembly

The gear coupling at the rotor end is a modification of a standard design because of the special mounting flange with scallops to clear the pitch change mechanism. At the gearbox end, however, the coupling is of standard design and is mounted on the gearbox stub shaft. A nonstandard feature is the internal seal to prevent lubricating grease from entering the internal shaft bore. The Sier Bath Gear Co. of North Bergen, NJ, was selected to design and manufacture this shaft assembly.

The drive shaft is shown in Figure 5.4-2 (Drawing 163C5353). The ends are tapered to permit hydraulic mounting or removal of coupling hubs. An interference fit of approximately 0.002 inch per inch diameter will permit full torque transfer without the stress concentration of a keyway. The 15-inch outside diameter shown provides a stiffness that results in a first torsional frequency for the entire drive train of 3.5P, off-line (12.72 r/s, 2.02 Hz).

5.4.2.2 Speed Increaser Gearbox

The gearbox is a three-stage, tandem articulated, parallel shaft gearbox with input and output shafts on a vertical centerline, and horizontal casing splits. The tandem articulated shafts permit the load path to be split with equal sharing of the load. The manufacturer is Philadelphia Gear Corporation of King of Prussia, PA. The envelope and external features are shown in Figure 5.4-3 (Drawing 132D6275). The gearing is designed for strength and durability for 30-year life to AGMA specifications with periodic maintenance.

The low speed stub shaft is tapered for keyless mounting and hydraulic removal of a rigid hub and has a 6-inch internal bore for passage of cables from the rotor to a slipring assembly, which is bolted to the face of the shaft extension on the upwind side of the gearbox. The slipring stator is supported by a bracket on the gearbox casing.

Bearings and gears are lubricated by an electric pump-driven spray system. The pump has sufficient excess capacity to supply lubricating oil to the rotor bearing. The gearbox incorporates internal heaters in the sump for startup under ambient conditions of low temperatures.

There is an oil cooler external to the nacelle that cools the lubricating oil when operating a high temperature.

The gearbox third stage is designed with a casing split horizontally at the center line of the third stage shafts. This is intended to facilitate a change in the third stage speed ratio by installing a different set of pinions. The upper casing section can be lifted so the pinion can be replaced on site. This feature allows a speed adjustment of up to 10% to correct for any undesirable frequency placement that may be defined when operation begins at the site.

5.4.2.3 High Speed Shaft Assembly

The high speed shaft assembly includes the high speed brake disk, a slip clutch and a floating shaft that connects the speed increaser gearbox to the generator. A toothed wheel bolts to one face of the rotor brake disk; it provides the means to sense the rotational speed of the shaft electromagnetically. A hydraulically

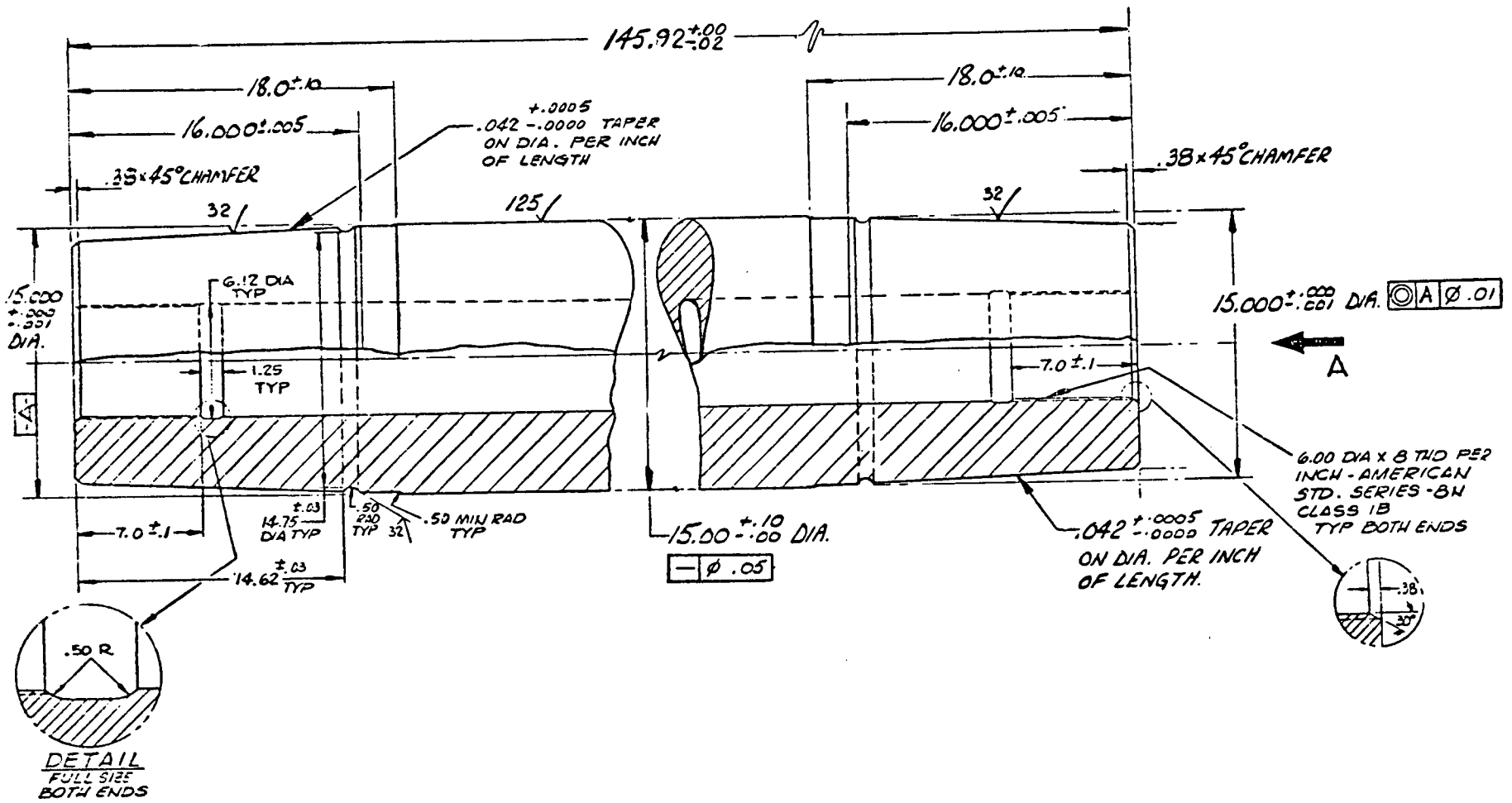

Figure 5.4-2 Low Speed Drive Shaft

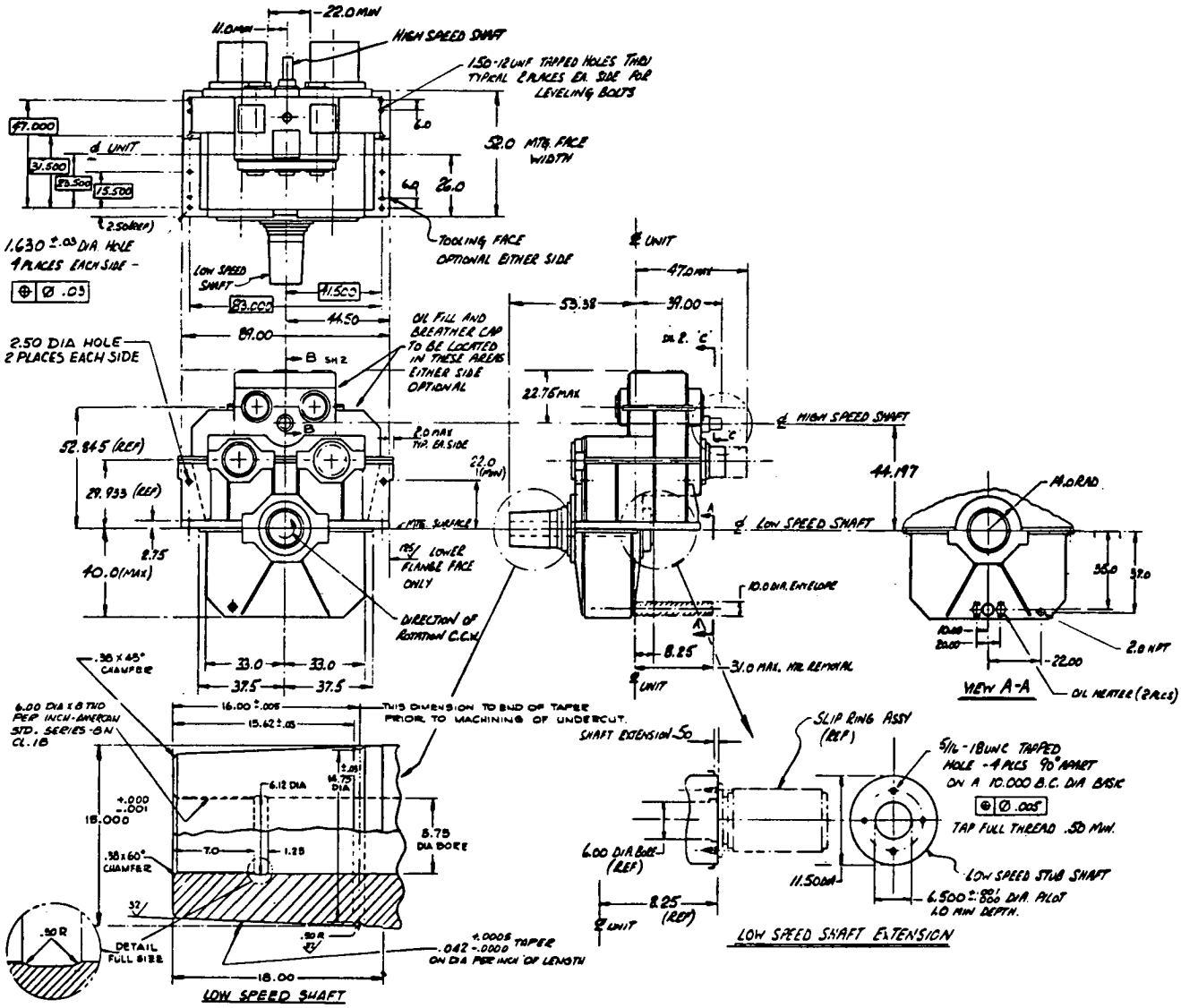

Figure 5.4-3. Gearbox Envelope

operated brake caliper is mounted from a bracket on the gearbox casing. The slip clutch provides overload protection for the entire drive train by slipping when torque exceeds 188% of rated torque, or 15,400 ft-lb. The slip clutch is the dry type with metallic friction plates, adjustable for torque level by means of adjusting bolts. Figure 5.4-4 shows the high speed shaft assembly less the rotor brake disk.

The two flexible half couplings, separated by a floating spacer shaft, accomodate both angular and offset misalignment between the gearbox and generator. Thrust plates and buttons on the spacer limit axial float. This is a common optional variation on couplings of this type, used when axial float must be limited because of the lack of thrust capability in the generator bearings. The spacer is removable by unbolting flanges at each end. Removing the spacer also permits access for removal of the other coupling components, including the clutch.

5.4.2.4 Rotor Brake

The brake used to bring the rotor to a stop and position the blades in a 3 - 9 o'clock position, consists of a stainless steel disk mounted on the high speed shaft and a hydraulically operated brake caliper attached to the gearbox housing. The brake caliper is a standard unit made by the Goodyear Corporation, Berea, Kentucky, for off-road vehicles, and is shown in Figure 5.4-5. The brake disk was made from stainless steel to avoid the possibility of irregular operation caused by rust build up during non-operating periods, as experienced on Mod 0.

The brake caliper is operated from an accumulator charged by the yaw drive hydraulic supply. Nominal pressure is 1300 psi and minimum 1000 psi. The brake torque is given by:

$$T = \mu A r p$$

where μ = coefficient of friction = .21
A = total piston area = 24 in^2
r = effective moment arm = 1 ft.
p = brake pressure = 1000 psi

$$T = .21 \times 24 \times 1 \times 1000$$

$$= 5240 \text{ ft-lb}$$

This torque is well below the setting on the slip clutch, 15,440 ft-lb so that inadvertant brake operation cannot overload drive train components.

The kinetic energy dissipated by the brake in bringing it to a stop from 5 rpm (.523 radians/sec) is

$$KE = I\omega^2/2$$

$$= 2211 \times 10^3 \times (.523)^2 / 2$$

$$= 301{,}000 \text{ ft-lb.}$$

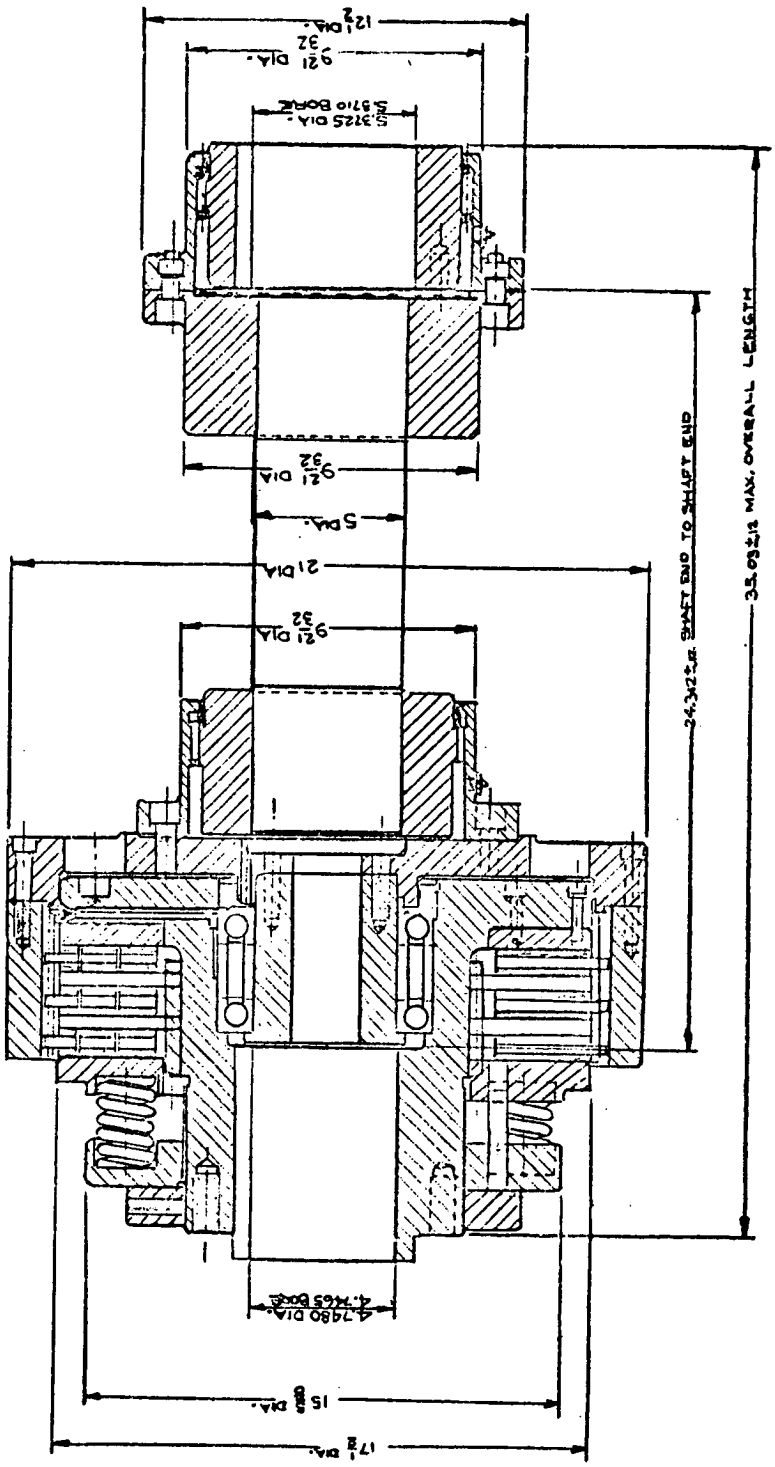

Figure 5.4-4. High Speed Shaft Assembly - Less Brake Disc

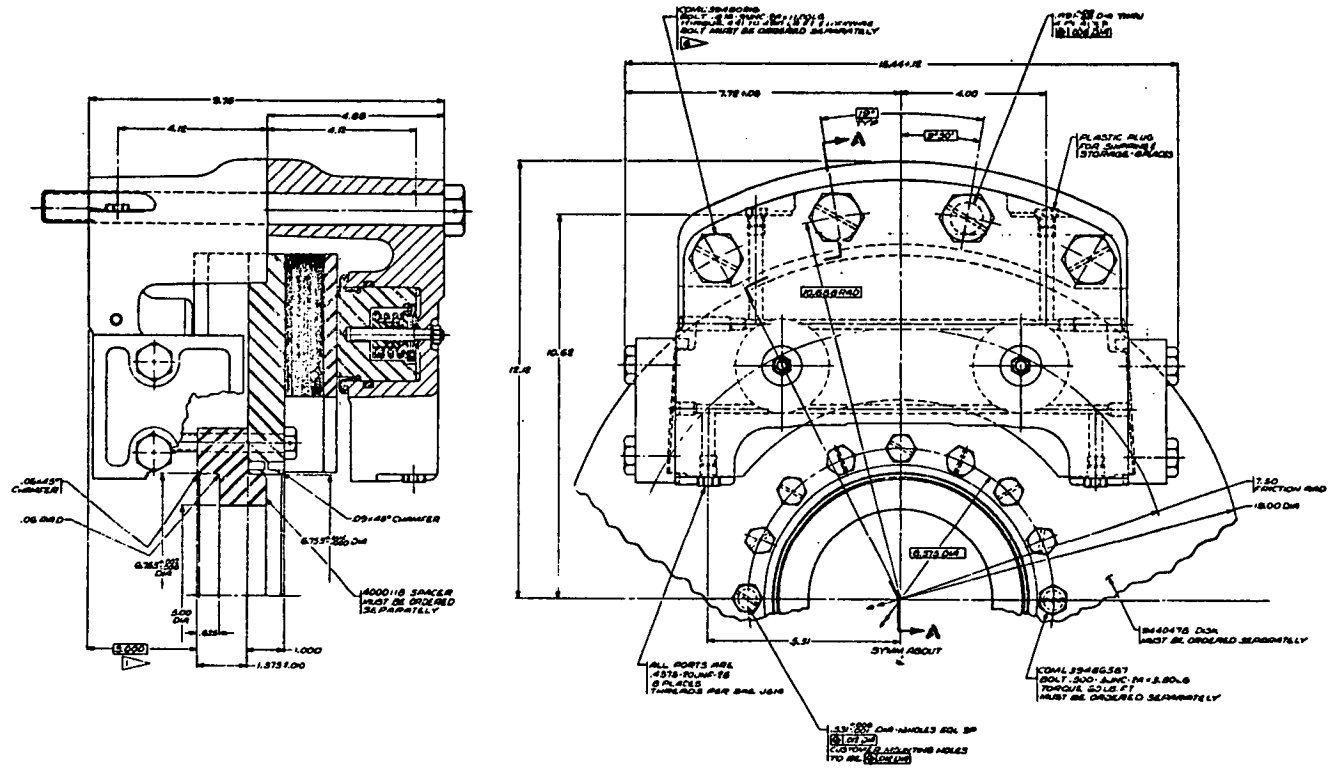

Figure 5.4-5 An Assembled Caliper Brake

Although the published value for continuous operation without degradation is only 133,500 ft-lb., this value is based on a very conservative temperature rise of 8°F. If operation is intermittent (adequate cooling time between applications) and the disk temperature is allowed to rise 50°F, 327,000 ft-lb of energy can be dissipated. When the energy level exceeds 3×10^6 ft-lb, brake operation remains normal, although some reduction in brake life may occur. At higher energy levels, brake effectiveness will be lost, but not catastrophically. The limit is reached when the brake disk overheats and permanently distorts. Tests performed with this brake by General Electric's Locomotive Products Department showed that over 12×10^6 ft-lb could be dissipated in an emergency. Allowing for the smaller disk diameter used in these tests, it is estimated that over 20×10^6 ft-lb could be absorbed in an emergency shutdown of the wind turbine. This corresponds to a rotor speed of 61 rpm or 64% overspeed.

During normal operation, the time to come to a stop from 5 rpm will be:

$$t = \frac{I\omega}{TN} \qquad \text{where } N = \text{speed ratio}$$

$$= 2211 \times 10^3 \times .523 \; / \; 5240 \times 52$$

$$= 4.2 \text{ seconds}$$

During this time the blade would travel 120°.

The static holding torque of the brake will be higher than the dynamic torque by virtue of the coefficient of friction (0.3 versus 0.21).

$$T_s = .3 \times 24 \times 1 \times 1300$$

$$= 9350 \text{ ft-lb}$$

This corresponds to 114% of rated torque.

5.4.3 DRIVE TRAIN MAINTENANCE

The drive train will be assembled, aligned and tested before it is shipped to the operational site. Although all components are designed for a 30-year life, provisions have been made to replace components without the need of removing the rotor or nacelle from the tower.

The gear couplings on both the low speed and high speed shaft are lubricated with grease and they will require relubrication annually. Grease fittings are provided in each coupling.

The lubricating oil in the gearbox requires only periodic checking, and the oil must be replaced only when it becomes contaminated. The sump heaters are mounted in a glycol-filled well and can be replaced without loss of lubricating oil.

The brake on the high speed shaft will require periodic inspection to measure wear. Although anticipated wear rates are low, replacement of brake pads can be done routinely, and even replacement of the brake disk is relatively simple. Inspection of the brake will include examination of hydraulic connections and seals for indication of fluid leakage.

All components of the drive train except as previously noted are designed for a 30-year life, using conservative criteria that are standard for industrial components. Wear points are gear teeth and bearings. Gear durability is based on American Gear Manufacturers Association (AGMA) specifications, which provide for stress levels below endurance limits. The gear couplings will benefit by operating at less than maximum misalignment limits under normal operation. Similarly, bearing life is based on conservative Anti-Friction Bearing Manufacturers Association (AFBMA) criteria.

Overload conditions that cause torques reaching 1.88 times rated values are expected to occur only infrequently. Under these conditions, stress levels throughout the drive train remain below yield so that no permanent damage will be incurred. The drive train is protected against overload torques by the slip clutch in the high speed shaft assembly should torques exceed 1.88 rated.

5.4.4 DRIVE TRAIN STRESS ANALYSIS

All components of the drive train were analyzed for stresses at peak loading and for fatigue. Detailed analyses were performed of the gear teeth in the low speed shaft coupling by the supplier, Sier-Bath, and Philadelphia Gear Corporation used their proprietary computer codes to check strength and durability of the gears in the gearbox. Critical sections in the drive train occur at the couplings on the load speed shaft. Further discussion of the stresses in these areas follows; in all other areas positive margins of safety of 50% or more were calculated by conservative analysis or were judged adequate by inspection.

Where the coupling hubs are installed by interference fit on the low speed shaft, the first concern is that the contact pressure between hub and shaft is sufficient to transmit the design torque of 995,000 ft-lb., which includes a 1.20 safety factor. The contact pressure is given by:

$$P = \frac{2T}{\pi d^2 L \mu}$$

where T = torque (in-lb)

d = diameter of fit
= (14.978 + 14.309) x 1/2
= 14.644 in.

L = length of contact
= 15.62 - .38
= 15.34 in.

μ = 0.2

The use of 0.2 for coefficient of friction is appropriate for carefully degreased surfaces. Substitution yields

$$p = 11{,}600 \text{ psi}$$

The interference fit required to achieve this pressure can be computed using Birme's equations:

$$\frac{\Delta}{d} = \frac{p}{E_e}\left[\frac{1+c_e^2}{1-c_e^2} + \nu_e\right] + \frac{p}{E_i}\left[\frac{1+c_i^2}{1-c_i^2} - \nu_i\right]$$

where Δ = diametrical interference

E = elastic modulus

ν = Poisson's ratio

c = $\frac{\text{inside diameter}}{\text{outside diameter}}$

e, i are subscripts referring to outer ring (hub) and inner ring (shaft), respectively

where $E_e = E_i$, $\nu_e = \nu_i$

$$\frac{\Delta}{d} = \frac{p}{E}\left[\frac{1+c_e^2}{1-c_e^2} + \frac{1+c_i^2}{1-c_i^2}\right]$$

for $c_e = \frac{14.644}{23.5}$, and $c_i = \frac{5.75}{14.644}$

$$\Delta = .0206 \text{ in.}$$

The actual interference fit was obtained by heating the hub to a temperature of 300°F, or a differential temperature of 230°F, which provided approximately 10 mils clearance over a cold fit up. The hub was then moved axially a measured distance of .495 inches, corresponding to the correct interference fit on the conical surfaces having a taper of .0418 in/in.

The hoop stress in the hub at its bore can be computed by Lame's equation:

$$\sigma_x = p\left(\frac{1+c_e^2}{1-c_e^2}\right)$$

$$= 25{,}200 \text{ psi}$$

This stress occurs in a 4140 steel hub having a minimum tensile yield strength of 132,000 psi, providing a very large margin of safety. Similarly, the hoop stress (compressive) in the shaft due to the interference fit, occurring at the bore, is 27,400 psi in a 4340 steel having a minimum tensile strength of 140,000 psi.

The critical section for the shaft is just beyond the hub where compressive hoop stresses are absent and fatigue cracks can propagate. At this section, the torque at rated power of 2945 hp and 34.7 rpm is:

$$T = \frac{63025\ P}{n}$$

$$= 5.30 \times 10^6 \text{ in-lb}$$

The torsional shear stress is

$$\tau = \frac{T_c}{J} = \frac{16 T d_o}{\pi (d_o^4 - d_i^4)}$$

$$= 8200 \text{ psi}$$

Assuming an alternating load of $\pm$ 10% rated load, the maximum stress is 10,000 psi and the stress ratio R = .82. Bending stress due to the weight of the shaft will combine with torsional stresses; however, at the ends of the shaft these stresses are negligible.

In order to compute a margin of safety in fatigue, it is first necessary to compute an allowable alternating shear stress based on bending fatigue data, and apply appropriate stress reduction factors. The allowable tensile fatigue stress for unnotched 4340 steel at R = .82 and 10^8 cycles is 15,000 psi, corresponding to an alternating shear stress (one-half of the stress range) of 8667 psi. The factors to be applied are

k_R = reliability factor = .76
(This factor relates the average value from test data to the 3 σ value normally used for design)

k_s = size factor = .6
(This factor relates test data for small diameter specimens to the 15 in. shaft diameter)

k_{SF} = surface finish factor = .9
(Appropriate for ground surface)

k_T = shrink fit concentration factor = .57

k_f = fretting factor = .5

The result is a combined factor k = .117, giving a reduced allowable of = 1010 psi, and a margin of safety:

$$MS = \frac{1010}{820} - 1 = +.23$$

Although this margin of safety may appear to be low, it is based on very conservative assumptions in both the loading and allowable stress. A similar fatigue analysis of the high speed shaft shows a margin of safety of +2.18.

5.4.5 DRIVE TRAIN STIFFNESS SENSITIVITY ANALYSIS

A sensitivity analysis was performed to assess the off-line torsional frequency of the drive train and to evaluate the effect on this frequency of critical system parameters (e.g. gearbox stiffness, generator inertia, and coupling stiffnesses and inertias). The baseline model was selected to represent the dynamic model used to calculate dynamic loads. The critical parameters were varied individually and the resulting frequencies evaluated. The analysis results indicated that the gearbox stiffness and the generator inertia have the greatest influences on the system frequency. It was also determined that if the gearbox stiffness is reduced from 8.62×10^8 in-lb/rad to 2.155×10^8 (75% drop), the off-line torsional frequency will reduce from 3.9P to 2.8P.

The drive train was modeled as a lumped mass and spring system to enable several iterations of model configurations to be evaluated in a convenient and economical manner. This model, shown in Figure 5.4-6, contained inertia representations for the blades, low-speed shaft coupling, gearbox and brake, high-speed shaft slip and flex couplings, and the generator. Inertia values were calculated based on the latest available drawings of the various components and from vendor data. Spring data were obtained in a similar manner and are listed along with the inertia data in Table 5.4-1.

In each case, the parameter of interest was varied to obtain its sole affect on the system torsional frequency. All the other baseline model parameters were held constant while the parameter being examined was modified. These modified values were divided by their baseline value to obtain a "parameter ratio". This ratio was used as the scale on the horizontal axis of the sensitivity analysis graph in Figure 5.4-7. The new resulting first torsional frequency was divided by the baseline first torsional frequency (i.e., 3.255 cycles/rev.) to obtain the frequency ratio which was used as the scale on the vertical axis of the graph.

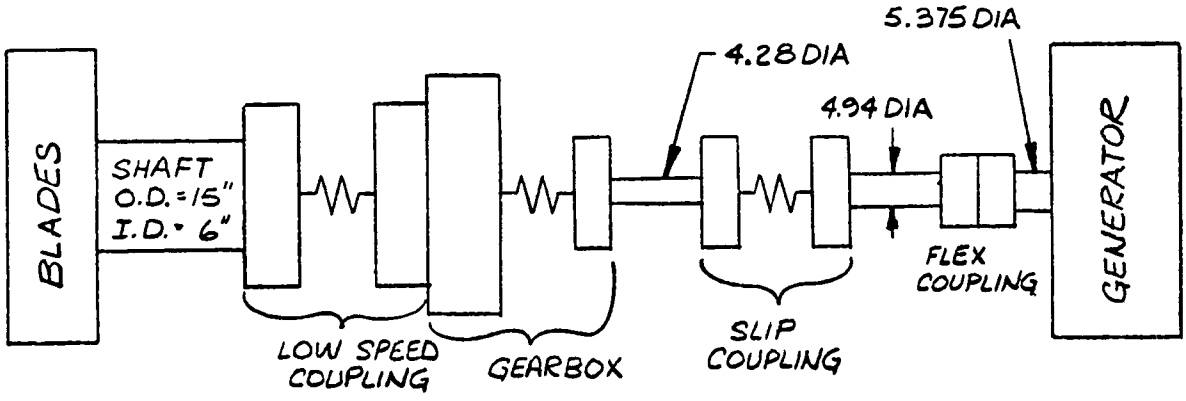

Figure 5.4-6. Baseline Drive Train Model

Table 5.4-1. Baseline Model Value

Values referenced to low speed shaft:

• Total Blade Inertia		1.721×10^7 in-lb sec^2
• Overall Low Speed Coupling	Stiffness	9.0×10^9 in-lb/rad
	Inertia	1046.0 in-lb sec^2
• Gearbox	Stiffness	3.38×10^8 in-lb/rad
	Inertia	105,500 in-lb sec

Values referenced to high speed shaft:

• Overall High Speed Slip Coupling	Stiffness	1.0×10^7 in-lb/rad
	Inertia	57.5 in-lb sec^2
• High Speed Flex Coupling	Stiffness	1.0×10^8 in-lb/rad
	Inertia	5.95 in-lb sec^2
• Generator Inertia		474.0 in-lb sec^2

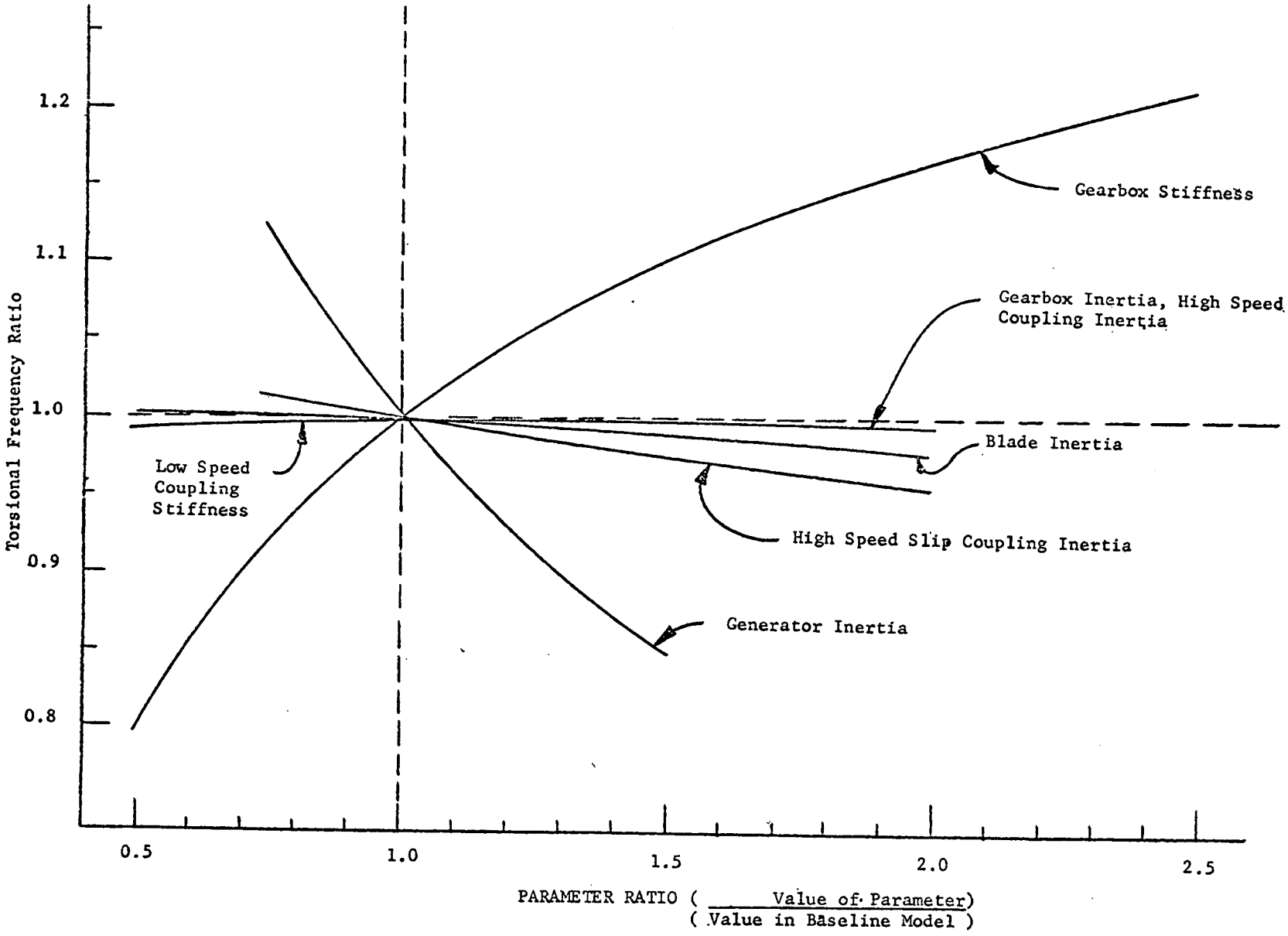

Figure 5.4-7. Stiffness Sensitivity Analysis

5.5 NACELLE

5.5.1 BEDPLATE AND FAIRING

5.5.1.1 Requirements

The bedplate supports the rotor and transfers all loads to the tower through the yaw bearing and yaw structure. Its stiffness must be such that, when attached to the tower, tower bending modes satisfy the requirements for frequency placement as discussed in Section 2. The bedplate must also provide a stiff foundation for all equipment mounted in the nacelle, particularly sufficiently stiff in bending to limit misalignment of the drive train under loading to the capabilities of the shaft couplings. A further stiffness requirement is that deflections at the yaw bearing should not severely degrade bearing life or induce large friction torques; this requirement is of the order of .010 to .020 inch maximum deflection out of plane under maximum loading.

The stress criteria for the bedplate are dictated by the NASA Statement of Work and the AISC code. Critical conditions are those which occur frequently covering a range of operating wind speeds, inflow and gust dispersion (Case A). For these loadings, stress levels must be maintained below the fatigue stress limits defined by Appendix B of the AISC code. Maximum loads are defined by the peak loads of Case B, up and down gust, from 35 to 50 and 35 to 20 mph. Application of the AISC code to the bedplate design represents a conservative approach that will provide adequate Margins of Safety.

The nacelle fairing is not treated as primary structure and is not subjected to the same dynamic loading as the bedplate. Criteria for design of the fairing follows standard commercial practice and is based on loading at maximum wind conditions. No permanent deformation is permitted at maximum loads (limit loads) and no failure allowed at 1.5 times design loads.

The NASA SOW requires the following provisions of the nacelle bedplate and fairing:

1. Provide environmental protection for equipment mounted in the nacelle.
2. Allow access from the top of the tower for maintenance.
3. Permit placement of equipment within the nacelle to locate the center of gravity on the tower axis.
4. Lightning protection.
5. Ventilation of the interior.
6. Exterior paint as defined by NASA.
7. Interior lights, convenience outlets and intercom.

A further design requirement for the bedplate and the fairing is that provisions be included for access to all components for maintenance and removal, even though components may be capable of a 30-year life without replacement.

5.5.1.2 Design Definition

The bedplate is defined by the assembly of Figure 5.5-1 (Drawing 298E460) and consists of several major subassemblies; a forward section shown in Figure 5.5-2 (Drawing 298E471), and Figure 5.5-3, an aft section (Drawing 298E472) and a rotor adapter structure Figure 5.5-4 (Drawing 298E473). The base section is built up from plate and standard structural shapes to form a rectangular box. Transverse members distribute the principal loads to the yaw bearing structure and allow for interruption of longitudinal beams to accomodate the gearbox. A hatch through the base permits access to the nacelle from the upper level of the tower. At the forward end, members support the generator and associated equipment. The rotor support adapter provides a transition from the circular bearing to the square section of the base section. Local stiffness is provided around the bearing bolting surface to limit out-of-plane deflections.

The fairing assembly is made up of five flat panels (four walls and a roof) that are bolted at the edges to form a rigid enclosure for the nacelle. Construction consists of frame-stiffened skins with thermal insulation between framing members. Joints are sealed by the use of elastomeric tape between faying surfaces. The roof may be removed as a unit to permit access to the nacelle for replacement of major components such as the gearbox or generator.

The bedplate supports and interfaces with all equipment mounted in the nacelle. However, the critical interfaces are those with major subsystems, including:

1. Rotor assembly
2. Pitch control mechanism
3. Yaw Structure
4. Fairing
5. Gearbox
6. Generator

The rotor interface is through the rotor bearing adapter structure, as shown in Figure 5.5-5 (Drawing 298E456). The rotor bearing housing bolts directly to the structure and the alignment of the rotor is determined entirely by the squareness of this surface with the remainder of the bedplate structure.

The pitch control mechanism interfaces with the bedplate structure at four clevis fittings on the rotor adapter. At these points, the pitch control actuator thrusts are reacted directly into the rotor bearing. The forward swing links that support the pitch change mechanism and react out-of-line thrusts from the actuators, are supported at three clevis fittings, shown in Section C-C of Figure 5.5-5.

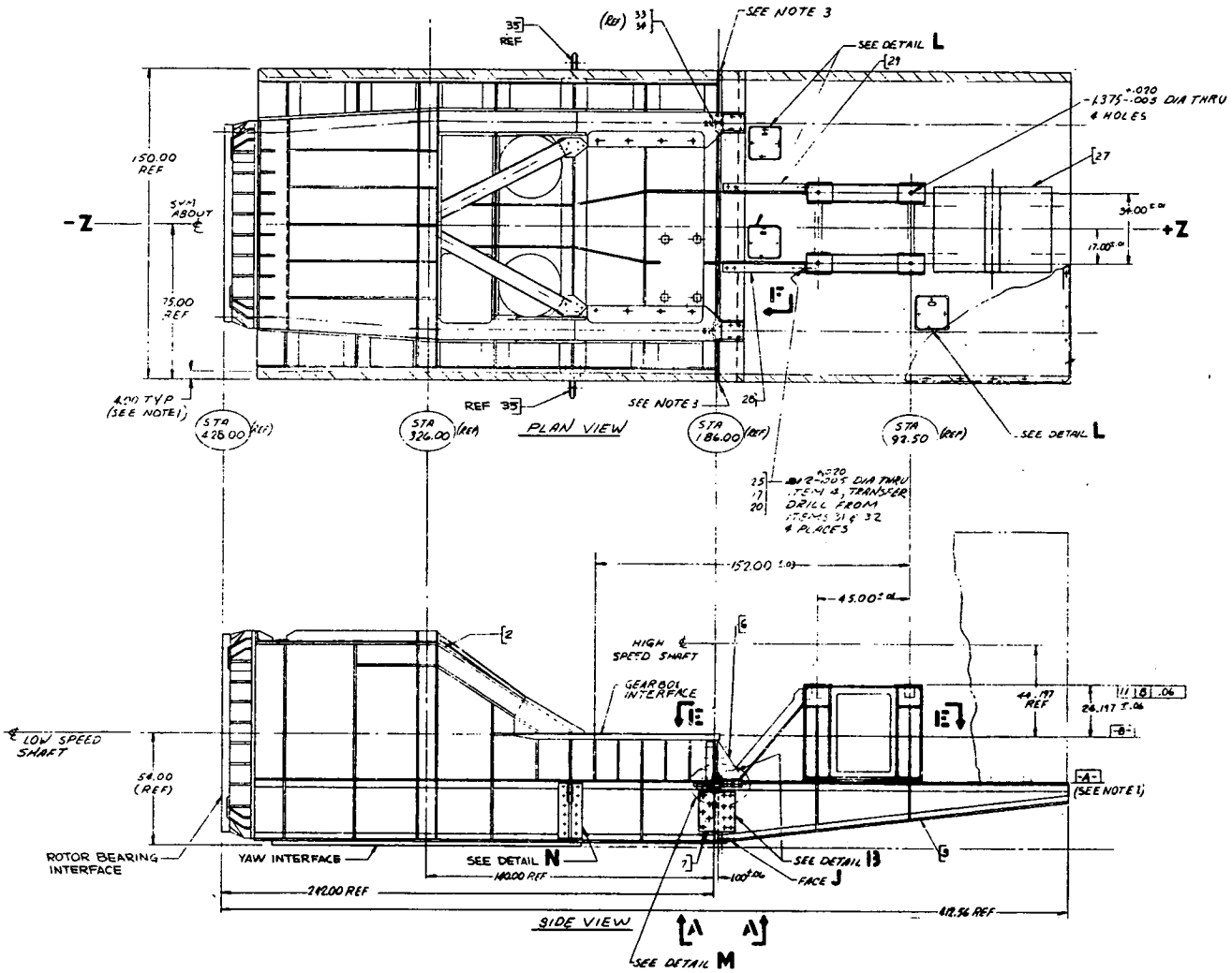

Figure 5.5-1. Bedplate Definition

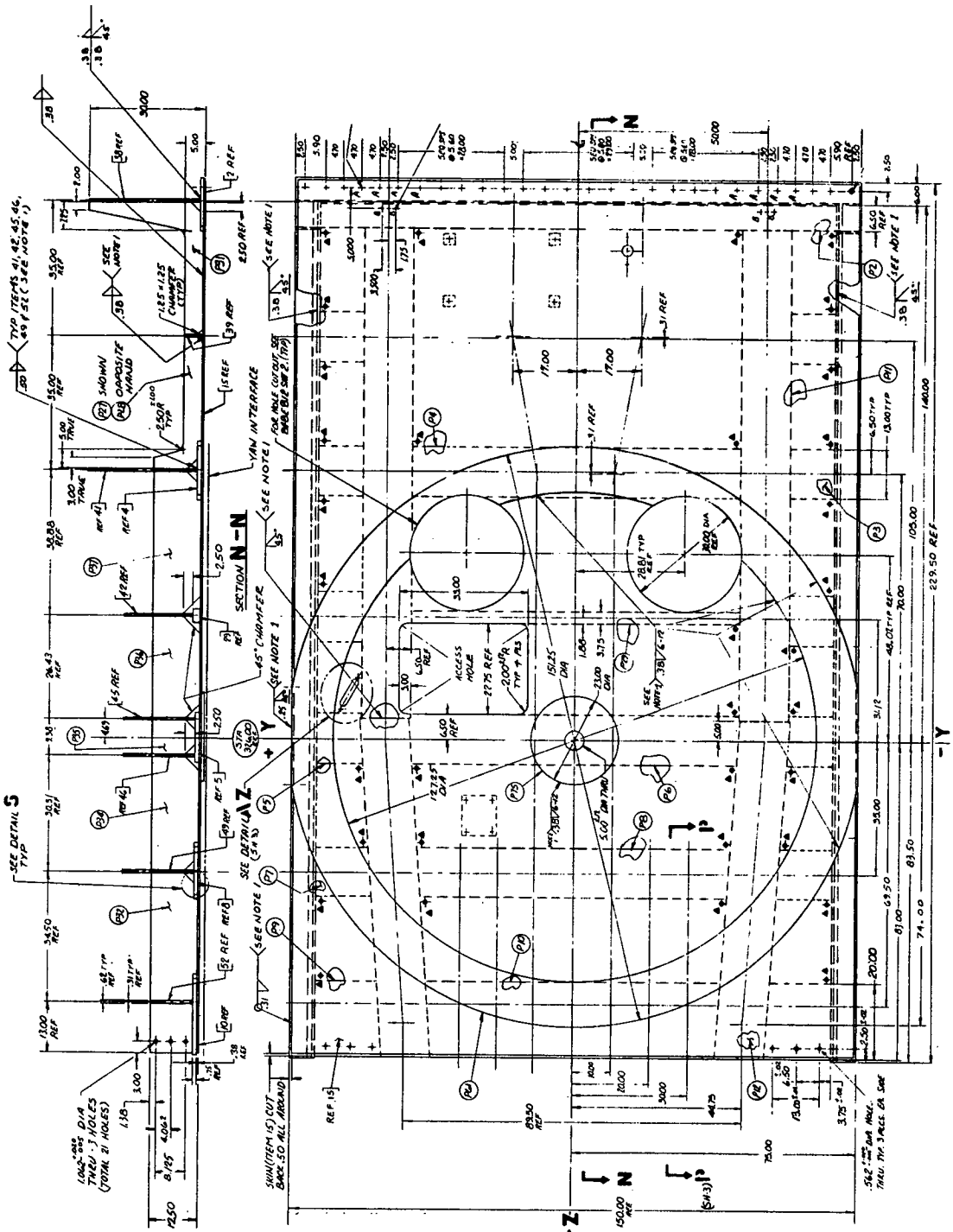

Figure 5.5-2 Aft Bedplate, Bottom View

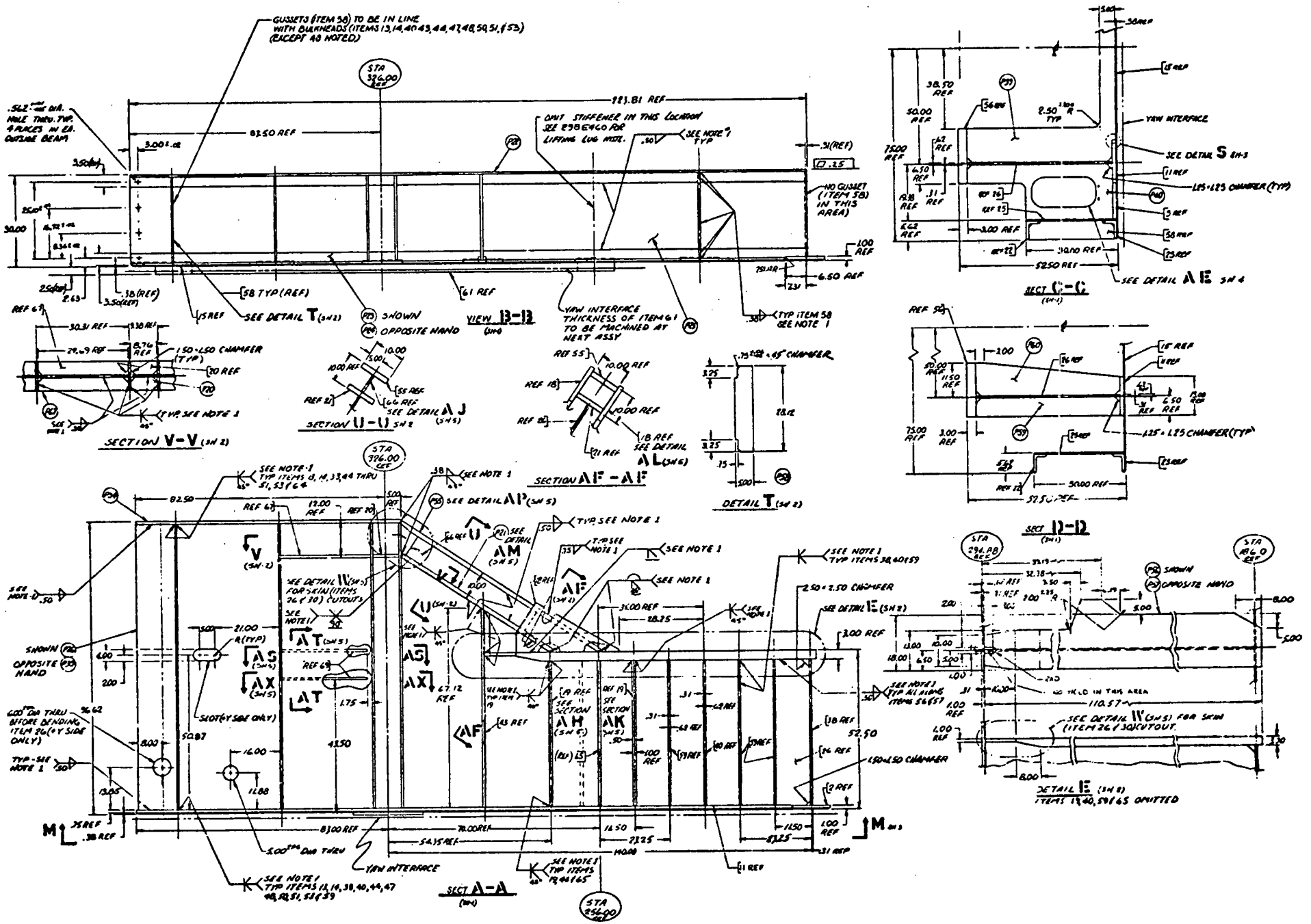

Figure 5.5.3 Aft Bedplate Section

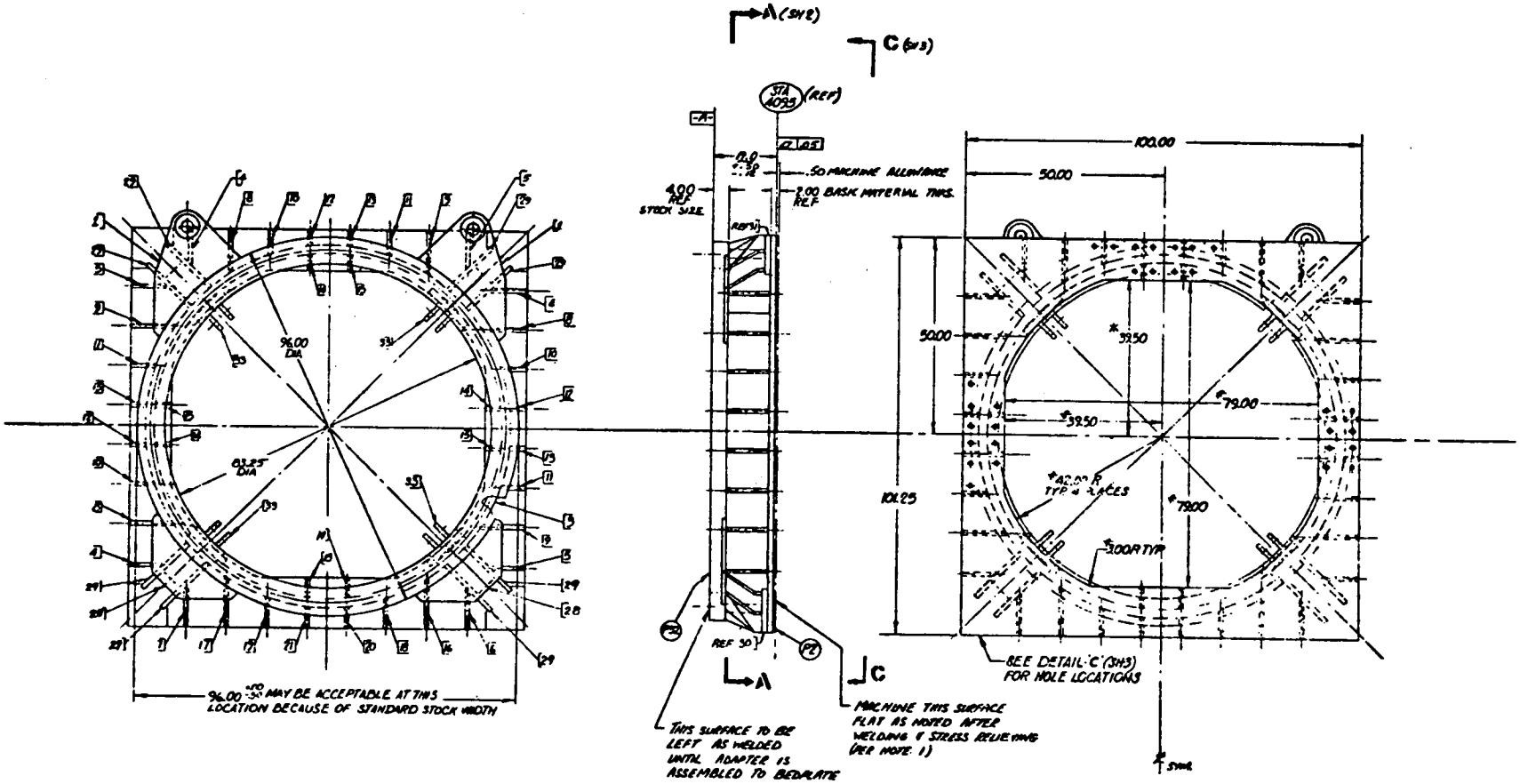

Figure 5.5-4 Rotor Adapter Structure

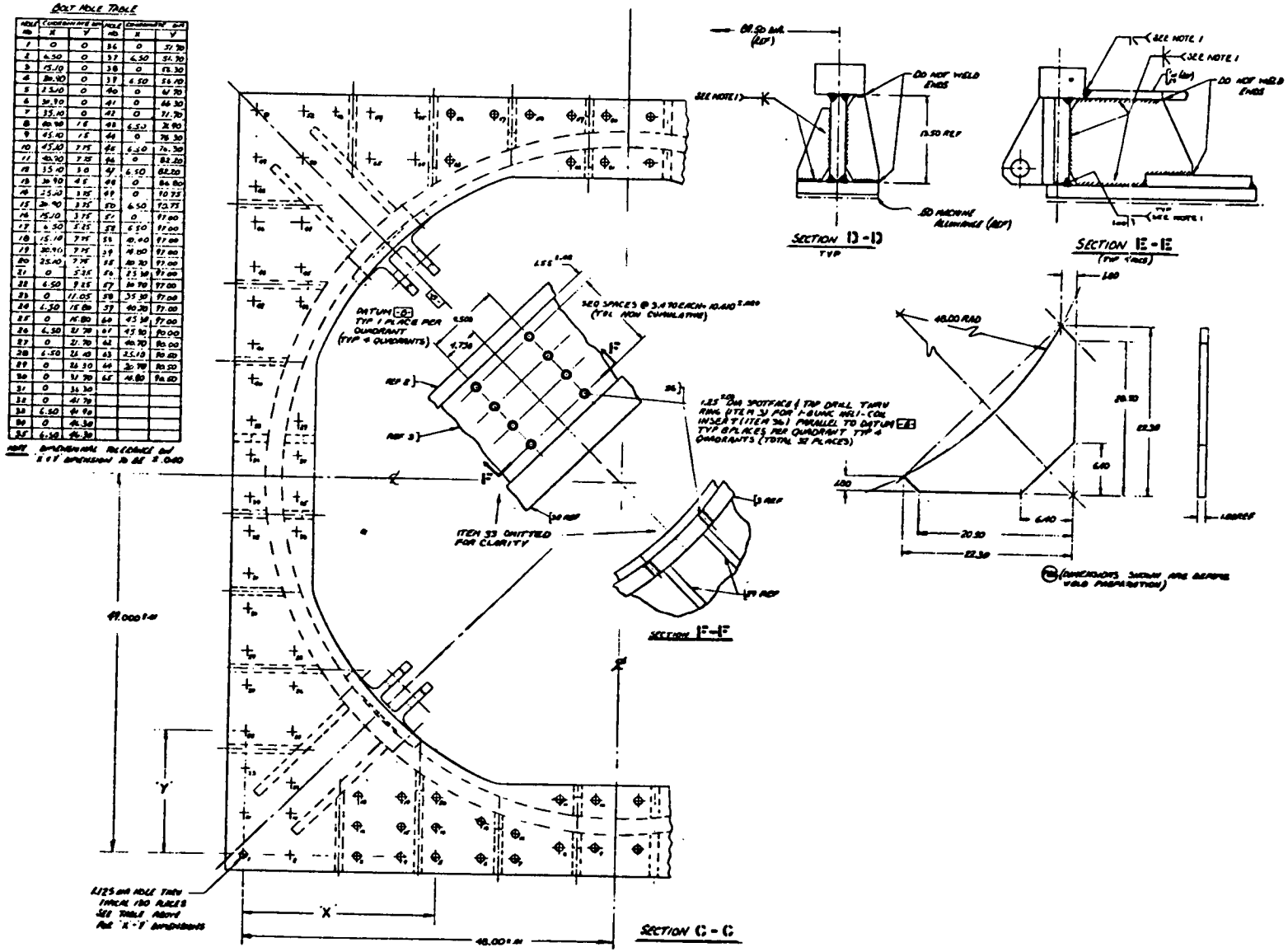

Figure 5.5-5 Rotor Interface

The yaw structure is bolted directly to the bottom face of the bedplate. This face is machined flat and parallel to the gearbox mounting surfaces.

The fairing interfaces with the bedplate around its perimeter as a bolted connection through the sill plates of the fairing.

5.5.1.3 Assembly and Maintenance

The bedplate is comprised of three major subassemblies: a forward section, aft section and rotor adapter structure. Each of these subassemblies is a steel weldment designed in accordance with AISC requirements. Where members are required to be removable for maintenance or replacement of components, they are fastened by bolting.

The most critical alignment in the bedplate assembly is to maintain the mounting face of the rotor adapter structure perpendicular with the mounting pads for the gearbox. This alignment will ensure that the rotor assembly, defined by the rotor hub bearing forward face (on the outer bearing race) is perpendicular to the low speed shaft of the gearbox. Alignment is obtained by making a final machine cut of the rotor adapter structure after it has been installed to the bedplate. Tolerances on this alignment will result in a change in slope of the drive shaft between the rotor and the gearbox and must be accommodated by the flexible gear coupling halves on the drive shaft. The drive shaft couplings will also permit a certain degree of lateral misalignment between the two mounting surfaces; however, this subject is more appropriately discussed as part of the rotor assembly installation requirements.

Misalignments between the gearbox mounting feet and the low speed stub shaft can be corrected for, to the extent that they are known in advance, by machining the bedplate mounting surfaces. However, the horizontal mounting pads also allow for shimming to reduce this misalignment, if required. Precise grinding is not required; a tolerance of 0.10 inch over the 100-inch diameter of the rotor adapter structure results in a slope error of 1 in 1000. This is well within the anticipated capability of the shaft coupling of 1/2 degree per engagement that will be required to accommodate dynamic deformation of the bedplate.

Since the drive shaft couplings can also accept some longitudinal misalignment, tolerances that locate the gearbox with respect to the rotor adapter structure in the longitudinal direction are not critical and will require no final machining of the bedplate assembly.

The fairing assembly will consist of a series of welded panel assemblies that ean be stacked for shipment. After a trial fit during the systems test, the fairing may be broken down for shipment. At the site, the fairing will be assembled by bolting and attached to the bedplate assembly.

Since the bedplate and fairing assemblies are essentially static structures, maintenance will consist of inspection for indications of fatigue cracks, buckling or other deformations, loose fasteners, corrosion, or other damage. It is anticipated that restoration of anticorrosive protection and external painting will be required at intervals from five to ten years.

5.5.1.4 Bedplate Design Evolution

The final bedplate design differs considerably from the concept originally presented at the Preliminary Design Review. This is a result of a change in the design approach that occurred during the early stages of final design definition. The concept originally presented was a complex truss, composed of standard rolled sections (mostly wide flange beams) of A36 low carbon steel. As the detail design progressed, it became apparent that this concept presented several problems:

1. Weight. The use of standard sections for all members meant that it would not be possible to optimize each member for the design loads. This implied the need to overdesign, resulting in an inefficient, overweight structure.

2. Growth Capability. During the early stages of design, the entire wind turbine design exhibited a steady growth, as each new load analysis resulted in the addition of more structural weight. The use of standard sections required a complete redesign and new geometrical arrangement with each load increase.

3. Welded Joint Configurations. The intersection between standard sections defined complex weld joints that would be difficult to weld and inspect. Review of preliminary drawings by consultants at Lehigh University pointed out the difficulty in establishing an appropriate stress concentration factor to apply to such joints in order to design for cyclic loading. Without the benefit of a second order finite element model of each joint configuration, the only option was to assign the lowest allowable range stress specified by AISC requirements. This constituted a severe design penalty in attempting to minimize structural weight.

4. Material Selection. Structural steel shapes are widely available in A36 steel. However, if suitable impact strength for low temperature operation is required, then testing costs added to A36 steel offset the low cost advantage of this steel as compared with other steels specifically intended for low temperature applications. The use of sheet or plate forms would open the selection to many other classes of steels that are not normally provided as structural shapes.

As a result of these considerations, the bedplate was reconfigured to a box girder type construction, using plate forms for all but a few secondary details. A516 Grade 70 steel was chosen, a material with good impact strength at low temperature, and less vulnerable to poor welding characteristics that sometimes occur as a result of the liberal chemical composition limits of A36. The plate design did not reduce the amount of welding required, but more of the welds could be accomplished as a continuous pass and could be categorized for higher allowable stresses. Since the configuration more closely resembled the box girder construction commonly used in bridge construction, it became easier to identify the appropriate weld joint category according

to AISC fatigue requirements (which are based largely on bridge construction). Optimization and design changes could be incorporated more easily by changing only the plate thicknesses without redefining the basic geometry.

5.5.1.5 Life

Failures affecting the life of the bedplate and fairing assemblies are fatigue, cracking and corrosion. The use of conservative strength criteria for these structures ensures that stress levels will remain below endurance limits and infinite fatigue life should be achieved. Periodic inspection of joints and other areas of high stress concentration should identify potential failures before they occur and while the damage is still repairable.

The bedplate structure follows standard practices for prevention of corrosion in steel structures as defined by AISC code. Design details consider the necessity for drainage holes and avoiding enclosed spaces that can collect water or are difficult to protect and inspect. Concealed joints that are likely starting points for crevice corrosion are avoided. Protective coatings include a shop-applied zinc-rich primer and enamel finish coat, with an on site touch up.

5.5.2 LUBRICATION AND ENVIRONMENTAL CONTROL

5.5.2.1 Requirements

The lubrication oil system provides lubricant for the rotor bearing as well as the gearbox. The system is required to maintain a sufficient flow of oil within an acceptable viscosity range of 340 to 5,000 SUS at all operating temperatures. During startup when ambient temperatures are below 55°F, the oil must be heated and circulated before rotation can begin; at oil temperatures above 150°F, the oil must be cooled by circulation through an external cooler.

The heat dissipated in the gearbox and rotor bearing varies with the amount of power generated, which is a function of wind speed. As shown in Figure 5.5-6, the maximum heat dissipated is 147 hp or 374,000 Btuh. The temperature rise through the system, based on a flow rate of 66 gpm is 30.6°F.

The environmental control system, operating in conjunction with the oil lubrication system, is required to maintain the air temperature within the nacelle within acceptable limits. The most sensitive equipment within the nacelle is the nacelle multiplexer unit, which must operate within an ambient air temperature of 0° to 130°F. The generator draws cooling air from within the nacelle and exhausts externally, utilizing a built-in fan.

5.5.2.2 System Description

The lubrication system is shown schematically in Figure 5.5-7. The lube oil and ventilation systems have three operational modes that include: startup, normal operation, and shutdown.

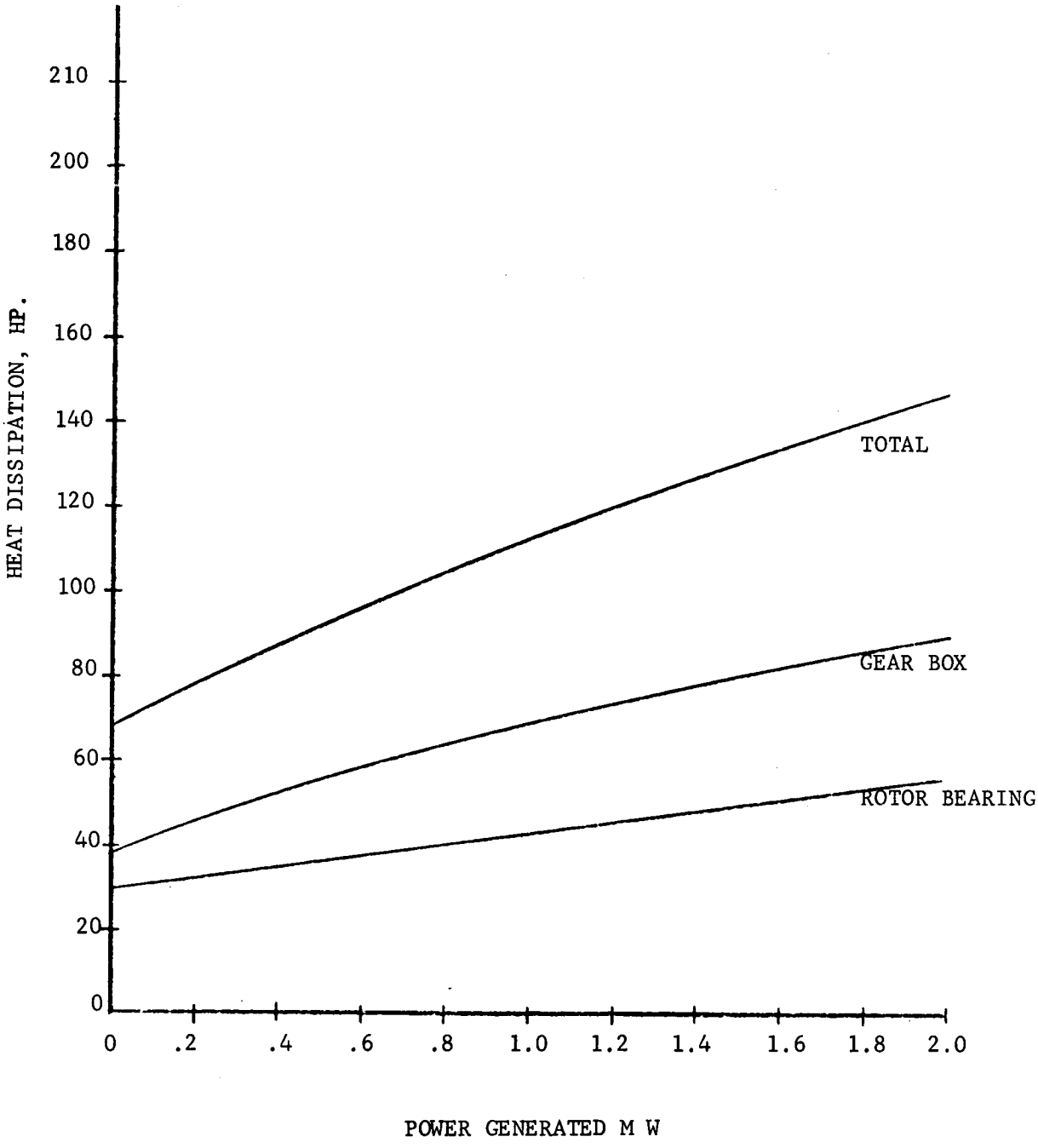

Figure 5.5-6. Heat Dissipation

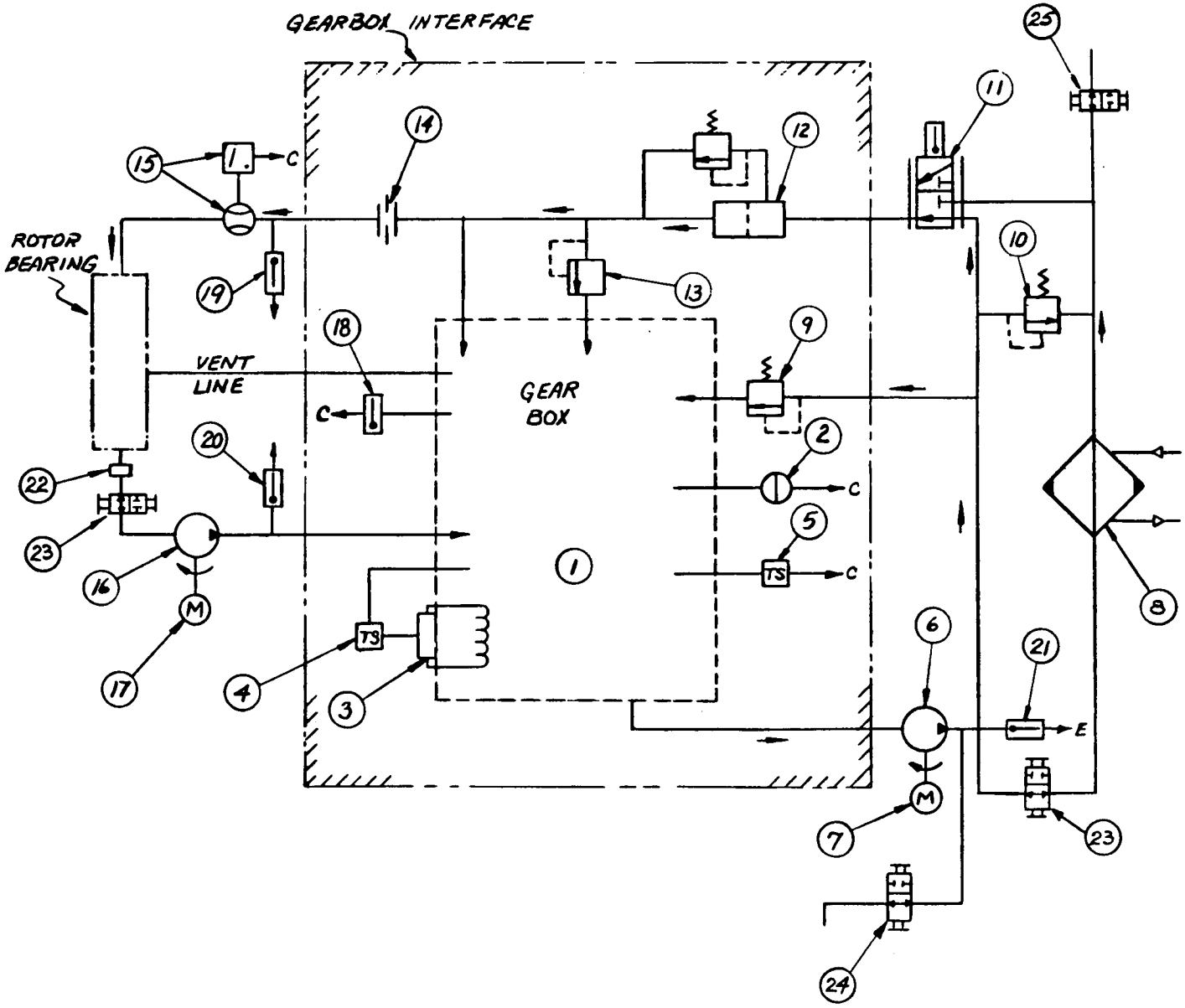

SYSTEM DESCRIPTION TABLE

ITEM NO	NAME	SYSTEM IDENT. NO	REMARKS
1	RESERVOIR		80 GAL CAPACITY
2	LEVEL CONTROL SWITCH	LM30LLS1	OPENS WHEN LEVEL < 70 GAL
3	SUMP HEATER	-	2 REQD. THERMO-STAT CLOSES WHEN TEMP < 240°F
4	SUMP OIL TEMP CONTROL SWITCH	-	OPENS WHEN OIL TEMP > 70°F
5	PUMP CONTROL SWITCH	LM26TS5	CLOSES WHEN OIL TEMP > 60°F
6	MAIN LUBE PUMP	-	60 GPM - 200 PSI MAX.
7	MAIN LUBE PUMP MOTOR	-	15 HP - 480 VOLT 3Ø
8	OIL COOLER	-	375,000 BTUH CAPACITY
9	PRESSURE RELIEF VALVE	-	SET AT 90 PSI
10	PRESSURE RELIEF VALVE	-	SET AT 75 PSI
11	THERMOSTATIC MIXING VALVE	-	FLOW BY-PASS COOLER OIL TEMP <120°F
12	FILTER	-	25 MICRON - 60 GPM SET TO BY-PASS 25 PSI
13	PRESSURE RELIEF VALVE	-	SET AT 30 PSI
14	FLOW CONTROL ORIFICE	-	15 GPM - ORIFICE DIA = .457 IN.
15	FLOW CONTROL SWITCH	LM31FS1	SHUTDOWN FLOW <13.5 GPM
16	RETURN (SCAVENGE) PUMP	-	15 GPM - 10 PSI 1800 RPM
17	RETURN PUMP MOTOR	-	3 HP - 208 VOLTS 3Ø 1750 RPM
18	TEMP SENSOR	LM29RTD1	SHUTDOWN - OIL TEMP 55°F >T> 170°F
19	TEMP SENSOR	EM63TS2	-
20	TEMP SENSOR	EM67TS6	-
21	TEMP SENSOR	EM64TS3	-
22	MAGNETIC PLUG	-	SELF CLOSING
23	VALVE	-	MANUAL ISOLATION 2 REQD
24	VALVE	-	MANUAL - DRAIN
25	VALVE	-	MANUAL - VENT

Figure 5.5-7 Lubrication System Schematic

5.5.2.2.1 Startup

Startup is the interval between shutdown and normal operation during which time the oil is heated or cooled to the operating range of 60°F to 170°F, as measured at the high speed bearing of the gearbox.

(a) Cold Start (oil temperature in sump less than 70°F)

As soon as power is supplied by the utility the gearbox sump heaters and pipe trace heaters are turned on and continue to heat until their respective thermostats register 70°F. When the main lube pump thermostat located in the gearbox sump registers 60°F or greater, the main lube pump and the return pump will start pumping, if CODAS has supplied the enabling power. The main lube pump pumps oil from the sump to the gearbox and rotor bearing, and the return pump returns the oil from the rotor bearing to the gearbox sump.

When the sensor located in the exit port of the critical high speed bearing in the gearbox registers between 60°F and 170°F, CODAS will interpret this signal to mean that the lube oil system is ready and capable of providing adequate lubrication to the gearbox and rotor bearing.

(b) Hot Startup (oil temperature in the gearbox reservoir is equal to or greater than 70°F)

The main lube pump and return pump will start pumping as soon as CODAS supplies the enabling power.

When the temperature sensor located in the exit port of the high speed bearing in the gearbox registers between 60°F and 170°F, CODAS will interpret this signal to mean that the lube oil system is ready for operation.

5.5.2.2.2 Normal Operation

Normal operation follows from a successful completion of a startup sequence and continues until a shutdown occurs.

5.5.2.2.3 Shutdown

Shutdown dictated by a lube oil system symptom will occur during startup or normal operation when one of the following signals is received by CODAS:

a. Oil level sensor in the gearbox sump indicates that the running oil level is 10 gallons below the normal value.

b. The high speed bearing sensor in the gearbox indicates that the temperature is less than 60°F or greater than 170°F after startup.

c. The flow sensor at the inlet to the rotor bearing registers flow less than 13.5 gpm after the main lube pump has started pumping.

The ventilation system consists of two inlet louvers on the forward face of the nacelle fairing, an exhaust fan with automatic louvers on the aft face of the fairing, and an exhaust duct that carries cooling air from the hood of the generator to the outside. The inlet louvers have fixed vanes and are protected by wire screens. They are sized to accommodate an inlet flow of 10,000 cfm. The exhaust fan is rated at 5,000 cfm and an additional 5,000 cfm is drawn by the generator for cooling. The exhaust fan is thermostatically controlled to operate when the nacelle temperature exceeds 90°F.

5.5.3 YAW SUBSYSTEM

5.5.3.1 Function and Requirements

The yaw subsystem (YS) functions discussed in this section are at an overall subsystem level. Functions of the individual components of the YS are described in succeeding paragraphs.

The YS primary requirement is to position and align the nacelle assembly with the wind velocity vector. Changes in the wind direction would require the YS to follow the wind by repositioning the nacelle/rotor accordingly. The YS also provides the structural interface and transition between the top of the tower, and the rotating bedplate/nacelle.

During the design effort investigations into various wind cases, plus Mod-0 experience, indicated that structural load amplification would occur if the YS permitted any "free-play" in the rotational drive mechanism. Therefore, pressure is applied to the brakes at all times: 1,000 psi while yawing, 3,000 psi when no yaw maneuver is taking place.

Another function provided by the YS is automatic relief from rotational overload conditions that may occur from sudden changes in wind in-flow angles.

Additional design requirements of the YS are:

1. Provide ample stiffness, when attached to the tower and bedplate, so that the stiffness characteristics shall satisfy the frequency placement requirements.

2. Provide stiffness requirement of the primary structural members to limit deflections at the yaw bearing interface to .010 to .020 inch. This deflection prevents degradation of the bearing performance in terms of long life and increased friction torques.

3. Provide support structure for all YS components.

4. Provide manned access for maintenance, repair, installation and removal of all YS components.

5. Provide ingress/egress for the nacelle.

6. Satisfy AISC, ASTM, AFBMA and AWS requirements.

7. Compliance with NASA SOW:

   a. Crossed roller bearing with internal gear

   b. Worm drive or hydraulic drive

   c. Yaw rate shall not exceed 2^{o}/second

5.5.3.2 Design Description

GE Drawing 47J240701 (Figure 5.5-8) shows the overall yaw subsystems assembly. The basic YS occupies an envelope size of 176 inches in diameter by 93-7/8 inches high. The YS is positioned on the centerline of the tower which establishes the centerline of rotation in a horizontal plane for yaw maneuvers. Positioning the nacelle/rotor assembly by a yaw maneuver is provided by a bull gear/ring bearing driven by two pinion gears at a constant rate of 0.25^{o}/second.

The lower support structure for the bearing, referred to as the lower yaw structure, is provided by an annular ring weldment that attaches to the top of the tower. This ring serves to distribute the load reactions from the eight tower supports to the inner race of the yaw bearing, attached via a total of forty-eight 1-1/4 - 7 UNC high strength bolts. The upper flange is extended radially outward to form a circular disk for the yaw brakes to engage.

The upper yaw structure, located above the ring bearing, is also a weldment. The structure attaches to the outer race of the bearing via a total of forty-eight 1-1/4 - 7 UNC high strength bolts. The upper surface of the structure is then bolted to the nacelle bedplate structure. The nacelle, structure and outer bearing race assembly presents an integral configuration that is capable of rotating about the centerline of the tower. The upper structure also supports the two hydraulic drive motors with a pinion and shaft subassembly, via two individual bearings. These two bearings remove an overhung load condition from the shaft bearings in the hydraulic drive motor. Thus, extended life is gained for these bearings. The output shaft of the hydraulic drive motor is joined to the pinion drive shaft with flexible gear couplings, which are key mounted onto their respective shafts.

The yaw bearing will be manually lubricated using the grease fittings accessible from inside of the yaw structure.

5.5.3.2.1 Yaw Structure

GE Drawing 298E483 (Figure 5.5-9) shows details of the lower support structure for the YS. It is an annular ring weldment that serves to distribute the load reactions from the eight tower support points to the inner race of the yaw bearing. ASTM A516 Grade 70 structural steel is utilized for the fabrication and welding in accordance with Appendix B of the

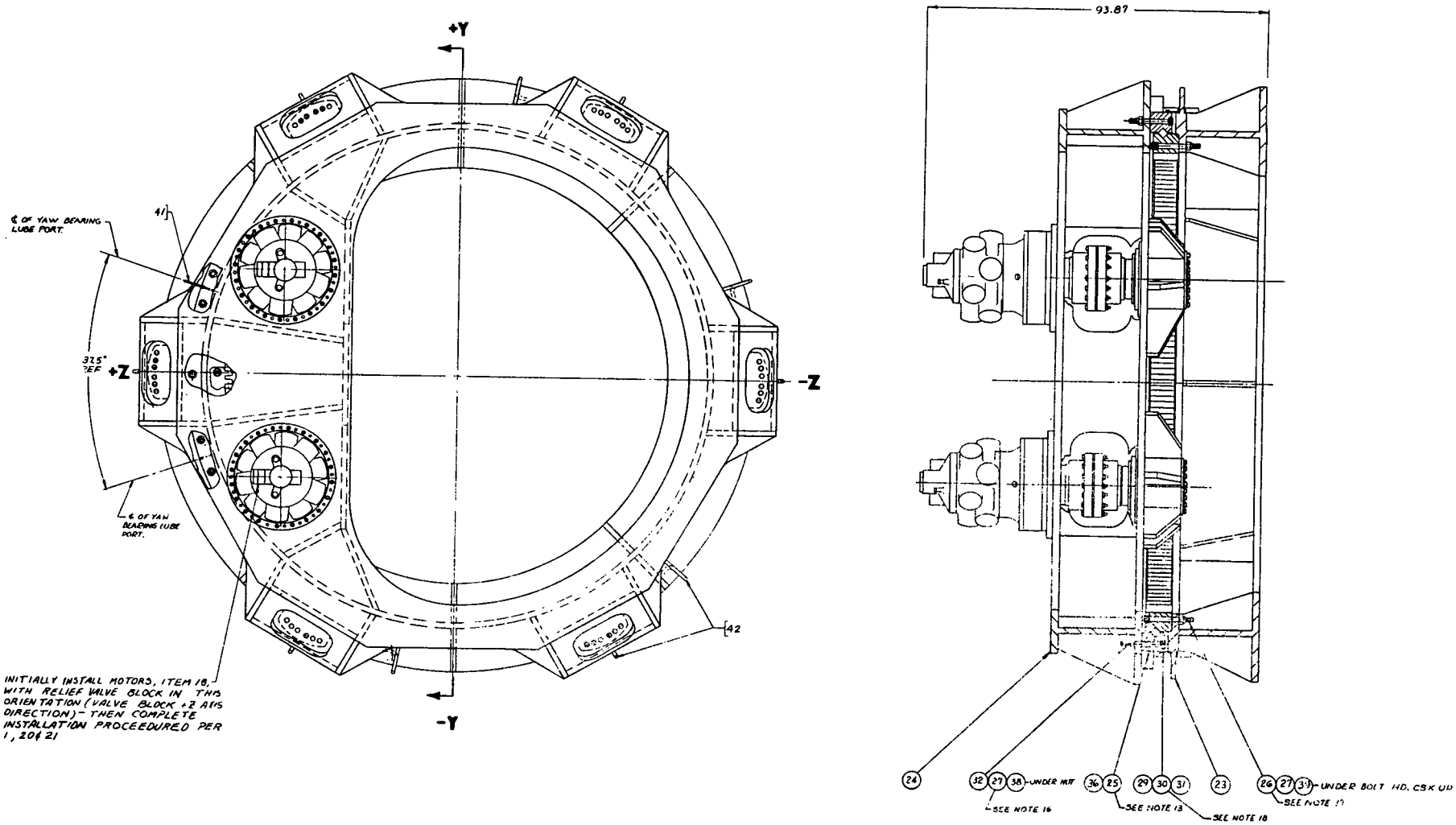

Figure 5.5-8 Yaw Subsystem Assembly

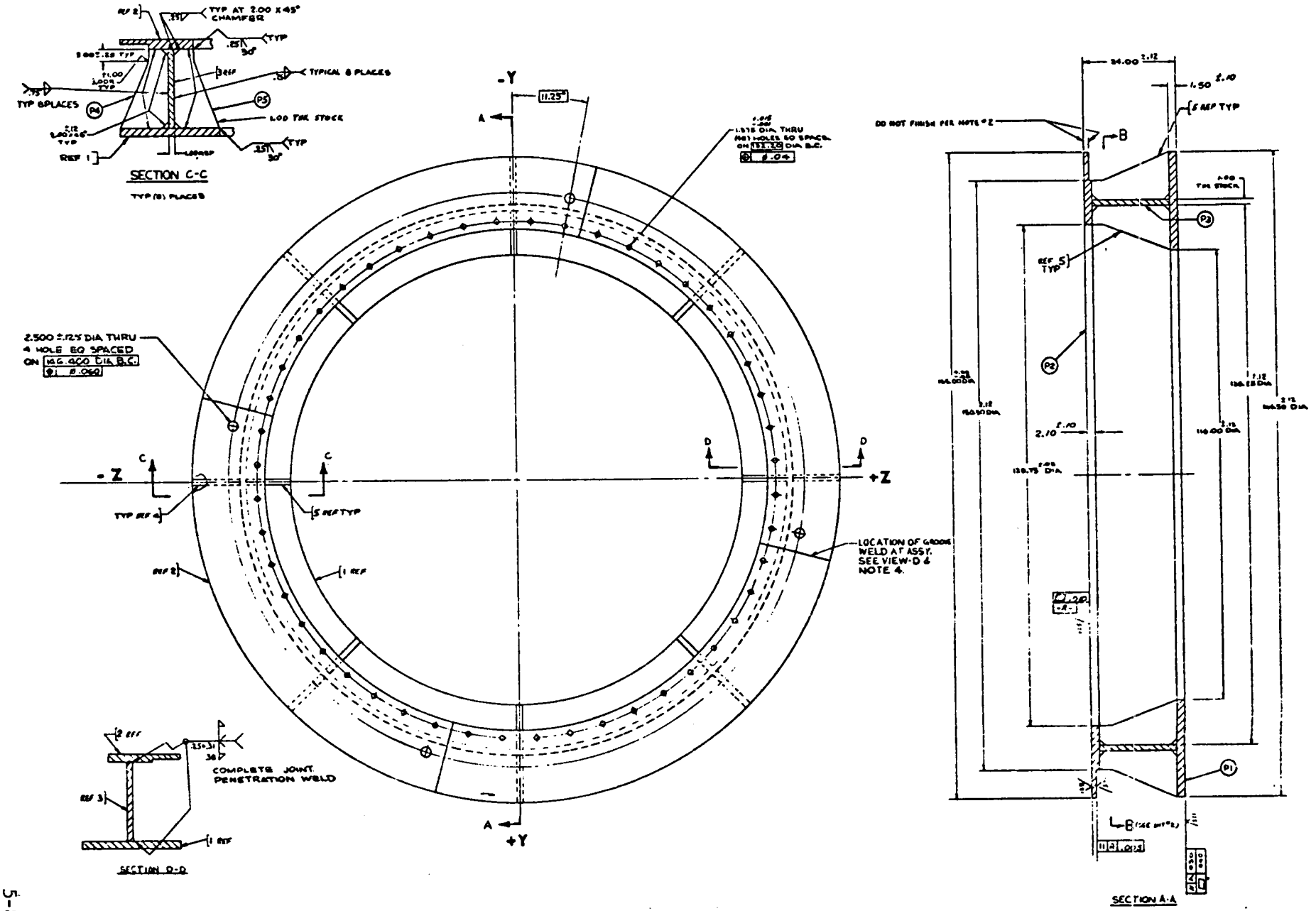

Figure 5.5-9 Lower Yaw Structure

AISC Specification for fatigue loading.

All welded joint preparation, type of welding and heat treating and inspection procedures are in accordance with the Structural Welding Code published by the American Welding Society. Generally, all welding is full penetration using submerged arc technique, ultrasonically inspected and stress relieved prior to final machining.

The annular ring is 166.5 inches in diameter by 25 inches high. One lower flange is bolted to a prepared fitting that terminates the tubular structure at the top of the tower. The upper flange is extended radially outward and machined on both sides to form the disk for the yaw brake. Cap and web thicknesses that provide the desired section properties were determined by stress analyses shown in paragraph 5.5.6.

A shroud encircles the yaw bearing and serves to retain the bearing grease. The shroud will rotate with the nacelle. A second closure is installed in a horizontal plane at the tower/YS interface. It also serves as a work platform for the YS. A hatch is provided in this closure for ingress/egress to and from the nacelle. Neither of the closures are sealed, but will weather protect the YS components and keep birds and animals from entering.

A ladder is provided from the upper section of the tower to reach the door in the lower yaw closure. The YS structure provides an extension of the ladder through to the lower hatch located in the nacelle bedplate.

The hydraulic power system, and controls for the yaw brakes and yaw drive motor, are located in the nacelle.

A cable raceway provides support for electrical cables from the slip ring to the junction boxes at the top of the tower. The cable raceway also serves as the anti-rotational structure that restrains the lower portion of the slip ring assembly in a fixed position.

If a total failure of the YS should occur (i.e., loss of driving, holding and braking pressure), a manually operated pump can be used to pressurize each yaw brake and thus provide the holding power. This feature can be used for emergency application and for repair/maintenance services during a normal shutdown period.

GE Drawing 298E481 (Figure 5.5-10) shows the upper support structure for the YS. It is similar to the lower support structure in that it also is a fabricated annular ring weldment. Welded joint configurations were also designed in accordance with AISC, ASTM and AWS requirements.

The annular ring is 175.7 inches across the brake support structure by 28.4 inches high. Secondary beams and branches have been welded, drilled and machined to provide the required mounting provisions for the hydraulic drive motor, pinion bearings, yaw brakes, external shield, hydraulic lines, and lubrication lines. (Reference GE Drawing 47J240701, Figure 5.5-8).

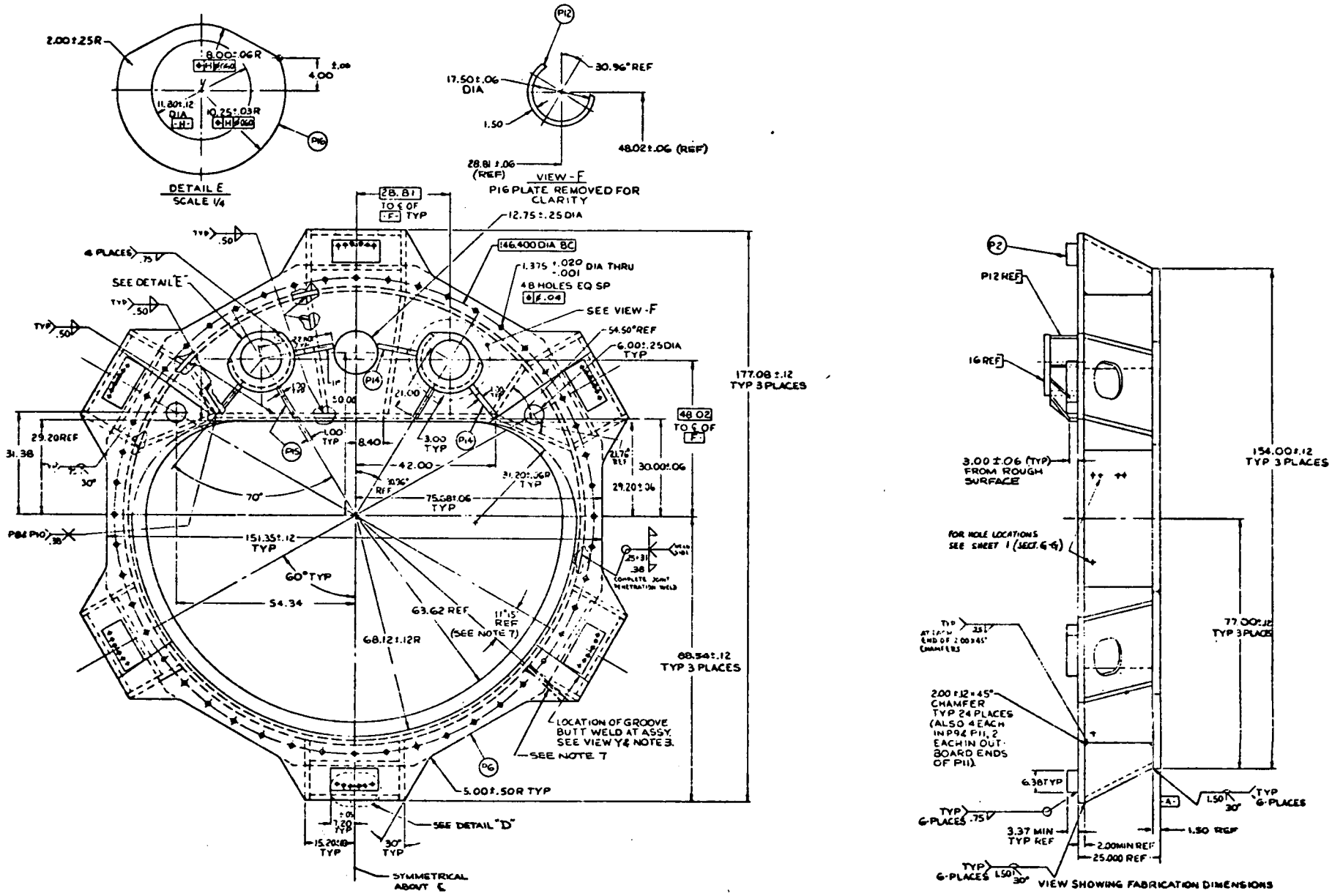

Figure 5.5-10 Upper Yaw Structure

The primary load carrying members are the upper cap-to-bedplate interface and the lower cap-to-yaw bearing interface.

5.5.3.2.2 Yaw Drive Train

All elements that provide the motive power to turn the nacelle about the yaw axis are included under the term "yaw drive train". By extension, the yaw brakes, which provide damping to the yaw drive, and locking forces when the nacelle is at rest, are included in this discussion. The yaw drive train consists of a hydraulic supply (including accessories described below), hydraulic motors with integral gearbox, splined coupling, drive pinion and bull gear integral with the yaw bearing. Yaw brakes are pressurized by the yaw hydraulic supply, located in the nacelle.

5.5.3.2.3 Yaw Bearing and Mating Pinion

GE Drawing 298E478 (Figure 5.5-11) shows the basic cross section of the crossed roller type bearing with an internal gear. This drawing accompanies Specification 273A6416 as an outline configuration control document. All critical areas of the bearing design and definition that appear in the Specification 273A6416 were analyzed and confirmed by Mr. John Rumbarger of Franklin Institute Research Laboratories, a recognized authority in large bearing design.

The major contributor to the final envelope size of the bearing is the gear face size required to accommodate the tangential force that develops the torque necessary to position the nacelle.

The maximum yaw torque each motor is capable of generating is 550,000 ft-lb. or a combined total of 1.1×10^6 ft-lb. This driving torque, in combination with the damping torque of 760,000 ft-lb. provided by the yaw brakes, is sufficient to overcome the external dynamic torques. In calculating the gear tooth configuration, a torque of 600,000 ft-lb. was assumed.

With the gear pitch diameter at 124 inches, the tangential force requirement is calculated to be 58,064 pounds per pinion. Using the Lewis formula:

$$FW = \frac{TF}{SY/DP} \quad \text{where}$$

FW = Gear face width in inches

TF = Tangential force in pounds

S = Allowable fatigue stress = 48,000 psi (R_c = 30, 100,000 cycles)

Y = Form factor for 20° full depth involute tooth pinion = 0.264

DP = Diametrial pitch = 1.0

Therefore, the FW = 4.58 inches for a single pinion load application. (The yield strength of the gear teeth at R_C 30 will equal a minimum of 117,000 psi.) Thus there will be a positive margin of safety with the actual face width of 7.00 inches.

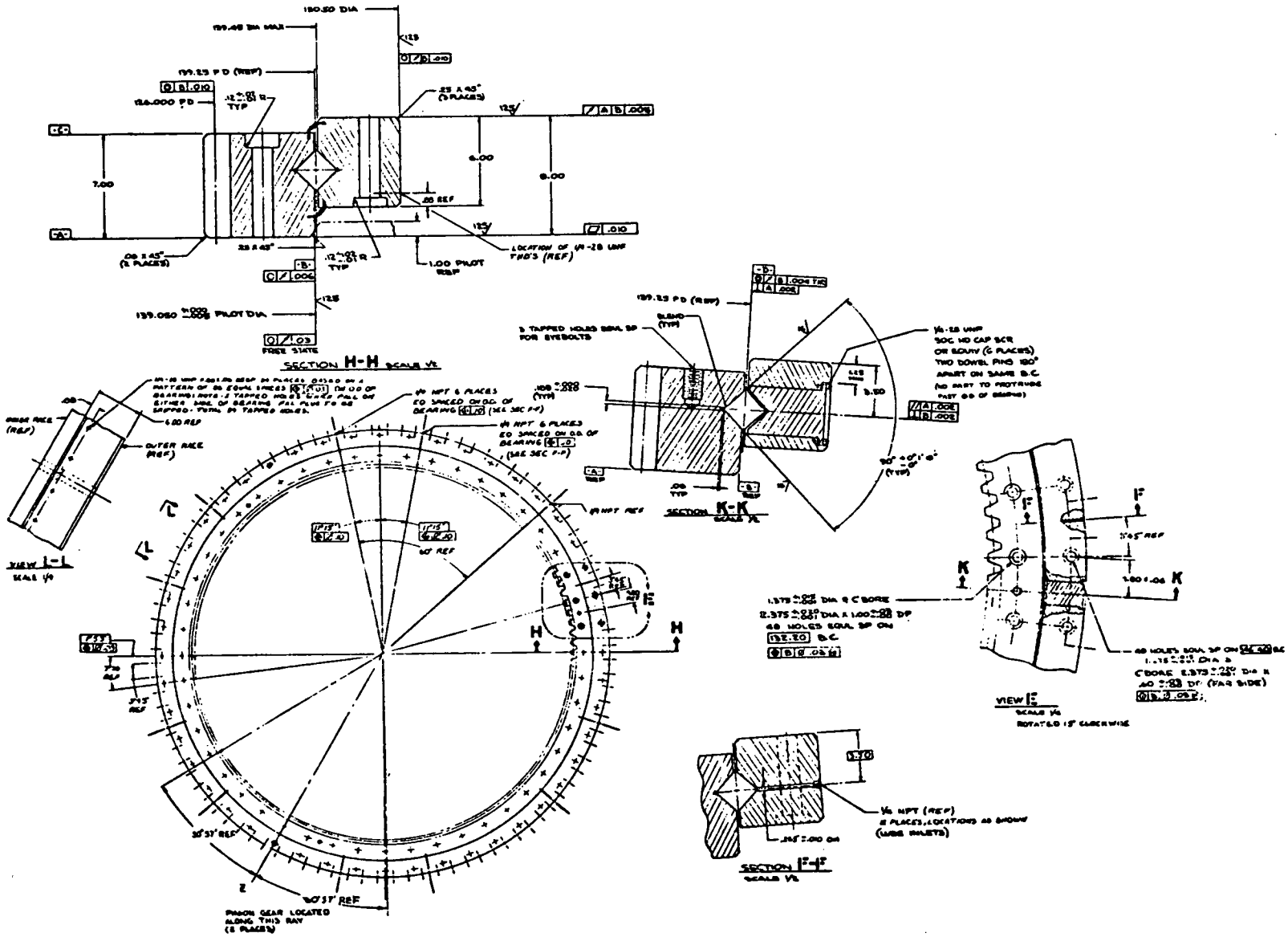

Figure 5.5-11 Yaw Bearing

As a result of the trade-off involving the parameters shown above, and optimizing fatigue characteristics to achieve the long life requirement, a bull gear design incorporating 126 teeth was arrived at. For the pinion, thirteen involute gear teeth were accomodated on a minimum pinion pitch diameter at 13 inches, with a DP of 1.0. The objective here was to minimize the torque requirements on the pinion drive shaft and subsequent requirements placed on the hydraulic drive motor. Thus, the gear ratio of 9.7 was established for the pinion to bull gear.

5.5.3.2.4 Yaw Brake

The rationale for the use of these brakes is as follows:

1. Locks out backlash (free-play) in the yaw drive train during the static and maneuvering modes.
   Advantages:

   a. Increases stiffness in the yaw direction, thus eliminates dynamic loading of the WTG system.

   b. Reduces fatigue loading on the gear teeth of the bearing bull gear and mating pinion gear, thus increasing their design life.

   c. Removes fatigue loading on the gears and bearings located in the hydraulic motor, thus increasing their design life.

2. Reduces maximum loads for extreme wind conditions for the entire yaw drive train.
   Advantages:

   a. Assists the hydraulic motors in overcoming peak yaw dynamic torques.

   b. Eliminates the need for a safety clutch.

   c. Maintains a gear face height that is compatible with the required bearing forging size.

3. Provides a yaw locking feature during maintenance periods.

4. Provides emergency stop.

The yaw brake is defined by GE Drawing 163C5355 (Figure 5.5-12). The cyclic yaw torques, as defined by dynamic analysis, can reach as high as 1.8×10^6 ft-lb. The torque generated by both yaw motors is 1.1×10^6 ft-lb. If the polarity of the external yaw torque is in opposition to the driving torque of the motor, a worst case deficit of 700,000 ft-lb. of torque exists, with the possiblity that the nacelle would be driven, momentarily, counter to the commanded direction of rotation. With 1,000 psi on all brakes, an additional retarding torque of 760,000 ft-lb. is provided to oppose the external torque,

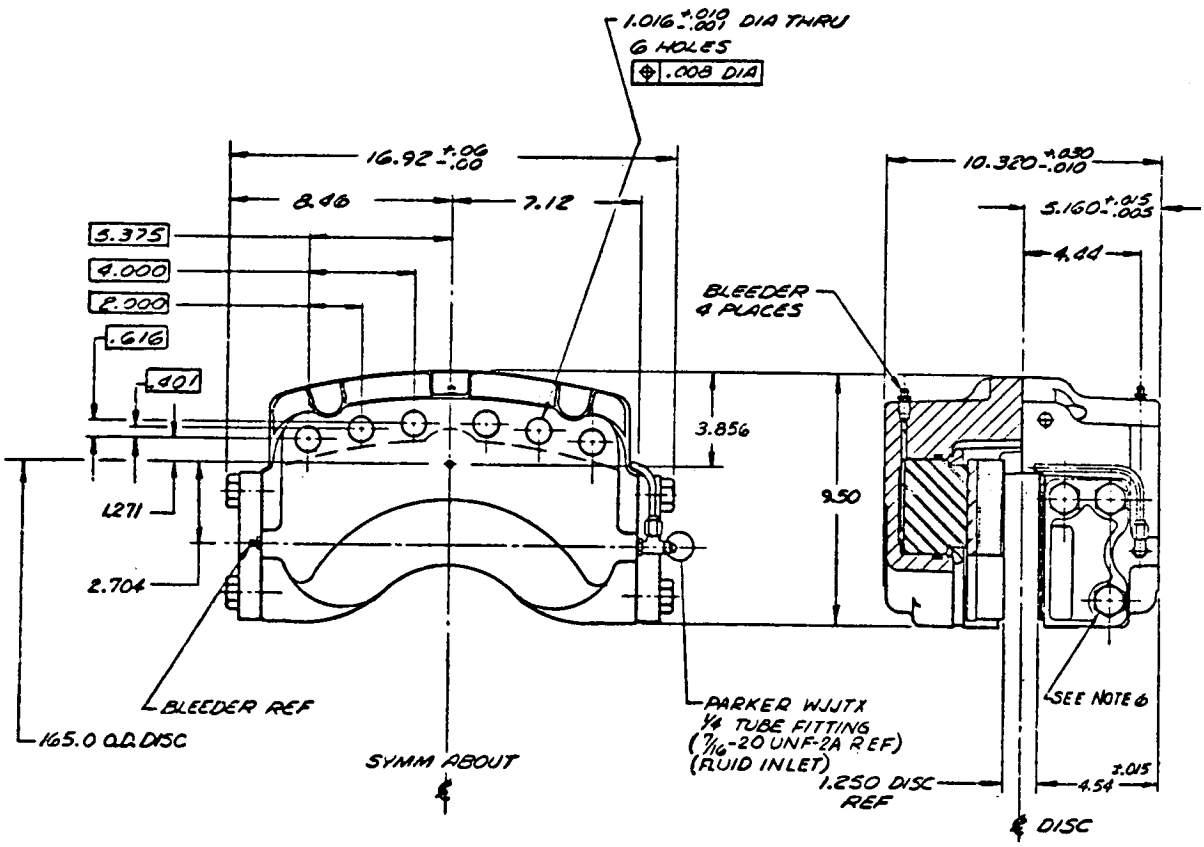

Figure 5.5-12. Yaw Brake

thus the net torque on the nacelle, with 1,000 psi pressure, is zero, preventing a potential regressive motion of the nacelle. Similarly, when the polarity of the external yaw torque is of the same sign as the polarity of the yaw motor driving torque, an excessive torque level can be generated. The retarding torque of the engaged yaw brakes acts as a modifying factor in this respect. It should be remembered that the yaw drive motors rotate at a constant speed. If the external torques should drive the nacelle ahead of the motor, the motor torque will be reduced to zero, and even provide negative (retarding) torque of up to a maximum of 1.1×10^6 ft-lb. This system has been evaluated with a computer simulation and appears satisfactory.

During shutdown periods and non-maneuvering modes, all six brakes are engaged in a static configuration that produces a holding force of 2.1×10^6 ft-lb. at an applied pressure of 3,000 psi.

The selected brake is an off-the-shelf, hydraulic actuated, disk caliper brake manufactured by the Goodyear Corp., Berea, Kentucky. It occupies an envelope size 17 inches long by 10.4 inches wide by 9 inches high. The total weight is approximately 2,000 pounds. This brake has been in service for over four years on 200-ton trucks and earth moving equipment. Clark Equipment Co. and Unit Rig Equipment Co. are the largest users of this brake. Goodyear Corp. has tested the brake with 200,000 on/off cycles at the rate of 3 cycles per minute using 3,000 psi hydraulic pressure without a failure. The brake has been successfully operated at 3,500 psi and pressurized to 8,000 psi in an attempt to burst the piston and/or cylinder housing, without failure. The operating pressure range for the WTG application is 1,000 to 3,500 psi.

5.5.3.2.5 Hydraulic Drive Motor

The requirements for a hydraulic drive motor were established as 55,000 ft-lbs. of torque at 2.5 degrees/second. The selected motor was manufactured by Chamberlain Industries Limited, Staffa Works, London, England. It is available through a central office at Double A Products Co., Manchester, Michigan, and over 25 distributors throughout the United States. GE Drawing 132D6380 (Figure 5.5-13) is an outline envelope of a GB 1400 Series Staffa Motor. Looking at the left-hand profile view, the double bank of ten cylinders/pistons are identified. In the central portion of the same view, a planetary gear transmission, with a 3.625 ratio, is connected to the output shaft of the Staffa motor. On the extreme right end of the same view, one half of a modified Koppers gear coupling presents the interface that will attach to a mating hub that will connect to the pinion shaft shown in Paragraph 5.3.2. The overall size of the GB 1400 motor assembly is approximately 2 feet in diameter by 4 feet long.

Characteristics of Staffa Motors include:

1. High energy conversion efficiency: 94 to 98% overall energy conversion efficiency is attainable in the operating torque and speed range.

2. High starting torques: up to 94% of maximum running torque at dead shaft stall.

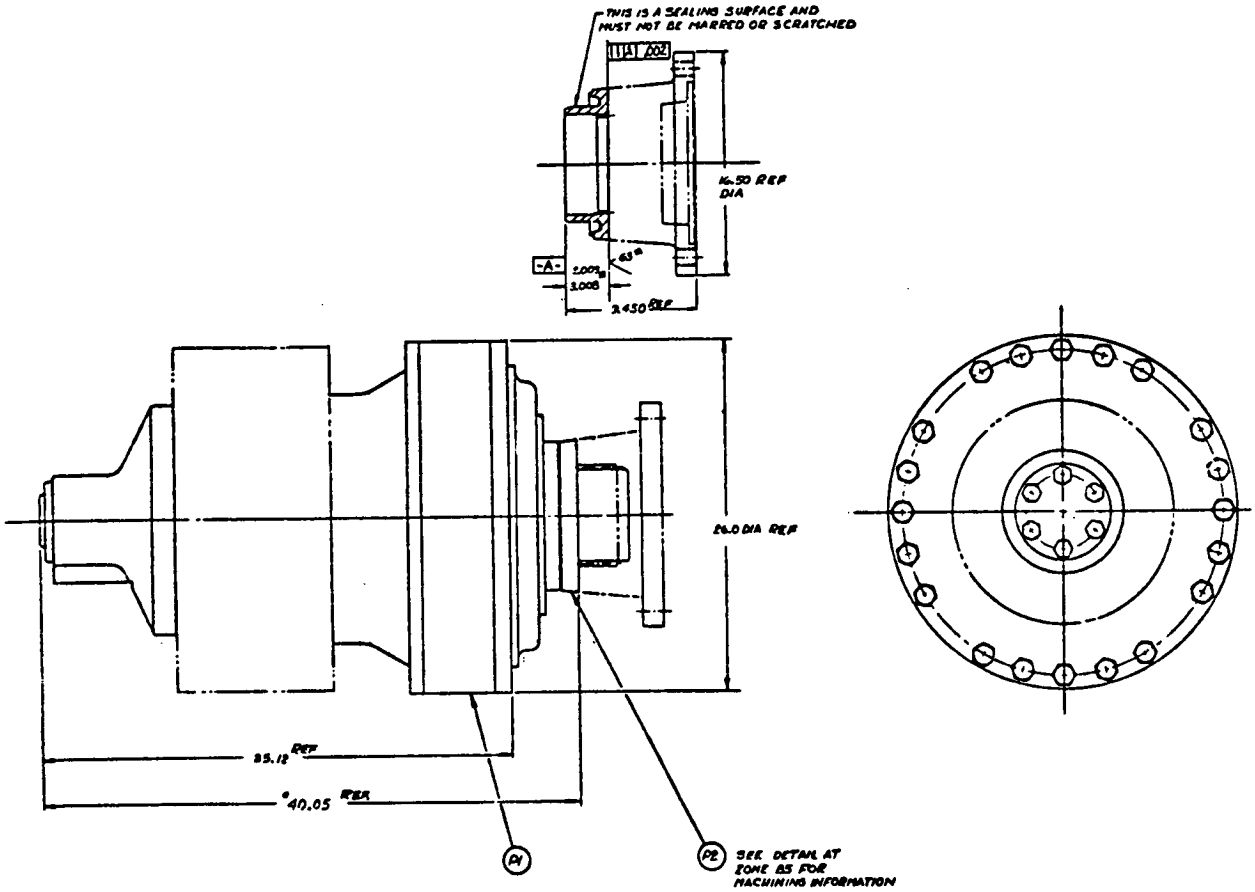

Figure 5.5-13. GB 1400 Series Staffa Motor

3. High reliability and long life due to balanced design and wear compensating sealing rings.

4. Low speed and high torques without the need for additional gearing.

5. Virtually silent operation throughout the speed and torque range.

For this motor, B-10 bearing life calculations are based on the formulas provided by the Timken Bearing Co. (Note: B-10 life is the number of hours at which 10% of the bearings may be expected to show some evidence of the end of their useful life.) However, Timken's formulas are intended for more severe operating conditions than normally encountered by hydraulic motors and the duty cycle of the Yaw Subsystem (YS). Experience among the hydraulic equipment manufacturing companies indicates that actual bearing life exceeds calculated values by a factor of 2 to 3. The YS design discussed in paragraph 5.3.2 removed the side load conditions that would have been seen by the Staffa motor by isolating the pinion on a separate shaft and bearings. Therefore, the B-10 bearing life is estimated to be 18,000 hours. This is based on a speed factor of 10 rpm, the lowest number listed in the speed factor table, for calculating bearing life.

Conservative calculation for 1 rpm would equal 70,800 hours of B-10 bearing life. The YS cycle of 30 years is assumed to be 12 minutes/day of operation or a total of 2,200 hours.

5.5.3.2.6 Hydraulic Pressure System

GE Drawing 298E479 (Figure 5.5-14) shows the overall schematic of the hydraulic pressure system. The pressure system depicts commonality in that hydraulic power from a central source is used to service three areas. These areas are: 1) yaw drive motors, 2) yaw brakes, and 3) high speed shaft brake. The requirements for operating the motors differ from the two-brake systems since a closed loop servo system controls the motor functions, and a displacement fluid system operates both brakes. The operating fluid specifications are compatible for the motor and brakes.

To determine yaw hydraulic system performance over the expected temperature range, a thermal analysis indicates that oil and equipment temperatures less than $0^{o}F$ can only be reached after prolonged soaking in a below-zero condition. Once the system has been started and is operating, equipment and oil temperature will reach normal condition. To assist the pumps under low temperature conditions, the reservoir has been equipped with a 2 kW heater that will be turned on every time the oil temperature in the reservoir falls below $20^{o}F$. The Sundstrand pump is capable of pumping fluid with viscosity as high as 6,000 SSU. The pump and motor can operate with fluid viscosity as low as 100 SSU.

5.5.3.3 Yaw Drive System Stiffness

To evaluate the adequacy of the yaw drive, its stiffness was determined by calculations using the latest design data for the shaft and yaw drive pinion and manufacturer's data for the motor. Motor data included a stiffness value

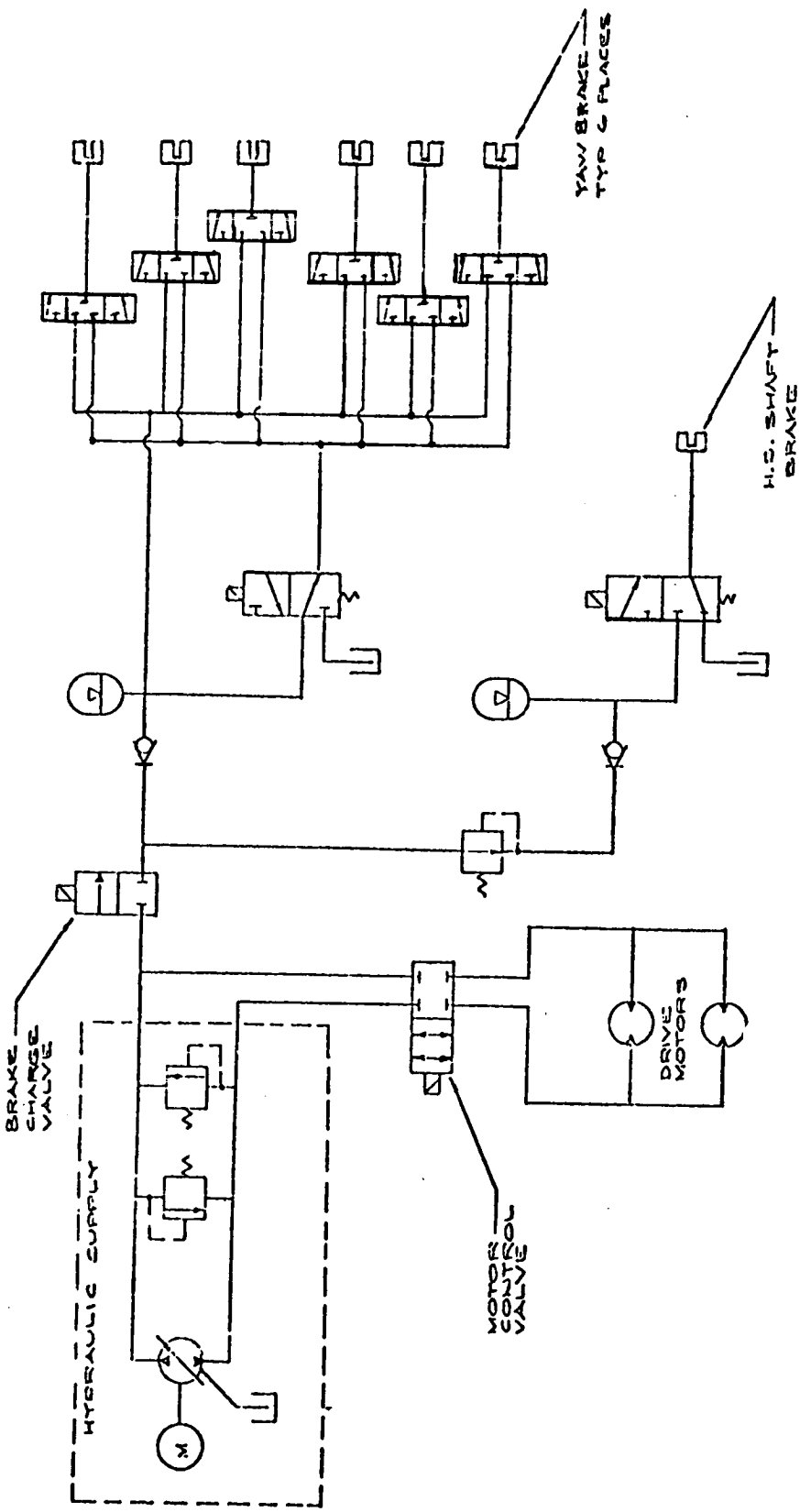

Figure 5.5-14 Yaw Hydraulic Pressure System Schematic

for the gearbox, and geometry and drawings for the remaining items. Using these data a combined or total sum for the system stiffness was calculated.

Figure 5.5-15 represents, in block diagram form, the individual components that make up the entire yaw drive train. The 20 hp electric motor is the prime mover, driving a hydraulic pump. The elastic elements in the pump and motor are their respective shafts and the compressibility of the fluid in the motor. The emf in the electric motor was considered to be a "damping" rather than "spring" force since an induction motor is used, and for that reason emf coupling can be ignored in the stiffness calculation. Anchoring of the electric motor and pump housing to ground is extremely stiff and for this reason it can also be ignored in the calculation. The transmission line contains two elements that contribute to compliance: 1) the compressibility of the fluid, and 2) the strain of the tubing. Compressibility of fluids in the transmission line was lumped together with the fluid in the hydraulic motor and valves, and the fluid in the pump, for compliance calculations. Compliance due to tubing strain was calculated separately, but, as shown in Table 5.5-1 and the attached calculations, it was two orders of magnitude lower than compliance due to compressibility.

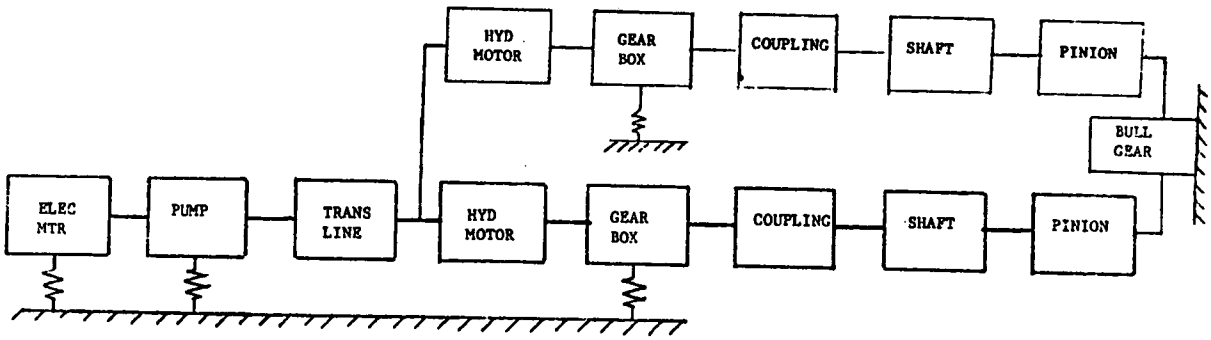

Figure 5.5-15. Yaw Drive Block Diagram for Stiffness Analysis

Table 5.5-1. Stiffness Values of Yaw Drive Components

		Raw Number	Combined Stiffness (in-lb/rad) at Pinion	In-lb/rad at Tower
Electric Motor	Shaft Torsion (including Armature)	1.75×10^{-6} rad/in-lb	6.85×10^{13}	9×10^{14}
Pump	Shaft Swash Plate (Stiff - Ignore) Motoring Torque Hydraulic Fluid Compr. (1 in^3)	2.1×10^{-6} rad/in-lb Negligible 0.0607 in-lb/psi *	5.9×10^{13}	7.7×10^{14}
Transmission Line	Bulk Modulus (134 in^3) Tubing Strain	* 7.4×10^7 in-lb/rad	9.8×10^8	1.0×10^{11}
Hydraulic Motor	Bulk Modulus (212 in^3) Piston Strain (Very Stiff - Ignore) Shaft	2.26×10^6 (incl. *) Negligible 4.62×10^9 in-lb/rad	2.95×10^7	3.00×10^9(x2)
Gearbox	Input Shaft Gear Teeth (ref. to Pinion) Planetary Gear Pin Bending Output Shaft Torsion of Planetary Gear Support	2.1×10^7 in-lb/rad 3.3×10^9 in-lb/rad 1.51×10^9 in-lb/rad 2.74×10^8 in-lb/rad 4.9×10^9 in-lb/rad	11.85×10^7	12.3×10^9(x2)
Housing/Support Structure	Torsion Thru Housing & Adapter Plate	1.22×10^{11} in-lb/rad	1.22×10^{11}	1.3×10^{13}
Coupling	Torsion	1294×10^6 in-lb/rad	17.94×10^9	19.25×10^{11}(x2)
Shaft	Torsion	5.0×10^8 in-lb/rad	2.88×10^8	3.0×10^{10}(x2)
Pinion	Gear Teeth	δ = .0062/tooth with Pinion Torque = 10^6 in-lb	5.15×10^8	5.35×10^{10}(x2)

*Compressibility of fluid in pump and transmission line is included in hydraulic motor stiffness.

The hydraulic motor contains three major compliance contributors: compressibility of the fluid trapped in the motor, strain of piston and cylinder, and shaft compliance.

In calculating the effect of compressibility of the fluid in the motor, only 30% of the swept volume of the motor was included, since at any one time only five of the ten pistons are being pressurized, and these are at various stroke positions, such that the resulting "live" piston volume is a maximum of 30% of swept volume. To this value is added the amount of fluid trapped in the five (of ten) internal feed lines between valve and pistons. In calculating the effect of fluid compressibility, the fluid volume trapped in the motor was lumped with the fluid volume in the hydraulic lines and pump. Piston and cylinder strain was found to be insignificant and was ignored. Due to its geometry, compliance of the hydraulic motor shaft was very low. The gearbox (3.625:1) is coupled directly to the Staffa motor and contains five elements that contribute to compliance: the input and output shafts, torsion of the planetary gear support structure, bending of the gear teeth, and bending of the planetary gear pinion. The gearbox, forming an integral structure with the hydraulic motor housing, is bolted to the nacelle platform. Compliance of the combined housing and housing/support structure interface was looked into and found to be extremely small (two orders of magnitude smaller than compliance of the gearbox) and was consequently ignored. The remaining components in the drive train are the coupling, pinion shaft and bending of pinion and bull gear teeth.

Examining the calculated compliances, shown in Table 5.5-1, it is apparent that the "controlling" compliance is that due to hydraulic fluid compressibility. It is four times higher than the compliance of the next "softest" element, the gearbox (or to look at it another way, the stiffness of the hydraulic fluid column is one fourth of the stiffness of the gearbox). In calculating hydraulic column stiffness (or compliance) a realistic figure for bulk modulus was used. Conventional, published data puts the bulk modulus of hydraulic oil at 225,000. However, actual user experience has shown that the bulk modulus, due to entrainment and absorption of gases can be much lower, with 140,000 being a more realistic number. This lower number was used in calculating hydraulic column stiffness. In calculating the overall stiffness, it is apparent that only the hydraulic motor stiffness (consisting primarily of hydraulic fluid compressibility effects), the gearbox, and, to a lesser extent, the pinion (shaft and gear teeth) have any effect on the overall number. The "bottom line" of overall stiffness is 4.5×10^9 in-lb/rad, a value that offers sufficient margin for safe system operation.

The above analytical derivation of yaw drive stiffness value was confirmed by an actual stiffness test of key elements: the pump, hydraulic lines, and yaw drive hydraulic motor. Two different tests were performed. In one test, the output shaft was vibrated and resonances were recorded. These resonances are related to stiffness by the equation

$$f = \frac{1}{2\pi}\sqrt{\frac{K}{J}}$$

Stiffness is thus obtained from the measured natural frequency and calculated moments of inertia.

The second was a static test in which the output shaft and gearbox frame were bolted to a common frame, thus restraining all movement in the output shaft. A differential pressure was applied to the input ports to power the motor (apply torque). Since the output shaft was restrained, the applied torque caused rotational strain of the motor crankshaft. This "twist" was measured by instrumenting the top end of the motor (shaft extension through modified end cap) with a mirror. The movement of a reflected laser beam on a far wall yielded the indication of motor strain.

In the first test (vibratory excitation) the hydraulic tubing was duplicated to fully simulate the actual nacelle installation. Thus, hydraulic fluid compressibility was included in the observed stiffness value. The second test, on the other hand, reflected mechanical component stiffness only. Test results yielded a structural stiffness for the Staffa motor assembly of 9.7×10^7 in-lb/rad (vs 11.85×10^7 calculated) and a hydraulic fluid stiffness of 3.61×10^7 in-lb/rad (vs 2.95×10^7 calculated). The corresponding bulk moduli are 165,000 and 140,000, respectively. The above results indicate that the required overall stiffness will be met.

5.5.4 YAW HYDRAULIC SYSTEM

5.5.4.1 Yaw Hydraulic Pressure Supply

The hydraulic supply for the yaw motors and yaw brakes is provided by a separate hydraulic pressure system (HPS) shown schematically on GE Drawing 298E479 (Figure 5.5-14). The HPS consists of an electric motor driven, variable displacement hydrotransmission pump, Sundstrand Type 20, a 45 gallon hydraulic fluid reservoir, containing a level switch, high and low oil temperature switches, suction filter and 10 micron supply filter. Since the pump is reversible, a filter is located in both output lines. The filters contain a return by-pass such that the filter which is carrying the return flow is not being back flushed. Cross-over relief valves in the pump and in the motor protect against over pressures in excess of 3,300 psi and 3,700 psi respectively. A low pressure alarm switch on the motor closes when the pump charge pressure drops below 155 psi and opens when the charge pressure exceeds 185 psi. A Dennison through-flow, four port valve controls the flow from the pump to the motor in an "on" - "off" mode. However, this valve does not by itself determine motor operation.

5.5.4.2 Yaw Brake Circuits

The pressures to the yaw brakes, and to the high speed shaft brake, are supplied from a set of accumulators, each provided with pressure switches and pressure regulators (high speed shaft brake only). When any of the pressure switches serving a particular accumulator closes, indicating a low pressure condition, the pump is started and a two-way, two-port solenoid valve (N.C.), located in a branch line of the CW pump supply line, opens (simultaneously with pump startup) to recharge the accumulator. The recharging continues until all pressure requirements are satisfied, i.e., pressure switch opens indicating desired accumulator

pressure has been reached. An interlock in the computer, however, puts priority on yaw drive demand, i.e., whenever the system is in a yaw maneuvering mode, the system ignores accumulator recharging demand signals.

The 600 in^3 yaw brake accumulator stores hydraulic fluid at 3,500 psig. It is p protected by a relief valve set to open at 3,850 ± 75 psig. A low pressure switch closes when the accumulator presssure drops to 3,000 ± 50 psig and opens at 3,450 ± 50 psig. Closure of this switch starts the accumulator recharge action. A low pressure alarm switch, set to close when the pressure drops to 2,400 ± 50 psig, will generate a warning signal when the accumulator is not being recharged, or is losing pressure for any reason. The six brakes are supplied from either of two pressure manifolds. One manifold is connected to the accumulator directly. The other manifold is connected to the accumulator by means of a two-way, three-port solenoid valve. A set of six manual selector valves (one valve per brake) is provided to allow connection to the proper manifold. Under normal operation, manual selector valves serving brakes No. 1 and No. 4 are positioned such that these brakes are "on" continuously. Selector Valves dedicated to brakes No. 2, No. 3, No. 5 and No. 6 are set to the manifold which is fed through the solenoid valve. An additional pressure switch downstream of the solenoid valve indicates the state of the brakes (brakes are "on" when the pressure is high).

5.5.4.3 Rotor Brake Supply

The high speed shaft brake is served by a separate accumulator circuit at 1,150 psi nominal pressure. Decelerating the blade from 5 rpm and holding it once it stopped is accomplished with this single pressure setting. The accumulator has a capacity of 1 gallon and is charged through a 1,300 psig (nominal) regulator. The signal for charging is generated by a pressure switch which closes at 1,050 ± 50 psig and opens at 1,250 ± 50 psig. A separate low pressure alarm switch closes at 800 ± 50 psig to warn of any pressure losses or failure to recharge. A relief valve set for 1,500 psi protects this circuit from overpressure. Pressure is applied to the brake manifold through a two-way, three-port solenoid valve. The brake is engaged (pressurized) when power is applied to the solenoid valve and is "off" (depressurized) when the solenoid valve is de-energized.

A pressure switch is provided downstream of the solenoid valve to indicate presence or absence of high pressure in the brake manifold.

5.5.4.4 Yaw Hydraulics Failure Modes

Electrical Power Failure - In the event of loss of electrical power, the result will be loss of yaw maneuver capability, since the pump will be inoperative. The yaw brakes, however, will be "on" since the control valve,"B", in the deenergized position, pressurizes the brakes.

The high speed brake will be "off" to prevent the rotor from stopping suddenly (loss of power also feathers the blades). The valve controlling this brake connects the high speed brake to the return line when deenergized.

If the hydraulic power supply becomes disabled for any reason, the effect will be loss of yaw maneuvering capability. This failure will be detected immediately since the pump contains a pump failed alarm switch that closes when the charge pressure drops below 160 psi. Since the brakes operate from their respective accumulators, the brake circuits will have sufficient reserve for ten "on-off" cycles, sufficient for a shutdown sequence. Failure in the yaw drive circuit for any other reason, such as a catastrophic leak, failure of one motor, or failure of control valve "A", to open (or close) is not catastrophic but will initiate a shutdown. Pressure loss in the yaw brake circuit will initiate a shutdown, but the yaw motors will aid in holding yaw position, since they act as a brake up to a yaw moment of 1.3 million foot-pounds, and thus provide a measure of redundancy to the yaw brakes.

5.5.5 PCM HYDRAULIC SYSTEM

The function of the PCM Hydraulic System is to provide the actuation to the pitch change mechanism and to permit feathering of the blades during an emergency situation.

The system shown schematically in GE Drawing 848E810 (Figure 5.5-16) consists of five distinct elements, all interconnected and acting as an integral unit:

1. Hydraulic Supply
2. Emergency Feather Control
3. Servo Valve
4. Accumulators
5. Actuators

5.5.5.1 PCM Hydraulic Pressure Supply

The hydraulic supply located in the nacelle as shown on GE Dwg. 298E457 contains a slew and the accumulator charging pump, both connected to a common reservoir. The pumps are located below the reservoir to assure a net positive suction head at all times. The slew pump is a pressure compensated type and is running continuously during normal operation. It delivers 20 gpm between 0 and 1,500 psi. The slewing flow control is accomplished by the servo valve which receives its signal from the CODAS. In the event that the slewing control flow exceeds pump capability, the flow is supplemented by the main accumulators. The charging pump also operates continuously through an unloading valve to charge the accumulator when pressure drops to 2,550 psi (nominal) and to return the charging flow to the reservoir when accumulator pressure exceeds 2,950 psi (nominal). The reservoir contains an immersion heater, low oil level switch, high and low oil temperature switches and an oil cooler (heat exchanger). The oil is filtered through a 74 micron filter on the suction side, and a 10 micron filter on the discharge side of both pumps. A separate filter in the servo valve pilot supply line filters the oil to a level of 3 microns. The slew pump is protected by a "motor failed alarm" switch which closes when slewing pump pressure drops below 200 psi. The charging system is protected by a "low pressure alarm" switch which closes when feather accumulator pressure drops below 2,250 psi.

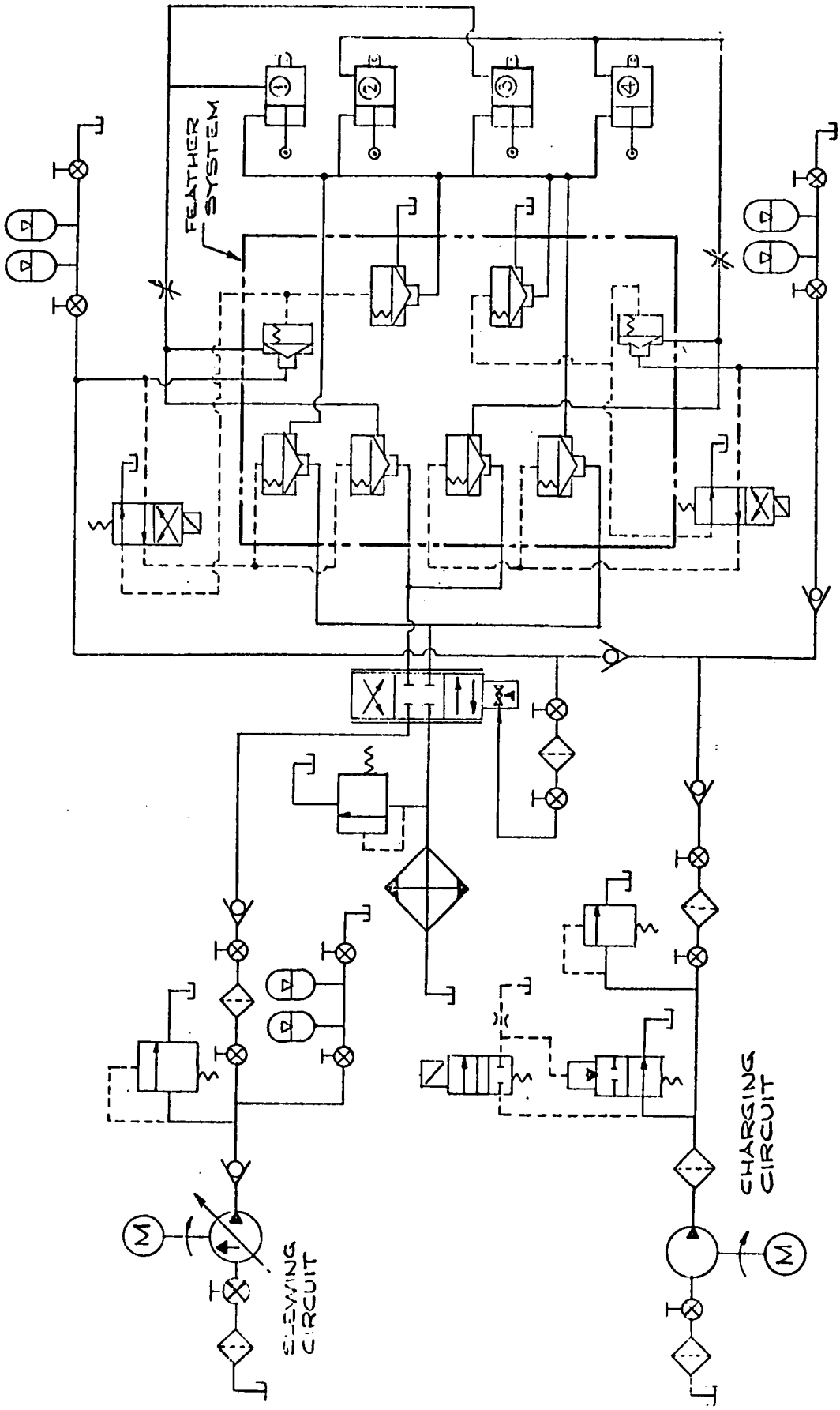

Figure 5.5-16 PCM Hydraulic System-Simplified Schematic

The emergency feather control permits slewing control flow to pass from the servo valve to the actuators without restriction. In an emergency, (or on command), the emergency feather control blocks the servo valve, by closing the block check valve and the feather lock valve, opens the feather dump valves and the feather valve. Opening the feather valve admits hydraulic fluid to the blind end of the actuators, precipitating actuator movement in the direction to feather the blades. Hydraulic fluid from the rod ends of the actuators is permitted to return to the hydraulic reservoir via the feather dump valve. Two separate, but identical, circuits are provided in the emergency feather control to assure reliability. Each circuit serves two actuators. Each actuator pair is capable of independently accomplishing blade feathering. The four-part, two-way solenoid valve, the feather solenoid valve in each circuit controls the piloted check valves. Hydraulic flow through each circuit is provided by two pairs of accumulators, each pair dedicated to a pair of actuators.

5.5.5.2 PCM Hydraulics Startup

In the dormant mode, all valves and motors are deenergized, the blades are in the "feather" condition and the feather lock is engaged to prevent retraction of the PCM. All hydraulic lines are filled, but depressurized. The actuators are fully extended.

To startup, the following sequence of events takes place: Remove power from all electrically actuated or power components. Check oil temperature - reservoir oil temperature should be above $0^{o}F$. If oil temperature is below $0^{o}F$, turn on the immersion heater in hydraulic reservoir. When temperature rises above $0^{o}F$, generate, and apply to servo valve, a control signal corresponding to blade feathering. Start charge and slewing pumps. Observe output pressures. When emergency feather accumulators are fully charged ($2,950 \pm 50$ psig), apply power to both feather solenoid valves. This precipitates the following action: The pitch lock mechanism is retracted, the feather dump valves and feather valves are closed, and the pitch lock and block check valves are opened. At this point, the system is effectively under control of the servo valve. A controlled blade pitch change can now be initiated.

5.5.6 NACELLE STRESS ANALYSIS

Stress analyses were performed for all structural elements of the nacelle. These analyses had several objectives:

1. Provide a detailed analysis of internal loads, stresses, and deflections.

2. Demonstrate the structural integrity by compliance with the requirements of AISC and other applicable codes.

3. Provide the mathematical models and stiffness matrices for the major structural elements, required for dynamic simulation analyses.

Where possible, analysis was performed with manual computations, using classical or recognized empirical formulas. However, for the major substructures, bedplate and rotor hub, due to their complexity and their critical roles in determining system stiffness, it was necessary to use finite element computer techniques. The

NASTRAN computer program was used to model and analyze both the bedplate and rotor hub. MASS, a similar program, was used to analyze the tower, as described in paragraph 5.6. Results of the rotor hub analysis are presented in paragraph 5.2.

5.5.6.1 Bedplate Analysis

The first step in analyzing the bedplate structure using NASTRAN was to define a finite element model. The model is shown graphically in Figure 5.5-17, consisting of 557 grid points, 714 beam elements (identified as CBAR), 538 quadrilateral plates (CQUAD), and 108 triangular plates (CTRIA). These elements have the following characteristics:

CBAR: A simple beam capable of resisting tensile or compressive axial load, bending about both axes, and torsion. It is used to represent cap members, structural angles, and panel intersections.

CQUAD: Quadrilateral panels, capable of resisting axial load and bending about both in-plane axes. It is used to represent regular bulkheads and webs.

CTRIA: Triangular panels, with capabilities the same as CQAD members, used to represent segments of irregularly shaped panels.

The critical design conditions used for analysis of the bedplate are cases A and B as defined in Appendix B. Case A is the cyclic load condition, used for fatigue analysis. Case B is an upgust case with inflow, resulting in peak loads. In addition to the shear loads and moments defined at the bedplate interfaces, inertia loads due to dynamic response were added. As a conservative simplification, accelerations at the bedplate extreme corners were averaged, and these values applied to all elements in three principal directions.

Results of the NASTRAN analysis are summarized in Table 5.5-2. This table was assembled by scanning all output data for low margins of safety, based on arbitrarily assigned allowable stresses. Figure 5.5-18 shows a typical computer print-out page for beam elements. Listed are bending stresses about the principal axes of the element, and the axial stress (column 6). In column 8, it may be noted that the extreme fiber stress for member 759 is 7038 psi. The conservative assumption is made that the stress is completely reversed and that the computed value can be compared with one-half of the allowable stress range per Appendix B of AISC. Table 5.5-3 is a summary of stress range allowables, as amended by AISC in 1978. For member CBAR 759, located as shown in Figure 5.5-19, the allowable stress range is determined by the joint to the rotor adapter structure, typified by Example No. 8 of the AISC code, shown in Figure 5.5-20. For this joint and Loading Condition 4 (over two million cycles), the allowable stress range is Category B, 16,000 psi, or the margin of safety is:

$$MS = \frac{8000}{7038} - 1 = +.14$$

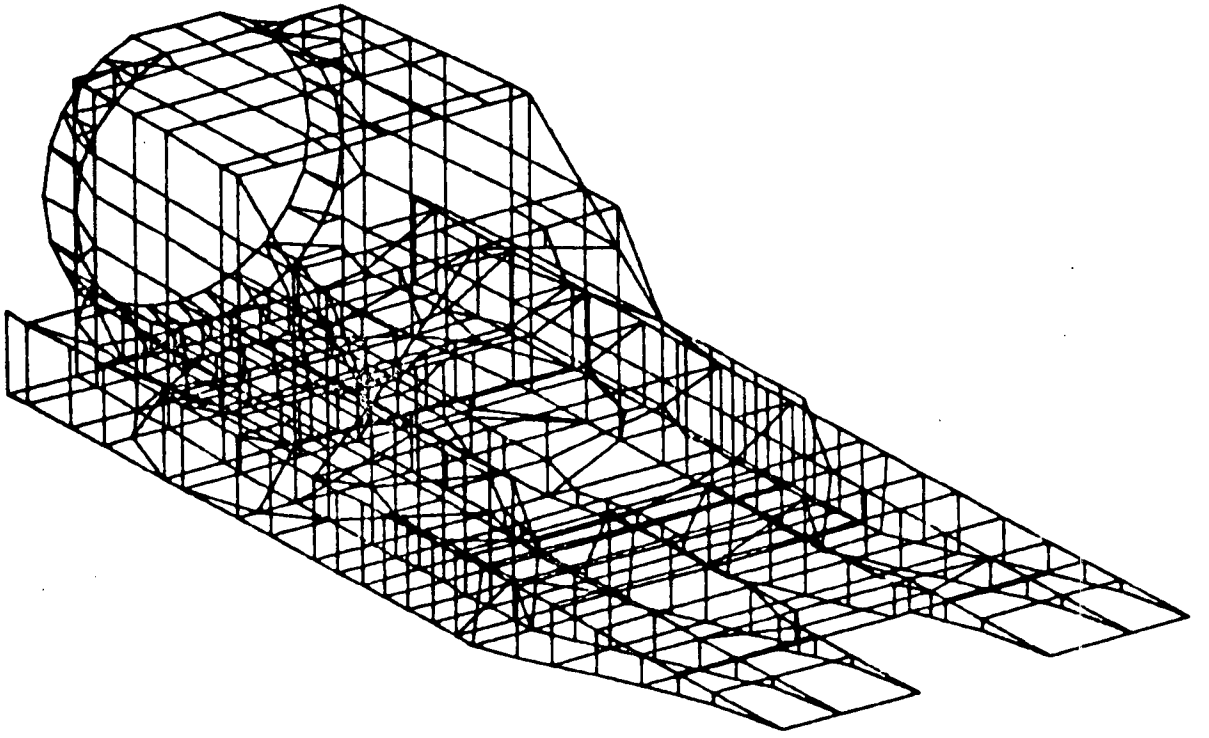

Figure 5.5-17 Finite Element Model of Bedplate

Table 5.5-2. Summary of Stress Analysis, Bedplate

Component/Grid & Element Number		Maximum Stress (psi)	Allowable Stress (psi)	Critical Stress Type	Minimum Margin of Safety
CBAR 712	FATIGUE LOADING	< 5000	±5000	Bending	See Note #1
CBAR 755		±6174	±8000	Bending	+.31
CBAR 759		±7038	±8000	Bending	+.14
CBAR 773		±4858	±8000	Bending	+.65
CBAR 776		±4295	±8000	Bending	+.86
CBAR 2087		±3426	±3500	Bending	+.02
CBAR 2090		< 5000	±5000	Bending	See Note #1
CQUAD 1708		±1773	±2500	Bending	+.41
CQUAD 1722		±1622	±2500	Bending	+.54
CTRIA 1825		±1298	±2500	Bending	+.93
CTRIA 1825		±3154	±4000	Shear	+.27
CTRIA 1855		±1020	±2500	Bending	+1.45
CTRIA 1855		±2400	±4000	Shear	+.67
CBAR 759	PEAK LOADING	15,943	22,800	Bending	+.43
CBAR 773		16,685	22,800	Bending	+.37
CBAR 776		20,432	22,800	Bending	+.11
CBAR 790		15,723	22,800	Bending	+.45
Bolts at Joint Sta. 428		21,612 lbs	41,390 lbs.	Tension	+.96
Backup Angle at Sta. 409.5		19,631 psi	21,600 psi	Bending	+.10

Notes:

1. Stresses predicted by NASTRAN on these elements (CBAR 712 and CBAR 2090) are unrealistically high due to modeling induced eccentricity. The stresses are conservatively determined to be less than 5,000 psi.

FATIGUE LOADS

SUBCASE 1

STRESSES IN BAR ELEMENTS (CBAR)

ELEMENT ID.	SA1 / SB1	SA2 / SB2	SA3 / SB3	SA4 / SB4	AXIAL STRESS	SA-MAX / SB-MAX	SA-MIN / SB-MIN	M.S.-T / M.S.-C
746	1.554726E+02	-6.925688E+02	2.165114E+02	-6.887844E+02	-4.434516E-01	2.160680E+02	-6.930122E+02	1.6E-01
	-5.113120E+02	2.151154E+03	-6.450221E+02	2.142864E+03		2.150710E+03	-6.454655E+02	2.6E+00
747	-1.346107E+02	2.195343E+03	-1.032760E+03	2.139658E+03	-6.837400E+02	1.511604E+03	-1.716500E+03	6.5E-01
	1.420897E+02	-1.700683E+03	7.634877E+02	-1.662156E+03		7.974770E+01	-2.384423E+03	4.8E-02
748	7.025405E+02	5.155750E+02	-9.525846E+02	4.129572E+02	-3.009281E+02	4.016124E+02	-1.253513E+03	4.1E-01
	-4.980371E+02	-2.994120E+03	2.067769E+03	-2.835040E+03		1.766841E+03	-3.295048E+03	-2.4E-01
751	2.658266E+02	2.572626E+02	-2.324412E+03	3.049940E+03	-6.701508E+02	2.379789E+03	-2.994563E+03	5.1E-02
	-1.714949E+02	-3.181837E+02	2.863160E+03	-4.006087E+03		2.193009E+03	-4.676237E+03	-4.7E-01
752	1.336140E+02	1.827306E+03	-1.069302E+03	1.675956E+03	-1.270422E+03	5.568848E+02	-2.339724E+03	3.5E+00
	1.528123E+02	-2.243878E+03	1.013080E+03	-2.121279E+03		-2.573414E+02	-3.514300E+03	-2.9E-01
753	9.353176E+01	-3.761770E+02	1.055462E+02	-3.691804E+02	-6.771626E+00	9.877460E+01	-3.829486E+02	4.2E-01
	-5.354762E+02	1.770115E+03	-4.063767E+02	1.756227E+03		1.763343E+03	-5.422478E+02	3.6E+00
754	-6.719475E+01	1.773240E+02	-2.787940E+01	1.786381E+02	-2.356064E+01	1.550775E+02	-9.075539E+01	1.5E+01
	9.949625E+01	-3.808171E+02	1.022938E+02	-3.746945E+02		7.873316E+01	-4.043777E+02	5.2E+00
755	-6.319921E+02	2.295456E+02	-2.009407E+03	4.013970E+03	-1.085105E+03	2.928865E+03	-3.094512E+03	-1.5E-01
	6.220509E+02	-3.109544E+02	2.739438E+03	-5.089416E+03		1.654333E+03	-6.174521E+03	-6.0E-01
756	3.230355E+02	1.443305E+03	-1.050497E+03	1.280344E+03	-1.579165E+03	-1.358593E+02	-2.629661E+03	
	1.015097E+03	-1.966710E+03	5.376223E+01	-2.035149E+03		-5.640680E+02	-3.614313E+03	-3.1E-01
757	9.880839E+01	-3.509121E+02	8.751531E+01	-3.466927E+02	-3.328587E+01	6.552252E+01	-3.841980E+02	9.2E-01
	-4.360505E+02	1.334828E+03	-2.759123E+02	1.330794E+03		1.301543E+03	-4.693364E+02	4.3E+00
758	-9.006951E+01	1.726577E+02	-3.816588E+00	1.788563E+02	-4.252233E+01	1.363340E+02	-1.325913E+02	1.7E+01
	1.027219E+02	-3.639617E+02	9.054342E+01	-3.596331E+02		6.019962E+01	-4.064840E+02	5.2E+00
759	5.661981E+02	4.403633E+02	-3.987020E+03	5.055327E+03	-1.432172E+03	3.623155E+03	-5.419191E+03	-3.1E-01
	-1.127286E+02	-4.310830E+02	3.870191E+03	-5.605435E+03		2.438020E+03	-7.037607E+03	-6.4E-01
760	-3.247372E+01	-5.184617E+01	5.749278E+01	-4.182637E+01	-6.404001E+01	-6.547238E+00	-1.158862E+02	4.8E+00
	-5.792076E+01	4.978956E+02	-2.020602E+02	4.754855E+02		4.338556E+02	-2.661002E+02	8.4E+00
761	-6.674869E+01	1.240590E+02	-8.191830E-01	1.289184E+02	-7.078665E+01	5.813171E+01	-1.375353E+02	4.2E+01
	-2.934645E+01	-5.523629E+01	5.628139E+01	-4.560943E+01		-1.450526E+01	-1.260229E+02	1.7E+01
762	-2.996360E+01	-8.038031E+01	6.983889E+01	-6.891465E+01	-2.292530E+01	4.691358E+01	-1.033056E+02	2.1E+01
	2.076780E+01	1.341816E+02	-8.889255E+01	1.208807E+02		1.112563E+02	-1.118179E+02	2.1E+01
763	-3.832834E+01	-1.605971E+02	1.191461E+02	-1.419884E+02	1.108000E+01	1.302261E+02	-1.495171E+02	1.4E+01
	5.914101E+01	1.503867E+02	-1.335810E+02	1.283201E+02		1.614667E+02	-1.225010E+02	1.6E+01

Figure 5.5-18 Sample Output from NASTRAN Analysis of Bedplate

Table 5.5-3. Allowable Stress Range from AISC Code (1978 Edition)

Category (From Table B2)	Allowable Range of Stress, F_{sr} (ksi)			
	Loading Condition 1 F_{sr1}	Loading Condition 2 F_{sr2}	Loading Condition 3 F_{sr3}	Loading Condition 4 F_{sr4}
A	60	36	24	24
B	45	27.5	18	16
C	32	19	13	10*
D	27	16	10	7
E	21	12.5	8	5
F	15	12	9	8

*Flexural stress range of 12 ksi is permitted at the toe of stiffener welds on girder beams or flanges.

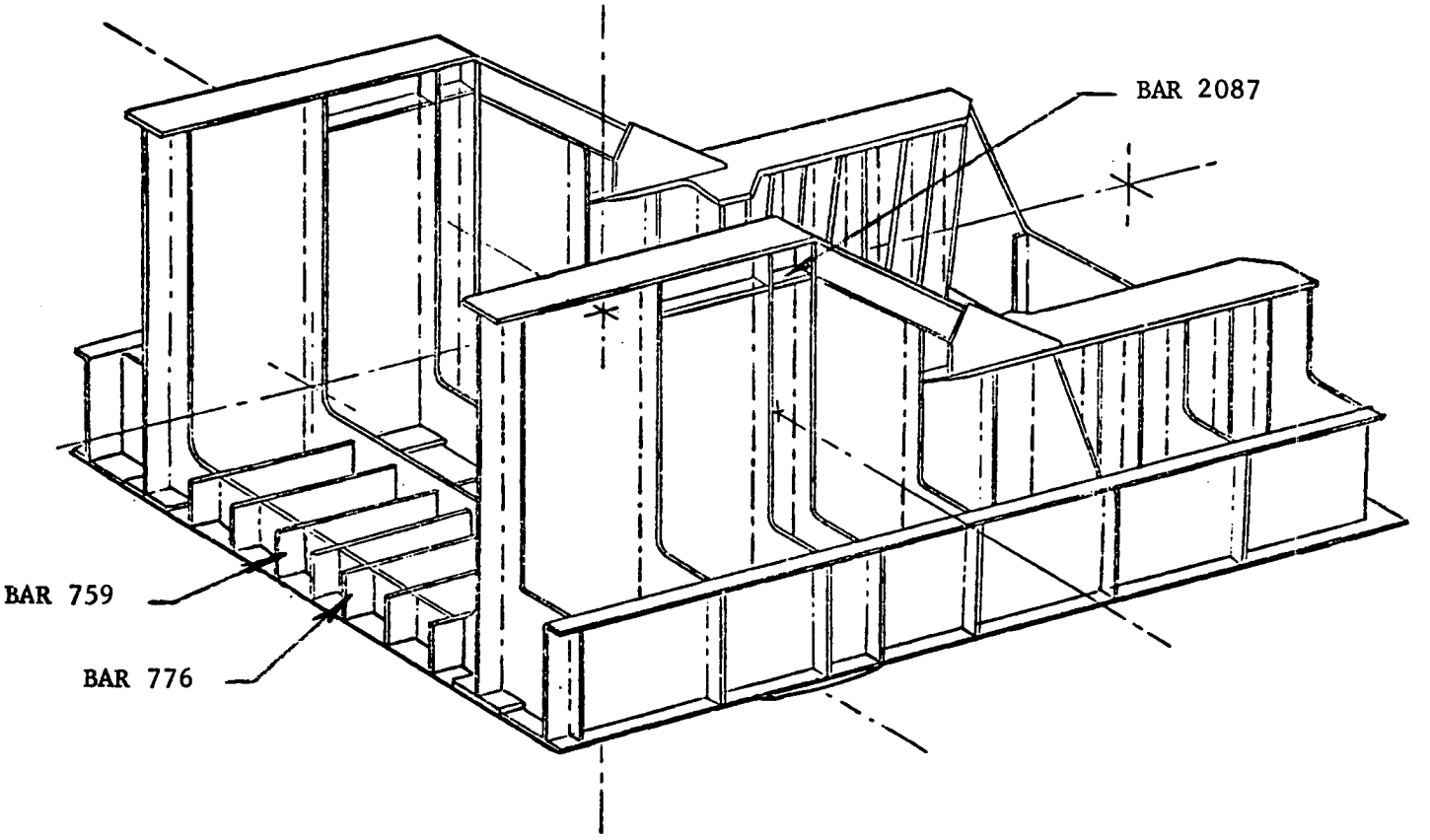

Figure 5.5-19 Location of Critical Elements in Bedplate Structure

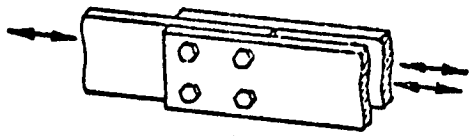

Figure 5.5-20. Illustrative Example of Type 8 Joint from AISC Code

The margins of safety listed in Table 5.5-2 were computed using steps similar to this illustrative example. For peak loads, the allowable stress is 60% of yield strength or 22,800 psi, or for bolted joints, the allowable shear stress per Table 5.5-4, taken from the AISC code.

The minimum margin of safety in fatigue occurs at member CBAR 2087, located as shown in Figure 5.5-19. For this member, the weld joint is Category D with an allowable stress range of 7000 psi.

5.5.6.2 Yaw Section Analysis

It was not necessary to use a finite element computer analysis of the yaw structure because its simplicity and symmetry made it amenable to manual calculations. The upper and lower structures were treated as curved circular beams and analyzed using simple formulas. In addition, detailed analyses were made of secondary structural elements, such as the yaw brake mountings, yaw drive pinion supports, and yaw drive motor mountings. In this report, only the critical sections of the primary structural elements will be discussed.

The loading conditions considered in analysis of the yaw structure were:

1. Cyclic loading per Case A

Table 5.5-4. Allowable Working Stresses (ksi) for Bolted Joints(1)

Class	Surface Condition of Bolted Parts	Standard Holes		Oversize Holes and Short Slotted Holes		Long Slotted Holes	
		A325	A490	A325	A490	A325	A490
A	Clean mill scale	17.5	22.0	15.0	19.0	12.5	16.0
B	Blast-cleaned carbon and low alloy steel	27.5	34.5	23.5	29.5	19.5	24.0
C	Blast-cleaned quenched and tempered steel	19.0	23.5	16.0	20.0	13.5	16.5
D	Hot-dip galvanized and roughened	21.5	27.0	18.5	23.0	15.0	19.0
E	Blast-cleaned, organic zinc rich paint	21.0	26.0	18.0	22.0	14.5	18.0
F	Blast-cleaned, inorganic zinc rich paint	29.5	37.0	25.0	31.5	20.5	26.0
G	Blast-cleaned, metallized with zinc	29.5	37.0	25.0	31.5	20.5	26.0
H	Blast-cleaned, metallized with aluminum	30.0	37.5	25.5	32.0	21.0	26.5
I	Vinyl wash	16.5	20.5	14.0	17.5	11.5	14.5

Values from this table are applicable only when they do not exceed the lowest appropriate allowable working stresses for bearing-type connections, taking into account the position of threads relative to shear planes and, if required, the 20% reduction due to joint length.

(1) Reference "Specification for Structural Joints Using ASTM 325 or A490 Bolts", February 4, 1976, AISC.

Table 5.5-5. Design Loads at Yaw Bearing

(Units are Lbs. for Shear
and Ft-Lbs. for Moment)

	Loads	Mean	Cyclic	Peak	
CASE A					
Fatigue	V_x	--	± 82161	--	
	V_y	--	± 28046	--	
	V_z	--	± 35903	--	
	M_x	--	± 984780	--	
	M_y	--	± 539953	--	
	M_z	--	± 150945	--	
CASE B					
	V_x	- 339730	± 51158	- 390888	
Peak	V_y	- 55	± 21051	- 21106	
35-50 mph	V_z	- 48533	± 18458	- 66991	
+41° Inflow	M_x	157300	±1326800	1484100	
	M_y	1274900	± 661170	1936070	
	M_z	- 728445	± 121360	- 849805	
CASE D				Headwind	Sidewind
	V_x	--	--	- 338387	- 338387
Hurricane	V_y	--	--	--	- 38644
	V_z	--	--	- 14523	--
	M_x	--	--	--	288638
	M_y	--	--	245333	138831
	M_z	--	--	--	- 283389

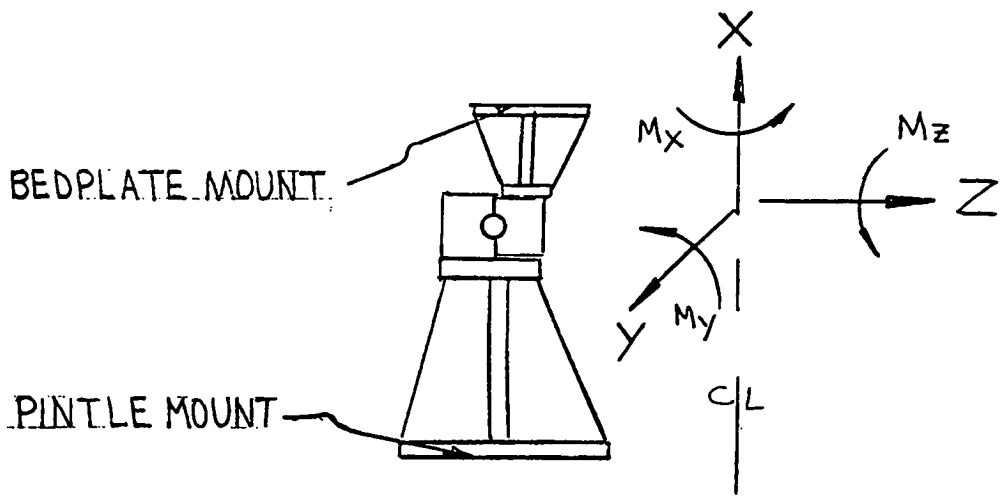

2. Peak loading per Case B

3. Hurricane loading per Case D

4. Maximum torque output of yaw hydraulic drive motors (55000 ft-lb)

5. Maximum brake loads due to hydraulic overpressure (3500 psi)

The critical loads appropriate to the yaw structure are summarized in Table 5.5-5 for Cases A, B, and D. Further details of these cases may be found in Appendix B. For bolted connections, the influence of tension preload was considered, based on the AISC recommendation of preloading all high strength bolts to approximately 70% of their minimum tensile strength.

Margins of safety were computed for all structural elements, based on the allowable stresses that have now been incorporated in the 1978 AISC code. A summary of the critical margins for both the upper and lower yaw structures is given in Table 5.5-6. Margins listed as "adequate" are greater than 100%; "very adequate" are greater than 200%.

The following is a sample calculation for bending of the upper yaw structure, lower flange. The loading condition for cyclic loading is Case A, summarized in Table 5.5-5. It is convenient to convert the loading as a uniformly distributed load, equal to the peak intensity. This is accomplished by expressing the moments M_y and M_z as equivalent axial loads, then adding them to the vertical loading V_x.

$$N_m = \frac{M_y \leftrightarrow M_z}{\pi R^2}$$

where R = radius of yaw bearing = 69.6 in

$$N_m = \frac{560 \times 10^3 \times 12}{\pi \times (69.6)^2}$$

$$= 442 \text{ lb/in}$$

$$N = N_m + \frac{V_x}{2\pi R}$$

$$= 442 + \frac{82 \times 10^3}{2\pi \times 69.6}$$

$$= 630 \text{ lb/in}$$

Local bending occurs at the lower flange because the inner race of the bearing, where the loads are introduced to the upper structure, is offset from the web of the upper structure. The lower flange is treated as a cantilever beam of

Table 5.5-6. Summary of Margins of Safety for Upper and Lower Yaw Structures

Location	Loading Condition	Minimum Margin of Safety
Upper Structure, web	Case A, bending	+.65
Upper Structure, upper flange	Case A, bending	+.42
Upper Structure, lower flange	Case A, bending	+.63
Brake outrigger	Brake force, bending	Very adequate
Motor support beam, flange	Motor torque, bending	Very adequate
Cross beam	Motor torque, bending	Very adequate
Pinion bearing support	Motor torque, bending	Adequate
Lower Structure, web	Case A, bending	+.65
Lower Structure, upper flange	Case A, bending	+.42
Lower Structure, lower flange	Case A, bending	+2.29
Lower Structure, gussets	Case A, tension	+.90
Brake disk	Brake force, buckling	Very adequate

unit width, with free edges (see Figure 5.5-21).

$$f_b = \frac{Mc}{I}$$

$$= \frac{630 \times 2.863 \times 2.100/2}{(2.1)^3 / 12}$$

$$= 2450 \text{ psi}$$

The stress range is then double this value, or 4900 psi. The allowable stress range is conservatively taken as 8000 psi, assuming that the weld between the web and the lower flange classifies the joint as Type 21 by the AISC code, or Category F. It might be argued that the joint more closely resembles Type 15a, Category B, with a 16,000 psi allowable stress range.

$$MS = \frac{8000}{4900} - 1 = +.63$$

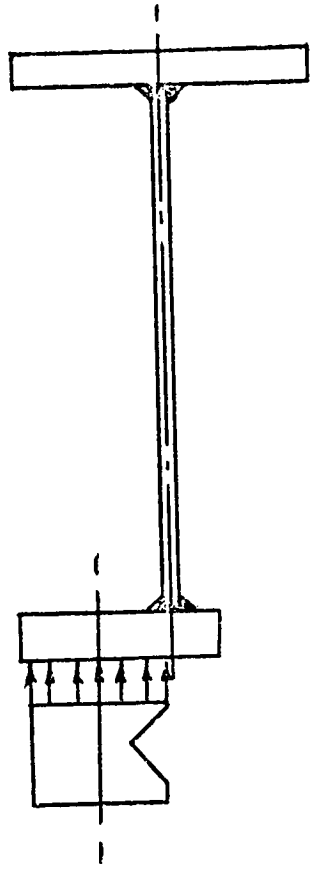

Figure 5.5-21. Lower Flange of Upper Yaw Structure

5.6 TOWER

5.6.1 REQUIREMENTS

The design requirements for the tower specified in the NASA Statement of Work can be summarized as follows:

1. Open truss construction with members of structural carbon steel
2. Bracing generally designed for bolted field assembly
3. Provide a lift device of half-ton capacity for access to the nacelle
4. Provide a means for evacuation of personnel in the event of failure of the lift device
5. Maximum design wind load of 150 mph (at hub height)
6. Seismic loads per Zone 3
7. First bending frequency shall be at least 2.8 times the rotor operating frequency
8. First torsional frequency shall be at least 6.5 times the rotor operating frequency.

In addition, the tower is required to have a design life of 30 years, operating in a range of environmental conditions, including temperature extremes from -31°F to +120°F. The low-temperature requirement is significant because it places the fracture-toughness requirements for the steel in the most severe class, Zone 3.

Comparison with loads determined by the system dynamic simulation has shown that the critical design conditions are Case A for fatigue and Case B for peak stresses, rather than the hurricane wind loads or seismic loading defined in the SOW.

5.6.2 DESIGN DEFINITION

The final design of the tower is illustrated in Figure 5.6-1 or GE Drawing 848E834. This drawing defines overall geometry, member sizes, materials, and general joint design. From this drawing and detailed loads data extracted from the finite element computer program, shop drawings were prepared by the tower fabricator for each member and joint in accordance with AISC specifications. The characteristics of the tower are summarized in Table 5.6-1.

5.6.3 DESIGN EVOLUTION AND TRADE-OFFS

During the detail design phase, the tower design evolved through several iterations in an attempt to satisfy strength and stiffness requirements at minimum cost, in the face of continual growth in system weight and design loads. As part of this design evolution, several trade-off studies were made on the selection of overall geometry, grade of steel, and structural form of members. To gain maximum bending stiffness, the tower height was reduced and the width increased as far as adequate blade clearances would allow. Beyond that point, it would have been necessary to introduce a tilt in the rotor axis or increase the rotor overhang in order to maintain clearance with the tower when the blade is at its maximum tip deflection. Having established the overall geometry, the only parameter to be varied to achieve the desired strength and stiffness was the cross-sectional area of the primary members.

For the four tubular leg members that comprise most of the tower weight, the selection of steel grade became a tradeoff between fracture toughness and cost.

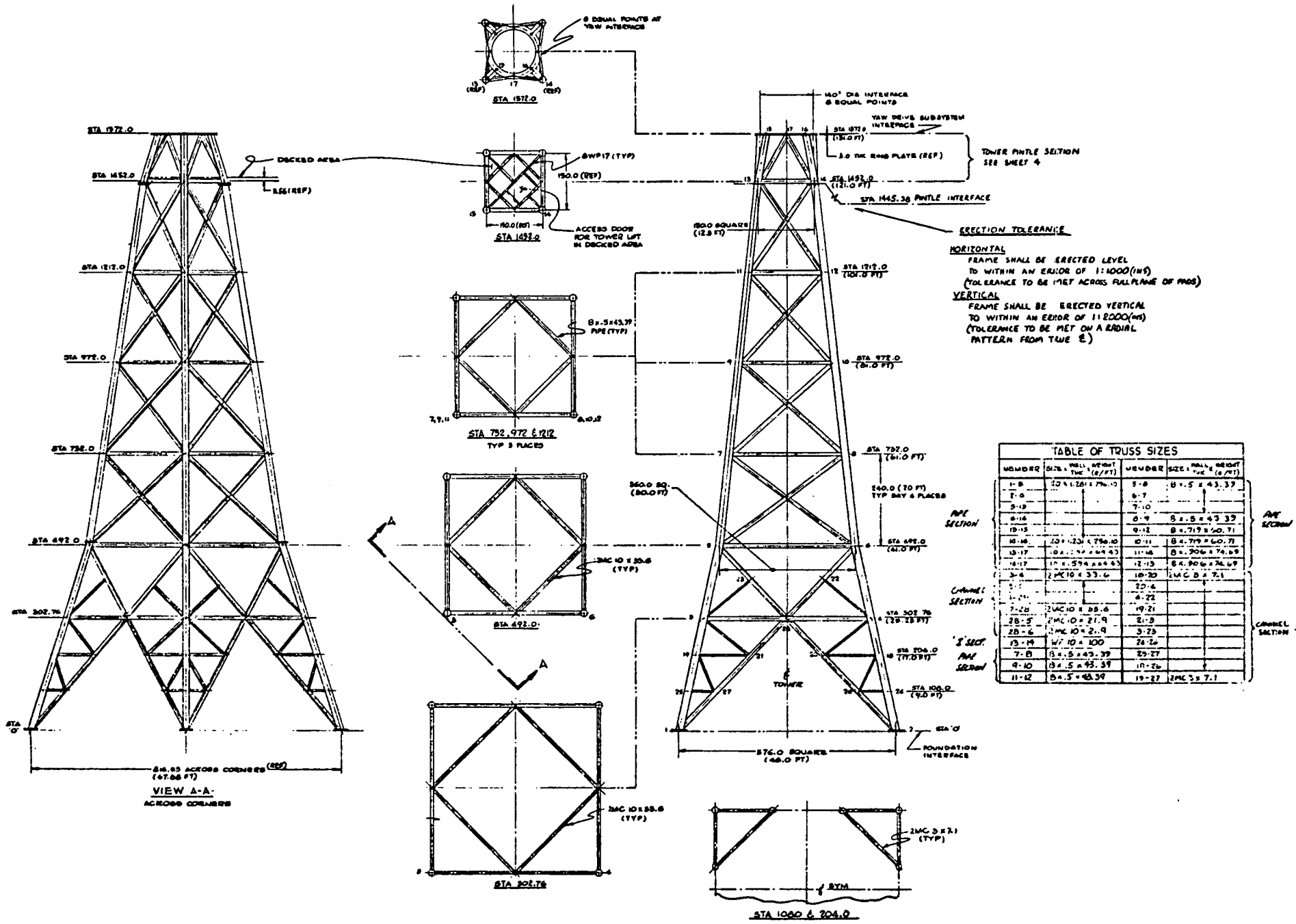

TABLE OF TRUSS SIZES

MEMBER	SIZE x WALL THK (in) x WEIGHT (#/FT)	MEMBER	SIZE x WALL THK (in) x WEIGHT (#/FT)
1-5	30 x 1.281 x 384.10	5-8	8 x .5 x 43.39
2-6		6-7	
3-19		7-10	
4-14		8-9	8 x .5 x 43.39
13-15		9-12	8 x .719 x 60.71
14-16	30 x 1.234 x 296.10	10-11	8 x .719 x 60.71
15-17	24 x .594 x 69.43	11-16	8 x .906 x 74.69
16-17	24 x .594 x 69.43	12-13	8 x .906 x 74.69
3-4	2 MC 10 x 33.6	18-20	2MC 8 x 7.1
5-21		20-4	
1-22		4-22	
7-23	2MC 10 x 33.6	19-21	
23-5	2MC 10 x 21.9	21-3	
23-6	2MC 10 x 21.9	3-23	
13-19	W 10 x 100	24-24	
7-8	8 x .5 x 43.39	25-27	
9-10	8 x .5 x 43.39	10-26	
11-12	8 x .5 x 43.39	19-27	2MC 5 x 7.1

Figure 5.6-1A Tower Configuration, Sheet 1

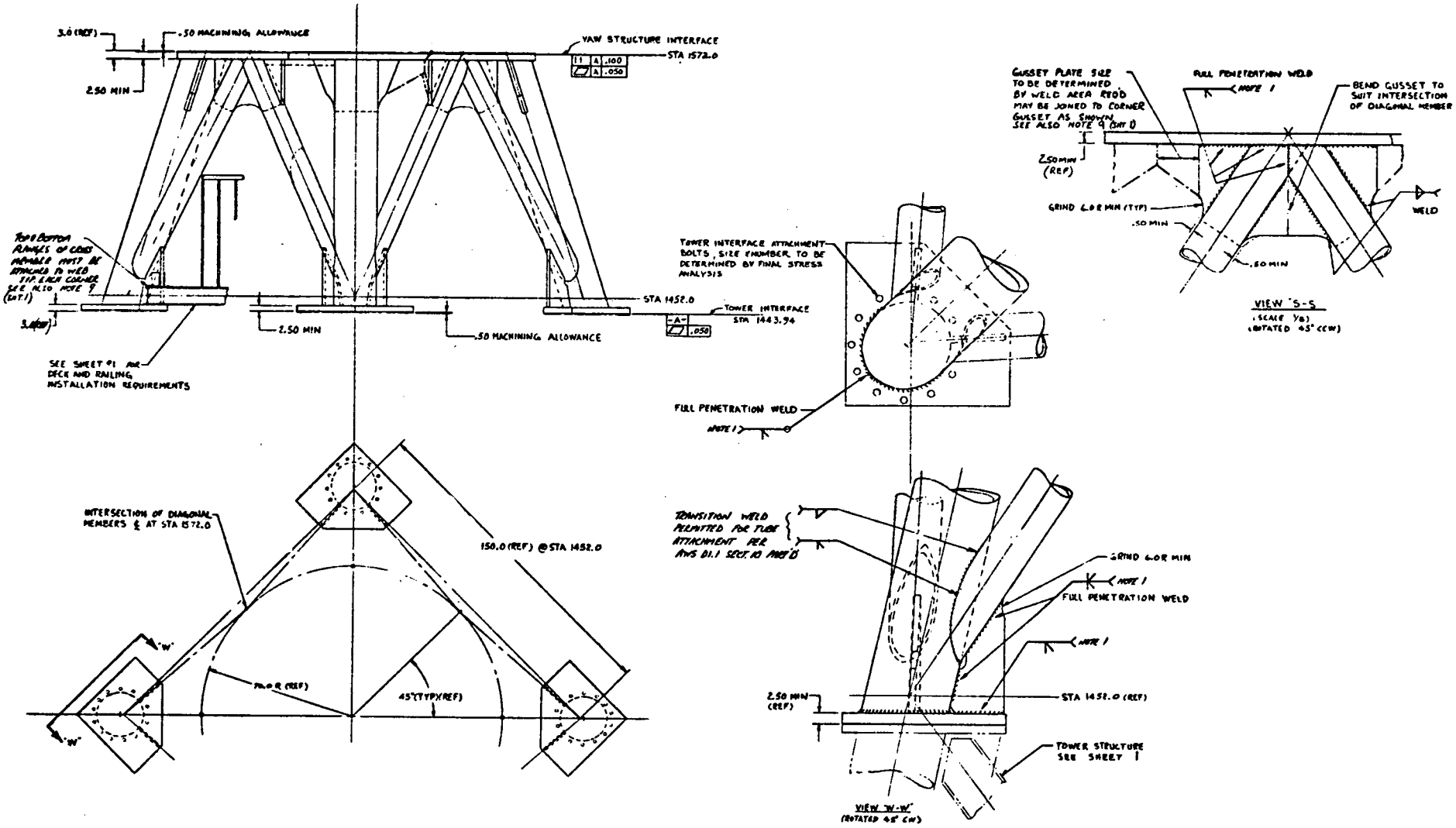

Figure 5.6-1B Tower Configuration, Sheet 2

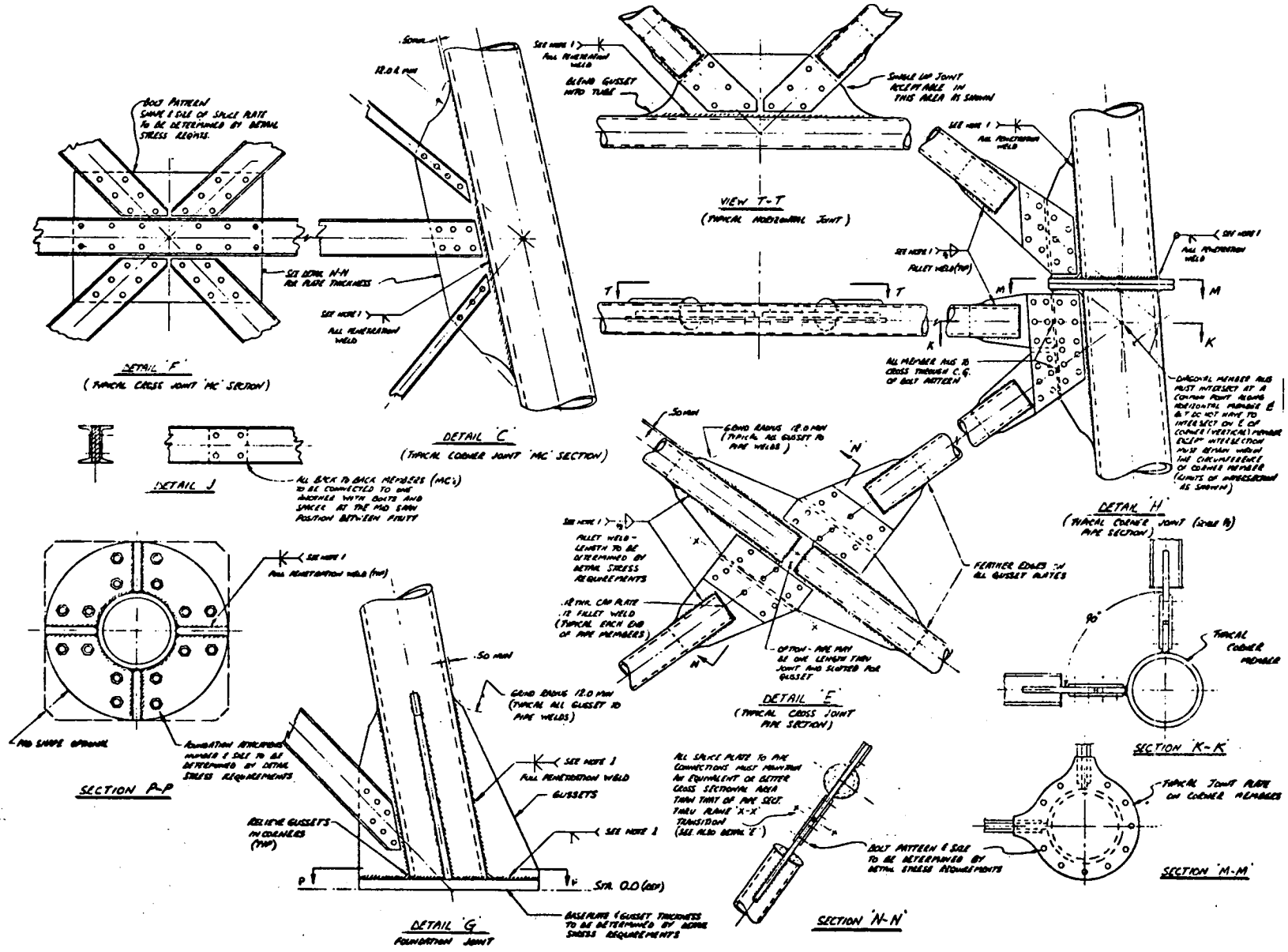

Figure 5.6-1C Tower Configuration, Sheet 3

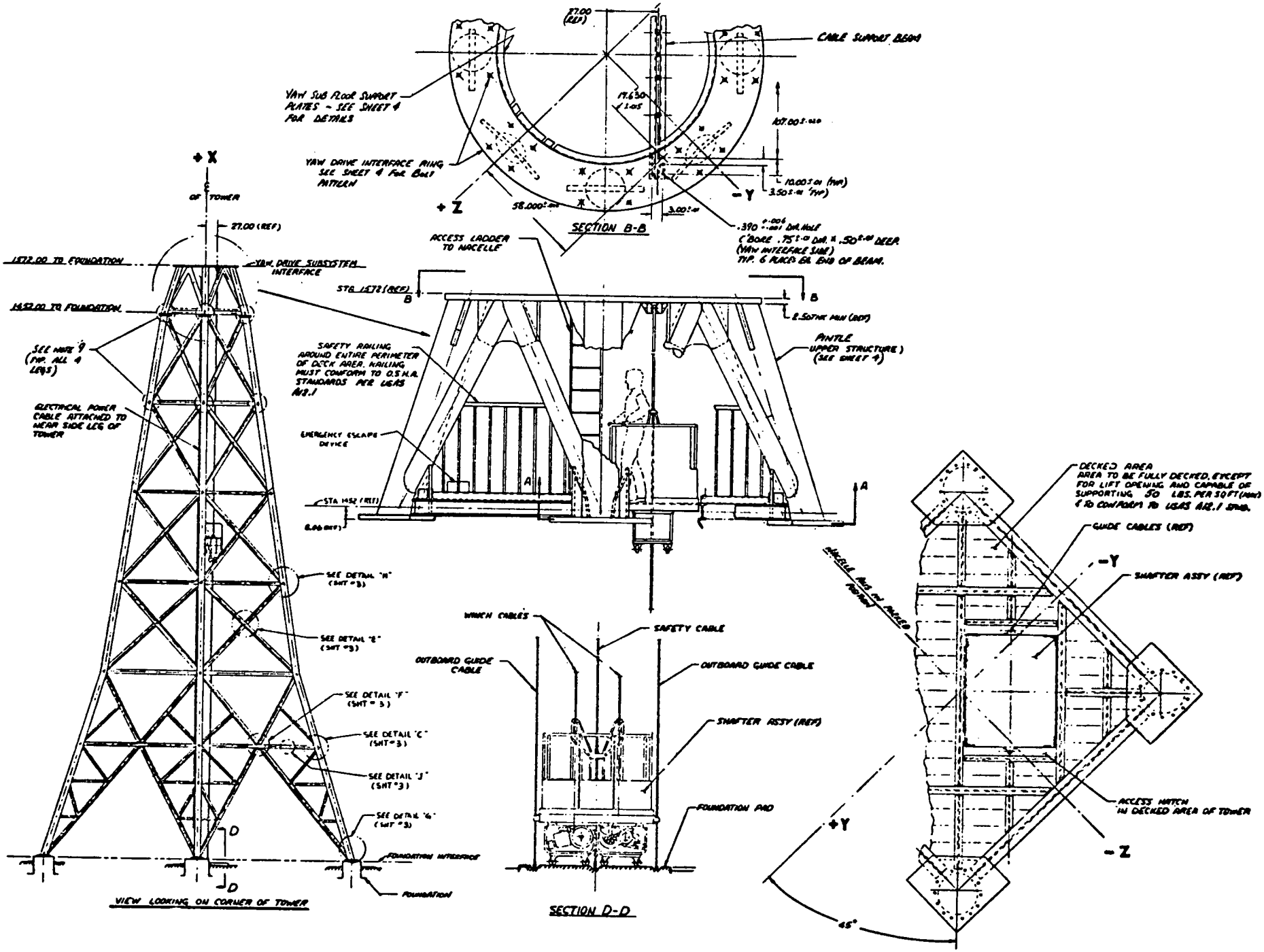

Figure 5.6-1D Tower Configuration, Sheet 4

Table 5.6-1. Mod-1 Tower Engineering Characteristics

Total Height	131 ft
Width at Base	48 ft
Width at Pintle	12 ft
Design Life	30 yrs
Total Weight	360,000 lbs
Materials	
Tubes	ASTM A333
Shapes	ASTM A36
First Bending Natural Frequency	3.2 P
First Torsional Natural Frequency	7.2 P
Design Codes	AISC, AASHTO

Pipe of the required diameter and wall thickness is normally available to a limited number of specifications. The two candidate materials for the tower were ASTM specifications A53 and A333. As shown by the comparison summarized in Table 5.6-2, A333 has good, well-established fracture toughness but is higher in cost than A53 when compared for Zone 1 service temperatures (0°F and above). However, for Zone 3 service, the cost difference becomes uncertain. Suppliers are unwilling to guarantee the results of Charpy V-notch tests on A53 pipe because of the latitude in chemical composition of steel to this specification. Experience with bridge failures due to brittle fracture has led AASHTO (American Association of State Highway and Transportation Officials) to specify the test temperature for standard impact tests with steels similar to A36 at 70°F above the intended service temperature. For Zone 3 (-31 to -60°F), toughness must exceed 15 ft-lb at a test temperature of 10°F. As shown in Table 5.6-2, A333 would have no difficulty meeting this requirement while test results for A53 would be marginal and only selected heats would be expected to pass. When a review of system requirements confirmed that service temperature limits were not to be compromised, selection of A333 for the tubular members of the tower became essential.

Table 5.6-2. Comparison of Pipe Specifications

	A53 Grade B	A333 Grade 6
Tensile Strength, Min(ksi)	60	60
Yield Strength, Min (ksi)	35	35
Minimum Impact Test Temperature	Not required	-50°F
Impact Strength, 10°F(ft-lb)	5 to 15	20 to 30
Carbon, Max. (%)	.30	.30
Manganese, Max. (%)	1.20	.29 - 1.06
Phosphorus, Max. (%)	0.05	.048
Sulfur, Max. (%)	0.06	.058
Silicon, (%)	NA	.10 Min.
Cost*, $/lb. (Zone 1 Service)	.39	.51

*Costs quoted April, 1977, for 20" diameter pipe.

Tubular members for the tower were specified because of their low drag coefficient as compared with other structural shapes. The objective was to keep the velocity decrement in the tower wake acceptably small, and to have confidence in the estimate of tower shadow by being able to relate it to wind tunnel measurements for all-tubular tower models and other data. Within the framework of overall geometry and section properties selected to meet strength and stiffness requirements,

a study was made to determine if some of the members could be standard structural shapes. The question to be answered was, would the lower cost of standard shapes such as I's or channels justify a possible increase in the magnitude of the tower shadow and hence, the magnitude of cyclic loading? Several variations were considered, but the choice narrowed to the two configurations compared in Table 5.6-3. The use of channel shapes for diagonal members below the blade tips does not significantly affect tower shadow and is economic.

Table 5.6-3. Tower Concept Comparison

	Concept "B"	Concept "D"
Tower height, ft.	131	131
Legs, size and type	20 in. pipe	20 in. pipe
Material	A333	A333
Weight, 10^3 lb	128	128
Projected area, Ft^2	309	309
Drag coefficient	.42	.42
Diagonal Members, Pintle Section, Size and Type	12 in. pipe	12 in. pipe
Material	A333	A333
Weight, 10^3 lb	30	30
Projected area, Ft^2	38	38
Drag coefficient	.40	.40
Diagonal Members Below Pintle, Size and Type	8 & 10 in. pipe	8 & 10 in. channel
Material	A333	A36
Weight, 10^3 lb	112	128
Projected area, Ft^2	311	311
Drag coefficient	.90	2.0
Diagonal Members Below Blade Tips, Size and Type	3 & 10 in. channel	3 & 10 in. channel
Material	A36	A36
Weight, 10^3 lb.	50	50
Total Weight, 10^3 lb	320	336
Total Projected Area, Ft^2	658	658
Average Drag Coefficient	.66	1.17
Relative Wake Energy	1.0	1.76
Relative Velocity Decrement	1.0	1.33

The cost difference for channel members in bays above the blade tips is summarized in Table 5.6-4. Because channel members are less efficient in buckling, a weight increase results when these members are used. Note that the cost figures in this comparison were quoted in April, 1977, and may not reflect prices actually paid. Tower shadow characteristics of the two concepts were compared by calculating an average drag coefficient, weighted

Table 5.6-4. Tower Concept Cost Comparison

	Concept "B"	Concept "D"
Diagonal Members	Pipe	Channel
Material	A333	A36
Weight, 10^3 lb	112	128
Material Cost, $/lb	.40	.215
Fabrication Cost $/lb	.525	.462
Cost Difference, $10^3$$	+16.9	--
Cost of Fairing Installation, 10^3 $	--	+15 to 20

NOTE: Comparison only diagonal members below pintle and above blade tips. All other members are the same.

according to the projected areas of each member shape. These calculations are summarized in Table 5.6-3, which shows that the wake energy for concept "D" would be 76% higher for "B", or the velocity decrement 33% higher. If service experience were to show that the more severe tower shadow were unacceptable, a solution would be to install sheet metal fairings to all channel members which would reduce the drag coefficient from 2.0 to perhaps 1.0 or less. However, the costs of such modification are estimated at 15 to 20 thousand dollars and several weeks time. Because the risk was not justified by the potential cost savings, concept "B" was selected.

An estimate of the anticipated velocity decrement can be made by comparison with wind tunnel data

$$\Delta V = \Delta Vo \times (k \times C_{D_1}/C_{D_0})^{\frac{1}{2}}$$

where ΔVo = velocity decrement from wind tunnel test
= .225
k = solidity factor = 1.51
C_{D_1} = Mod 1 drag coefficient = .66
C_{D_0} = Model drag coefficient = 1.2
ΔV = .205

This value agrees with the conservative assumption of a 24% tower shadow effect used in the system dynamic simulation.

5.6.4 FOUNDATION DESIGN

The tower is supported by separate foundations for each of its four legs, typically shown in Figure 5.6-3. Borings at the Boone, North Carolina, site showed the presence of foundation quality rock just below the surface. The foundation was designed by J.E. Sirrine Company, Raleigh, North Carolina, based on the core sample properties. Because of the dead weight of the wind turbine, relatively small tension loads are developed in the foundation. Each leg is secured by eight 1.50 in. diameter anchor bolts, hooked at a depth of 30 in.

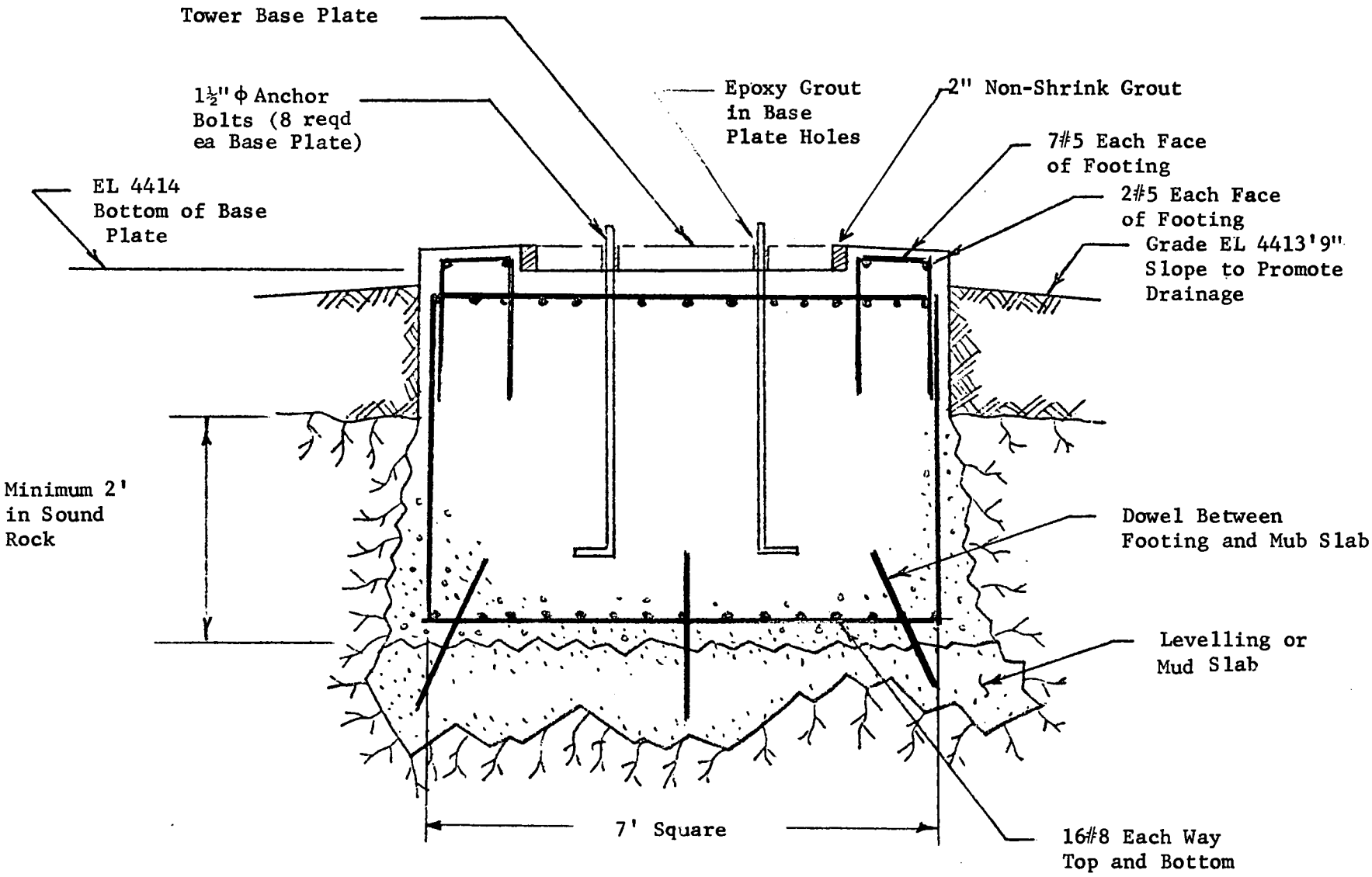

Figure 5.6-3

Typical Tower Footing Design

in the foundation. The shear load is reacted from the tower base plate through non-shrink grout to a lip on the foundation tied with No. 5 reinforcing bars to to the primary reinforcing bars in the foundation. Shear load is also transferred to the anchor bolts through friction and epoxy grout in the base plate holes.

5.6.5 PERSONNEL LIFT AND ACCESS PROVISIONS

A personnel and equipment transfer device will be installed and used as a means of gaining access from ground level to a platform located approximately 120 feet above grade. Figure 5.6-2 (GE Drawing 298E458) shows the overall installation of this transfer device. It is identical to the unit installed by NASA on the Mod-0 WTG at Sandusky, Ohio. It is Model No. ST-27 (Shafter) as manufactured by Spider Staging Sales Company, Renton, WA.

In the event of failure of the lift device, personnel can be evacuated from the tower by means of an emergency escape device supplied for use with Model ST-27. This unit is called "Rescumatic" and is an off-the-shelf device that meets OSHA requirements, ANSIB30.1, ANSIB30.2, ANSIB30.3 and ANSIB30.11, "Emergency Egress from Elevated Work Stations". It is a fully automatic, nonpowered device that provides a safe, constant descent speed of 3 fps. There is a personnel sling at each end of the descent cable whereby continuous operation can be offered without the need to rewind. Two of these units are planned for use with the lift device and another would be stored in the platform area at the base of the nacelle. A training program is recommended for potential users of the "Rescumatic" unit.

The Rescumatic unit has undergone life expectancy tests conducted by Underwriters Laboratory. Rescumatic was operated continuously for three months at 24 hours/day. At the end of this period, the linings were worn out, but the unit was capable of safe use without the clutch lining. (The unit operated rather loudly, and the descent was not a smooth ride.)

Translating the life test to comparable WTG application, the Rescumatic unit could be used 20 times a month for 30 years before it showed signs of wear.

5.6.6 TOWER STRESS ANALYSIS

The analytical approach was to develop a detailed finite element computer model. The analysis of the model was performed with the use of the GE computer program called MASS.

The finite element computer model represents the entire 130-foot tower including every structural member plus the yaw bearing support. This model consists of 117-grid points having 701 degrees of freedom. The corner members and all upper bay diagonal and horizontal members are tubular. The bottom bay diagonal

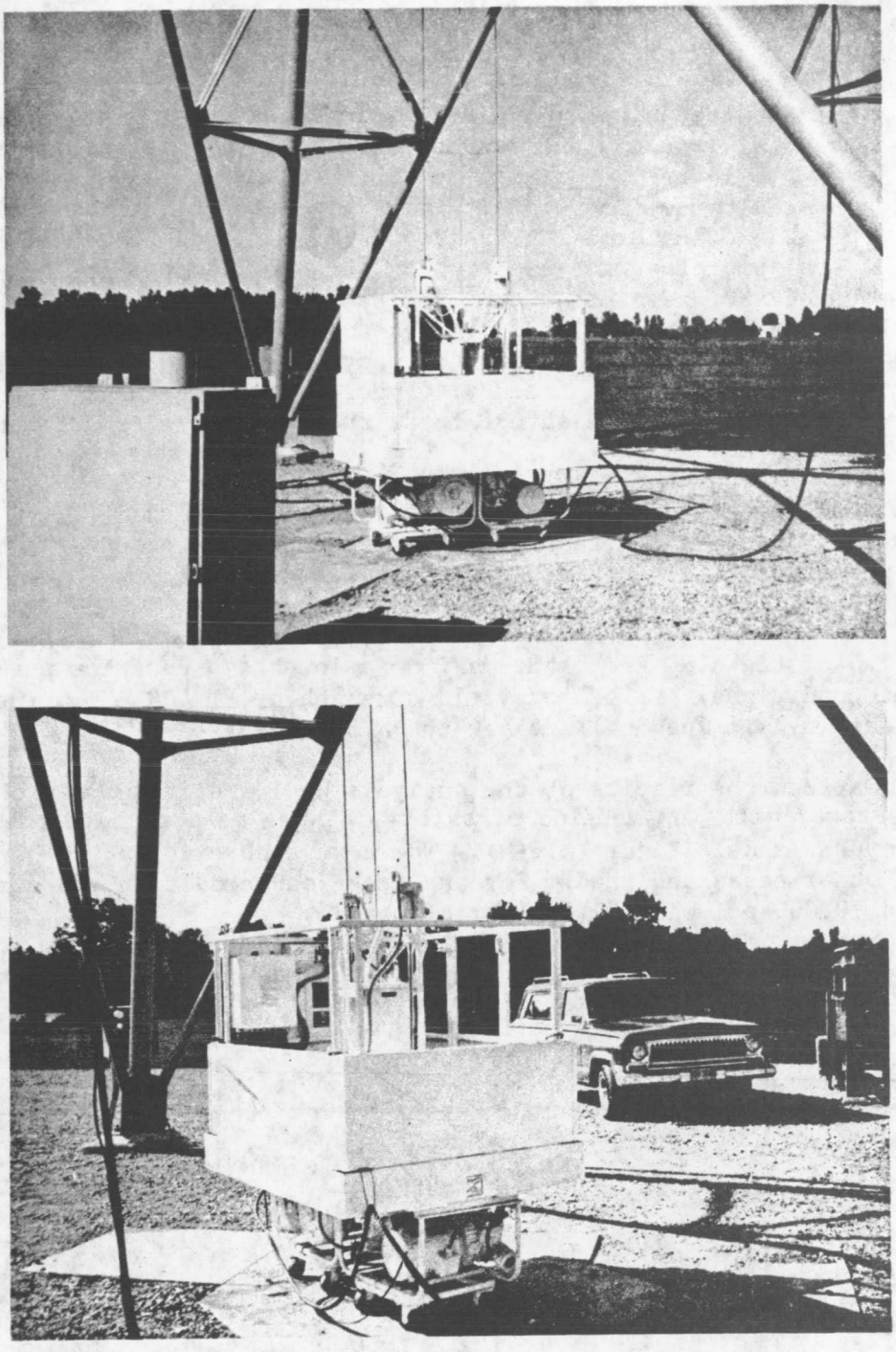

Figure 5.6-2 Personnel Transfer Device

and horizontal members are back-to-back channels. Figure 5.6-4 shows the tower grid point locations. Figure 5.6-5 is a computer printout of this model.

Critical load cases for the tower were: Case A (fatigue) and Case B (peak dynamic load), as defined in Appendix "B".

The major area of concern is the range stress due to the oscillatory loading for the 30-year life requirement. Referring to the AISC code as shown in Figure 5.5-3, the range stress allowable depends on the number of cycles and type of joint. For a plate welded joint (Category E) having 2×10^6 stress reversals (Loading conditions 4), the range stress allowable is 5,000 psi.

The MASS program uses a three-dimensional finite element stiffness matrix solution and is capable of determining the static/dynamic and thermal behavior of a structure. Analysis of a wide spectrum of structural types including trusses, frames, shells of revolution and pressure vessels, as well as combinations of these can be accomplished. The capability of the program is 20 substructures. Each substructure can have as many as 200 nodes for a total of 4,000, each with six degrees of freedom. Types of loading include point or lumped mass, distributed or pressure forces, thermal gradients and maneuver forces.

The program is most generally used to provide a detailed internal stress and distortion analysis based on the resultant load/thermal environment. A second purpose is to provide a stiffness matrix for specified nodes to be used in subsequent dynamic analysis.

Using Section 1.5 of the AISC Code, the maximum allowable stress for peak loading (infrequent conditions), is 60% of yield strength or 21,600 psi. The range stress allowables (cyclic loading) are per the AISC code.

Table 5.6-5 summarizes the results of the analysis by identifying only the members in the tower with low margins of safety. These members have been identified on the computer model (Figure 5.6-4). There were no critical members or joints for the other cases analyzed. For the peak load condition, no combined stress exceeded 10,000 psi with 21,600 psi allowable.

Table 5.6-5. Summary of Critical Margins of Safety in Tower Members

Member	Stress Range (psi)	Allowable Stress Range (psi)	Margin of Safety
477-486	2940*	5000**	.70
479-486	2540*	5000**	.97
481-490	2130*	5000**	1.35
483-492	3170*	5000**	.58
477-492	2590*	5000**	.93
401-516	4730	7000	.48
516-412	5130	7000	.36
404-514	6570	7000	.07
514-504	5340	7000	.31

All members had high margins of safety in buckling.

*Diagonal members at the top of the tower are reinforced with gussets providing an additional area of 30 in^2 at the location of the Category "E" weld.

**Category "E", loading condition 4, per AISC Code, 1978 Edition (in press)

As an illustrative example, consider member 404-514, which is a section of one of the four leg members, from the foot (404) to the intersection with the first horizontal brace members (514). Figure 5.6-6 is the computer printout for this member, analyzed for Case A cyclic loads. Note that the maximum combined stress of 3285 psi occurs at joint 404, due primarily to the bending stresses introduced by diagonal members 404-513 and 404-515. Conservatively, the cross section at joint 404 is assumed to be that of the 20 in. diameter pipe only, with no credit taken for the added area of the four stiffening gussets. The stress range is assumed to be double* the maximum combined stress, or 6570 psi. The allowable range stress for a Category D weld joint, loading condition 4 is 7000 psi. (Category D is applicable to base metal adjacent to a detail of limited length attached by a groove weld subjected to tranverse loading, when the detail length is less than 4 in., with no transition.) The margin of safety is:

$$MS = \frac{7000}{6570} - 1 = + .07$$

* To simplify computations, the loading was assumed to be completely reversed so that the stress range was conservatively taken as double the maximum combined stress, or 6570 psi.

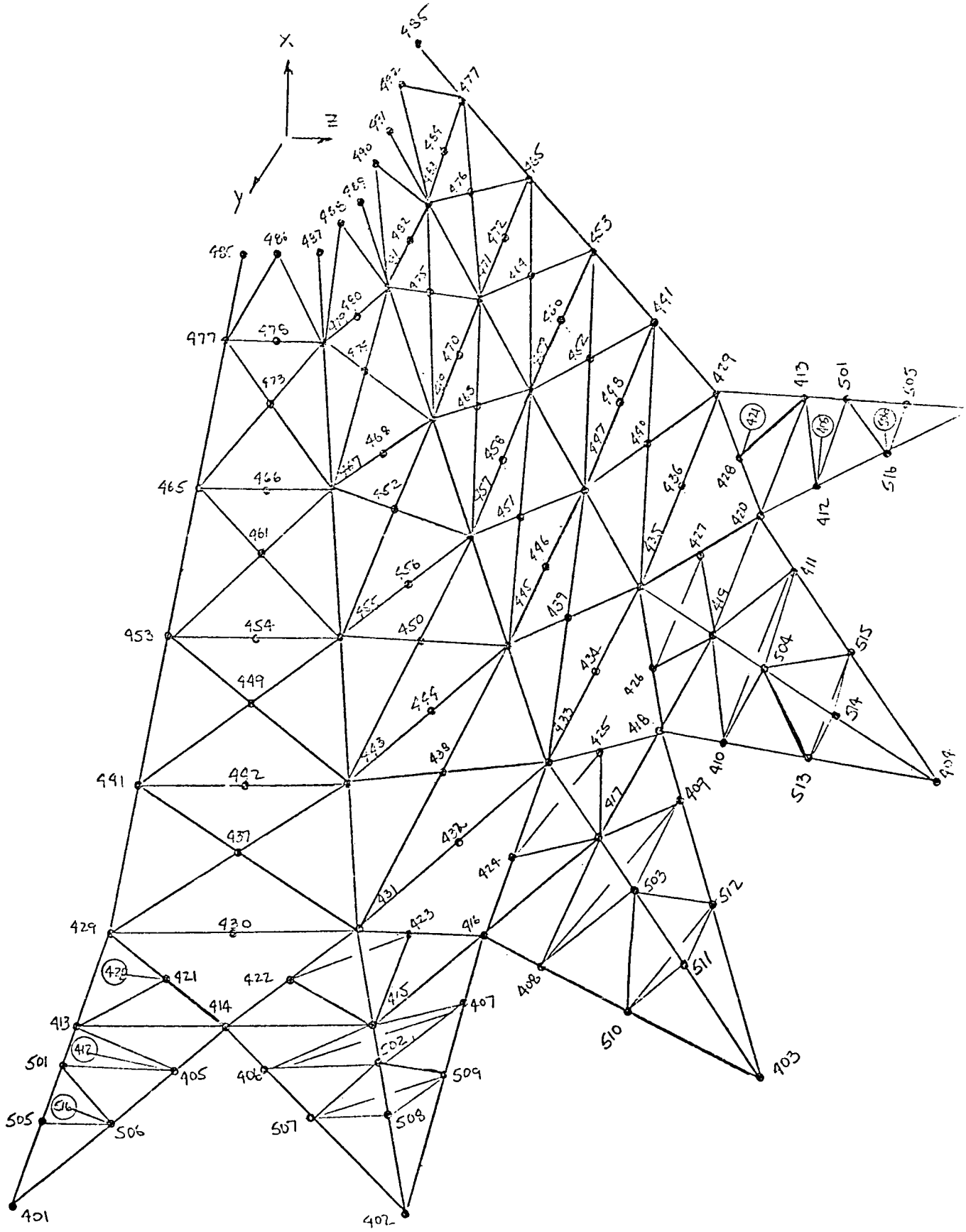

Figure 5.6-4 Node Identification for Tower Finite Element Model

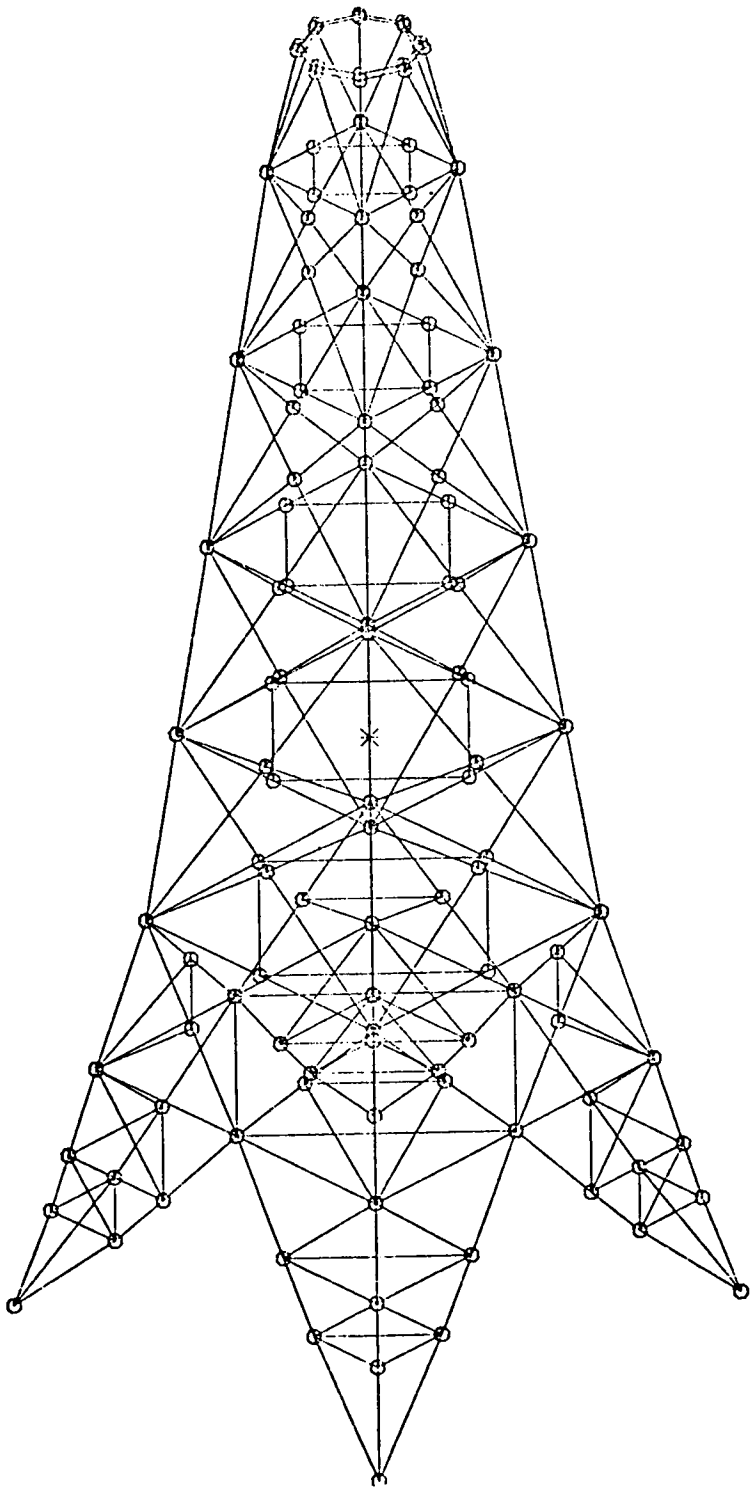

Figure 5.6-5 Computer Plot of Tower
Finite Element Model

```
                                MEMBER  404  514 ( STRAIGHT TUBE )                    FREQUENCY = 0.

      I JOINT, JOINT  404 - COORDINATES (     -1680.,     -288.0,     -288.0) - RESTRAINT CODE ( 0, 0, 0, 0, 0, 0)
      J JOINT, JOINT  514 - COORDINATES (     -1558.,     -258.0,     -258.0) - RESTRAINT CODE ( 0, 0, 0, 0, 0, 0)
      O JOINT, REFERENCE - COORDINATES (     -1188.,      180.0,     -180.0)

  REFERENCE  TEMP      = 0.                TOTAL MEMBER WEIGHT  =      2919.      TOTAL MEMBER LENGTH  =      129.2
  RATIO                = 0.                ROTOR  SPEED         = 0.

  YOUNGS  MODULUS      = 0.3000E 08        WEIGHT  DENSITY      = 0.3000E 00      DISTRIBUTED LOADS  1 = 0.
  SHEAR   MODULUS      = 0.1000E 08        TEMPERATURE  GRAD 1  = 0.                                 2 = 0.
  THERMAL COEFFICIENT  = 0.                TEMPERATURE  GRAD 6  = 0.                                 3 = 0.
  OUTSIDE  RADIUS      = 0.1000E 02        TEMPERATURE AVERAGE  = 0.                                 4 = 0.
  TUBE  THICKNESS      = 0.1281E 01                                                                  5 = 0.
                                                                                                     6 = 0.

                                        * * *  CALCULATIONS  * * *

                              DIRECTION 1     DIRECTION 2     DIRECTION 3     DIRECTION 4     DIRECTION 5     DIRECTION 6

  X,Y,Z LOADS   JOINT  404 (I) 0.1301E 06     0.2705E 05     -0.3535E 06     0.3350E 05     0.3415E 06     0.2781E 05
                JOINT  514 (J)-0.1296E 06    -0.2750E 05     -0.2147E 06    -0.2499E 05     0.1918E 06    -0.2732E 05

  NORM. DEFLS.  JOINT  404 (I) 0.             0.              0.             0.             0.             0.
                JOINT  514 (J) 0.1434E-01    -0.7739E-02     -0.8482E-04    -0.9910E-04    -0.5627E-04    -0.1586E-01

  NORM. LOADS   JOINT  404 (I)-0.4424E 04     0.1357E 06     0.3382E 06     0.3570E 06     0.2885E 05     0.4236E 04
                JOINT  514 (J) 0.3830E 04    -0.1352E 06     0.1948E 06     0.2115E 06    -0.2892E 05    -0.4567E 04

  POTENTIAL  ENERGY  = 0.5687E 03                                                          KINETIC  ENERGY  = 0.

  ========================================  STRESS  CALCULATION  1051  ========================================

      INPUT  CONSTANT                                                  JOINT  404      MID  POINT      JOINT  514

      PRESSURE = 0.                                  COMBINED  STRESS   0.3285E 04                     0.2663E 04
                                                LONG. BENDING STRESS   0.1483E 04                     0.8675E 03
```

Figure 5.6-6 Computer Output for Tower Stress Analysis

SECTION 6

POWER GENERATION SUBSYSTEM

SECTION 6

POWER GENERATION SUBSYSTEM

This section describes the electrical system of the Wind Turbine Generator. The main power transfer path through the generator, main breaker and step-up transformer are covered. In addition, the auxiliary power supply, control system interface equipment, interconnecting wiring, the ground control enclosure, and various protective devices are also described.

6.1 REQUIREMENTS AND SYSTEM OVERVIEW

6.1.1 STATEMENT OF WORK REQUIREMENTS

Requirements, as paraphrased from SOW NAS-320058, are:

Exhibit B

1.1	2000 kWe Rated Power, 60 Hertz synchronous generator, 30-year life
1.4	Availability, life, general environment
1.6.5	NEMA Standards
1.7.3	100,000 Startups
2.4.8.4.1	Nacelle Lightning Protection
2.4.8.5	Nacelle Lights, outlets & intercom
2.5.1	4160V, 2188 kVA, 40°C, .8 pf, more than 90% efficient, 105°C Rise for Class F, MG1-22 generator requirements.
2.5.2	Safe shutdown power
2.5.3	Slip rings
2.5.4	Mutual fault protection
2.5.5	Lightning protection of electrical equipment
2.5.7	FAA approved illumination
2.7.1.1	Synchronize
2.9	Lightning model for 2.4.8.4.1 of Exhibit B

Additionally, interconnection with the site utility and wiring of the Engineering Data Acquisition System (EDAS) is required.

6.1.2 SYSTEM OVERVIEW

A simplified one-line diagram of the basic power circuit is shown in Figure 6-1. The utility connection with Blue Ridge Electric Membership Cooperative (BREMC) is stepped down from 12.47 kV to 4.16 kV. Auxiliary power is obtained from the 4.16 kV bus through transformers to 4 and 208Y120 Volt distribution systems. The generator is connected or disconnected from the 4.16 kV bus depending on whether or not the wind is blowing.

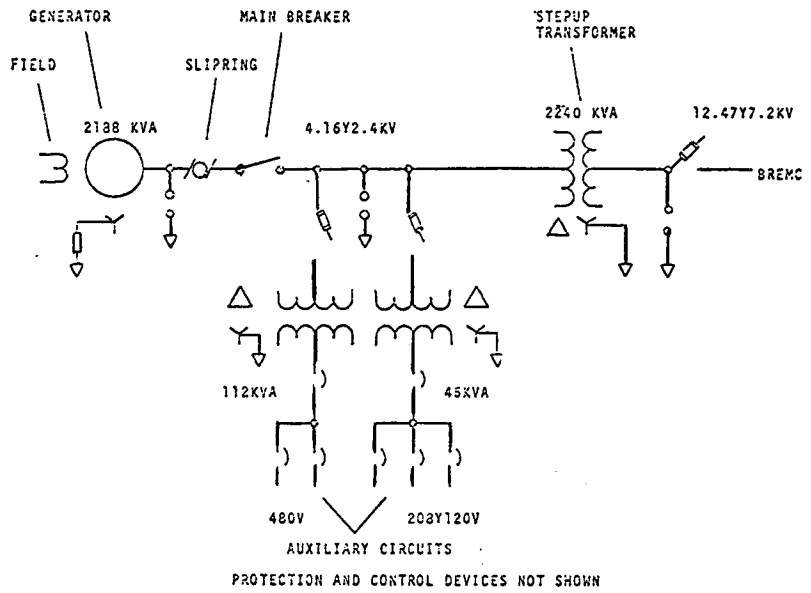

Figure 6-1 Simplified One-Line Diagram

The full one-line diagram of power distribution and relaying is shown in Figure 6-2. A description of the function of each device appears in Paragraph 6.3. The relaying represents an economical protection scheme utilizing standard components and electrical utility practices.

A block diagram of the system location of major elements is shown in Figure 6-3. The generator and associated exciter, sensing and protective devices are located in the nacelle. An auxiliary control and power distribution box, several discrete sensors, and the nacelle multiplexer unit (NMU) are interconnected and wired to the tower slip rings which provides for yaw rotation.

On the tower side of the slip ring, conduit enclosed wiring runs to the control enclosure at the base of tower. The enclosure houses the remainder of the control system, the generator main breaker, additional sensing and indicating devices, and the auxiliary power transformers and distribution. A separate pad is located under the tower for mounting of the Generator Step-up (GSU) Transformer which connects to the enclosure and to the BREMC.

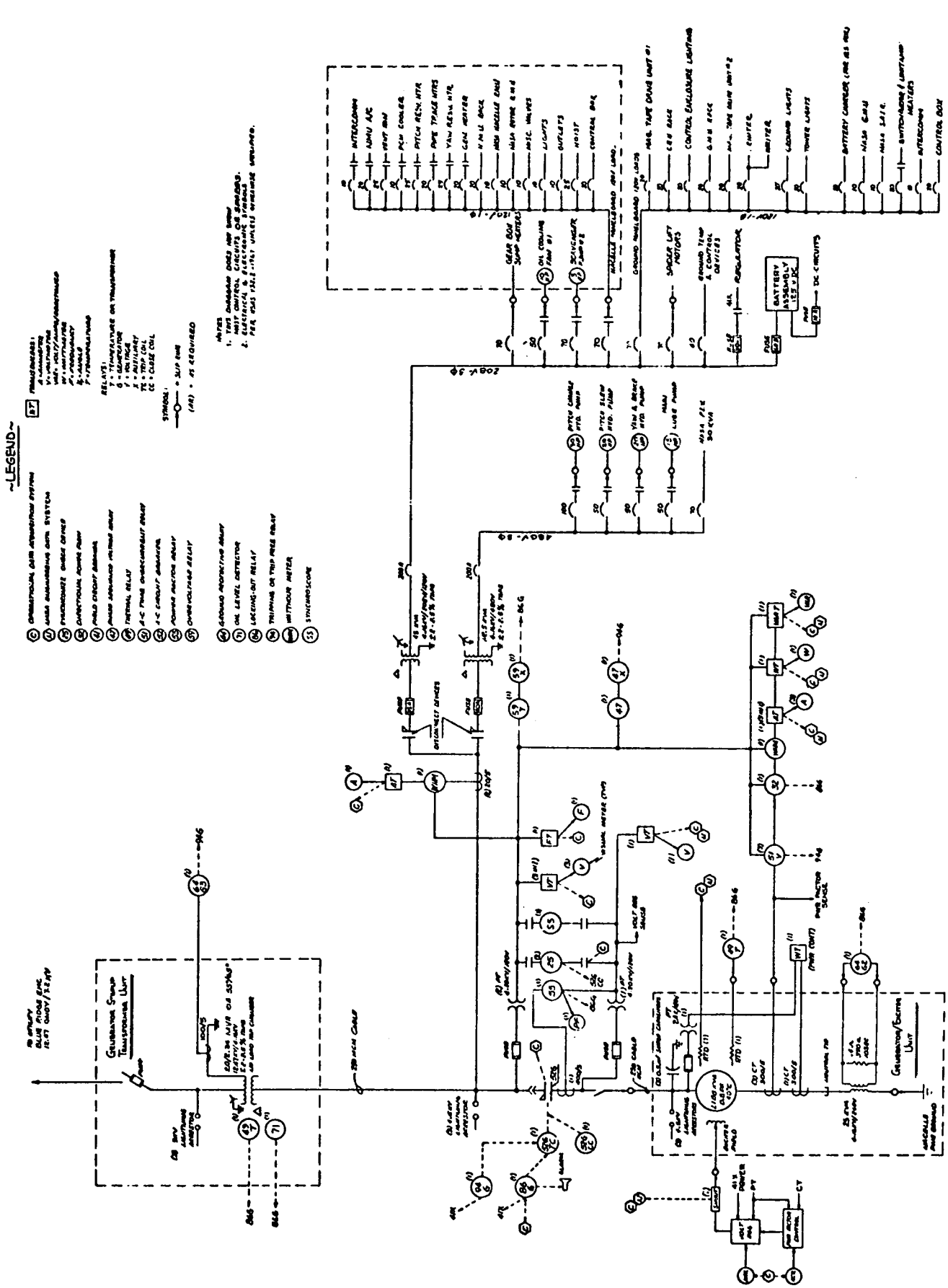

Figure 6-2 One-Line Diagram

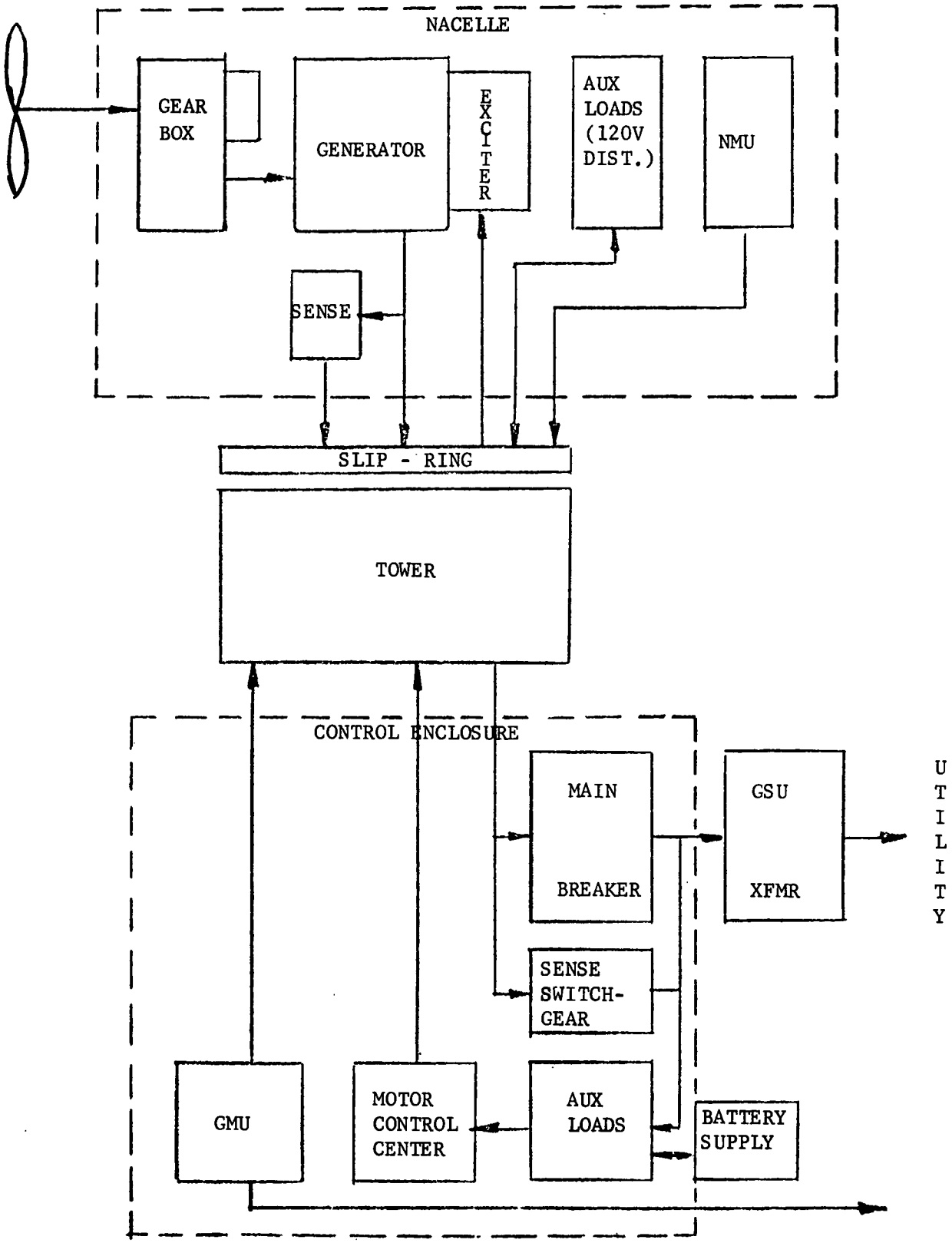

Figure 6-3 Mod-1 WTG Block Diagram

The individual elements of the Wind Turbine Generator system are described in the following paragraphs.

6.2 GENERATOR AND POWER GENERATION AUXILIARIES

The generator, shown in Figure 6-4, is a 4-pole, 1800 rpm, 4160 Volt, Wye connected unit with shaft-mounted exciter. Class F (105°C rise over 40°C ambient) insulation is used. The generator is rated 2188 kVA, .8 power factor and the exciter is rated at 25 kW at standard ambient. A cutaway illustration of the unit's construction is shown in Figure 6-5.

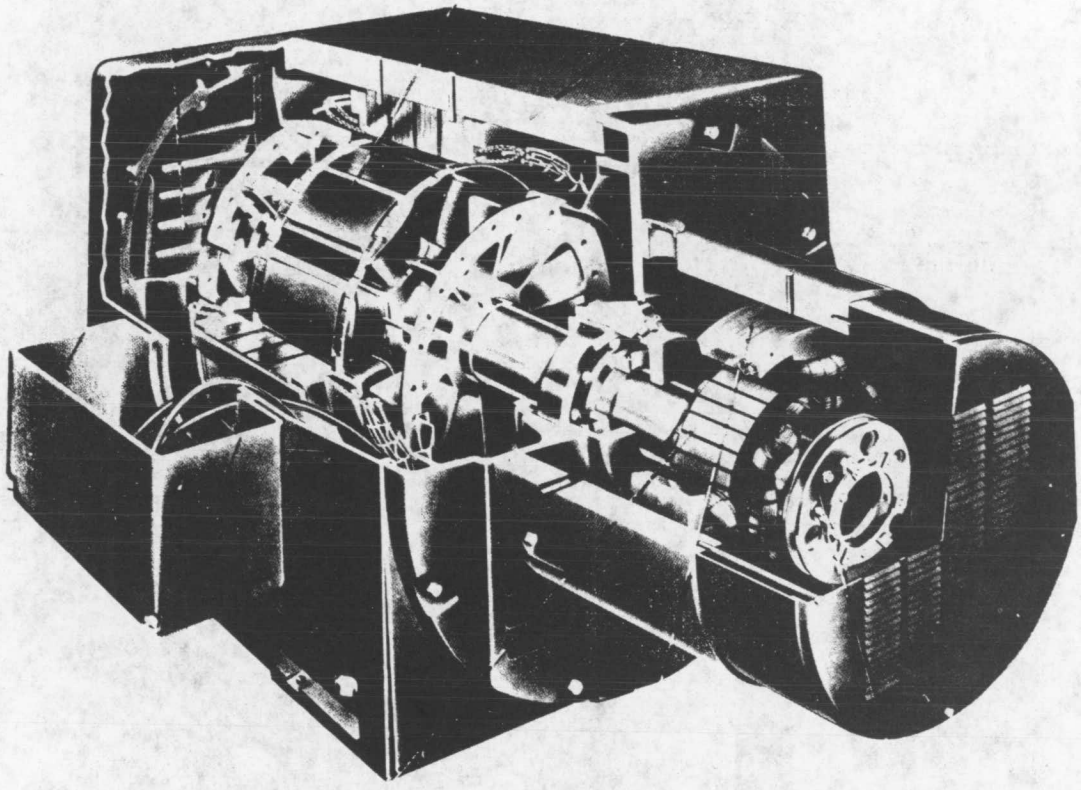

Figure 6-5 The Cutaway of Generator

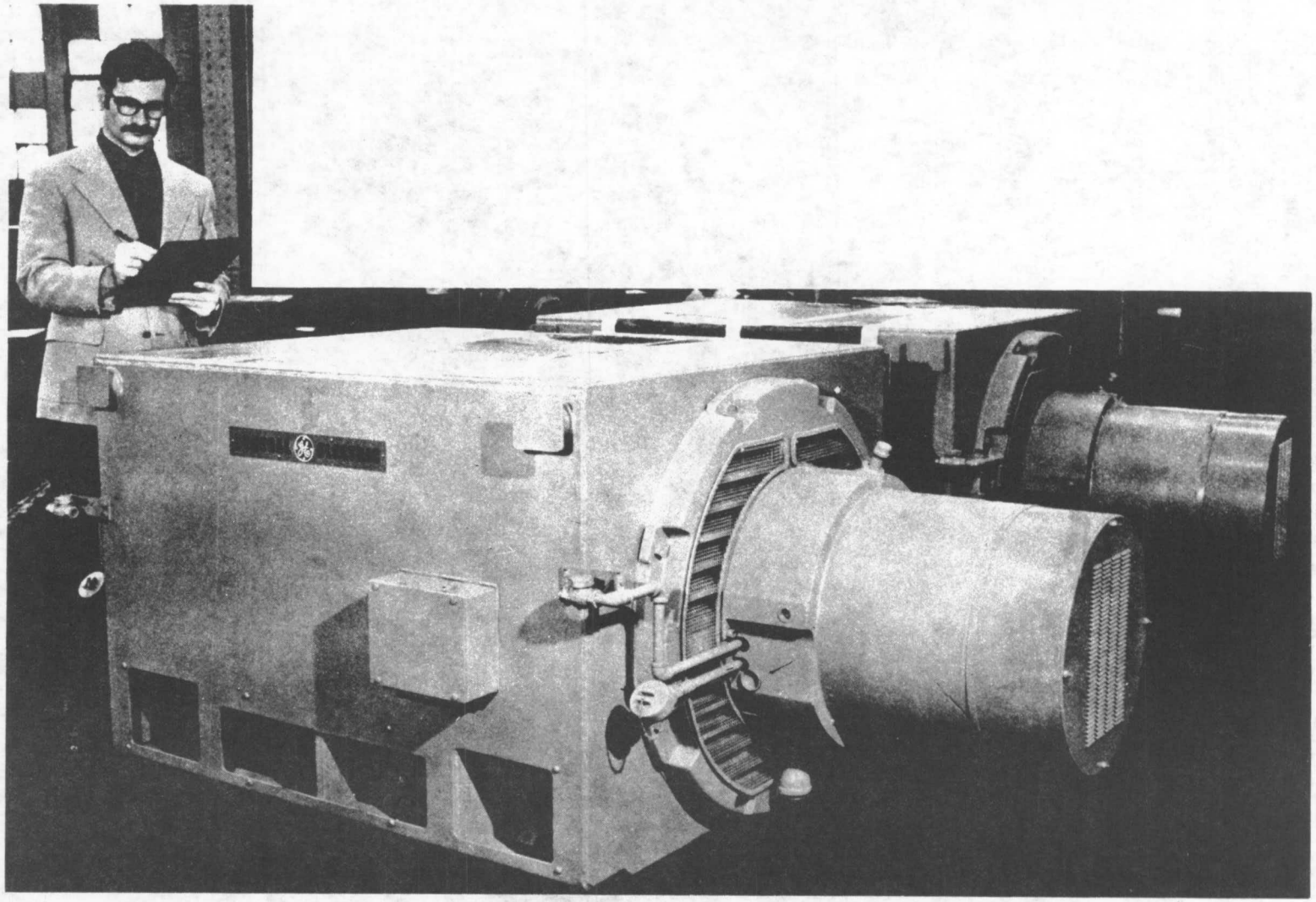

Figure 6-4 Generator

Due to the above average number of starts anticipated, provisions have been made to supplement the normal sleeve bearing oil ring lubrication system with a flood-type system. The hydraulic package is not provided but can readily be added if field experience indicates one is needed.

The sleeve-type bearings and their mounting are split for ease of replacement and this type of bearing has an excellent life record. Synchronous machines of this size have a relatively large air gap, on the order of 0.125 inches and considerable bearing wear can be tolerated before replacement is mandatory.

Generator characteristics and saturation curves are shown in Paragraph 4.2 of this report.

The generator with accessories weighs 11,500 pounds in a frame that occupies 120 cubic feet of space. An open top frame construction is used with cooling air drawn in from the ends and discharged through the top via ducting.

RTD detectors are provided for monitoring stator winding and bearing temperatures. A space heating coil is also provided to prevent condensation. It will be energized when the unit is not generating.

Special tests are not called for as the machine design is mature. Design problems are not anticipated. Standard commercial tests have been performed by the manufacturer and consist of:

1. Resistance of armature and field check
2. High potential and insulation resistance test
3. Phase rotation check
4. Shaft current check
5. No load excitation check
6. Mechanical balance check at rated speed
7. Bearing end play check

Auxiliary equipment is mounted in a caged area under the generator and consists of primary winding protective lightning arrestors and surge capacitors, a potential transformer, neutral side mounted current transformers, and a grounding transformer. The all six generator leads are brought out in order to mount the phase current transformers. A grounding resistor associated with the transformer is mounted on top of the generator. Current transformer and potential transformer ratios and the resistor rating are shown on the one-line, Figure 6-2.

6.3 SWITCHGEAR AND TRANSFORMER

6.3.1 ELEMENTS OF SWITCHGEAR

Switchgear for control, protection and instrumentation of the system are mounted in the control enclosure and basically consist of:

1. Generator Circuit Breaker and Isolation Switch
2. 4160 Volt Bus and Protection Equipment
3. Instrument Transformers

4. Protective Relays
5. Transducers for signals to Data Systems
6. Auxiliary Power Supply Transformers
7. Main Protection for Auxiliary Power Supply
8. Terminations for High Voltage Cable
9. Grounded Metallic Enclosure
10. Visual Indicating Instruments
11. Generator Control Devices

6.3.2 GENERATOR CIRCUIT BREAKER AND ISOLATION SWITCH

The generator circuit breaker 52G is based on a large motor starter rated at 4160 Volts, 360 Amperes continuous, with 50 mVA interrupting capability without fuses.

The WTG generator switching device will be operated frequently. Conventional air magnetic breakers (such as the GE AM 4.16 - 250) have a somewhat limited repetitive duty capability as defined by industry standards. For example, the maximum number of breaker operations between minor servicing is 2000. Furthermore, conventional breakers are required to sustain no more than 10,000 no-load mechanical operations, or 5000 full-load non-fault operations before major servicing is required.

The breaker used is the air break contactor employed in GE Limitamp^{R} motor starters shown in Figure 6-6. This device is designed specifically for repetitive operations and tests have shown that major maintenance of the contactor would not be required for at least one-half million operations.

The Limitamp contactor is frequently employed as an inexpensive small breaker substitute in situations where its 50 mVA symmetrical interrupting capability is sufficient (or where the use of fuses for current limiting in association with the contactor is satisfactory) and the contactor has a ten-cycle blocked withstand capability of 18,810 Amperes rms. A short circuit study was performed on the wind turbine generator system to verify that a Limitamp contactor would be satisfactory. This study assumed a stiff 1000 mVA source at the transformer and indicated that the interrupting duty on the contactor would be approximately 29 mVA and the momentary duty would be approximately 6963 Amperes, both of which are well within the tested capability of a Limitamp contactor.

Another consideration in using a Limitamp contactor for a generator breaker is that during synchronization, the voltage across the contactor tips will be twice system voltage. The 5 kV Limitamp contactor has an AC one-minute hipot rating across the contact tip of 20 kV, which is more than sufficient for this application.

In critical applications, it is advisable to employ a special form of contactor which includes two coils. One coil is a solenoid closing coil which causes the main contacts to close under control of the synchronizer and which engages a mechanical latch. After the main contacts are closed and the latch is engaged, the closing-coil circuit is interrupted. The contactor may be opened by energizing the second coil which releases the mechanical latch. Therefore, the mechanically latched contactor performs just as a conventional stored-energy circuit breaker with close and trip coils. An antipump circuit is provided to prevent more than one closing operation for each close circuit pickup.

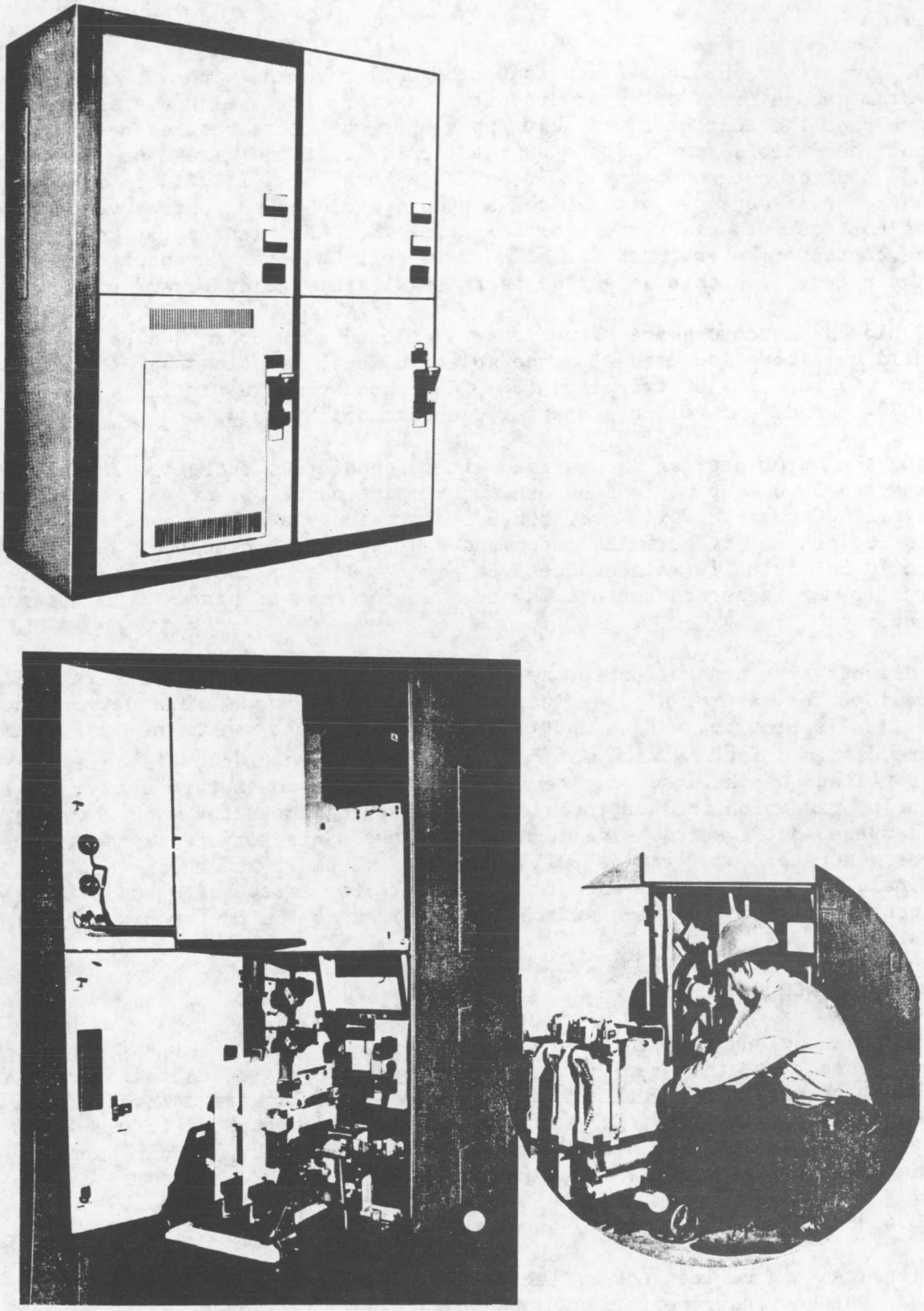

Figure 6-6. Main Contactor

The use of a mechanical latch contactor will make the wind turbine generator system secure from contactor dropout. However, it is also necessary to make sure that the contactor can be tripped open when this becomes necessary. During fault conditions, the voltage at the terminals of the generator will be depressed, and for a three-phase fault on the 4.16 kV bus, it will be zero. If the contactor is equipped with AC coils, there would be no control voltage to trip the contactor to clear the short circuit. For this reason, it is necessary that the contactor be equipped with a DC trip coil that can be operated from the station battery, which also serves as the system emergency power source.

DC-closed contactors are slower than AC-closed contactors due to the current build-up time associated with the solenoid, but, by using 208V AC closing (52 GCC) and 125V DC tripping, (52 GTC), the advantages of rapid closing (about 0.070 second) and reliable opening can both be obtained.

When the motor starter is provided with a separately energized latch, it has an expected 50,000 operations before major maintenance, or over 4 operations per day for 30 years. While over 500,000 operations have been demonstrated, contact tip replacement is normally recommended at 200,000 operations. The Limitamp should be virtually maintenance free for the life of the WTG. The auxiliary transformer feeder contactors may be used for renewal parts if maintenance is required.

A drawout-type connection to the network bus and WTG generator terminals is provided for ease of starter inspection and maintenance. The network bus connection is provided with a shutter to prevent contact with the bus. Contactors are designed for use with motors where, when the contactor is open, there is no voltage on the load side terminals. Limitamp contactors are provided in enclosures which include interlocks to trip the contactor when the enclosure is opened but the load side terminals of the contactor are exposed. Synchronous generators can provide full voltage if running, and thus, the "load" terminals can have voltage when the main contactor is open; therefore, a key interlock system and isolating switch are required so the contactor may be inspected safely.

6.3.3 POWER EQUIPMENT

An insulated bus structure is provided for the line side of the contactors. The bus connects to the step-up transformer by cable and connects to the auxiliary supply transformers, potential transformers, and lightning arrestors in adjacent compartments. As previously noted, the generator connects to the "load" side of the contactor. The arrangement of components within a four-bay lineup in the control enclosure is shown in Figure 6-7.

6.3.4 SWITCHBOARD

A freestanding cabinet houses the protective relays, generator excitation equipment and instrumentation transducers and indicating devices. The device locations are shown in Figure 6-8.

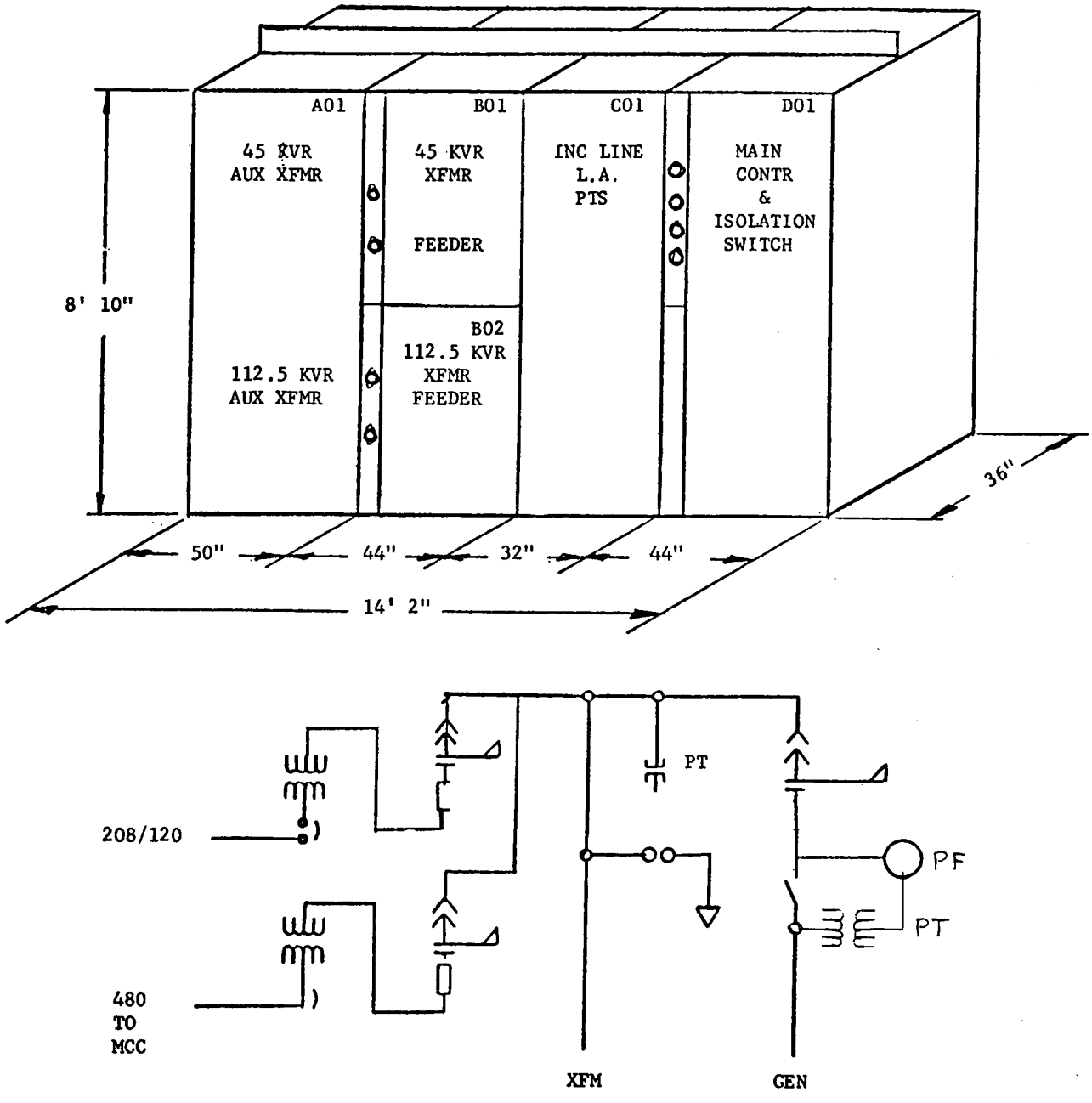

Figure 6-7. Power Equipment Arrangement

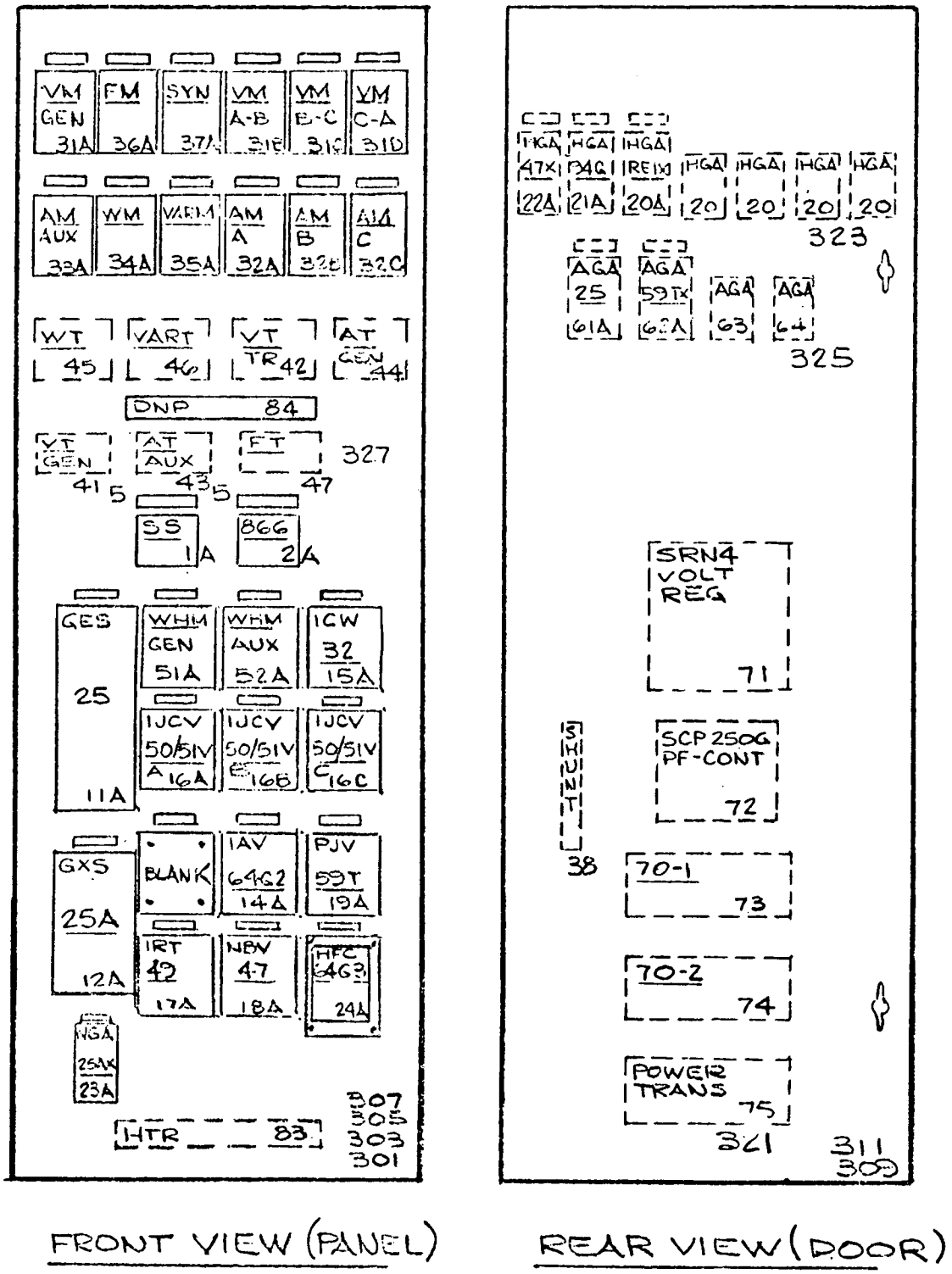

Figure 6-8 Switchboard Arrangement

6.3.4.1 Protective Relays

A cost-effective minimum set of protective relays is provided. Their designation, function and operation follows. Device numbers are from American National Standards Institute (ANSI) C37.2 and types are GE designations. The relays are mostly utility type drawout case devices that can be readily tested and maintained. A typical relay is shown in Figure 6-9.

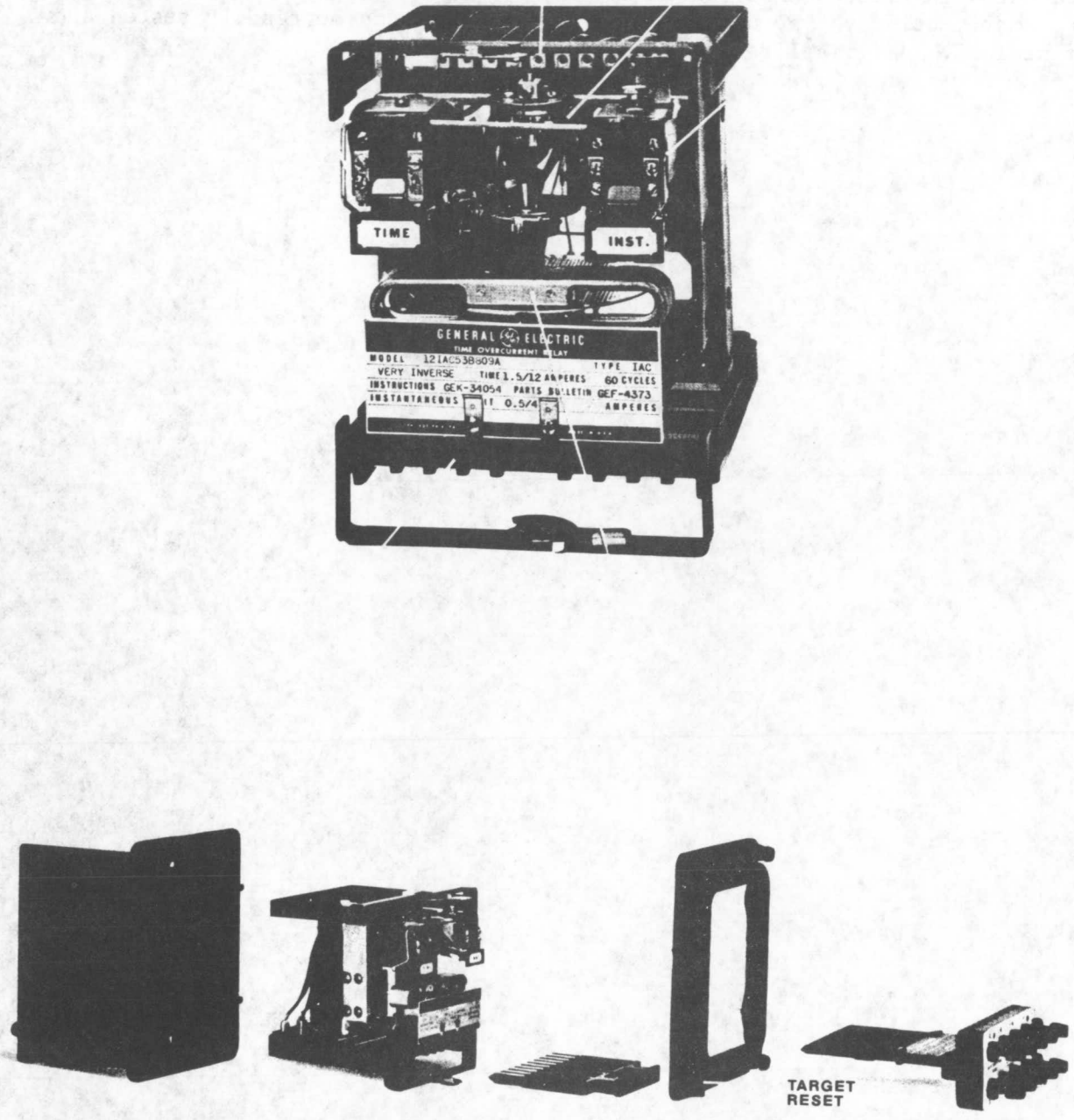

Figure 6-9. Protective Relay

1. Device 25A, Synchronism Check, Type GXS. An up to 30 degree adjustable, slip cutoff relay which closes its output contact to permit circuit breaker closure when generator and utility frequency and angle are in the accept band. If the 52G circuit breaker/contactor is closed outside an angle of about ± 10 degrees, potentially damaging torque levels could be imposed on the mechanical drive system; therefore, the 25A device acts as a backup to the 25 device.

2. Device 25, Automatic Synchronizing Type GES. When enabled by the computer system, this relay compares frequency and angle across the 52G and outputs a close command anticipating the 52G closing time.

3. Device 32, Anti-Motoring, Type ICW. Operates through a time delay when directional power sensing indicates the generator is operating as a motor and taking, rather than delivering, power from the utility. This condition may occur due to power control loop error or minicomputer malfunction and is undesirable. Operation of the 32 device locks out the main contactor.

4. Device 41, Field Circuit Breaker. A motor starter in the Power Control and Distribution unit controls the voltage regulator system input power. While not strictly a "Field" circuit breaker control, it serves the same function because the brushless exciter static regulator combination cannot have the regulator output to the exciter field disconnected.

5. Device 47, Negative Sequence Voltage. Type NBV. Operates through an auxiliary time delay relay when either a phase-to-phase fault occurs on the utility connection or a fuse is blown on the step-up transformer primary. This device operates on negative sequence voltage which is only present during unbalanced conditions as noted. Initial operation of the 47 device will not lock out the main contactor since utility recloser operation will remove. A blown fuse will cause lockout by continuous pickup of the 47 device.

6. Device 49, Thermal Overload, Type IRT. Operates on excessive generator winding temperature caused by overloads as indicated by an embedded RTD. The 49 device acts as a backup to the control system in order to protect the generator. Operation causes lockout.

   The step-up transformer also has an overtemperature contact that causes lockout.

7. Device 51V, Overcurrent, Type IJVC. Three relays, one on each phase, with current transformers on the neutral side of the generator operate on fault caused excessive current. These devices have instantaneous and time over-current functions with voltage restraint such that they become about four times more sensitive to current when voltage is less than normal. The instantaneous attachment provides high-speed operation for generator terminal faults.

Internal generator faults are detected with the field energized before the main 52G is closed due to the CT placement, and operation of the 51 V effectively causes lockout of the system for a cable fault between the generator and main contactor. The output contact wiring goes to the 94G trip relay.

8. Device 55, Power Factor, Type IC3655A100. A synchronous motor loss of excitation relay is connected to detect generator loss of excitation or out of step and causes lockout. Loss of excitation detection by exciter field current monitoring is not reliable because exciter faults could cause loss of field without significant change in exciter field current. Operation cannot be tolerated unexcited as induced rotor currents will rapidly overheat the field damper windings and cause an unacceptable Var flow due to the large generator reactive power requirements from the connected distribution line.

9. Device 59T, Overvoltage, Type PJV. Operates on overvoltage on the 4.16 kV system to protect the step-up transformer and auxiliary transformers from excessive flux due to voltage regulator malfunction of utility overvoltage. Operation causes lockout.

10. Device 64G2, Ground Protective, Generator, Type IAV. Operates on voltage across the generator grounding resistor which permits 20 Amperes of fault current to flow. This device will operate on 4.16 kV system ground faults and cause lockout of the main contactor.

11. Device 64G3, Ground Protective, Utility, Type NGV. An instantaneous current relay, sensing neutral current on the grid side of the transformer, is set above the normal unbalanced load level and responds to utility ground faults. The main contactor is not locked out on 64G3 operation.

12. Device 71, Liquid Level, Transformer. Operates on loss of transformer oil to lockout the main contactor. If a fault subsequently develops, the fuses at the transformer will clear the fault.

13. Device 86G, Lockout. This device is a spring-operated, electrically released contact multiplying relay responsive to any of several parallel inputs and requiring manual reset.

14. Device 94G, Trip Relay. This device is provided for non-lockout main contactor operation such as initiated by the 47 or 64G3 devices.

15. Utility Recloser Voltage Block. The automatic circuit recloser which protects the feeder circuit to which the WTG connects will be modified to incorporate a voltage block. If the recloser opens, but the WTG main contactor does not, there will be voltage on the feeder due to the WTG and the recloser will be prevented from possible asynchronous closing by the block.

6.3.4.2 Transducers and Meters

Transducers with current source output are mounted in the switchboard to provide

isolated signals to the operational and engineering data system. The indicated quantities are:

1. Utility frequency
2. Real power
3. Reactive power
4. Three-phase utility voltage
5. Single phase generator voltage
6. Three-phase primary current
7. Single phase auxiliary current
8. Exciter field current

Indicating DC milliameters with appropriate scales are provided for the transducers. Conventional utility practice is to provide a switch for most meters in order to read currents and voltages on only two meters by switching between phases. This practice reduces panel space and provides a slight cost saving. Panel space is not critical on the Mod-1 WTG, and three meters will be provided, each for voltage and current, to minimize manual switching. While multiple unattended sites could justify meter elimination, the type specified is inexpensive and desired for the Mod-1 WTG's.

Watthour meters are provided for the main generator circuit and for the auxiliary power circuit. They back up the minicomputer totals kept on the same quantities. The indicating instruments and scales consist of:

1. Real Power - Kilowatts (-500/0/+2500)
2. Reactive Power - Kilowatts (-500/0/+1500)
3. Voltage - 3 Phases (0-6 kV) plus 1 phase generator (0-6 kV)
4. Current - 3 Phases (0-300A)
5. Current - Auxiliary (0-20A)
6. Synchroscope - Utility to generator
7. Frequency - (55 - 65 Hz) Utility and Generator
8. Power Factor - (-0.6/0/+0.6) on Device 55

6.3.4.3 Other Controls

Both the regulator and power factor controllers have reference operated motor-driven potentiometers for adjustment of no-load voltage and on-line VARS, respectively. The stabilizer system mounted in the ground peripheral rack provides additional damping of the drive train by varying the excitation with speed. The regulator is supplied with a special center tapped transformer and can negative field force. Frequency transduced signals are available to the control system in addition to shaft speed to control frequency with suitable software implementation. When on-line, the signals will be monitored to detect over/under frequency drift and trip the 52G main circuit breaker should a utility recloser operation go undetected by the relay protection sensing voltage.

6.3.5 TRANSFORMER

The generator step-up (GSU) transformer provides voltage matching between BREMC 12,470-Volt distribution and the WTG 4160 Volt system. An oil-filled distribution type unit with accessories in air insulated connection compartments is utilized with 2,000 kVA and 2240 kVA ratings at 55°C and 65° C rise respectively.

In Figure 6-10, the basic transformer tank and cooling tubes are shown.

A grounded wye connection is utilized on the BREMC side to limit line-to-ground potential imposed on the system. Lightning protection is provided for the transformer and a fused interlocked manually-operated air switch provides disconnect capability. A line-side neutral current transformer is provided to feed the 64G3 current relay to sense line faults.

The secondary is Delta connected. A no-load tap changer and four primary taps, each 2.5 percent apart, are provided.

Accessories provided with the transformer include:

1. Resealing fault pressure vent
2. Ground pad
3. Handhole
4. Oil sampling device mounted on drain valve
5. Liquid level gage with alarm contacts
6. Temperature gage with alarm contacts
7. Anti-condensation heater
8. Key interlock on high-voltage fuse compartment

6.4 AUXILIARY POWER DISTRIBUTION

6.4.1 LOAD BUSES

480 Volt, Three Phase - A 112.5 kVA, 3-phase transformer is used to supply a 480 Volt bus. The principal loads on this bus are:

1.	Pitch change hydraulic pump	20 hp
2.	Pitch slew hydraulic pump	20 hp
3.	Yaw and brake hydraulic pump	20 hp
4.	Gear and rotor lube pump	15 hp
5.	EDAS PIV	30 kVA

208/120 Volt - A 45 kVA transformer supplies a 3-phase, 208 Volt bus that is also utilized to supply 120 Volt single phase loads by line to neutral connections. The principal loads are:

1.	Nacelle 120 Volt power distribution	10 kVA
2.	Scavenger pump	3 hp
3.	Oil cooling fan (if required)	10 hp
4.	Lift and gearbox heaters	8 kVA
5.	Control enclosure 120 Volt power distribution, 15 kVA	

6.4.2 PROTECTION AND CONTROL

A factory-wired motor control center is utilized for branch circuit protection and control. This unit is illustrated in Figure 6-11 and the individual element locations are shown in Figure 6-12.

Plug-in-type motor starters having circuit breaker protection, overload relays and main contactors with indicating lights are furnished for the hydraulic pump motors, the Portable Instrument Vehicle (PIV) power feed, and heavy heaters where computer control is needed. Manually-controlled circuits have protection and control combined in plug-in-type circuit breakers.

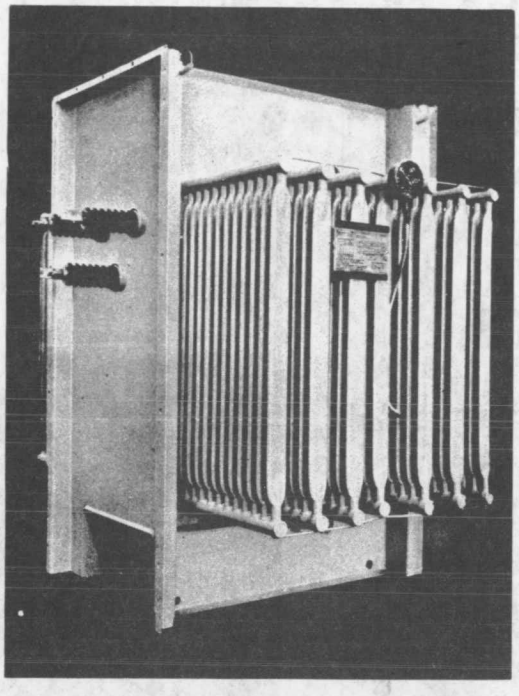

Figure 6-10. Step-up Transformer

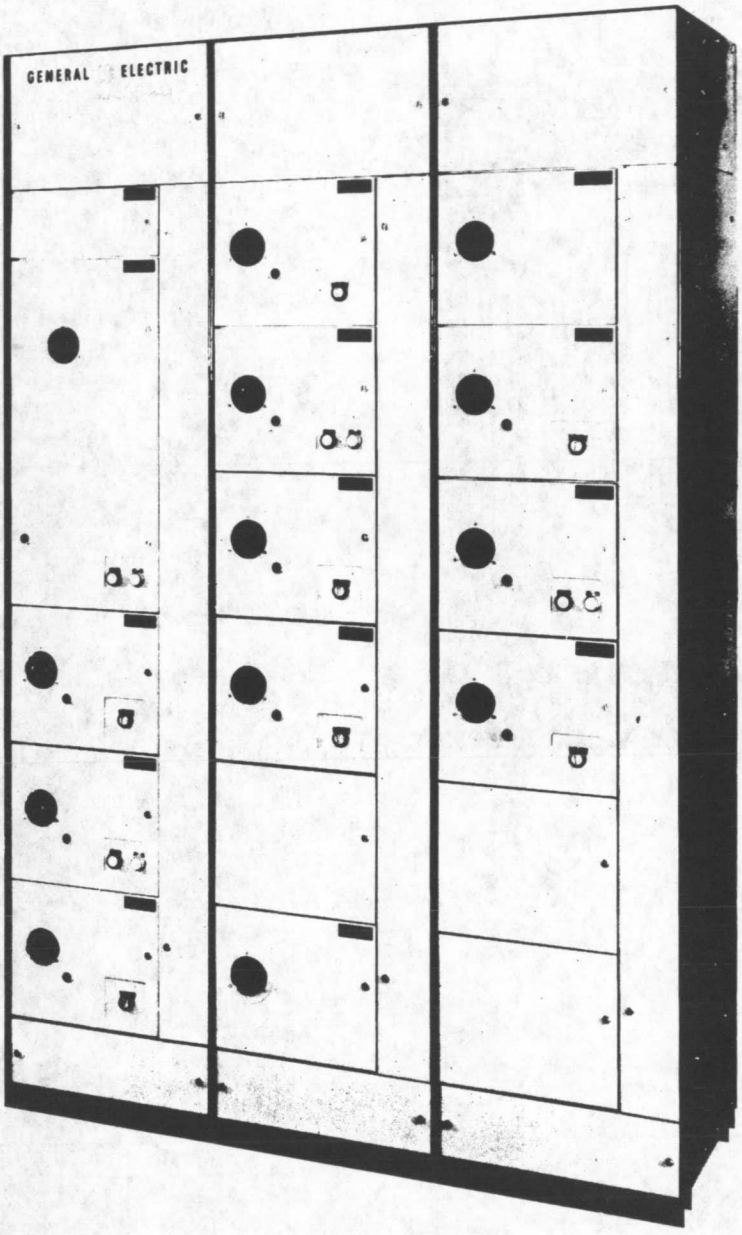

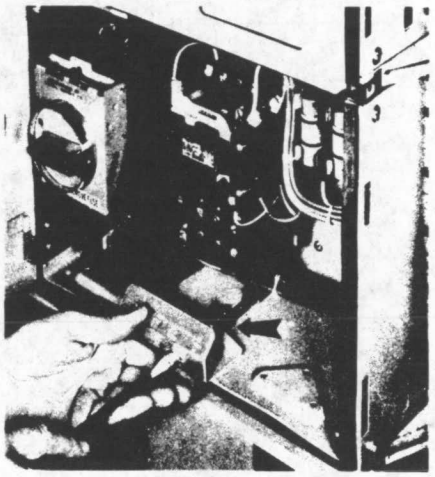

Figure 6-11. Motor Control Center

The rear of the control center has a control panel, illustrated in Figure 6-13, with interposing relays between the computer and the starters. A second panel is utilized as a master terminal board for all tower and nacelle circuits except the 4,160 Volt and shielded signal leads.

6.5 STATION BATTERY AND FAA LIGHTING

A 50-Ampere hour, 125-Volt lead calcium station battery assembly with charger is provided in an insulated and heated enclosure mounted on the outside wall of the control enclosure. Appearance of this unit is shown in Figure 6-14. The dc supply provides tripping power for the main breaker, operates assorted relaying in the switchboard, and powers the aircraft warning lighting. A float charge at 2.12 Volt dc per cell is maintained to eliminate equalizing the battery periodically. The charger has a 9 Ampere continuous supply capability and is powered by a single phase 208 Volt ac supply.

Due to lack of room in the control building and to eliminate the concern for possible hydrogen collection, the batteries are mounted in a separate cabinet. The cabinet is a two-tiered device, providing access to all the cells and charger for ease of maintenance. Because of the -31°C ambient specification, heaters are supplied in the cabinet as well as insulation. This cabinet arrangement is standard.

Wind turbine FAA construction approval will be sought by BREMC based on providing a double red obstruction light on the nacelle per prior discussion and recommendation with FAA-Washington and NASA. This lighting is based on the

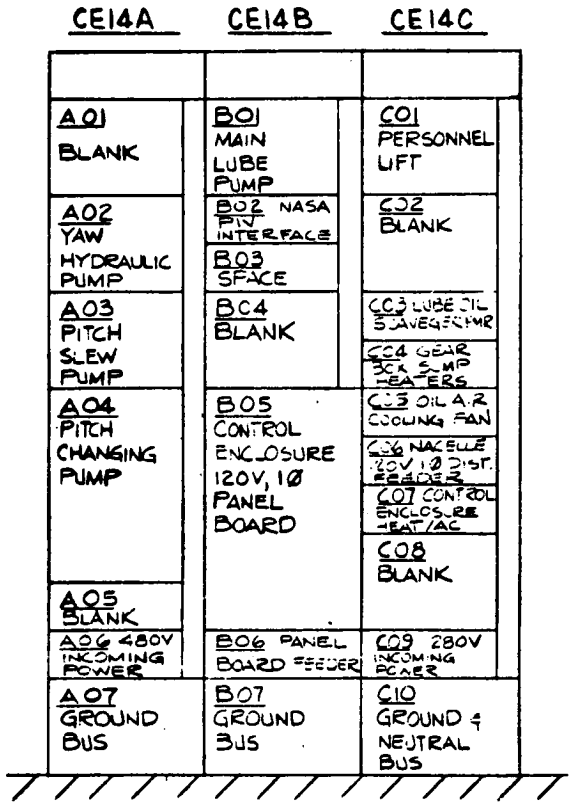

Figure 6-12. Bus and Starter Location Motor Control Center

CONTROL INTERPOSING RELAYS

CONTACTORS

FUSE BLOCK

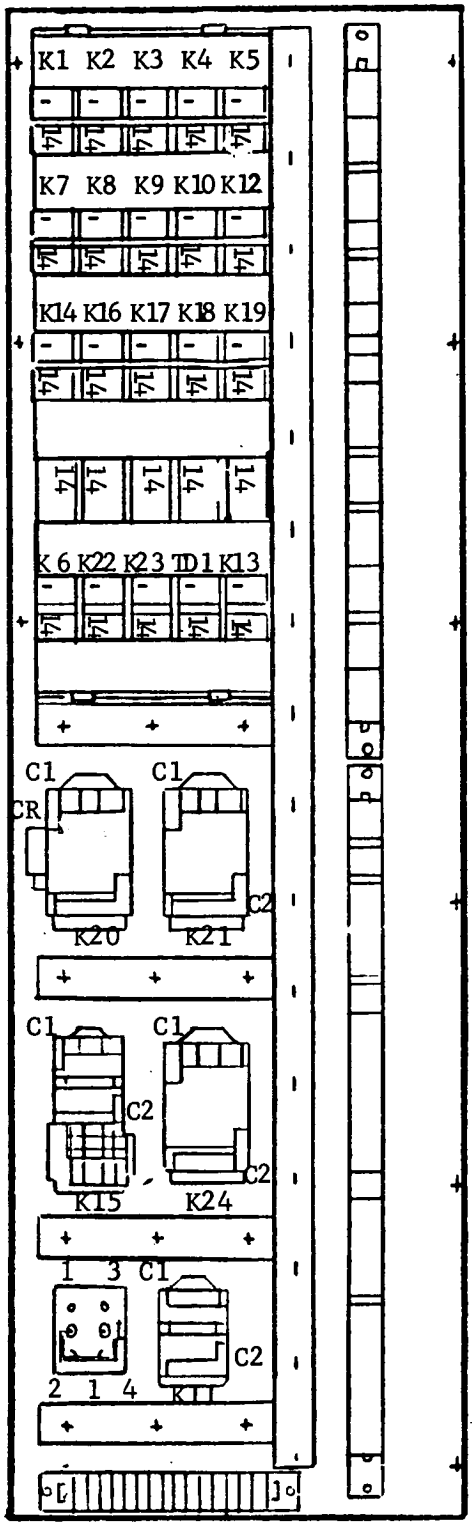

WIRE DUCT

TERMINAL BOARDS

Figure 6-13 Control Panel

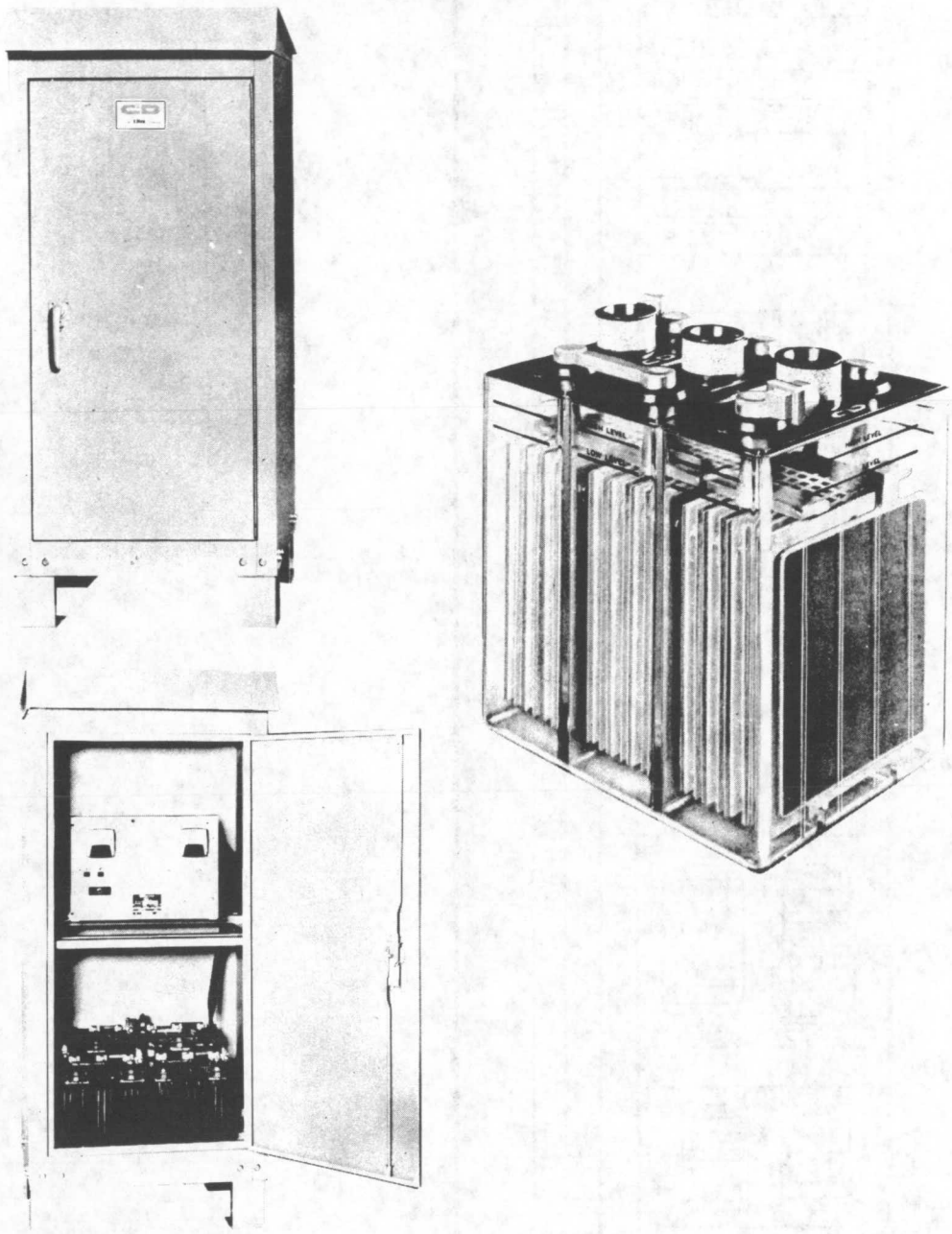

Figure 6-14. Station Battery and Charger

presence of a meterorological tower with lighting within 500 feet of the WTG tower. A standard FAA approved Fresnel lensed, double lamp assembly is mounted near the center top of the nacelle.

6.6 WIRING AND SLIP RINGS

This section describes interconnecting wiring. A slip ring is used on the tower to nacelle yaw interface to provide continuous rotation capability. Another yaw electrical interface, utilizing the limited rotational ability of a cable wrap, was considered during preliminary design, but set aside in favor of slip rings due to development cost and risk for Mod-1.

6.6.1 WIRING

Tower wiring is routed in voltage separated metallic conduit for protection from physical damage, electromagnetic interference, lightning strikes and contact with personnel.

Junction and pull boxes are located on the tower legs at approximately 20-foot intervals. Insulating wire wedges are used to limit the length of free hanging wire, thus limiting strain on the wires induced by the vertical run.

The nacelle is prewired as much as possible using metallic conduit or wireway. The control enclosure interior is also prewired with a tower interface terminal board for ease of field wiring. Crimp lugs are used for terminal board type terminations and crimp pins are used for plug insert-type terminations. A dead-break-type connector is used on the slip ring terminations and air stress-cone termination is used elsewhere on the 4,160 Volt cables.

All high voltage (4,160 Volt) is wired with General Electric type "MV-90" Vulkene Power Cable with 15 kV shielded construction. Power wiring below 600 Volts is type THHN building wire. Series 44 Raychem wire is used for all instrumentation wiring due to the integrity and ease of shield terminations.

Belden coaxial and triaxial cables are used for all multiplexing functions.

6.6.2 SLIP RINGS

6.6.2.1 Yaw Slip Ring

The yaw slip ring assembly shown in Figure 6-15 handles the electrical interface for all wire and cables between the nacelle and ground or tower. A position sensor gives the relative position between the tower and the nacelle. The characteristics are listed as follows:

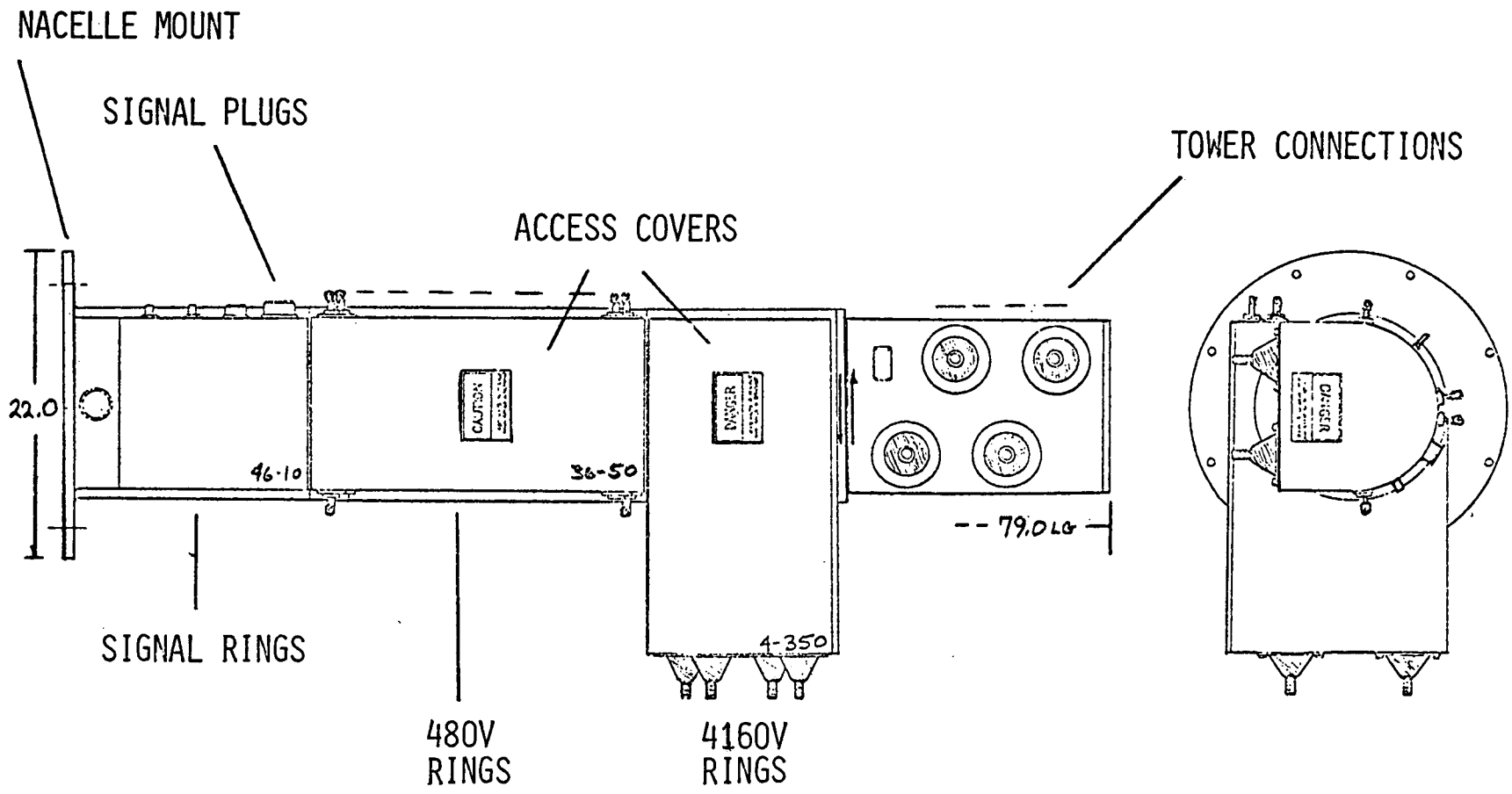

Figure 6-15. Yaw Slipring

Item	Type
Power 4 rings	350 Ampere Capacity, 4,160 Volts, 60 Hz
Auxiliary 36 rings	50 Amperes, 480 Volts, 60 Hz
Signal 44 rings	10 Amperes, 150 VAC 60 Hz
Ring Material	Coin Silver
Brush Material	Silver Graphite

6.6.2.2 Rotor Slip Ring

The rotor slip ring assembly shown in Figure 6-16 is located on the gearbox in the nacelle. It is driven by the low speed shaft. A position sensor is built into the assembly as a means of determining the rotor position.

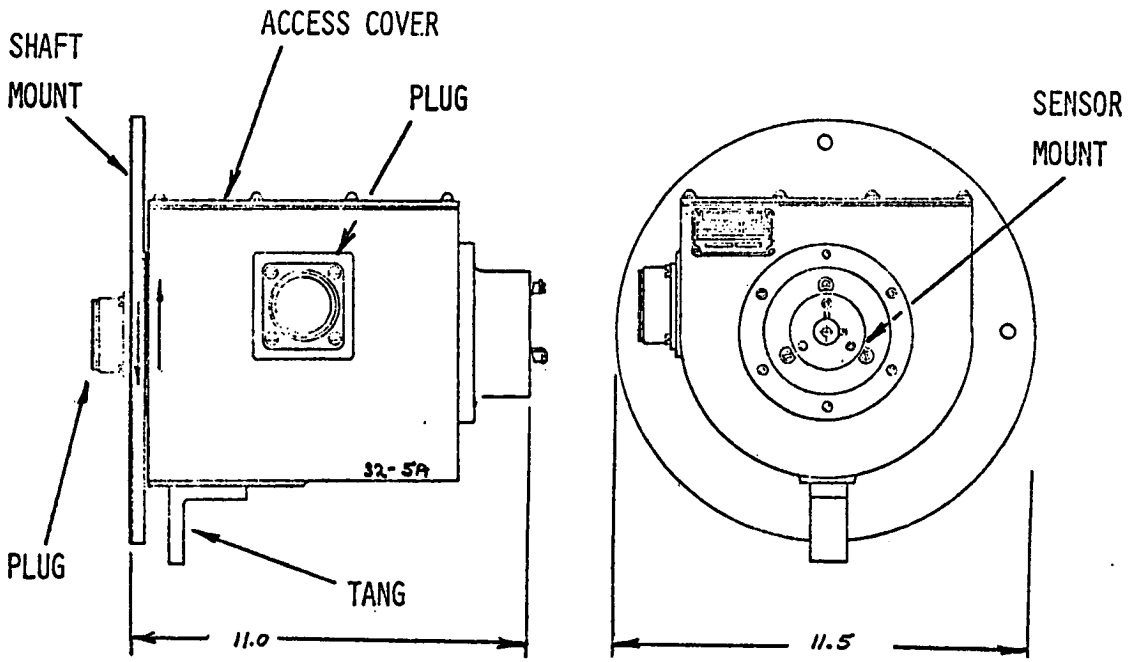

Figure 6-16. Rotor Slipring

The characteristics of the rotor slip ring are listed as follows:

Item	Type
Revolution Rate	34.7 rpm
Number of Rings	30
Current	5 Amperes
Voltage	125 V ac or dc
Ring Material	Coin Silver
Brush Material	Silvered Graphite

6.6.3 CABLE REEL

A cable take-up reel is utilized to manage power and control wires to the personnel lift. This unit is illustrated in Figure 6-17.

6.7 INSTRUMENTATION

The method of routing of the various sensor wires from the individual sensors to either the operational (CODAS) or engineering (EDAS) data system interface is covered in Paragraph 6.6.1 and a description of electrical transducers and meters is covered in Paragraph 6.3.4.

The EDAS system wiring is separable from CODAS either because a sensor is used only in EDAS or because it is used in both systems and routed first to CODAS with a buffered output from CODAS to EDAS. Additional instrumentation discussion is given in Section 7.

6.8 LIGHTNING PROTECTION

The most probable lightning events are direct strikes on the WTG structure or electrical circuit incoming voltage surges due to strikes on the overhead distribution lines.

A ground wire-shielding scheme or rod attractor was discarded as too cumbersome to practically implement and structure strikes are accepted on the blade, nacelle, and tower structure.

Minimum earth resistance is specified at less than 5 Ohms and is provided by rods at the site. Each tower leg is tied to the rod arrangement and bridging straps are used at the main leg joints.

The blade, hub, and yaw bearings are potential current carrying paths for a lightning strike and are protected with an outer diameter located gap which will break down and carry most of any large discharge current due to the high rate of rise of current and inductive path through the bearing proper. A low-resistance brush bypass scheme is also being evaluated.

The lightning model specified (shown in Figure 6-18) has an initial peak current of 200 kA at a rate of rise of 100 kA/microsecond. Most data available indicates 100 kA or more peak is reached only 2 percent of the time and that a 50 percent

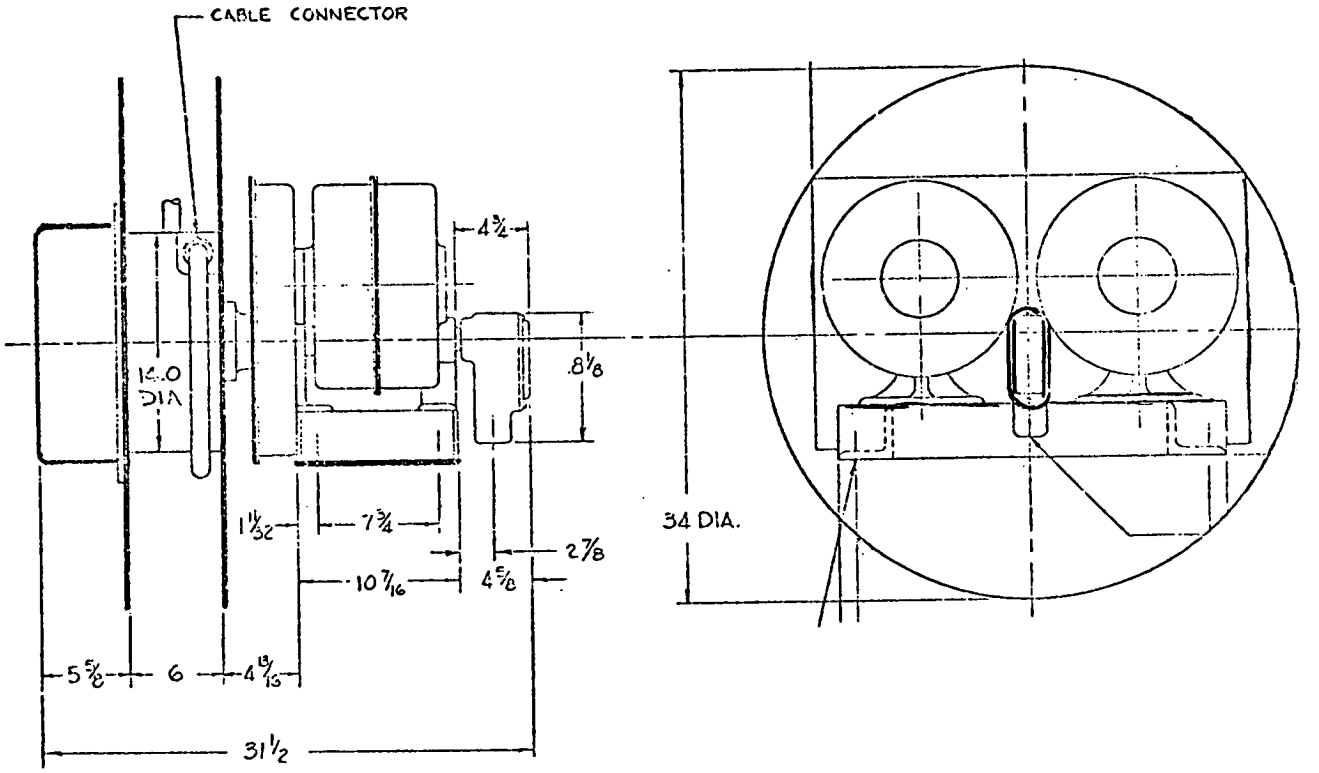

Figure 6-17. Cable Reel

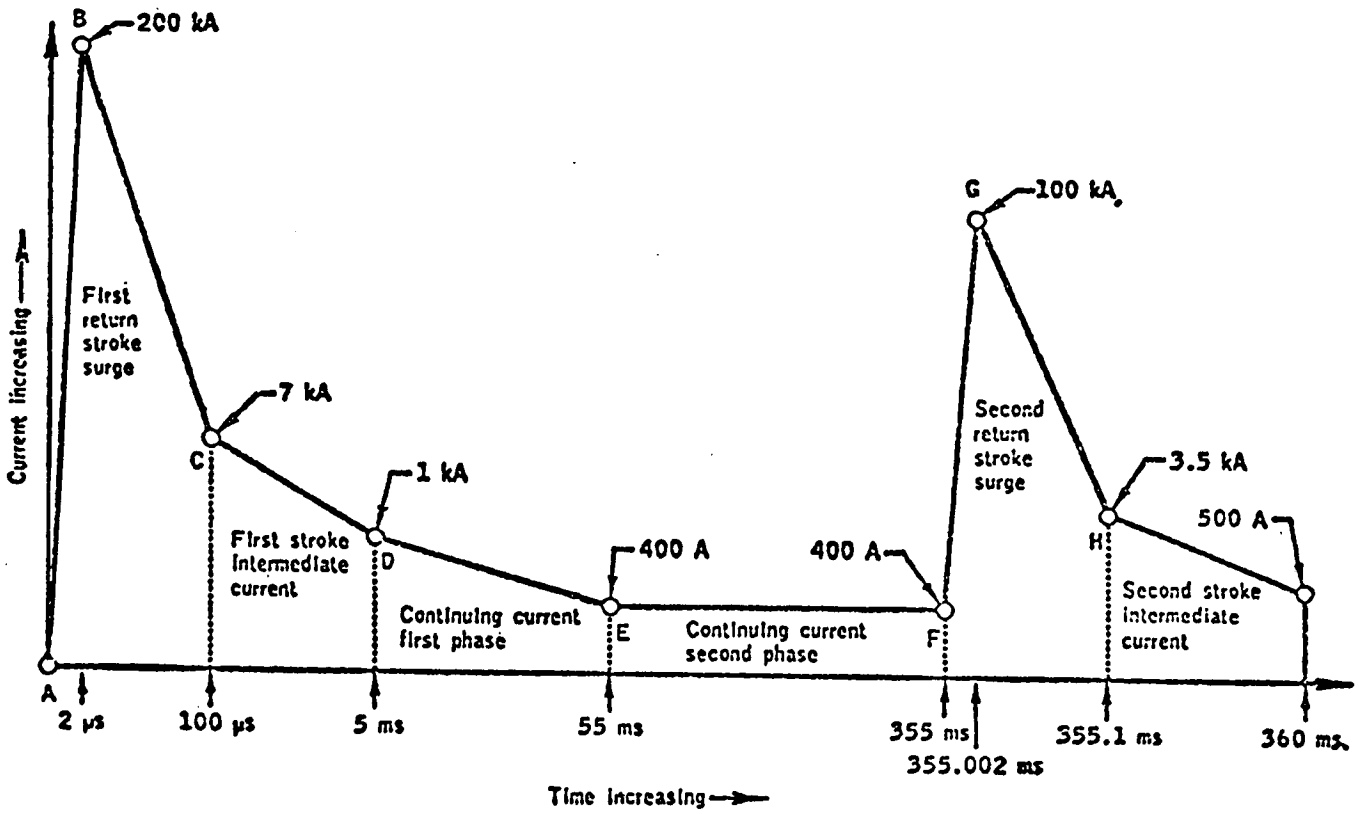

Figure 6-18. Lightning Model

probable value is about 20 kA. Intense local heating will occur where the streamer strikes the structure but only superficial damage is expected.

A Faraday cage effect is present for equipment within the nacelle and local potential differences should not occur unless the current path is badly asymmetric. A strike on a tower leg will introduce some "near-strike" electromagnetic coupling into conduit enclosed wiring and optical isolators have been applied to sensitive circuits. Gas discharge tubes are being evaluated as high energy bypass devices for an added measure of protection. Low-voltage motors are not protected as their insulation level is normally adequate to survive surges unless directly connected to an overhead line.

The higher voltage apparatus is more sensitive to steep front surges due to larger size and capacitive division of a large percentage of the surge onto the first winding section. A lower ratio of test-to-normal voltage exists and lightning arrestors are applied at the BREMC terminals within the control enclosure at the 4,160 Volt bus, and at the generator terminals. A surge capacitor is also mounted at the generator terminals. This protection is deemed adequate for strikes on the incoming line or induced "near-strike" surges.

6.9 CONTROL ENCLOSURE

A van-type enclosure, shown in Figure 6-19, is used to house ground-mounted equipment. The interior arrangement is shown in Figure 6-20 with control electronics equipment mounted at one end and the previously described power equipment disposed at the other end to minimize EMI.

The construction, typically used for drilling platform or gas turbine control enclosures, is built up of a self-supporting base channel structure to which interior equipment is secured. A subfloor provides ample wiring space with separate trays run for signal level and power leads. Conduit interfaces are provided in the channel base for external wiring.

An insulated roof and wall structure is secured to the base with window-type air conditioners and resistance heaters to provide environmental control. Convenience outlets and interior and exterior lights are installed in the wall structure. The battery assembly mounts on the outside wall.

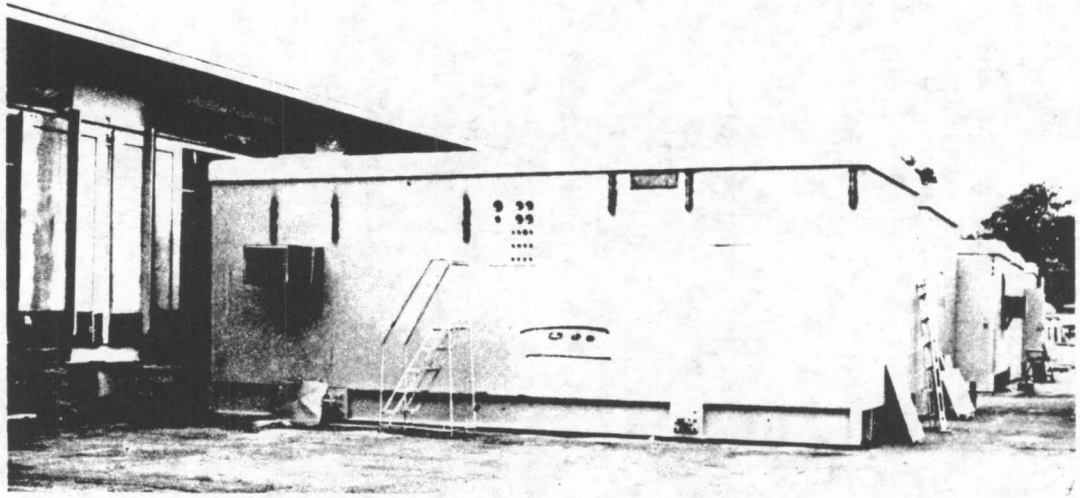

Specification:	273A6507
Drawing:	138D6861
Vendor:	General Electric Company Drive Systems Department
Weight:	33,000 lb. with equipment
Dimensions:	126.4 W x 128 H x 334 L inches
Location:	Ground

Figure 6-19. Control Enclosure

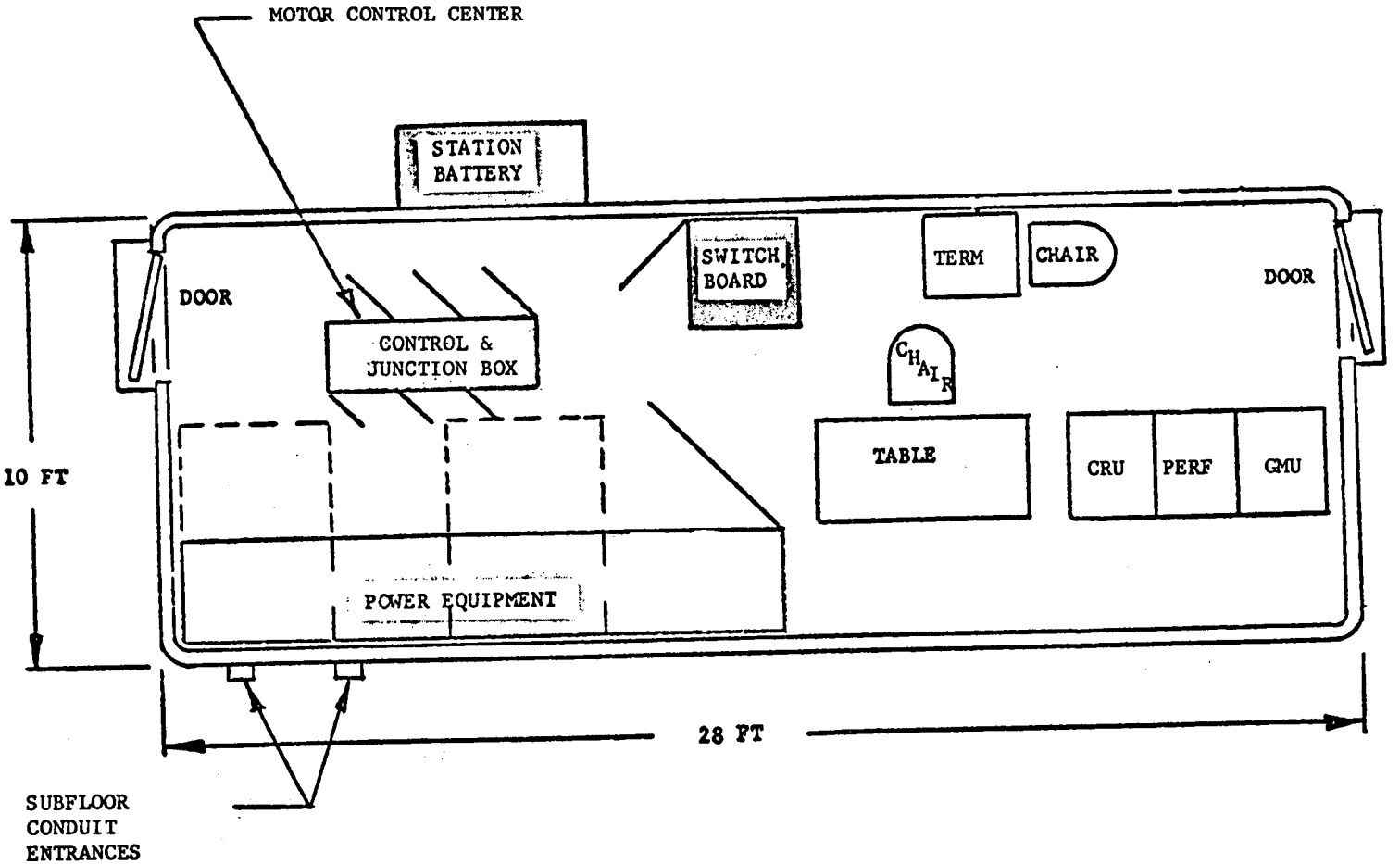

Figure 6-20. Enclosure Interior

SECTION 7

CONTROL AND INSTRUMENTATION SUBSYSTEM

SECTION 7

CONTROL AND INSTRUMENTATION SUBSYSTEM

7.1 OVERVIEW

The Control and Instrumentation Subsystem performs all sensing (except switchgear), recording, utility communication, signal conditioning and buffering, and control functions for the WTG. Figure 7-1 shows the overall functional arrangement of the equipment excluding the Engineering Data Acquisition System (EDAS). In the Nacelle, there are sensors, the Nacelle Control Electronics (NCE), the Digital Interface Panel (DIP), and the Servo Controller which are described in Paragraph 7.3. On the ground, the Control Subsystem consists of sensors, the Ground Control Electronics, and the Ground Digital Interface Panel (DIP).

The WTG system requires: precision analog control of blade angle to satisfy power quality requirements, yaw position, generator excitation, power output and switching functions in response to wind speed, wind direction, machine capability, utility demand, and output power quality. The control of most functions is dependent on multiple inputs and varying "logic" depending on operating modes. Accordingly, the Control Subsystem, with its data gathering and processing capability is the system master controller. Central Processing Unit (CPU) logic is used to determine availability of power from wind conditions, as shown in Figure 7-2, the update of yaw position, when to enable the main circuit breaker, and when conditions require immediate WTG shutdown for safety purposes.

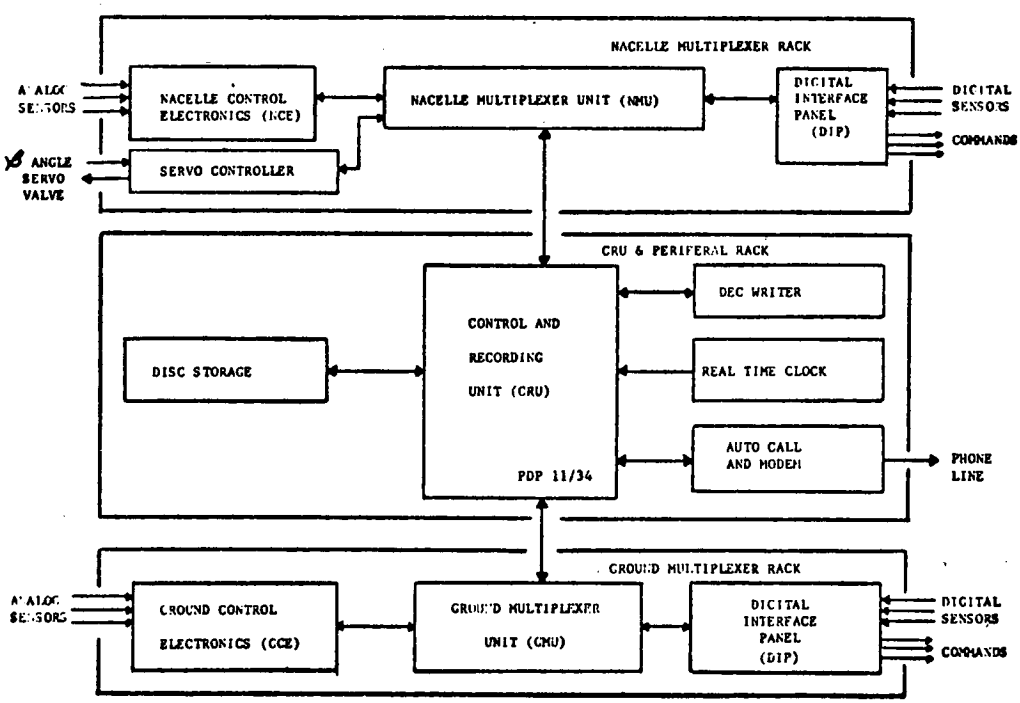

Figure 7-1. Control Subsystem Block Diagram

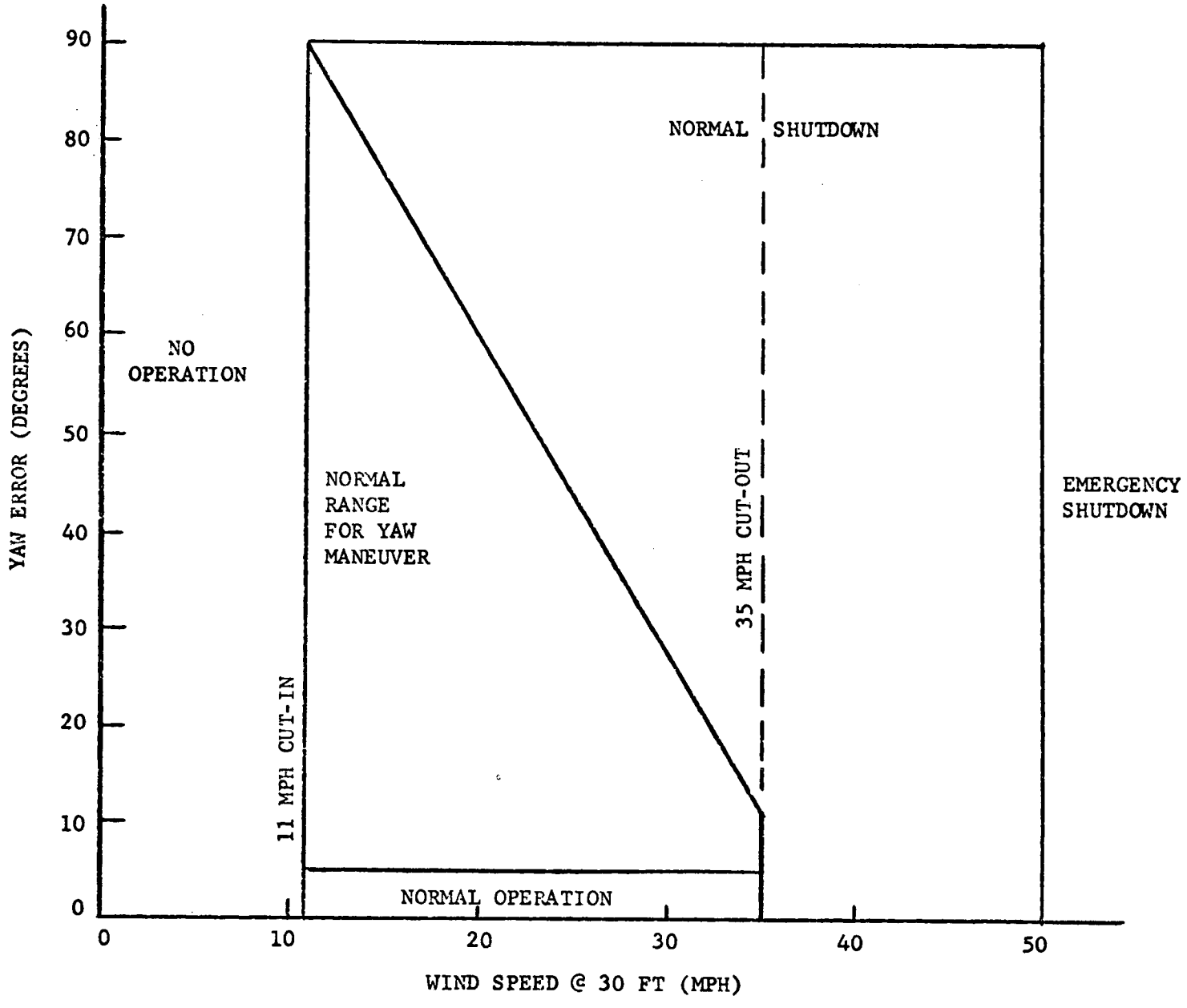

Figure 7-2. Wind Performance Envelope

Manual control is also processed through CPU logic to preclude unsafe operation. Output power level is controlled by commands to the analog pitch control loop in the Servo Controller. This permits considerable flexibility in operation. A discrete power level can be maintained, the system can track wind speed and maximize power output continuously, the system can be programmed to come on-line automatically and autonomously when wind conditions permit, or the system can be "manually" operated by keyboard inputs.

The Control Subsystem provides maximum energy capture capability with subrated wind speed while maintaining safe control of rotor speed and load. A remote dispatcher can receive data and issue commands over a conventional phone line. Sufficient diagnostic data is automatically recorded so that the cause of shutdowns can be readily determined.

Alternate implementation approaches were considered for logic and data processing. The Digital Equipment Corporation PDP-11 line was chosen to provide lowest program cost and highest operational flexibility both in system testing and at site.

7.2 FUNCTIONAL DESCRIPTION

7.2.1 CONTROL FUNCTIONS

The Control Subsystem has the following basic functions:

1. Control the rotor blade pitch angle to start up, supply subrated power at wind speeds between 11 and 24.6 mph, and rated power at wind speeds between 24.6 and 35 mph;

2. Control the yaw drive and brake hydraulic subsystem to drive the Nacelle in yaw and apply the yaw and generator shaft brakes;

3. Condition and buffer sensor signals for internal use and the NASA Engineering Data Aquisition System;

4. Provide operator interface;

5. Record data, commands and status for diagnostic purposes;

6. Provide dispatcher control over telephone line.

These functions are performed fully automatically and unattended to accommodate internal system variables as well as wind changes in speed and direction. A detailed set of functions with descriptions is listed in Table 7-1.

The pitch control function is designed to control pitch angle to regulate

Table 7-1. Control System Functions

Function	Description
Monitor Enable	Process Lockout Sensors, Initialize Commands
Initialization	Initialize Yaw, Pitch, and Lube Subsystems
Site Enable	Process Automatic Restart Sensors
Anti-Stall	Limit β as a f(Vw) to Prevent "Stall"
Overstress	Limit Structural Stress as a f(Vw, Yaw Error)
Yaw Correct	Align Nacelle With Wind Vector
Pitch Ramp	Ramp β 90^{o} to 72^{o} - Maximum Coefficient of Lift
Speed Ramp	Ramp Generator Speed 0 to 1800 rpm
Rate Sync	Set Freq. Generator = Freq. Utility
Voltage Sync	Set Voltage Generator = Voltage Utility
Angle Sync	Enable Switch Gear Synchronizer, Wait for Breaker Close
Power Ramp	Step Power in 75 kW Increments 1 Sec. Apart
Shutdown	Disengage Utility, Feather Blades, Brake, Park Rotor
Power Peaking	Iterate Power Set - Point to Max. Value for $11 \leq VW \leq 24.6$

generator output to match the power reference. This is the main stream function which directly controls the power, but five other functions are required to make the machine practical. Table 7-2 describes all the pitch control modes of operation and lists their operating conditions. Figure 7-3 shows control functions required to perform "STARTUP".

Table 7-2. Pitch Control Modes of Operation

Mode	Functional Description	Operating Conditions	
		Control Parameters	Wind Speed (mph)
Startup	Ramp Blade Pitch Angle to +72° With Shaft Brake On. Accelerate Rotor to Rated Speed by Pitching Blade Using Speed Schedule.	o Time o Shaft Speed o Blade Angle	11 to 35
Rate Sync	Closed Loop Control of Pitch to Make f Utility = f Generator	o Utility Frequency o Generator Speed	11 to 35
Angle Sync	Closed Loop Control of Pitch to Make Ø Utility = Ø Generator	o Utility Phase Angle o Generator Phase Angle	11 to 35
Power Control	CPU Ramps Power Reference Command to Set Desired Power Output	o Time o Generator Power o Blade Angle	11 to 35
Manual	For Testing and Periodic "exercising", the Blade can be commanded Over the Full Range.	o Manual o Blade Angle o Time	0 to 10.9
Pitch Jam	"Pitch Jam" Status to NMU if Pitch Mechanism does not Respond to Position Control	o Time o Voltage	Any
Power Down	CPU Ramps Reference to Zero Power	o Time o Generator Power o Blade Angle	11 to 35
Slow Down	Reduce Rotor Shaft Speed to 5 rpm by Slewing Blade at 1 Deg/Sec	o Blade Angle o Shaft Speed	Any

The Nacelle must rotate about its vertical yaw axis to be able to collect the most wind energy possible. The second control function is involved with actuating the hydraulic yaw motor and yaw brake that holds the Nacelle when it is not being driven. Control logic for the four wind speed regimes is given in Table 7-3. After the average yaw error has been above five degrees for five minutes, the yaw hydraulic motors are turned on, in the appropriate direction, until the corrected angle is less than one degree. Because of

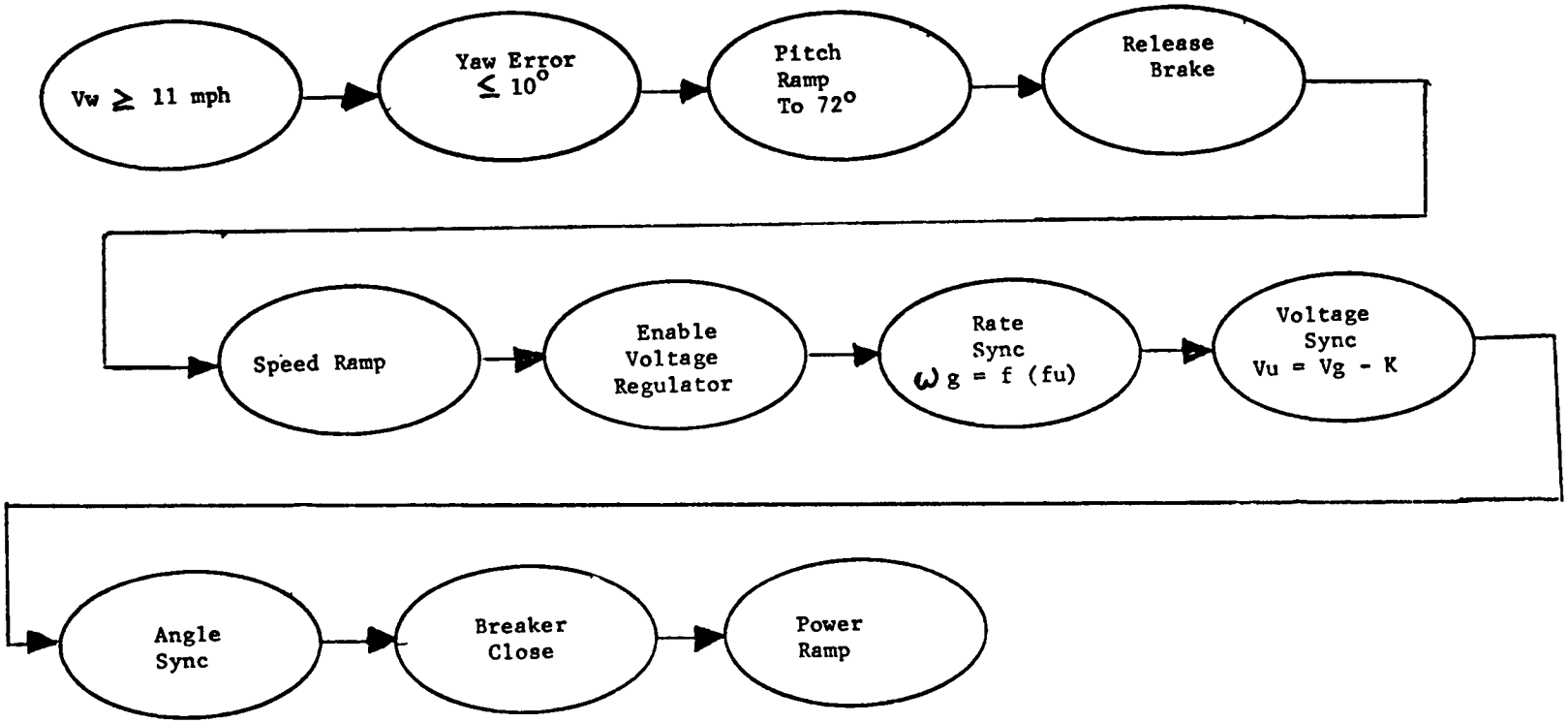

Figure 7-3. Startup Control Functions

1/4 degree per second yaw rate, higher sensitivity is selected as the yaw error increases as shown in Figure 7-4. This change in sensitivity allows higher energy capture in a rapidly changing wind direction.

Table 7-3. Yaw Control

Wind Speed (mph)	Drive	Brake	Notes
0 to 11	Off	On	No Operation
11 to 35	Corrects for Yaw error of 5^{o} for 5 minutes	Off when driving	0.25 deg/sec
Above 35	Off	On	Shutdown
0 to 25	Manual - to any angle	Manual	For test

The generator shaft brake can be controlled in three ways. During normal operation, the brake is applied after the generator shaft speed has dropped below 265 rpm. With brake applied, the deceleration (Δ rpm/ Δ T is computed while the shaft is coming to a stop. The brake is then released, the servo controller ramps the generator shaft speed up to 35 rpm, and applies the brake to stop at the 3-9 position after computing the required brake applica- angle.

There are also two manual control modes. The on-site operator can position the rotor hub to any angle. This works by ramping the generator shaft speed to 35 rpm, using the last deceleration value and applying the brake to stop at the selected angle. In addition, the brake can be turned on and off manually from the keyboard.

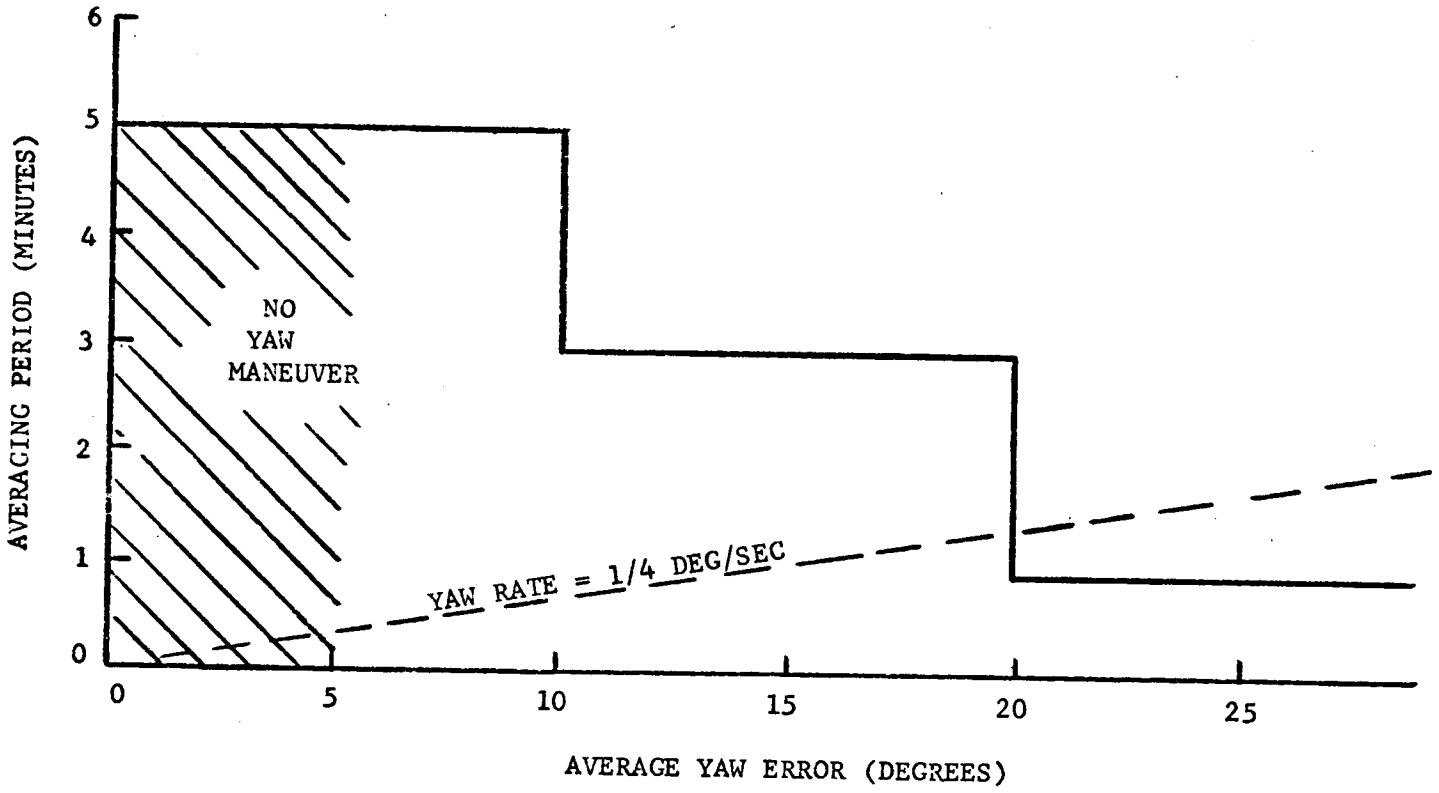

Figure 7-4. Yaw Correction Averaging Logic

Because the WTG is a complex electromechanical system, it must be protected from internal and external equipment failures, which would propagate into expensive damage, and wind speed/direction change combinations that could inflict damaging stresses or cause the pitch subsystem to lose control. For this reason, logic has been designed into the WTG for safe operation. Table 7-4 describes the types of system shutdown and gives the criteria for each. Figures 7-5 and 7-6 show the logic flow for normal and emergency shutdowns.

At present, the remote dispatcher has the capability to "reset" the software after a shutdown so that the system will attempt to restart. If the attempt finds an anomalous sensor value left over from the previous shutdown, the system will simply not proceed to startup. This logic will preserve safety and equipment in all cases except one. If a failure or other condition causes sufficient vibration at one of the three accelerometer locations to trigger a shutdown (lockout), it may be dangerous to attempt a restart from a remote location. One possible cause could be a shaft, bearing, PCM linkage, or blade failure which could propagate at the next restart. Therefore, on-site inspection and testing is advisable and on-site restart is required.

7.2.2 MANUAL FUNCTIONS

Manual functions required for debug, calibration and test operations are listed in Table 7-5. These functions may be used by the on-site operator, one at a time, and will be continuously monitored by the computer to prevent any dangerous combinations.

7.2.3 BACKUP OVERSPEED SHUTDOWN

A separate circuit is used to bypass all software to feather the blades. Figure 7-7 is a functional block diagram of the design approach. If, for any reason (including any computer failure), the hub should reach 105% to 110% of rated speed (field adjustable), the "Backup Overspeed Shutdown" device will open a contact in series with the emergency feather solenoid coil. Since these redundant solenoids are arranged in a "deadman" configuration where coil current is required to keep them closed, the interruption of the power line redundantly initiates emergency feather action. Startup is never permitted unless the hydraulic accumulators are full. In addition, since the Backup Overspeed reset action is momentary, a reset signal failure in the "ON" mode does not prevent the device from opening the feather solenoid circuit in response to an overspeed.

7.2.4 SUPPORT FUNCTIONS

7.2.4.1 Reporting

An unsolicited on-site report will be automatically generated once an hour. Figure 7-8 is a representation of this report which will be printed out on the LA 36 DEC writer if its switch is on.

In addition, for development only, critical system parameters will be displayed (reported) on site via the VT-52 video display. These parameters will include System State, System Mode, Control Source (Local or Utility), Wind Speed, Current Power Set, and Current kW's being generated.

Table 7-4. WTG Shutdown Logic

Type of Shutdown	Description	Criteria For Shutdown
Normal	1. Yaw Off if Failure 2. Power Down (Pitch Change) 3. Breaker Open 4. Slow Down (Speed Ramp) 5. 3-9 Stop	Manual Command Dispatcher Command Wind Speed Drops Below 11 MPH User Subsystem Failure Wind Speed - Yaw Error Out of Band Temperatures Out of Band Average Wind Speed Above 35 MPH Emergency Pitch Hydraulic Pressure Low
Emergency	1. Yaw Off if Failure 2. Pitch Emergency Feather 3. Breaker Open 4. 3-9 Stop	Frequency Out of Band Shaft Speed too High Main Breaker Open Utility Voltage Dip Below Limit Wind Speed - Yaw Error Out of Band Any Vibration Above Limit Data Link Anomoly
Utility Outage	Emergency Feather, Yaw Motor Off, Brake On, Shaft Brake Off	Utility Voltage Drops Out
Pitch Jam	1. Pitch Emergency Feather 2. Yaw 90° to Wind and Track	Blade Will Not Respond

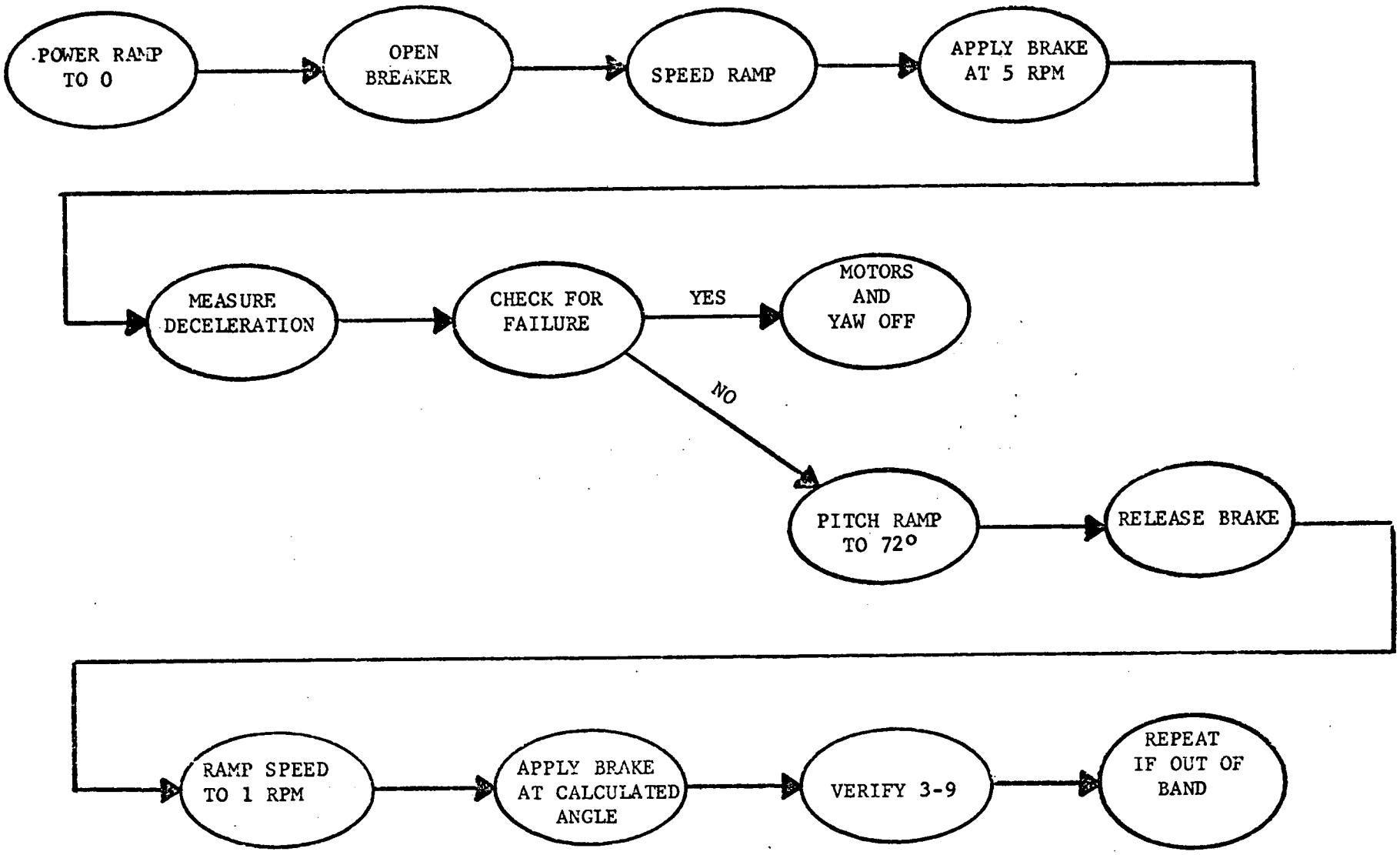

Figure 7-5. Normal Shutdown Logic Flow

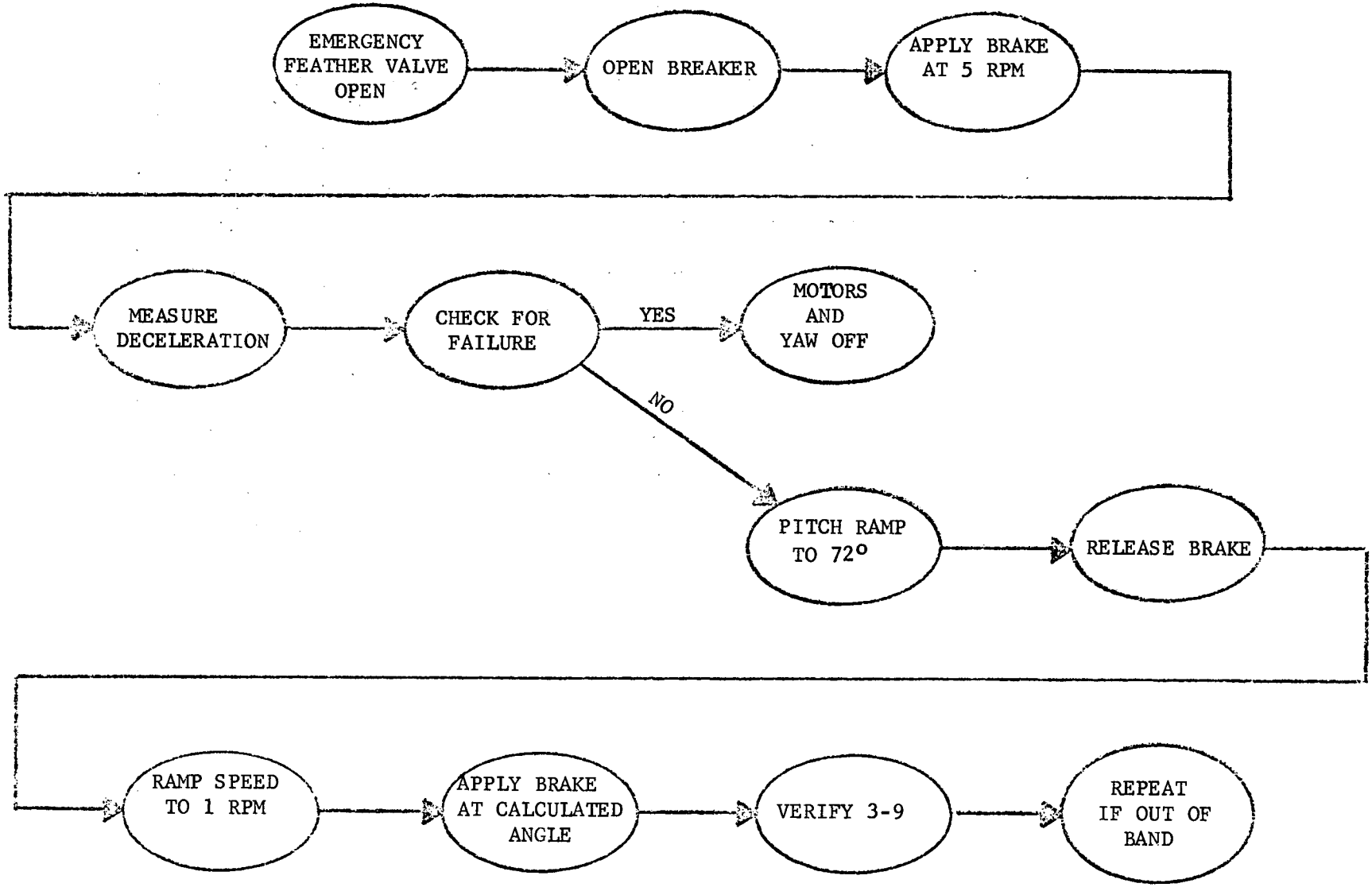

Figure 7-6. Emergency Shutdown Logic Flow

Table 7-5. Manual Functions

Function*	Additional Restrictive Conditions**
Pitch to Any Angle ($\bar{+}5^{o}$)	Wind Speed $<$ 15 mph
Yaw to Any Angle ($\bar{+}5^{o}$)	Wind Speed $\leq$ 35 mph
Release/Apply Shaft Brake	Hub Speed $\leq$ 2 rpm β = Feather
Rate Sync	-
Voltage Sync	-
Yaw Hydraulics Pump Motor On/Off	-
Hub to Any Angle ($\bar{+}10^{o}$)	Wind Speed $\leq$ 25 mph
PCM Charge Pump Motor On/Off	-
PCM Slew Pump Motor On/Off	-
Release/Apply Yaw Brake	Wind Speed $\leq$ 25 mph
Main Lube Pump On/Off	-
Auxiliary Power On/Off	-
Hub to Any Speed ($\pm$0.5 rpm)	Break Away $\leq$ Wind Speed $\leq$ 25 mph

* One at a Time

** In Addition to Subsystem Permissives Enabled, No Lockout Condition and Keys On

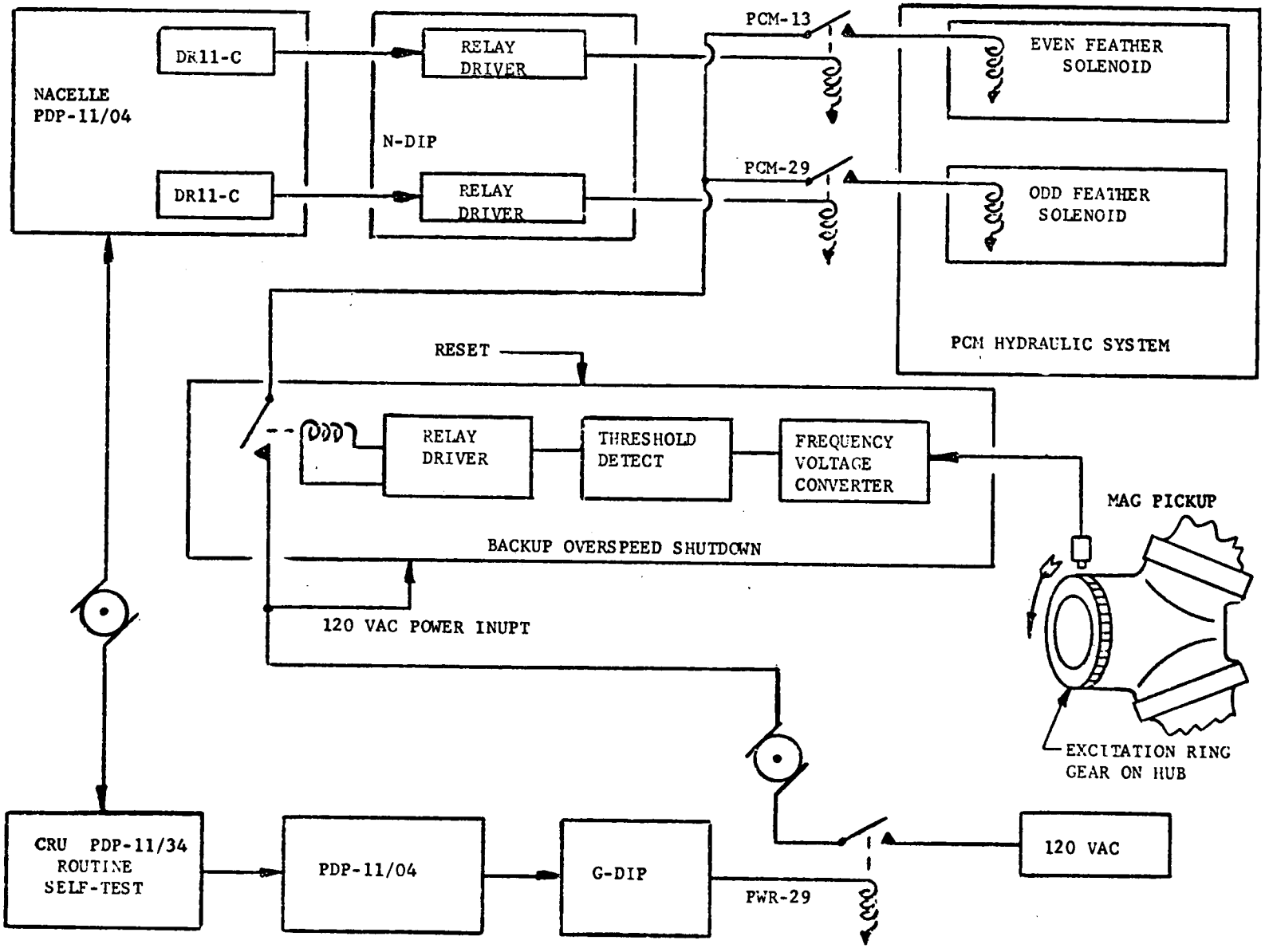

Figure 7-7. Emergency Shutdown Redundancy

CUMULATIVE DATA

1.75329E+04 HOURS

GENERATED KW HRS	2.6298E+07
KVAR HRS	1.9285E+06
AUXILIARY KVA HRS	3.2123E+03
ELECTRICAL EFFICIENCY	0.2345 OVER TOTAL TIME
WIND MPH-HRS	3.8570E+05
AVERAGE KW/MPH	6.9876E+01
TOTAL BREAKER OPERATIONS	8.7650E+03
BREAKER OPERATIONS PER HOUR	4.9999E-01
OVERSPEEDS	51 ABOVE 105 PERCENT

Figure 7-8. Report Example

7.2.4.2 Recording

For development only, historical operational data will be recorded on magnetic tape. The tape will consist of all traffic between the Control and Recording Unit (CRU) and each of the Remote Multiplexer Units (RMU's), all traffic between the CRU and the Utility, all interface between the CRU and the on-site operator when the system is in the Automatic Mode, and all internal state changes. Recorded data will be available to interested personnel via playback processor when the WTG system is not operating.

An RK05 disc is allocated to record operational data, in wrap-around fashion, to allow diagnosis of shutdowns when the magnetic tapes are no longer used.

7.2.4.3 Dispatcher Communications

Dispatcher Communications are comprised of a subset of Operator Communications and consist of:

1. Sign On/Sign Off - identify self to system
2. Utility Enable - authorize the system to go to Generate
3. Power Set - query and alter the level of generation to which the system is currently attempting to adhere
4. Shutdown - direct the system to idle and stay there until Utility Enable is received

7.2.5 TEST FEATURES

Tests are divided into two major categories: development and operational. Development testing involves module debug, subsystem test, system test and integration. To facilitate these activities, the DIP and the NCE/GCE interface panels provide the capability to select test data input from one of three sources: sensor simulation input, computer supplied input, or live sensor input. Sensor simulation is used in the module debug phase and part of the subsystem test activity; computer supplied input is used in subsystem and system level test; live sensor input is utilized at integration time.

Operation testing involves hardware validation and computer self-checking. Again, the DIP and the NCE/GCE play important roles. The hardware validation/fault detection activity can utilize the interfaces in the sensor simulation input mode. The periodically activated computer self-check mechanism utilizes the interface in the computer supplied input mode to determine the state of health of all of the system hardware interfaces.

7.3 EQUIPMENT DESCRIPTION

Hardware details of the Control and Instrumentation Subsystem are described in this paragraph in terms of circuit functions performed, hardward configuration and photographs of the equipment in its present state of development.

7.3.1 EQUIPMENT LOCATIONS

Except for the remote sensors, the Control and Instrumentation Subsystem equipment has been divided into two groups. As much of this equipment as possible is located on the ground in the Control Enclosure but, in the interest of minimizing tower communication, some of the equipment had to be packaged into the Nacelle. This equipment, referred to as the Nacelle Multiplexer (MUX) Unit Rack, is located against one Nacelle wall adjacent to the generator as shown in Figure 7-9. The rest of the equipment has been placed in one end of the Control Enclosure as indicated by the shaded boxes in Figure 7-10. The sensor locations are defined in various assembly drawings as indicated in Paragraph 7.4.

7.3.2 MULTIPLEXER RACKS

There are two multiplexer racks in the Control Subsystem, one in the Nacelle and one in the Control Enclosure. These racks are essentially alike except the Nacelle rack contains the Servo Controller, an air conditioner and heater, and is insulated with one-inch thick polyfoam. Therefore, the Nacelle Mux Unit Rack is described and a separate treatment of the Ground Mux Rack is not given. Figure 7-11 is a photograph of the NMU Rack with a description of each of the GE designed components on the right and the purchased components on the left side. The following paragraphs describe each of the components in the Nacelle Mux Rack.

7.3.2.1 Digital Interface Panel (DIP)

The Nacelle Digital Interface Panel (N-DIP) provides all the circuitry needed to interface 32 user subsystems' digital sensors, 32 command relays, and 32

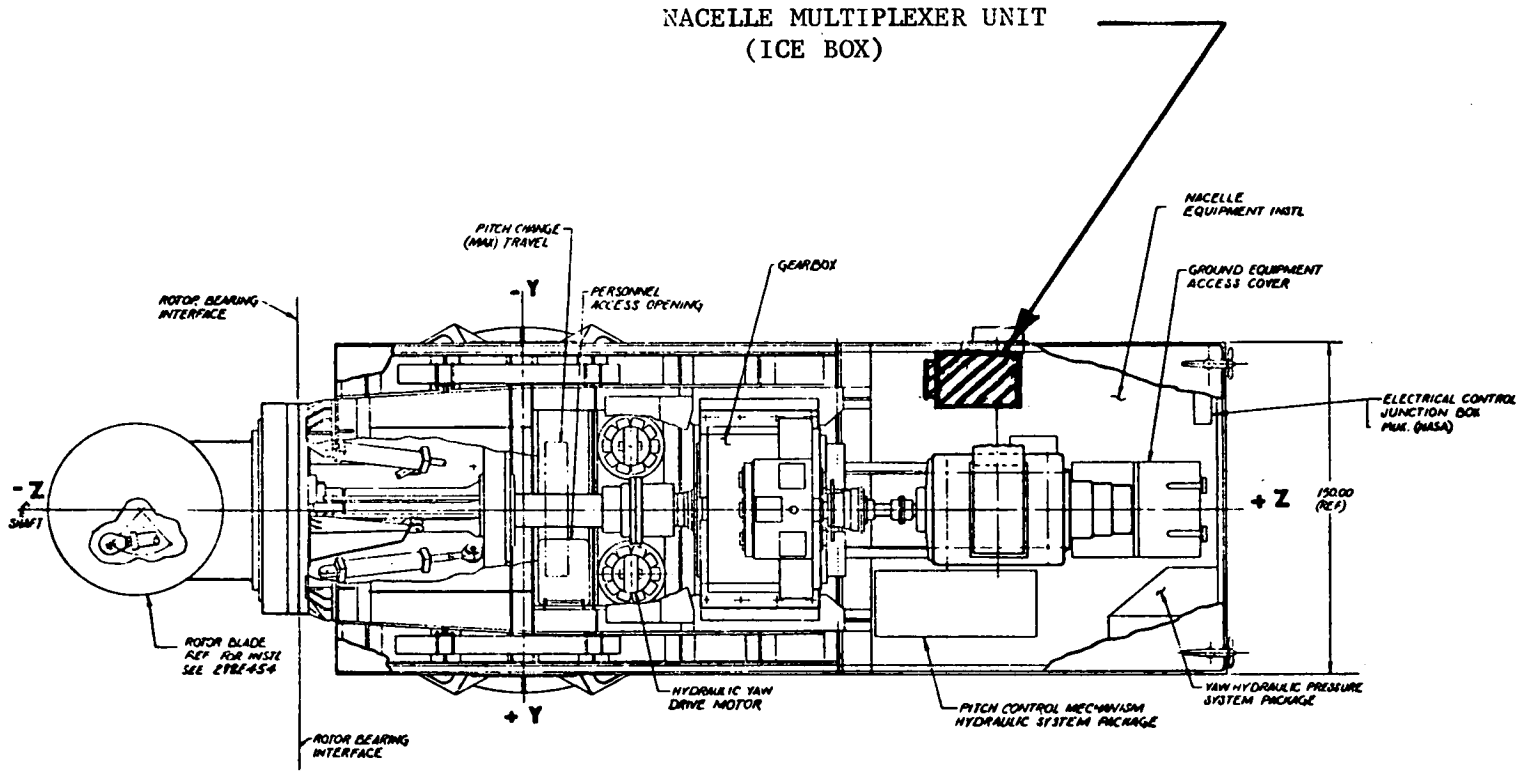

Figure 7-9 Nacelle Unit Showing Location of Control Equipment Subsystem

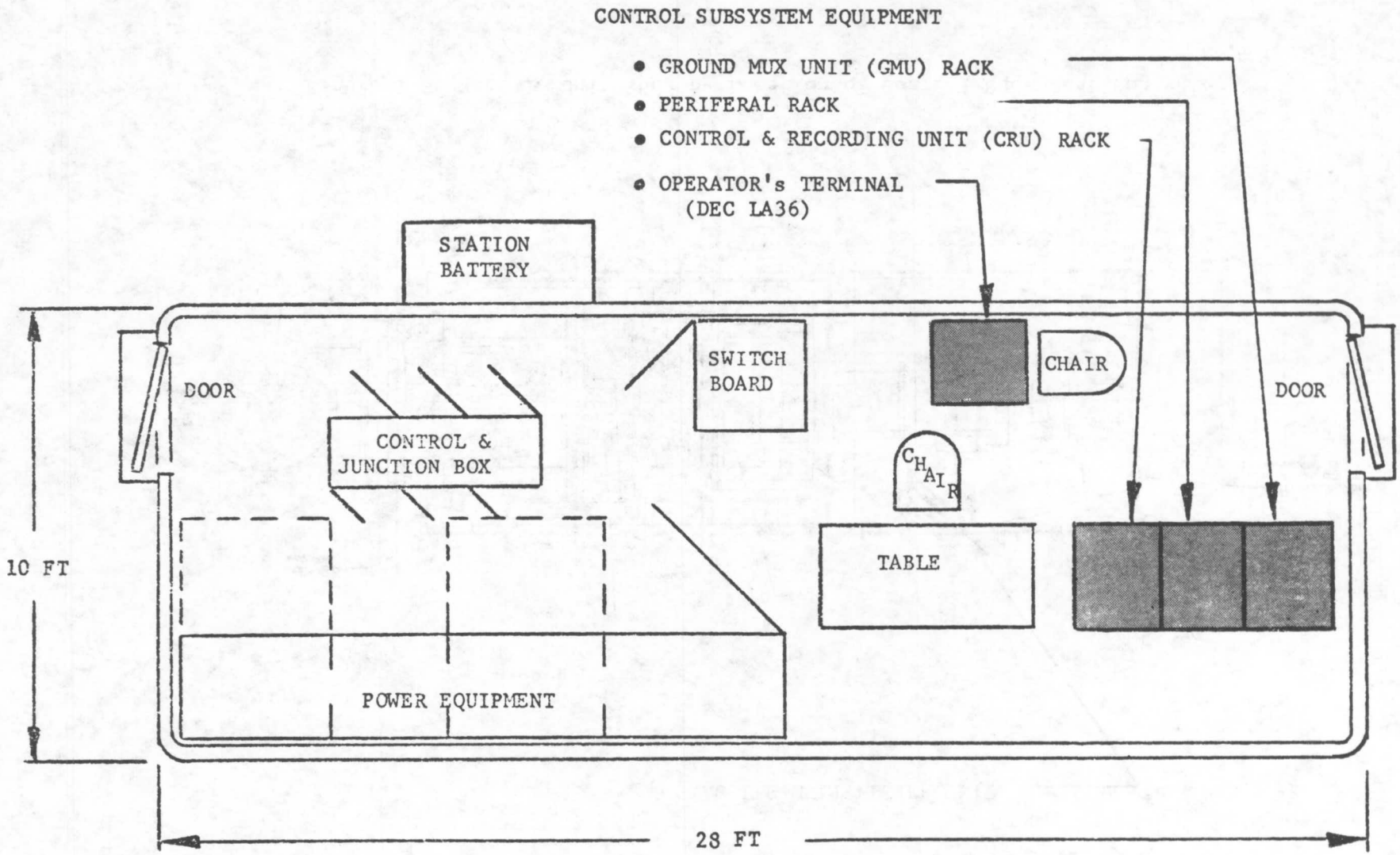

Figure 7-10. Control Enclosure Layout Showing Control Subsystem Equipment Locations

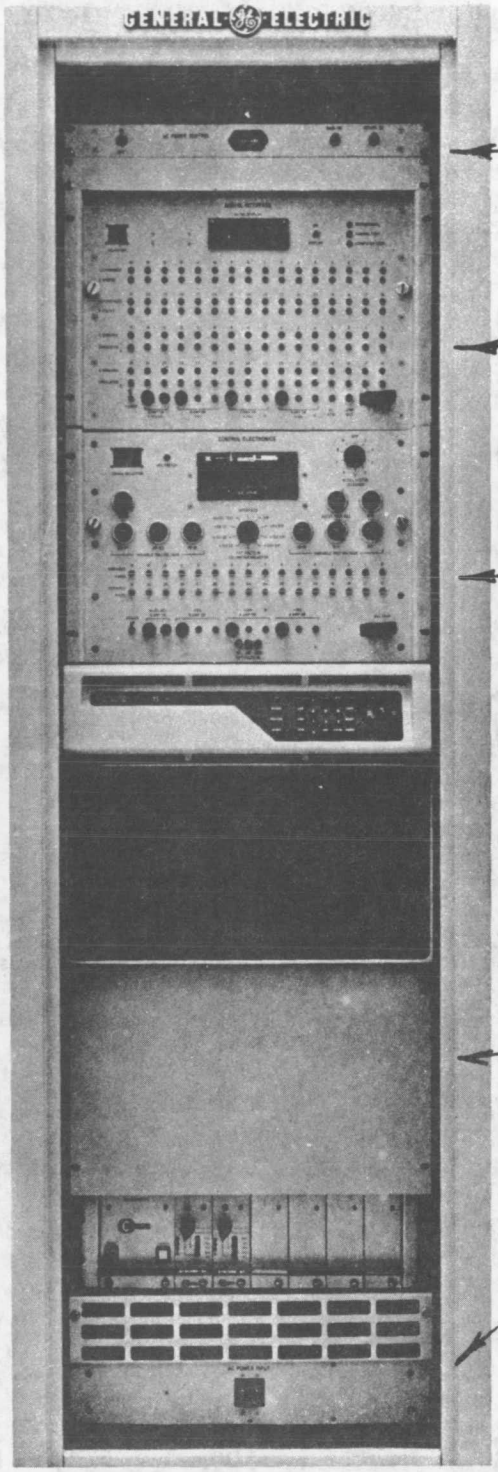

AIR CONDITIONER

RACK COOLING
RACK HEATING
TEMP. CONTROLS
KOOLTRONICS

MULTIPLEXER

DATA ACQUISITION
DATA COMPRESSION
RECEIVE & ISSUE CMDS
DEC PDP SELF TEST 11/04

INTERFACE BOX

PARALLEL 1/F
OPTO ISOLATORS
TEST 1/F
COMM. MICRO'S
DEC BA 11

WIND TRANSLATOR

SYNCHRO-DC
CLIMATRONICS

POWER CONTROL PANEL

RACK POWER CONTROL
RACK POWER STATUS
ELAPSED OPERATING TIME

DIGITAL INTERFACE PNL

DIGITAL CMD, STATUS, &
SENSOR INTERFACE
TEST CONTROL LOGIC
OCTAL WORD DISPLAY

CONTROL ELECTRONICS

AMALOG SENSOR COND.
EDAS BUFFERS
TEST CONTROL LOGIC
ACCEL. CALIB.
DVM

SERVO CONTROLLER

ANALOG BLADE CONTROL
RVDT MOD & DEMOD
SHAFT SPEED TACK (F/V)

AC POWER INPUT PNL

LINE FILTER
POWER CONTACTOR

Figure 7-11. Nacelle Mux Unit (NMU) Rack (Ice Box)

status feedback channels with the remote multiplexers in addition to test logic that allows both manual and automatic computer driven testing. Figure 7-12 illustrates how the N-DIP functions interface these signals from the user equipment to the multiplexer. The Ground DIP is identical except that the N-DIP has 32 channels and the G-DIP has 16 channels.

Figure 7-13 is a photograph of the DIP front panel showing the recessed design which allows a cover to protect the switch controls and displays when manual testing is not being performed. Two rows of switches are provided for manual sensor simulation. The four rows of lights at the top of the panel indicate the state of commands and their respective status. The lower two rows of lights indicate the state of each of the digital sensors. The DIGITAL INTERFACE OCTAL DISPLAY converts the binary word configuration to OCTAL for any selected command, status or sensor line as indicated on the Leverwheel switch. The covered "ALL STOP" button commands Emergency Shutdown.

Figure 7-14 shows the command and status logic for a single channel. The DIP, shown in the middle block, receives a command signal from the multiplexer, it lights the status light, and drives the corresponding relay coil in the commanded user subsystem. When the user status switch closes, the "debounce circuit" prevents ambiguity and the "driver" lights the status light and drives the multiplexer's opto-isolator.

Figure 7-15 shows one channel of the digital sensor interface logic which allows both manual and computer driven testing. The MUX sets up the "OPER/TEST" command so the DIP will receive either the real sensor signal or a test (simulated) signal. The "COMP/MAN" command determines whether the DIP receives a manual input from the front panel switch or a computer driven input. The "TEST CABLE" buffer allows the rest of the DIP to be tested in the absence of real sensors.

7.3.2.2 Control Electronics (CE)

The Control Electronics component is used to interface the analog sensor signals with the analog-to- digital (A/D) converters in the multiplexers, receive commands for test mode selection, and buffer Servo Controller commands and remote Engineering data NASA Mux signals.

Figure 7-16 shows how the CE functions interface the various signals. The CE has capability to monitor 32 analog signals making full use of two 16-bit computer words. The buffer circuitry, however, is implemented only as required. A manual calibration signal is provided to each accelerometer which injects an accurate current into the internal calibration coil. This current is correlated with a known output so that trouble shooting can be carried out without removing the accelerometer.

Figure 7-17 is a photograph of the CE front panel showing the recessed design similar to the DIP. Two rows of toggle switches are provided to select either fixed or variable simulated input. The potentiometers shown provide this variable input. The digital voltmeter shown can be selected to read any of the internal power supply voltages; any of the 32 analog signals at the interface, as selected by the "SIGNAL SELECTOR" thumb wheel switch; the accelerometer calibration currents; or it may be used to measure some external

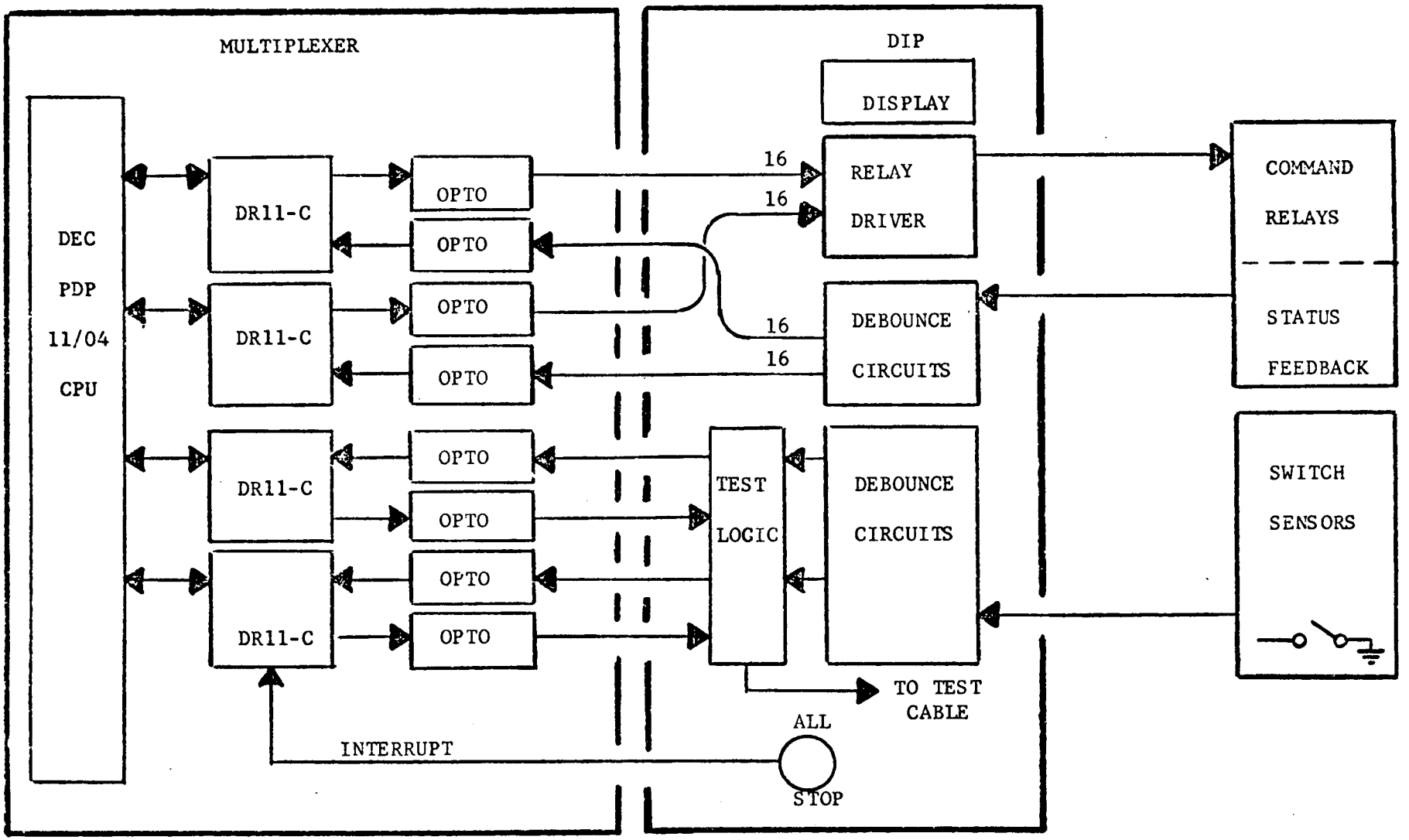

Figure 7-12. Nacelle Digital Interface Panel (DIP) Functions Showing Interfaces

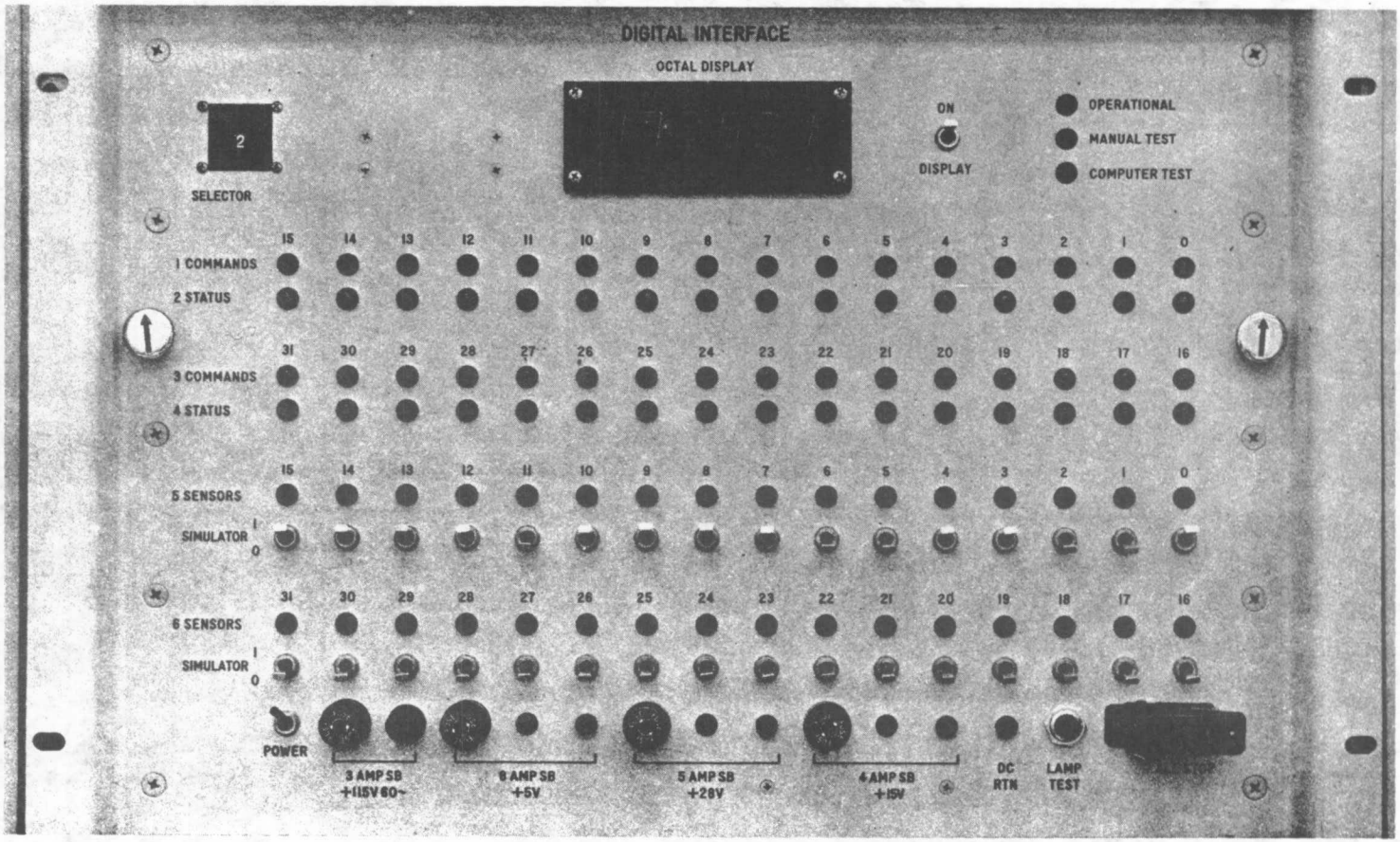

Figure 7-13. Digital Interface Panel (DIP)

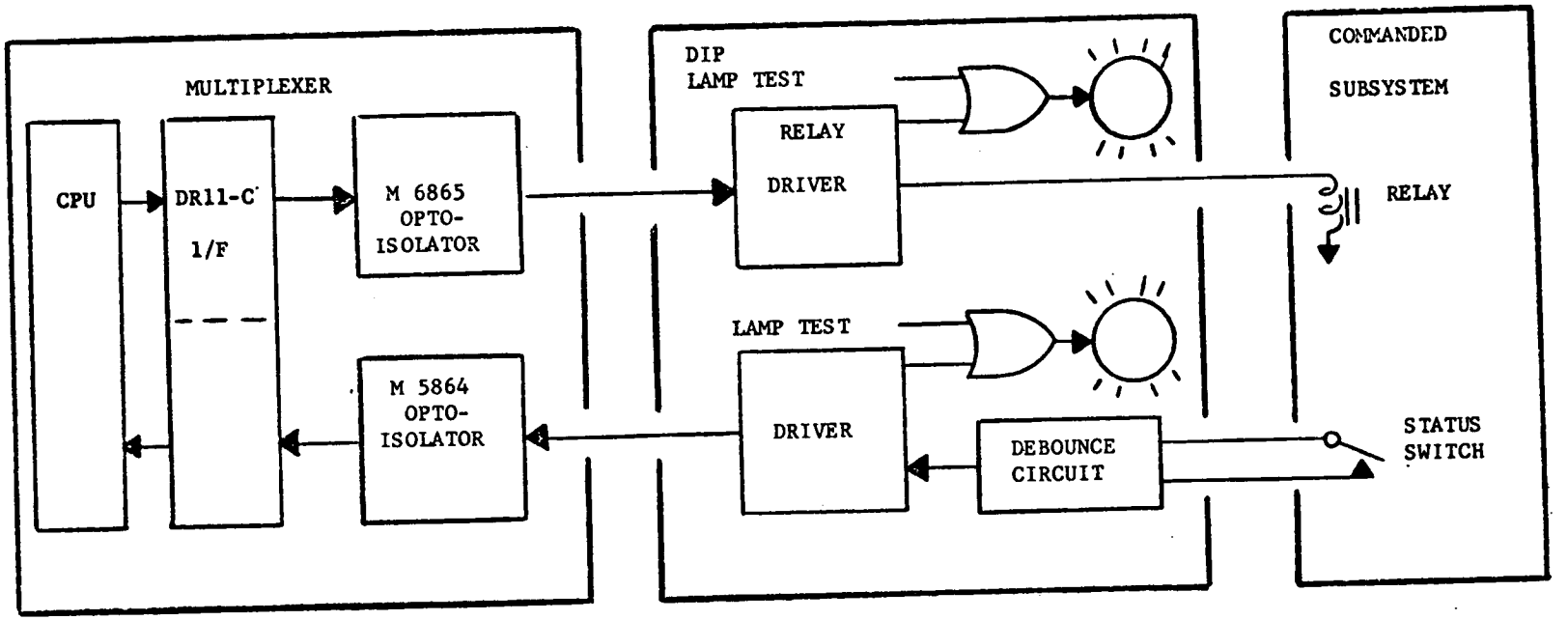

Figure 7-14. Digital Interface Panel (DIP) Showing Single Channel Command and Status Logic

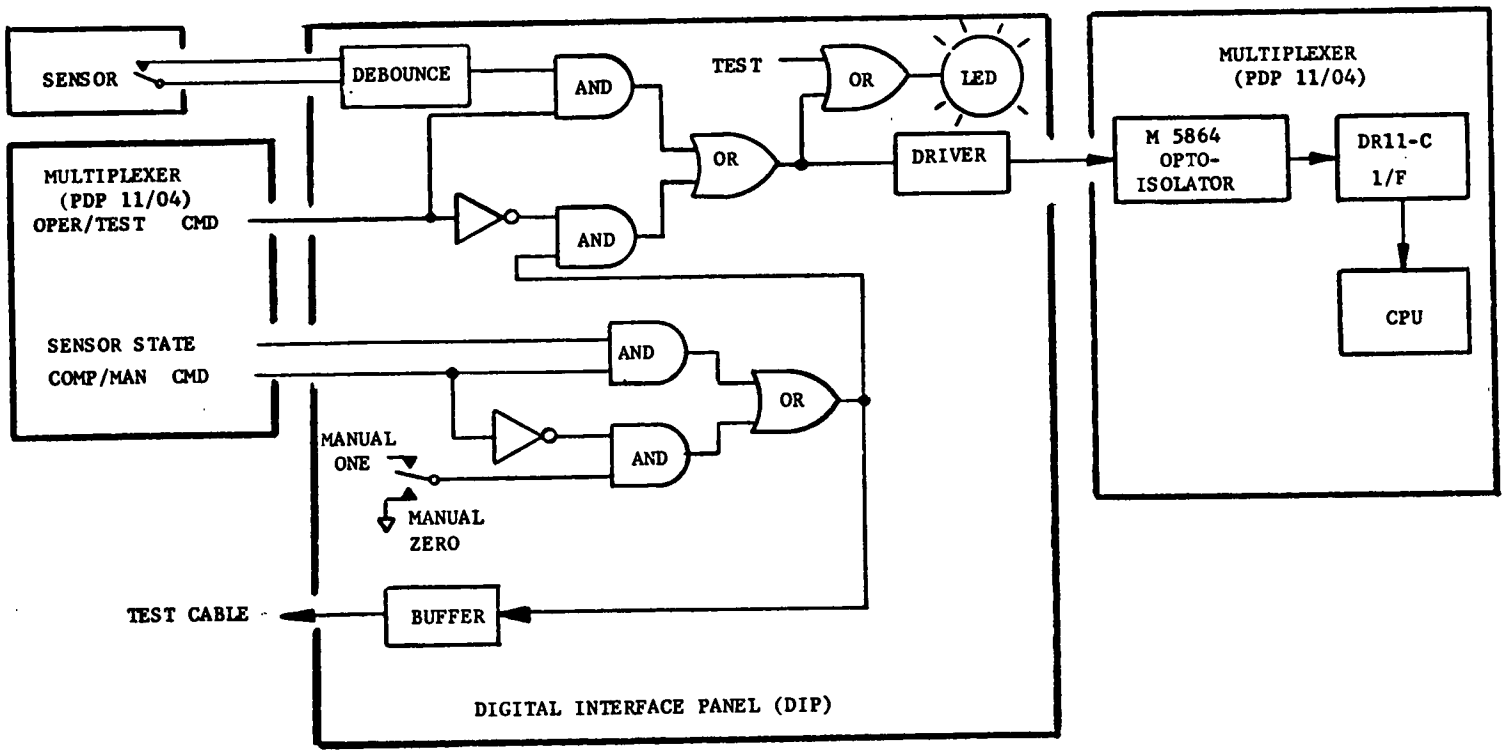

Figure 7-15. Digital Interface Panel (DIP) Showing Single Channel Sensor and Test Logic

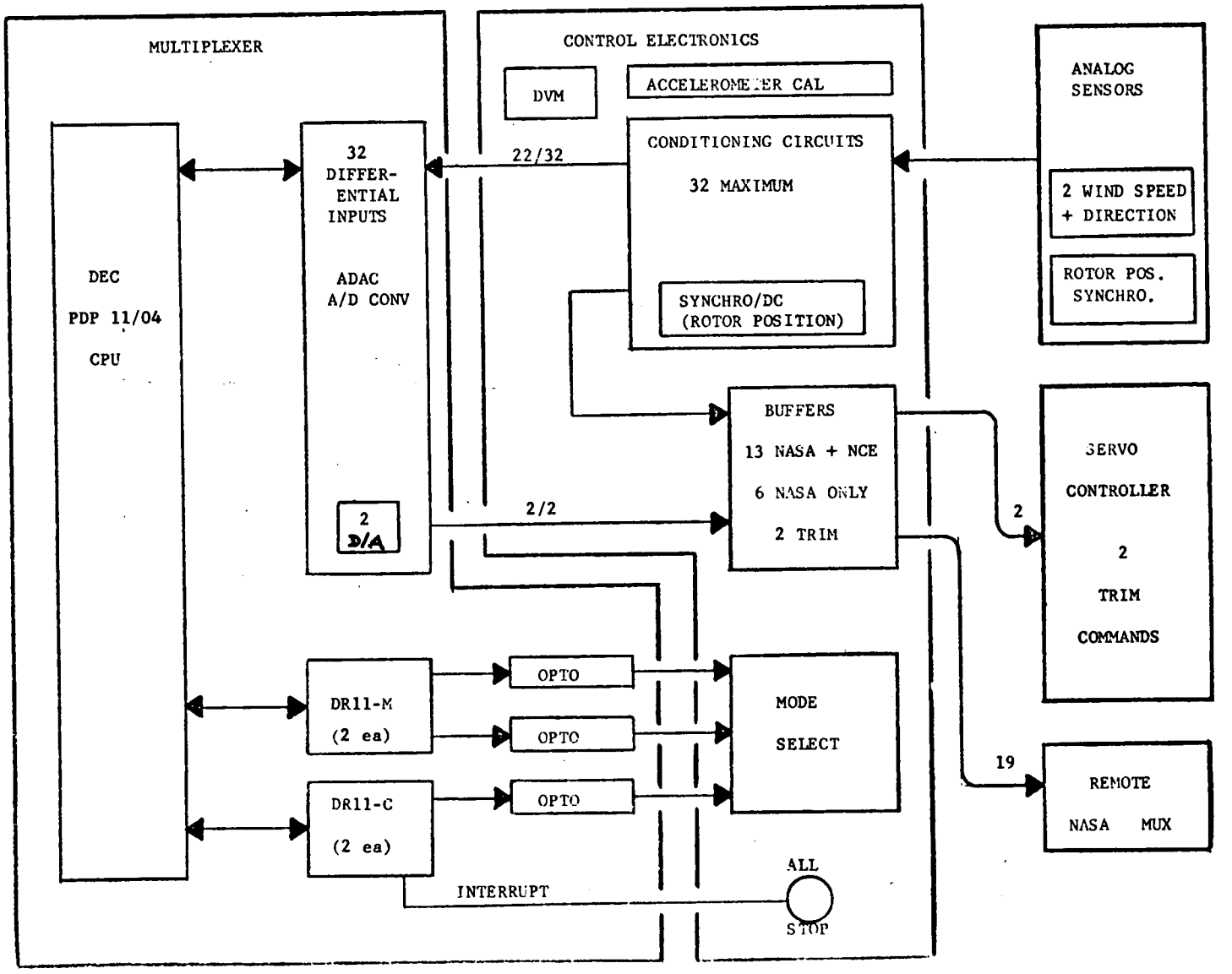

Figure 7-16. Nacelle Control Electronics (CE) Functions Showing Interfaces

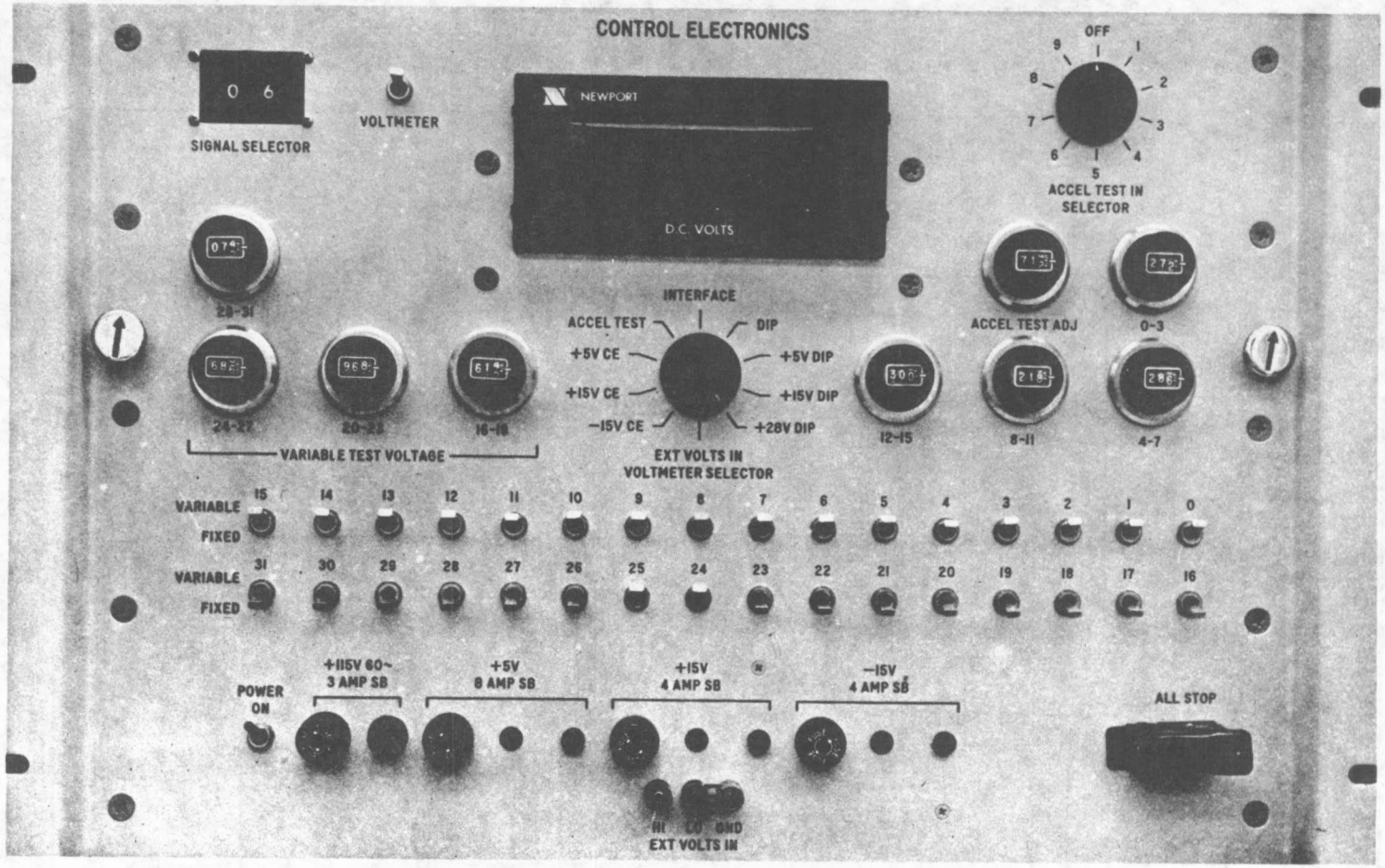

Figure 7-17. Control Electronics (CE)

voltage through the jacks provided at the bottom of the panel. As on the DIP, the covered "ALL STOP" button instantly commands Emergency shutdown.

Figure 7-18 shows one channel of the CE signal conditioning, buffering, and logic which allows both manual and computer driven testing. The MUX sets up the "OPER/TEST" command so the CE will receive either the real sensor signal or a test (simulated) signal. The "COMP/MAN" command determines whether the CE receives a manual value from the front panel or a computer driven value through the D/A converter. The "FIXED/VAR" command selects either +5 Volts or the computer driven value. If a manual front panel test value is selected, it can be set to +5 Volts or placed on one of the potentiometers so that any specified value can be dialed.

7.3.2.3 Remote Multiplexer Unit (NMU or GMU)

The Remote Mux Unit whose functional arrangement is shown in Figure 7-19 consists of a PDP 11/04 computer built by Digital Equipment Corporation. The PDP 11/04 has 32K words of parity MOS memory, with the battery backup feature (H775CA) so that data stored in MOS memory will be retained when power is off. The computer also has a KY11 LB programmer console so that the computer may be operated without a computer terminal. Figure 7-20 shows the hardware configuration. The RMU is directly connected to the CRU via a DMC11 Network Link. This communications link will allow the PDP 11/04 to be down line loaded from a host processor (CRU). This feature allows the PDP 11/04 to receive all of its programming from the CRU and pass data to the CRU at a date rate of 1Mbs. In order to run the RSX-11S operating system, a programmable real time clock is provided (KW11P). Interface between sensors and computer are accomplished via four DR11C parallel I/O interfaces and two DR11-M parallel output interfaces. All connections between sensors and interfaces are optically isolated via M5864 optical isolator input modules and M6865 optical isolator output modules.

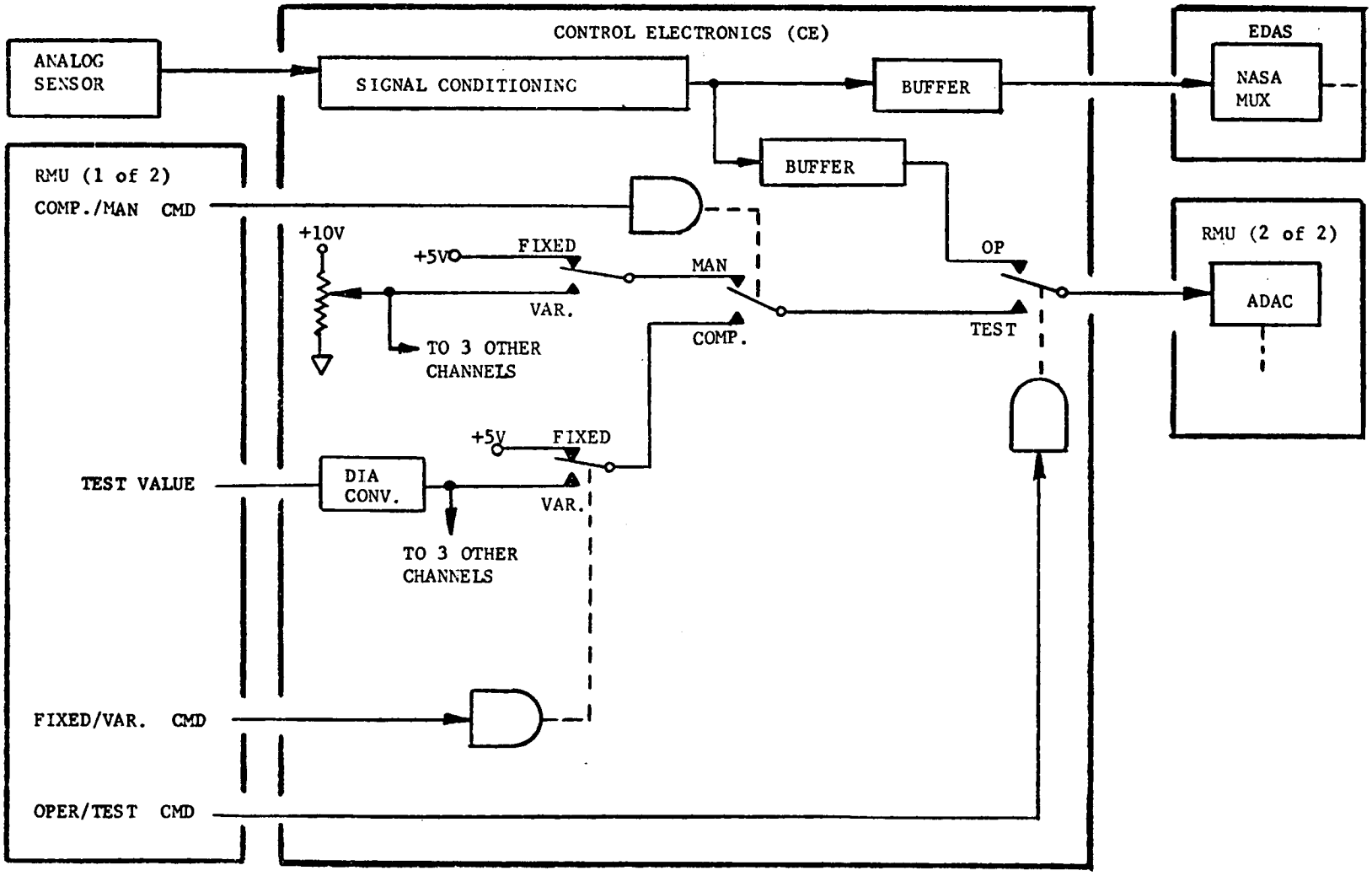

Figure 7-18. Control Electronics (CE) Showing Single Channel Signal Conditioning and Mode Select Logic

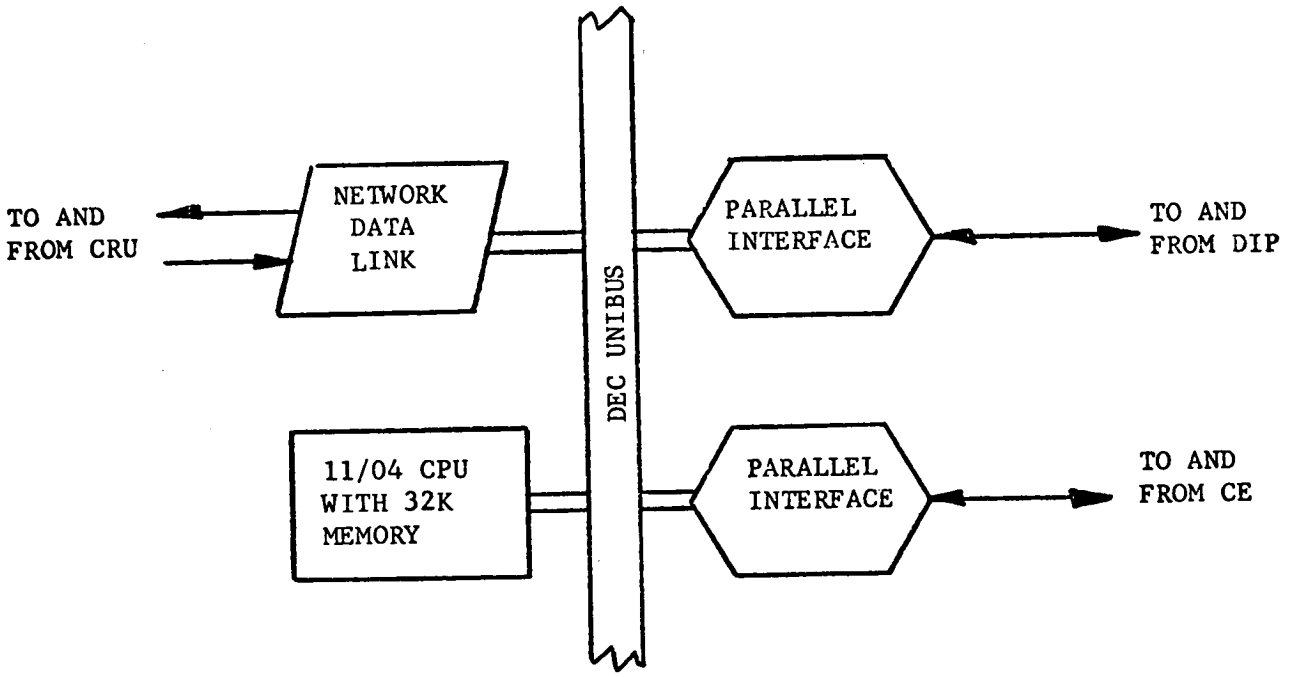

Figure 7-19. Remote Mux Unit (DEC PDP 11/04) Functional Arrangement

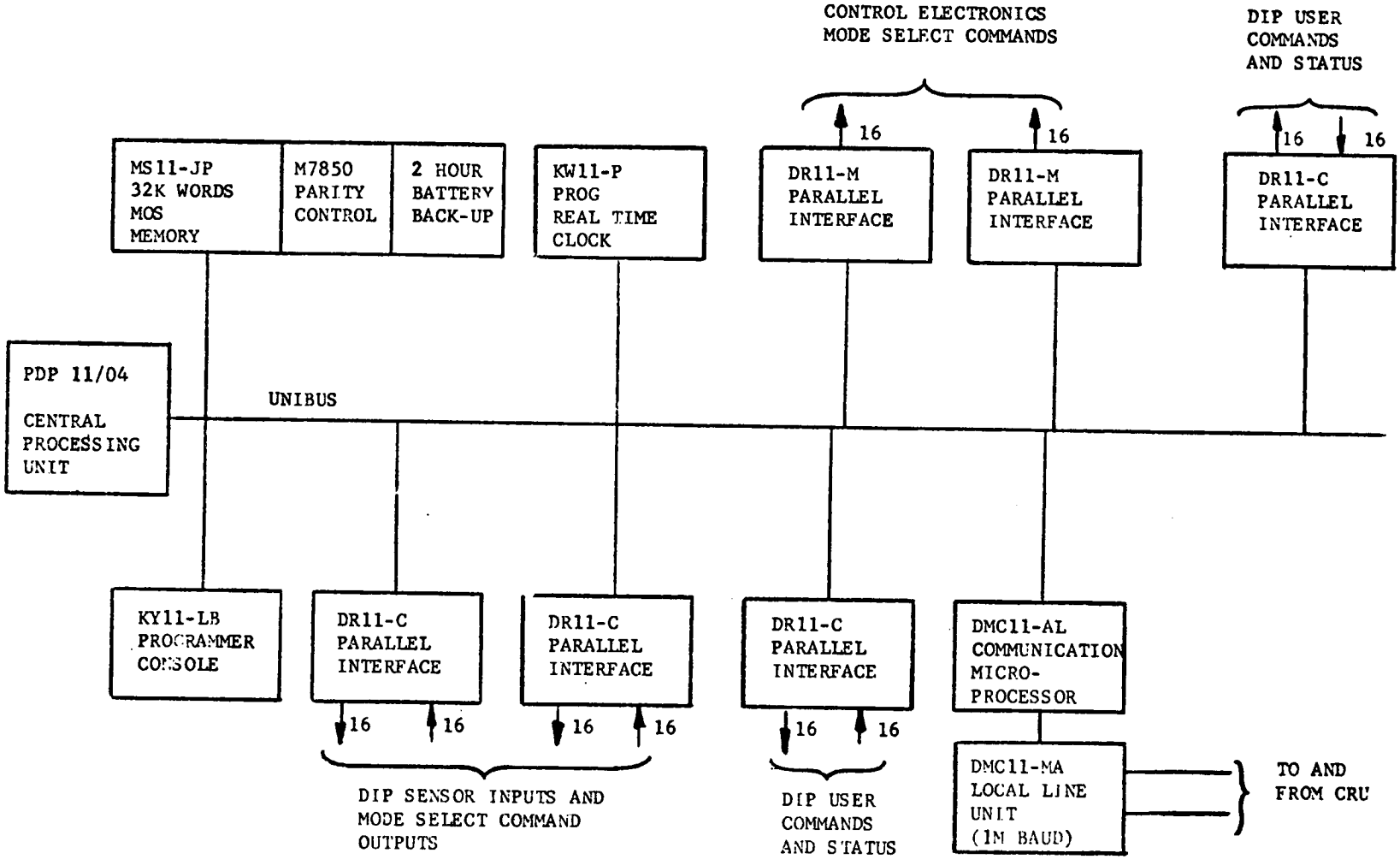

Figure 7-20. Remote Mux Unit (DEC PDP 11/04) Hardware Configuration Showing Interfaces

7.3.2.4 Servo Controller

The Servo Controller performs the analog control of blade pitch angle in response to mode and reference trim commands from the CRU and blade angle, hub speed, hydraulic valve spool position, and generator power from analog sensors as shown in Figure 7-21. The commanded modes of operation are listed and described back in Table 7-2.

Servo Controller regulates either generator shaft speed or power. A tachometer/precision reference combination provides an error signal when the generator speed does not match the reference. In power mode, the error signal is the difference between a CPU supplied reference and the output of a power transducer. The error signals are fed to an integrator and compensation circuits before they are amplified and converted to a current signal to drive the electro-hydraulic servo valve. The Nacelle Mux Unit transmits the analog speed and power trim signals which are used for rate sync and for limiting power to a value below rated capacity. Because of the specialized electrical requirements on the speed control tachometer, a second unit is used to provide generator speed to the CPU for logic and recording purposes.

The servo valve control loop electronic design includes two displacement transducers, a signal amplifier and a current amplifier. The main valve linear displacement transducer, an LVDT, provides a signal indicating hydraulic flow rate. The rotary displacement transducer, an RVDT, provides a signal indicating actual blade pitch angle. Both are magnetic devices requiring AC excitation and demodulation. The signal amplifier is an operational amplifier, which provides a summing junction, gain and compensation. The output is also used to provide status to the CPU when the hydraulic pitch change mechanism does not respond to the error signal in a prescribed time. This condition, called Pitch Jam, causes the CPU to issue emergency shutdown commands, which feather and lock the blades and stop the shaft with the blades in a 3-9 o'clock position. The current amplifier is simply a linear, voltage-to-current converter which produces the 15 milliamperes required to drive the servo valve.

The Servo Controller is a combination of analog and digital circuits using off-the-shelf components to produce a low-cost, reliable design. The digital commands from the Nacelle Mux and the status back to the Nacelle Mux are handled by TO5 relays. All resistors are low-temperature coefficient with 1% tolerance. The operational amplifiers are Bifet types (with high input impedance and low-drift characteristics with temperature and time) for long timing circuits like integrators and instrumentation types for critical offset circuits like closed loop feedback amplifiers. The tachometers are designed using a Frequency to Voltage chip and a 1-pole active filter. The oscillator/demodulators for the linear (LVDT) and angular (RVDT) motion sensors are purchased off the shelf components. All circuitry is designed to give minimum offset (both current and voltage) drift over the $\pm 20^{o}F$ temperature range controlled by the NMU Rack enclosure. Precision potentiometers are incorporated in all gain and feedback paths to allow field adjustment of critical parameters.

The generator control circuit consists of a tachometer which receives a signal from the generator shaft speed sensor and a reference. The tachometer has

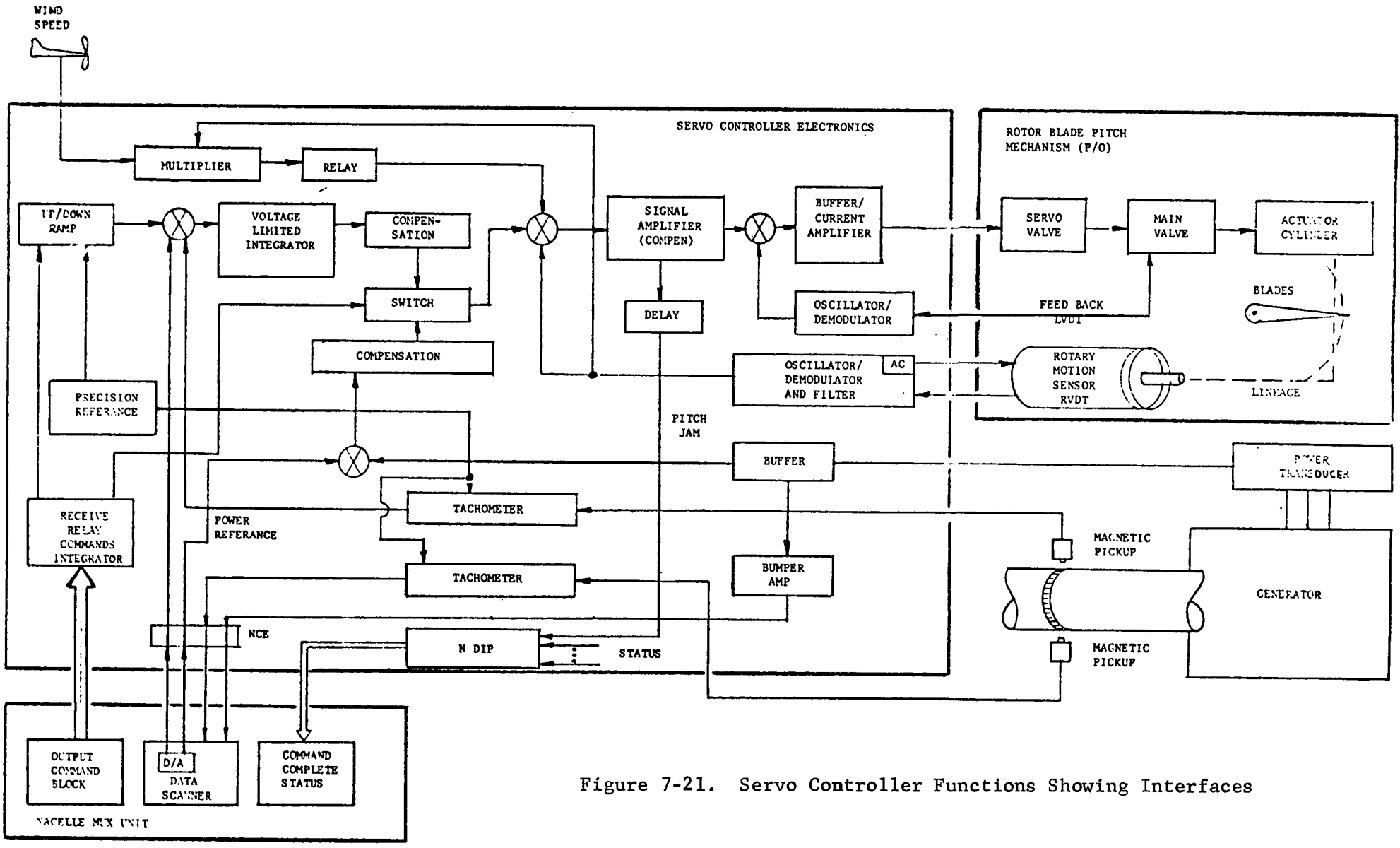

Figure 7-21. Servo Controller Functions Showing Interfaces

≃1% accuracy at 1818 rpm to assure setting a small positive power reference in the event of an erroneous CPU command. An 1818 rpm reference will be provided as the basic running reference. This reference and the tachometer user will use the same precision reference voltage to reduce drift errors. The tachometer basically consists of a precision charge dispenser that is triggered by the shaft speed pickup. On/off control of the loop will be controlled by a discrete command from the CPU via the NMUX. A ramp circuit controls the rise and fall of the speed reference signal to assure controlled startup and stopping. In addition to the reference signal, the CPU can set, via the D/A function of the NMUX, a trim on the speed reference to fine trim the speed to match the line frequency to enable breaker closure.

The error between the speed reference signal and the tachometer output is fed to an integrator along with the D/A output and the power signal. The integrator output voltage corresponds to a pitch angle setting on the rotor blades. Therefore, the integrator has a voltage limit to provide a maximum -0.5° pitch reference signal. This limit is required to assure rapid response to reduce pitch angle in the event of wind gusts or reduced speed commands. The summary junction/integrator function is accomplished with a single operational amplifier circuit. The clamp is done using an additional operational amplifier to clamp the integrator input when the voltage limit is reached. At normal operating speed, the error between speed reference and tachometer is nearly zero, so the integrator output is responding to the error between the D/A input (power reference) and the power signal, hence the generator output power is controlled.

7.3.2.5 Power Control and Input Panels

The power fed to the equipment racks is 115 Volts, single phase, 60 Hertz for all equipment except for the NMU rack air conditioner which is 208 Volts, single phase, 60 Hertz. The Power Control Panel at the top of the racks (see Figure 7-11) provides the on/off switch, status lights, and elapsed time meter. The AC Power Input Panel, together with its isolation transformer at the bottom of the rack, provides isolation, line filtering, and contains the power contactor which is controlled from the Power Control Panel.

7.3.2.6 Air Conditioner

The Nacelle Mux Unit Rack (Ice Box) is located in the Nacelle. It provides temperature control for its internal electronics. This heating and cooling is accomplished using a modified Model KAC-8 rear panel mounted electronic cabinet air conditioner produced by Kooltronic, Inc. The internal heater is needed only for cold startup when the ice box air temperature is below 50°F. The ice box is an insulated enclosure which houses the Nacelle Control Subsystem electronics, and contains the air conditioner (nominally rated at 8000 Btuh) with a 500-watt heater. The ice box provides the cooling and heating to establish and maintain the ice box interior at 50°F to 90°F over the range of outdoor ambient temperature of 0°F to 124°F. The ice box is insulated with one-inch thick urethane foam insulation and has a K value of 0.25 $\frac{\text{Btu - in}}{\text{hr - ft}^2\text{-°F}}$.

The electronics weight totals 750 lbs and, when operating continuously, generates 1500 Watts of heat. The most temperature sensitive components have a

maximum operating temperature limit of 90°F. The air conditioner, heater, and circulating fan are contained in a single housing which mounts on the rear of the ice box.

7.3.3 CONTROL AND RECORDING UNIT (CRU) AND PERIPHERAL RACKS

The CRU and Peripheral Racks, which are located in the Control Enclosure contain the main process control computer, the mass storage disc drives, the real time clock for time tagging data, and the telephone line modem and auto caller. Also included in this section is the operator input/output device. Figure 7-22 is a photograph of the CRU and Peripheral Racks and lists a short description of each of the components.

7.3.3.1 Control and Recording Unit (CRU)

The Control and Recording Unit consists of a PDP 11/34 computer built by Digital Equipment Corporation. Figure 7-23 is a diagram of the functional arrangement showing the peripheral interfaces. The PDP 11/34 has 64K words of parity MOS memory, with the battery backup feature (H775CA) so that the data stored in MOD memory will be retained when power is off. The PDP 11/34 also has memory management so that up to 128K words of memory may be used. The central processing unit is further augmented by the use of the KE11-B extended arithmetic element and the FP11AU floating point unit. Both KE11-B and FP11AU units are required to run FORTRAN IV PLUS. In order to run the RSX-11M operating system, a programmable real time clock is provided (KW11P). This unit provides interrupts up to 10 msec apart. Figure 7-24 is a diagram of the CRU hardware configuration showing the various interfaces.

7.3.3.2 Disc Units

The CRU utilizes two RK05 disc units as the system program mass storage. Each RK05 stores 2.5 megabytes of data. The RSX 11M system and all system software, as well as the archive disgnostic data, is stored on the disc units.

7.3.3.3 Real Time Clock

The CRU uses a Datum 9100 real time clock, with 1 msec resolution to indicate when events occur. The time is read using a DR11C interface. The Datum clock also has a battery backup to insure that an accurate time record may be maintained despite power failure lasting 60 hours.

7.3.3.4 Auto Call and Modem

The CRU may contact a utility terminal or receive system status inquires via a VADIC 1601 Auto Calling Unit (ACU) and VADIC 301 Modem. The ACU is controlled by a DEC DN11-DA ACU interface. Serial communication is accomplished via a DL11-E serial interface at a data speed of 300 baud.

7.3.3.5 Operator Terminal

The device used for operator input and output is the DEC LA36 "DECwriter" shown in Figure 7-25. This keyboard printer prints messages and reports from the CRU

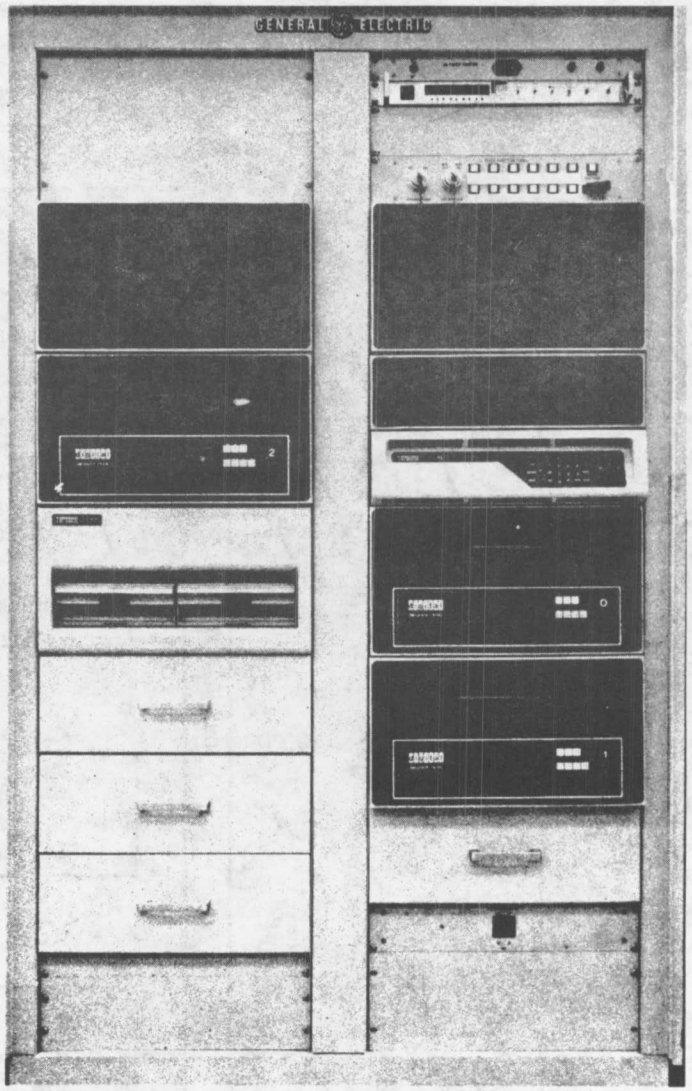

DISK DRIVES

OPERATING SYSTEM STORAGE
ARCHIVE
DEC RK 11 & RK05

REAL TIME CLOCK (NOT SHOWN)

DATA TIME TAG
DATUM 9100

POWER CONTROL PANEL

RACK POWER CONTROL
RACK POWER STATUS
ELAPSED OPERATING TIME

FIXED FUNCTION PANEL

ESD KILL BUTTON
SOFTWARE TEST
ENTRANCE ALARM KEY
LIFT INTERLOCK KEY

PHONE INTERFACE

AUTO CALL
MODEM
VADIC

CONTROL & RECORDING UNIT

PROCESS PARAMETERS
FORMAT DATA
MANUAL CONTROL
ISSUE COMMANDS
SELF TEST
DEC PDP 11/34

INTERFACE BOX

COMMUNICATION MICROPROCESSORS
DATUM CLOCK INTERFACE
FIXED FUNCTION INTERFACE
PHONE LINE INTERFACE
DEC BALL

AC POWER INPUT PANEL

LINE FILTER
POWER CONTACTOR

Figure 7-22. CRU and Periferal Rack Configuration

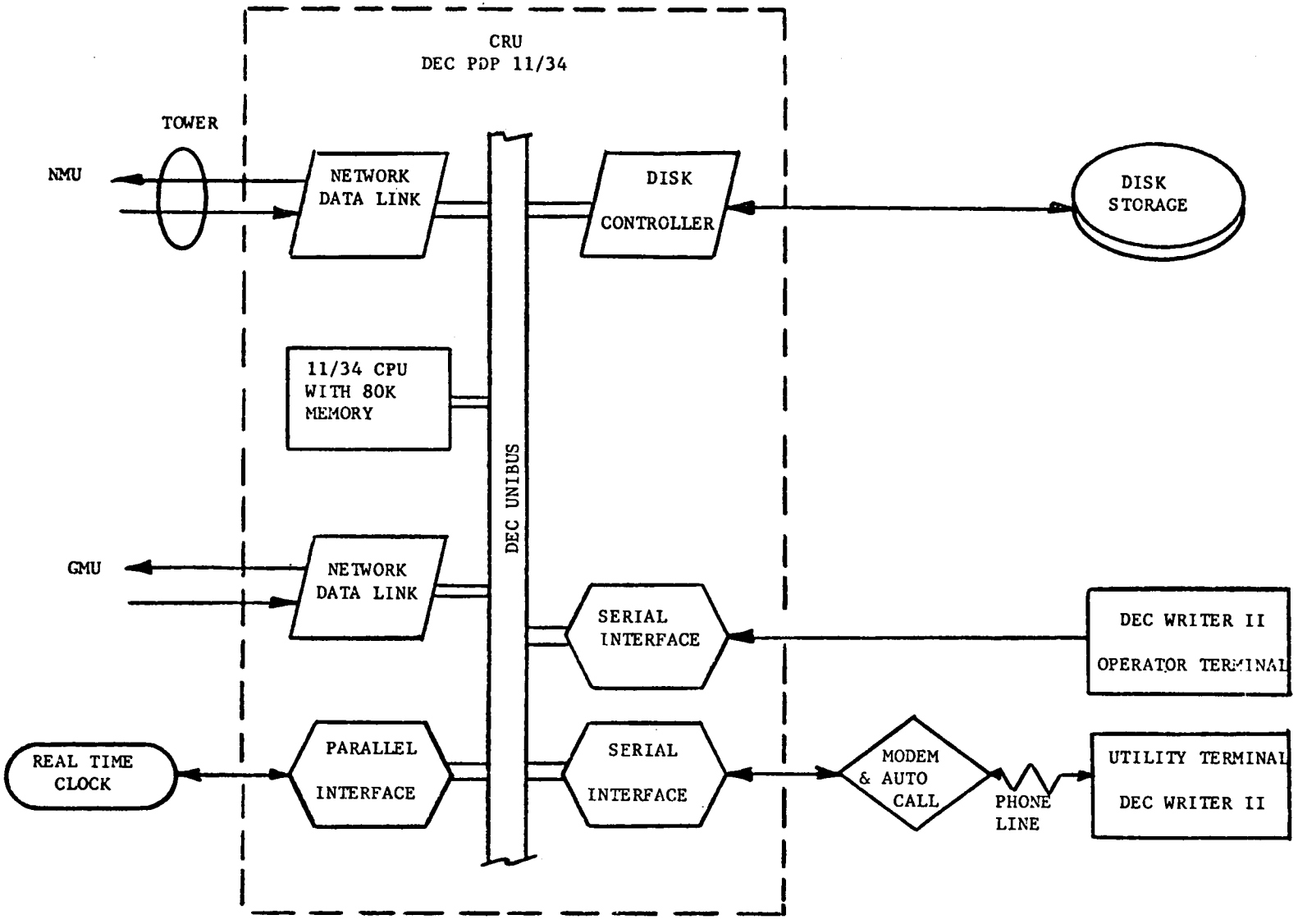

Figure 7-23. Control and Recording Unit (DEC PDP-11/34) Functional Arrangement

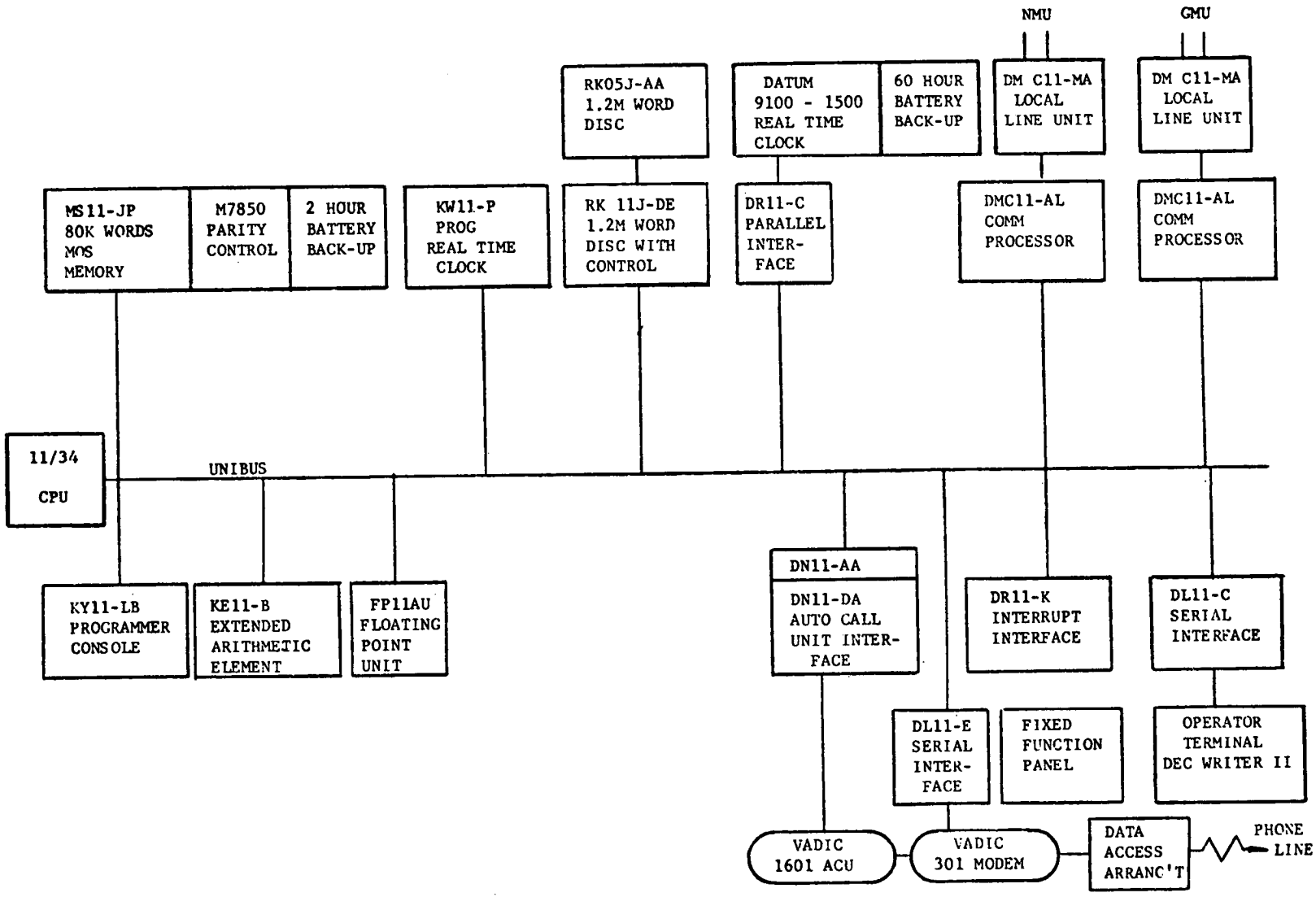

Figure 7-24. Control and Recording Unit (DEC PDP-11/34) Hardware Configuration Showing Interfaces

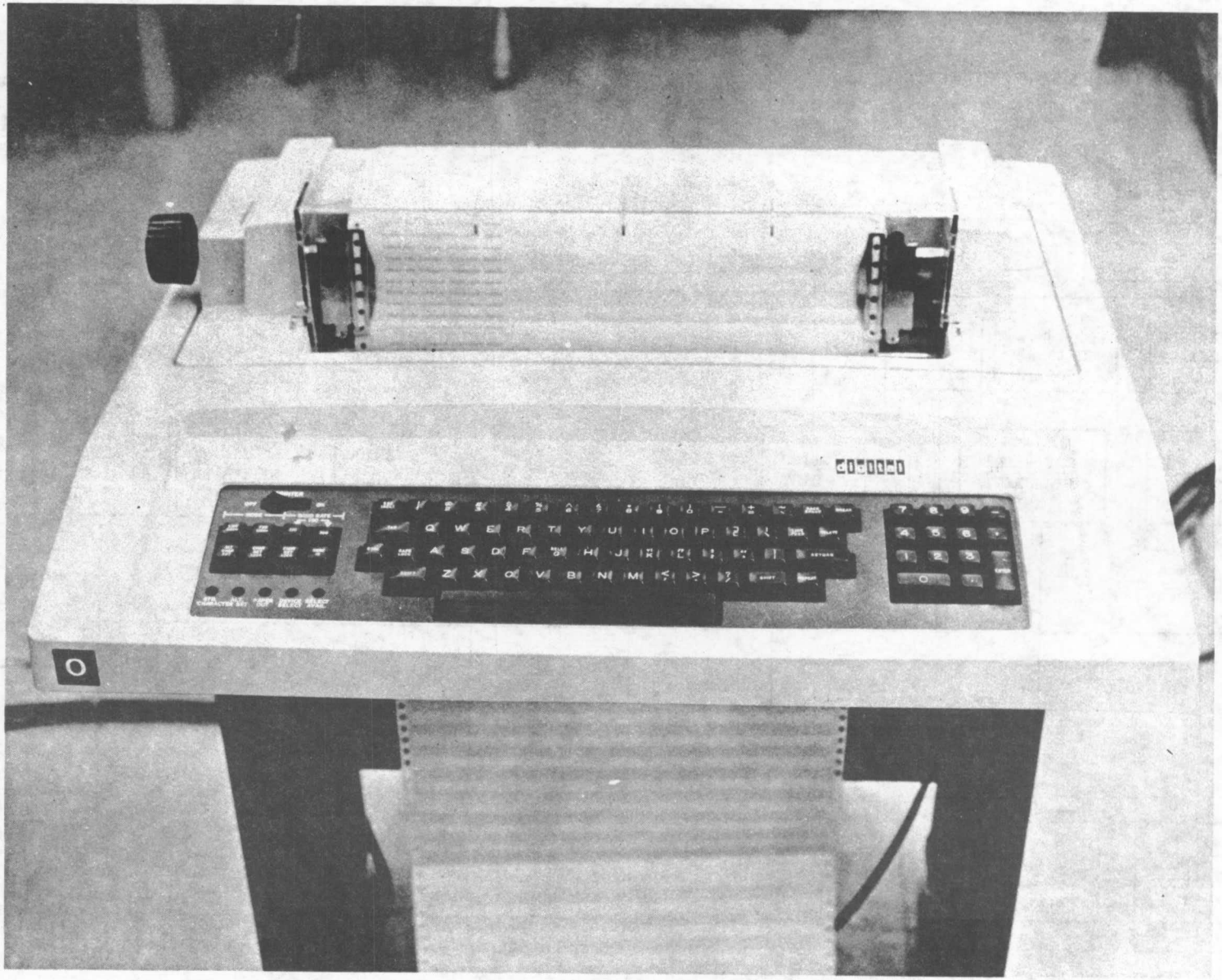

Figure 7-25. Operator Terminal (DEC LA 36)

and gives commands typed in by the operator.

7.4 SENSORS

The WTG sensors are listed by number, type and location in Tables 7-6, 7-7, 7-8, and 7-9.

A brief description of each of the more important sensors on the WTG appears in the following paragraphs.

7.4.1 WIND SPEED AND DIRECTION SENSOR

The Aerovane Transmitter is a combination anemometer and wind vane originally designed for the U.S. Navy as a durable and trouble-free instrument for measuring winds to 200 mph over a wide range of environmental conditions. The Aerovane has been used world-wide in applications related to government, industry, research, and education. In the transmitter, the direction transducer is a synchro that operates on 115V 60 Hz; the speed transducer is a rugged DC magneto with a linear output. The 12-inch diameter, three-bladed molded rotor, coupled to the DC magneto, has a maximum threshold of 2.5 mph and distance constant of 15 ft. The output of the magneto, filtered to prevent radio interference, is linear; 9.2 VDC, into 1150 Ohms, at 87.1 mph (1800 rpm), and 10.56 Volts at 100 mph. Wind direction, measured by a streamlined vane with a damping ratio of approximately 0.28 and a distance constant of 34 ft., is transmitted by a Type IHG synchro, operating on 115 Volts, 60 Hz, to a DC converter.

7.4.2 SHAFT SPEED TRANSDUCERS

Shaft speeds of both rotor and generator are measured by using an Electro Corporation Di-Mag magnetic sensor along with ferromagnetic gear teeth on the shafts.

Di-Mag digital magnetic sensors are versatile, non-contact sensing devices. They combine active electronics with a magnetic sensor in a single shell to produce a constant amplitude output signal suitable for direct use in digital equipment. This combination results in a much lower noise factor. Because the digital signal conditioning is performed internally, interface circuitry with its associated costs is eliminated. Di-Mag's performance also offers several other benefits, the most important are:

1. The establishment of an extremely precise relationship between the physical position of any sensed object and the electrical signal produced.

2. Increased sensitivity with the capability to produce full output of +5 to +15 Volts at speeds as low as 3 inches per second at gaps of 0.050 inch, or 1 inch per second at gaps of 0.010 inch.

3. Excellent resistance to water, oil, shock and vibration damage which assures longevity and operating reliability.

Table 7-6. Operational Sensor Definition

ID	Measured Item	Sensor Type	Sensor Location	Next Higher Assembly Dwg. No.	QDAS	EDAS	Sensor Drawing or Part Number
N-MA-PCM-01	Pitch Angle No.-1	RVDT	PCM Swing Link	175C9865 Item 3*	X	X	273A6520
N-MA-PCM-02	Pitch Angle No.2	RVDT	PCM Swing Link	175C9865 Item 3*	X		273A6520
N-MD-ROT-01	Rotor Bearing Oil Flow	Flow Switch		848E877 Item 39	X		273A6780 P1
N-MA-ROT-04	Rotor Bearing Vib	Accelerometer	Bearing Stator	848E885 Item 96	X		273A6616
N-MA-PCM-03	Pitch Odd Increase Press	Press Xducer	PCM Hydraulics	848E876 Item 2	X	X	132D6366
N-MA-PCM-04	Pitch Even Increase Press	Press Xducer	PCM Hydraulics	848E876 Item 2	X		132D6366
N-MA-PCM-05	Pitch Decrease Press	Press Xducer	PCM Hydraulics	848E876 Item 2	X		132D6366
N-MD-PCM-06	Odd Feather Accum. Press	Pressure Sw	PCM Hydraulics	848E876G1 Item P26	X		H210-CR-127-A4
N-MD-PCM-07	Even Feather Accum. Press	Pressure Sw	PCM Hydraulics	848E876G1 Item P26	X		H210-CR-127-A4
N-MD-PCM-08	Main Accum. Press.	Pressure Sw	PCM Hydraulics	848E876G1 Item P26	X		H210-CR-127-A4
N-MD-PCM-10	Hyd. Oil Low Level	Level Sw	PCM Hyd Res	77255354A Item P11	X		△
N-MD-YAW-02	Hyd. Oil Level	Level Sw	Yaw Hyd Res	0002759A Item P26	X		△
N-MD-YAW-03	Hyd. Pump Failed Alarm	Pressure Sw	Yaw Hyd Syst	0002759A Item P28	X		△
N-MD-DRT-01	Shaft Brake Accum. Low	Pressure Sw	2300 psi Accum	0002759A Item P30	X		△
N-MD-DRT-02	Shaft Brake Alarm	Pressure Sw	2300 psi Accum	0002759A Item P49	X		△
N-MD-YAW-04	Yaw Brake Accum. Low	Pressure Sw	3500 psi Accum	0002759A Item P14	X		△
N-MA-PWR-01	Gen Winding Temp ØA	RTD	Generator	132D6266	X		△
N-MA-PWR-04	Gen Bearing Shaft End Temp	RTD	Generator	132D6266	X	X	△
N-MA-PWR-05	Gen Bearing Aft End Temp	RTD	Generator	132D6266	X		△
G-MA-DRT-05	Rotor Shaft Speed	Magnetic	Torque Plate	848E885 Item 78	X	X	273A6506
N-MA-DRT-06	Rotor Shaft Position	Synchro	Rotor Slip Ring Assy	298E464 Item 30	X	X	273A6619
N-MA-DRT-07	Generator Shaft Speed	Magnetic	Generator Shaft	298E464 Item 8	X		273A6506
N-MA-DRT-08	Generator Vib	Accelerometer	Gen Shaft Bearing	298E463 Item 25	X		273A6616

△ Sensor Part of Purchased Assembly

Table 7-6. Operational Sensor Definition (Cont.)

ID	Measured Item	Sensor Type	Sensor Location	Next Higher Assembly Dwg. No.	QDAS	EDAS	Sensor Drawing or Part No.
[illegible]-MA-PCM-27	Pitch Change Bearing Vib	Accelerometer	Thrust Bearing	848E936 Item 23	X		273A6616 △
[illegible]-MD-DRT-13	Trans. Oil Level	Level SW	Transmission	03-160-0027-4G	X		△
[illegible]-MD-PCM-28	Slew Pump Failed Alarm	Press SW	Slew PMP Disch Line	77255354A P12	X		△
[illegible]-MA-DRT-14	Transmission Hi Spd Brng Temp	RTD	Trans	03-160-0027-4G	X		163C5360
[illegible]-MA-ENV-01	Wind Speed No.1	Magneto	Weather Boom	298E466 Item 21-L	X	X	163C5360
[illegible]-MA-ENV-02	Wind Speed No. 2	Magneto	Weather Boom	298E466 Item 21-R	X		163C5360
[illegible]-MA-ENV-03	Wind Direction No. 1	Synchro	Weather Boom	298E466 Item 21-L	X	X	163C5360
[illegible]-MA-ENV-04	Wind Direction No. 2	Synchro	Weather Boom	298E466 Item 21-R	X		163C5360
[illegible]-MA-ENV-05	Nacelle Temp	RTD			X		273A6612
[illegible]-MD-PWR-06	Aircraft Obstruction Lite	Shunt		132D6390G1 Item 28	X		RW31V2R0
G-MA-PWR-07	Generator ØA Current	Ct & Xducer	Switchboard	CT848E926 Item 2 XD848E899 Item 16 (50/51V)	X	X	163C5358 △
G-MA-PWR-08	Generator ØB Current	Ct & Xducer	Switchboard	CT848E926 Item 2 XD848E899 Item 16 (50/51V)	X	X	163C5358 △
G-MA-PWR-09	Generator ØC Current	Ct & Xducer	Switchboard	CT848E926 Item 2 XD848E899 Item 16 (50/51V)	X	X	163C5358
G-MA-PWR-10	Generator Voltage (ØA-ØB)	Pt & Xducer	Switchboard	PT175C9851 Item 3Pt XD848E899 Item 41 (VTGEN)	X	X	△ △
G-MA-PWR-11	Generator Power (KW)	Ct, Pt & Xducer	Switchboard	PT(2)175C9851 Item 1Pt & 2Pt CT(2)848E926 Item 2 XD848E899 Item 45 (WT)	X	X	△ 163C5358 △
G-MA-PWR-12	Generator Power (KVARS)	Ct,Pt & Xducer	Switchboard	PT(2)175C9851 Item 1Pt & 2Pt CT(2)848E926 Item 2 XD848E899 Item 46 (VART)	X	X	△ 163C5358 △
G-MA-PWR-13	Utility Voltage ØA-ØB	Pt & Xducer	Switchboard	PT(2)175C9851 Item 1Pt & 2Pt XD848E899 Item 42 (VT/VR)	X		△ △
G-MA-PWR-16	Utility Frequency	Xducer	Switchboard	PT175C9851 Item 1Pt XD848E899 Item 47 (ft)	X		△ △
G-MD-PWR-17	Transformer Temp Alarm	Temp Switch	Main Transformer		X		△

△ Sensor Part of Purchased Assembly

Table 7-6. Operational Sensor Definition (Cont.)

ID	Measured Item	Sensor Type	Sensor Location	Next Higher Assembly Dwg. No.	QDAS	EDAS	Sensor Drawing or Part Number
G-MD-PWR-18	Transformer Oil Level Alarm	Level Sw	Main Transformer		X		△
G-MD-PWR-19	Transformer Gnd. Curnt. Alarm		Switchboard		X		△
G-MA-ENV-07	Enclosure Temp	RTD			X		273A6612
G-MD-PWR-20	Main Breaker Position	Contacts	Main Circ. Breaker	175C9851 (I/055456)	X		△
G-MA-PWR-21	Auxiliary Current	Ct & Xducer	Switchboard	CT175C9851 11Ct & 13Ct	X		△
				XD848E899 Item 43 $\frac{\text{At}}{\text{AUX}}$	X		△
G-MA-PWR-22	Exciter Field Current	Xducer	Switchboard		X	X	913A-20-H
N-SD-PCM-09	Feather Latch Position	Switch, Position	Feather Latch	132D6037 Item 9	X		273A6677
N-MD-DRT-26	Shaft Brake Press	Switch,Press	Brake Hydraulics	0002759A Item P49	X		△
N-MD-YAW-05	Yaw Brake Alarm	Switch,Press	Brake Hydraulics	0002759A Item P29	X		△
N-MD-YAW-07N	Yaw Brake On/Off	Swith,Press	Brake Hydraulics	0002759A Item 29	X		△
N-MA-PWR-30	Nacelle PWR Sensor	Pt & Xducer		CT848E926 Item 2 PT848E926 Item 4 XD848E926 Item 6	X		CT163C5358 PT175C9902P1 XD50-4723 15MNDD1
G-MD-PWR-32	Battery Low Voltage Alarm	Switch	Batt. & Charger Enc	S-1889 LVAR	X		△
G-FF-ENV-12	Enclosure Door Alarm	Switch	Enc. Door		X		20-180S
G-FF-ENV-15	Security Alarm On/Off	Switch	Cru Rack	132D6288 Item 5	X		PTKBC2242R-B39
G-MD-ENV-15	Interlock Switch	Switch	Cru Rack	132D6288 Item 6	X		PTKBC2242R-B39
N-MD-DRT-22	Lube Oil Temp	Temp Switch	Xmission Pump	03-160-0027-4G	X		△
N-MA-DRT-29	Generator Speed (1400-2200)	Magnetic	Hi Spd Shaft	298E464 Item 8	X		273A6506
_____	Rotor Shaft Over Speed	Magnetic	Torque Plate	848E885 Item 28	X		273A6505

△ Sensor Part of Purchased Assembly.

Table 7-7. Engineering Sensor Definition - NASA Rotor Mux

Line No.	Measured Item	Sensor Type	Sensor Location	Next Higher Assembly Dwg. No.	EDAS	ODAS	Sensor Drawing or Part Number
1	Blade No. 1 0% Flatwise Bending	4 Leg Str. Ga.	0		X		
2	Blade No. 1 0% Edgewise Bending	4 Leg Str. Ga.	0		X		
3	Blade No. 1 0% 45° L.D.	4 Leg Str. Ga.	0 % of Blade		X		
4	Blade No. 1 0% Torsion	4 Leg Str. Ga.	0 Length From		X		
5	Blade No. 1 50% Flatwise Bending	4 Leg Str. Ga.	50 Root		X		
6	Blade No. 1 50% Edgewise Bending	4 Leg Str. Ga.	50		X		
7	Blade No. 1 50% Torsion	4 Leg Str. Ga.	50		X		
8	Blade No. 2 0% Flatwise Bending	4 Leg Str. Ga.	0		X		
9	Blade No. 2 0% Edgewise Bending	4 Leg Str. Ga.	0		X		
10	Blade No. 2 0% 45° L.E.	4 Leg Str. Ga.	0 % of Blade		X		
11	Blade No. 2 0% Torsion	4 Leg Str. Ga.	0 Length From		X		
12	Blade No. 2 50% Flatwise Bending	4 Leg Str. Ga.	50 Root		X		
13	Blade No. 2 50% Edgewise Bending	4 Leg Str. Ga.	50		X		
14	Blade No. 2 50% Torsion	4 Leg Str. Ga.	50		X		
15	Hub Tension/Compression	½ Br. Str. Ga.	Hub	848E925 Item No. 1	X		273A6610
16	Hub Tension/Compression	½ Br. Str. Ga.	Hub	848E925 Item No. 1	X		273A6610
17	Hub Tension/Compression	½ Br. Str. Ga.	Hub	848E925 Item No. 1	X		273A6610
18	Hub Tension/Compression	½ Br. Str. Ga.	Hub	848E925 Item No. 1	X		273A6610
19	Hub Tension/Compression	4 Leg Str. Ga.	Hub	848E925 Item No. 1	X		273A6610
20	Hub Tension/Compression	4 Leg Str. Ga.	Hub	848E925 Item No. 1	X		273A6610
21	Rotor Shaft Torsion	4 Leg Str. Ga.	Low Speed Shaft	848E925 Item No. 1	X		273A6610
22	Pitch Rod No. 1 Tens/Comp.	4 Leg Str. Ga.	Pitch Rod #1	848E925 Item No. 1	X		273A6610
23	Pitch Rod No. 2 Tens/Comp.	4 Leg Str. Ga.	Pitch Rod #2	848E925 Item No. 1	X		273A6610
24	Rotor Brng. Inner Race Temp.	Thermocouple	Rotor Brng.	848E885 Item No. 79	X		273A6620
25	Pitch Change Bearing Temp.	Thermocouple	Pitch Change Brng.	848E936 Item No. 21	X		273A6620

Table 7-8. Engineering Sensor Definition - NASA Nacelle Mux

Line No.	Measured Item	Sensor Type	Sensor Location	Next Higher Assembly Dwg. No.	EDAS	ODAS	Sensor Drawing or Part Number
1	Wind Speed	Magneto	Weather Boom		X	X	*
2	Wind Direction	Synchro	Weather Boom		X	X	*
3	Outside Air Temp	Thermocouple	External Nacelle	298E466* Item 42	X		273A6624
4	Blade Pitch Angle	RVDT	H/S Swing Link	*	X	X	*
5	Pitch Odd Increase Press	Transducer	PCM Inc. Manifold	848E876 Item 187	X	X	132D6386
6	PCM Hyd. Oil Temp	Thermocouple	PCM Hyd. Res.	77255354-A Item 10	X		273A6608P2
9	Rotor Shaft Position	Synchro	Low Spd. Slip Rings	*	X	X	*
10	Bedplate Bending	4 Leg. Str. Ga.		132D6085 Item 1	X		273A6610
11	Bedplate Bending	4 Leg. Str. Ga.		132D6085 Item 1	X		273A6610
12	Bedplate Bending	4 Leg. Str. Ga.		132D6085 Item 1	X		273A6610
13	Bedplate Tension, Compression			132D6085 Item 2	X		
14	Bedplate Tension, Compression	Rosette Str. Ga.		132D6085 Item 2	X		273A6617
15	Bedplate Tension, Compression			132D6085 Item 2	X		
16	Yaw Torque CW	Pressure Trans.	Yaw Motor Hyd. Line	848E875 Item 2	X		132D6386
17	Yaw Torque CCW	Pressure Trans.	Yaw Motor Hyd. Line	848E875 Item 2	X		132D6386
18	Inlet Lube Temp	Thermocouple		848E877 Item 33	X		273A6608P1
19	Transmission Outlet Lube Temp.	Thermocouple		848E877 Item 33	X		273A6608P1
20	Yaw Position	Synchro	Yaw Slip Ring Assm	848E877 Item 26	X		273A6619
21	Bedplate Vibration (X)						
22	Bedplate Vibration (Y)	3 Axis	Top Corner N.W.	132D6382/132D6084-G1 (AFT)	X		273A6616
23	Bedplate Vibration (Z)	Accelerometer					
24	Bedplate Vibration (X)						
25	Bedplate Vibration (Y)	3 Axis	Top Corner S.E.	132D6382/132D6084-G2 (FWD)	X		273A6616
26	Bedplate Vibration (Z)	Accelerometer					
27	Rotor Bearing Outer Race Temp	Thermocouple	Rotor Brng	848E885 Item 79	X		273A6620
28	Rotor Bearing Oil Outlet Temp	Thermocouple	Oil Outlet	848E877 Item 33	X		273A608P1
29	Yaw Hyd. Oil Temp.	Thermocouple	Yaw Hyd. Res.	E0002759A Item 22	X		273A6608P2
30	Gen. Winding Temp ØB	Rtd.	Gen. Winding	132D6266	X		*
31	Gen. Shaft Brng. Temp.	Rtd.	Gen. Bearing	*	X	X	*

* = SEE OPERATIONAL LIST

Table 7-9. Engineering Sensor Definition - NASA Ground Mux

Line No.	Measured Item	Sensor Type	Sensor Location	Next Higher Assembly Dwg. No.	EDAS	ODAS	Sensor Drawing or Part Number
1	Generator Current ØA	CT & Transducer	Switchboard	*	X	X	*
2	Generator Current ØB	CT & Transducer	Switchboard	*	X	X	*
3	Generator Current ØC	CT & Transducer	Switchboard	*	X	X	*
4	Generator Power (DW)	CT, PT & Transducer	Switchboard	*	X	X	*
5	Generator Power (KVAR)	CT, PT & Tranducer	Switchboard	*	X	X	*
6	Tower Vibration Site No.1X						
7	Tower Vibration Site No.1Y	3 Axis Accel.	Tower	132D6047G1	X		273A6616
8	Tower Vibration Site No.1Z						
9	Tower Vibration Site No.2X						
10	Tower Vibration Site No.2Y	3 Axis Accel.	Tower	132D6047G1	X		273A6616
11	Tower Vibration Site No.2Y						
12	Exciter Field Current	Shunt	Switchboard	*	X	X	*
13	Generator Voltage (ØA-ØB)	PT & Transducer	Switchboard	*	X	X	*
17	Rotor Shaft Speed	Magnetic	Torque Plate	*	X	X	*

7.4.3 BLADE POSITION ANGLE TRANSDUCER

A KAVLICO RVDT (Rotary Variable Differential Transformer) is used to measure blade pitch angles by sensing the swing link position in rotation. The R502 type has been chosen with modifications to accommodate the 0 to +10 Volt output for 0 to 80° rotational range.

7.4.4 ROTOR SHAFT AND NACELLE POSITION SENSOR

The sensors for both Nacelle position and rotor shaft position are size 23 standard military 23Cx6D, 60 Hz control transmitters (synchros) manufactured by the Vernitron Corporation. These units are accurate to 6 minutes of arc. The output signal is converted to a 0 to 10 Volt DC level by Interface Engineering's Model SA810-B Synchro-to-Linear DC Converter.

7.5 ENGINEERING DATA ACQUISITION SYSTEM (EDAS)

The Engineering Data Acquisition System (EDAS) provides data for structural, aerodynamic, and electrical performance evaluation of the WTG System.

General Electric provides sensors, signal conditioning, buffering where necessary, and cabling to the Mobile Data Acquisition System supplied by NASA.

This system is described in detail in NASA Statement of Work No. 3-783203, dated April 15, 1976. Basically, the system hardware consists of three 32-channel Remote Multiplexer Units (RMU), a Stand-Alone Instrument Recorder (SAIR), and a Portable Instrument Vehicle (PIV).

7.5.1 REMOTE MULTIPLEX UNITS

Three RMU's are used on each 2000 kW WTG, one in the rotor, one in the Nacelle and one in the control enclosure. Each RMU can process up to 32 inputs consisting of sensors or previously conditioned and buffered signals.

7.5.2 STAND-ALONE INSTRUMENT RECORDER (SAIR)

When the PIV is not at the WTG site, the SAIR is available to record approximately 40 minutes of preselected inputs from each RMU on a continuous tape loop. Sixteen channels of data can be recorded from each RMU on each of 3 tracks; the fourth track records an internally generated time code. Signals and the remote stop command enter the SAIR via one 18-pin connector. The remaining 3-pin connector is for 120 Volt AC power input.

A momentary contact closure between pins B and C of the 18-pin connector stops the recorder, saving the last 40 minutes of data. Recording can be started again only by pushing the manual reset button.

7.5.3 PORTABLE INSTRUMENT VEHICLE (PIV)

The PIV provides data reduction facilities for the Engineering Data Acquisition System either in a real-time mode or in an off-line mode with playback of recorded data.

Interfacing of the PIV to the WTG is through connectors on the exterior of the vehicle. Power (480 Volts, 3 Phase, 30 kVA) enters on the left side of the PIV while FM multiplexed signals from the RMUX enter on the right side through J1 through J9 (6 jacks for signals and 3 for expansion capability). Calibration commands to the RMUX are provided by J17.

7.6 SOFTWARE DESCRIPTION

7.6.1 FUNCTIONAL FLOW

The WTG software system is comprised of two parts, Process Control and Auxiliary Functions as shown in Figure 7-26.

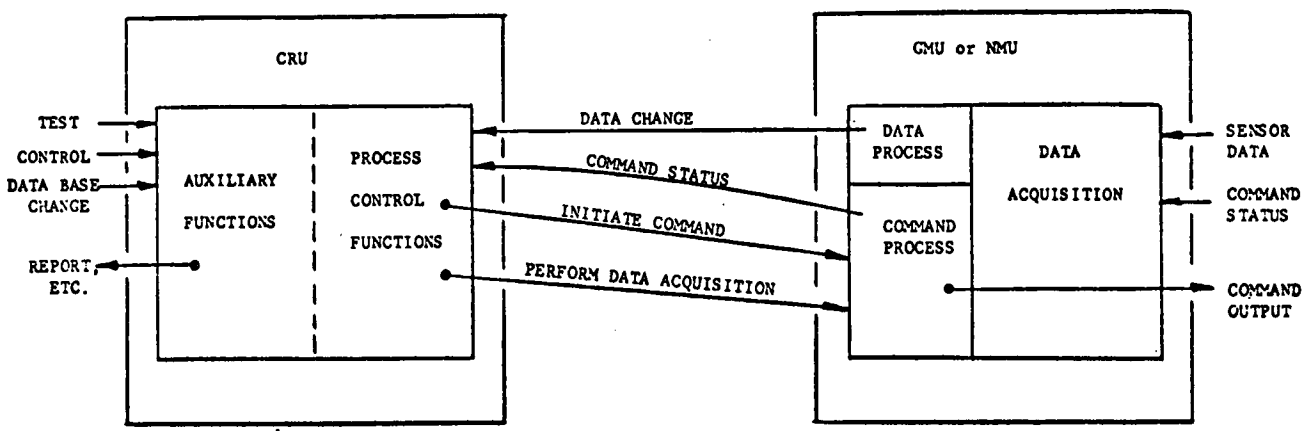

Figure 7-26. Software Overview Diagram

The Process Control function is performed in three computers, the Control and Recording Unit (CRU), the Nacelle Multiplexer Unit (NMU) and the Ground Multiplexer Unit (GMU). The GMU and NMU are used for data collection and data concentration. They provide the system link to the commands and sensors in the WTG. The CRU performs the analysis of sensor change data, and causes commands to be dispatched by the NMU and GMU as circumstances require. The Process Control function is clock-driven as opposed to interrupt-driven. A request is dispatched by the CRU to the GMU and NMU every 100 millisecond, which directs these multiplexers to sample data, compress it and report predetermined changes to the CRU. Commands initiated by the CRU are output by the multiplexers. Command completion is monitored; retry, when necessary, is performed; status, either pass or fail, is reported back to the CRU. Conditions resulting in shutdown are monitored by

the CRU; when detected, the appropriate command sequences are initiated and sent to the GMU and NMU. All inter-computer discourse and all significant events are recorded in the Archive file by the CRU.

Auxiliary Functions (which consist of operator interface routines, utility interface routines, data base inspect and change routines, archive replay, report control, and manual system exercise) are handled primarily in the CRU. They are implemented as "background" tasks and executed during time remaining between end of Process Control function and the next tick of the 100 millisecond Process Control Clock.

A functional representation of the Data Acquisition cycle and of the Command Output and Process cycle is contained in Figures 7-27 and 7-28 respectively. Figure 7-29 depicts the start to finish process of sensing an abnormal condition, generating the command to correct that condition, and sensing the fact that the command was initiated properly by the hardware.

7.6.2 SYSTEM FUNCTIONAL ALLOCATION

Three basic functions are performed by the WTG software system. They are: Process Control, Data Recording, and Auxiliary Functions. The Process Control Function is carried out in all three processors; the CRU, GMU and NMU. In the CRU, Process Control is performed by Data Acquisition, Control Task, State Enable and Data Process Modules. In the GMU and NMU, Process Control is performed by Data Acquisition, Data Process, Output, Command Acquisition, Command Process, and Controls Interface Driver. Data Recording is performed entirely in the CRU via the Archive processor. Auxiliary functions are likewise carried out primarily in the CRU. The modules involved in the CRU include Display, Manual (Functions), Test (Build), Modify, Playback, Startup, and Report. Test Execute module executes in each of the CRU's.

7.6.3 MODULE FUNCTIONAL DESCRIPTIONS

7.6.3.1 Control and Recording Unit (CRU)

Data Acquisition/Control Task. Data Acquisition is activated whenever a data buffer is received in the CRU. It schedules ARCHIVE and the Control Task. The Control Task examines the buffer, strips out the data, event by event, and enters each event occurrence in the CRU Event Table. It then cycles through the Event Table, scheduling Data Process Modules (DPMS) for each newly tabled event. Four services are provided to the Data Process Modules. They are: the issuance of commands to the GMU/NMU, the initiation of one Data Process Task by another, the changing of the status of the runability of other DPMS, and the saving of computed variables for use by other DPMS.

State Enable. State Enable is the module which remembers which tasks must consent for the system to go from the IDLE state to the GENERATE state and remembers which modules still have not consented. When the system is in the

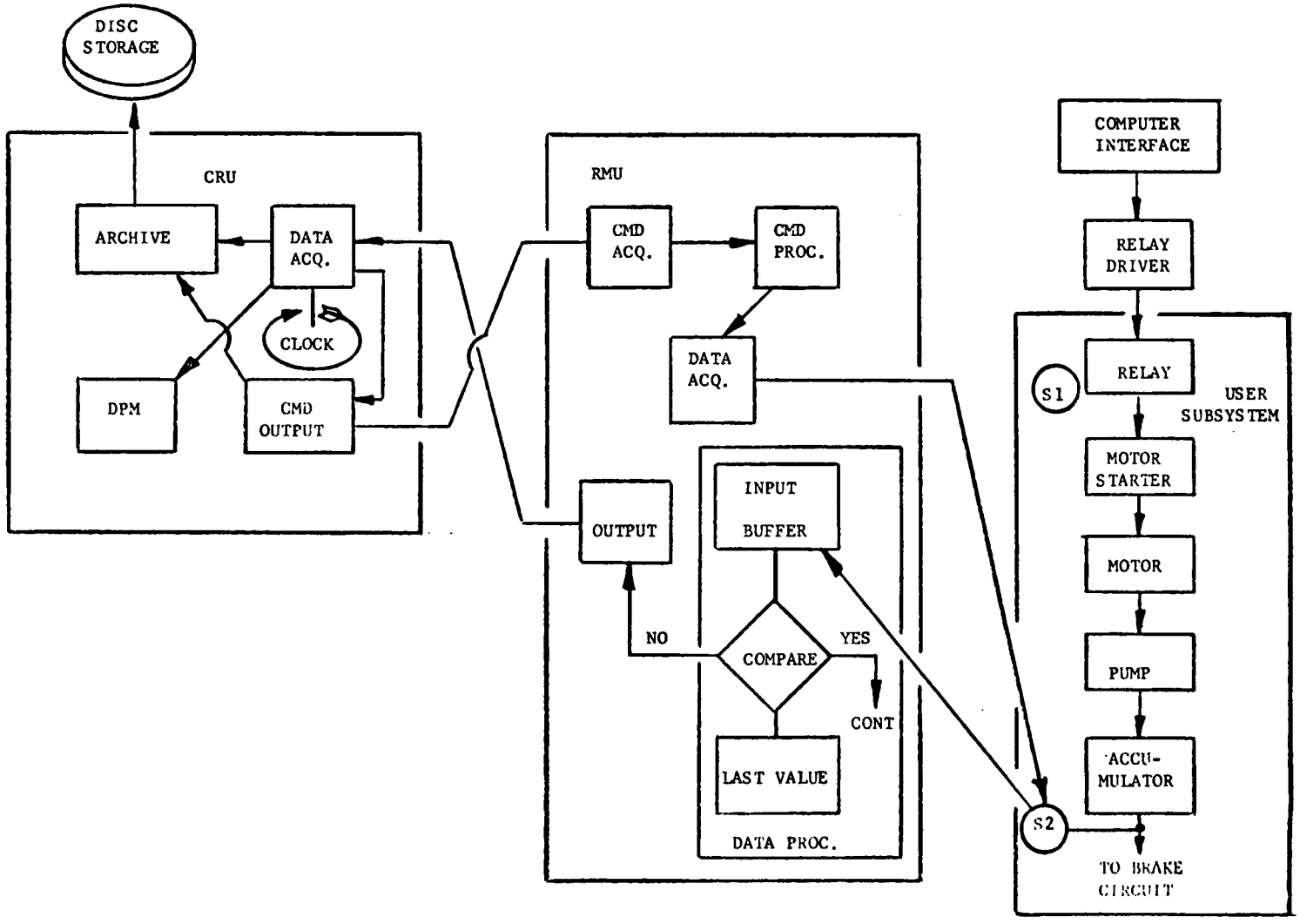

Figure 7-27. Data Acquision and Compression

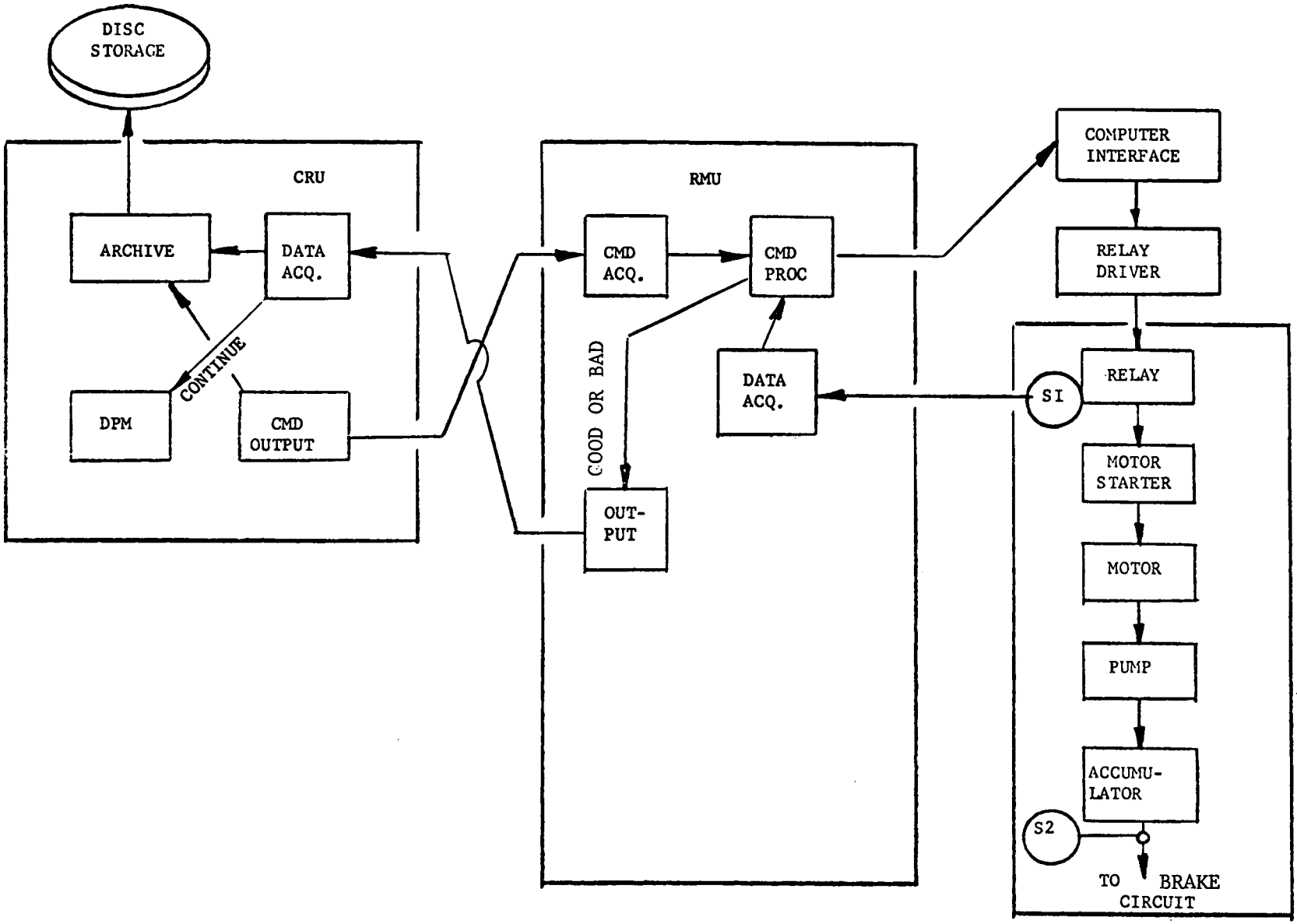

Figure 7-28 Command Generator

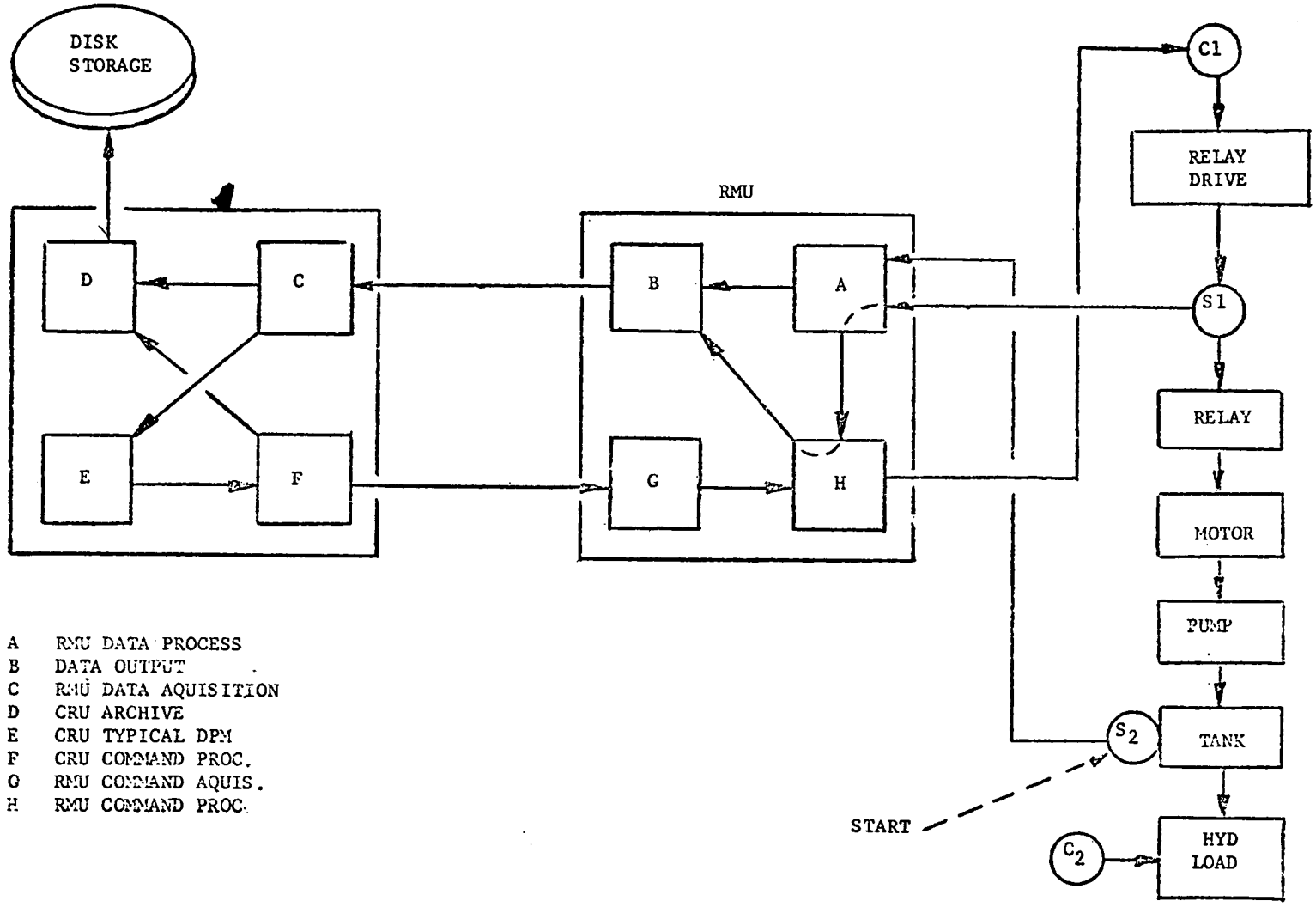

Figure 7-29. Typical WTG Control Loop

AUTOMATIC mode of operation, it is either in the GENERATE state trying to stay there, or in the IDLE state trying to go to GENERATE when conditions permit.

Data Process Modules. Data Process Modules examine change conditions as reflected in sensor status changes being reported by the RMUS and react to them as necessary. These reactions can include Command output, process shutdown, or notification to other modules.

Archive. Archive records all pertinent system data. This data includes traffic to and from the RMUS, discourse with the operator when the system is in AUTOMATIC mode, interface with the Utility, and internal changes of state.

Display. Displays predefined groups of system (collected and monitored) data on the CRT and/or DEC writer. As the sensors that contribute to any current display change, the display is also updated.

Manual. Manual provides the on-site operator with the facility to exercise various component parts of the WTG environment. These manually exercisable functions are Pitch, Yaw, Blade Rotation Enable, Rate Sync, Angle Sync, and Normal Shutdown. This module prevents the operator from performing any function which could conceivably cause damage to any part of the system.

Test. Test provides the on-site operator with the capability to alter the system sensor scan frequency and to alter the source of the incoming sensor data. Sensor data source can be Manual, Computer, or Live (Sensor).

Modify. Modify provides the operator with the capability of altering critical system parameters. Those items which the operator can modify include the present power setting, the present sample rate, the periodicity of the Self-Check function and individual sensor parameters.

Startup. Startup provides the linkage for the operator or utility dispatcher to take the system from a cold start to a condition of Automatic operation in the Idle mode: the scan cycle is initiated, the system is commanded to a known initial condition, and the system will try to go to Generate if all is satisfactory.

Playback. Playback provides site personnel with the capability of looking at the archived data. The operator is queried, via the CRT or DEC writer when the WTG is nonoperational, for guidelines on what to extract from the ARCHIVE file and for what time frame. The operator can choose an event-related report or a statistical summary.

7.6.3.2 GMU/NMU

Data Process. Data Process is scheduled by the Data Acquisition Module at the termination of a sensor scan cycle. It first determines whether any discrete sensors have changed since the last cycle. If they have, the specific change sensor(s) are identified, their System Identification code is extracted from the RMU Data Process Table, and a notification of change is sent to OUTPUT. The Data Process Table is then updated to reflect the most current state of the sensor.

The final task is to determine if any analog sensors have either exceeded their permissible aperture change or crossed a predefined band limit. If either condition has occurred, OUTPUT is notified, and the Analog Process Table is updated.

Output. Output is entered by all other RMU modules to send data in an orderly, buffered fashion, to the CRU. Data is buffered, and when Data Process completes its sensor scan, OUTPUT checks its current output buffer. If it is not empty, the buffer is terminated and sent to the CRU.

Command Acquisition. Command Acquisition receives all traffic coming from the CRU. Commands which alter process parameters such as Change Sample Rate and Force Route are executed immediately. Hardware commands, such as PCM Servo On/Off and Power Trim, are recorded in the Command Process Table. Command Process is scheduled to output the command.

Command Process. Upon being activated by Command Acquisition, the Command Process presents the command to the control interface. When activated by Data Process, Command Process scans the Command Process Table looking for Active commands. When found, the Running Delay Time field is decremented. When Delay Time goes to zero, the latest value of the related Command Completion sensor is extracted from the Data Process Table. If the latest status equals the desired status, OUTPUT is activated to send a Successful Command Completion to the CRU. Otherwise, retry procedures are initiated.

Controls Interface. The Control Interface is a group of general service routines used by various RMU functions to communicate with the Windmill Command and sensor functions. These routines can be entered by RMU processors to perform the following tasks:

1. Output a command
2. Write to all interfaces
3. Read from all interfaces
4. Alter the input source of the interfaces

7.6.3.3 Test Modules

Software test modules are provided to generate test data and to distribute test data in the Remote Units for the Final Software Validation Test.

Test Build/Modify accepts engineering data values for the analog sensors and ones and zeroes for the discrete sensors and will form the State Time data blocks. This module converts all the analog engineering data into their equivalent 12-bit analog values and places the analog and discrete data onto the RX01 Floppy Discs for both the GMU and the NMU. Initial raw data will be input from the VT52. Later, this data can be modified on the Floppies through the VT52. Test Build/Modify will also list the test data contents of the Floppy for verification purposes.

In order to run the Operational Scenario Test and Anomalous Shutdown Tests. Test Execute will be down-line loaded to each remote. TXQT will retrieve the State Time data blocks and temporarily store them in the PDP 11/04 MOS memory for sequential processing. Upon receipt of a Data Acquisition request from the CRU, both Remote Units distribute a State Time data block to the appropriate input parts of their respective analog and discrete interface units. Then, control is passed back to the operational acquisition module to scan, acquire, and process the data as usual. TXQT continues to process all the State Time data blocks through last State Time when it signals the CRT and printer that the test is over.

An operational test capability for the various hardware interfaces is provided by the Self-Test function. The sensor and command interfaces are periodically presented with known data values. They are then read and the input is compared to the output. Any detected anomolies between the two data sets result in an RMU initiated shutdown. This process is depicted in Figure 7-30.

7.6.4 STORAGE ALLOCATION

The RKØ5 disc will contain the following file structures:

1. CRU Initialization Data Base
2. GMU Initialization Data Base
3. NMU Initialization Data Base
4. DISPLAY skeleton tables
5. The DISC Archive file
6. The RSX11-S and RSX11-M operating systems
7. The RMU Test Execute Processors
8. A File of Error Code Expansions for reporting to the Utility and ON-site operator.

7.6.5 FINAL SOFTWARE VALIDATION

7.6.5.1 Introduction

The purpose of the Final Software Validation Test is to insure that the developed software meets all the operational and safety requirements of the Wind Turbine Generator. This means that the software system acquires and processes all sensor signals from the WTG, that it outputs the correct commands to the WTG subsystems at the right time, that it properly archives, displays and prints out all messages and data for both the site and the utility operators and that it properly responds to all operator requests from either the site or the utility.

7.6.5.2 Test Processors

A test philosophy for the WTG process control system was developed predicated

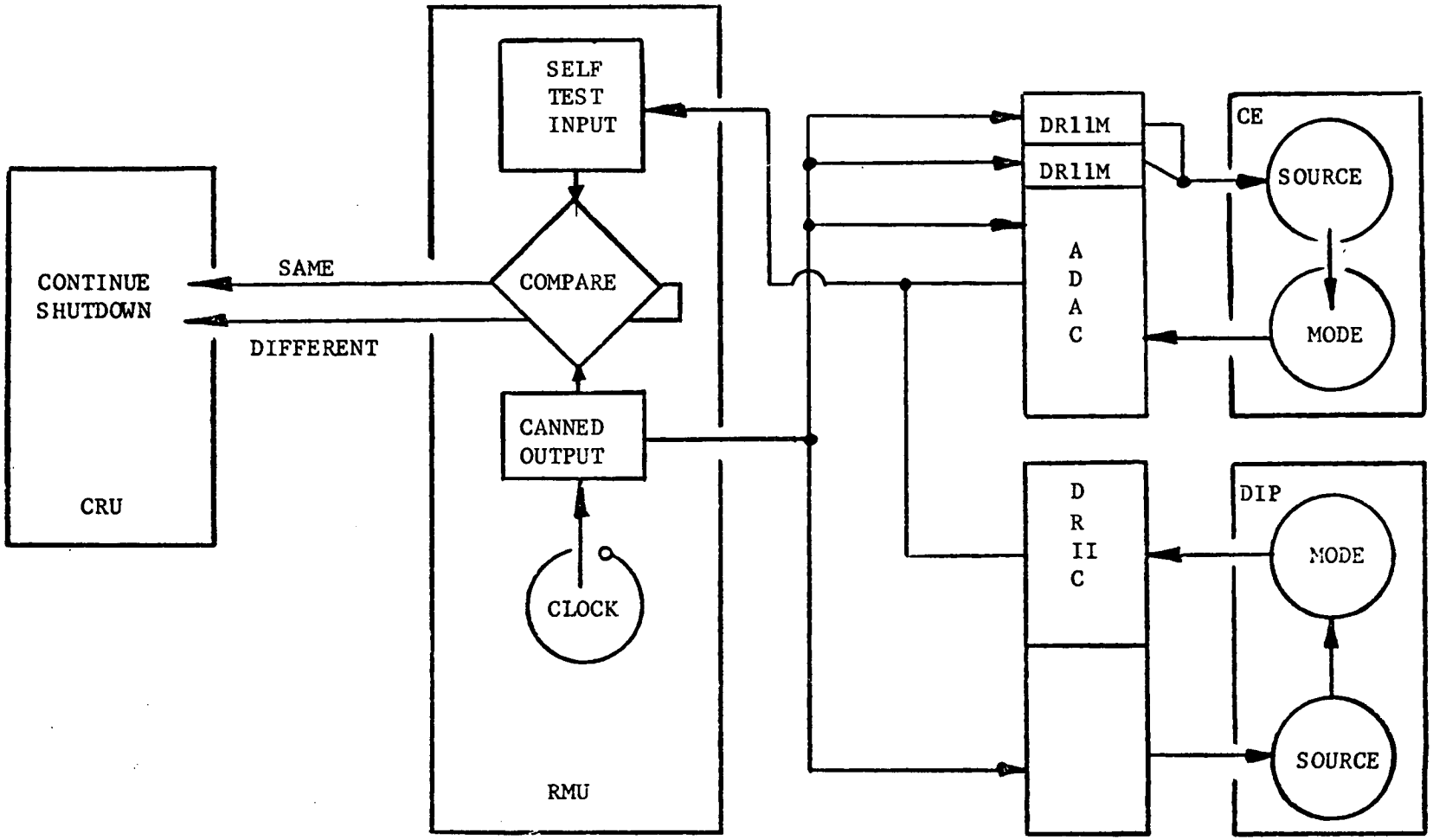

Figure 7-30 Self Test

upon the following two assumptions:

1. Sensor rates of change (in particular, analog sensors) are constant and predictable over most of the WTG operational range and can, therefore, be described in a test data base.

2. Commands, when enacted, affect finite areas of interest and can, therefore, be associated in a test data base with sensors which are affected by the initiation of the command.

In short, the test processor for the WTG system has the capability of allowing the test initiator to command sensor(s) to change at a rate compatible with the known characteristics of the sensor and with the characteristics of the parameter which the sensor is measuring; furthermore, the processor incorporates methods of simulating actual hardware response to the many and varied commands that the WTG software system has at its disposal for the purpose of controlling WTG operation.

The data designs required to implement the preceding are incorporated in the Command Profile Table and the Sensor Profile Table. These two tables will be built once and stored on the RK05 disc. When test scenarios are defined and converted to records for inclusion ona floppy disc test input file, these two tables will be inserted at the beginning of the file on the floppy. They will be utilized by the test processor (TXQT) at test initialization time for defining the initial test operational environment. All subsequent sensor alteration records (Figure 7-31) included on the test data base will be applied against one or both of these tables. These records will be reread whenever a Reinitialization record is encountered while reading the Test Data Base during execution of TXQT.

TBLD is a stand-alone processor that executes in the PDP 11/34 under RSX11-M. Its purpose is to build and/or modify test data bases on floppy discs. TXQT is a run-time routine that is down-line loaded from the RK05 to each RMU when the tester directs the TEST processor (under OIF) to do this. It performs Initialization, Sensor Modification, and Command Processing.

Initialization. Reads in (from the Test Floppy), the HDR record and prints pertinent information contained in it on whatever terminal is attached to the PDP 11/04. It then reads the Sensor Profile Table (SPT) and Command Profile Table (CPT) from the floppy and initializes them in memory. These two records provide TXQT with the initial baseline sensor and command environment for test initiation.

Sensor Modification. This code is executed each time the RMU receives a Data Acquisition request from the CRU. First, any sensor modification records for this cycle are read from the floppy disc and processed. Then, Sensor Parameter Table entries are examined to determine SOURCE (of data). If required, the interface is changed to read from LIVE or DIP. These values are inserted, where required, in the proper Sensor Profile Table entries.

Next, any necessary Command Completion Sensors are processed for this cycle. The Sensor Profile Table is then cycled, and each value is moved to the TXQT output buffer. Finally, the interface is set to MODE MANUAL, SOURCE COMPUTER,

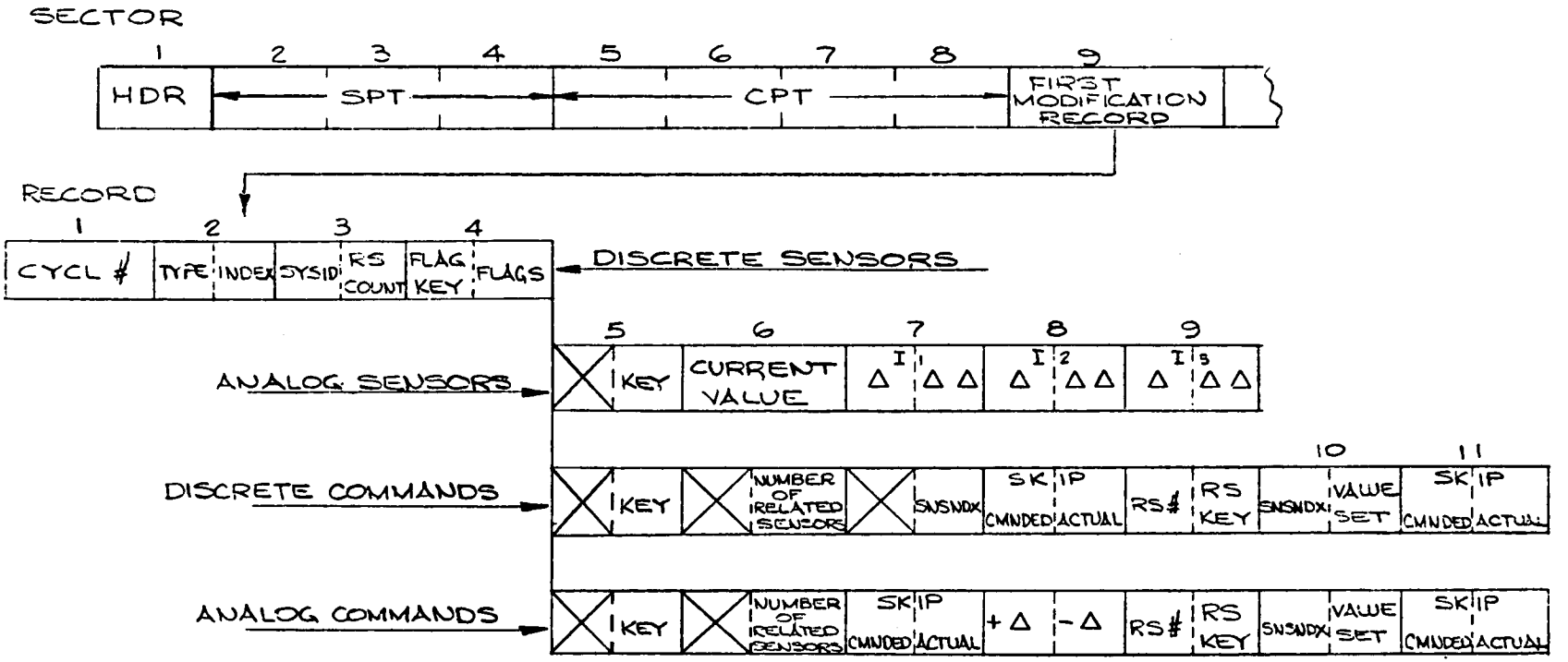

Figure 7-31 Floppy Disc Test Data Base

and the updated buffer is written. TXQT then exits for this cycle.

Command Processing. This code is executed whenever a "REAL" command is received in the RMU. If the command is being turned ON, sensor-related to the command are also turned on.

If the command is being turned OFF, the related sensors are likewise turned off.

Figure 7-32 presents an overall block diagram of the test process from Data Base Build through Test execute. Figures 7-33 and 7-34 are representations of the WTG command/sensor interface relationship and the relationship in the test environment, respectively.

7.6.5.3 Test Philosophy

Rigorous testing of a real-time sample data control system is complex by virtue of the time dependent nature of the system. The system being sampled is the WTG which provides approximately 60 unique and independent data sources to the computer. Upon receipt of these signals, the computer exercises control over the WTG by sending it analog and discrete commands which change the WTG physical state. The changed state data is then returned to the computer for further evaluation and processing which may result in the issuance of additional commands. However, at the time of software validation, there will be no WTG to either provide the time varying input data or to respond to commands. Therefore, in order to validate the software, the WTG data sources must be simulated. The planned tests permit a software self-test approach by which the WTG environment is simulated and which insures testing of all the computer software functions.

The approach in testing the software of CODAS is to exercise every automatically controlled and every manually controlled function through sets of known input conditions that will evoke known required responses. This exercise is accomplished by a combination of actual manual inputs from site and utility (test) operators and by simulated sensor inputs representing the WTG subsystems. The test data will be input from the floppy test data base augmented by the manual sensor inputs of the digital interface panel and the control electronics panel. The test processor will then feed data to the remotes in a real time simulation.

This test scheme is also used for on-site testing. Once on site, all initial checkout or any required software changes in the parameter tables or CRU processing would have to be checked out before reconnecting to and driving any WTG subsystem hardware. By running CODAS from the simulated sensor data on the floppy discs, it can be verified that CODAS has been properly reconfigured and is outputting the correct command responses under the newly imposed requirements. Such a procedure is essential to protect system hardware from any software errors that could possibly occur whenever a programming change in the field becomes necessary.

7.6.5.4 Operational Scenario Test

The Final Software Validation Test is designed to reflect as nearly as possible the same procedures and conditions that are found in the operational system.

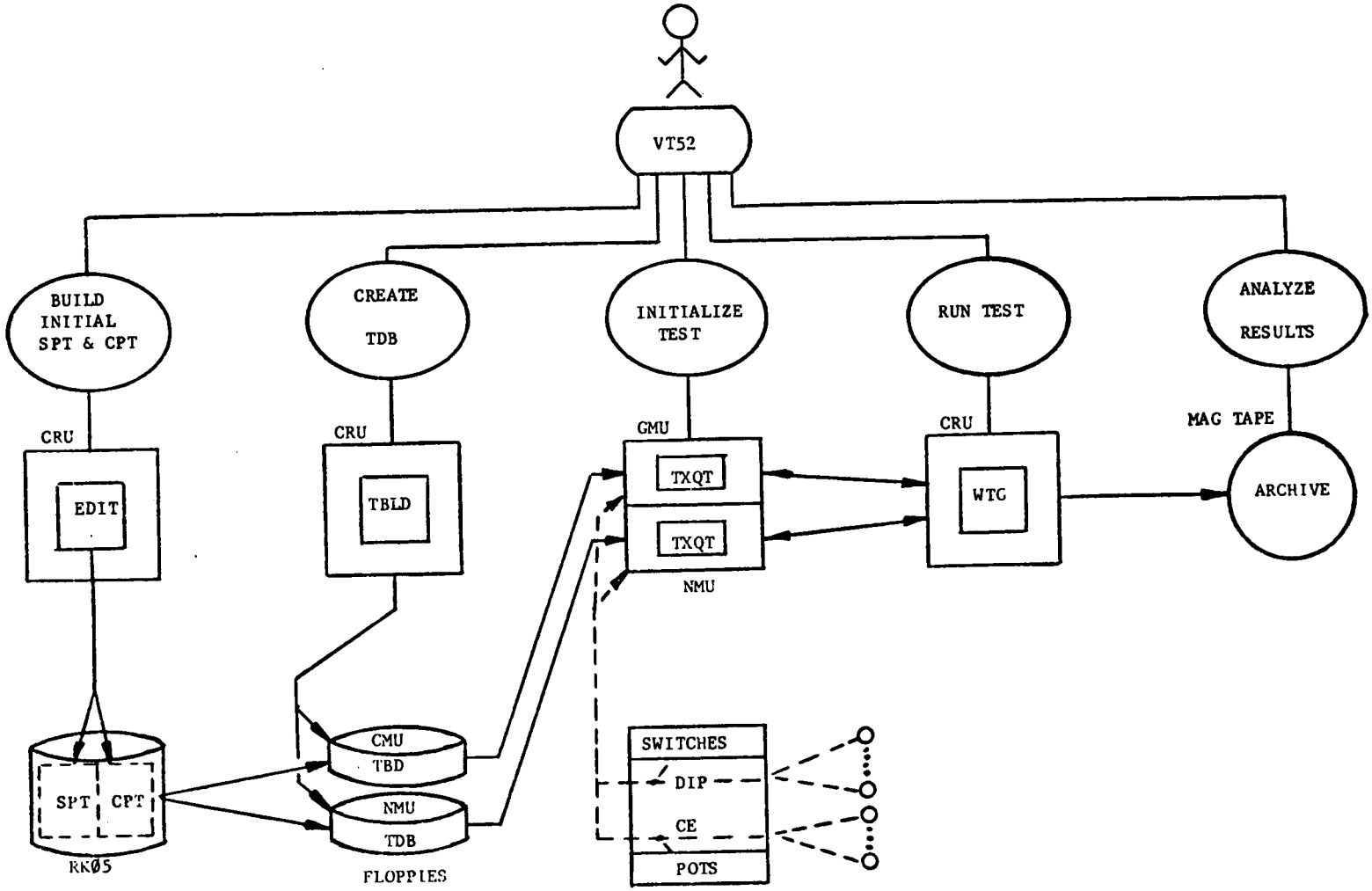

Figure 7-32. Elements of Test System

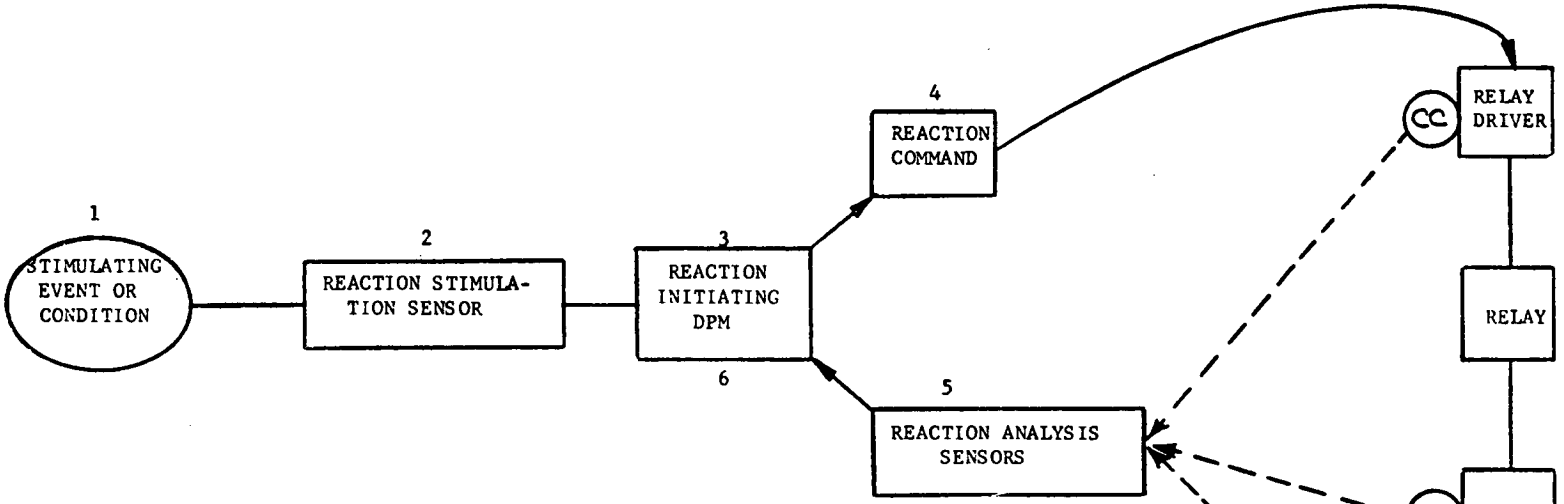

1. An event or condition occurs
2. A sensor monitoring that condition changes
3. The DPM responsible for correcting the condition is activated as a result of the sensor change.
4. The DPM issues a command to correct the condition.
5. As sensors associated with the command loop change, they are fed to the DPM to analyze.
6. When satisfied that the condition has been corrected, the DPM turns the command off and exits.

Figure 7-33. Normal WTG System Action/Reaction

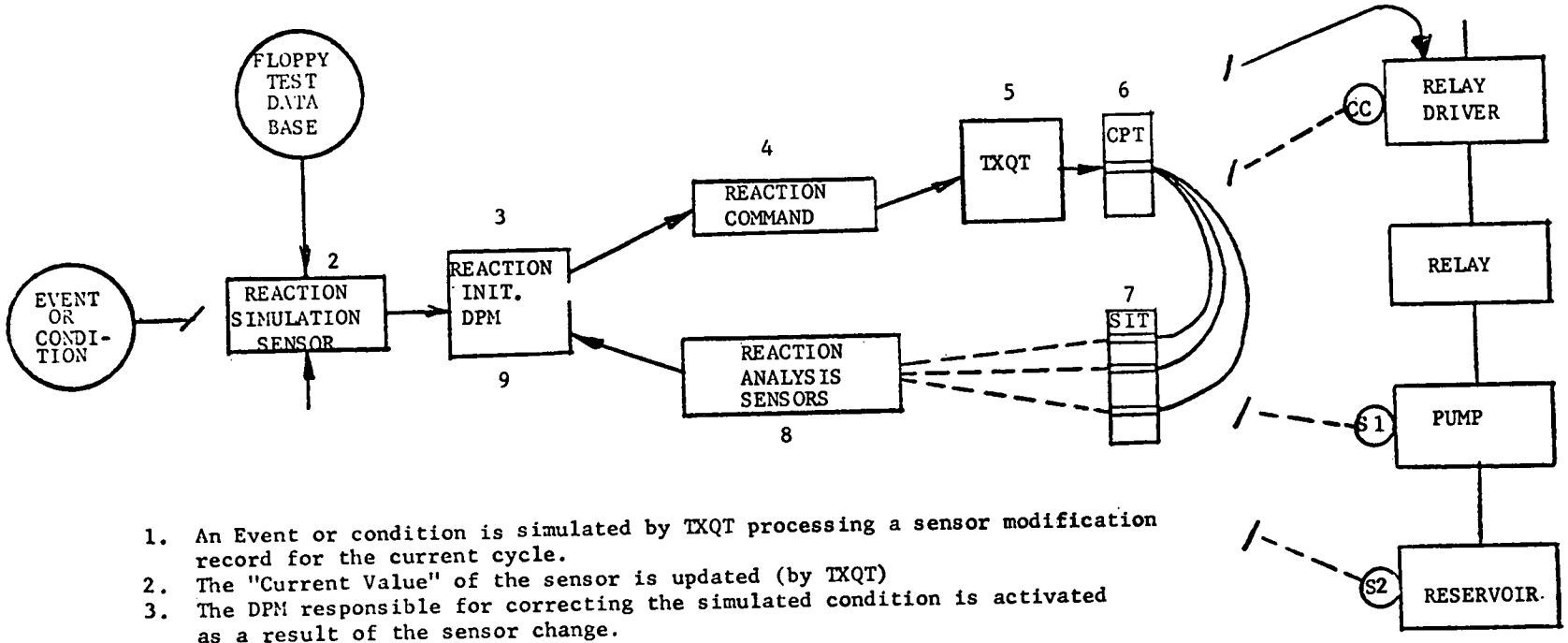

1. An Event or condition is simulated by TXQT processing a sensor modification record for the current cycle.
2. The "Current Value" of the sensor is updated (by TXQT)
3. The DPM responsible for correcting the simulated condition is activated as a result of the sensor change.
4. The DPM issues a command to correct the condition.
5. TXQT is given the command.
6. The command is activated in the CPT & the related sensors are extracted.
7. The related sensors are activated in the SPT and sensor modification is initiated.
8. As sensors associated with the command loop change, they are routed to the DPM to be analyzed.
9. When satisfied that the condition has been corrected, the DPM turns off the command & exits.

Figure 7-34 WTG System Action/Reaction Under Test Interface

This means that every manual and automatic software procedure to run the actual WTG hardware is tested. Each test is designed to reproduce a distinct portion of the operational system. For example, in its simplest form, a test data base issues all commands and checks responses. In a more complex format, a test data base will simulate actual real time conditions in idle or generate state and simulate system and/or environmental failures. The archived data will be used to verify that the software operation is correct.

It should be noted that all data to be processed as part of the Operational Scenario is an accurate representation of all WTG subsystems, assuming that all equipment is operating perfectly. The software will be evaluated against this data. Once the data has been thoroughly and accurately prepared, and bugs are removed from the operational software, the computer will successively command the simulated WTG through the modes of WAIT, IDLE, GENERATE, AND SHUTDOWN.

7.6.5.5 Anomalous Shutdown Tests

In contrast to the Operational Scenario, the test data associated with the Anomalous Shutdown Tests reflects equipment malfunctions and out-of-limit conditions of environmental parameters (wind speed, wind direction, ambient temperatures). It is estimated that there are 70 such test cases which will force normal shutdown, normal shutdown with lockout, emergency shutdown and emergency shutdown with lockout. Each of these cases will be tested in turn. After each shutdown, the simulated WTG is set in GENERATE mode to prepare for the next anomalous shutdown. The process is repeated until all the shutdown test cases have been run.

SECTION 8
GLOSSARY

SECTION 8

GLOSSARY

AGMA	American Gear Manufacturers' Assn.
AISC	American Institute of Steel Construction
β	Blade Pitch Angle
BREMC	Blue Ridge Electric Membership Cooperative
CG	Center of Gravity
CODAS	Control Operational Data System
CPU	Central Processing Unit
CRU	Control and Recording Unit
DEC	Digital Electronics Corporation
DIP	Digital Interface Panel
DOF	Degrees of Freedom
DPM	Data Processing Module
EDAS	Engineering Data Aquisition System
EMI	Electromagnetic Interference
FMEA	Failure Modes and Effects Analysis
GCE	Ground Control Electronics
GMU	Ground Multiplexer Unit
GSU	Generator Step-up Transformer
LVDT	Linear Variable Differential Transformer
MS	Margin of Safety
NCE	Nacelle Control Electronics
NMU	Nacelle Multiplexer Unit
P	Per Revolution Frequency
PCM	Pitch Control Mechanism
PDR	Preliminary Design Review
PIV	Portable Instrumentation Vehicle
PSS	Power System Stabilizer
PU	Per Unit
RTD	Resistance Temperature Detector
r/s	Radian/sec
RVDT	Rotary Variable Differential Transformer
SAIR	Stand Alone Instrument Recorder
SOW	Statement of Work
TC	Thermocouple
T/C	Thickness to Chord Ratio
TE	Trailing Edge
WFF	Wind Feed Forward
YS	Yaw Subsystem

1. Report No.	2. Government Accession No.	3. Recipient's Catalog No.
NASA CR-159495		

4. Title and Subtitle	5. Report Date
MOD-1 WIND TURBINE GENERATOR ANALYSIS AND DESIGN REPORT	May 1979
	6. Performing Organization Code
7. Author(s)	8. Performing Organization Report No.
	10. Work Unit No.
9. Performing Organization Name and Address General Electric Co. Space Division PO Box 8661 Philadelphia, Pa. 19101	11. Contract or Grant No. NAS 3-20058
	13. Type of Report and Period Covered Contractor Report
12. Sponsoring Agency Name and Address US Department of Energy Division of Distributed Solar Technology Washington, DC 20545	14. Sponsoring Agency Code Report # DOE/NASA/0058-79/2-Vol I

15. Supplementary Notes Final Report - Vol. I
Prepared under Interagency Agreement EC-77-A-29-1010
Project Manager, R. Puthoff Wind Energy Project Office
NASA Lewis Research Center, Cleveland, Ohio 44135

16. Abstract

The MOD-1 program is being conducted in six phases: Analysis and Preliminary Design (culminating in a Preliminary Design Review), Detail Design (ending with a Final Design Review), Fabrication and Assembly, System Testing, Site Preparation, and Installation and Checkout. Major milestone dates for these phases are shown in Table 1-1. This report is intended to describe only the results of the first two phases; that is, activities leading to the completion of Detail Design. Although this report places emphasis on a description of the design as it finally evolved, it also traces the steps through which the design progressed in order to understand the major design decisions. This report is Vol. I; the Appendix containing supporting analyses and back-up material too voluminous for the Final Report is issued as Vol. II.

17. Key Words (Suggested by Author(s))	18. Distribution Statement
Wind Turbine Generator; MOD-1 WTG Final Report	Unclassified - unlimited STAR Category 44 DOE Category UC-60

19. Security Classif. (of this report)	20. Security Classif. (of this page)	21. No. of Pages	22. Price*
Unclassified	Unclassified	320	

* For sale by the National Technical Information Service, Springfield, Virginia 22161

☆ U.S. GOVERNMENT PRINTING OFFICE: 1980-657-145/5227